10 February 2012 | $10

Science

Gordon Research Conferences

AAAS

CONTENTS

Volume 335 Issue 6069

CONTENTS continued >>

page 651

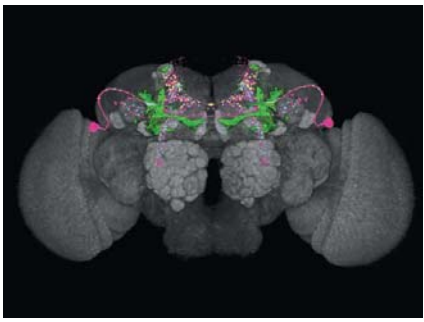

pages 664 & 678

COVER

Colorized scanning electron micrograph of a blood clot, removed from the coronary artery of a patient with acute myocardial infarction, showing the fibrin meshwork (brown) with trapped red blood cells (average ~7 micrometers across) and a cholesterol crystal (yellow). Regulated clotting of blood is essential for preserving life in vertebrates. The Gordon Research Conference on Hemostasis will be held 22 to 27 July 2012 in Waterville Valley, New Hampshire. See page 728 for the conference schedule and preliminary programs.

Image: Chandrasekaran Nagaswami and John W. Weisel, University of Pennsylvania

DEPARTMENTS

Published by AAAS

CONTENTS

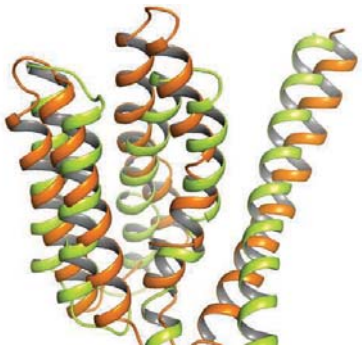

pages 669 & 686

page 690

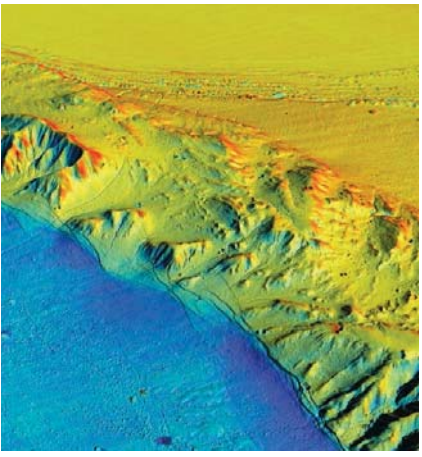

page 702

SCIENCEONLINE

SCIENCEXPRESS
www.sciencexpress.org

ApoE-Directed Therapeutics Rapidly Clear β-Amyloid and Reverse Deficits in AD Mouse Models
P. E. Cramer et al.
Bexarotene counters the effects of neurodegenerative disease in mice.
10.1126/science.1217697

Triggering a Cell Shape Change by Exploiting Preexisting Actomyosin Contractions
M. Roh-Johnson et al.
Morphogenesis in developing worms and flies harnesses ongoing cortical motility.
10.1126/science.1217869

The Alarmin Interleukin-33 Drives Protective Antiviral $CD8^+$ T Cell Responses
W. V. Bonilla et al.
A danger signal released from dying cells is required for antiviral immunity in mice.
10.1126/science.1215418

Plant UVR8 Photoreceptor Senses UV-B by Tryptophan-Mediated Disruption of Cross-Dimer Salt Bridges
J. M. Christie et al.
A tryptophan pyramid allows a dimeric protein to perceive ultraviolet light without an additional chromophore.
10.1126/science.1218091
>> Science *Podcast*

Intensifying Weathering and Land Use in Iron Age Central Africa
G. Bayon et al.
Savannas abruptly replaced rainforests around 3000 years ago on account of both climate and human land-use changes.
10.1126/science.1215400

The Obligation to Prevent the Next Dual-Use Controversy
R. R. Faden and R. A. Karron
10.1126/science.1219668
>> *Policy Forums pp. 660 and 662*

TECHNICALCOMMENTS

Comment on "Phonemic Diversity Supports a Serial Founder Effect Model of Language Expansion from Africa"
M. Cysouw et al.
Full text at www.sciencemag.org/cgi/content/full/335/6069/657-b

Comment on "Phonemic Diversity Supports a Serial Founder Effect Model of Language Expansion from Africa"
C.-C. Wang et al.
Full text at www.sciencemag.org/cgi/content/full/335/6069/657-c

Comment on "Phonemic Diversity Supports a Serial Founder Effect Model of Language Expansion from Africa"
R. Van Tuyl and A. Pereltsvaig
Full text at www.sciencemag.org/cgi/content/full/335/6069/657-d

Response to Comments on "Phonemic Diversity Supports a Serial Founder Effect Model of Language Expansion from Africa"
Q. D. Atkinson
Full text at www.sciencemag.org/cgi/content/full/335/6069/657-e

SCIENCENOW
www.sciencenow.org
Highlights From Our Daily News Coverage

Did Easter Islanders Mix It Up With South Americans?
Genetic evidence suggests that Polynesians may have mingled with pre-Columbian Native Americans.
http://scim.ag/Easter_Islanders

Air Guns Shake Up Earthquake Monitoring
A new device may help researchers keep an eye on changing stresses along fault zones.
http://scim.ag/Earthquake_Monitoring

Primed for Addiction?
People with brains wired for drug abuse do not necessarily become addicts.
http://scim.ag/Primed-Addiction

SCIENCETRANSLATIONAL MEDICINE
www.sciencetranslationalmedicine.org
Integrating Medicine and Science
8 February issue: http://scim.ag/stm020812

RESEARCH ARTICLE: AAV2 Gene Therapy Readministration in Three Adults with Congenital Blindness
J. Bennett et al.
Repeat administration of gene therapy to the contralateral retina of three congenitally blind patients was safe and resulted in improved vision.

RESEARCH ARTICLE: Simultaneous Targeting of Toll- and Nod-Like Receptors Induces Effective Tumor-Specific Immune Responses
J. Garaude et al.

FOCUS: Improving Immunotherapy—Revisiting the Immunologist's Little Secret
J. A. Berzofsky
A cancer vaccine of irradiated tumor cells expressing flagellin primes effective NLRC4/NAIP5- and TLR5-dependent antitumor immune responses.

RESEARCH ARTICLE: Mechanisms of Acquired Crizotinib Resistance in ALK-Rearranged Lung Cancers
R. Katayama et al.

PERSPECTIVE: Escaping ALK Inhibition—Mechanisms of and Strategies to Overcome Resistance
C. M. Lovly and W. Pao

PODCAST
J. Engelman and O. Smith
Multiple mechanisms of crizotinib resistance were identified in lung cancer patients, including new secondary ALK mutations and activation of receptor tyrosine kinases.

SCIENCESIGNALING
www.sciencesignaling.org
The Signal Transduction Knowledge Environment
7 February issue: http://scim.ag/ss020712

RESEARCH ARTICLE: Protein Kinase CK2 Triggers Cytosolic Zinc Signaling Pathways by Phosphorylation of Zinc Channel ZIP7
K. M. Taylor et al.

PODCAST
K. M. Taylor and A. M. VanHook
The kinase CK2 promotes the generation of intracellular zinc waves by stimulating the zinc channel ZIP7.

RESEARCH ARTICLE: PTEN Directly Activates the Actin Depolymerization Factor Cofilin-1 During PGE_2-Mediated Inhibition of Phagocytosis of Fungi
C. H. Serezani et al.
The protein phosphatase activity of PTEN impairs macrophage phagocytosis of a fungal pathogen.

PERSPECTIVE: An "Inordinate Fondness for Transporters" Explained?
D. J. Eide
The presence of low- and high-affinity transporters enables cells to adequately prepare for nutrient fluctuations.

FORUM: Highlights of Selected Talks Related to Posttranslational Modifications in Cell Signaling
N. R. Gough
These are summaries of presentations from the Cell Signaling Networks 2011 meeting.

SCIENCECAREERS
www.sciencecareers.org/career_magazine
Free Career Resources for Scientists

Taken for Granted: How to Live With Danger
B. L. Benderly
As the Sangji case moves toward a legal judgment, will the academy learn its lessons?
http://scim.ag/TFG_Danger

Translational Research Finds a New Center
M. Price
A new NIH center aims to set the national agenda on translational research, but budget constraints mean not much change for now.
http://scim.ag/TransCenter

Perspective: Questing for Blue Oceans
J. Garcia-Martinez
A Spanish molecular nanotechnology researcher, TR35 Innovator of the Year, company founder, and policy adviser encourages early-career scientists to incite scientific revolutions.
http://scim.ag/BlueOceans

SCIENCEPODCAST
www.sciencemag.org/multimedia/podcast
Free Weekly Show

On the 10 February *Science* Podcast: ultraviolet light sensing in plants, investigating earthquakes with LIDAR, indoor microbe populations, and more.

SCIENCE (ISSN 0036-8075) is published weekly on Friday, except the last week in December, by the American Association for the Advancement of Science, 1200 New York Avenue, NW, Washington, DC 20005. Periodicals Mail postage (publication No. 484460) paid at Washington, DC, and additional mailing offices. The title SCIENCE is a registered trademark of the AAAS. Domestic individual membership and subscription (51 issues): $149 ($74 allocated to subscription). Domestic institutional subscription (51 issues): $990; Foreign postage extra: Mexico, Caribbean (surface mail) $55; other countries (air assist delivery) $85. First class, airmail, student, and emeritus rates on request. Canadian rates with GST available upon request, GST #1254 88122. Publications Mail Agreement Number 1069624. **Printed in the U.S.A.**

Change of address: Allow 4 weeks, giving old and new addresses and 8-digit account number. **Postmaster:** Send change of address to AAAS, P.O. Box 96178, Washington, DC 20090–6178. **Single-copy sales:** $10.00 current issue, $15.00 back issue prepaid includes surface postage; bulk rates on request. **Authorization to photocopy** material for internal or personal use under circumstances not falling within the fair use provisions of the Copyright Act is granted by AAAS to libraries and other users registered with the Copyright Clearance Center (CCC) Transactional Reporting Service, provided that $30.00 per article is paid directly to CCC, 222 Rosewood Drive, Danvers, MA 01923. The identification code for *Science* is 0036-8075. *Science* is indexed in the *Reader's Guide to Periodical Literature* and in several specialized indexes.

AAAS
ADVANCING SCIENCE, SERVING SOCIETY

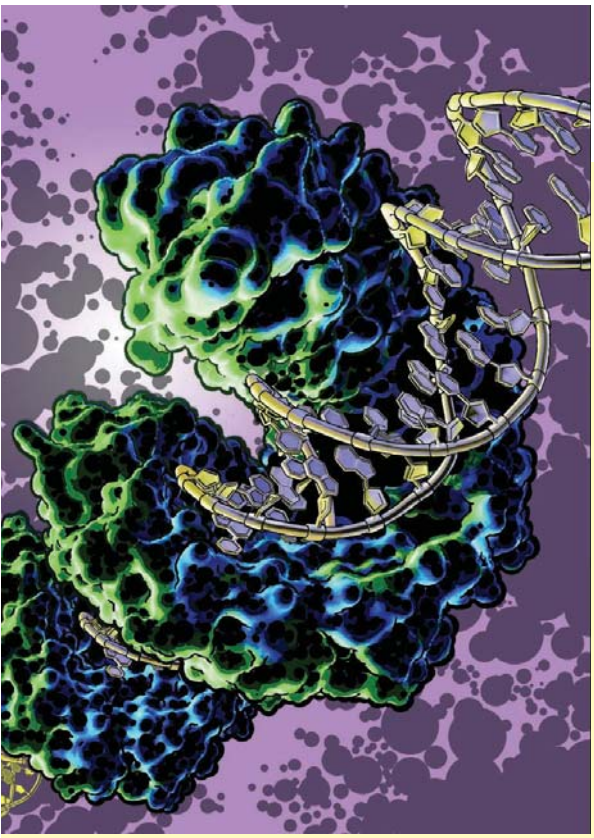

<< Wrapped DNA

TAL effectors are proteins that bacterial pathogens inject into plant cells that bind to host DNA to activate expression of plant genes. The DNA-binding domain of TAL proteins is composed of tandem repeats within which a repeat-variable diresidue sequence confers nucleotide specificity. **Deng *et al.*** (p. 720, published online 5 January) report the structure of the TAL effector dHax3, containing 11.5 repeats, in DNA-free and DNA-bound states, and **Mak *et al.*** (p. 716, published online 5 January) report the structure of the PthXo1 TAL effector, containing 22 repeats, bound to its DNA target. Together, the structures reveal the conformational changes involved in DNA binding and provide the structural basis of DNA recognition.

Spring Bloom

The spring bloom of plankton in northern seas develops apparently in response to increasing light and to winter weather, which make nutrients available at the surface. This seasonality is important on a global scale because it reflects a tipping point, driven by phytoplankton growth, between CO_2 production and carbon storage. The phenomenon is thus of particular interest in this era of carbon excess. **Giovannoni and Vergin** (p. 671) review what is known about the dynamics of these highly ordered microbial plankton communities, discuss the specialist roles of certain taxa, and reflect on predictions for anthropogenic changes to the oceans and what these might mean for geochemical cycles driven by ocean microbiota.

Earthquakes from Above

Preparing for risks and hazards associated with large earthquakes requires detailed understanding of their mechanical properties. In addition to pinpointing the location and magnitude of earthquakes, postmortem analyses of the extent of rupture and amount of deformation are key quantities, but are not simply available from seismological data alone. Using a type of optical remote sensing, Light Detection and Ranging (LiDAR), **Oskin *et al.*** (p. 702) surveyed the surrounding area that ruptured during the 2010 M_w 7.2 El Mayor–Cucapah earthquake in Northern Mexico. Because this area had also been analyzed in 2006, a comparative analysis revealed slip rate and strain release on the shallow fault zone and a number of previously unknown faults. As remote imaging becomes cheaper and more common, differential analyses will continue to provide fault-related deformation data that complements modern seismological networks.

CREDITS (TOP TO BOTTOM): JON BOGDANOVE; KARUNADASA *ET AL.*

Edging In on MoS_2

Molybdenum disulfide is a widely used catalyst in the petrochemical industry that has recently shown promise for water-splitting applications. Its activity appears to be confined to edge sites with exposed disulfide groups, although the precise geometric details underlying the chemistry remain uncertain. **Karunadasa *et al.*** (p. 698) prepared a molecular complex modeling one of these edge sites, in which a triangular Mo-S-S unit is supported by metal coordination to five tethered pyridine rings. The molecule was characterized crystallographically and proved robustly active toward electrochemical generation of hydrogen from water, even when applied to crudely filtered seawater.

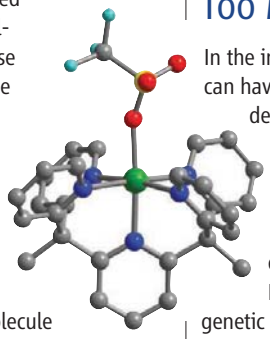

Challenging the Mushroom Bodies

Early memory is labile and is gradually consolidated over time into long-lasting, stable memory. In several species, including mammals, memory consolidation depends on protein synthesis. In *Drosophila*, long-term memory is produced by spaced repetitive training, which induces cyclic adenosine monophosphate (cAMP)–response element–binding protein (CREB)–dependent gene transcription and de novo protein synthesis. Using a large number of genetic tools, **Chen *et al.*** (p. 678; see the Perspective by **Dubnau**) localized this CREB-dependent induction of de novo protein synthesis to two dorsal-anterior-lateral neurons in the adult brain. Importantly, protein synthesis was not required within the mushroom bodies, which are usually considered to be the site of associative learning and memory in insects.

Maintaining Equilibrium

Na^+/Ca^{2+} exchangers (NCX) are membrane transporters that maintain the homeostasis of cytosolic Ca^{2+} and play an essential role in Ca^{2+} signaling. Despite a long history of physiological work and a large body of functional data, the structural basis underlying the ion exchange mechanism of NCX is poorly understood. **Liao *et al.*** (p. 686; see the Perspective by **Abramson *et al.***) present a high-resolution crystal structure of an NCX from *Methanococcus jannaschii* and demonstrate that this archaeal NCX catalyzes Na^+/Ca^{2+}-exchange reactions similar to its eukaryotic counterpart. The structure clarifies the mechanism of ion exchange proteins and reveals the basis for the stoichiometry, cooperativity, and bidirectionality of the reaction.

Too Much Tolerance?

In the immune system, loss of tolerance to self can have devastating consequences, such as the development of autoimmune diseases. In some cases, however, we may wish to be able to break tolerance, for example, to activate immune cells to fight tumors. **Schietinger *et al.*** (p. 723, published online 19 January; see the Perspective by **Lee and Jameson**) used a combination of genetic mouse models and adoptive immune cell transfers to better understand the mechanisms regulating tolerance in T lymphocytes. In contrast to the prevailing paradigm, the maintenance of T lymphocyte tolerance did not require the continuous presence of antigen. Tolerance was able to be broken when previously tolerized cells were placed in an environment depleted of immune cells. However, when lymphocyte numbers were restored, cells were once again tolerized, even in the absence of antigen. These data, together with gene expression profiling, suggest that tolerance

Continued on page 634

Continued from page 633

is associated with a specific gene expression program that, although possible to override temporarily, is reimposed by epigenetic mechanisms.

Be My Guests

For a range of applications, including medical diagnostics or drug delivery, it is necessary to encapsulate one or more components into a microcapsule. While there are many methods that can do this, most either produce a range of capsule size or are not easily scalable for making large quantities. **J. Zhang *et al.*** (p. 690) developed a microfluidic-based system for making capsules using host-guest chemistry. Cucurbit[8]uril, which readily forms complexes in water, was used as the host molecule and could accommodate two different guest molecules. Rapid complexation was observed of methyl viologen–modified gold nanoparticles and a naphthol-containing copolymer.

Ties That Bind

Almost by definition, effective catalysts bind their substrates for a very short time—releasing them quickly after helping them react and then moving on to bind new, as yet unreacted, substrates. This property engenders an efficient cycle, but it hinders study of the binding motif. **Garand *et al.*** (p. 694, published online 19 January; see the Perspective by **Zwier**) devised a technique to extract bound complexes from solution and freeze their conformations in cold, gas-phase clusters. Probing these clusters by vibrational spectroscopy in conjunction with theoretical calculations then allowed the sites of hydrogen bonding that hold the complexes together to be pinpointed.

Close-Up of DNA Methylation

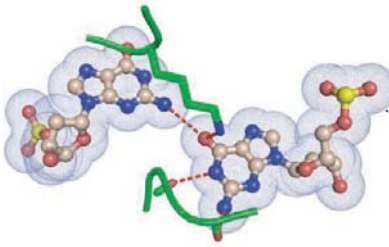

In eukaryotes, maintenance of genomic CpG methylation patterns is required for imprinting, retrotransposon silencing, and X-chromosome inactivation. The epigenetic mark needs to be faithfully maintained and propagated during repeated cell divisions in somatic cells by selective methylation of hemi-methylated CpG dinucleotides following DNA replication, which is carried out by the enzyme DNMT1. **Song *et al.*** (p. 709) determined the crystal structure of mouse DNMT1 bound to a DNA duplex containing a hemimethylated CpG on the parental strand, such as would be found immediately after DNA replication. Together with a previous structure of the autoinhibited structure, the findings suggest that a combination of active and auto-inhibitory mechanisms ensures the high fidelity of DNMT1-mediated maintenance of DNA methylation.

Before Tohoku-Oki

Recordings by Japan's dense seismic network in the days and weeks before the 2011 M_w 9.0 Tohoku-Oki earthquake provide an opportunity to interrogate what caused the dynamic rupture of one of the largest earthquakes on record. Using a method to extract small earthquakes that are often obscured by overlapping seismic waves, **Kato *et al.*** (p. 705, published online 19 January) identified over a thousand small repeating earthquakes that migrated slowly toward the hypocenter of the main rupture. Based on the properties of these foreshocks, the plate interface experienced two sequences of slow slip, the second of which probably contributed a substantial amount of stress and may have initiated the nucleation of the main shock.

Keeping a Kinase in Check

Cyclic adenosine monophosphate (cAMP)–dependent protein kinase (PKA) is involved in the regulation of several key metabolic pathways. It exists in mammalian cells as an inactive tetramer composed of a regulatory (R) subunit dimer and two catalytic (C) subunits. cAMP binding causes activation by releasing the C subunits. Insight into PKA regulation has come from structures of R and C subunit heterodimers; however, further understanding requires knowledge of the holoenzyme structure. **P. Zhang *et al.*** (p. 712) report a high-resolution structure of the $RII\beta_2{:}C_2$ tetramer. The structure reveals interactions at an interface between the two RC heterodimers and provides insight into the mechanism of allosteric activation upon cAMP binding.

CREDIT: SONG *ET AL.*

Gottfried Schatz is professor emeritus at the Biozentrum of the University of Basel and former head of the Swiss Science and Technology Council. His work dealt mainly with the biogenesis of mitochondria. E-mail: gottfried.schatz@unibas.ch.

The Endangered Bond

CREATIVE IDEAS ARE CHILDREN OF SOLITUDE, YET ARE RARELY CONCEIVED IN ISOLATION. THIS IS particularly true in science, which thrives on reliable and precise communication across linguistic, social, and cultural barriers. The digital age has given us instant global communication, yet scientists still prefer to talk about shared values and scientific issues face to face. As a unifying bond for our scientific culture, nothing rivals the spoken word.

This bond, however, is not invulnerable. Science was once part of a much broader intellectual effort that included the humanities, but at some time in the 19th century, a breakdown in communication made the two go their separate ways. The British physicist and writer Charles Percy Snow deplored this split in his influential Rede Lecture "The Two Cultures," delivered on 7 May 1959 in the Senate House at the University of Cambridge. His words ring as true today as they did half a century ago: "I constantly felt I was moving among two groups . . . who had almost ceased to communicate at all . . ." The same words can also be used to alert us to the fact that a degradation of verbal communication is now threatening to open up rifts even within the sciences. This degradation is especially noticeable in biology and other rapidly evolving fields that have a strong descriptive component. From my detached view as a retired biochemist, most lectures on biological topics appear so overloaded with unnecessary information, so obsessed with technical detail, and so cluttered with abbreviations, jargon, and acronyms as to be nearly incomprehensible to anyone but the specialist. More often than not, I also wait in vain for a concluding remark that would reveal the broader implications and long-term goals of the work. When attending lectures was still part of my daily routine, I had become accustomed to this insane newspeak, but now I recognize it as a serious threat to our scientific culture. A lecture designed to impress rather than inform usually does neither. Instead, it drives a wedge between different disciplines and promotes scientific fragmentation.

There is no quick fix for today's dire lecturing habits, but we could improve them through two approaches. One of them is teaching. Not all students are gifted lecturers, but most of them can be taught the basics of public speaking. Such teaching ought to be central to every science curriculum, yet it is usually ignored or done in only a perfunctory way. Its major goal should not be producing polished orators but scientists who understand the difference between the important and the unimportant and who will focus their lectures on the essence of their findings. The second approach could aim at the profusion of monikers and acronyms that have made biological fields such as gene transcription, signal transduction, or immunology such uninviting territories to eager newcomers. Deciphering the chemical structure of our genome and its roughly 25,000 genes has exacerbated this dilemma by triggering an avalanche of new gene names and abbreviations, which are often applied indiscriminately, with different names used to describe the same gene in different species.* Gordon Research Conferences and similar special meetings could serve as efficient settings for researchers to work out a consistent and rational nomenclature for their scientific discipline.

We should no longer tolerate lectures that drown the audience in a flood of unnecessary information and technical terms. Effective communication is a bridge between different disciplines and is essential to the advance of science. Agreement on a standard terminology should also stimulate discovery, because standardization is a proven motor for innovation. According to the Austrian logician Ludwig Wittgenstein, "Alles, was sich aussprechen lässt, lässt sich klar aussprechen" ("Whatever can be said can be said clearly"). In science, simple and clear language in both spoken and written communication is not only a matter of style—it is also a matter of substance.

– Gottfried Schatz

10.1126/science.1219756

*B. Bennani-Baiti, I. M. Bennani-Baiti, *Gene* **491**,103 (2012).

Published by AAAS

EDITORS' CHOICE

EDITED BY KRISTEN MUELLER AND JAKE YESTON

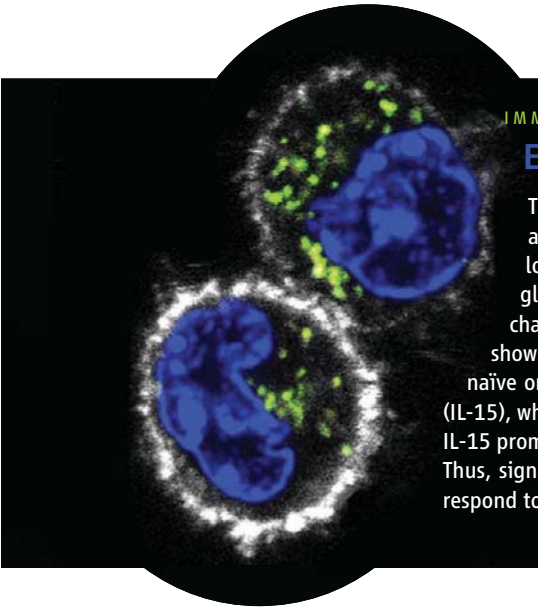

IMMUNOLOGY

Energy to Burn

The life of a T cell can be very demanding—at least as far as metabolism is concerned. An encounter with a pathogen calls for rapid proliferation and, for the subset of cells that go on to become memory cells, long-term survival. How do cells manage such metabolic demands? Upon activation, T cells switch to glycolysis. Largely quiescent memory cells, however, use oxidative phosphorylation but do have the extra challenge of being able to respond under conditions of increased work or stress. van der Windt *et al.* now show that mouse $CD8^+$ memory T cells have substantial mitochondrial spare respiratory capacity compared to naïve or effector T cells, which helps them keep up with their energetic demands. The cytokine interleukin-15 (IL-15), which is critical for memory T cell differentiation, was required for this elevated spare respiratory capacity. IL-15 promoted mitochondrial biogenesis and expression of a metabolic enzyme necessary for fatty acid oxidation. Thus, signals encountered along the way to becoming a memory T cell also endow these cells with the ability to respond to future energetic demands. — KLM

Immunity **36**, 68 (2012).

APPLIED PHYSICS

Magnetized at the Interface

Magnetism arises when electron spins in a solid align parallel (ferromagnetism) or antiparallel (antiferromagnetism) to each other. Especially useful in today's computer industry is the so-called exchange bias, a somewhat counterintuitive phenomenon whereby an antiferromagnet (AFM) interfaced with a ferromagnet (FM) biases the preferred direction of the magnetization of the FM despite having zero net magnetization of its own. Gibert *et al.* now demonstrate the exchange bias effect in an artificial lattice consisting of alternating thin layers of the normally nonmagnetic $LaNiO_3$ and the magnetic $LaMnO_3$. When sliced thinly, $LaMnO_3$ is a FM, and the authors show that its magnetization curve is shifted by the presence of $LaNiO_3$, as is typical in exchange bias systems; this suggests that $LaNiO_3$ develops magnetic ordering as well. Previous work has indicated the presence of AFM order in thin films of $LaNiO_3$; the authors' numerical modeling suggests that a modulated spin distribution resembling a spin wave is created in the nickelate. — JS

Nat. Mater. **11**, 10.1038/nmat3224 (2012).

GENETICS

Mom's in Charge

Imprinting is a genetic mechanism that directs an offspring to use only one copy of a parental gene. Typically, this occurs through the directed expression of an allele from only one parent. In the mammalian placenta, imprinting ensures proper nutrient allocation to the developing offspring. Costa *et al*. investigated whether this was also the case in the endosperm, the nutritive accessory tissue found in the seeds of flowering plants. In maize plants, the imprinted gene *Maternally expressed gene1* (*Meg1*), which encodes a small peptide known to control cell differentiation in plants, regulated nutrient allocation and affected embryo growth. *Meg1*

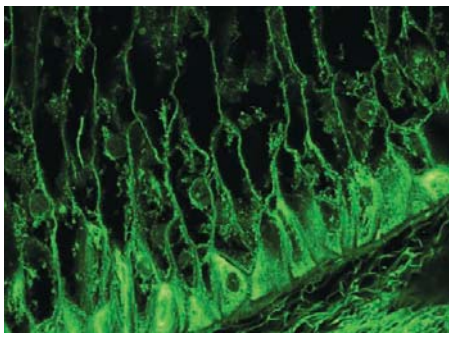

promoted the development and differentiation of the endosperm nutrient transfer tissue, which is responsible for the uptake and partitioning of sugars within the seed. In this system, imprinting was necessary for fine-balancing nutrient allocation from the maternal tissue to both the embryo and endosperm. These findings suggest that, similar to their roles in the mammalian placenta, imprinted genes function in the plant endosperm to control the nourishment of the embryo. — LMZ

Curr. Biol. **22**, 160 (2012).

MATERIALS SCIENCE

A Model for Aging

When cooled below the glass transition temperature, amorphous polymers show a sudden and rapid increase in viscosity, which macroscopically manifests as a hardening or solidifying of the material. Nonetheless, even at these temperatures, local segmental motion is possible, and the polymers thereby age with time as the chains relax into a lower-energy state. Recent experiments have shown that when deformed at a constant load, glassy polymers initially flow rapidly but then suddenly stop, with a striking decrease in the segmental relaxation time, but the basis for this behavior has not been well understood. Fielding *et al.* tackle this problem by developing a simple model of elastic polymer dumbbells immersed in a glassy solvent, in effect. Under a constant load, rejuvenation of the glassy segments occurs as initial fluidization leads to an accelerated rate of motion. However, the associated increase in the stress borne by the polymer segments then causes an arrest in the strain, allowing the glassy segments to resolidify. The authors note that the unloading behavior of the glassy chains is not well captured by the simple model, as the collapsing polymer chains carry enough stress to cause the glassy solvent to flow. By including a simple modification of the effective modulus of the polymer to reflect more realistic conditions, they are able to capture much of the behavior seen experimentally. — MSL

Phys. Rev. Lett. **108**, 48301 (2012).

CREDITS (TOP TO BOTTOM): *IMMUNITY* **36**, *68* (2012); J. YUAN

Published by AAAS

EVOLUTION

Getting from One to Two

Life on Earth was initially unicellular, but at some point these morphologically simple organisms started forming cooperative clusters of cells that allowed them to overcome the limited size and complexity of their single-celled brethren and thus colonize new environments.

To explore how this transition might have occurred, Ratcliff *et al.* subjected the unicellular yeast *Saccharomyces cerevisiae* to a gravity selection protocol. Heavy (and therefore more rapidly sinking) "snowflake" clusters of cells arose through dividing cells remaining stuck together. The close genetic relatedness of the cells in the clusters reduced the potential evolutionary conflict. Further selection resulted in larger snowflake clusters, which nonetheless grew to a specific size limit and reproduced through the production of smaller, but still multicellular, daughter snowflakes. The asymmetric divisions needed to generate the daughter snowflakes were driven by the formation of specialized apoptotic (self-killing) cells that allowed fragmentation of the interconnected cluster of parent snowflake cells. Higher rates of apoptosis correlated with smaller, more numerous daughter snowflakes, which, given their relatively fast growth rates, probably increased the chance of cluster survival through the next selection step. These results suggest that multicellularity may have arisen early in the evolution of life, and indeed there is evidence of filamentous and mat-like organisms dating back to over 3 billion years ago. — GR

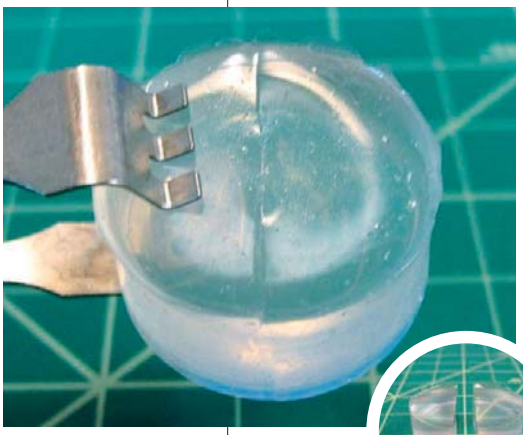

Proc. Natl. Acad. Sci. U.S.A. **109**, 10910.1073/pnas.1115323109 (2012).

BIOMEDICINE

All Eyes on Epigenetics

Cancer geneticists who are cataloging the genes mutated in human tumors have encountered a recurring theme: Many tumor types carry mutations in genes implicated in epigenetic mechanisms that regulate gene expression. New work on a rare childhood eye cancer called retinoblastoma reinforces the notion that the development and behavior of tumors involve both genetic and epigenetic mechanisms. Retinoblastoma arises when both copies of a tumor suppressor gene called *RB1* are inactivated. It had been postulated that *RB1* loss destabilizes the genome, leading to the accumulation of additional mutations that increase tumor aggressiveness. Through whole-genome sequencing of four retinoblastoma samples, Zhang *et al.* instead discovered that these tumors have a low mutation rate and a stable genome. However, several known oncogenes and tumor suppressor genes were found to have epigenetic changes that correlated with changes in their expression pattern in tumor versus normal tissue. Thus, *RB1* mutational status appears to affect the epigenetic mechanisms that turn genes on and off. One of the genes overexpressed in retinoblastoma encodes the protein tyrosine kinase SYK, and experiments with preclinical models suggest that SYK inhibitors may be useful drugs for targeting this type of tumor. — PAK

Nature 10.1038/nature10733 (2012).

CHEMISTRY

Polymer, Heal Thyself

Damage to a polymer, such as a cut or crack, can be repaired if it's possible to recover the reactive groups that initiate and sustain polymerization. Zheng and McCarthy show that one of the oldest polymerization schemes—the formation of silicones from cyclic siloxanes—can be used in this fashion. An 80:1 mixture of octamethylcyclotetrasiloxane (D4) and its ethylene-linked dimer (bis-D4) was polymerized with an anionic initiator by heating at 90°C for 4 hours. The resulting polymers contained active silanolate end groups under ambient conditions. The rubbery material could be cut with a knife and then repaired by holding the pieces in place next to one another and reheating at 90°C for 4 hours. When the repaired material was stressed by bending, it split at a location different from the knife cut. The authors note that this propensity was probably evident ~60 years ago when these polymerization methods were originally explored. — PDS

CREDIT: ZHENG AND MCCARTHY, *J. AM. CHEM. SOC.* **134**, 10.1021/JA2113257 (2012)

J. Am. Chem. Soc. **134**, 10.1021/ja2113257 (2012).

Published by AAAS

AROUND THE WORLD

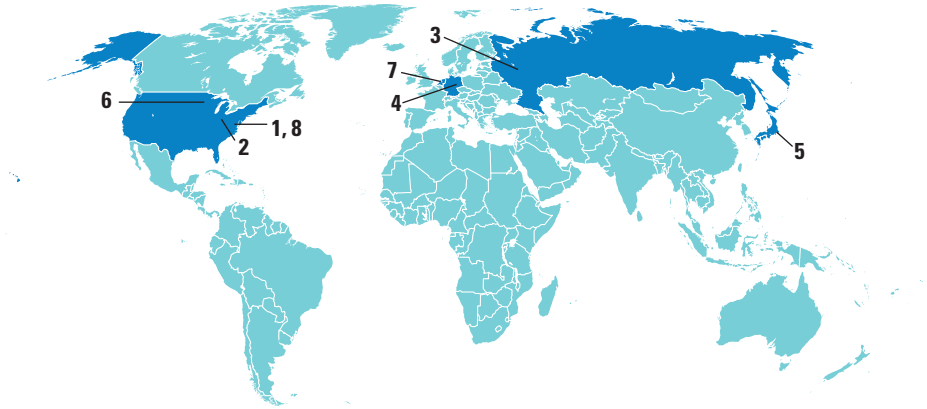

Washington, D.C. **1**

Whistleblowers' Lawsuit Puts Focus on FDA

A senior U.S. Senator wants to know why officials at the U.S. Food and Drug Administration (FDA) monitored the personal e-mail of six technical staffers who complained to the White House, Congress, and the press about the agency's approval process for cancer-screening devices. The 31 January letter to FDA from Senator Charles Grassley (R–IA), the top Republican on the Senate Committee on the Judiciary, came shortly after the six whistleblowers filed a lawsuit against FDA, alleging officials improperly monitored their computers and retaliated against them for publicizing their complaints.


Grassley

The lawsuit was filed by two doctors, one M.D./Ph.D., a scientist, an engineer, and a statistician. All served on scientific review committees for FDA's Center for Devices and Radiological Health. In 2008, they were among nine FDA reviewers who told Congress that agency officials had approved devices despite negative reviews. Freedom of Information Act requests revealed that FDA began monitoring government computers used by the "FDA nine," even capturing personal photos. Some of the staffers have since left FDA or been fired. Among other things, Grassley wants to know if FDA is still monitoring those who remain.

Indianapolis **2**

Creationism School Bill Unlikely to Advance

The Indiana state Senate last week approved a bill specifying that any classroom discussion of creationist views must include origin-of-life stories from "multiple religions." But the Indiana House of Representatives seems unlikely to go along after the House speaker described the legislation as "someplace where we don't need to go."

The original bill cited creation science as a topic that teachers could include in any discussion of "various theories on the origins of life." An amendment broadened the bill's scope to include "Christianity, Judaism, Islam, Hinduism, Buddhism, and Scientology." Opponents said the legislation, if enacted, would violate a 1987 Supreme Court ruling against the teaching of religion in public schools.

One veteran Indiana science teacher says the controversy is a reminder that some students might regard any lesson on evolution as a threat to their beliefs and that educators should be prepared to handle any questions in a sensitive manner. Says Bruce Kendall of Mt. Vernon High School in Fortville, Indiana, "I tell my teachers, 'Please don't kill God just to make your point.' "

http://scim.ag/Indiana_bill

Moscow **3**

New Fobos-Grunt Mars Mission?

Russian space scientists this week floated the idea of building a new version of the Fobos-Grunt sample return spacecraft after the first model failed to escape Earth orbit and crashed in the Pacific on 15 January. Fobos-Grunt was launched on 9 November with the aim of bringing back samples from


Phobos

Mars's moon Phobos. But once in orbit it failed to respond to commands from the ground and did not ignite rockets which would set it on course for Phobos. Its orbit eventually degraded.

Lev Zelenyi, director of Moscow's Space Research Institute, said at a 1 February press conference that the team behind the mission wanted to try again. Fobos-Grunt-2 would be "improved and simplified," he says, and would save money by using much of the original craft's infrastructure. But Russian Space Agency chief Vladimir Popovkin told the press that this all depends on ExoMars. This ESA/NASA project will send an orbiter to Mars in 2016 followed by a large lander in 2018. Last year the agencies asked Russia to join too and discussions are expected to be concluded this month.

Leipzig, Germany **4**

Extinct Human Genome Goes Online

Researchers in Germany posted the first high-resolution version of an extinct human's genome this week on the Web site for the Max Planck Institute for Evolutionary


Nice view. Denisova Cave attracted three kinds of humans.

Anthropology (www.eva.mpg.de/denisova/). A year after extracting ancient DNA from the finger of a girl who lived in Denisova Cave, Siberia, at least 30,000 years ago, paleogeneticist Svante Pääbo's team has now sequenced every position in her genome at least 30 times. They can compare even small differ-

CREDITS (TOP TO BOTTOM): NASA/JPL-CALTECH/UNIVERSITY OF ARIZONA; U.S. SENATE; ANN GIBBONS

Published by AAAS

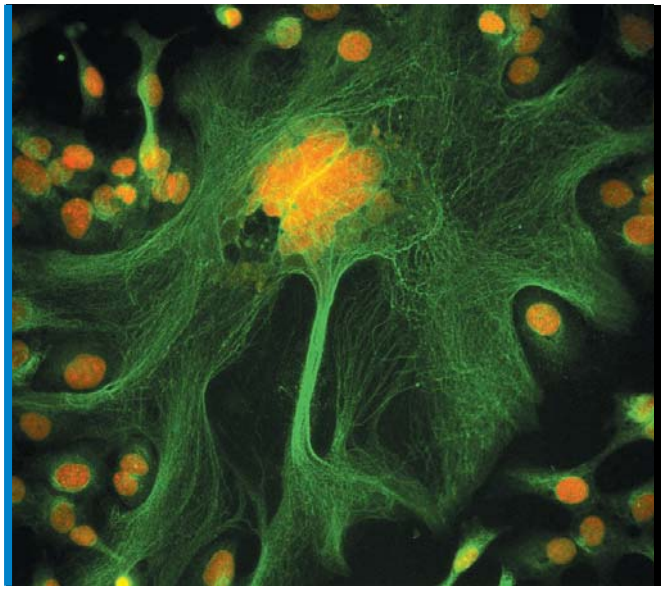

Microscopy on Broadway

Geoffrey V. Grandjean's elegant, colorful image of human ovarian cancer cells could become a tourist attraction this spring: From 20 to 22 April, Grandjean's image, along with two other regional winners of GE's 2011 IN Cell Analyzer Image Competition, will appear on NBC Universal's high-definition screen at Times Square in New York City.

The company announced its three regional winners 2 February. Grandjean, a research assistant at MD Anderson Cancer Center at the University of Texas, Houston, won the regional prize for the Americas for his image of cancer cells stained to show DNA (in red) and microtubules (in green). Marie Neguembor from the San Raffaele Scientific Institute in Italy took the European prize for her image of a myoblast, a precursor to a muscle cell. And research scientist Leslie Caron at Genea in Australia won for the Asia/Pacific region, for her image of vascular smooth muscle cells derived from human embryonic stem cells.

ences in copies of genes that this ancient girl inherited from her mother and father—and differences in her DNA and that of living humans and Neandertals.

Tokyo **5**

Kavli's First Endowment in Japan, For Physics of the Universe

The Kavli Foundation, known for supporting basic research in targeted fields, is endowing its first institute in Japan, giving $7.5 million to University of Tokyo's Institute for the Physics and Mathematics of the Universe (IPMU). "They are doing excellent science" in theoretical physics, astrophysics, and cosmology, says Kavli Foundation President Robert Conn. In addition, the foundation wants to support the institute's example of "a new way for science to be done in Japan," he says. IPMU is among the most international of Japan's research institutes. English is the official language, and more than half of its 200 researchers are non-Japanese.

This is also the first time a Japanese research institution's endowment has received such a large international contribution, says IPMU Director Hitoshi Murayama. "It's a new model of support for science in Japan," he says. IPMU was established in 2007 as one of Japan's World Premier International Research Center Initiatives, which are receiving about $17 million per year for 10 years (*Science*, 14 September 2007, p. 1493). The Kavli grant will ensure permanent funding and hopefully lead to more contributions, says Murayama.

St. Paul, Minnesota **6**

Minnesota Discards Newborn Blood Records

Minnesota bowed to the state's supreme court ruling last week and began destroying blood samples collected in its newborn-screening program. Minnesota and Texas are among the latest states to yield to families who sued, arguing that retaining and studying such samples—even anonymously—is a violation of privacy if consent isn't obtained first (*Science*, 10 April 2009, p. 166). Minnesota Health Commissioner Edward Ehlinger issued a statement saying, "We're going to begin destroying a valuable public health resource, the residual blood spots from about 200 babies born in Minnesota each day."

Screened. A newborn is tested for phenylketonuria.

For nearly 2 decades, the state health department has taken a few drops of blood from every newborn to check for rare congenital and heritable disorders that can be treated, such as phenylketonuria. The state lab also retained samples for test validation and disease research. But last week Minnesota put into effect its new policy of holding samples only 71 days for screening, then destroying them. Some positive test results may be retained for medical use, and some older records are being held until the court says what should be done with them.

Amsterdam, the Netherlands **7**

Scientists Boycott Elsevier To Protest Pricing

More than 4000 researchers and students have signed an internet petition pledging to boycott scientific publishing giant Elsevier because of its journal pricing. At thecostofknowledge.com, the signers vow not to publish papers in Elsevier's journals, referee other researchers' studies, or do other types of editorial work for the company.

The petition was initiated on 23 January by Fields medalist and blogger Timothy Gowers, a mathematician at the University of Cambridge in the United Kingdom. It highlights a number of gripes including the "exorbitantly high prices" of Elsevier's journals and the publisher's support of legislative proposals in the U.S. Congress that would roll back "open access" policies at the U.S. National Institutes of Health.

Elsevier, however, said in a written statement that its prices "have been among the industry's lowest for the past ten years," and that it has taken steps to make more of its material freely available. "We respect the freedom of authors to make their own decisions," the publisher wrote. "We hope the ones who sign the boycott >>

Published by AAAS

Giant Eye on the Sky

On 2 February, scientists at the European Southern Observatory's Paranal Observatory in Chile for the first time successfully linked together all four telescopes of the observatory's Very Large Telescope (VLT) array. In a technique called interferometry, light beams collected by each telescope are routed through tunnels and combined in a central laboratory. Researchers at Paranal tried such a linkup in March 2011 but failed. Together, the telescopes of the VLT array form the largest ground-based optical telescope in the world, with a diameter of 130 meters and high spatial resolution high enough to see details up to 25 times finer than the individual telescopes can.

>>AROUND THE WORLD

reconsider their position, however, and we are keen to engage to discuss their concerns." **http://scim.ag/_Elsevier**

Washington, D.C. **8**

Report Outlines Steps to More U.S. Science Degrees

Making sure that college students interested in earning science and engineering degrees don't switch fields or drop out is the fastest and least expensive way to meet the future needs of the U.S. workforce, says a new report from the President's Council of Advisors on Science and Technology (PCAST).

To retain them, the PCAST report says that faculty in STEM (science, technology, engineering, and mathematics) fields need to be trained to become better teachers. The report calls for a national program to improve the math skills of all entering students, noting that inadequate preparation in math is preventing many of them from pursuing STEM degrees. It also suggests that students be given more ways to earn a STEM degree than the traditional route of attending one school full time for 4 or 5 years.

The report got a shout-out this week at a White House science fair, the second event President Obama has hosted to demonstrate the administration's commitment to STEM education. The PCAST report follows a 2010 study on how to improve precollege instruction. **http://scim.ag/sci-degree**

FINDINGS

Study Fails to Find Arsenic In Microbial DNA

The debate over whether a bacterium can incorporate arsenic into its DNA flared up again last week, with the posting of a paper refuting the idea on arXiv, an electronic preprint archive primarily used by physical scientists. The December 2010 report online in *Science* describing a microbe that grew in arsenic and seemed to incorporate the toxic element into its biomolecules had already elicited eight critical technical comments (*Science*, 3 June 2011, p. 1149).

Now one vocal critic, Rosemary Redfield, a microbiologist at the University of British Columbia, Vancouver, in Canada, and colleagues at Princeton University have grown the bacterium in the presence of arsenic, mimicking the original paper's methodology. After stringent purification steps, Redfield and her colleagues tested the bacterium's DNA for arsenic using liquid chromatography mass spectrometry. Contrary to the original report, they found that arsenic did not stimulate growth of the microbe, and they saw no evidence of its uptake in the microbe's genetic material. Now, says Redfield, "The burden of proof is back on the authors." **http://scim.ag/Redfield**

THEY SAID IT

"Contrary to circulating online reports, Komen has not 'defunded' any grantee based on human embryonic stem cell research conducted at their institution."

—A statement from Susan G. Komen for the Cure, a charity embroiled in a firestorm over abortion politics last week. Komen's cancer research grants total about $300 million, but it has never specifically funded work on human embryonic stem cells.

CREDIT: ESO/F. KAMPHUES

Published by AAAS

BY THE NUMBERS

$294,000 Amount per year that a new cystic fibrosis drug approved by the U.S. Food and Drug Administration will cost (see p. 645).

$32.26 million Amount raised by a disco dance party on 4 February for pediatric cancer research at Texas Children's Cancer and Hematology Centers.

Telltale Isotopes Hint At North Korea Weapons Test

In mid-May 2010, monitoring stations near North Korea belonging to the Comprehensive Nuclear-Test-Ban Treaty Organization (CTBTO) detected radionuclides in the air, suggesting a nuclear weapons test. There were no seismic signals of an explosion, however, and the ratio of nuclides did not fit the usual pattern for a weapons test. "It was a mystery for most in the field," says Lars-Erik De Geer of the Swedish Defense Research Agency.

De Geer suggests an explanation in an upcoming issue of *Science & Global Security*. North Korea may have carried out a low-yield underground test on 11 May that leaked some radionuclides immediately and more on two later occasions. An excess of xenon-133 suggests the test cavity was contaminated by an earlier blast, hinted at in a government report that mentions a nuclear "success" on 15 April. The 11 May blast, which may have been too small to be picked up seismically, appeared to use uranium-235 rather than plutonium-239.

Richard Garwin of the Federation of American Scientists says other, simpler explanations could account for the radionuclides detected, such as reprocessing spent nuclear fuel to make isotopes for medical imaging. "There's a big burden of proof to show it's not reprocessing," he says.

New Malaria Death Toll Disputed

A new attempt to calculate the global number of malaria deaths claims that 1.2 million people died of the disease in 2010, twice as many as the estimates from the World Health Organization (WHO). But many experts question the new figures, especially the higher death toll for adults.

Lifesaver. Treated bed nets have reduced malaria mortality.

Calculating the number of malaria deaths is difficult because public health records in the hardest-hit areas are scarce. Christopher Murray of the University of Washington, Seattle, and his colleagues combed through data on causes of death between 1980 and 2010 in the 105 countries with malaria transmission. They then developed computer models that included factors like drug resistance and weather patterns to estimate the worldwide toll.

Their report in the 4 February issue of *The Lancet* concludes that 435,000 Africans over age 5 died of malaria in 2010—eight times WHO's number. That's too high, says malaria epidemiologist Robert Snow of the Kenya Medical Research Institute in Nairobi; severe malaria is rare in adults, he says, because exposure to the disease helps build partial immunity. Malaria is a common misdiagnosis, he adds, so records can be misleading. Snow hopes the debate will highlight the need for better surveillance. "We need to be honest … in saying we don't know," he says. "This is another example of guessing."

Science LIVE

Join us next week for a series of live chats from the annual AAAS meeting in Vancouver, on topics from the fate of the oceans to the food of the future. **http://scim.ag/aaas_2012**

Random Sample

Pluto's Second Shot At Post Office Fame

Will Pluto rise again? Yes, if Alan Stern and Dan Durda get their way. Stern, the principal investigator of NASA's New Horizons mission to the dwarf planet, and Durda, an astronomer and space artist, have posted a petition on the website change.org urging the U.S. Postal Service (USPS) to issue an official stamp in 2015 honoring the mission's arrival at Pluto.

It's been a long time coming. In the 1990s, when USPS issued a series of stamps commemorating the first missions to visit the planets in the solar system, "Poor old Pluto didn't have anything," Durda says. All Pluto got was a sad little stamp featuring a nondescript white ball floating in darkness above the slogan, "Not yet explored."

Now, with New Horizons (which launched in 2006) on its way, Stern and Durda, both of the Southwest Research Institute's Department of Space Studies in Boulder, Colorado, want Pluto to get another taste of postal glory.

In designing a stamp for the petition (pictured), Durda says, he steered clear of a standard "looking back toward the sun" shot. "I said, nope, not this time. It's not just some boring iceball; we know it has an atmosphere, a lot of potential for interesting atmospheric phenomena, a lot of albedo contrast. So let's try to indicate that it's going to be an interesting world."

The petition went online 1 February and closes 15 March. Success won't guarantee that Durda's design makes the final post office cut, but he says "it would be a great honor to have the artwork."

Meanwhile, the original 1991 stamp is on its way to Pluto itself, one of nine mementos in New Horizons's payload. So "not yet explored" will fly past Pluto, even as the message becomes obsolete.

CREDITS (TOP TO BOTTOM): © DAN DURDA; PHILONG SOVAN/XINHUA/LANDOV

Published by AAAS

FRANCE

€22 Billion Stimulus Brings Worries About *Egalité*

Building boom. A new research building is one of several construction projects at the Strasbourg campus.

STRASBOURG, FRANCE—If you want to know how President Nicolas Sarkozy's government is changing the research and higher education landscape in France, start in this city on the German border. In 2009, its three existing universities merged; the resulting University of Strasbourg, home to more than 42,000 students, has since then been showered with new money from the French government. A major campus renovation has started, new buildings are on the drawing board, and several labs have received extra euros to buy modern equipment, embark on new projects, or boost existing ones.

Strasbourg has been one of the biggest winners so far in Investments for the Future, a stimulus package announced by the French government in 2009 to shore up the economy after the global financial crisis and turn France into a more competitive, innovative nation. Altogether, €21.9 billion of the program's €35 billion budget—which was raised in the financial markets and is better known as the Big Loan—is allocated to research and higher education.

On 3 February, French Prime Minister François Fillon announced five new winners in the flagship component of the stimulus, the €7.7 billion Excellence Initiatives (Idex), which aims to help create a group of five to 10 world-class research and higher education clusters. Strasbourg had won that honor last July, together with clusters called Idex Bordeaux and Paris Sciences et Lettres; they have now been joined by groups at Aix-Marseille, Toulouse, Paris-Saclay, Sorbonne Université, and Sorbonne Paris Cité, bringing the total to eight.

For the winners, the Idex label is more than a financial windfall. "It has improved our image internationally and also locally," says Alain Beretz, president of the University of Strasbourg. "It is like a sports victory for the general public."

But the wave of new investments has also generated anxiety and criticism. Smaller universities worry that they may become lower-tier educational and research outposts while Strasbourg and other sites blossom—a break with France's egalitarian tradition. Jacques Fontanille, the president of the University of Limoges, warns that a long-term concentration of funds in a few large clusters "will imperil more than half of France's [83] universities." And even Beretz worries that the scheme could be a financial trap if regular research and higher education budgets are cut.

> *"We needed to streamline what was the world's most fragmented higher education system."*
>
> —JEAN-RICHARD CYTERMANN, FRENCH OBSERVATORY OF SCIENCE AND TECHNOLOGY

Not all the stimulus money goes to a happy few. There is a €1 billion program called Labex, which offers support for individual labs of international stature; €1 billion is reserved for expensive scientific instruments; and there are special components to support promising scientific fields, such as health and biotechnology, carbon-free and nuclear energy, and aerospace.

But concentration into fewer, better universities is one of Sarkozy's key objectives; it is also the idea behind Operation Campus, a program to give fewer than a dozen research centers—including Strasbourg and several other Idex winners—funds to spruce up their aging campuses. The concentration strategy was driven in part by worries about France's poor performance in global university rankings; in 2011, for instance, only two French universities made the top 50 in the so-called Shanghai ranking. The large number of universities, elite *Grandes Écoles*, and government labs is seen as part of the problem. "We needed to streamline what was the world's most fragmented higher education system," says Jean-Richard Cytermann, president of the French Observatory of Science and Technology in Paris.

Candidates for the Idex money had to put together plans detailing how they hope to climb up the university rankings—for example, by recruiting top researchers and students, or creating new, innovative multidisciplinary degrees. How much more money the new Idex universities will end up with is not entirely clear, because the competition's rules are complex. For instance, the funds that universities have bagged in Labex will be deducted from their Idex funding. Moreover, much of the stimulus isn't given to the universities directly but put into a special Treasury account yielding 3.4% interest. In Strasbourg's case, that means an extra €30 million or so on top of its €600 million annual budget. "That will enable us to go faster, and to plan better in the long term than we can with annual grants, which the government does not always deliver on time," Beretz says.

Predictably, the selection process triggered discontent among the losers, such as a cluster in Montpellier, known for its environmental and agricultural science, which failed even to be short-listed for Idex. "This is disappointing and infuriating," says Danièle Hérin, president of the University of Montpellier 2 for Science and Technology. "The fact that we came fourth among French universities in the last Times Higher Education rankings shows we are recognized internationally." Part of the problem was that the Idex jury valued consolidation; despite plans to merge, Montpellier's five universities have so far failed to reach an agreement, and they have partnerships with 10 research agencies. "This is a major advantage, but it's compli-

CREDIT: E. MANINI AND R. FISCHKANDL

Published by AAAS

cated to manage," Hérin says.

The government has promised not to interfere with the Idex jury's decisions, but Fillon said last week that two clusters that almost made it in the second round of funding—Lyons-St. Etienne and Paris Novi Mundi Université—will receive cash from the program to help carry through their "high-quality projects." Harvard University economist and Idex jury member Philippe Aghion hopes there will be a third round of Idex awards as well—there are other deserving candidates, he says—but that will be up to the government that takes over after elections this spring.

To biochemist Patrick Monfort, general secretary of the research union SNCS-FSU, the entire spectacle is a bit unseemly. "We have always been against the principle of competition among institutions and individuals," he says. So are most scientists, he says—but they feel they have to go along to prevent worse. Whether the program will really boost France's university rankings or lead to an explosion of good research remains to be seen. "We will have to wait at least 4 years to be able to judge," Cytermann says. Idex winners are "put on probation," he notes; if they don't deliver, they could lose their funding.

–BARBARA CASASSUS

Barbara Casassus is a writer in Paris.

PERSONALIZED MEDICINE

New Cystic Fibrosis Drug Offers Hope, at a Price

Last week, the news that U.S. regulators had approved a new drug for cystic fibrosis (CF) cheered patients and the biomedical research community. The drug, called Kalydeco and made by Vertex Pharmaceuticals, is the first to target the genetic defect discovered 23 years ago that causes a protein to malfunction in cystic fibrosis, resulting in a sticky buildup of mucus in the lungs and digestive tract that eventually causes fatal health problems.

"This is something we've all waited a long time for. So it is wonderful," says Francis Collins, director of the National Institutes of Health, who helped lead the team that discovered the CF gene in 1989. He says he was in a coffee shop in downtown Washington, D.C., last week when a man approached him and said that his 13-year-old grandson with CF had just learned that he is eligible for the drug. "His grandfather started crying and I started crying. We've gotten to the point where an amazing potential future exists for this boy," Collins says.

But as Collins acknowledges, the approval of Kalydeco illustrates both the promise and peril of personalized medicine, which in this case has resulted in a drug that's extremely expensive and helps only 4% of people with the disease, or 1200 patients.

Cystic fibrosis affects about 30,000 people in the United States; patients typically live only into their late 30s. When scientists discovered the causative gene—cystic fibrosis transmembrane conductance regulator (*CFTR*), which codes for a membrane protein—many thought a cure would soon follow. But early efforts focused on inserting a corrective DNA sequence with gene therapy, which has not yet worked (*Science*, 19 June 2009, p. 1504). Scientists moved ahead, however, on studying how hundreds of mutations cause defects in the CFTR protein that prevent chloride and water from passing through the cell membrane.

In the late 1990s, the Cystic Fibrosis Foundation decided to fund a search for small molecules that might correct these defects. Academic labs weren't doing high-throughput screening, says foundation CEO Robert Beall: "We had to move faster." The foundation gave $75 million to a company called Aurora Biosciences in San Diego, California, later bought by Vertex Pharmaceuticals. Aurora-Vertex screened 230,000 compounds using cell assays—an unusual approach at the time, says Vice President for Discovery Biology Paul Negulescu. They found a compound that could target a rare mutation, *G551D*, that makes the CFTR protein structure open too slowly. Two clinical trials found that a version of the compound, VX-770, "helps the gate open," Negulescu says. It improved lung function and weight gain and resulted in fewer infections in patients 6 years and older with the *G551D* mutation. Last week, the U.S. Food and Drug Administration approved VX-770, Kalydeco, after an unusually fast 3-month review.

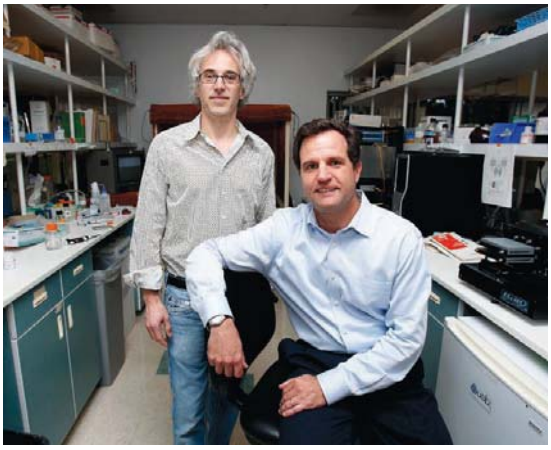

On target. Fred Van Goor (*left*) and Paul Negulescu of Vertex Pharmaceuticals helped develop the first drug aimed at the gene defect that causes cystic fibrosis.

CREDIT: JOHN GASTALDO/UT SAN DIEGO/AP PHOTO

Vertex is now testing Kalydeco in combination with another new compound that targets a more common mutation carried by 90% of cystic fibrosis patients. This defect, ΔF508, prevents the CTFR protein from folding properly and moving to the cell surface. Although correcting this problem is more challenging, some are encouraged by the Kalydeco results: "This provides a proof of concept suggesting that if you can repair a CFTR defect, you can have an impact on this disease," says cystic fibrosis researcher Michael Welsh of the University of Iowa in Iowa City, who was not involved with the trial. Results from an efficacy trial are expected later in 2012.

Some have been taken aback by the price of Kalydeco, which will cost $294,000 a year for the twice-daily pill, to be taken for a lifetime. Beall says this is "not totally out of line" with prices for other drugs for rare diseases. His group is encouraged that Vertex will make the drug available for free to uninsured patients with household incomes below $150,000 and will cover up to 30% of copayments for some with insurance.

Still, Kalydeco joins other drugs targeted to patients with a particular disease mutation—such as a wave of new cancer drugs—that cost upward of $100,000. As more such costly drugs emerge, "there's going to have to be a reality check," Collins says. He anticipates a "complicated conversation" between companies, insurers, and "society as a whole" to make the drugs an affordable part of health care.

–JOCELYN KAISER

Published by AAAS

PALEONTOLOGY

More Than One Way for Invaders to Wreak Havoc

Ravenous pythons and anacondas invading the Florida Everglades are ravaging the local ecology. But a study published last month suggests that invasive species can have a more insidious effect on natural systems.

About 380 million years ago in the Devonian period, invasive species reigned rampant in the world ocean as the number of marine animal species plummeted. That ecological crisis has been classed as one of the Big Five mass extinctions. But paleontologists think the main problem was not that existing species died out but that new ones failed to form.

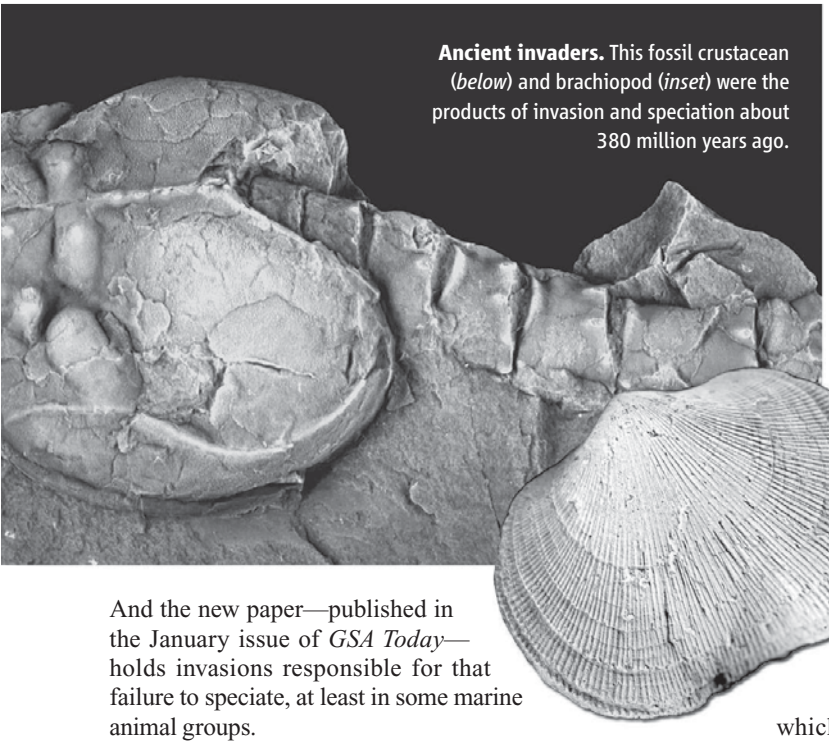

Ancient invaders. This fossil crustacean (*below*) and brachiopod (*inset*) were the products of invasion and speciation about 380 million years ago.

And the new paper—published in the January issue of *GSA Today*—holds invasions responsible for that failure to speciate, at least in some marine animal groups.

The new look at the Devonian "has hit on something very interesting," says paleontologist George McGhee of Rutgers University in Piscataway, New Jersey. "We don't know where modern invasives will lead us," McGhee says, but the study raises the possibility that recovering from the current human-induced mass extinction could be much more difficult than thought.

For insights into what long-term legacy today's invasions might have in store, paleontologist Alycia Stigall of Ohio University in Athens went back 380 million years to the Frasnian stage of the late Devonian period, a geologic interval roughly 7 million years long. In those ancient times, the diversity of marine animals plunged, but not because an asteroid impact or a series of humongous volcanic eruptions had wiped out most species.

Species are always going extinct, even between crises. In the Frasnian, the pace of extinction was only slightly elevated above the background rate. Instead, diversity fell because the rate of appearance of newly evolved animal groups such as genera and families fell. Stigall recently confirmed that even at the level of species, Frasnian diversity plunged because the appearance of new species slowed, not because of elevated rates of extinction of species.

To sort out what slowed speciation while only modestly elevating extinction, Stigall analyzed the fossil records of four commonplace groups of shallow marine animals, including a group of clams and two groups of brachiopods, which are bottom-dwelling shelled animals on stalks. By tracking their evolutionary history as well as their movements around what is now eastern North America, she could determine which of two styles of speciation detectable in the fossil record was at work: vicariance or dispersal.

Vicariance takes place when a new geographic barrier such as mountains or a river splits the existing range of a species, leaving members of the species on either side free to evolve into two new species. In dispersal, a species becomes geographically isolated when it migrates across a barrier to a new range where it can become a new species. Speciation by vicariance has always been found to be more common in the early history of life and dominates by a ratio of 3 to 1 today. But Stigall found that the Frasnian turned the pattern upside down: Speciation occurred by vicariance only 28% of the time and by dispersal 72% of the time.

Stigall thinks that reversal shows that invasions are hard on speciation. Three major invasion episodes were triggered in the Frasnian when sea level rose to create connected inland seas across eastern North America. During such onslaughts, she notes, ecological generalists—species that can make do under a wide range of environmental conditions—make the most successful invaders. And on the receiving end, generalists that are invaded do better than native specialists tolerant of only a narrow range of conditions. So generalists fare better all around, but they have fewer species and lower speciation rates, Stigall says. Combined with the lower survival rate of native specialists, that would have depressed speciation in the Frasnian, she says.

Her deep-time study holds timely lessons for modern humans, Stigall says. Loss of habitat and the introduction of new predators and diseases may be driving the current mass extinction, she says, but "we're looking at a worse outcome than currently predicted." Whenever the human-induced mass extinction has run its course, invasives will be seriously inhibiting the creation of new species and retarding recovery. And the greater vulnerability of specialist species compared with generalists means that "even if tremendous resources are devoted to [specialist] species, they probably won't be sustained in the long term." Given limited resources, she says, conservationists should give more-resilient species in the middle range the highest priority.

"Alycia's work is extremely important," says ecologist Daniel Brooks of the University of Nebraska, Lincoln. It "is showing that we can literally learn from the past to adapt to the future." Paleontologists, however, are still looking for more answers. "This is an interesting hypothesis," says paleontologist Peter Harries of the University of South Florida in Tampa; "now let's test it." For example, "what does the [ancient] invasion process look like?" he asks.

Modern ecologists have their concerns as well. "These broader [paleo] patterns could certainly inform our modern conservation strategies," says ecologist Edwin Grosholz of the University of California, Davis, but "paleontologists may be missing some of the complexities of their arguments." Those would include the way invaders increase diversity by adding themselves to the species count. Paleontologists and neontologists, all agree, could benefit by spending more time talking with each other.

–RICHARD A. KERR

CREDITS: ALYCIA STIGALL/OHIO UNIVERSITY

Published by AAAS

In trouble. The Croatian government provided a historic building for MedILS but little other support.

EASTERN EUROPE

High Hopes for Croatia's 'Warm Spring Harbor' Remain Unfulfilled

It was supposed to be a rising star in Eastern European science, an incubator of young talent and an international magnet for Croatia. But today, the Mediterranean Institute for Life Sciences (MedILS), housed in a historic building in Split overlooking the Adriatic Sea, is mired in controversy and appears to be on the brink of collapse.

The director and founder, Miroslav Radman, said on a national talk show in December that he was paying bills out of his own pocket. Funding has almost run dry, and key staffers have left. "I can't wait to get my hands off that steering wheel," Radman said. But critics say his autocratic management style and other missteps may have led to the institute's undoing.

Radman, an internationally renowned geneticist at Paris University V and a member of the French Academy of Sciences, together with his former professor, now-retired microbiologist Marija Alačević, founded MedILS in 2003 as a center of excellence in high-risk innovative research. Politicians loved it. The Croatian government paid about $4.2 million to renovate an army building within the summer home complex of former Yugoslav President Marshal Tito and gave the institute a free 40-year lease. Radman ambitiously nicknamed it Warm Spring Harbor Laboratory—a wink to the famed lab in Cold Spring Harbor, New York.

MedILS attracted several researchers, although most were part-timers who kept an appointment abroad. Their work started appearing in high-impact journals. The lab was becoming a "hotspot of high-quality science," MedILS group leader Ivan Đikić and Scientific Director Bojan Žagrović wrote in a 2008 *Nature Biotechnology* article.

But within 2 years, both had left, driven away, Đikić says, by fierce behind-the-scenes power struggles, discontent over management structures, and differing visions of the institute's direction. Đikić became scientific director of the Frankfurt Institute for Molecular Life Sciences, where he had remained on the faculty; Žagrović—the only group leader to be fully based at MedILS—left for the Max F. Perutz Laboratories in Vienna. A key problem, says Janoš Terzić, who co-led Đikić's group and is now the vice-dean for science at the University of Split's Medical School, is that Radman leads the institute like "a one-man show." Those who criticized his decisions were accused of plotting against him, Đikić says.

The institute's first management council resigned en masse in 2006 because it felt it "was not really in charge of managing the institute," says Vlatko Silobrčić, who headed the council at the time. Another entire management council stepped down in 2008, and Radman fired a third one in 2009, "because they were trying to remove me," Radman says.

Expat. MedILS Director Miroslav Radman.

Meanwhile, money began running short. Radman and Alačević counted on the Croatian government to support the lab's operating costs, but that never happened; an official at the Croatian research ministry who asked not to be named says "it was not logical" for the state to cover running costs of a private institution. Radman's critics say he was supposed to ensure that the institute found funding.

They also took aim at Radman for spending less time at the institute than at his base in Paris. Some said this made it very difficult to organize the day-to-day running of the institute, obtain signatures on documents, or apply for grants. "It wasn't possible to lead the institute from a distance," says Stjepan Marčelja, a visiting fellow in mathematics at the Australian National University in Canberra and a member of MedILS's scientific advisory board.

Radman acknowledges that key researchers have left and that the number of MedILS's staff has shrunk from over 25 to just 12, most of them absent much of the time. But he defends his record and management style. The money from the Croatian government "was for my vision, not for someone else's vision," he says. "People were free not to come to the institute, but if they did, then loyalty was a minimum expected," he says. Radman admits that "it's less than ideal" he can't be at MedILS full-time but says that limited support from the Croatian government made him reluctant to relocate.

Dimitri Krainc, an associate professor at Harvard Medical School in Boston who heads one of three groups at the institute, says expectations about the institute were too high—and support too little—from the beginning. "The scientists were expected to build an institute from scratch," he says. Similar new initiatives elsewhere in Europe had more start-up money; "everything else was the consequence of this misguided starting point."

What will happen now is uncertain. Đikić says Croatian officials are aware of the problems, but no one is interested in tackling them. Alačević, Radman's co-founder, says that Radman is scrambling for funds abroad. Radman hopes the left-wing government that took over in December will provide new funds. Licensing some of MedILS's patents will also help, he says, and he has just signed a contract to start a new center for aging research, which will be co-funded by the French Center for Scientific Research. "I don't have a pessimistic outlook," he says.

Terzić is more guarded. He once hoped that MedILS would become "a Croatian mini-Harvard or Max Planck Institute"; now, he says, only a change in management and leadership style, along with a strong and independent scientific advisory board and new international projects, can salvage the institute. "MedILS should be started again, from the beginning," Marčelja adds. **–MICO TATALOVIC**

Mico Tatalovic is a writer in London.

CREDITS (TOP TO BOTTOM): COURTESY OF MEDILS

Published by AAAS

Indoor Ecosystems

The microbial ecology of buildings gets a boost from a foundation and researchers trying to better understand the invisible communities in our homes, hospitals, and workspaces

What's inside? Buildings are ecosystems in their own right and are now being studied as such.

UNTIL 3 YEARS AGO, NOAH FIERER WAS your typical microbial ecologist. At the University of Colorado, Boulder, he focused on the outdoors, studying the microbes inhabiting soils and leaf litter. Then he tackled ecological questions closer to home—first in the microbes living in humans and next in mundane places like computer keyboards. After realizing how much time he spends indoors, he began thinking bigger. While many scientists have counted the germs on indoor surfaces, few had systematically tried to assess the biodiversity of interior spaces. He and Rob Dunn, an ecologist at North Carolina State University in Raleigh, have just mounted a large citizen-science survey to do just that.

Volunteering to be its first participant, I rubbed 10 cotton-tipped swabs along surfaces of my apartment—including my door sills, toilet, pillowcase, and counters—and sent them back to Fierer for DNA sequencing. His analysis showed that my home hosts a wide variety of microbes.

Hardy *Acinetobacter* are burrowed into the crevices of my cutting boards. Countertops are biodiversity hot spots of bacteria and fungi, including sphingomonads that may have settled out of the tap water used to wipe the counter. The toilet seat is coated with bacteria associated with human skin, and doorsills are crawling with fungi and grass pollen. The front doorknob and TV screen harbor unusual bacteria not typically found in water, soil, or the human body—perhaps representing entirely new communities unique to those surfaces.

Online
sciencemag.org
Podcast with author Courtney Humphries.

Fierer and Dunn plan to compile similar microbial survey data from the homes of thousands of volunteers like myself from different parts of the world. The pair wants to explore whether the microbial makeup of homes differs depending on location, the density of the surrounding population, or whether a home is freestanding or an apartment. It will be the first comparison of houses from a wide geographic range.

This "basic Lewis and Clark exploration" will offer new information. But the real goal, Dunn says, "is to understand not just what is there but why, and to see the extent to which these species are associated with our lifestyles, geography, and climate."

While some scientists worry that such efforts may simply lead to meaningless lists of microbes, new information is pouring in about the microbial denizens of other kinds of buildings as well. In work that blends microbial ecology, indoor air science, and building engineering, researchers have begun scouring classrooms, offices, and hospitals for microbial life and analyzing the factors that affect human exposure to it.

So far, most of this work on indoor microbial ecology has been funded by the Alfred P. Sloan Foundation, not by the U.S. or other governments. Since 2004, the foundation has spent more than $23 million on dozens of such research projects. While novel molecular techniques have made it possible to study microbes in many environments, the interiors of buildings rarely drew the attention of microbial ecologists, says Sloan Program Director Paula Olsiewski. At the same time, building scientists were assessing chemicals and particles in indoor air but ignoring its biology. "We thought it was important to study where people live," Olsiewski says.

A needed field

The 2001 National Human Activity Pattern Survey estimated that people in the developed world spend nearly 90% of their time indoors; yet "so much funding and effort goes into thinking about ecosystems in which we spend 10% of our time," complains Jessica Green, a microbiologist at the University of Oregon, Eugene. She heads the Biology and the Built Environment (BioBE) Center, which was created in 2010 with a $1.8 million grant from the Sloan Foundation.

There are certainly health reasons to pay more attention to the microbes inside our buildings. The air circulated by heaters and air conditioners can spread infectious diseases, for example, and some cases of so-called sick building syndrome can stem from unchecked mold. Fungi in buildings are also associated with allergies, asthma, and other pulmonary conditions.

And then there's the impact on the edifices themselves. Microbes contribute to the deterioration of buildings by breaking down wood, stone, concrete, and other materials.

Yet little is known about what microbes live in buildings and why they reside in certain places but not others. As a result, homeowners and building managers who invest time, money, and energy cleaning surfaces and filtering air do not really know the effects of these activities. Choices in construction materials, ventilation systems, building design, and maintenance also influence an interior's microbial complement, but how? "In order to understand what shapes the diversity and function of microbes indoors, you must understand the indoor environment from an abiotic context—its chemistry, structure, and dynamics," Green says.

Green's background provides her with a strong appreciation of the need to blend abiotic and biotic factors. She began her studies in civil engineering and earned a Ph.D. in nuclear engineering, but eventually switched to microbial ecology because of a passion for biodiversity. Before coming to Oregon, she had focused on microbial diversity in soils and oceans. But attracted to the university's program in sustainable building design and inspired by the potential of Sloan support, she joined forces with two university colleagues,

CREDIT: JESSICA GREEN



Systematic study. Researchers collected microbes from air (*left, middle*) and surfaces (*right*) in a campus building to understand its microbial ecology.

microbiologist Brendan Bohannan and architect G. Z. "Charlie" Brown, to launch BioBE.

Because indoor ecology is an emerging field, Green and other researchers must struggle with developing effective protocols for assessing these ecosystems and finding practical applications for their insights. For example, Fierer and Dunn are taking steps to standardize their citizen-science microbial survey; they'll place extra weight on samples from a core set of participants—including other scientists—who will provide more in-depth data by sampling the same spots several times. Fierer and Dunn hope to identify reproducible patterns in their results that will yield real insights into what factors determine the microbial residents, rather than just a census.

"That's my criticism of the field, that you're just getting a list," says Jordan Peccia, an environmental engineer at Yale University who studies how moving air affects microbes in buildings. But, Fierer counters, "without that basic knowledge, it's hard to take the next step."

Anybody home?

To help them take that next step, Fierer and others in the field turn to software programs that help match the microbial DNA sequences from their surveys with known bacteria and the other environments in which those microbes have been found. As genome sequencing costs have come down, the databases of microbial DNA have exploded. These resources help researchers track whether microbes that live indoors come from soil, outside air, humans, other animal occupants, or some other source.

Using these databases, Fierer's group recently identified the probable sources of microbes from several surfaces in 12 public bathrooms. The results, published on 23 November 2011 in *PLoS ONE*, were not surprising: Bacteria associated with human skin abound on surfaces people touch; bacteria from the gut occupy toilet seats; and a higher level of vaginal microbes was found in women's bathrooms than men's. But Fierer says the study shows it's possible to see spatial patterns in the origins of microbes, and his team is now working on a project to create a detailed atlas of the typical spatial patterns of microbes found in kitchens.

For Green's latest project, she and her colleagues conducted a classical ecological study on the microbial diversity in one University of Oregon building. Similar to how Green and others have examined microbes in natural environments, the researchers repeatedly took samples from the building, hoping to provide enough data to make inferences about the causes and consequences of microbial diversity indoors. For example, they collected air from six rooms at different times of the day to understand the dynamics of microbes over time and their response to human presence. They also gathered dust from each of the building's more than 300 rooms to understand how microbial populations vary across an entire building. To study the microbial variability within individual rooms, Green's team chose different "habitats"—floors, walls, desktops, and seats—and used square sample plots set up the same way as those historically used to study plant biodiversity.

Microbe collector. Jessica Green is applying ecological methods and theory to indoor spaces.

The analysis by the Oregon group is ongoing, but part of the goal is to model relationships between building use and design and microbial diversity. The team is also trying to discover whether ecological theories developed from studying plant and animal diversity on islands, a well-researched topic, can help them make sense of the ecology of microbes indoors.

"You can think of a building as a collection of islands," Bohannan says. Although individual rooms are somewhat self-contained environments, like islands are, they are linked through ventilation and the movement of occupants. If this island model turns out to be true, Bohannan says, it would mean that the movement of microbes between rooms affects their ecology as much as the conditions of the room, and building design and management could be manipulated to control this dispersal.

Moving air moves microbes

Green and Bohannan have already begun to look at how ventilation affects indoor microbes. Over the past few decades, the push to reduce energy use has created buildings that are highly sealed to outside air, and the Oregon researchers are trying to understand the consequences of this reduced air exchange. To do that, Green's team recently turned to an Oregon hospital, because hospitals typically have ventilation that is tightly controlled. They initially surveyed the microorganisms in mechanically ventilated rooms with windows closed and repeated the census after opening the rooms' windows for 2 hours.

CREDITS: (TOP LEFT TO RIGHT) ANGIE PONSO; JESSICA GREEN (2); (BOTTOM) ANGIE PONSO

Published by AAAS

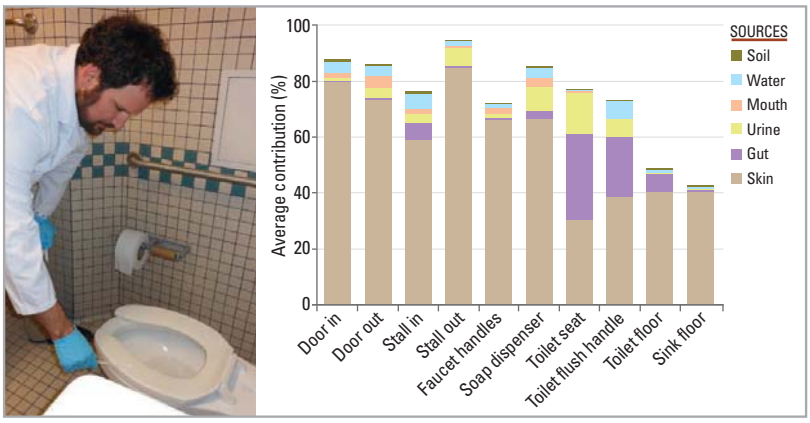

Bathroom biogeography. By swabbing different surfaces in public restrooms, researchers determined that microbes vary in where they come from depending on the surface (chart).

In just that short time, the microbes had begun to take on a "signature" of outside air (more types from plants and soil), and 2 hours after the windows were shut again, the proportion of microbes from the human body increased back to previous levels.

The study, which appeared online 26 January in *The ISME Journal*, found that mechanically ventilated rooms had lower microbial diversity than ones with open windows. The availability of fresh air translated into lower proportions of microbes associated with the human body, and consequently, fewer potential pathogens. Although this result suggests that having natural airflow may be healthier, Green says answering that question requires clinical data; she's hoping to convince a hospital to participate in a study to see if the incidence of hospital-acquired infections is associated with a room's microbial community.

For his part, Peccia, who is also a Sloan grantee, is merging microbiology and the physics of aerosols to look more closely at how the movement of air affects microbes. Peccia says his group is building on work by air-quality engineers and scientists, but "we want to add biology to the equation."

Outside influence. Students prepare to sample air outside a classroom in China as part of an indoor ecology study.

Bacteria in air behave like other particles; their size dictates how they disperse or settle. Humans in a room not only shed microbes from their skin and mouths, but they also drum up microbial material from the floor as they move around. But to quantify those contributions, Peccia's team has had to develop new methods to collect airborne bacteria and extract their DNA, as the microbes are much less abundant in air than on surfaces.

In one recent study, they used air filters to sample airborne particles and microbes in a classroom during 4 days during which students were present and 4 days during which the room was vacant. They measured the abundance and type of fungal and bacterial genomes present and estimated the microbes' concentrations in the entire room. By accounting for bacteria entering and leaving the room through ventilation, they calculated that people shed or resuspended about 35 million bacterial cells per person per hour. That number is much higher than the several-hundred-thousand maximum previously estimated to be present in indoor air, Peccia reported last fall at the American Association for Aerosol Research Conference in Orlando, Florida.

His group's data also suggest that rooms have "memories" of past human inhabitants. By kicking into the air settled microbes from the floor, occupants expose themselves not just to the microbes of a person coughing next to them, but also possibly to those from a person who coughed in the room a few hours or even days ago.

Peccia hopes to come up with ways to describe the distribution of bacteria indoors that can be used in conjunction with existing knowledge about particulate matter and chemicals in designing healthier buildings. "My hope is that we can bring this enough to the forefront that people who do aerosol science will find it as important to know biology as to know physics and chemistry," he says.

Still, even though he's a willing participant in indoor microbial ecology research, Peccia thinks that the field has yet to gel. And the Sloan Foundation's Olsiewski shares some of his concern. "Everybody's generating vast amounts of data," she says, but looking across data sets can be difficult because groups choose different analytical tools. With Sloan support, though, a data archive and integrated analytical tools are in the works.

To foster collaborations between microbiologists, architects, and building scientists, the foundation also sponsored a symposium on the microbiome of the built environment at the 2011 Indoor Air conference in Austin, Texas, and launched a Web site, MicroBE.net, that's a clearinghouse of information on the field. Although Olsiewski won't say how long the foundation will fund its indoor microbial ecology program, she says Sloan is committed to supporting all of the current projects for the next few years. The program's ultimate goal, she says, is to create a new field of scientific inquiry that eventually will be funded by traditional government funding agencies focused on basic biology and environmental policy.

Matthew Kane, a microbial ecologist and program director at the U.S. National Science Foundation (NSF), says that although there was interest in these questions prior to the Sloan program, the Sloan Foundation has taken a directed approach to funding the research, and "I have no doubt that their investment is going to reap great returns." So far, though, NSF has funded only one study on indoor microbes: a study of *Pseudomonas* bacteria in human households.

As studies like Green's building ecology analysis progress, they should shed light on how indoor environments differ from those traditionally studied by microbial ecologists. "It's important to have a quantitative understanding of how building design impacts microbial communities indoors, and how these communities impact human health," Green says. But it remains to be seen whether we'll someday design and maintain our buildings with microbes in mind.

–COURTNEY HUMPHRIES

Courtney Humphries is a freelance writer in Boston and author of *Superdove*.

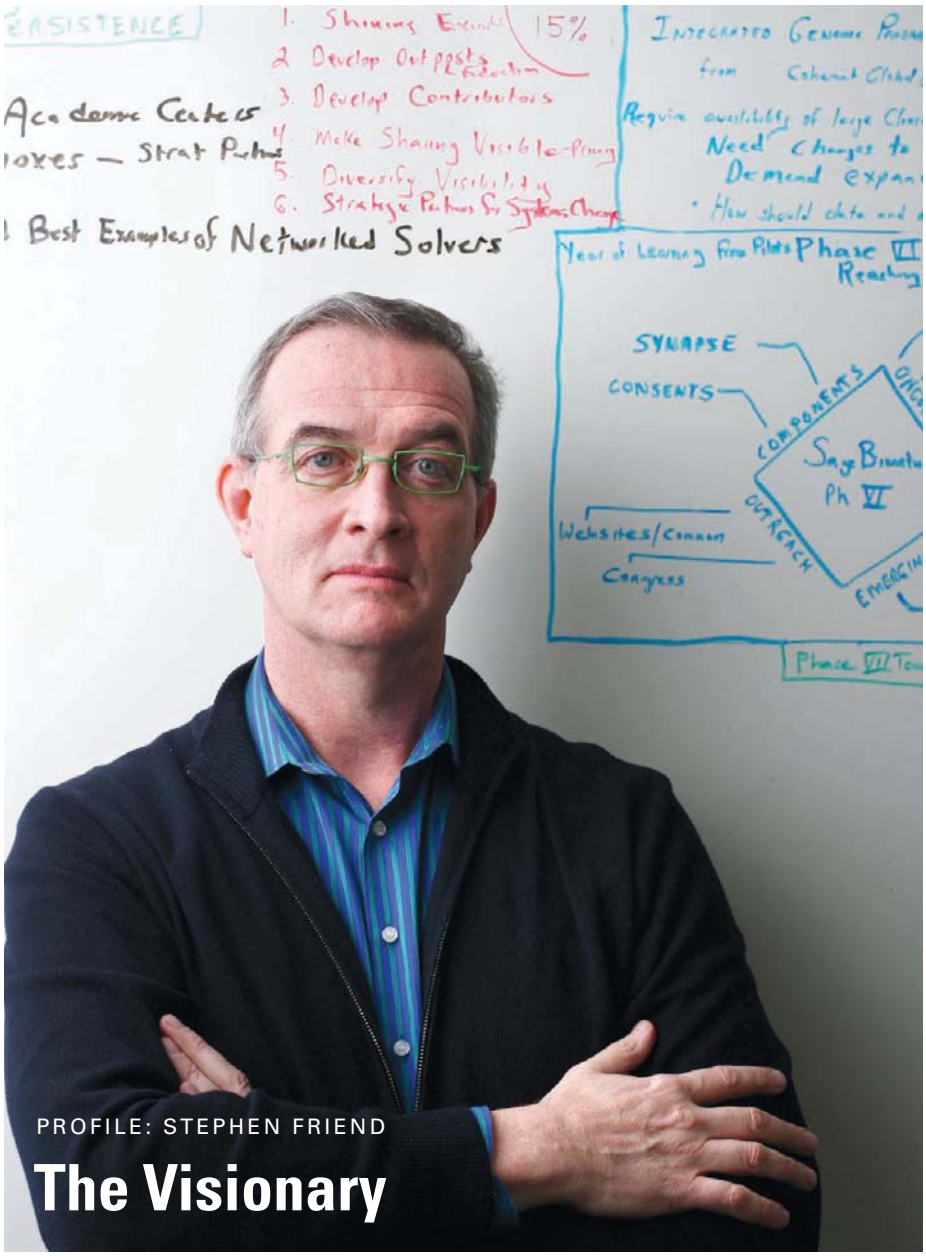

PROFILE: STEPHEN FRIEND

The Visionary

Seeking to spur drug development, Stephen Friend has launched a daring series of initiatives to make biomedical research more open and effective

It's late afternoon and everyone's heading home after an open-access conference in suburban Maryland where Stephen Friend has just delivered yet another of his signature stump speeches. In the past 10 days, his dizzying schedule included stops in Norway, New York City, Boston, and the nearby National Institutes of Health (NIH) in Bethesda, Maryland. But he's more than willing to hop on his soapbox again when a reporter asks. Most biomedical researchers are hunter-gatherers, holding their data close until they've published their findings, Friend says. But that won't lead to the development of new drugs or therapies, he insists: Untangling the biology of diseases such as cancer and diabetes requires finding patterns in enormous amounts of data, such as the torrent of information now pouring out of big genomics projects. Identifying the needles in such haystacks—culprit proteins or genes causing disease—demands a new kind of science. "The scale of and scope of the problem will need to be solved by sharing the data and networking."

Friend should know something about what's needed for biomedical science: He's treated children with cancer, helped discover a new class of cancer genes while an academic at Harvard University, and co-founded a biotech company that Merck bought for more than $600 million and, as part of the deal, hired him to head its cancer research. Now he's trying to do nothing less than change the competitive culture of science.

Three years ago, frustrated by the constraints of working in a big company, Friend negotiated a friendly separation from Merck and co-launched a nonprofit called Sage Bionetworks, based at the Fred Hutchinson Cancer Research Center in Seattle, Washington. Among its goals, Sage wants to persuade drug companies, academics, clinicians, and patients to share genomic and other biomedical information freely in a huge database. Other researchers would download and work on it together, mapping out the intracellular pathways that contribute to human diseases and building computational models of those conditions that would be better than the animal models now used in preclinical drug development. In short, Friend wants to bring to biomedical science the same open-source ethos embraced by the computer programmers who wrote the Linux operating system and by the people who contribute information to Wikipedia.

"What I realized was that drug discovery would continue to be consistently hampered by the lack of good models of disease. And to build those models was going to take massive amounts of data being shared over many iterations, over decades," says Friend, 58, who enlivens his usual semicasual attire—sport coat, button-down shirt, no tie—with green metal-rimmed glasses.

Friend isn't the only researcher who wants colleagues to take a more open approach to biomedical problems, but he is one of the most driven and persuasive. Thanks to his legendary persistence, dozens of big names in biomedical research have signed on to various Sage projects. "He's able to galvanize people to do things," says cancer biologist Robert Weinberg of the Whitehead Institute for Biomedical Research in Cambridge, Massachusetts, who once trained Friend and has followed his career. In his new position, Friend has also forged ties beyond the scientific community: He works with open-access activists on data-sharing rules, gets free cloud-computing space from Amazon, and collaborates with major patient advocacy groups.

Even some of the scientists who have signed on, however, are skeptical. Several point out that systems biology, the disease-modeling approach that Sage promotes, is still a young and evolving field. Others are confused by Sage itself, which Friend admits is "big, ill-defined," and has

"Stephen has a very idealistic vision of how we as scientists in the bioarena should be working together and why that hasn't happened."

—ERIC SCHADT, MOUNT SINAI MEDICAL CENTER

CREDIT: JOHN LOK

Published by AAAS

yet to hit a home run that might clarify its purpose.

But many believe Friend is on to something—or at least trust his track record enough to give him the benefit of the doubt. "He's an incredible innovator. He's always at the forefront of new things," says William Chin, executive dean for research at Harvard Medical School in Boston and a former senior vice president at Eli Lilly. Friend is a "machine on ideas," adds Eric Schadt, a longtime scientific collaborator. "Stephen has a very idealistic vision of how we as scientists in the bioarena should be working together and why that hasn't happened."

FRIEND'S PRESCRIPTION FOR A BIOMEDICAL REVOLUTION

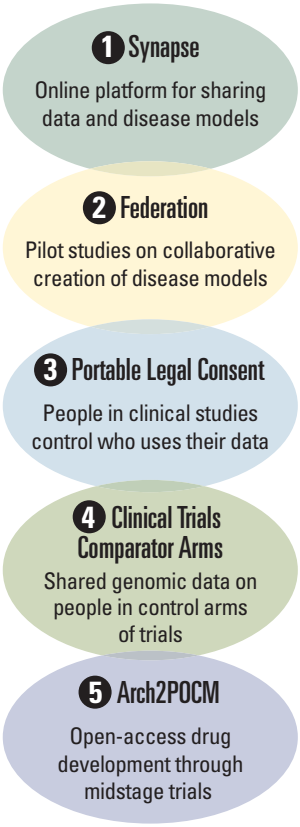

A change in philosophy

Friend didn't expect to become a scientist; he majored in philosophy in college, veered toward medical ethics, and wound up in medical school and graduate school as part of an M.D.-Ph.D. program. As a pediatric oncologist, Friend was moved by the patients he saw, including a boy and his father who had both lost an eye to a rare inherited cancer called retinoblastoma. Frustrated by how little was known about the disease, he accepted a postdoc position in Weinberg's lab with the goal of finding the gene behind retinoblastoma.

One small problem: "He had no idea how to do it," Weinberg says—Friend's doctorate was in biophysics. "I taught him, basically," says René Bernards of the Netherlands Cancer Institute, a fellow postdoc in the Weinberg lab. Yet within 2 years, Friend was first author of a *Nature* paper on the cloning of *RB1*, the first tumor suppressor gene—a major milestone in cancer research.

At the time, Bernards was struck by Friend's sense of direction. "He said he would divide his life into three parts: basic science, drug development, and art collecting," Bernards recalls. "I thought he was bullshitting." (Friend now collects art and creates it himself, working on a new project each year with artists in the Seattle area.)

After starting his own lab at the Harvard-affiliated Massachusetts General Hospital, Friend later moved to Seattle to work with geneticist Leland Hartwell of the Hutchinson Center, who later shared the Nobel Prize for work on the cell cycle. They eventually teamed up with University of Washington, Seattle, immunologist Leroy Hood, one of the early pioneers of systems biology, to make inexpensive gene expression arrays—chiplike devices that were becoming increasingly popular for measuring gene activity—and look for differences in gene expression in healthy and diseased tissue. That led the three to found the biotech company Rosetta Inpharmatics and, in collaboration with Bernards, to develop the first commercial gene expression test, MammaPrint, which was approved by U.S. regulators in 2007 for predicting whether breast cancer will recur.

In 1999, Friend hired Schadt, a young, maverick mathematician, to expand Rosetta's bioinformatics efforts. Schadt worked on combining DNA mutation data with gene expression levels in particular tissues from healthy animals or people and those with a disease. Massive computations using a supercomputer revealed networks of genetic interactions that pointed to genes that play a key role in the disease. These could then become potential targets for drugs or indicate which patients would not benefit from a treatment. In an influential 2005 *Nature Genetics* paper, for example, the Schadt team used their approach to find a network of genes active in obese mice.

Hoping to use Rosetta's gene expression analysis for drug development, Merck bought the company in 2001 for $620 million, netting Friend over $10 million. The company also made Friend its director of oncology drug development. The network analysis yielded a string of papers in top journals and new drug candidates for diseases such as diabetes and heart disease.

Friend and Schadt saw the next step as taking their network analyses from animals—the source of much of their data—into humans. But because people are much more genetically diverse than strains of mice, and diseases such as depression come in many subtypes, Friend realized they would need a wide variety of data from tens or hundreds of thousands of patients to reach the needed statistical strength for human studies. "It became apparent that you would need these megascale analyses," he says. So Friend began several Merck collaborations with academic cancer centers to build massive databases, eventually to be open to all, that could be used to identify which subsets of cancer patients might benefit from a treatment.

Friend says he and Schadt realized, however, that "no one company" could do what was needed. So 3 years ago, when Merck decided to close down much of Rosetta as part of a companywide downsizing, Friend, according to Hartwell, now at Arizona State University in Tempe, "talked Merck into letting him" take Rosetta's bioinformatics division and an estimated $150 million in computers, software, data, and intellectual property and create Sage Bionetworks.

An uncommon approach

Sage, which has grown from 15 to 35 staff members and has a modest $5 million budget, has some characteristics of a conventional nonprofit research organization. Its team of computational biologists have NIH and foundation funding and collaborate with academics and companies on network modeling studies. Schadt, now at Pacific Biosciences in Menlo Park, California, and Mount Sinai Medical Center in New York City, is one such partner. And Sage has inked a deal with Pfizer to use its modeling approach to develop cancer drugs.

But Sage is also part think tank, one with a grand vision of creating what Friend calls a "commons" where researchers come together to share and analyze vast amounts of biomedical data. At Sage's invitation-only annual meetings, participants refine their ideas for breaking down cultural barriers. For example, Sage and outside experts are working on data-sharing rules that Friend calls "a set of principles about what is good behavior, what is bad behavior."

Indeed, those who collaborate with Sage, including companies, agree to share data and models online within a year of the end of a project. The mandatory policy is reminiscent of the so-called Bermuda rules developed to compel DNA sequencing centers to release their data within a reasonable period, says Robert Cook-Deegan of the Duke Institute for Genome Sciences & Policy in Durham, North Carolina, who collaborates with Sage. "I think the way they're doing it is really smart."

As scaffolding for the commons, Sage is building an online repository for data sets. It differs from existing databases such as

NIH's GenBank because the data sets are more extensively curated, Friend says, and the repository will also host the software underlying their computer models of diseases. That is important and "much more complicated than genomic data," says David Haussler of the University of California (UC), Santa Cruz, who led the way in developing tools for sharing human genome data. "I applaud Sage for taking on this task."

But building the repository has gone slowly. When Sage staffers set out to gather 100 or so data sets that they had their eye on, such as gene expression and proteomics data from cancer patients, more than half were not available or were missing key underlying data such as annotations describing how and when clinical measurements were collected. Often the consent forms signed by patients did not allow even data stripped of personal identifiers to be shared publicly. "I've been disappointed in how difficult sharing data is," says Sage staffer Lara Mangravite. Sage is now working on a tiered access system to its gathered data sets that would comply with privacy rules.

Data-sharing frustrations have driven another project that Sage supports: an online consent form that allows people to control which scientific studies use their genomic and health data. "It's a shift from giving data to institutions where they really can't share it to shifting control to the patient," Friend says.

The project's leader is Sage board member John Wilbanks, formerly with Creative Commons, the nonprofit group that works to eliminate copyright issues and other factors limiting the exchange of information. Friend is convinced that only "patient-oriented, citizen-oriented projects" will generate enough data to build disease models complete enough to help suggest or test treatments. Volunteers are now testing a draft version of the form, and several patient groups will begin using it this spring.

Sage is also experimenting with a version of "networked" science. Friend recruited five research teams to work together on "superhard problems" in aging, cancer, and diabetes, such as finding genes driving the Warburg effect, a metabolic process used by tumor cells. "It was a pilot to see whether science got done faster and whether people felt as though their ideas were benefiting by sharing them or whether they felt robbed," Friend says. After more than a year of work, the so-called Federation has submitted two papers to journals—one, for example, found patterns in methyl groups attached to DNA that correlate with a person's age. Friend says the result "would have taken much longer and may never have come about" without the Federation.

But Stanford University bioinformatics researcher Atul Butte, a Federation member, says that although members "learned to trust each other," the lack of specific funding for the collaboration slowed progress. "The jury is out on whether we did more than we could have as individual labs collaborating" with an NIH grant, he says.

A successor project will use a new software platform under development at Sage to make it easier to build disease models together in real time the way software engineers now do, Friend says. Other efforts at Sage aim to coax data out of drug companies. One that is furthest along invites companies to contribute genetic and clinical data on people with a disease who were enrolled in the control arms of drug clinical trials. The companies have little incentive to keep these data proprietary, yet they could be a gold mine as a shared resource for studying mechanisms of disease, Friend says. Seven companies initially agreed to submit data sets, and two, GlaxoSmithKline and Johnson & Johnson, have begun to do so, but the rest realized that the consent forms signed by the patients wouldn't allow the companies to share the data. That experience, too, has underscored the need for a new kind of consent, Friend says.

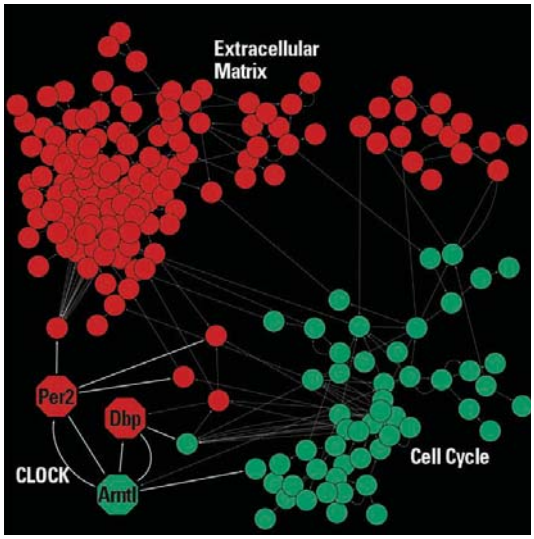

Muscular model. Sage wants to spur modeling of cell networks, such as this one showing how in muscle cells, circadian clock genes modulate expression of other genes, such as those involved in the cell cycle and extracellular matrix (red indicates genes with increased activity, green decreased).

CREDIT: JONATHAN DERRY/SAGE BIONETWORKS

Climbing a big hill

Friend's most ambitious project attempts to speed drug development and reduce its financial risk to companies by bringing companies and academics together for the initial testing of potential drugs. Dubbed Arch2POCM and led by Friend, Aled Edwards of the University of Toronto, and Chas Bountra of the University of Oxford, participants will freely share compounds and data until a potential drug has shown safety and efficacy in a phase II clinical trial. (The unwieldy acronym stands for Archipelago to Proof of Clinical Mechanism, with the initial word symbolizing groups collaborating.) The reasoning is that companies don't need intellectual property protection up to that point because they will want to modify and improve any compounds that work in this initial efficacy trial, says Harvard's Chin, who is not directly involved. But compared with other public-private partnerships, Arch2POCM would reach much further into the drug-development pipeline. "It's a very good idea" but "risky," Chin says.

Arch2POCM's leaders are talking to five companies and hope to have commitments by midsummer for projects involving drug candidates for cancer, autism, and schizophrenia. "Stephen has a big hill to climb," says molecular biologist Keith Yamamoto of UC San Francisco, who is helping run Arch2POCM. "But I think we're at a stage where we need to be trying new experiments."

Some researchers who aren't disease modelers themselves but would contribute data to Sage caution that its systems biology approach is still experimental. Cardiologist Eric Topol, director of the Scripps Translational Science Institute in San Diego, California, says that until one of the drugs Merck found using network analysis reaches the market, the approach "isn't validated yet." Still, Topol calls systems biology "increasingly important" in human genomics. And although the diagrams in a disease-modeling paper can be bewildering to a clinician, he expects "that the juice we'll get out of it will be useful."

If that happens, Friend may have already moved on to something else equally ambitious. Sage's mission is deliberately fuzzy so that it can "evolve," he says. "We are not under the illusion that our solution has to be what happens." And claiming success for specific projects is not the objective but rather being a "catalyst for others doing it," Friend says. Once projects are set up, "our hope is that Sage drops out of the picture, and in 5 to 10 years no one knows what Sage is."

–JOCELYN KAISER

Published by AAAS

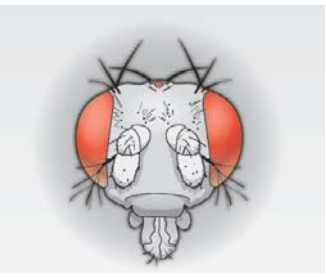

LETTERS

edited by Jennifer Sills

Carbon Shifted But Not Sequestered

Release. Carbon dioxide returns to the atmosphere as speleothems form.

THE NEWS & ANALYSIS STORY "AN UNSUNG CARbon sink" (C. Larson, 18 November 2011, p. 886) states that the erosion of limestone by carbonic acid formed from atmospheric carbon dioxide may constitute an "underappreciated carbon sink," partially mitigating the increase of carbon dioxide from anthropogenic sources. This mitigation is only possible if the captured carbon dioxide is sequestered in an unreactive form. In this case, it is not.

Weathering of limestone consumes carbon dioxide to form soluble bicarbonates in solution. If redeposited as calcite (e.g., as travertine or speleothems), the associated carbon dioxide will be returned to the atmosphere. If carried into the oceans, it may be sequestered as shells or reefs, again with the release of the carbon dioxide. There will therefore be no net sequestration of carbon dioxide, but rather a transfer to the oceans, where it will equilibrate over time with the atmosphere.

Because a mole of fossil carbon dioxide from limestone is remobilized by the reaction of a mole of atmospheric carbon dioxide, there is also a net increase in the carbon dioxide cycling between the atmosphere and the oceans.

Chemical weathering of basic igneous rocks, where there can be net sequestration of carbon dioxide to form insoluble carbonates, is the substantial inorganic "carbon sink," as shown by the enormous deposits of carbonate rocks worldwide.

RANE L. CURL

Department of Chemical Engineering, University of Michigan, Ann Arbor, MI 48109–2136, USA. E-mail: ranecurl@umich.edu

Response

CURL MAKES A VALID POINT ABOUT THE BEHAVior of carbonate minerals on multimillion-year time scales. Our interest, though, is in the much shorter time scales of decades to centuries. Considering remaining uncertainties in measuring some aspects of the global carbon cycle and the relatively rapid environmental changes under way in the atmosphere and oceans, quantifying carbon budgets in relevant geological systems for these shorter time periods may be more complicated (*1*). Our task is to better understand rates and processes associated with mineral weathering and impacts on carbon cycling.

C. GROVES,[1]* J. CAO,[2] C. ZHANG[2]

[1]Hoffman Environmental Research Institute, Western Kentucky University, Bowling Green, KY 42101, USA. [2]International Research Centre on Karst under the auspices of UNESCO and Key Laboratory of Karst Geology, Institute of Karst Geology, Chinese Academy of Geological Sciences, Ministry of Land and Resources, Guilin, Guangxi, 541004, China.

*To whom correspondence should be addressed. E-mail: chris.groves@wku.edu

Reference

1. Z. Liu, W. Dreybrodt, H. Liu, *Appl. Geochem.* **26**, S292 (2011).

Ecosystem Services: Heed Social Goals

IN THEIR POLICY FORUM "PAYING FOR ECOsystem services—Promise and peril" (4 November 2011, p. 603), A. P. Kinzig *et al.* identify a series of conditions that would need to be satisfied for payments for ecosystem services (PES) to succeed. They also highlight the reasons that potential ecosystem service buyers feel uncertain about the system, potentially choking the demand for services. However, Kinzig *et al.* fail to account for the role of service providers and the factors that might spur or undermine their willingness to supply ecosystem services in exchange of payment. Growing evidence shows that non-economic factors are highly influential in shaping service providers' sustained participation in PES (*1*).

Kinzig *et al.* describe PES as an instrument that primarily pursues cost-effective conservation goals regardless of collateral social implications. Such decoupling is ethically untenable in a growing number of places where top-down PES schemes are quickly spreading without proper understanding of service providers' needs and the potential impacts of PES on their livelihoods. When parachuted into rural communities of the developing world without market power or political voice, PES—including payment related to clean development mechanisms and REDD (Reducing Emissions from Deforestation and Forest Degradation)—can enhance existing inequalities in income, access to resources, and decision-making if pro-poor management measures are not considered (*2*, *3*). On the ground, institutional complexities can easily lead to misrepresentation of the poor and "elite capture" (in which some benefit more from the services than others) (*4*).

Taking fairness and participation issues into account might be somewhat discomforting to some scientists and practitioners working on market-based instruments for conservation. Nonetheless, PES that separate conservation effectiveness from distributive and procedural impacts risk delegitimizing the tool. Furthermore, such an approach may be counterproductive for PES effectiveness, insofar as the joint provision of positive outcomes for conservation and livelihoods is more likely when users participate actively

in transparent rule-making aspects of ecosystem governance (*5*, *6*). In the actual global economic climate where markets are disproportionally burdening the poor, PES should thus not become a source of environmental and social injustice.

ESTEVE CORBERA[1]* AND UNAI PASCUAL[2,3]

[1]Institute of Environmental Science and Technology, Universitat Autònoma de Barcelona, Bellaterra, 08193, Spain. [2]Ikerbasque Foundation for Science, Basque Centre for Climate Change (BC3), Bilbao, 48008, Basque Country, Spain. [3]Department of Land Economy, University of Cambridge, Cambridge, CB39EP, UK.

*To whom correspondence should be addressed. E-mail: esteve.corbera@uab.cat

References

1. G. van Hecken, J. Bastiansen, *Dev. Change* **41**, 421 (2010).
2. L. Rico García-Amado *et al*., *Ecol. Econ*. **14**, 216 (2011).
3. D. Melick, *Conserv. Biol*. **24**, 359 (2010).
4. L. Pesett, D. Huberman, E. Bowen-Jones, G. Edwards, J. Brown, "Making REDD work for the poor: Report prepared on behalf of the Poverty Environment Partnership" (Overseas Development Institute, London, 2008).
5. L. Persha, A. Agrawal, A. Chhatre, *Science* **331**, 1606 (2011).
6. W. M. Adams *et al*., *Science* **306**, 1146 (2004).

Ecosystem Services: Free Lunch No More

IN THEIR POLICY FORUM "PAYING FOR ECOsystem services—Promise and peril" (4 November 2011, p. 603), A. P. Kinzig and colleagues cite the Millennium Ecosystem Assessment report's finding that 60% of the world's ecosystem services have declined over the past 50 years, and declare the statistic unsurprising given that "we get what we pay for." Yet, the very concept of ecosystem services stems from the fact that these services are provided, pro bono, by the natural environment. There is such a thing as a free lunch.

This helps explain the lack of emerging markets for ecosystem services. As any salesperson can attest, trying to raise the cost of a good or service with existing customers is generally a more difficult task than raising the cost for new customers. This is because consumers are more willing to pay additional costs for services they do not currently possess, or for an increase in quality of services already received, than simply paying for services that were previously free (*1*). Creating markets for ecosystem services that already exist for free (even if those services are deteriorating) was never going to be an easy task.

Given these difficulties, it is not surprising that many existing ecosystem services markets, such as the SO_2 example cited by Kinzig *et al*., have required regulatory enforcement to at least kick-start the process. Many currently scarce ecosystem services were previously abundant, and it will take time and often regulatory prodding to move these services into a true incentive-based economy. Integrating an understanding of consumer psychology will help overcome the barriers to success.

LUCAS N. JOPPA

Microsoft Research, Computational Ecology and Environmental Sciences, Cambridge, UK. E-mail: lujoppa@microsoft.com

Reference

1. J. Loomis, P. Kent, L. Strange, K. Fausch, A. Covich, *Ecol. Econ.* **33**, 103 (2000).

Response

WE AGREE WITH CORBERA AND PASCUAL that payments for ecosystem services (PES) should be deployed only if they improve overall human wellbeing. We also agree that the credibility and acceptability of PES schemes likely require that participants view both the process and the outcomes as fair. We do not, however, agree with Corbera and Pascual's idea that the payments made to providers of ecosystem services can simultaneously signal the scarcity of those resources, meet the poverty alleviation goals of governments, and reduce income inequality. Multiple objectives require multiple mechanisms.

The central argument in our Policy Forum is that if people have no measures of the scarcity (the true social opportunity cost) of environmental resources, those resources will be misused, with potentially serious consequences for current and future human wellbeing. PES schemes have the potential to enhance the ways ecosystem services are used and protected by signaling the scarcity of environmental resources, and that should be their goal. Using PES to address social justice or poverty alleviation at the same time means that they will likely miss this goal. In the most comprehensive review of the successes and failures of PES schemes to date, Pattanayak, Wunder, and Ferraro report that government-funded schemes with prominent distributional goals are significantly less effective than user-funded schemes in securing additional ecosystem service flows (*1*).

Poverty alleviation and income redistribution are both important objectives and may well be critical to the acceptability of PES schemes, as Corbera and Pascual say, but payments made for ecosystem services will not be effective in meeting those objectives. The payments made under existing PES schemes have been shown to help the poor in some cases, but the benefits of participation are generally very small relative to governments' poverty-alleviation targets (*1*). Poverty alleviation and income redistribution are better met through other mechanisms, such as investment in public goods that benefit all members of a community, technology transfer, retraining programs, cash "dividends," and annual enrollment benefits.

The evidence gives little comfort to those who want to kill two birds with one stone. The main advantage of PES schemes is to signal the scarcity of environmental resources. Redistributing income requires a different mechanism. Although both may be part of the same package, they should not be conflated.

Joppa suggests that implementation of PES schemes is difficult in part because people are reluctant to pay for things they previously got for free. It is true that people are reluctant to give up rights that give them positions of privilege. However, when such rights no longer serve current needs, societies have frequently found the political will to abrogate them, increasing well-being in the process. The earliest modern examples include the curtailment of historic rights to pollute both air and water and to harvest marine resources (*2*). All address the overexploitation that comes from open-access rights to common pool environmental resources (*3*). The effectiveness of such an approach is sensitive to the design of new rights, as we argued in the case of the U.S. SO_2 control. However, it has been shown that the abrogation of open-access

Letters to the Editor

Letters (~300 words) discuss material published in *Science* in the past 3 months or matters of general interest. Letters are not acknowledged upon receipt. Whether published in full or in part, Letters are subject to editing for clarity and space. Letters submitted, published, or posted elsewhere, in print or online, will be disqualified. To submit a Letter, go to www.submit2science.org.

NextGenVOICES

Definition of Success: Last Call

You have one more week to respond to our second NextGen VOICES survey! Share your thoughts about these questions:

What is your definition of a successful scientist? How has this definition changed between your mentor's generation and your own?

To submit, go to http://scim.ag/NextGen_2.

Deadline for submissions is 17 February. A selection of the best responses will be published in the 6 April issue of *Science*. Submissions should be 250 words or less. Anonymous submissions will not be considered. Please submit only once.

Published by AAAS

rights to marine resources has averted the collapse of many wild capture fisheries (*4*). We expect such changes to occur again. Rights to a free ride on ecosystem services provided by others are inefficient—they reduce global well-being. Corbera and Pascual would argue that they are also unfair. For both reasons, it is worth the effort to overcome the reluctance of people to lose a position of privilege.

ANN P. KINZIG,[1] CHARLES PERRINGS,[1]* F. STUART CHAPIN III,[2] STEPHEN POLASKY,[3] V. KERRY SMITH,[4] DAVID TILMAN,[5] B. L. TURNER II[6]

[1]School of Life Sciences, Arizona State University, Tempe, AZ 85287, USA. [2]Department of Biology and Wildlife, University of Alaska Fairbanks, Fairbanks, AK 99775, USA. [3]Department of Applied Economics, University of Minnesota, St. Paul, MN 55108, USA. [4]W. P. Carey School of Business, Arizona State University, Tempe, AZ 85287, USA. [5]Department of Ecology, Evolution, and Behavior, University of Minnesota, St. Paul, MN 55108, USA. [6]School of Geographical Sciences and Urban Planning, and School of Sustainability, Arizona State University, Tempe AZ 85287, USA.

*Author for correspondence. E-mail: charles.perrings@asu.edu

References

1. S. K. Pattanayak, S. Wunder, P. J. Ferraro, *Rev. Environ. Econ. Pol.* **4**, 254 (2010).
2. T. Tietenberg, *Oxford Rev. Econ. Pol.* **19**, 400 (2003).
3. G. Hardin, *Science* **162**, 1243 (1968).
4. C. Costello, S. D. Gaines, J. Lynham, *Science* **321**, 1678 (2008).

CORRECTIONS AND CLARIFICATIONS

Reports: "Fear erasure in mice requires synergy between antidepressant drugs and extinction training" by N. N. Karpova *et al.* (23 December 2011, p. 1731). An author was left out of the author list. Amine Bahi should be listed between Yumiko Akamine and Regina Sullivan. Bahi's affiliation is the Department of Anatomy, Faculty of Medicine and Health Sciences, United Arab Emirates University, Al-Ain, United Arab Emirates.

Reports: "Formation and spread of aircraft-induced holes in clouds" by A. J. Heymsfield *et al.* (1 July 2011, p. 77). The photo used in Fig. 1A was incorrectly credited. The credit should read, "Photo provided by Eric M. Brown, technical background by Michael Carmody." The credit has been corrected in the HTML version online.

TECHNICAL COMMENT ABSTRACTS

Comment on "Phonemic Diversity Supports a Serial Founder Effect Model of Language Expansion from Africa"

Michael Cysouw, Dan Dediu, Steven Moran

We show that Atkinson's (Reports, 15 April 2011, p. 346) intriguing proposal—that global linguistic diversity supports a single language origin in Africa—is an artifact of using suboptimal data, biased methodology, and unjustified assumptions. We criticize his approach using more suitable data, and we additionally provide new results suggesting a more complex scenario for the emergence of global linguistic diversity.

Full text at www.sciencemag.org/cgi/content/full/335/6069/657-b

Comment on "Phonemic Diversity Supports a Serial Founder Effect Model of Language Expansion from Africa"

Chuan-Chao Wang, Qi-Liang Ding, Huan Tao, Hui Li

Atkinson (Reports, 15 April 2011, p. 346) reported a declined trend of phonemic diversity from Africa that indicated the African exodus of modern languages. However, his claim was only supported when the phonemic diversities were binned into three or five levels. Analyses using raw data without simplification suggest a decline from central Asia rather than from Africa.

Full text at www.sciencemag.org/cgi/content/full/335/6069/657-c

Comment on "Phonemic Diversity Supports a Serial Founder Effect Model of Language Expansion from Africa"

Rory Van Tuyl and Asya Pereltsvaig

Atkinson (Reports, 15 April 2011, p. 346) concluded that language originated in western Africa and that, due to a serial founder effect, languages repeatedly lost phonemes the farther they moved from the African point of origin. Independent examination of the published data tends to refute both these claims.

Full text at www.sciencemag.org/cgi/content/full/335/6069/657-d

Response to Comments on "Phonemic Diversity Supports a Serial Founder Effect Model of Language Expansion from Africa"

Quentin D. Atkinson

Concerns have been raised about my proposal that global phonemic diversity was shaped by a serial founder effect during the human expansion from Africa. I welcome this discussion of new data and alternative interpretations. Although this work highlights interesting questions for future research, it does not undermine support for a serial founder effect model of expansion of language from Africa.

Full text at www.sciencemag.org/cgi/content/full/335/6069/657-e

Comment on "Phonemic Diversity Supports a Serial Founder Effect Model of Language Expansion from Africa"

Michael Cysouw,[1]*† Dan Dediu,[2,3]† Steven Moran[1]

We show that Atkinson's (Reports, 15 April 2011, p. 346) intriguing proposal—that global linguistic diversity supports a single language origin in Africa—is an artifact of using suboptimal data, biased methodology, and unjustified assumptions. We criticize his approach using more suitable data, and we additionally provide new results suggesting a more complex scenario for the emergence of global linguistic diversity.

Recently, Atkinson (*1*) reported a negative correlation between the size of the phonemic inventory of a language and its geographic distance from western Africa. He proposed that this is the result of a repeated linguistic founder effect accompanying the migration of modern humans out of Africa some 50,000 to 70,000 years ago. According to this proposal, the original languages spoken in western Africa would have had a large phoneme inventory, which became reduced during the spread of modern humans over the globe because of imperfect transmission in the small founder populations involved. From a linguistic perspective, this result is surprising and contradicts our intuitions. Although we agree that there is clear nonrandom geographic patterning in the distribution of phoneme inventory sizes among the world's languages, we very much doubt that it shows any detectable remnant of the proposed demographic scenario.

In summary (*2*), we see the following problems with Atkinson's findings. First, his data are coarse-grained summaries of the UCLA Phonological Segment Inventory Database (UPSID) (*3*) as reported in the *World Atlas of Language Structures* (WALS) (*4*). To illustrate our concerns, we used the original UPSID database (which is freely available online) together with tone data from WALS. Atkinson's WALS-based estimates of phoneme inventory size turn out to be only imperfectly correlated with the actual number of phonemes as specified in UPSID ($r = 0.60$, $P < 2.2 \times 10^{-16}$). Specifically, his WALS-based data give unjustified weight to the number of vowels and tones at the expense of the number of consonants, strongly biasing the resulting geographic patterning toward western Africa's having large phoneme inventories (figs. S3 and S4). When the UPSID data are appropriately corrected for speaker community size and linguistic genera through a mixed-effects model, the largest phoneme inventories are actually found in North America (fig. S8).

Second, Atkinson methodologically follows previous work reporting clines of decreasing genetic and phenotypic diversity with increasing distance from Africa (*5*, *6*). Accordingly, he uses the term "phonemic diversity" interchangeably with the more accurate "phoneme inventory size," but this seems misplaced. In the original papers (*5*, *6*) "diversity" refers to variation within populations of individuals, whereas Atkinson's linguistic diversity refers to differences between languages. In fact, the languages of western Africa and New Guinea/Australia in UPSID show the lowest variability in inventory sizes (fig. S5). On the basis of the proposed serial founder effect, low variability might have been expected in New Guinea/Australia, but surely not in the supposed origin in western Africa.

In practice, Atkinson's biologically inspired method searches for the geographic location

[1]Research Unit Quantitative Language Comparison, Ludwig Maximilian University, Geschwister Scholl Platz 1, D-80539 Munich, Germany. [2]Language and Genetics Department, The Max Planck Institute for Psycholinguistics, Wundtlaan 1, 6525 XD, Nijmegen, Netherlands. [3]Donders Institute for Brain, Cognition and Behaviour, Kapittelweg 29, 6525 EN, Nijmegen, Netherlands.

*To whom correspondence should be addressed. E-mail: cysouw@lmu.de

†These authors contributed equally to this work.

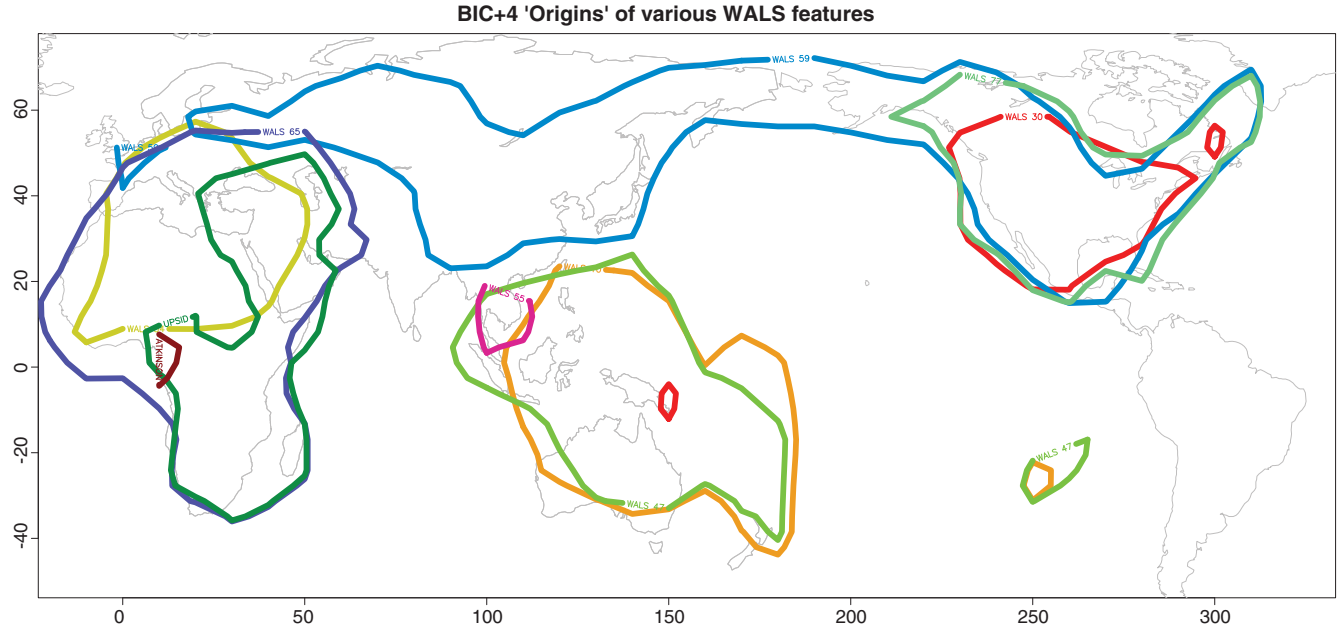

Fig. 1. Areas of "origin" of various other inventory-like linguistic characteristics as identified using Atkinson's methodology. Notably, the origins are dispersed over the whole globe and not concentrated in Africa. The dark red area in Africa is the origin of phoneme inventories as proposed by Atkinson. The dark green area in Africa and the Near East is the corresponding area based on the UPSID phoneme inventory data. The small red area on the eastern tip of New Guinea is the origin for the UPSID phoneme inventory data using a quadratic geographical distance model. Details about the other areas can be found in (*2*).

minimizing the Bayesian information criterion (BIC) (*7*) of the regression between phonemic inventory size and geographic distance, including further control variables. Atkinson selects those locations at most four BIC units away from this optimum as having considerable support in being the origin of the expansion. A quick computation shows that this implies accepting models that are at most $e^2 \sim 7.4$ times less likely than the optimal one (*2*), which strikes us as rather arbitrary. Further, this BIC optimization method necessarily "spreads" any origin across a contiguous geographic region, even in the case of totally random data (fig. S12).

Notwithstanding this criticism, we replicated Atkinson's method using the UPSID data, but instead of a single origin in western Africa, we found two separate "origins," one in eastern Africa and one in the Caucasus (fig. S10). The BIC+4 range of possible origins covers a large area, including also the Middle East and southern Africa. Although this finding does not necessarily contradict an expansion from Africa, it does not provide clear support in its favor, either. Further, adding a quadratic distance factor to the model substantially improves the fit and suggests an alternative origin located in New Guinea with a small phoneme inventory (fig. S10). Even more problematic, when we apply the original method to other inventory-like linguistic characteristics from WALS (Fig. 1), we find origins of global clines all over the world, not just in Africa, and not always corresponding to the highest structural "complexity" (fig. S11). Therefore, the observation of an Africa-based phoneme inventory cline does not generalize to other linguistic characteristics of a similar kind.

Third, Atkinson's explanation crucially depends on a positive correlation between phonemic inventory size and speaker community size, which, unfortunately and contrary to his own claim [see figure S1 in (*1*)], does not hold for small populations when using UPSID data ($r = 0.04$, $P = 0.64$) (fig. S6). This correlation reaches significance at the 5% level only when languages with speaker populations above 10^5 are included, but such large speaker community sizes only arose in the context of agriculture long after the peopling of most of the globe (*8*).

Fourth, the geographic patterning of tone might be influenced by a genetic bias postdating the out-of-Africa migration by tens of thousands of years (*9*). Moreover, consonant inventories (and to a lesser extent, vowel inventories) do not seem to be phylogenetically stable enough (*10*) to conserve the kind of deep signal necessary for the proposed scenario, whereas other, more stable, features show non-African "origins" (fig. S11).

Finally, we believe that Atkinson's interpretation of the reported worldwide cline in terms of a linguistic serial founder effect is problematic because of the extraordinary large amount of horizontal processes affecting language (*11*, *12*) and because the underlying mechanism proposed by Atkinson is linguistically not plausible (*13*). Further, global clines in linguistics, like in genetics, do not necessarily equate with a serial founder effect and can have other causes (*2*, *14*).

Summarizing, the reported linguistic evidence for an expansion from Africa is unfortunately an artifact of various methodological decisions and biased interpretations. We consider this to be unfortunate, because we would very much welcome any new insights into human prehistory based on geographic patterns of linguistic diversity. In this respect, we applaud Atkinson for further developing this approach (*15*) and renewing the methodological discussion, because only explicit testing and refutation opens the way for the formulation of more specific hypotheses concerning the identification of possible linguistic signatures of ancient demographic events.

References and Notes

1. Q. D. Atkinson, *Science* **332**, 346 (2011).
2. Materials and methods are available as supporting material on *Science* Online.
3. I. Maddieson, K. Precoda, The UCLA Phonological Segment Inventory Database (1990); http://web.phonetik.uni-frankfurt.de/upsid_info.html.
4. M. Haspelmath, M. S. Dryer, D. Gil, B. Comrie, Eds., *The World Atlas of Language Structures* (Oxford Univ. Press, Oxford, 2005).
5. A. Manica, W. Amos, F. Balloux, T. Hanihara, *Nature* **448**, 346 (2007).
6. L. Betti, F. Balloux, W. Amos, T. Hanihara, A. Manica, *Proc. Biol. Sci.* **276**, 809 (2009).
7. G. E. Schwarz, *Ann. Stat.* **6**, 461 (1978).
8. S. Mithen, *After the Ice* (Orion Books, London, 2003).
9. D. Dediu, D. R. Ladd, *Proc. Natl. Acad. Sci. U.S.A.* **104**, 10944 (2007).
10. D. Dediu, *Proc. Biol. Sci.* **278**, 474 (2011).
11. S. G. Thomason, T. Kaufman, *Language Contact, Creolization, and Genetic Linguistics* (Univ. of California Press, Berkeley, CA, 1988).
12. T. F. Jaeger, P. Graff, W. Croft, D. Pontillo, *Linguist. Typol.* **15**, 281 (2011).
13. C. Bowern, *Linguist. Typol.* **15**, 207 (2011).
14. I. Maddieson, T. Bhattacharya, D. E. Smith, W. Croft, *Linguist. Typol.* **15**, 267 (2011).
15. J. Nichols, *Linguistic Diversity in Space and Time* (Univ. of Chicago Press, Chicago, 1992).

Acknowledgments: The authors declare no conflict of interests. M.C., D.D., and S.M. designed the research; M.C. and S.M. organized the data; M.C. and D.D. performed the analysis and wrote the paper. M.C. and S.M. are funded by European Research Council starting grant 240816 QuantHistLing.

Supporting Online Material

www.sciencemag.org/cgi/content/full/335/6069/657-b/DC1
Materials and Methods
SOM Text
Figs. S1 to S12
Table S1
References

24 May 2011; accepted 3 January 2012
10.1126/science.1208841

Response to Comments on "Phonemic Diversity Supports a Serial Founder Effect Model of Expansion from Africa"

Quentin D. Atkinson[1,2]

Concerns have been raised about my proposal that global phonemic diversity was shaped by a serial founder effect during the human expansion from Africa. I welcome this discussion of new data and alternative interpretations. Although this work highlights interesting questions for future research, it does not undermine support for a serial founder effect model of expansion of language from Africa.

I hypothesized that phoneme inventory size is subject to a serial founder effect like that observed in population genetics (*1*). The plausibility of such a process is grounded in theoretical models of cultural and linguistic transmission, which predict that small populations should carry fewer phonemes (*2*–*4*), and an observed positive correlation between phonemic diversity and speaker population size (*1*, *5*). If phonemes are more likely to be lost in small founder populations, a succession of founder events during range expansion should progressively reduce phonemic diversity with increasing distance from the point of origin. I show that global variation in phonemic diversity is clinal and, like our genetic diversity, fits a serial founder effect model of expansion from Africa. As for any correlational finding, it is important to consider alternative causal explanations, and so much of the paper (*1*) and subsequent discussion (*6*–*10*) is devoted to examining potential alternatives. Here, I continue this process, addressing a number of concerns that relate to the data and assumptions on which the result is based (*11*–*13*). Although these warrant consideration and raise interesting questions for future research, I argue that they do not undermine the hypothesis presented in the paper.

Cysouw *et al.* criticize my use of the term "phonemic diversity" to describe the number of phonemes in a language, arguing that although phenotypic or genetic diversity measure within-population variation, phonemic diversity measures between-population variation. Phonemic diversity is a convenient shorthand, but I am agnostic about the use of the term, particularly if it engenders confusion. To be clear, phonemic diversity is not a measure of variation between populations; it is simply a property of populations—the measured number of phonemes carried by speakers. Although phonemic diversity is measured in a different way from genetic diversity, the analogy holds in the sense that the link with population size that predicts a serial founder effect in genetic diversity can also be applied to phonemic diversity.

The results I reported are based on phoneme counts derived from the *World Atlas of Language Structures* (WALS) (*14*), combining binned estimates of relative vowel, consonant, and tone inventory size and assigning equal weights to each. This equal weighting was criticized as being inappropriate (*11*–*13*) because, for example, there are many more consonants in languages than vowels or tones, and the binning procedure used in WALS may lose information in a way that biases results.

Cysouw *et al.*'s serial founder analysis of reweighted WALS data, controlling for population size and language affiliation, also supports an African origin. Residuals from a regression of population size and language affiliation against their UCLA Phonological Segment Inventory Database (UPSID) (*15*) data are highest in North America, but this does not speak to the independent effects of population size and distance from Africa on phonemic diversity. When the UPSID data are used in a serial founder analysis controlling for population size and language affiliation, Cysouw *et al.* also find support for an African origin, even when the two most highly diverse Khoisan languages are excluded, although the inferred origin is expanded to include the Caucasus.

Wang *et al.* analyze a selection of languages from their own source of phonemic diversity data and show that although the relationship between total phonemic diversity and distance from Africa remains significant, there is a stronger relationship with distance from Europe and central Asia. However, this result is dependent on four closely related outliers in Wang *et al.*'s data from southeast Asia (two Tai-Kadai languages and two Wu dialects). Removing these nonindependent outlier languages again favors an origin in Africa ($r = -0.471$, $P < 0.001$) over central Asia ($r = -0.455$, $P < 0.001$) or Europe ($r = -0.461$, $P < 0.001$). Including all languages in the same hierarchical linear modeling approach used in the original paper to control for population size and account for relatedness between languages within the same family, Wang *et al.*'s data also favors an African origin [Bayesian information criterion (BIC) = 776.9), over central Asia (BIC = 787.4), or Europe (BIC = 777.7)], although the improvement over a European origin is not decisive.

Van Tuyl and Pereltsvaig use Wikipedia to identify some cases of possible disagreement in levels of phonemic diversity. There is clearly some ambiguity or discrepancy in phoneme assignments and what exactly is counted between sources. As I have advocated elsewhere (*6*), the way to resolve this is to continue work to standardize phoneme inventory data and evaluate the serial founder effect model and its alternatives against multiple sources. This work has already begun (*6*), and Cysouw *et al.* and Wang *et al.* continue this process.

In line with previous genetic and phenotypic studies (*16*), I used a BIC threshold of four units to identify the credible origin area. This value is more conservative (allowing greater uncertainty in any inferred origin area) than the value of two suggested by Cysouw *et al.* The fact that the method I used identifies spatially contiguous areas of origin is not a disadvantage. This emerges naturally from the fact that model fit for different putative origins is spatially autocorrelated, but the method need not identify a single origin area or any clearly defined area. As Cysouw *et al.*'s own simulations show, when the method is applied to random data, the area supported using a BIC threshold of four includes the whole world, correctly indicating that the random data do not point to any particular origin location.

Van Tuyl and Pereltsvaig make much of the fact that the global cline in phonemic diversity does not hold within all continents. However, looking for individual within-continent trends greatly reduces statistical power and is more affected by recent population movements and nonindependence due to relatedness between languages in a region. Such a pattern does not undermine the global trend. When effects of continent and by-continent variation in the relationship with distance from Africa are added to a hierarchical linear model that incorporates language affiliation information, model fit is decisively worse than when region is ignored (BIC is 807.1 with region effects and 773.2 without). Even in the regional model, the global effect of distance from Africa remains significant [$\beta = -7.34$ to -2.05×10^{-5} (95% highest posterior density); $P < 0.001$]. Further, Van Tuyl and Pereltsvaig's own analysis shows a significant stepwise decline in phonemic diversity between continents with increasing distance from Africa.

Van Tuyl and Pereltsvaig also focus on the precise location of the best-fit origin in Africa, questioning the level of support for a western African origin. Although this is an interesting

[1]Department of Psychology, University of Auckland, Private Bag 92019, Auckland 1142, New Zealand. [2]Institute of Cognitive and Evolutionary Anthropology, University of Oxford, 64 Banbury Road, Oxford OX2 6PN, UK. E-mail: q.atkinson@auckland.ac.nz

line of inquiry, particularly given the view that eastern Africa represents the cradle of humanity, none of the interpretation in my paper relates to the specific origin location within Africa; as I make clear, the family-level analysis identified an origin area spanning all of Africa.

Cysouw *et al.* report the fit of a model of phonemic diversity as a quadratic function of distance. Rather than the gradual global cline predicted under a serial founder effect, fitting a quadratic model will tend to identify steeper localized gradients in phonemic diversity. This model finds an African best-fit origin for the WALS data, but the best-fit model for the UPSID data is a positive quadratic function with distance from New Guinea (i.e., phonemic diversity is lowest in New Guinea and increases with distance). Although these more complex models may identify previously unrecognized patterns, unlike arguments for a simple serial founder effect model of phonemic diversity, we have no a priori reason to think a positive quadratic function of distance is a good model of how phonemes change. Likewise, there is no reason to expect that aspects of language "complexity," like the assortment analyzed by Cysouw *et al.*, should all show a founder effect. Such features can be expected to behave quite differently. Indeed, as Cysouw *et al.* mention, loss of complexity in one domain is thought to be compensated with elaboration in other domains. There are clearly interesting large-scale geographic patterns in some of these features that warrant further research. Although I am in favor of the rigorous examination of these patterns, the blanket application of a founder analysis to such features tells us little about the processes that generated them and does not refute the findings with regard to phonemic diversity.

Cysouw *et al.* also suggest that levels of between-language variation in phonemic diversity (which they measure as the standard deviation in phonemic diversity across a language and its five nearest neighbors) contradict the predictions of a founder effect model. The founder effect model is a prediction about mean levels of diversity that we expect to see across an expansion—the result of a balance between merging, splitting, and borrowing processes (*1*). Variance in phonemic diversity between neighbors will depend largely on their statistical independence (due to relatedness, recency of expansion, borrowing, and the density of sampling), whether there are upper or lower limits on diversity, and variation in other factors such as population size and the nature of local language formation mechanisms. Hence, although a low standard deviation in New Guinea/Australia and western Africa is interesting, it is does not contradict a serial founder effect from Africa.

The relationship I report between population size and phonemic diversity also holds for Cysouw *et al.*'s reweighted WALS and UPSID data. When restricted to small speaker population sizes, this relationship is in the correct direction, but Cysouw *et al.* point out that the trend is not statistically significant for their measures. Likely distortions of smaller population sizes since European colonial expansion combined with fewer data points may undermine the ability to detect a significant relationship among small populations. For the full data set, phonemic diversity appears to relate reliably to demography in the manner predicted by simulations of cultural evolution (*2*–*4*) and consistent with a serial founder effect. More detailed analysis of a larger sample of smaller populations may be needed to determine whether the nature of the relationship is fundamentally different among small groups.

Wang *et al.* and Cysouw *et al.* question whether phonemic diversity is stable enough to reflect migration events on the scale of the human expansion from Africa. Cysouw *et al.* point out that tone may be influenced by genetic variants that postdate the African expansion, but together these genes explain only 7% of the variance (*17*). Studies examining typological stability on phylogenies indicate that rates of phoneme replacement vary across families but are generally comparable to other structural features (*18*). Cysouw *et al.* cite evidence that consonant inventories may be less stable than other features, including vowel and tone inventory (*19*). However, these inferred rates are contingent on the binning procedure used to code the data and so do not provide an absolute estimate of long-term stability. Moreover, horizontal transmission due to borrowing can inflate rates of evolution on a phylogeny without disrupting geographic patterning. As I highlighted in my paper, phonemic diversity appears highly stable at the language-family level, with family affiliation explaining about 50% of the variance around the globe (*1*).

Admixture or horizontal transfer of phonemes between languages due to borrowing is not, as Cysouw *et al.* and Van Tuyl and Pereltsvaig claim, problematic for the serial founder effect model. In fact, as is the case in population genetics (*20*), horizontal transfer can help to maintain a cline, because neighboring populations at similar points in the expansion (e.g., in Africa versus in Australia) are more likely to encounter similar phonemes and levels of diversity. Nonetheless, I agree with Cysouw *et al.* that there is more to language change than phoneme inventories and serial founder effects; I do not expect this result to be the last word on language origins. Some of the most promising avenues of future research address questions touched on in these and other commentaries (*6*–*10*), including explicitly modeling rates of evolution of individual sound changes (*21*), rates of borrowing on a phylogeny (*22*), and determining population structure without assuming a tree-like model of evolution (*23*). I look forward to more research applying these and other quantitative methods to identify the key drivers of global variation in human language.

References

1. Q. D. Atkinson, *Science* **332**, 346 (2011).
2. B. De Boer, *The Origins of Vowel Systems: Studies in the Evolution of Language 1* (Oxford University Press, New York, 2001).
3. P. Trudgill, in *The Handbook of Language Variation and Change*, J. K. Chambers, P. Trudgill, N. Schilling-Estes, Eds. (Blackwell, Oxford, 2002), pp. 707–728.
4. J. Henrich, *Am. Antiq.* **69**, 197 (2004).
5. J. Hay, L. Bauer, *Language* **83**, 388 (2007).
6. Q. D. Atkinson, *Linguist. Typol.* **15**, 321 (2011).
7. T. F. Jaeger, P. Graff, W. Croft, D. Pontillo, *Linguist. Typol.* **15**, 281 (2011).
8. C. Bowern, *Linguist. Typol.* **15**, 207 (2011).
9. I. Maddieson, T. Bhattacharya, E. Smith, W. Croft, *Linguist. Typol.* **15**, 267 (2011).
10. D. Ringe, *Linguist. Typol.* **15**, 223 (2011).
11. M. Cysouw, D. Dediu, S. Moran, *Science* **335**, 657 (2012); www.sciencemag.org/cgi/content/full/335/6069/657-b.
12. C.-C. Wang, Q.-L. Ding, H. Tao, H. Li, *Science* **335**, 657 (2012); www.sciencemag.org/cgi/content/full/335/6069/657-c.
13. R. Van Tuyl, A. Pereltsvaig, *Science* **335**, 657 (2012); www.sciencemag.org/cgi/content/full/335/6069/657-d.
14. M. Haspelmath, M. S. Dryer, D. Gil, B. Comrie, *The World Atlas of Language Structures Online* (Max Planck Digital Library, Munich, 2008).
15. I. Maddieson, K. Precoda, *UCLA Working Papers in Phonetics* **74**, 104 (1990).
16. A. Manica, W. Amos, F. Balloux, T. Hanihara, *Nature* **448**, 346 (2007).
17. D. Dediu, D. R. Ladd, *Proc. Natl. Acad. Sci. U.S.A.* **104**, 10944 (2007).
18. S. J. Greenhill, Q. D. Atkinson, A. Meade, R. D. Gray, *Proc. Biol. Sci.* **277**, 2443 (2010).
19. D. Dediu, *Proc. Biol. Sci.* **278**, 474 (2011).
20. L. J. L. Handley, A. Manica, J. Goudet, F. Balloux, *Trends Genet.* **23**, 432 (2007).
21. A. Bouchard-Côté, P. Liang, T. Griffiths, D. Klein, paper presented at the Advances in Neural Information Processing Systems 20 (NIPS), Vancouver, BC, Canada, 8 to 12 December 2008.
22. S. Nelson-Sathi *et al.*, *Proc. Biol. Sci.* **278**, 1794 (2011).
23. G. Reesink, R. Singer, M. Dunn, *PLoS Biol.* **7**, e1000241 (2009).

8 July 2011; accepted 3 January 2012
10.1126/science.1210005

Comment on "Phonemic Diversity Supports a Serial Founder Effect Model of Language Expansion from Africa"

Chuan-Chao Wang, Qi-Liang Ding, Huan Tao, Hui Li*

Atkinson (Reports, 15 April 2011, p. 346) reported a declined trend of phonemic diversity from Africa that indicated the African exodus of modern languages. However, his claim was only supported when the phonemic diversities were binned into three or five levels. Analyses using raw data without simplification suggest a decline from central Asia rather than from Africa.

Atkinson (*1*) analyzed the phoneme numbers of 504 languages around the world and found a strong inverse relationship between the phonemic diversity and distance from an inferred origin in Africa, which supports an African origin of modern languages. Although a statistically significant declined trend of phonemic diversity from Africa can be observed from the analyses of his normalized data set, his conclusion was questionable because of the simplification of the phoneme inventories.

The simplified data used in Atkinson's analyses were obtained directly from the *World Atlas of Language Structures* (WALS) (*2*), where the phoneme numbers of the languages were simply binned into three or five levels. However, this kind of simplification of the data lost most information of the phonemic diversity and might have resulted in bias conclusion. For example, the consonant inventory varies from less than 10 to more than 80 among the world languages (*3*), while only five levels were counted in Atkinson's analyses.

We collected a new data set of world phonemic diversity, including 579 languages from 95 linguistic families (table S1). The phoneme inventories were displayed without any simplification. To balance among the linguistic families, we excluded 69 samples of some well-studied linguistic families (i.e., Indo-European, Austronesian, and Sino-Tibetan) from our analyses. This made our data comparable to Atkinson's (table S2). Our analyses were based on the remaining 510 languages.

Judged from the original WALS maps and Atkinson's normalized data set, the diversities of vowel quality, tone, and consonant (Fig. 1A) all exhibit significant declines from Africa to the rest of the world. However, the declines from Africa will not be that pronounced when the data are not simplified (the exact counts of vowel qualities, tones, and consonants). Languages from Eurasia show higher diversities of vowel qualities and tones (Fig. 1B). Therefore, we argued that Atkinson's statistics were distorted by WALS's data simplification, which truncated the high ends of the scales (*2*).

For example, WALS binned the vowel quality inventories into three groups: small (2 to 4 qualities), medium (5 to 6 qualities), and large (7 to 14 qualities). Actually, the basic vowel quality inventory varies from 2 to 20 and is distributed unequally among the geographic regions (*4*). Most large vowel quality inventories appear in Eurasia, whereas only small inventories can be found in the Americas and Australia. The Germanic languages and the Wu Chinese dialects have the largest vowel quality inventories in the world, mostly larger than 10—for example, the Standard Swedish has at least 16 vowel qualities, and the Dôngdăc Wu spoken in southern Shanghai has 20 vowel qualities. In contrast, few languages from Africa have more than 10 vowel qualities (Fig. 1B). Therefore, a lower limit of seven qualities for large inventory in WALS's

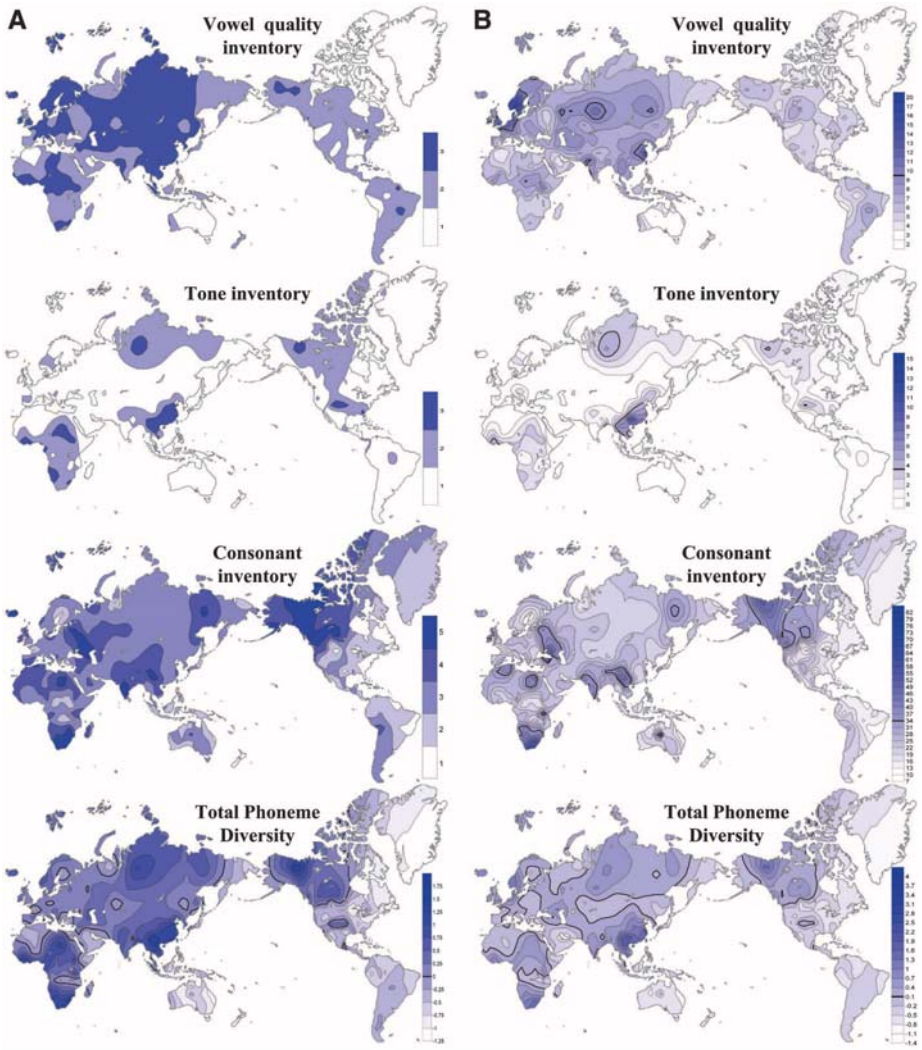

Fig. 1. Geographic distribution of the phonemic diversities of the world's languages. **(A)** Simplified phonemic diversities used by WALS. **(B)** Exact phoneme inventory counts and the corresponding total phoneme diversity.

Ministry of Education Key Laboratory of Contemporary Anthropology, School of Life Sciences, and Department of Chinese Language and Literature, Fudan University, Shanghai 200433 China.

*To whom correspondence should be addressed. E-mail: lihui.fudan@gmail.com

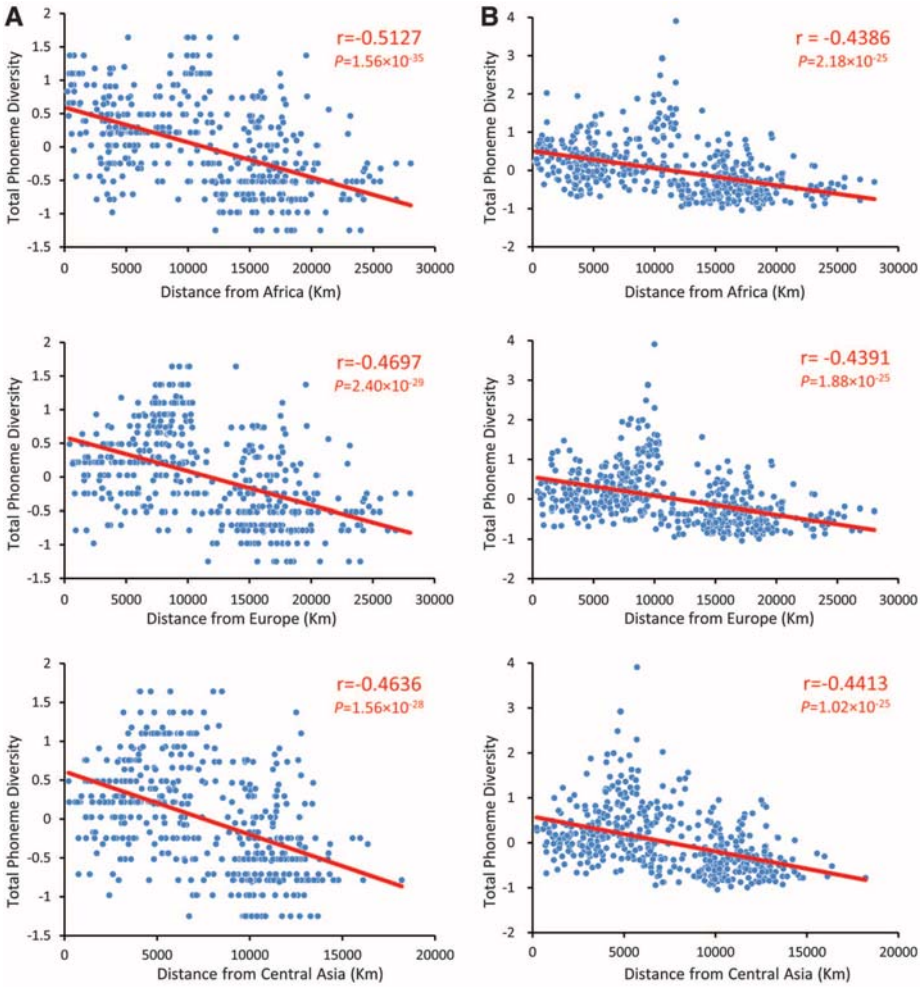

Fig. 2. Correlation between the distance from the best-fit origin of the languages and total phoneme diversity. Red lines are the fitted regression lines. Pearson correlation *r* and *P* values are shown in the upper right. **(A)** Estimated from simplified phoneme inventories. **(B)** Estimated from exact phoneme inventory counts.

data set eliminated the difference about the vowel diversity levels between the African and Eurasian languages. Besides the curtness in the vowel inventory counts, Atkinson's analysis ignored all other phonetic features of the vowels, such as nasalization, diphthong, and length, which vary tremendously among the world's languages (*5*).

Similar problems happened to the simplification of tone diversity. Most tonal languages in Africa have less than four tones, whereas most tonal languages in Asia have more than four. The Kam spoken in southwest China has the largest tone inventory (15 tones). The difference of tone diversity between the two continents is also screened in WALS. Using the raw data of all phonemes of the 510 languages without simplification, we analyzed the total phoneme diversity (table S1). The highest diversity is demonstrably in Asia (Fig. 1B), and the top three languages are Dôndäc (3.91), Kam (2.87), and Buyang (2.49).

We further redid the correlation analyses between the total phoneme diversity and distance from the "best-fit origin." Different regions were chosen as potential best-fit origins. Interestingly, stronger negative correlation was observed when choosing central Asia (the exact locus was Ashgabat) (Pearson correlation, $r = -0.4413$) or Europe ($r = -0.4391$) as the origin than choosing Africa ($r = -0.4386$) (Fig. 2B). Moreover, when using mean diversity across language families, central Asia ($r = -0.5503$, $P = 5.08 \times 10^{-5}$) exhibited even stronger correlation than Europe ($r = -0.4945$, $P = 3.54 \times 10^{-4}$) or Africa ($r = -0.5053$, $P = 2.49 \times 10^{-4}$). However, when the WALS simplification was applied to our data set, the strongest negative correlation was still found between the diversity and distance from Africa (Fig. 2A).

To further test the robustness of these findings, we repeated regressions after controlling for modern speaker population size (*6*). Africa never exhibited strongest correlation unless the data were simplified (table S3). Because there are some clear outliers among the sampled languages, we applied a robust linear model to minimize the possible influence of outliers (*7*). In this model, the best-fit origin also turned from Africa to Asia when the data was not simplified (table S4).

Thus, we demonstrated that WALS's data simplification has distorted Atkinson's results. Apparently, the results without simplification should be more reliable. Therefore, Asia (where the Babel was supposed to be) might be a more appropriate best-fit origin for modern languages if modern languages have a common origin.

References and Notes

1. Q. D. Atkinson, *Science* **332**, 346 (2011).
2. I. Maddieson, in *The World Atlas of Language Structures Online*, M. S. Dryer, M. Haspelmath, Eds. (Max Planck Digital Library, Munich, 2011); chaps. 1, 2, and 13.
3. P. Ladefoged, I. Maddieson, *The Sounds of the World's Languages* (Blackwell, Oxford, 1996).
4. H. Li, *Commun. Contemp. Anthropol.* **2**, 42 (2008), 10.4236/coca.2008.21007; http://comonca.org.cn/Abs/2008/007.htm.
5. International Phonetic Association, *Handbook of the International Phonetic Association* (Cambridge Univ. Press, Cambridge, 1999).
6. L. Excoffier, G. Laval, S. Schneider, *Evol. Bioinform. Online* **1**, 47 (2005).
7. W. N. Venables, B. D. Ripley, *Modern Applied Statistics with S* (Springer, New York, 2002).

Acknowledgments: This work was supported by Shanghai Commission of Education Research Innovation Key Project (11zz04) and Shanghai Professional Development Funding (2010001). Y. Hu helped with some of the statistics.

Supporting Online Material

www.sciencemag.org/cgi/content/full/335/6069/657-c/DC1
Tables S1 to S4
References

3 May 2011; accepted 3 January 2012
10.1126/science.1207846

Comment on "Phonemic Diversity Supports a Serial Founder Effect Model of Language Expansion from Africa"

Rory Van Tuyl[1]* and Asya Pereltsvaig[2]

Atkinson (Reports, 15 April 2011, p. 346) concluded that language originated in western Africa and that, due to a serial founder effect, languages repeatedly lost phonemes the farther they moved from the African point of origin. Independent examination of the published data tends to refute both these claims.

Recently, Atkinson (*1*) plotted total normalized phoneme diversity (TNPD), a synthetic measure of language complexity, against distance from a putative point of origin (PO) in western Africa. By forcing a linear least-squares fit to the data and adjusting the PO location, he observed a maximum negative correlation when the PO was set to latitude 1°18′S, longitude 9°46′E on the equatorial west coast of Africa (*2*). He interpreted this maximum-correlation linear regression fit as evidence for a serial founder effect (SFE), a hypothesis that assumes small bands of isolated pioneers repeatedly tend to develop languages with fewer phonemes than that of their progenitors, and he interpreted the location of the PO as evidence that language most likely originated in western Africa.

A plot of data (*3*) for the human migration path from Africa to South America (Fig. 1) shows a better fit when data are linearly regressed continent by continent, revealing none of the downward slope associated with an SFE for any continent but Africa (*4*). An SFE must surely have existed in settling the vast expanse of Eurasia and the Americas, but there seems to be no evidence of it in these data. Why then should an SFE be considered the cause of TNPD regression slope within Africa?

Because distance was measured through fixed waypoints between continents, two-dimensional interaction between the PO and data points outside Africa was lost, so adjusting the location of the PO has no effect on the correlation for data outside Africa [Fig. 1 and supporting online material (SOM)]. Therefore, one would expect the PO to have been determined based solely on African data, and it was. When correlation is maximized using African data only, the PO changes negligibly, demonstrating that non-African data are irrelevant to determination of the extrapolated point of maximum phoneme diversity within Africa.

Linear regression centered at the western African PO is weak and may be adventitious. Such trends can occur purely by chance in meaningless locations. For example, the point of maximum correlation for the north Asian data is in northern Burma (an unlikely origin for human language), and for Nilo-Saharan languages it is far south of their range, in the middle of the Congo rainforest. Thus, an extrapolated PO based on maximum correlation can signal something other than a logical point of language origin, and the zone of putative western African language origin shown in Atkinson's figure 2A may be an artifact of analysis. Our Fig. 2 shows that correlation contours surrounding the PO may largely be due to

[1]Independent Scholar, Los Altos, CA 94022, USA. [2]Department of Linguistics, Stanford University, Stanford, CA 94305, USA.

*To whom correspondence should be addressed. E-mail: roryvantuyl@gmail.com

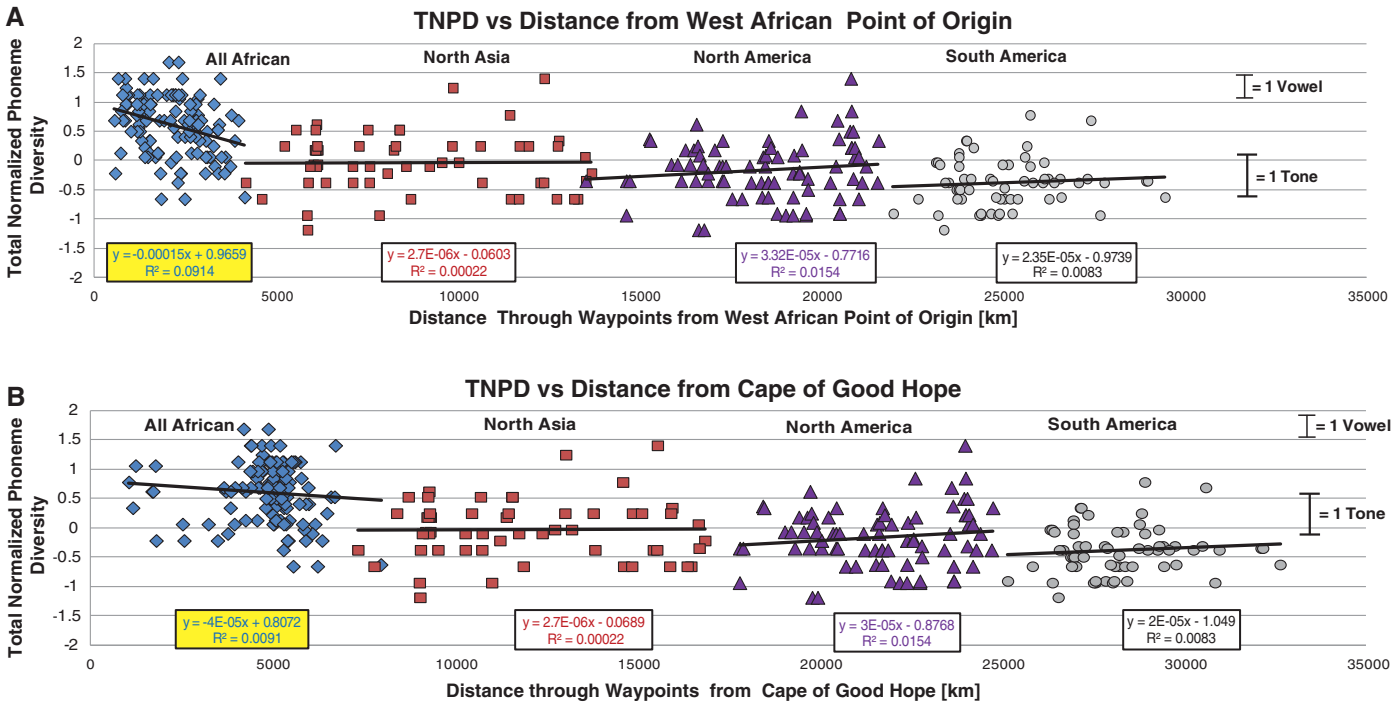

Fig. 1. TNPD for sub-Saharan Africa, north Asia (latitude > 30°, longitude > 30°), North America, and South America, versus (**A**) distance from the African point of origin and (**B**) distance from Cape of Good Hope. Continents outside Africa show no continuous phoneme loss versus distance. Africa shows a maximum decline (A) of about 1 SD of the data (0.48) with poor correlation (R^2 = 0.091) when a western African PO is chosen (A) and little decline for a southern African PO (B). When the PO within Africa is changed, the slopes and correlations for the African data change but non-African continents remain constant, showing that they have no active contribution to determining a maximum-correlation PO within Africa (see SOM).

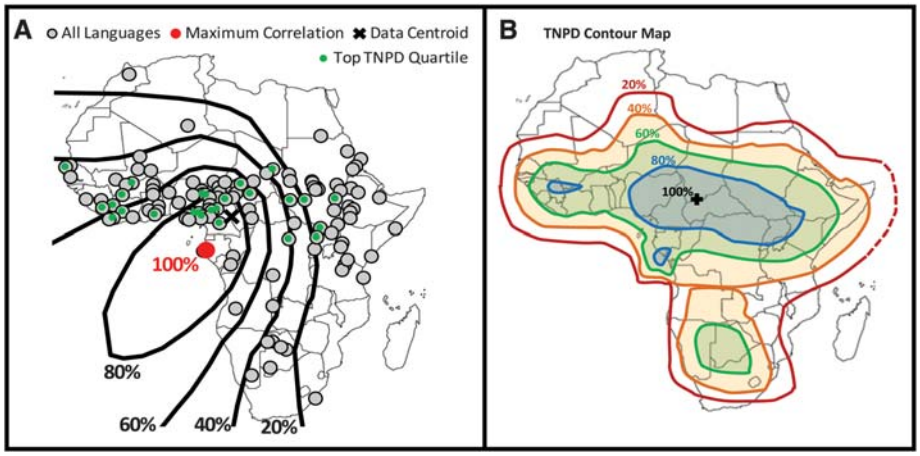

Fig. 2. (**A**) Map of African languages with contours of constant normalized correlation coefficient centered about a peak value (100%). These contours are similar to those for "likely area of language origin" in Atkinson's figure 2A. Language data are mostly in an equatorial swath, with fewer data to the south and very few to the north. (**B**) Map showing contours of normalized TNPD values (1000-km resolution). We see that the correlation contours in (A) do not accurately portray the distribution of TNPD (which stretches across the continent at about 7.5° north latitude) or the actual TNPD data peaks. Instead, the correlation method indicates elevated regions of correlation coefficient well into the Atlantic Ocean. The TNPD contour map shows peak TNPD near the data centroid, evidently a direct result of the data's geographic distribution.

the way the correlation technique interacts with the geographic distribution of data points, regardless of data's values (see SOM).

In addition to the above data analysis problems, there are reasons to doubt the data itself. TNPD as a measure of language complexity is highly problematic with regard to how phonemes are counted and how different phoneme types are combined. There are significant variations in phoneme counts reported from different sources, especially with respect to tones (*5*). TNPD calculations involve all consonant phonemes, some vowel phonemes (phonemic distinctions based on nasality and length are ignored), and tone features (tones are a suprasegmental feature on a par with length or stress and not a phoneme per se). Furthermore, assigning numerical values to the *World Atlas of Language Structures* (WALS) categories is questionable: In the TNPD scoring system, each vowel is on average worth 2.6 consonants, each tone worth 5.7 consonants. These ratios seem arbitrary, as is averaging vowels, consonants, and tones to calculate TNPD. As a result, consonant inventory plays virtually no role in the regression versus distance, and tones dominate the correlation (*6*). Furthermore, the TNPD measure also conceals that languages typically acquire or lose not single phonemes but whole (natural) classes of phonemes, such as clicks or ejectives, long or nasal vowels, or tonal distinctions.

Difficulties arise when a single numerical score is assigned to each WALS category, because with quantized categories the addition or subtraction of but a single phoneme can result in the same TNPD change as with multiple phonemes. Small changes in phoneme counts can have a substantial effect on analytical outcome. We conducted a study of 10 sub-Saharan languages that showed a discrepancy in 11 out of 30 counts (three for each language) between the WALS data and other sources, resulting in 8 of 10 languages changing TNPD quartile and the regression slope disappearing when the non-WALS data were used (*7*). [One African language, despite having 122 consonants (*8*), ranked in the second TNPD quartile.]

An SFE presupposes that languages change incrementally, in isolation from their neighbors. However, it is hard to see how the number of phonemes in a given language can be unambiguously attributed to a founder effect because languages are known to change in response to influences from neighbors (e.g., some Bantu languages acquired click sounds under the influence of Khoisan languages, and some Indo-Aryan languages acquired retroflex consonants from their Dravidian neighbors). Furthermore, DNA research argues for modern human origin in either eastern Africa (*9*) or southern Africa (*10*), and we can assume language originated with these people. Whatever the locations and phoneme inventories were for African languages in antiquity, the situation is surely different today, some 50,000 years after the modern human exodus. Migrations, conquests, and borrowings—many of which occurred long after the era of the founder effect—can explain the present state of African languages more credibly than simple diffusion of small founder groups.

References and Notes

1. Q. D. Atkinson, *Science* **332**, 346 (2011).
2. Triangulation of published data.
3. www.sciencemag.org/cgi/content/full/332/6027/346/DC1.
4. Overall fit to data is about 7% better to the segmented trend line shown (s = 0.473) than to an overall linear trend line (s = 0.505). The differences between mean values for adjacent continents are statistically significant between African and all non-African languages (t test; P = 0.000) and between North and South American (t test; P = 0.004), but not between north Asian and North American (t test; P = 0.175).
5. I. Maddieson, in *The World Atlas of Language Structures Online*, M. S. Dryer, M. Haspelmouth, Eds. (Max Planck Digital Library, Munich, 2011); chaps. 1, 2, and 13 (accessed 5/21/2011); http://wals.info.
6. Tones make up 59%, vowels 40%, and simple consonants 1% of the African regression slope.
7. Alternate data were obtained from Wikipedia Articles (accessed 5/23/2011) on the following languages: Swahili, Zulu, Jul'hoan, Sandawe, Khoekhoe, Maasai, Dinka, Luo, Igbo, and Yoruba. We do not assert these data to be correct; we merely note that they are different from the WALS data and reveal variation in phoneme counts between sources. Alternate data for the entire language set were not available and may not exist.
8. The language is !Xóõ. It has more than five times the average number of consonants, but fewer than five vowels [WALS (*5*), chapter 1].
9. D. M. Behar *et al.*; Genographic Consortium, *Am. J. Hum. Genet.* **82**, 1130 (2008).
10. B. M. Henn *et al.*, *Proc. Natl. Acad. Sci. U.S.A.* **108**, 5154 (2011).

Supporting Online Material

www.sciencemag.org/cgi/content/full/335/6069/657-d/DC1
Materials and Methods
Figs. S1 and S2
Table S1
References

1 June 2011; accepted 3 January 2012
10.1126/science.1209176

HISTORY OF SCIENCE

Paradoxical Roots of "Social Construction"

David Kaiser

Michael Polanyi and His Generation
Origins of the Social Construction of Science
by Mary Jo Nye
University of Chicago Press, Chicago, 2011. 427 pp. $45, £29. ISBN 9780226610634.

Fifteen years ago, scientists, historians, and sociologists traded salvos in what was termed the "science wars." Passions ran high; "social construction of science" became a battle cry. Critics like physicist Alan Sokal pointed an accusing finger at various humanists who had suggested that science was an inherently social phenomenon riven by rival interests rather than a rational pursuit of objective facts about the natural world. Some blamed the French sociologist Bruno Latour and his writings from the 1980s. Others highlighted members of the Edinburgh school of the sociology of scientific knowledge and their writings from the 1970s. Still others singled out Thomas Kuhn's remarkably influential little treatise, *The Structure of Scientific Revolutions* (*1*), first published in 1962.

How remarkable, then, to learn in historian Mary Jo Nye's *Michael Polanyi and His Generation* that the core notion of the social construction of science antedates the eras of Kuhn, the Edinburgh school, or Latour by several decades. Not only is the idea of social construction considerably older than usually recognized, as Nye deftly demonstrates, it was developed as part of a passionate plea for the autonomy of science from societal meddling. The hue and cry in the 1990s represented what Nye calls a "paradoxical legacy" of the earlier work.


Polanyi in the late 1950s.

Nye's book centers on Hungarian polymath Michael Polanyi, who became a principal architect of the notion that science proceeds by something other than strict rationality or algorithmic procedure. Born in 1891, Polanyi joined a generation of Central European scholars whose thinking about science and knowledge took form amid the political riptide of the early decades of the 20th century. Polanyi experienced the bloody crises of World War I and its aftermath, as the crumbling Austro-Hungarian empire gave way to a short-lived Bolshevik regime, itself toppled by a right-wing, counterrevolutionary revolt. By 1920, rampant antisemitism forced young Polanyi to leave his homeland and to pursue his career as a physical chemist in Berlin. In that cosmopolitan, intellectual setting, he rubbed shoulders with Albert Einstein, Max Planck, Fritz Haber, and others. Their tight-knit community fell apart once the Nazis rose to power in 1933. Within months, Polanyi fled to Manchester, England.

Polanyi had always enjoyed debating politics, economics, and social theory with other energetic thinkers from his childhood circle, including his older brother, the economist Karl Polanyi, and the sociologist Karl Mannheim. Yet he began to turn more squarely to philosophy soon after his relocation to Manchester. Like his geographical migrations, his professional shift had everything to do with politics. Polanyi made several visits to the Soviet Union during the early 1930s to visit scientific colleagues. He came away convinced that centralized, planned economies, symbolized by Stalin's Five-Year Plans, led inexorably to widespread privations and misery. Polanyi was therefore scandalized when in 1939 the prominent left-wing British crystallographer J. D. Bernal proposed that Britain adopt a kind of national planning for science. Bernal called for scientific efforts to be more overtly steered toward addressing societal needs. Around the same time, Polanyi grew suspicious—earlier than most—of what came to be known as the "Lysenko affair": the heavy-handed intrusion by Soviet authorities to squash research into genetics (on charges that genetics diverged from the official doctrine of dialectical materialism) and instead to prop up agronomist Trofim Lysenko's vaguely Lamarckian notions of inheritance.

To Polanyi, each of these episodes revealed the treachery of central planning, for science or any other part of society. He became convinced that advocates of central planning—even scientists like Bernal—made their political error because they had fundamentally misunderstood the nature of scientific practice. Central planning of scientific research could only work, Polanyi argued, if scientific discovery was the product of specifiable, rule-driven methods—that is, if it were wholly rational. Reflecting on his own scientific career, Polanyi concluded instead that scientific knowledge arose from a mélange of social processes that no purported method could capture.

In place of scientific method, Polanyi trumpeted the importance of "tacit knowledge." No practicing scientist learned the craft of research from books or articles, Polanyi argued. Rather, they had to practice craftlike skills, which they internalized via social relationships like apprenticeship training. Scientists developed an aesthetic sense for what counted as good science, according to Polanyi, and used any means available to convince colleagues from rival research schools to believe a given result. Scientists often formed their beliefs from an immersion in particulars that resisted explicit articulation; he likened the experience to religious conversion. To Polanyi, the routines of scientific research could never be captured by recipes, and therefore any effort to steer the direction of research, or subject science to central planning, was bound to fail.

Polanyi developed his philosophical program in a series of books and articles in the 1930s and 1940s, culminating in his best-known books, *Personal Knowledge* (*2*) and *The Tacit Dimension* (*3*). Kuhn read several of these works while writing *Structure*; so did early practitioners of 1970s-style sociology of scientific knowledge, including Harry Collins. To later interpreters, Polanyi's insights into the social foundations of scientific practice spoke to different political priorities: not the midcentury fears of totalitarianism, but the 1960s and 1970s disenchantment with the military-industrial complex.

In assessing the "paradox and irony" of later scholars' appropriation of Polanyi's ideas, Nye concludes, "Each generation of readers can select what it likes from the past." Her rich, impressive book recasts the science wars barbs of the recent past by illu-

The reviewer, the author of *How the Hippies Saved Physics: Science, Counterculture, and the Quantum Revival*, is at the Program in Science, Technology, and Society, Massachusetts Institute of Technology, Cambridge, MA 02139, USA. E-mail: dikaiser@mit.edu

Published by AAAS

minating the searing politics, intellectual passions, and spirited debates that drove Polanyi and his generation to think about science in social terms.

References

1. T. Kuhn, *The Structure of Scientific Revolutions* (Univ. Chicago Press, Chicago, 1962).
2. M. Polanyi, *Personal Knowledge: Towards a Post-Critical Philosophy* (Univ. Chicago Press, Chicago, 1958).
3. M. Polanyi, *The Tacit Dimension* (Doubleday, Garden City, NY, 1966).

10.1126/science.1214357

SOCIOLOGY

Imaginary Identities

Marta Tienda

Between 1960 and 1980, the American Indian population surged from 524 thousand to 1.3 million (*1*). Rather than natural increase, most of this impressive demographic growth resulted from changes in census practices that allowed respondents instead of enumerators to designate their identity. The U.S. Census requires Native Americans to specify their tribal affiliation but does not stipulate other markers of membership, such as language or residence, which some Indian nations require as a condition of membership. The question of who is an Indian transcends genetics and determines access to goods and services. Thus, as David Treuer (an Ojibwe) recently noted, tribal identity is (silly as it seems) often measured in "teaspoons of blood" (*2*).

More than instrumental ends, humans' obsession with their genealogy is rooted in a desire to forge social identities. With the possible exception of establishing paternity, these social identities, imagined or real, have little to do with biology or genetics, as Eviatar Zerubavel convincingly argues in *Ancestors and Relatives*. Yet, because science evokes conceptions of truth, grounding genealogy in biology is used to validate even far-fetched claims about relatedness. The proliferation of DNA testing firms and online programs to build family trees attests to the public's fascination with genealogical roots (*3*). To lure genealogy enthusiasts into discovering their past, for example, Ancestry.com boasts 7 billion genealogical records from across the globe, ranging from vital statistics and census and military records to immigration and vital statistics. The Web site also offers cheek-swab DNA test kits to help in locating "genetic cousins" (*4*).

From the outset Zerubavel (a sociologist at Rutgers University) engages readers with provocative questions like "Are sixth cousins still family?" and "Why do we consider Barack Obama a black man with a white mother rather than a white man with a black father?" Drawing on a vast range of sources—from scriptures to academic disciplines—Zerubavel aims to uncover the "transcultural and transhistorical" principles that underlie conventional understandings of genealogical relatedness. He argues, simply put, that culture trumps biology in establishing ancestry and kinship ties, as well as group boundaries that define clans, tribes, communities, and even nations.

The claim that ancestry and ethnicity are social rather than biological constructs is not new. Nonetheless, the book artfully debunks restraining myths about the salience of biology in human differentiation. Zerubavel exposes strong parallels between diagrams used to establish codescent and those used to illustrate splintering and differentiation, and he demonstrates how the ties that link relatives are similar to those that connect humans to other animals. In his words, "The modern academic compartmentalization of knowledge has evidently kept [scholars] from realizing that they were actually all looking at different manifestations of the genealogical principle of co-descent." Unlike humans, however, other animals are at most interested in immediate, not distant, relatives. Zerubavel reminds us that the "search for common ancestors is effectively boundless … basically we are all cousins."

Understanding the social construction of descent requires both questioning assumptions about the cognitive underpinnings of genealogy and deciphering the social norms, conventions, and classification practices that define relatedness and group membership. Even though biologists have improved upon the measurement of genealogical distances between organisms and entire populations, the absence of natural boundaries separating recent from distant ancestors, or even close relatives from nonrelatives, leaves ample space for cultural engineering of genealogical lineation. And, as Zerubavel demonstrates, there is no shortage of creativity in crafting genealogies.

To delineate distant ancestral ties, genealogists use norms and culturally defined classification schemes, but with hefty doses of selective amnesia and strategic "adjustment" of kinship ties. The inevitable results are fictive genealogies and imaginary identities. Zerubavel pokes fun at the pseudoscience of genealogy by using vernacular terms to characterize how genealogies are culturally tailored to derive fictive kinship lines. In a chapter aptly titled "Politics of descent," he amply illustrates the art of genealogical fabrication in practice. Using wit and punchy exposition, he discusses how "cutting and pasting" is used to suppress temporal inconsistencies in ancestral ties; how "stretching" is used to legitimize putative ties to the Daughters of the American Revolution; how "clipping" allowed Nazis to ignore the Jewish ancestors of Aryan Germans; and how "splitting," "pruning," and "marginalizing" tactics conveniently remove undesirable ancestors from genealogies. In short, ancestor worship is impervious to scientific advances in biology and genetics.

Ancestors and Relatives
Genealogy, Identity, and Community
by Eviatar Zerubavel
Oxford University Press, Oxford, 2011. 238 pp. $24.95, £15.99. ISBN 9780199773954.

If genealogies are largely fabricated cultural narratives about social descent rather than accurate histories of ancestors and descendants (and if the boundaries demarcating race, ethnicity, and nationality are chimerical), why do they resonate with experts and lay audiences alike? And looking to the future—especially in the face of growing social complexity and uncertain kinship ties due to immigration, remarriage, blended families, surrogacy, adoption, and artificial insemination—why should anyone care about genealogy? According to Zerubavel, "Genealogy, in short, is first and foremost a way of thinking. … [and] one of the distinctive characteristics of human cognition. As the very objects of our genealogical imagination, ancestors and relatives therefore deserve a prominent place among the foundational pillars of the human condition." An erudite treatise about how culture drives human cognition about near and remote relations, *Ancestors and Relatives* offers lay and academic audiences alike a great read.

References and Notes

1. C. M. Snipp, *American Indians: The First of This Land* (Russell Sage Foundation, New York, 1989).
2. D. Treuer, *New York Times*, 21 December 2011, p. A39.
3. My sister learned from a now-defunct DNA testing firm that the Tiendas are 68% European, 25% Native American, and 7% Sub-Saharan African. The results were accompanied with a detailed manual and a map explaining the migration patterns undergirding the statistical estimates.
4. http://dna.ancestry.com/welcome.aspx.

10.1126/science.1217669

The reviewer is at the Office of Population Research, Wallace Hall, 2nd Floor, Princeton University, Princeton, NJ 08544, USA. E-mail: tienda@princeton.edu

Published by AAAS

PUBLIC HEALTH AND BIOSECURITY

Adaptations of Avian Flu Virus Are a Cause for Concern

Members of the National Science Advisory Board for Biosecurity explain its recommendations on the communication of experimental work on H5N1 influenza.

Kenneth I. Berns,[1]* Arturo Casadevall,[2] Murray L. Cohen,[3] Susan A. Ehrlich,[4] Lynn W. Enquist,[5] J. Patrick Fitch,[6] David R. Franz,[7] Claire M. Fraser-Liggett,[8] Christine M. Grant,[9] Michael J. Imperiale,[10] Joseph Kanabrocki,[11] Paul S. Keim,[12]† Stanley M. Lemon,[13] Stuart B. Levy,[14] John R. Lumpkin,[15] Jeffery F. Miller,[16] Randall Murch,[17] Mark E. Nance,[18] Michael T. Osterholm,[19] David A. Relman,[20] James A. Roth,[21] Anne K. Vidaver[22]

We are in the midst of a revolutionary period in the life sciences. Technological capabilities have dramatically expanded, we have a much improved understanding of the complex biology of selected microorganisms, and we have a much improved ability to manipulate microbial genomes. With this has come unprecedented potential for better control of infectious diseases and significant societal benefit. However, there is also a growing risk that the same science will be deliberately misused and that the consequences could be catastrophic. Efforts to describe or define life-sciences research of particular concern have focused on the possibility that knowledge or products derived from such research, or new technologies, could be directly misapplied with a sufficiently broad scope to affect national or global security. Research that might greatly enhance the harm caused by microbial pathogens has been of special concern (*1*–*3*). Until now, these efforts have suffered from a lack of specificity and a paucity of concrete examples of "dual use research of concern" (*3*). Dual use is defined as research that could be used for good or bad purposes. We are now confronted by a potent, real-world example.

Highly pathogenic avian influenza A/H5N1 infection of humans has been a serious public health concern since its identification in 1997 in Asia. This virus rarely infects humans, but when it does, it causes severe disease with case fatality rates of 59% (*4*). To date, the transmission of influenza A/H5N1 virus from human to human has been rare, and no human pandemic has occurred. If influenza A/H5N1 virus acquired the capacity for human-to-human spread and retained its current virulence, we could face an epidemic of substantial proportions. Historically, epidemics or pandemics with high mortalities have been documented when humans interact with new agents for which they have no immunity, such as with *Yersinia pestis* (plague) in the Middle Ages and the introduction of smallpox and measles into the Americas after the arrival of Europeans.

> *"Communication … should be greatly limited in terms of the experimental details and results."*

Recently, several scientific research teams have achieved some success in isolating influenza A/H5N1 viruses that are transmitted efficiently between mammals, in one instance with maintenance of high pathogenicity. This information is very important because, before these experiments were done, it was uncertain whether avian influenza A/H5N1 could ever acquire the capacity for mammal-to-mammal transmission. Now that this information is known, society can take steps globally to prepare for when nature might generate such a virus spontaneously. At the same time, these scientific results also represent a grave concern for global biosecurity, biosafety, and public health. Could this knowledge, in the hands of malevolent individuals, organizations, or governments, allow construction of a genetically altered influenza virus capable of causing a pandemic with mortality exceeding that of the "Spanish flu" epidemic of 1918? The research teams that performed this work did so in a well-intended effort to discover evolutionary routes by which avian influenza A/H5N1 viruses might adapt to humans. Such knowledge may be valuable for improving the public health response to a looming natural threat. And, to their credit and that of the peer reviewers selected by the journals *Science* and *Nature*, the journals themselves, as well as the U.S. government, it was recognized before their publication that these experiments had dual use of concern potential.

The U.S. government asked the National Science Advisory Board for Biosecurity (NSABB) (*5*), to assess the dual-use research implications of two as-yet-unpublished manuscripts on the avian influenza A/H5N1 virus, to consider the risks and benefits of communicating the research results, and to provide findings and recommendations regarding the responsible communication of this research.

Risk assessment of public harm is challenging because it necessitates consideration of the intent and capability of those who wish to do harm, as well as the vulnerability of the public and the status of public health preparedness for both deliberate and accidental events. We found the potential risk of public harm to be of unusually high magnitude. In formulating our recommendations to the government, scientific journals, and the broader scientific community, we tried to balance the great risks against the benefits that could come from making the details of this research known. Because the NSABB found that there was significant potential for harm in fully publishing these results and that the harm exceeded the benefits of publication, we therefore recommended that the work not be fully communicated in an open forum. The

[1]Genetics Institute, University of Florida, Gainesville, FL 32611, USA. [2]Albert Einstein School of Medicine, Bronx, NY 10461, USA. [3]Frontline Healthcare Workers Safety Foundation, Ltd., Atlanta, GA 30338, USA. [4]University of Texas Medical Branch, Galveston, TX 77555, USA. [5]Princeton University, Princeton, NJ 08544, USA. [6]Battelle National Biodefense Institute, LLC, Frederick, MD 21702, USA. [7]MRIGlobal, Frederick, MD 21702, USA. [8]University of Maryland School of Medicine, Baltimore, MD 21201, USA. [9]InfecDetect Rapid Diagnostic Tests, LLC, Princeton, NJ 08540, USA. [10]University of Michigan Medical School, Ann Arbor, MI 48109, USA. [11]University of Chicago, Chicago, IL 60637, USA. [12]Northern Arizona University, Flagstaff, AZ 86011, and Translational Genomics Research Institute, Phoenix, AZ 85004, USA. [13]University of North Carolina School of Medicine, Chapel Hill, NC 27599, USA. [14]Tufts University School of Medicine, Boston, MA 02111, USA. [15]The Robert Wood Johnson Foundation, Princeton, NJ 08540, USA. [16]University of California–Los Angeles, Los Angeles, CA 90095, USA. [17]Virginia Polytechnic Institute and State University–Virginia Tech Resource Center, Arlington, VA 22203, USA. [18]GE Healthcare, Princeton, NJ 08540, USA. [19]University of Minnesota, Minneapolis, MN 55455, USA. [20]Stanford University School of Medicine, Stanford, CA 94305, USA. [21]Center for Food Security and Public Health, Iowa State University, Ames, IA 50011, USA. [22]University of Nebraska, Lincoln, NE 68588, USA.

*The authors are members of the U.S. National Science Advisory Board for Biosecurity. †Author for correspondence. E-mail: Paul.Keim@nau.edu

Published by AAAS

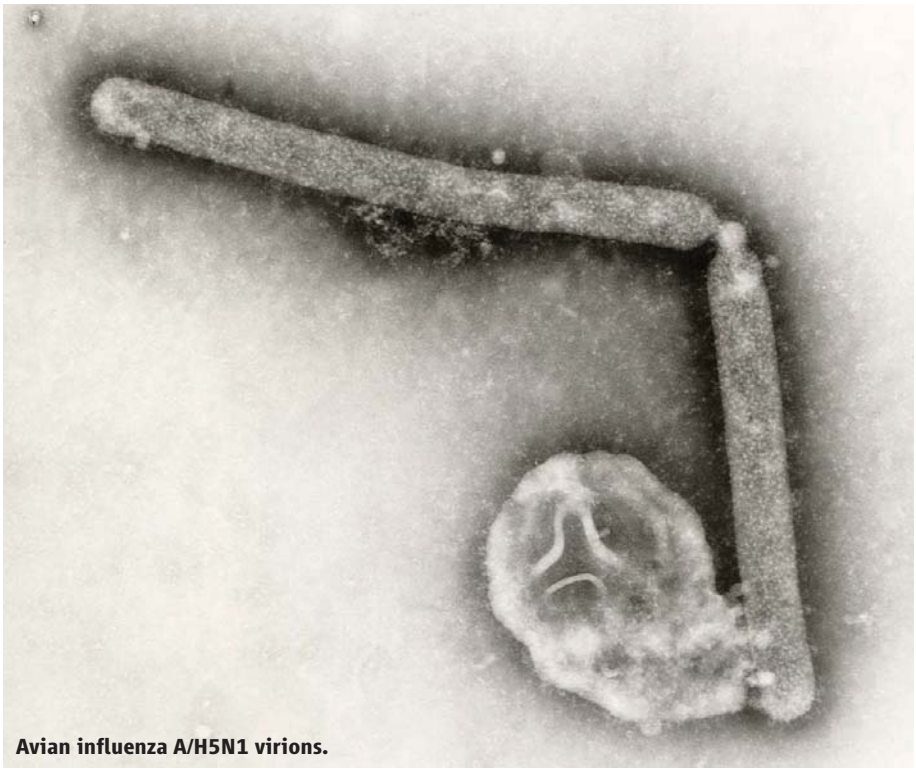

Avian influenza A/H5N1 virions.

CREDIT: CYNTHIA GOLDSMITH AND JACKIE KATZ/CENTERS FOR DISEASE CONTROL AND PREVENTION

NSABB was unanimous that communication of the results in the two manuscripts it reviewed should be greatly limited in terms of the experimental details and results.

This is an unprecedented recommendation for work in the life sciences, and our analysis was conducted with careful consideration both of the potential benefits of publication and of the potential harm that could occur from such a precedent. Our concern is that publishing these experiments in detail would provide information to some person, organization, or government that would help them to develop similar mammal-adapted influenza A/H5N1 viruses for harmful purposes. We believe that as scientists and as members of the general public, we have a primary responsibility "to do no harm" as well as to act prudently and with some humility as we consider the immense power of the life sciences to create microbes with novel and unusually consequential properties. At the same time, we acknowledge that there are clear benefits to be realized for the public good in alerting humanity of this potential threat and in pursuing those aspects of this work that will allow greater preparedness and the potential development of novel strategies leading to future disease control. By recommending that the basic result be communicated without methods or details, we believe that the benefits to society are maximized and the risks minimized. Although scientists pride themselves on the creation of scientific literature that defines careful methodology that would allow other scientists to replicate experiments, we do not believe that widespread dissemination of the methodology in this case is a responsible action.

The life sciences have reached a crossroads. The direction we choose and the process by which we arrive at this decision must be undertaken as a community and not relegated to small segments of government, the scientific community, or society. Physicists faced a similar situation in the 1940s with nuclear weapons research, and it is inevitable that other scientific disciplines will also do so.

Along with our recommendation to restrict communication of these particular scientific results, we discussed the need for a rapid and broad international discussion of dual-use research policy concerning influenza A/H5N1 virus with the goal of developing a consensus on the path forward. There is no doubt that this is a complex endeavor that will require diligent and nuanced consideration. There are many important stakeholders whose opinions need to be heard at this juncture. This must be done quickly and with the full participation of multiple societal components.

We are aware that the continuing circulation of the highly pathogenic avian influenza A/H5N1 virus in Eurasia—where it is constantly found to cause disease in animals of particular regions—constitutes a continuing threat to humankind. A pandemic, or the deliberate release of a transmissible highly pathogenic influenza A/H5N1 virus, would be an unimaginable catastrophe for which the world is currently inadequately prepared. It is urgent to establish how best to facilitate the much-needed research, as well as minimize potential dual use.

To facilitate and motivate this process, we also discussed the possibility of the scientific community participating in a self-imposed moratorium on the broad communication of the results of experiments that show greatly enhanced virulence or transmissibility of such potentially dangerous microbes as the influenza A/H5N1 virus, until consensus is reached on the balance that must be struck between academic freedom and protecting the greater good of humankind from potential danger. With proper diligence and rapid achievement of a consensus on a proper path forward, this could have little detrimental effect on scientific progress but significant effect on diminishing risk.

There are many parallels with the situation in the 1970s and recombinant DNA technologies (*6*–*8*). The Asilomar Conference in California in 1975 was a landmark meeting important to the identification, evaluation, and mitigation of risks posed by recombinant DNA technologies. In that case, the research community voluntarily imposed a temporary moratorium on the conduct of recombinant DNA research until they could develop guidance for the safe and responsible conduct of such research. We believe that this is another Asilomar-type moment for public health and infectious-disease research that urgently needs our attention.

References and Notes

1. National Research Council, *Biotechnology Research in an Age of Terrorism* (National Academies Press, Washington, DC, 2004); www.nap.edu/catalog.php?record_id=10827.
2. National Research Council, *Globalization, Biosecurity, and the Future of the Life Sciences* (National Academies Press, Washington, DC, 2006); www.nap.edu/catalog.php?record_id=11567.
3. NSABB, *Strategic Plan for Outreach and Education on Dual Use Research Issues* (NSABB, NIH, Bethesda, MD, 2008); http://oba.od.nih.gov/biosecurity/PDF/FinalNSABBReportonOutreachandEducationDec102008.pdf.
4. World Health Organization, Confirmed human cases of H5N1 2003–2012; www.who.int/influenza/human_animal_ interface/EN_GIP_20120116CumulativeNumberH5N1cases. pdf.
5. Office of Biotechnology Activities, About NSABB; http://oba.od.nih.gov/biosecurity/about_nsabb.html.
6. M. Singer, D. Soll, *Science* **181**, 1114 (1973).
7. P. Berg, D. Baltimore, S. Brenner, R. O. Roblin, M. F. Singer, *Proc. Natl. Acad. Sci. U.S.A.* **72**, 1981 (1975).
8. M. Singer, P. Berg, *Science* **193**, 186 (1976).

9. R. G. Webster (St. Jude Children's Research Hospital, Memphis, TN) and J. W. Curran (Emory University, Atlanta GA) contributed substantially to the content of this Policy Forum.

Published online 31 January 2012

10.1126/science.1217994

PUBLIC HEALTH AND BIOSECURITY

Restricted Data on Influenza H5N1 Virus Transmission

Authors of a debated flu transmission study discuss why such work is important and should be published.

Ron A. M. Fouchier,* Sander Herfst, Albert D. M. E. Osterhaus

Since its first detection in 1997, highly pathogenic avian influenza (HPAI) H5N1 virus has devastated the poultry industry of numerous countries of the Eastern Hemisphere. As of January 2012, HPAI H5N1 virus caused 577 laboratory-confirmed human cases of infection, of which 340 were fatal. Sustained human-to-human transmission has not been reported. Whether this virus may acquire the ability to be transmitted via aerosols and cause a future pandemic has been a matter of intense debate in the influenza field and in public health research communities.

Scientific advice about the risk of HPAI H5N1 virus to cause a future pandemic is largely based on expert opinion rather than facts. Some experts have judged this risk to be low on the basis of the following assumptions stemming from historical data: (i) only virus subtypes H1, H2, and H3 cause pandemics; (ii) influenza viruses do not cause pandemics without reassortment ("genetic mixing") of human and animal viruses; and (iii) pigs are required as an intermediate host to yield pandemic viruses (*1*). Partly as a consequence of inconsistent scientific advice, H5N1 virus outbreaks in poultry are not always stamped out with a sense of urgency for human health (*2*).

Estimates of the impact—including the death toll—of a possible future H5N1 virus pandemic for use in (inter)national pandemic preparedness plans do not generally exceed those of the H1N1 Spanish influenza pandemic of 1918 (*3*). Although it is recognized that the case-fatality rate of current H5N1 infections is much higher than that of the Spanish influenza pandemic, experts have argued that an aerosol-transmissible H5N1 virus would probably be less virulent than the currently circulating HPAI H5N1 viruses. However, there is no scientific evidence to support this assumption.

Our research program on H5N1 virus transmission, which led to submission of one of the papers that has stirred up so much recent controversy, aimed to investigate whether and how HPAI H5N1 virus can acquire the ability to be transmitted via aerosols among mammals and whether it would retain its virulence. If H5N1 virus can acquire the ability of aerosol transmission with few mutations without significantly losing virulence, existing assumptions should no longer be used as the basis for scientific advice. Furthermore, pandemic preparedness plans would need to be revised globally to account for much higher numbers of hospitalized cases and deaths. These are important issues in risk communication and in preventing a future pandemic or handling it as well as possible if prevention fails.

In addition, our research project has direct practical implications. Currently, our knowledge of determinants of airborne transmission of influenza virus is virtually nonexistent. If we knew which mutations and biological traits can change the zoonotic H5N1 virus into a virus with major public health impact, detection of specific mutations in circulating avian viruses should trigger more aggressive control programs than those employed currently. Moreover, if a HPAI H5N1 virus has the potential to cause a future pandemic, our last resort would consist of implementing societal measures (such as quarantine and travel restrictions), surveillance, vaccination, and the use of antiviral drugs. Diagnostic tests, antiviral drugs, and prepandemic H5N1 vaccines are currently evaluated using HPAI H5N1 strains with biological properties that are similar (but may not be identical) to the strain that would cause the pandemic. Because surveillance and effectiveness of vaccination and antiviral drugs may depend on virus lineage and specific mutations, these measures need to be evaluated in the context of viruses with the most relevant genetic and biologic properties.

Oversight, Biosafety, and Biosecurity

Our work on aerosol transmission of HPAI H5N1 virus was done completely openly, and the decision to perform the work was reached upon serious local, national, and international consultation. The work has been discussed among staff members of the Department of Virology at Erasmus Medical Center (MC) since 1997, followed by consultation with local biosafety officers and facility managers. Over several years, numerous international influenza specialists and other virologists operating in class-3 and-4 facilities were consulted, and a plan was drawn to obtain adequate research facilities in Rotterdam.

After a Broad Agency Announcement of the National Institute of Allergy and Infectious Diseases and National Institutes of Health (BAA NIH-NIAID-DMID-07-20) in 2005, the Department of Virology, along with U.S. partners, drafted a research proposal to become an NIAID NIH Center of Excellence for Influenza Research and Surveillance (CEIRS) to support the research agenda of the U.S. Department of Health and Human Services (DHHS) Pandemic Influenza Plan. The proposal was reviewed favorably with the help of external reviewers, and the research contract was awarded.

An explicit permit to work with aerosol-transmissible H5N1 virus was obtained from the Dutch Ministry for Infrastructure and the Environment (I&M) in 2007. To this end, I&M was advised by the Commission on Genetic Modification (COGEM), an independent scientific advisory committee for the Dutch government. I&M and COGEM concluded that the proposed work could be performed with negligible risk to humans and the environment under the conditions outlined in the application.

The facility designed for the research consists of a negative-pressurized laboratory in which all work is carried out in class-3 isolators or class-3 biosafety cabinets, which are also negative pressurized. Only authorized personnel who have received appropriate training can access the facility, which has state-of-the art security systems. All facilities, personnel, procedures, and records are subject to inspection and oversight by institutional biosafety officers of Erasmus MC in close consultation with the facility management. In agreement with the U.S. select agent regulations for oversees laboratories, the facilities, personnel, procedures, and records are further inspected by the U.S. Centers for Disease Control and Prevention every 3 years. The most recent inspection

Department of Virology, Erasmus Medical Center, Rotterdam, the Netherlands.

*Author for correspondence. E-mail: r.fouchier@erasmusmc.nl

Published by AAAS

took place in February 2011, at which time no shortcomings in biosafety and biosecurity measures were identified.

Other research institutes—following similar but independent routes in the United States and elsewhere—have also come to the conclusion that this type of research is important, is of major interest to public health, and can be performed safely (*4*–*8*).

Dissemination of Results

After the decision was made that the research project was important and could be performed safely, the next question to address was whether the methods and results should be published in detail. We decided to describe our data, although not in complete detail, during a keynote lecture at the influenza conference organized by the European Scientific Working Group on Influenza (ESWI) in Malta in September 2011 to inform the influenza field, as well as policy-makers, of our results. About the same time, a manuscript was submitted for publication. We consulted with NIAID NIH staff, collaborators within our CEIRS center, and organizers of the ESWI meeting about the decision to make our results available to the public.

In agreement with the Dutch Code of Conduct for Biosecurity and the U.S. regulations on "dual use research of concern," *Science* first conducted its own biosecurity review and the manuscript was independently sent to the National Science Advisory Board for Biosecurity (NSABB) for advice. The NSABB drafted recommendations for the U.S. government suggesting that the conclusions of the manuscript could be published, but without experimental details and mutation data that would enable replication of the experiments. It was recognized by NSABB that detailed information about the results (specific mutations) should be shared under confidentiality with parties that "need to know."

Important questions that stem from the draft NSABB recommendations are who will identify the parties that need to know, how, and what mechanism can be used to share classified information? In our opinion, identification of relevant parties should be done liberally and should include the public health services of countries where H5N1 virus has infected humans, poultry, and other animals in recent history. According to the databases of the World Health Organization (WHO) and Food and Agriculture Organization (FAO), these countries span Bangladesh, Cambodia, China, Egypt, Hong Kong SAR-PRC, India, Indonesia, Iran, Israel, Japan, Korea, Mongolia, Myanmar, Nepal, Palestinian Autonomous Territories, and Vietnam (*9*, *10*). WHO and FAO reference laboratories around the world and other expert laboratories affiliated to affected countries need to know. Affected countries and affiliated laboratories require detailed knowledge of our results to ensure implementation of the most up-to-date molecular diagnostics and virus genome sequence interpretation. Companies and research organizations with research and development programs aiming at the development of diagnostic tests, vaccines, and antiviral drugs for H5N1 virus need to know if the effectiveness of such tools depends on the virus lineage or specific mutations. Finally, research laboratories that study H5N1 virus host adaptation, H5N1 virus in mammalian model systems, or use the virus lineage that was the subject of our studies have a need to know because they may unknowingly develop high-risk variants. The latter group is not hypothetical, as we have identified, from published literature, laboratories working with H5N1 viruses that may only require one to three mutations before the viruses used may become transmissible via aerosols.

The WHO-coordinated Pandemic Influenza Preparedness (PIP) Framework went into effect at the World Health Assembly in May 2011 after 4 years of intense international negotiations. The PIP was implemented to promote sharing of influenza viruses and to provide the member states access to vaccines and other benefits. Withholding information from countries that share influenza viruses and their sequence data would be a major step backward in the field of global infectious disease surveillance and research.

Biosecurity experts have argued that the methods we have used represent a recipe to create biological weapons and that information about the specific mutations that determine transmission of H5N1 virus could also be misused for this purpose. However, it is important to emphasize that we did not develop novel methods and that we only used information and methods that are available freely from the scientific literature. The logic in this work is sufficiently obvious that virologists could perform experiments similar to ours even if our method is not published.

Perspective on Dual-Use Research

The recent recommendation of the NSABB to restrict publication of research results is unprecedented and is a major deviation from common practice in the life sciences. Among thousands of manuscripts that describe potential dual-use research according to the NSABB guidelines (*11*), only a handful has raised questions (*7*, *8*, *12*) and none has triggered similar advice. In dual-use research, weighing risks and benefits of the research is the crux. Biosecurity experts are more likely to lean toward zero or near-zero tolerance with respect to risk, whereas for infectious disease specialists, incremental risks may be waived in light of potentially important public health benefits. Reaching consensus among scientific disciplines, let alone among the public at large, is virtually impossible.

We do not agree with the NSABB recommendations. Nevertheless, we have respected their advice. Together with the NSABB, NIAID NIH, and *Science*, and in close consultation with key parties in the public health field, we hope to find a solution for disseminating key information to those who need to know while shielding this information from potential misuse. However, we cannot rule out the possibility that new scientific research, outbreak events, political sensitivities, or other circumstances may call for deviation from this route.

As we compare the current threat posed by bioterrorism and our past experience with the threat of influenza, we would argue that nature itself should be considered the prime bioterrorist. Viruses emerging from animal reservoirs have killed many millions of people around the globe without the help of direct human interference, and we need to be prepared for other naturally occurring events similar to those caused by influenza A virus, HIV, SARS-coronavirus, West Nile virus, filoviruses, and henipaviruses. Infectious disease specialists have a moral obligation to perform dual-use research in the interest of public health and to communicate the results of their work responsibly.

References and Notes

1. E. M. Sorrell *et al.*, *Curr. Opin. Virol.* **1**, 635 (2011).
2. J. Domenech *et al.*, *Sci. Tech. (Paris)* **28**, 293 (2009).
3. D. H. H. S. Pandemic Influenza Plan (2005); www.hhs.gov/pandemicflu/plan/pdf/HHSPandemicInfluenzaPlan.pdf.
4. T. R. Maines *et al.*, *Proc. Natl. Acad. Sci. U.S.A.* **103**, 12121 (2006).
5. H. L. Yen *et al.*, *J. Virol.* **81**, 6890 (2007).
6. Y. Gao *et al.*, *PLoS Pathog.* **5**, e1000709 (2009).
7. T. D. Cline *et al.*, *J. Virol.* **85**, 12262 (2011).
8. L. M. Chen *et al.*, *Virology* **422**, 105 (2012).
9. WHO, www.who.int/influenza/human_animal_interface/EN_GIP_20111215CumulativeNumberH5N1cases.pdf.
10. Food and Agriculture Organization, H5N1 HPAI Global Overview, April-June 2011 (2011); www.fao.org/docrep/014/am722e/am722e00.pdf.
11. NSABB, Proposed framework (2007);http://oba.od.nih.gov/biosecurity/pdf/Framework%20for%20transmittal%200807_Sept07.pdf.
12. T. M. Tumpey *et al.*, *Science* **310**, 77 (2005).

10.1126/science.1218376

Published by AAAS

NEUROSCIENCE

Ode to the Mushroom Bodies

Neurons that stabilize memory storage are located outside of a region in the insect brain long thought to handle this task.

Josh Dubnau

Immediately after a behavioral experience, our memories are rich and vibrant but fragile. Over time, memory of an event or experience begins to fade, but we typically remember the important details because memories become consolidated into a form that is resistant to the passage of time and disruption. Invertebrate animal models, including the fruit fly *Drosophila melanogaster,* have been used to elucidate mechanisms of consolidation that rely on biochemical signaling within a neuron (*1*, *2*). By contrast, most investigations of communication between brain regions for systems-level consolidation have focused on vertebrate animals, based on the assumption that larger, more complex brains are capable of more elaborate processing of memory over time (*3*, *4*). However, several recent studies have provoked a systems view of fruit fly memory (*5*–*7*), and on page 678 of this issue, Chen *et al*. (*8*) provide an even stronger push in that direction.

Conversion of short-term memory (STM) to long-term memory (LTM) involves gene expression under control of the transcription factor cyclic adenosine monophosphate (cAMP)–response element binding protein (CREB) (*9*, *10*). In the *Drosophila* olfactory model, memory formation involves cAMP signaling within neurons of a brain region called mushroom bodies (MBs) (*1*, *2*). The surprising finding of Chen *et al*. is that CREB-dependent gene transcription and protein synthesis required for LTM does not occur in MBs, where olfactory learning takes place, but in a pair of neurons called DAL (see the figure). This result, and the additional role of ellipsoid body neurons (*6*), forces us to think of memory consolidation in the fly in the context of a larger brain system.

The perception of an odor in *Drosophila* is represented as a pattern of neural activity within the MB. If the odor is presented along with a strong reinforcement in the form of reward or punishment, the MBs receive neuromodulatory inputs (such as dopamine in response to an electric shock). The simultaneous stimuli (odor and dopamine) trigger a cellular mechanism called "coincidence detection." For example, stimulation of dopamine receptors in a MB neuron that also experiences an increase in intracellular calcium concentration driven by the odor leads to synergistic activation of an adenylyl cyclase (called *rutabaga*), leading to synthesis of cAMP. This boost in cAMP concentration results in local modifications of synaptic strength. Such coincidence detection likely occurs in the subset of MB neurons that respond to a particular odor and underlies changes in the responses of those neurons the next time the odor is presented.

How does consolidation take place in this model? It involves cAMP-dependent signaling to CREB, which orchestrates gene expression to stabilize the learning-driven modifications to the cell's synapses. This biochemical consolidation mechanism is thought to maintain changes that took place earlier within the same neurons when the coincidence detection occurred in MB neurons. This is why the requirement of CREB-mediated gene expression in DAL neurons and not in MB neurons for LTM is such a conceptual jolt.

Chen *et al*. pinpointed the site of new protein synthesis during memory consolidation in *Drosophila* through cell-specific genetic manipulation in the fly brain. The authors assessed the effect of blocking protein synthesis [by expressing a temperature-sensitive version of a toxin ($RICIN^{CS}$) to inhibit ribosomes] in different subsets of neurons or neuron cell types. This led to the identification of DAL neurons as a necessary location for protein synthesis during memory consolidation. More surprisingly, however, protein synthesis appears to be dispensable in MBs. This observation was validated using a photoconvertible fluorescent protein (KAEDA) to detect de novo protein synthesis. The gene encoding KAEDA was expressed in the subsets of neurons in the fly brain using regulatory regions of genes that are normally activated

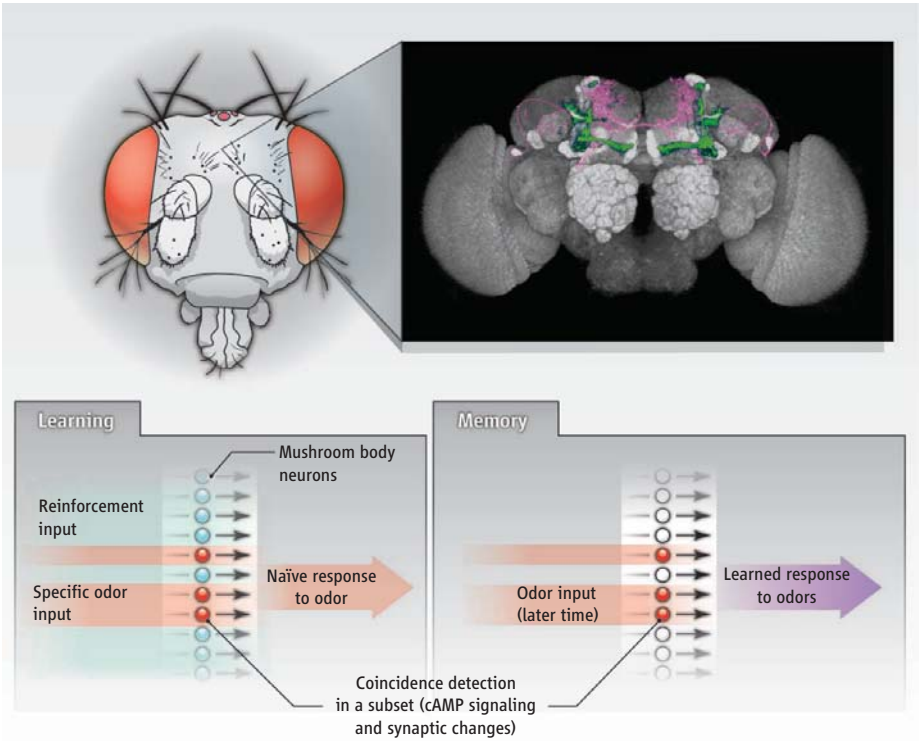

Memory consolidation. (**Top**) The synthesis of new proteins underlying olfactory memory storage takes place in a different anatomical location (DAL neurons, pink) than the brain region where memory is stored [mushroom bodies (MBs)]. DAL neurons appear to form synapses with a subset of MB pioneer α/β neurons (green). (**Bottom**) Odor inputs during learning are represented as a pattern of neural activity within a sparse subset (red) of MB neurons. Punishment drives neuromodulatory inputs (such as dopamine) to all MB neurons (blue). Coincidence detection occurs within neurons that receive both signals. This drives cAMP-dependent synaptic changes that alter the response of the network when the odor is encountered later.

Cold Spring Harbor Laboratory, Cold Spring Harbor, NY 11724, USA. E-mail: dubnau@cshl.edu

Published by AAAS

during memory formation. This revealed an acute induction of KAEDA expression in DAL neurons but not in MBs during memory consolidation. Thus, protein synthesis occurs and is required in DAL neurons but is neither required nor detected in MBs. It is possible that low levels of protein synthesis in MBs escape the RICIN^{CS} effect and are below detection with KAEDA. However, Chen *et al*. further investigated this question by genetic manipulations of CREB function. They demonstrated that CREB-mediated gene transcription is required for LTM in DAL neurons but not MBs as previously thought (*11*, *12*).

The role for CREB-dependent gene expression in DAL neurons but not MBs is at first hard to understand for two reasons. Expression of the adenylyl cyclase *rutabaga* in MBs is sufficient to support both STM (*13*, *14*) and LTM (*5*, *15*). Thus, CREB function in DAL neurons is not downstream in a signaling sense from *rutabaga* action in MB. There is much evidence that olfactory stimuli are represented as a pattern of activity within MBs and that the associative memory forms there. In principle, olfactory memory could be initiated in one place and then transferred to another during consolidation. But it seems implausible that a few DAL neurons can represent the olfactory percept and also "store" LTM. Instead, a view emerges in which the consolidated memory is distributed within a neural circuit that includes MBs, DAL neurons, and ellipsoid neurons (*6*). Indeed, Chen *et al*. report that DAL axons likely are presynaptic to a subset of MB neurons called pioneer α/β neurons. Although this suggests that MBs are postsynaptic to DAL neurons, the role of gene transcription and protein synthesis within DAL neurons that is driven by coincidence detection in MB neurons also suggests that MBs are upstream of DAL neurons (presynaptic). Taken together, the simplest interpretation is a MB-DAL-MB feedback loop, perhaps including ellipsoid body neurons (*6*). The next task will be to integrate the established biochemical and emerging systems views of consolidation.

References

1. A. C. Keene, S. Waddell, *Nat. Rev. Neurosci.* **8**, 341 (2007).
2. S. E. McGuire, M. Deshazer, R. L. Davis, *Prog. Neurobiol.* **76**, 328 (2005).
3. S. H. Wang, R. G. Morris, *Annu. Rev. Psychol.* **61**, 49, (C1) (2010).
4. P. K. Dash, A. E. Hebert, J. D. Runyan, *Brain Res. Brain Res. Rev.* **45**, 30 (2004).
5. A. L. Blum, W. Li, M. Cressy, J. Dubnau, *Curr. Biol.* **19**, 1341 (2009).
6. C. L. Wu *et al*., *Nat. Neurosci.* **10**, 1578 (2007).
7. M. J. Krashes, A. C. Keene, B. Leung, J. D. Armstrong, S. Waddell, *Neuron* **53**, 103 (2007).
8. C.-C. Chen *et al*., *Science* **335**, 678 (2012).
9. J. C. Yin, T. Tully, *Curr. Opin. Neurobiol.* **6**, 264 (1996).
10. A. J. Silva, J. H. Kogan, P. W. Frankland, S. Kida, *Annu. Rev. Neurosci.* **21**, 127 (1998).
11. D. Yu, D. B. Akalal, R. L. Davis, *Neuron* **52**, 845 (2006).
12. D. B. Akalal *et al*., *J. Neurosci.* **30**, 16699 (2010).
13. T. Zars, M. Fischer, R. Schulz, M. Heisenberg, *Science* **288**, 672 (2000).
14. S. E. McGuire, P. T. Le, A. J. Osborn, K. Matsumoto, R. L. Davis, *Science* **302**, 1765 (2003).
15. S. Trannoy, C. Redt-Clouet, J. M. Dura, T. Preat, *Curr. Biol.* **21**, 1647 (2011).

10.1126/science.1218171

MATHEMATICS

Critical Truths About Power Laws

Most reported power laws lack statistical support and mechanistic backing.

Michael P. H. Stumpf[1] and Mason A. Porter[2]

The ability to summarize observations using explanatory and predictive theories is the greatest strength of modern science. A theoretical framework is perceived as particularly successful if it can explain very disparate facts. The observation that some apparently complex phenomena can exhibit startling similarities to dynamics generated with simple mathematical models (*1*) has led to empirical searches for fundamental laws by inspecting data for qualitative agreement with the behavior of such models. A striking feature that has attracted considerable attention is the apparent ubiquity of power-law relationships in empirical data. However, although power laws have been reported in areas ranging from finance and molecular biology to geophysics and the Internet, the data are typically insufficient and the mechanistic insights are almost always too limited for the identification of power-law behavior to be scientifically useful (see the figure). Indeed, even most statistically "successful" calculations of power laws offer little more than anecdotal value.

By power-law behavior, one typically means that some physical quantity or probability distribution $y(x)$ satisfies (*2*, *3*)

$$y(x) \propto x^{-\lambda} \text{ for } x > x_0,$$

where λ is called the "exponent" of the power law. In the equation, the power-law behavior occurs in the tail of the distribution (i.e., for $x > x_0$). A power-law distribution has a so-called "heavy tail," so extreme events are far more likely than they would be in, for example, a Gaussian distribution. Examples of such relationships have been reported in a wide range of situations, including the Gutenberg-Richter law in seismology (*4*), allometric scaling in animals (*5*), the distribution of hyperlinks on the World Wide Web (*6*), the sometimes vehemently refuted (*7*) "scale-free" nature of the Internet (*8*), a purported unified theory of urban living (*9*), patterns of insurgent and terrorist activity (*10*), and (ironically) the paper publication rates of statistical physicists (*11*). A subtlety to note is that this list includes two different types of reported power laws: bivariate power laws like allometric scaling and power-law probability distributions like the paper publication rates.

Power laws in statistical physics emerge naturally from microscopic theories and can be related to observable macroscopic phenomena. A good example is magnetization (*3*). The derivation of a power law suggests that—in a certain ("critical") regime—phenomena do not possess a preferred scale in space, time, or something else: They are, in a sense, "scale free." However, as Philip Anderson pointed out in 1972 (*12*), one must be cautious when claiming power-law behavior in finite systems, and it is not clear whether power laws are relevant or useful in so-called "complex systems" (*13*, *14*). It is important to take a nuanced approach and consider not only whether or not one has or can derive a detailed mechanistic model of a system's driving dynamics, but also the extent of statistical support for a reported power law. One additionally needs to consider empirical support, as theories for power-law behavior arise from infinite systems, and real systems are finite.

The power law reported for allometric scaling stands out as genuinely good (see the figure) (*5*): Not only is there a sound theory underlying why there should be a power-law

[1]Centre for Integrative Systems Biology and Bioinformatics, Imperial College London, London SW7 2AZ, UK. [2]Oxford Centre for Industrial and Applied Mathematics, Mathematical Institute and CABDyN Complexity Centre, University of Oxford, Oxford OX1 3LB, UK. E-mail: m.stumpf@imperial.ac.uk; porterm@maths.ox.ac.uk

relationship between body size x and metabolic performance y, but this relationship has been supported empirically over many orders of magnitude (from bacteria to whales). The clear dependence of various biological characteristics on body size is, of course, insufficient by itself to infer a causal relationship, but few people would dispute the reality of such a relationship.

Purported power laws fall loosely into two categories: those with statistical support—by itself a nontrivial task (*15*)—and those without it. Numerous scholars have neglected to apply careful statistical tests to data that were reported to exhibit power-law relationships; so-called "scale-free" networks are perhaps the best known and most widely discussed examples (*2*, *6*, *13*). However, when formal statistical tools have been applied to network data, evidence favoring power-law relationships has almost always been negligible (*7*, *15*, *16*).

As a rule of thumb, a candidate power law should exhibit an approximately linear relationship on a log-log plot over at least two orders of magnitude in both the x and y axes. This criterion rules out many data sets, including just about all biological networks. Examination (*15*) of the statistical support for numerous reported power laws has revealed that the overwhelming majority of them failed statistical testing (sometimes rather epically). For example, a recent study found (*17*) that the number of interacting partners (i.e., the degree) of proteins in yeast is power-law distributed, but careful statistical analysis refutes this claim (*18*). Noise or incomplete data can further distort the picture (*19*). Trying to discern a power-law relationship by eyeballing straight lines (or even trying to find them using, for example, least-squares fitting) on log-log plots of data can be appealing, but the human ability to detect patterns from even the flimsiest of evidence might lead researchers to conclude the existence of a bona fide power law based on purely qualitative criteria.

Even if a reported power law surmounts the statistical hurdle, it often lacks a generative mechanism. Indeed, the same power law (that is, with the same value of λ) can arise from many different mechanisms (*3*). In the absence of a mechanism, purely empirical fitting does have the potential to be interesting, but one should simply report such results in a neutral fashion rather than provide unsubstantiated suggestions of universality. The fact that heavy-tailed distributions occur in complex systems is certainly important (because it implies that extreme events occur more frequently than would otherwise be the case), and statistically sound empirical fits of event data, when used with caution, can help in data interpretation (as it is certainly useful to estimate how often extreme events occur in a given system). However, a statistically sound power law is no evidence of universality without a concrete underlying theory to support it. Moreover, knowledge of whether or not a distribution is heavy-tailed is far more important than whether it can be fit using a power law.

Suppose that one generates a large number of independent random variables x_i drawn from heavy-tailed distributions, which need not be power laws. Then, by a version of the central limit theorem (CLT), the sum of these random variables is generically power-law distributed (*20*). Few people today would express amazement at finding that the CLT holds in a given context (when one adds up random variables drawn from distributions with finite moments), and the CLT is a vital tool in statistics, providing the basis for many rigorous scientific analyses. It also holds ubiquitously, including in situations in which random variables are drawn from heavy-tailed distributions; in such cases, however, power laws replace the Gaussian distribution as the limiting situation. One thus expects power laws to emerge naturally for rather unspecific reasons, simply as a by-product of mixing multiple (potentially rather disparate) heavy-tailed distributions. For example, it is possible to decompose a supposedly "power-law" degree distribution of a metabolic network into separate distributions of metabolites of different types (*16*). The degree distribution for each of these metabolite classes is different, reflecting the different roles that they play in the organism.

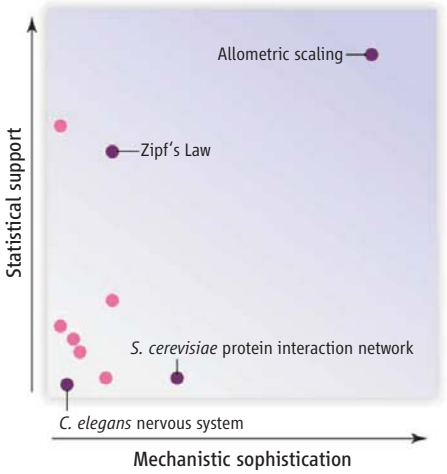

How good is your power law? The chart reflects the level of statistical support—as measured in (*16*, *21*)—and our opinion about the mechanistic sophistication underlying hypothetical generative models for various reported power laws. Some relationships are identified by name; the others reflect the general characteristics of a wide range of reported power laws. Allometric scaling stands out from the other power laws reported for complex systems.

Finally, and perhaps most importantly, even if the statistics of a purported power law have been done correctly, there is a theory that underlies its generative process, and there is ample and uncontroversial empirical support for it, a critical question remains: What genuinely new insights have been gained by having found a robust, mechanistically supported, and in-all-other-ways superb power law? We believe that such insights are very rare.

Power laws do have an interesting and possibly even important role to play, but one needs to be very cautious when interpreting them. The most productive use of power laws in the real world will therefore, we believe, come from recognizing their ubiquity (and perhaps exploiting them to simplify or even motivate subsequent analysis) rather than from imbuing them with a vague and mistakenly mystical sense of universality.

References and Notes

1. R. M. May, *Nature* **261**, 459 (1976).
2. M. E. J. Newman, *Am. J. Phys.* **79**, 800 (2011).
3. J. P. Sethna, *Entropy, Order Parameters, and Complexity* (Oxford Univ. Press, Oxford, 2010).
4. B. Gutenberg, C. F. Richter, *Seismicity of the Earth and Associated Phenomena* (Princeton Univ. Press, Princeton, NJ, ed. 2, 1954).
5. G. B. West, J. H. Brown, B. J. Enquist, *Science* **276**, 122 (1997).
6. A.-L. Barabási, R. Albert, *Science* **286**, 509 (1999).
7. W. Willinger, D. Alderson, J. C. Doyle, *Not. Am. Math. Soc.* **56**, 586 (2009).
8. R. Albert, A.-L. Barabási, *Rev. Mod. Phys.* **74**, 47 (2002).
9. L. Bettencourt, G. West, *Nature* **467**, 912 (2010).
10. N. Johnson *et al.*, *Science* **333**, 81 (2011).
11. N. Li ***et al.***, http://arxiv.org/abs/1108.0833 (2011).
12. P. W. Anderson, *Science* **177**, 393 (1972).
13. E. Fox, Keller, *Bioessays* **27**, 1060 (2005).
14. D. Avnir, O. Biham, D. Lidar, O. Malcai, *Science* **279**, 39 (1998).
15. A. Clauset, C. R. Shalizi, M. E. J. Newman, *SIAM Rev.* **51**, 661 (2009).
16. R. Tanaka, M. Csete, J. Doyle, *Syst. Biol.* **152**, 179 (2005).
17. H. Yu *et al.*, *Science* **322**, 104 (2008).
18. A. Clauset, Power laws in the mist (15 October 2008); Structure & Strangeness, www.cs.unm.edu/~aaron/blog/archives/2008/10/power_laws_in_t_1.htm.
19. M. P. Stumpf, C. Wiuf, R. M. May, *Proc. Natl. Acad. Sci. U.S.A.* **102**, 4221 (2005).
20. W. Willinger, D. Alderson, J. C. Doyle, L. Li, in *Proceedings of the 2004 Winter Simulation Conference*, R. G. Ingalls, M. D. Rossetti, J. S. Smith, B. A. Peters, Eds. (Institute for Operations Research and the Management Sciences, Hanover, MD, 2004), pp. 130–141; paper available at www.informs-sim.org/wsc04papers/016.pdf.
21. M. P. H. Stumpf, P. J. Ingram, *Europhys. Lett.* **71**, 152 (2005).

22. We thank J. Carlson, A. Clauset, and A. Lewis for useful discussions and Ch. Barnes, A. MacLean, and C. Wiuf for helpful comments on the manuscript.

10.1126/science.1216142

IMMUNOLOGY

Remembering to Be Tolerant

Self-tolerant T cells can be transiently reactivated.

June-Yong Lee and Stephen C. Jameson

We avoid potentially lethal autoreactivity because our adaptive immune system ignores normal, healthy tissues. Although multiple mechanisms induce self-tolerance, it is less clear how tolerance is maintained. On page 723 in this issue, Schietinger *et al*. (*1*) report that self-specific T lymphocytes can be driven to transiently break tolerance, but revert back to the tolerant state, even in the absence of the relevant self-antigen. This suggests that a "memory" of tolerance restrains autoreactive lymphocytes.

Various processes prevent damage by self-reactive T cells. Some auto-reactive T cells are deleted during development, whereas others survive but are functionally altered, becoming regulatory T cells (which restrain rather than promote immune responses), or are rendered nonresponsive (*2*, *3*). A key question is whether surviving tolerant T cells ever recover functionality. This is relevant not just for understanding autoimmunity, but also for immunotherapeutic approaches to cancer, in which selectively breaking T cell tolerance can be used to eradicate tumors.

To explore how self-tolerance can be broken (and reestablished), Schietinger *et al*. used an experimental model in which mouse $CD8^+$ T cells expressing a T cell receptor specific for an antigen called GAG (TCR_{GAG}) developed in the presence or absence of GAG as a self-antigen. In this particular system, exposure to GAG as a self-antigen does not delete TCR_{GAG} T cells but leaves them functionally defective, whereas TCR_{GAG} T cells that develop in the absence of GAG are fully competent (*4*, *5*).

Schietinger *et al*. found that simply removing tolerant TCR_{GAG} T cells from the source of toleragen failed to restore their ability to respond to the GAG antigen, suggesting that additional signals were needed. Many T cell populations respond to T cell deficiency (lymphopenia) by undergoing "homeostatic" proliferation, a process typically driven by cytokines [including interleukin-7 (IL-7) and IL-15] and weak ligands for the T cell receptor [peptides in a complex with major histocompatibility complex (MHC) proteins that are displayed by antigen-presenting cells]. Homeostatic proliferation enhances responses by self-reactive T cells in tumor immunotherapy models (*6*), and IL-15 transiently restores function of TCR_{GAG} T cells in vitro (*5*). Indeed, Schietinger *et al*. found that proliferation of tolerized TCR_{GAG} T cells in a lymphopenic environment restored responsiveness to the GAG antigen. This functional "rescue" occurred whether or not the lymphopenic host expressed GAG, indicating that self-tolerance was truly reversed during homeostatic proliferation (see the figure).

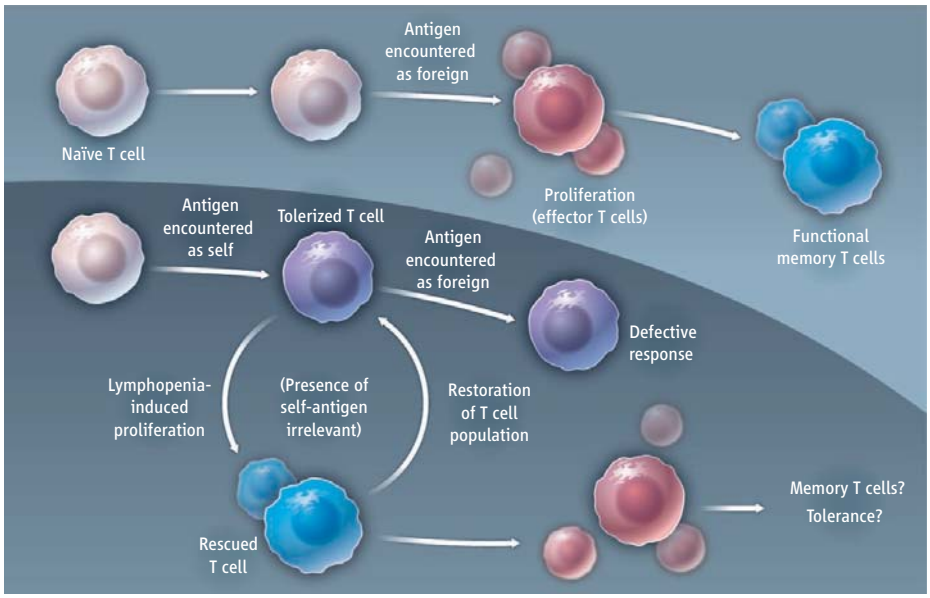

Memories of self-awareness. (**Top**) Naïve T cells that encounter the antigen specific for their T cell receptor under inflammatory conditions respond by activation and proliferation. (**Middle**) T cell tolerance ensues when the T cell receptor ligand is encountered as a self-antigen under nonstimulatory conditions, resulting in a defective T cell response. (**Bottom**) The function of tolerant T cells can be transiently restored through proliferation in response to T cell lymphopenia, but such rescued T cells become retolerized once T cell numbers have been restored to normal levels, even in the absence of continued encounter with self-antigen.

Such suspension of self-tolerance was short-lived, however: Once homeostatic proliferation restored the normal number of T cells, TCR_{GAG} cells reverted to a tolerant state, as indicated by an inability to respond to GAG by cytokine production or proliferation. Unexpectedly, expression of the GAG antigen in the host was irrelevant for reestablishing tolerance. These observations suggest that the self-reactive T cells had a "memory" of tolerance that reasserted itself—even without a tolerogenic cue—once homeostatic proliferation was complete. Intriguingly, "retolerized" T cells transferred into a new lymphopenic host could be functionally rescued a second time, suggesting that there can be cycles of functional rescue and retolerization as the state of lymphopenia changes.

Schietinger *et al*. also noted that the transition from tolerant to "rescued" T cells was accompanied by substantial alterations in gene expression, including changes in genes associated with nonresponsiveness. Many (although not all) of these patterns were reversed as the cells became retolerized (in the absence of tolerogen), suggesting reestablishment of a tolerant gene expression program.

How then is this persistent "memory" of tolerance imparted? Schietinger *et al*. found that expression of a microRNA (miR-181a) increased in tolerized and retolerized TCR_{GAG} T cells, and inversely correlated with expression of proposed miR-181a target genes. However, miR-181a expression enhances T cell receptor sensitivity during thymic development (*7*, *8*), which is difficult to reconcile with the prediction that miR-181a dictates the tolerant phenotype.

Center for Immunology, University of Minnesota Medical School, Minneapolis, MN 55414, USA. E-mail: james024@umn.edu

Published by AAAS

Further studies will be needed to decipher the mechanisms involved in both rescue and retolerization of self-reactive T cells.

Ironically, lymphopenia can contribute to autoimmunity (*9*, *10*), and the study by Schietinger *et al*. reinforces the view that homeostatic T cell proliferation may promote self-reactive T cell responses. It is interesting to speculate that the act of transitioning through cell cycle may be critical in releasing tolerant T cells from inhibitory networks, allowing subsequent changes in gene expression and functional rescue. However, these studies also suggest that homeostatic cues suspend rather than permanently break self-tolerance, and that the prevailing homeostatic signals dictate the current state of self-reactivity. Regulation of homeostatic cues could help lead self-reactive cells back to a default state of tolerance as a treatment for active autoimmunity. At the same time, these findings highlight the difficulties in sustaining self-reactive responses for cancer immunotherapy (in which a patient's immune system no longer recognizes a tumor as self tissue and can target tumor cells for destruction). It will be important to determine whether activation of T cells during their "rescue" from tolerance can establish long-term functional memory—and, if so, whether such cells cross the line into overt auto-aggression.

References

1. A. Schietinger, J. J. Delrow, R. S. Basom, J. N. Blattman, P. D. Greenberg, *Science* **335**, 723 (2012); 10.1126/science.1214277.
2. D. L. Mueller, *Nat. Immunol.* **11**, 21 (2010).
3. K. A. Hogquist, T. A. Baldwin, S. C. Jameson, *Nat. Rev. Immunol.* **5**, 772 (2005).
4. C. Ohlén *et al*., *J. Exp. Med.* **195**, 1407 (2002).
5. R. M. Teague *et al*., *Nat. Med.* **12**, 335 (2006).
6. C. A. Klebanoff, H. T. Khong, P. A. Antony, D. C. Palmer, N. P. Restifo, *Trends Immunol.* **26**, 111 (2005).
7. Q. J. Li *et al*., *Cell* **129**, 147 (2007).
8. P. J. Ebert, S. Jiang, J. Xie, Q. J. Li, M. M. Davis, *Nat. Immunol.* **10**, 1162 (2009).
9. T. Krupica Jr., T. J. Fry, C. L. Mackall, *Clin. Immunol.* **120**, 121 (2006).
10. S. Datta, N. Sarvetnick, *Trends Immunol.* **30**, 430 (2009).

10.1126/science.1218927

CHEMISTRY

Probing Frozen Molecular Embraces

The conformation of the complex formed by a catalyst and its substrate was determined with a method that combined mass spectrometry and infrared spectroscopy.

Timothy S. Zwier

The interaction of a catalyst with its substrate partner can coax the reactant into a new conformation that can stretch its bonds and rotate its functional groups. These changes can reduce the energetic costs of reaction and facilitate a specific approach for other reactants that favors a particular stereochemical product. Some of the new catalysts being developed demonstrate exquisite control even over the way that bulky substituents are assembled on a framework by trapping them in a stereochemical configuration from which they cannot be disengaged, thus avoiding unwanted rearrangements (*1*, *2*). Some of these catalysts clasp onto one of the reactants through multiple hydrogen-bonding (H-bonding) attachment points that complement those on the substrate, working cooperatively to produce the desired configuration in the binding partner (*1*, *2*). On page 694 of this issue, Garand *et al*. (*3*) submit a complex formed by a peptide-derived catalyst (C) and an aromatic substrate (S) (see the figure) to a detailed structural interrogation through a combination of mass spectrometry and infrared (IR) spectroscopy.

Department of Chemistry, Purdue University, West Lafayette, IN 47907–2084, USA. E-mail: zwier@purdue.edu

The work of Garand *et al*. is a prime example of a new wave of experimental methods (*4*–*7*) that directly combine the power of IR spectroscopy and mass spectrometry in a single experiment. Although the conditions of their experiment—unsolvated complexes in the gas phase—differ substantially from those of catalytic reactions in solution, the experimental observation of C···S complexes—and likely many other types of H-bonded ensembles—is now possible. By plucking the C···S complex out of solution into the gas phase and weighing it in a mass spectrometer, examination of only the desired complex is assured. Furthermore, the authors use a recently developed cooling and tagging scheme that stabilizes the complex in a low-energy configuration for detailed spectroscopic characterization.

Modern mass spectrometers combine high sensitivity and excellent mass resolution and, with the advent of electrospray sample introduction (*8*), can bring even large molecules into the gas phase as ions. Once in the gas phase, a molecule's chemical connectivity is typically probed by sequential fragmentation by using rare-gas collisions, reactions with electrons, or reactions with oppositely charged ions. These pro-

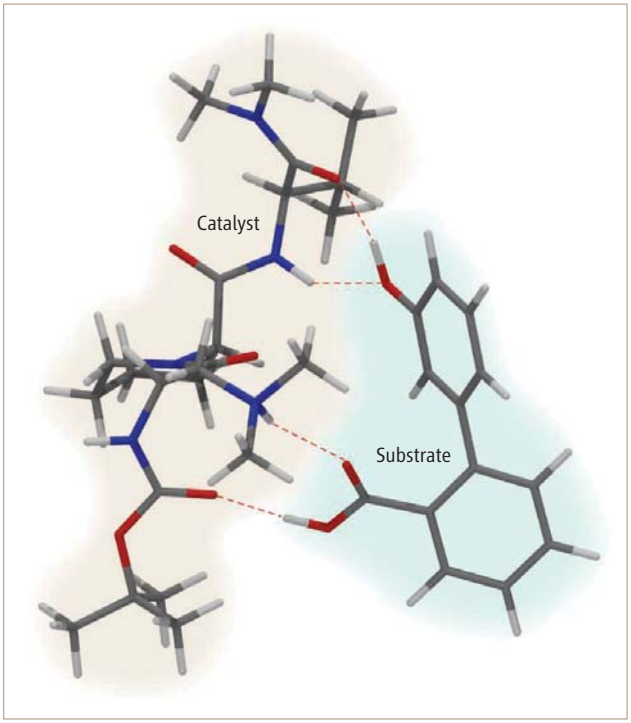

Details of a tiny hug. A ball-and-stick representation of the molecular complex studied by Garand *et al*. between a catalyst derived from a tripeptide and a biaryl substrate [atoms are colored blue (nitrogen), red (oxygen), white (hydrogen), and gray (carbon); H-bonds are depicted as red dashed lines].

Published by AAAS

cesses break specific covalent bonds in the molecule's structure, leading to fragmentation patterns that have imprinted upon them the identity and sequence of its molecular components.

Yet, there is a deeper level of structural characterization of these very same, structurally complex ions that has until recently been lacking. Large, complex molecules fold into particular secondary and tertiary structures that are held together not by covalent bonds but by a network of intramolecular H-bonds, suitably supported by weaker electrostatic and dispersive forces, and subject to steric constraints. Furthermore, the binding of one molecule to another, as occurs in the C···S complex, usually disrupts certain intramolecular H-bonds by forming a new set of stabilizing intermolecular and intramolecular H-bonds.

IR spectroscopy provides a powerful means for characterizing the structures formed by these soft but intimate molecular embraces. The vibrational motions of molecules occur at frequencies characteristic of particular functional groups (e.g., C=O or N-H stretches) that respond to complexation in complementary ways that reflect the strength and number of H-bonds in which each group is involved. Thus, the IR spectrum of the C···S complex can reveal much about its molecular embrace—if the spectrum of just a few ions present in a mass spectrometer can be recorded.

For bulk samples, an IR spectrum can be recorded by measuring the absorption of IR radiation as the reduction in incident light at a detector as a function of IR wavelength. However, in these experiments, the sample is an ensemble of gas-phase ions, so packing too many of them with like charge into too small a volume would cause them to repel one another and overcome the forces holding them in the trap. Also, typical ion traps, like the one used by Garand *et al*., hold no more than about 10,000 ions, a number far too small to produce a measurable decrease in the IR intensity.

The solution is to use mass analysis for detection. Absorption of IR light photofragments the complex ion, so absorption events are detected as changes in its mass. However, a single IR photon has insufficient energy to cause photofragmentation, even for the H-bonded complex. Also, if the complex has substantial internal energy, several conformers in addition to the lowest-energy state may be present, which would complicate the interpretation of the IR spectrum.

Garand *et al*. used a trick called "D_2 tagging" that addresses both these issues. The ion trap is cooled to exceedingly low temperatures (~10 K), and a D_2/He buffer gas mixture is pulsed into the trap, where it is cooled by collisions with the walls of the trap. When the cold neutrals arrive in the trap, they help cool the ions. The D_2 molecules also form molecular clusters by attaching to the complex and forming a series of $(C{\cdots}S)^+(D_2)_n$ ions separated to higher mass by multiples of 4 daltons. These weakly bound D_2 molecules do little to perturb the structure of the C···S complex, but the loss of one or more weakly bound D_2 molecules serves as a marker that IR absorption took place. An IR laser source with a wavelength range that spans most of the near-IR and fingerprint regions was operated at modest powers so that the observed fragmentation intensities reflected the true single-photon absorption spectrum.

The IR spectra obtained are notable for their wavelength coverage, high signal-to-noise ratio, and reproducibility. Garand *et al*. used these characteristics to their advantage in comparing spectra recorded for appropriately isotope-labeled C···S complexes. The chemical connectivity of the ions, as well as the much more subtle structural consequences of noncovalent binding, were determined with unprecedented accuracy, which suggests that studies of even larger complexes should be possible.

References

1. J. L. Gustafson, D. Lim, S. J. Miller, *Science* **328**, 1251 (2010).
2. R. R. Knowles, E. N. Jacobsen, *Proc. Natl. Acad. Sci. U.S.A.* **107**, 20678 (2010).
3. E. Garand *et al*., *Science* **335**, 694 (2012); 10.1126/science.1214948.
4. T. R. Rizzo, J. A. Stearns, O. V. Boyarkin, *Int. Rev. Phys. Chem.* **28**, 481 (2009).
5. K. Gulyuz, C. N. Stedwell, D. Wang, N. C. Polfer, *Rev. Sci. Instrum.* **82**, 054101 (2011).
6. N. C. Polfer, J. Oomens, *Mass Spectrom. Rev.* **28**, 468 (2009).
7. J. C. Poully *et al*., *Int. J. Mass Spectrom.* **297**, 28 (2010).
8. S. Nguyen, J. B. Fenn, *Proc. Natl. Acad. Sci. U.S.A.* **104**, 1111 (2007).

10.1126/science.1218285

STRUCTURAL BIOLOGY

It's All in the Symmetry

Jeff Abramson, Aviv Paz, Kenneth D. Philipson

The structure of a sodium-calcium exchange protein provides insight into the mechanism of Ca^{2+} transport through the cell membrane.

Calcium ion (Ca^{2+}) signaling is essential to many cellular processes, from fertilization to apoptosis (cell death). Stable Ca^{2+} levels are achieved through tightly regulated and coordinated cellular processes. Alterations in Ca^{2+} levels are involved in many pathological conditions, including stroke and heart failure (*1*). After Ca^{2+} stimulation, the Na^+/Ca^{2+} exchanger (NCX)—a ubiquitous Ca^{2+} export protein residing in the plasma membrane—participates in the restoration of resting levels of Ca^{2+} in excitable cells. On page 686 of this issue, Liao *et al*. (*2*) report the structure of a prokaryotic homolog of NCX, revealing a symmetrical protein scaffold and ion-binding pocket that provides detailed insights into the Na^+/Ca^{2+} exchange process.

Liao *et al*. screened more than 50 prokaryotic NCX homologs for their ability to be expressed in an *Escherichia coli* host. NCX from *Methanococcus jannaschii* (NCX_Mj) was the only homolog to reach an expression level suitable for structural studies. After purification, the authors resolved the structure of NCX_Mj using both conventional and lipidic mesophase (lipidic cubic phase) (*3*) crystallization, delivering the first high-resolution structure for this class of proteins.

NCX_Mj consists of 10 transmembrane helices, formed from two structural repeats of 5 transmembrane (5TM) helices with opposing topology (see the figure, panel A). 5TM inverted repeat proteins are a vast structural class of transmembrane transport proteins (*4*), but NCX_Mj has an entirely new structural fold with the same principal elements of structural symmetry.

Although the NCX sequences between species diverge widely, all NCX proteins have conserved α repeats in transmembrane helices 2 and 3 (α1) and 7 and 8 (α2) (*5*), which are critical for transport function (*6*). In the structure reported by Liao *et al*., the two α repeats are packaged in the

Department of Physiology and the Cardiovascular Research Laboratories, David Geffen School of Medicine at UCLA, Los Angeles, CA 90095, USA. E-mail: jabramson@mednet.ucla.edu

Published by AAAS

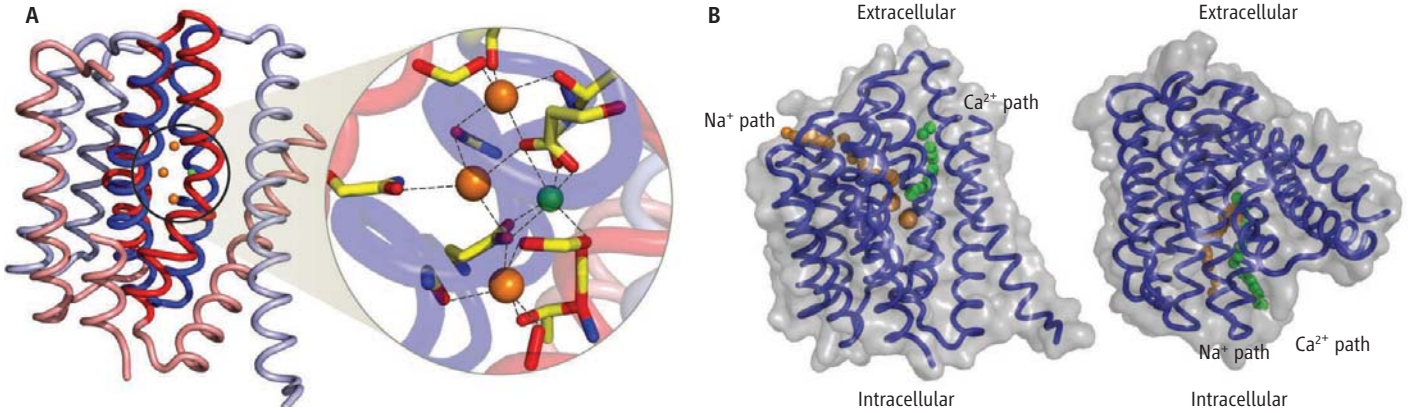

Calcium regulation. (**A**) The NCX_Mj structure reported by Liao *et al*. consists of two sets of five transmembrane helices, shown in shades of red and blue; the two α repeats that form the ion-binding pocket are highlighted in brighter shades of red and blue. (Inset) In the protein core, three Na^+-binding sites (orange) and one Ca^{2+}-binding site (green) are arranged symmetrically in a diamond shape. The coordinating residues are represented as ball and sticks. (**B**) The structure conforms to the alternating access mechanism providing access to either the extracellular side, as in the current structure (left), or to the intracellular side in an inverted model (right).

core of the protein, forming an ion-binding pocket with four cation binding sites that are arranged symmetrically in a diamond pattern (see the figure, inset to panel A). Two high-affinity Na^+ sites are located closest to the extracellular and intracellular surfaces. A two-fold rotational axis, centered on the plane connecting a low-affinity Na^+ site and a high-affinity Ca^{2+} site, coincides with the 5TM inverted topology of the protein. This arrangement is consistent with a three Na^+ to one Ca^{2+} stoichiometry. However, while the precise location of the Ca^{2+} ion was determined experimentally by Ca^{2+} anomalous scattering, it is difficult to unequivocally identify the position of Na^+ ions. Electron densities and ion-ligand coordination guided the positioning of the Na^+ ions. The four sites are in close proximity and have ideal ion coordination; all ligating residues reside in the two α repeats, in accord with biochemical data on NCX1 (*6*).

Consistent with kinetic data (*7*), the NCX_Mj structure suggests a transport mechanism in which a series of distinct conformational transitions ensure that the substrate-binding site is alternately accessible to either the extracellular or the intracellular face. The NCX_Mj structure resides in an outward-facing conformation, with two hydrophilic cavities leading from the extracellular face and penetrating the ion-binding pocket (see the figure, panel B). Using the "rocking bundle" mechanism (*8*), Liao *et al*. modeled the inward-facing state by swapping the conformations of the 5TM inverted repeats, generating two cavities facing the intracellular compartment. The inverted structural repeats demonstrate a common mechanism for achieving alternating access that appears to be shared by many classes of transport proteins (*8*).

Combining the structural information with known functional data, Liao *et al*. propose the following mechanism for Na^+/Ca^{2+} exchange: Beginning from an outward-facing conformation with Ca^{2+} bound at the high-affinity Ca^{2+} binding site, exchange is initiated as Na^+—entering from the extracellular side—occupies the three Na^+ sites in a concentration-dependent manner and competes for the Ca^{2+}-coordinating residues. This competition reduces the Ca^{2+} affinity and causes its release to the extracellular surface. Upon Ca^{2+} release, the "rocking bundle" conformational change transitions the protein to the inward-facing conformation, in which the Na^+ ions are exposed to the low intracellular Na^+ concentration and are released. As the Na^+ ions exit NCX, the high-affinity Ca^{2+} binding site is restored.

In addition to solving the structure, Liao *et al*. convincingly demonstrate that NCX_Mj facilitates transmembrane movement of Ca^{2+} in a Na^+-dependent manner consistent with Na^+/Ca^{2+} exchange. However, there is no evidence yet that NCX_Mj catalyzes an accumulation of Ca^{2+} beyond that which would be achieved by facilitated passive diffusion. Further kinetic data, as well as comparisons of features such as electrogenicity with those of the well-characterized mammalian NCX1, will be of much interest.

Beyond mechanistic insights, the NCX_Mj structure provides an opportunity to evaluate the extensive biochemical literature on the mammalian NCX1. First, there is a striking discrepancy between the NCX_Mj structure and the inferred topology of NCX1. Biochemical studies have indicated that NCX1 has 9, rather than 10, transmembrane segments (*9*). There is no sequence similarity between NCX_Mj and NCX1 outside of the conserved α-repeat regions, and there may be some deviation between structures. Nevertheless, the locations of the key ion-binding residues in the α-repeat regions of NCX1 can be readily modeled with the NCX_Mj structure, and the mechanistic insights gained for NCX_Mj are directly applicable to the distantly related NCX1.

Second, extensive mutational analyses of the α-repeat regions of NCX1 (*6*) help confirm that the modeled Na^+-binding sites of NCX_Mj are accurate. Given that the conserved α-repeat regions of members of the NCX family are only a small fraction of the proteins, it is striking that the reaction mechanism is so focused within these regions.

Liao *et al*. have generated the first structural blueprints of an NCX homolog that will aid the positioning of biophysical probes and further direct mutational studies in both prokaryotic proteins and their eukaryotic counterparts. This initial structure provides an exciting milestone, and although many questions have been answered, many more will certainly arise.

References

1. D. M. Bers, *Physiol* **21**, 380 (2006).
2. J. Liao *et al*., *Science* **335**, 686 (2012).
3. M. Caffrey, V. Cherezov, *Nat. Protoc.* **4**, 706 (2009).
4. J. Abramson, E. M. Wright, *Curr. Opin. Struct. Biol.* **19**, 425 (2009).
5. X. Cai, J. Lytton, *Mol. Biol. Evol.* **21**, 1692 (2004).
6. D. A. Nicoll, L. V. Hryshko, S. Matsuoka, J. S. Frank, K. D. Philipson, *J. Biol. Chem.* **271**, 13385 (1996).
7. D. W. Hilgemann, D. A. Nicoll, K. D. Philipson, *Nature* **352**, 715 (1991).
8. L. R. Forrest *et al*., *Proc. Natl. Acad. Sci. U.S.A.* **105**, 10338 (2008).
9. D. A. Nicoll, M. Ottolia, L. Lu, Y. Lu, K. D. Philipson, *J. Biol. Chem.* **274**, 910 (1999).

10.1126/science.1218696

Seasonality in Ocean Microbial Communities

Stephen J. Giovannoni* and Kevin L. Vergin

Ocean warming occurs every year in seasonal cycles that can help us to understand long-term responses of plankton to climate change. Rhythmic seasonal patterns of microbial community turnover are revealed when high-resolution measurements of microbial plankton diversity are applied to samples collected in lengthy time series. Seasonal cycles in microbial plankton are complex, but the expansion of fixed ocean stations monitoring long-term change and the development of automated instrumentation are providing the time-series data needed to understand how these cycles vary across broad geographical scales. By accumulating data and using predictive modeling, we gain insights into changes that will occur as the ocean surface continues to warm and as the extent and duration of ocean stratification increase. These developments will enable marine scientists to predict changes in geochemical cycles mediated by microbial communities and to gauge their broader impacts.

Seasonal dynamics in plankton communities emerge clearly in satellite observations of ocean color (*1*). At the largest scales, seasonal pulses of ocean surface chlorophyll can be discerned that are driven by dynamic, geographically variable, hydrographic processes that respond to day length. The magnitude of seasonality in the biosphere is so great that long-term measurements of atmospheric CO_2 reveal a rhythmic yearly imbalance in the ratio of carbon fixed by photosynthesis to carbon released by respiration. This ratio oscillates as carbon stored as plant biomass during the Northern Hemisphere summer is released again by respiration during autumn and winter.

Although marine microbial plankton contribute nearly half of gross yearly global photosynthesis, their contribution to the seasonal imbalance in the carbon cycle revealed by atmospheric CO_2 fluctuations is much less than that of land plants. This is because in the oceans, organic carbon production by phytoplankton is tightly coupled with its consumption by chemotrophic bacterioplankton, archaeoplankton, and protists (*2*). The catalysts of the ocean biological carbon cycle are dynamic communities of short-lived cells. Land plant biomass is about 600 Pg C (1 Pg = 10^{15} g), with turnover times of 15 years, whereas the biomass of marine phytoplankton is only about 2 Pg C, with a turnover time of 6 days.

Interest in the seasonality of ocean microbial communities overwhelmingly stems from the relationship between seasonality and global change. Disregarding complex hydrographic processes and weather, the main effect of warming on the oceans is to increase water column stratification (*3*), which occurs to some extent each year in temperate and subtropical seas as the ocean surface stratifies during the summer. Thus, studying seasonality can provide direct insights into how warming on broad scales can affect ocean microbial community functions. Although chlorophyll stocks and photosynthesis rates top the list of biological properties that are responsive to warming and stratification, concerns about rising atmospheric CO_2 have focused interest on the slight annual imbalance between photosynthesis and heterotrophy. This imbalance leads to net removal of atmospheric CO_2 and its long-term storage in the ocean (*4*). Biologically mediated ocean processes that remove carbon from the atmosphere are complex; they include sinking particulate organic matter (POM) and carbonates of biogenic origin, as well as the transport of dissolved organic matter from the upper euphotic zone (UEZ) into the upper mesopelagic (UMP) by turbulent mixing (*5*). One mechanism of carbon removal, sometimes referred to as "the microbial carbon pump," is the conversion of dissolved organic matter (DOM) to compounds that are recalcitrant to microbial oxidation (RDOM) and accumulate in the ocean (*6*, *7*). RDOM is a heterogeneous mixture that includes compounds, such as D–amino acids and lipopolysaccharides, that are found in microbial cell walls and membranes. The most abundant constituent of RDOM to be structurally characterized is carboxyl-rich alicyclic molecules (CRAM), a heterogeneous class of compounds that bear some structural similarities to terpenoids and may be partial oxidation products of sterols and hopanoids (*8*).

Single-celled microorganisms—the microbial plankton—are the main agents of ocean geochemical cycles. Dynamically changing communities of these organisms reduce and oxidize carbon, nitrogen, and sulfur. Ecological studies have used genetic markers for microorganisms to identify patterns of vertical stratification, latitudinal distributions, and variation with changing seasons. Powerful evidence of seasonality emerged from some ocean sites when genetic markers for microbial plankton diversity were used in oceanographic time series (*9*). One of the chief impediments to deciphering these communities is the difficulty of culturing their members, but this is being partially overcome by the development of methods for reconstructing genomes from fragments of community DNA or single cells taken from the environment (*10*–*12*).

Seasonality Is an Important Theme in Ocean Surface Ecology

Spring blooms of phytoplankton at mid- and high latitudes were the first manifestation of microbial plankton seasonality to be recognized, studied, and modeled (*13*). Several theories have been proposed to describe the physical, chemical, and biological interactions controlling the timing of vernal (spring) blooms of phytoplankton in seasonal seas. Sverdrup's critical depth hypothesis broadly serves as the conceptual foundation for understanding seasonal phytoplankton blooms. It predicts that blooms begin when the mixed layer shoals to the depth at which net phytoplankton growth exceeds net losses (*13*). An allied concept, the dilution-recoupling hypothesis, predicts the acceleration of phytoplankton growth in midwinter as mixing and dilution make grazing by protists less efficient (*14*).

Annual events at the Bermuda Atlantic Time-series Study (BATS) site in the western Sargasso Sea illustrate the principles of Sverdrup's critical depth hypothesis and the dilution-recoupling hypothesis (Fig. 1A). During the winter period of deep mixing, dilution of phytoplankton populations means less light, lower phytoplankton cell densities, and probably less efficient predation. Phytoplankton populations that are in the mixed layer as it shoals are exposed to higher light intensities, leading to pronounced phytoplankton blooms in the spring at higher latitudes. At lower latitudes, the picture is complicated by longer winter days and lower average nutrient (N and P) availability, which lead to increases in phytoplankton growth rates as soon as mixing moves N and P from the mesopelagic to the euphotic zone. The contrast between the critical depth hypothesis and the dilution-recoupling hypothesis illustrates two conceptual issues that broadly influence thinking about microbial plankton ecology: (i) To what extent are the compositions of microbial plankton communities determined by chemical and physical factors, such as macronutrient (N and P) flux and light, as opposed to being controlled by direct biotic interactions, such as predation by grazing protists and viruses? (ii) How do these processes vary between different ocean sites, or as climate change alters conditions?

The details of phytoplankton seasonality are continuously revealed as methods develop for monitoring populations of individual phytoplankton species. Flow cytometry studies of phytoplankton population dynamics in monthly samples at two long-term sites, the Hawaii Ocean Time-series (HOT; Fig. 1B), in the North Pacific subtropical gyre, and BATS (Fig. 1A), show that the unicellular cyanobacterium *Prochlorococcus* domi-

Department of Microbiology, Oregon State University, Corvallis, OR 97331, USA.

*To whom correspondence should be addressed. E-mail: steve.giovannoni@oregonstate.edu

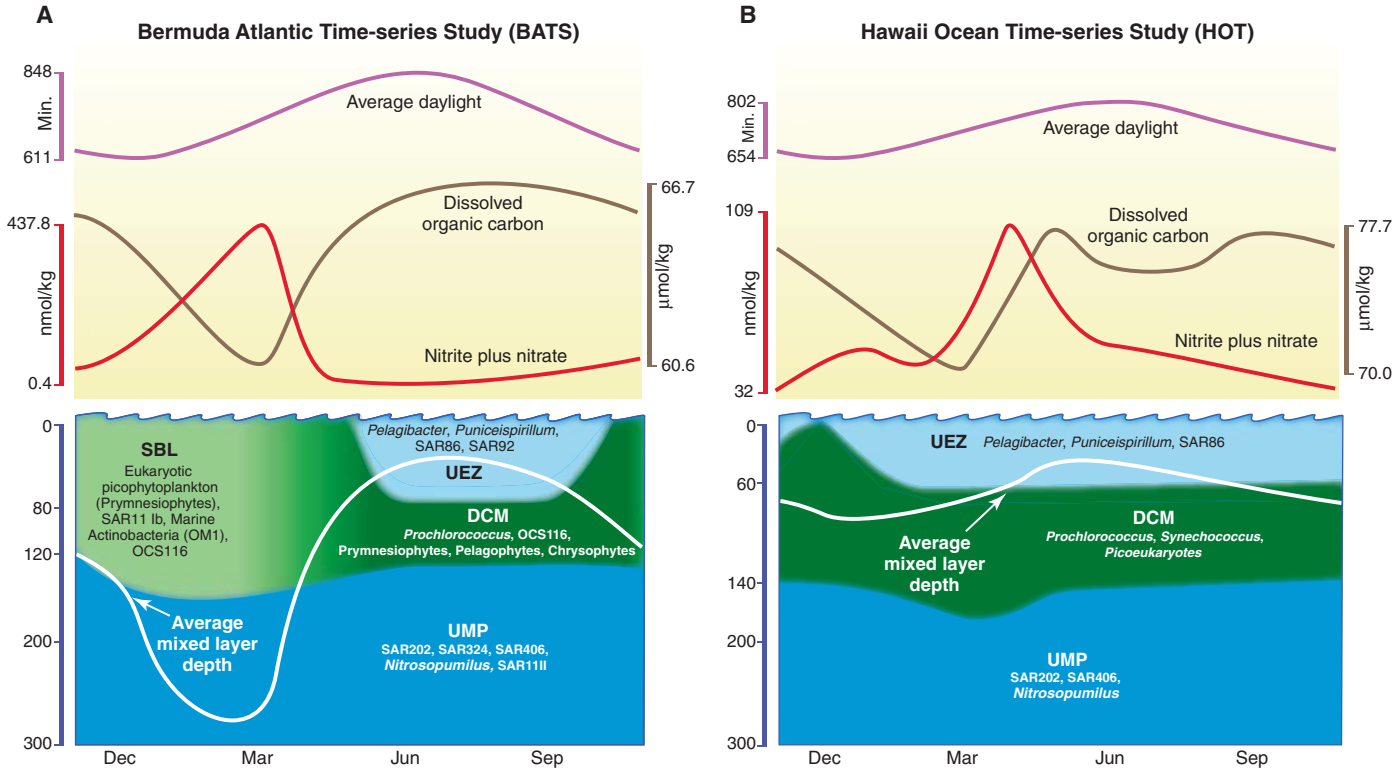

Fig. 1. Annual patterns of microbial community change in the surface layer (0 to 300 m) at BATS and HOT. (**A**) Four microbial communities have been resolved by their phylogenetic compositions. At BATS the euphotic zone community alternates between one dominated by eukaryotic phytoplankton in the winter and spring [spring bloom (SBL); light green] and a stratified pair of communities dominated by cyanobacteria in the summer and early autumn (see Fig. 2). Many important environmental variables change with these seasonal transitions: average monthly daylight (purple line), dissolved organic carbon (brown line), and nitrite plus nitrate (red line). At BATS, the SBL community begins developing late in autumn with the deepening of the mixed layer and intensifies in the spring as the mixed layer becomes shallow, exposing cells to higher incident light. The dilution-recoupling hypothesis predicts increasing phytoplankton populations due to relaxed predation during the early phase of the SBL. The critical depth hypothesis, which was developed to model events at higher latitudes, predicts phytoplankton blooms as sharply rising incident radiation causes increases in phytoplankton growth rates. Prymnesiophytes, marine Actinobacteria (OM1), OCS116, and SAR11 subclade Ib dominate the early SBL, but later, as the mixed layer shoals, other eukaryotic phytoplankton populations increase. As water column stratification increases and nutrients sink from the upper euphotic zone (UEZ; light blue), an oligotrophic community forms in the mixed layer that is dominated by *Pelagibacter*, *Puniceispirillum*, SAR86, and SAR92. During this period, a fourth community [deep chlorophyll maximum (DCM); dark green] forms near the chemocline. *Prochlorococcus* and the α-proteobacterium OCS116 (Fig. 2E) are characteristic members of the DCM community. The upper mesopelagic community (UMP; dark blue) is dominated by the distinct, early branching lineages SAR202, SAR324, SAR406, SAR11 subclade II, and *Nitrosopumilus* sp. (**B**) Less seasonal change in stratification of the water column at HOT results in less pronounced blooms of phytoplankton and more stable communities throughout the year. These communities resemble those found during summer stratification at BATS (*62*, *63*). There are other differences between BATS and HOT, including higher phosphate in the North Pacific. Values for dissolved organic carbon (brown line) and nitrate plus nitrite (red line) were averaged over the mixed layer and plotted on the same scale to emphasize their relative relationships. White lines indicate mixed-layer depth. Data were taken from the HOT-DOGS website (*64*) and the BATS website (*65*) and included years 2001–2009 (HOT) and 1996–2003 (BATS) averaged over the mixed-layer depth at station 2 (HOT).

nates phytoplankton in the summer and autumn when the water column is most stratified (*15*). The larger cyanobacterium *Synechococcus* is more abundant in the winter at HOT and in the spring at BATS, and is nearer to the surface than *Prochlorococcus* (*16*). Photosynthetic picoeukaryotes [cell diameter <3 µm (*16*); 2 to 4 µm (*15*)] are most common in the spring, but at BATS the spring bloom is more pronounced, probably because of the deeper mixed layer established during winter (100 m at HOT versus 250 m at BATS) (*15*, *16*). Note that measurements of cell size obtained from light scattering enabled these studies to calculate carbon biomass; often this information is not available from studies that use environmental gene frequencies as proxies for cells. Similar patterns were observed in the Gulf of Aqaba, a deep, oligotrophic region of the Red Sea, where Cryptophyceae and Chlorophyceae were abundant in winter and *Prochlorococcus* was abundant in summer (*17*).

Phytoplankton are better understood than their nonphotosynthetic counterparts because pigments provide a means to track them, but seasonal patterns of phytoplankton populations are still only partly known for several reasons, including ongoing discoveries of new taxa. For example, a previously unrecognized group of eukaryotic phytoplankton that branches deeply in evolutionary trees, close to haptophytes, was recently described and named Rappemonads (*18*). As with nonphotosynthetic species, genetic data and time series are bringing more resolution to the study of phytoplankton. A recent analysis of BATS data relied on plastid 16*S* ribosomal RNA (rRNA) genes as genetic markers for eukaryotic phytoplankton. It revealed previously unseen seasonal patterns among photosynthetic picoeukaryotes, including a prominent bloom of prasinophytes, which are unicellular organisms related to green plants, in the winter, during mixing of the water column (Fig. 1) (*19*).

Bacterioplankton and archaeoplankton are largely responsible for the oxidative side of the carbon cycle, and also for oxidizing reduced forms of N and S of biotic origin. Time-series measurements of rRNA gene markers have led to remarkable progress in identifying annual patterns in their distributions. The wide use of rRNA gene markers for uncultured microbial diversity in the 1990s identified many new lineages of nonphotosynthetic microbial plankton and provided the

first evidence of patterns of microbial community variation between the open and coastal ocean, between the euphotic and mesopelagic zones, and with latitude (*20*). Some studies focused on specific populations—for example, in Antarctic coastal waters (*21*)—and fluorescence in situ hybridization (FISH) detected a shift from lower archaeal abundances in the summer to higher abundances in the late winter. Similarly, in the North Sea and southeast coastal waters of the United States (*22*), fewer *Roseobacter* clade cells were observed in the winter than during the summer.

Two large studies have used discriminant function analysis (DFA) and time-series analysis (TSA) to examine annual patterns in surface bacterial communities collected monthly for 4.5 years at the San Pedro Ocean Time Series (SPOTS) study site, in the coastal waters of southern California (*23*), and a 6-year study in the western English Channel (*24*). These studies revealed monthly turnover in community composition that recurred on an annual basis with remarkable precision, indicating that community composition is indeed determined by seasonal factors. Smaller studies have reached similar general conclusions; for example, a 2-year study off the New Jersey coast detected seasonal patterns of bacterioplankton communities with distinct clusters of samples separated by season for each year and a distinction between summer and winter communities evident in the entire data set (*25*).

Long ocean time series at BATS and HOT are providing insights into links between ocean conditions and microbial communities. Over the entire BATS data set, statistical ordination resolved three microbial communities—spring bloom (SBL), summertime UEZ, and UMP ("twilight zone")—and provided evidence of a fourth community found near the chemocline in the vicinity of the deep chlorophyll maximum (DCM) (Fig. 1A) (*26*). At BATS these communities, and their relationships to important environmental variables, change markedly during the annual transition from spring to summer conditions, as sinking POM carries nutrients such as N and P out of the UEZ (Fig. 1A). The phytoplankton community shifts from eukaryotic to prokaryotic dominance, and a suite of organisms adapted to the extremely low-nutrient, high-light conditions of the summer surface takes over (Fig. 2, A and B). Evidence from HOT indicates stable UEZ and UMP communities throughout the year and lesser seasonal expansions of phytoplankton, mainly associated with the DCM (*27*).

During stratified periods, the UEZ of the tropics and mid-latitudes is an extreme, high-light, low-nutrient environment. Studies at BATS and HOT (*26*) show that the UEZ community is dominated by the heterotrophic proteobacteria *Candidatus* Pelagibacter (SAR11 subclade Ia), *Candidatus* Puniceispirillum (SAR116; Fig. 2E), SAR86 (Fig. 2D), SAR92, and the cyanobacteria *Synechococcus* and *Prochlorococcus* (*15*, *16*). Genome-enabled research, including metaproteomics, has shown that *Pelagibacter* competes for labile DOM (LDOM) compounds such as amino acids, organic acids, polyamines, osmolytes (such as glycine betaine, dimethylsulfoniopropionate, and taurine), and one-carbon (C1) compounds (such as formaldehyde, methanol, and methylamine) (*28*). C1 metabolism potentially enables these organisms to demethylate osmolytes, as well as to use C1 compounds that are produced abiotically from DOM by photochemical reactions (*29*). The genome of the SAR116 isolate *Puniceispirillum marinum* indicates it can also oxidize a variety of LDOM compounds including C1 compounds (*30*). Unlike *Pelagibacter*, *Puniceispirillum* is motile, an adaptation that may give it a role in the geochemically important process of POM colonization and oxidation. *Pelagibacter*, *Puniceispirillum*, and SAR92 all have light-dependent proteorhodopsin proton pumps that appear to benefit cells by augmenting respiration as a source of energy when oxidizable substrates are scarce.

A biochemical perspective on the oxidation of semilabile DOM (SLDOM) exported from the euphotic zone is slowly emerging from the studies of twilight-zone microbial communities. At BATS and HOT, these communities are similar in composition and relatively stable throughout the year (Fig. 1, A and B, and Fig. 2F) (*26*). Fluctuations in the twilight-zone microbial community at BATS have been observed during periods of organic matter export from the UEZ (*31*). Twilight-zone taxa are strikingly more diverse in their evolutionary origins than the UEZ community. The SAR202 clade of Chloroflexi (Fig. 2F), the SAR324 clade of δ-Proteobacteria, and the ammonia-oxidizing archaean *Nitrosopumilus* occur throughout the aphotic zone (*32*). Neither SAR202 nor SAR324 have been cultured, but several partial genomes amplified from single SAR324 cells have been reported recently (*8*, *33*). In one study, ribulose-1,5-bisphosphate carboxylase-oxygenase (RuBisCO) and sulfur oxidation genes were identified, suggesting a chemolithoauto-

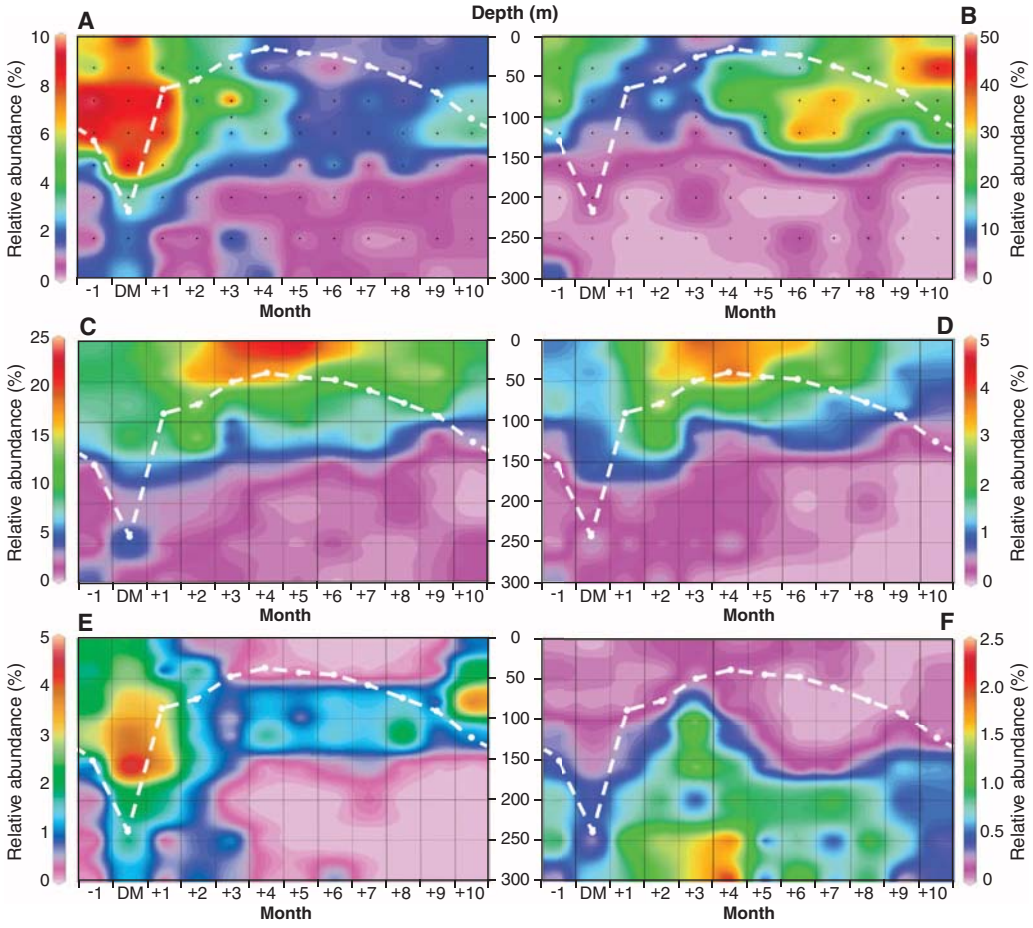

Fig. 2. (A to F) Ocean Data View (ODV) plots indicating average temporal and spatial distributions of microbial plankton at BATS. The graphs show relative abundance of (A) plastid 16*S* rRNA genes, (B) Cyanobacteria (*Prochlorococcus* and *Synechococcus*), (C) *Puniceispirillum*, (D) SAR86, (E) OCS116, and (F) SAR202. [Modified from (*19*, *26*)]

trophic lifestyle (*8*). Another SAR324 genome assembly contained 18 putative phytanoyl dioxygenases, which are predicted to catalyze the degradation of the lipid chain on chlorophyll a (*33*). The presence of motility genes in SAR324 genomes and direct microscopic observations suggest that these organisms swim toward and attach to sinking POM (*6*, *8*).

Microbial communities are known to vary across the ocean surface, differing between coastal and open ocean regions, with latitude, and in regions where mesopelagic waters upwell to the surface. Therefore, it is important to ask whether findings from a few well-studied sites can be extrapolated to broad geographical scales. Mounting evidence suggests that some themes of microbial community organization apply in different oceans: Most major microbial plankton groups are cosmopolitan, and their vertical relationships are similar across broad latitudinal transects (*34*). But there is clearly a complex relationship among latitude, upwelling, and seasonality that remains incompletely explored. A cruise in the boreal spring Atlantic from South Africa to the United Kingdom counted cells with FISH and found latitudinal variation in many of the most abundant groups of marine bacteria (SAR11, *Prochlorococcus*, Bacteroidetes, γ-Proteobacteria, and SAR202) (*34*). Other studies, using samples collected in all months across the world ocean, described latitudinal variation discerned through 16*S* rRNA gene phylogeny (*35*) and DNA fingerprinting (*20*).

Lessons from SAR11

The SAR11 group of α-Proteobacteria (Pelagibacteraceae) are the dominant bacterial group in the oceans and have emerged as major players in all time-series studies (*24*, *31*, *34*, *36*–*39*). They illustrate three important problems that must be addressed before a global view of ocean microbial community seasonality can fully emerge: (i) the need for a standard system of measuring and describing microbial diversity, (ii) the need to attach ecologically meaningful functions to units of microbial diversity, and (iii) the need for more sampling. Molecular phylogenies indicate that the SAR11 clade evolved long ago and diverged into several major subclades [i.e., Ia (*Pelagibacter*), Ib, II, III, and IV] and probably into many minor ecotypes (*5*, *19*, *31*). "Ecotypes" are genetic variants that can be distinguished phylogenetically and by their differing spatiotemporal distributions in environments. The correlation between phylogenetic branching and spatiotemporal distributions of SAR11 is evidence that early in their evolution the marine environment was partitioned among SAR11 specialists (*37*, *39*). At BATS, SAR11 subclade Ib blooms in the spring mixed layer, coincident with phytoplankton, followed by subclade Ia (*Pelagibacter*) in the summer. Subclade II blooms with the remineralization of dissolved organic carbon (DOC) in the mesopelagic each spring. Some of these relationships emerged in early studies reliant on a few depth profiles, but others were not revealed until more extensive time-series data were used to examine seasonal change in spatial relationships.

There is no agreement in the field about schemes for classifying SAR11 or other taxa. Most workers use a sequence divergence threshold (*10*, *40*), but some emphasize phylogenetic structure (*26*, *39*). An unfortunate consequence of this is that it has been difficult to compare the data obtained in different studies to identify common patterns in the distribution of SAR11 diversity. But by summing all SAR11 into a single unit of diversity, some comparisons can be made. At HOT (*38*) and in the western English Channel (*24*), their relative abundance peaks in the winter, whereas at BATS, both relative abundance and cell numbers peak in the summer (*26*, *36*).

Oceanographers are concerned with geochemistry at broad scales, so microbial diversity classification systems also must be attached to the functional properties of cells to achieve their potential usefulness. The SAR11 subclades referred to above can diverge at 16*S* rRNA loci by more than 15%, which suggests multiple species and potentially complex variation in function. One theory is that ancient events represented by deep branches in phylogenomic trees correspond to evolutionary changes that retain their ecological impacts today. For example, this is true of the cyanobacteria (Cyanophyta), a lineage that includes all cells and organelles that photochemically split water to produce oxygen. The correlation between deep branches in SAR11 phylogenetic trees and spatiotemporal partitioning of the BATS environment also supports this theory. Alternatively, frequent lateral gene transfer provides a path for organisms to evolve into new habitats, potentially scrambling the ecological meaning of phylogenetic origins. Ample evidence indicates that this does occur; for example, phosphate acquisition genes are highly variable, and both *Prochlorococcus* and SAR11 have more phosphate acquisition genes at BATS than at HOT, presumably as a result of selection caused by less availability of P in the North Atlantic (*41*). Comparative genomics is expanding rapidly because of inexpensive next-generation sequencing, and we can expect powerful new studies that aim to identify genomic determinants of function that are associated with deep phylogenetic branches and distinguish them from variable genomic properties. It will be particularly interesting to apply this approach to the UMP community, which is home to anciently diverged clades of δ-Proteobacteria (SAR324), Chloroflexi (SAR202), Fibrobacteres/Acidobacteria (SAR406), and Archaea that directly or indirectly must play a role in remineralizing DOM.

Connecting Seasonal Communities to Geochemistry

Despite caveats related to variability between ocean provinces, observations of ocean surface microbial communities are making it possible to predict changes that are likely to occur as the oceans warm. Prolonged stratification means diminished seasonality, the spread of oligotrophic ocean conditions, and an expansion of the UEZ communities like those at HOT and BATS. The impact of such changes on phytoplankton productivity has received broad attention, but much less is understood about how seasonal changes in populations of nonphotosynthetic organisms might affect carbon sequestration processes such as the biological carbon pump and the microbial carbon pump, both of which are focused on the small fraction of organic matter that escapes oxidation by a gauntlet of microorganisms.

Despite increasing resolution of microbial community dynamics, as yet little information is available that connects community composition to variation in geochemical processes. One of the clearest examples of geochemical specialization is the ammonia-oxidizing archaean *Nitrosopumilus marinus*. Summer blooms of *Nitrosopumilus* coincident with maximal rates of ammonia oxidation to nitrate have been detected by FISH and quantitative polymerase chain reaction (qPCR) measurements of the *Nitrosopumilus* ammonia monooxygenase gene (*amoA*) taken biweekly at a North Sea coastal site (*42*). Although such findings help us to understand the biology behind the nitrogen cycle, so far they have not been of much use in geochemical models.

Examples that tie variations in microbial populations to seasonal geochemical data from the environment, like that of *Nitrosopumilus*, remain rare. One of the biggest challenges is the carbon cycle. For example, at BATS, DOC accumulates annually in the UEZ in the summer, subsequently oxidizing when winter storms mix surface water into the UMP (*43*). DOC export by mixing is important; it accounts for about half of oxygen consumption in the UMP. Why is a fraction of DOC refractory to oxidation at the ocean surface in the summer, but labile when exported to the dark, nutrient-rich environment of the UMP? DOM composition has been shown to change with depth, correlating with shifts in community structure (*31*, *44*). Is it the unique properties of organisms residing in the UMP, the chemical properties of the environment, or both that cause the refractory DOC to become labile? A BATS study to address these questions found that populations of the α-proteobacterium OCS116 (Fig. 2E), SAR11 subclade II, and the marine Actinobacteria (OM1) increase in the mesopelagic after spring mixing (*31*). Although this study showed that a unique mesopelagic microbial community responds annually to DOC export, it has not yet been possible—even with the availability of metagenomic data—to identify specific biochemical mechanisms that explain the change in susceptibility of DOC to oxidation when it is exported.

So far, we have focused on the interplay between seasonally changing microbial communities and geochemical cycles, but an alternative perspective is to consider, at the level of populations of organisms, how the environment selects. Ecologists refer to ordered patterns in community composition as nonrandom assembly. One cause of nonrandom assembly is environmental

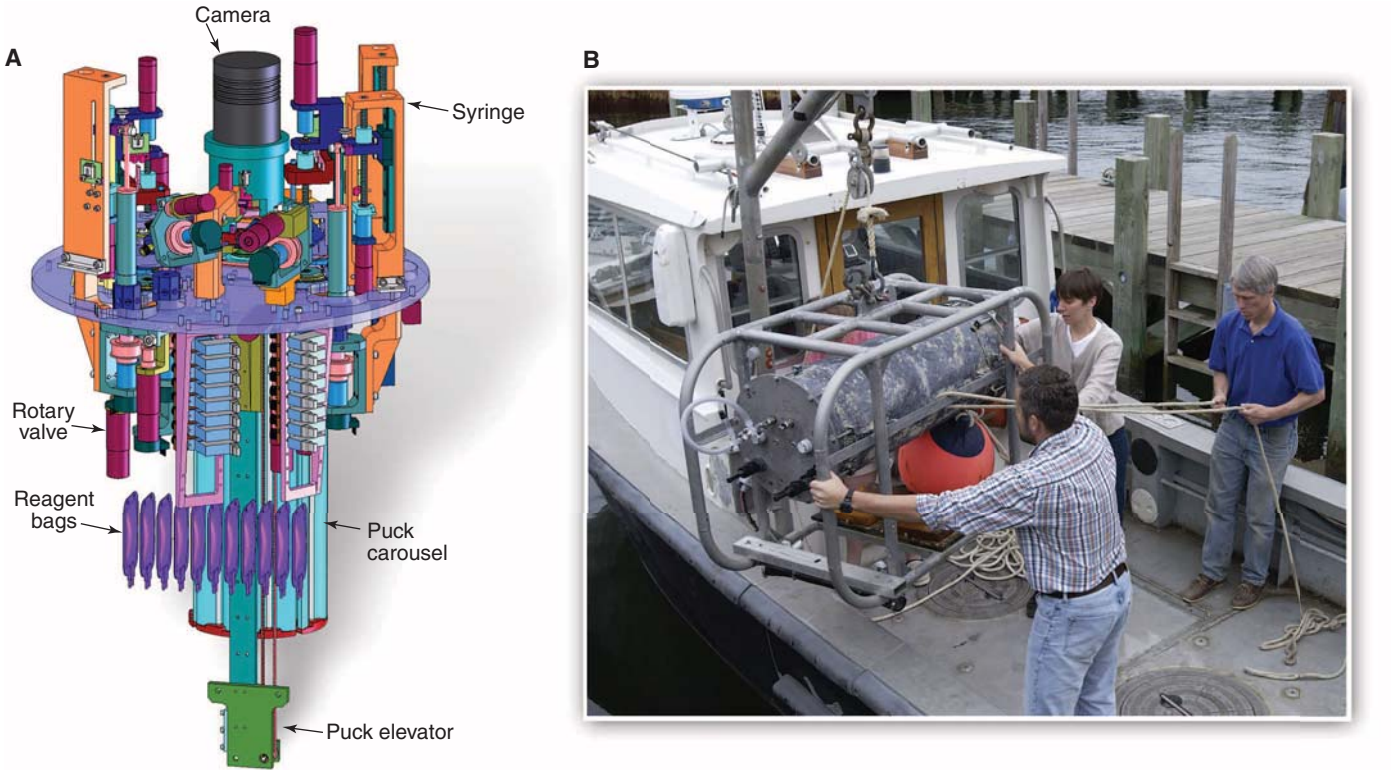

Fig. 3. (**A** and **B**) Autonomous devices, such as the Environmental Sample Processor [ESP; schematic illustration shown in (A)] and the FlowCytobot [deployment shown in (B)], were designed for in situ monitoring of microbial plankton. The ESP can conduct qPCR assays; the FlowCytobot can monitor phytoplankton by flow cytometry. In the future, devices like these may replace monthly cruises to ocean sites for the purpose of monitoring patterns of change in microbial communities. In a recent deployment, the ESP was used to monitor *Nitrosopumilus*, SAR11, and marine cyanobacteria 16*S* rRNA molecules. In parallel, qPCR was used to monitor the 16*S* rRNA genes from SAR11, *Nitrosopumilus*, and the large subunit RuBisCO gene (*rbc*L) from marine *Synechococcus* sp. during a 28-day deployment in Monterey Bay (*55*). [Images courtesy of Monterey Bay Aquarium Research Institute (ESP) and Tom Kleindinst, Woods Hole Oceanographic Institution (FlowCytobot)]

filtering—the selection pressure exerted on populations by abiotic factors. Nitrogen, phosphorus, and (to a lesser extent) iron have dominated oceanographic thinking about the environmental control of microbial populations. However, unusual nutrient requirements for trace metals, vitamins, and other organic growth factors, as well as allelopathic compounds that inhibit competitors and predators, are increasingly being studied to understand ocean microbial population dynamics (*45*, *46*). Growing evidence suggests that complex biotic interactions play a major role in shaping microbial community dynamics. Such interactions can be positive or negative; for example, the production of growth factors by one species, stimulating the growth of another, or growth inhibition due to predation, siderophore piracy, and other types of interference.

Patterns of variation caused by biological interactions were studied in the large SPOTS data set with methods designed to detect patterns in correlation tables (*37*). A follow-up study at SPOTS that included viruses, archaea, and protists provided stronger evidence that ocean microbial communities are highly interconnected ecological networks (*47*). Using methods familiar to systems biologists, SPOTS investigators detected a web of potential interactions between organisms, including interactions with abiotic factors. The DFA and TSA analyses include statistical support for interactions to examine delays of up to 6 months to find potential time-lagged interactions. Observing highly correlated community behavior is an important step toward understanding communities, but the process is far from complete and awaits work that will experimentally confirm patterns of connectivity and explain them with mechanisms. Very few examples of biotic interactions between microbial plankton can be demonstrated using live organisms, providing few opportunities to study underlying mechanisms experimentally (*46*). Validation is important because so many environmental factors in the ocean are functionally linked to seasonal changes in incident light. Hence, the concerted response of communities may include many organisms with unrelated biology that covary simply because abiotic factors covary, rather than because they are tied together by a specific interaction.

Nonetheless, organisms that have evolved in an environment where abiotic factors provide a strong driving rhythm do have the opportunity to coevolve. Insights emerged from the genome streamlining theory, which explains the small size of genomes in some abundant groups of marine bacteria, such as *Prochlorococcus* and *Pelagibacter* (*48*), as an adaptation that enables these cells to use limiting resources efficiently in oligotrophic regions of the oceans. For example, unusual requirements for reduced sulfur compounds (*49*) and glycine (*50*) have been described in *Pelagibacter*, indicating that during the evolution of its small genome, the biosynthesis of some essential compounds was "outsourced" to other members of the microbial community. Complex nutritional requirements caused by genome reduction can lead to increased food web connectivity and less versatility in cells, which could explain why so many abundant taxa of marine bacteria are challenging to cultivate. The cultivation of other abundant organisms that also have reduced genomes and unusual nutritional requirements will determine how broadly genome streamlining theory can be applied to explaining patterns observed in ocean surface plankton ecology.

Food web connectivity caused by nutritional dependence and other types of interactions has important consequences for predicting ecosystem responses to change (*51*). Microbial plankton communities are sensitive to perturbations, one class of which, referred to as "bottle effects," result in rapid changes in microbial community composition when water is collected and confined (*52*). The stability of microbial plankton communities is directly relevant to a host of environmental concerns, where interest focuses critically on whether environmental functions are maintained in response

to changing inputs. There is some good news, albeit incomplete, on this topic, from the 2011 Gulf of Mexico oil spill disaster, where the microbial plankton community showed an unexpected capacity to convert petroleum to carbon dioxide (*53*).

Outlook

Seasonal patterns of microbial community turnover have emerged prominently in satellite observations of chlorophyll from different ocean provinces, but as yet there is no consensus whether the same patterns occur at different sites, or about the factors that control community composition. Next-generation sequencing technology is playing an important role in the expansion of ocean microbial diversity measurements (*11*, *40*). To identify generalities that apply across systems, researchers will first have to reach a consensus about how to classify microbial diversity. To overcome the obstacles of ship expenses and weather, which impede collection of time-series data, scientists are testing a new generation of instruments that can be left in the ocean to monitor microbial communities in situ (Fig. 3) (*54*, *55*). Oceanographers will be particularly interested in using these data to develop a better understanding of how latitude, weather, pollution, nutrients, pH, and other factors alter the rhythms of microbial communities. Moving from descriptively assessing ocean surface microbial community structure to understanding factors that determine community structure and predicting how communities will respond to changing inputs is the long-range goal of most workers in the field (*9*). The best illustration of this idea is the Darwin Project, a marine ecosystem model that predicts the distribution of *Prochlorococcus* ecotypes according to physiological traits (*56*).

Metagenomics and allied technologies, including single-cell genome amplification (*11*, *30*) and population sorting (*12*), are leading to progress in associating uncultured microorganisms with functions, and a growing list of microbial plankton taxa can be grown and studied in laboratories (*30*). But so far, no comprehensive metagenomic studies of ocean seasonality have been published. Limited by data and methods, studies still have difficulty identifying anciently evolved genome characteristics that might link major branches of microbial plankton evolution with distinct functional roles in the environment (*57*). This goal is important because microbial diversity is dauntingly complex, making it imperative to find principles that simplify.

Highly resolved information about patterns of microbial community turnover has the potential to provide important refinements to models of geochemical cycles. For example, the partitioning of organic carbon among structured microbial communities that vary in seasonal patterns has been linked to the microbial carbon pump (*5*, *31*). But current models rarely take transitions in community structure into account because of insufficient information about the geochemical properties of organisms. One of the impediments to progress is the difficulty of determining geochemical function from genome information alone, without passing through a labor-intensive period of laboratory investigation for each organism. Another is the difficulty of resolving geochemical processes at finer chemical scales—that is, breaking broad chemical classes down to specifics. Current efforts to identify specific components of dissolved organic nitrogen (DON) and dissolved organic phosphorous (DOP) illustrate the challenges. Only recently was it understood that a fraction of DOP is in the form of phosphonates that have C–P bonds and thus are harvested by pathways that differ from those used to assimilate P from typical phosphate esters (*58*). A variety of new tools are emerging that provide more highly resolved chemical information. Some use high-performance liquid chromatography or mass spectroscopy to resolve complex mixtures of molecules at high resolution (*59*), to measure specific molecules with high sensitivity and precision (*60*), or to track the isotopic composition of molecules with either naturally occurring or introduced isotopes (*61*).

Some microbial communities, such as those that dominate the low-nutrient, high-irradiance environment of the euphotic zone in ocean gyres, are more accessible, have been more heavily sampled, and are at a more advanced stage of study. If the methods of systems biology are going to be successfully expanded to encompass communities of interacting microorganisms, it seems likely that early milestones will emerge from further studies of the stratified, upper euphotic zone community. Some potential advances that might require highly integrated approaches include the description of adaptations that determine success in this extreme environment, the refinement of geochemical cycles to finer scales of molecular specificity, and the identification of factors and interactions that control community structure.

Understanding fundamental aspects of microbial plankton biology, such as seasonal processes, may be important to understanding ocean responses to long-term changes, such as global warming, as well as short-term impacts, such as pollution events. It is important not to underestimate the complexity of this problem: A large-scale, long-term effort will be needed to understand seasonality and other dynamic aspects of ocean microbial communities, and to gauge their resilience to environmental perturbations.

References and Notes

1. www.youtube.com/watch?v=sQvYvlonu7Y
2. M. J. Behrenfeld *et al.*, *Nature* **444**, 752 (2006).
3. J. M. Lyman *et al.*, *Nature* **465**, 334 (2010).
4. D. A. Hansell, C. A. Carlson, D. J. Repeta, R. Schlitzer, *Oceanography* **22**, 202 (2009).
5. C. A. Carlson *et al.*, *Deep Sea Res. II* **57**, 1433 (2010).
6. F. Azam, *Science* **280**, 694 (1998).
7. N. Jiao *et al.*, *Nat. Rev. Microbiol.* **8**, 593 (2010).
8. B. K. Swan *et al.*, *Science* **333**, 1296 (2011).
9. D. K. Steinberg *et al.*, *Deep Sea Res. II* **48**, 1405 (2001).
10. D. B. Rusch *et al.*, *PLoS Biol.* **5**, e77 (2007).
11. T. Woyke *et al.*, *PLoS ONE* **4**, e5299 (2009).
12. M. L. Cuvelier *et al.*, *Proc. Natl. Acad. Sci. U.S.A.* **107**, 14679 (2010).
13. H. U. Sverdrup, *J. Cons. Perm. Int. Explor. Mer.* **18**, 287 (1953).
14. M. J. Behrenfeld, *Ecology* **91**, 977 (2010).
15. M. D. DuRand, R. J. Olson, S. W. Chisholm, *Deep Sea Res. II* **48**, 1983 (2001).
16. L. Campbell, H. B. Liu, H. A. Nolla, D. Vaulot, *Deep Sea Res. I* **44**, 167 (1997).
17. T. Al-Najjar, M. I. Badran, C. Richter, M. Meyerhoefer, U. Sommer, *Hydrobiology* **579**, 69 (2007).
18. E. Kim *et al.*, *Proc. Natl. Acad. Sci. U.S.A.* **108**, 1496 (2011).
19. A. H. Treusch *et al.*, *ISME J.* (2011).
20. J. A. Fuhrman *et al.*, *Proc. Natl. Acad. Sci. U.S.A.* **105**, 7774 (2008).
21. A. E. Murray *et al.*, *Appl. Environ. Microbiol.* **64**, 2585 (1998).
22. A. Buchan, J. M. González, M. A. Moran, *Appl. Environ. Microbiol.* **71**, 5665 (2005).
23. J. A. Fuhrman *et al.*, *Proc. Natl. Acad. Sci. U.S.A.* **103**, 13104 (2006).
24. J. A. Gilbert *et al.*, *ISME J.* **6**, 298 (2011).
25. J. D. Nelson, S. E. Boehme, C. E. Reimers, R. M. Sherrell, L. J. Kerkhof, *FEMS Microbiol. Ecol.* **65**, 484 (2008).
26. A. H. Treusch *et al.*, *ISME J.* **3**, 1148 (2009).
27. A. Eiler, D. H. Hayakawa, M. S. Rappé, *Front. Microbiol.* **2**, 140 (2011).
28. J. Sun *et al.*, *PLoS ONE* **6**, e23973 (2011).
29. K. Mopper *et al.*, *Nature* **353**, 60 (1991).
30. H.-M. Oh *et al.*, *J. Bacteriol.* **192**, 3240 (2010).
31. R. M. Morris *et al.*, *Limnol. Oceanogr.* **50**, 1687 (2005).
32. E. F. DeLong *et al.*, *Science* **311**, 496 (2006).
33. H. Chitsaz *et al.*, *Nat. Biotechnol.* **29**, 915 (2011).
34. M. Schattenhofer *et al.*, *Environ. Microbiol.* **11**, 2078 (2009).
35. T. Pommier *et al.*, *Mol. Ecol.* **16**, 867 (2007).
36. R. M. Morris *et al.*, *Nature* **420**, 806 (2002).
37. J. A. Fuhrman, J. A. Steele, *Aquat. Microb. Ecol.* **53**, 69 (2008).
38. A. Eiler, D. H. Hayakawa, M. J. Church, D. M. Karl, M. S. Rappé, *Environ. Microbiol.* **11**, 2291 (2009).
39. C. A. Carlson *et al.*, *ISME J.* **3**, 283 (2009).
40. M. L. Sogin *et al.*, *Proc. Natl. Acad. Sci. U.S.A.* **103**, 12115 (2006).
41. M. L. Coleman, S. W. Chisholm, *Proc. Natl. Acad. Sci. U.S.A.* **107**, 18634 (2010).
42. C. Wuchter *et al.*, *Proc. Natl. Acad. Sci. U.S.A.* **103**, 12317 (2006).
43. C. A. Carlson *et al.*, *Limnol. Oceanogr.* **49**, 1073 (2004).
44. S. J. Goldberg, C. A. Carlson, D. A. Hansell, N. B. Nelson, D. A. Siegel, *Deep Sea Res. I* **56**, 672 (2009).
45. E. M. Bertrand *et al.*, *Limnol. Oceanogr.* **52**, 1079 (2007).
46. A. Vardi *et al.*, *Science* **326**, 861 (2009).
47. J. A. Steele *et al.*, *ISME J.* **5**, 1414 (2011).
48. S. J. Giovannoni *et al.*, *Science* **309**, 1242 (2005).
49. H. J. Tripp *et al.*, *Nature* **452**, 741 (2008).
50. H. J. Tripp *et al.*, *Environ. Microbiol.* **11**, 230 (2009).
51. T. Gross, L. Rudolf, S. A. Levin, U. Dieckmann, *Science* **325**, 747 (2009).
52. B. M. Fuchs, M. V. Zubkov, K. Sahm, P. H. Burkill, R. Amann, *Environ. Microbiol.* **2**, 191 (2000).
53. T. C. Hazen *et al.*, *Science* **330**, 204 (2010).
54. R. J. Olson, H. M. Sosik, *Limnol. Oceanogr. Methods* **5**, 195 (2007).
55. C. M. Preston *et al.*, *PLoS ONE* **6**, e22522 (2011).
56. M. J. Follows, S. Dutkiewicz, S. Grant, S. W. Chisholm, *Science* **315**, 1843 (2007).
57. G. C. Kettler *et al.*, *PLoS Genet.* **3**, e231 (2007).
58. S. T. Dyhrman *et al.*, *Nature* **439**, 68 (2006).
59. B. P. Koch, K. U. Ludwichowski, G. Kattner, T. Dittmar, M. Witt, *Mar. Chem.* **111**, 233 (2008).
60. E. B. Kujawinski *et al.*, *Environ. Sci. Technol.* **45**, 1298 (2011).
61. J. D. Neufeld, M. Wagner, J. C. Murrell, *ISME J.* **1**, 103 (2007).
62. Y. Shi, G. W. Tyson, J. M. Eppley, E. F. DeLong, *ISME J.* **5**, 999 (2011).
63. T. D. Mullins, T. B. Britschgi, R. L. Krest, S. J. Giovannoni, *Limnol. Oceanogr.* **40**, 148 (1995).
64. http://hahana.soest.hawaii.edu/hot/hot_dogs/interface.html
65. http://bats.bios.edu/bats_form_bottle.html

Acknowledgments: We thank M. Behrenfeld, C. Thrash, and K. Halsey for critical comments. Supported by a grant from the Marine Microbiology Initiative of the Gordon and Betty Moore Foundation and NSF Microbial Observatory grants MCB-0237713 and OCE-0802004.

10.1126/science.1198078

Pigment Pattern Formation by Contact-Dependent Depolarization

Masafumi Inaba, Hiroaki Yamanaka, Shigeru Kondo*

The zebrafish, a tropical freshwater fish, has distinctive pigmented stripes that span the length of the body. Molecular genetic studies with this model organism have identified and characterized many genes involved in the formation of skin patterns and suggest that the interactions between the two pigment cell types, melanophores and xanthophores, play a key role (*1*–*3*). However, this molecular interaction network is unclear. Because the formation of pigment patterns occurs only in the skin of adult fish, most experiments have been performed by observing the distribution or migration of pigment cells in intact fish. However, these observations do not allow for the elucidation of specific interactions. To overcome this difficulty, we used gene mutation analysis to examine pigment cell interactions in an in vitro system.

In wild-type fish, melanophores and xanthophores segregate precisely (Fig. 1A). However, these cells intermingle in some regions of fish with a mutation in the *jaguar* gene (Fig. 1A), suggesting that communication between the pigment cells is disturbed (*2*, *4*). The *jaguar* gene encodes an inwardly rectifying potassium channel 7.1 (Kir7.1) (*5*), and this gene is expressed and required in melanophores (fig. S1). Prior works have shown that loss of Kir channels often leads to the depolarization of cells (*6*). Therefore, mutation of *jaguar* may result in the depolarization of melanophores. To test this hypothesis, we studied cell membrane potential by using a voltage-sensitive dye, $DiBAC_4(3)$. Pigment cells were dissociated from the fins and incubated with $DiBAC_4(3)$. As expected, the intensity of fluorescence was much higher in the *jaguar* melanophores than in the wild-type melanophores, indicating that the membrane undergoes constant depolarization in the *jaguar* melanophores (fig. S2). Moreover, we observed wild-type melanophores undergo transient depolarization when in contact with the dendrites of a xanthophore (Fig. 1B and movie S1). On the other hand, collision of fibroblasts did not induce contact-dependent depolarization of melanophores (movie S1), suggesting that a specific membrane-associated signal exists within the dendrites of the xanthophores. Long-term observation also revealed that most melanophores rarely migrate when they were not in contact with xanthophores. However, when melanophores were depolarized by contact with a xanthophore, they frequently (6 out of 10) moved away from the xanthophore (Fig. 1C and movie S3). This "repulsive" behavior should be considered important, because melanophores from the *jaguar* mutant always (10 out of 10) maintained contact with the xanthophore (movie S4). The repulsive behavior between melanophores and xanthophores may be responsible for the segregation of the two cell types in the skin of zebrafish.

Contact-dependent depolarization as well as the repulsion behavior shown by the melanophores may form part of the interaction network for stripe patterning. Mathematical studies have suggested that animal skin patterns can be formed by a reaction-diffusion (RD) mechanism (*7*, *8*). Theoretically, diffusion can be replaced by the combination of other signaling mechanisms that have long and short functional distances (*9*). If the interaction observed in this study serves as a short-range interaction, it does not contradict the RD hypothesis. Signal transfer via dendrites is more likely to be the mechanism underlying zebrafish skin pattern formation rather than diffusion because it is a more stable and direction-oriented process compared to a concentration gradient.

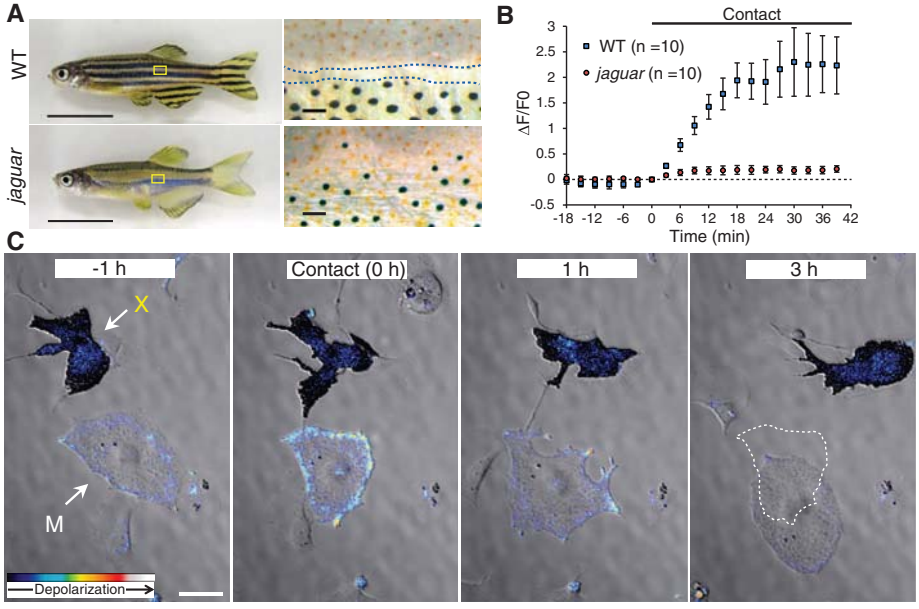

Fig. 1. (**A**) Pigment pattern of wild-type (WT) and the homozygous kir7.1 mutant (*jaguar*). Black cells and yellow cells are melanophores and xanthophores, respectively. Scale bars in overall views indicate 1 cm; enlarged views, 100 μm. Blue dotted lines indicate the edge of each group of pigment cells. (**B**) Time course of melanophore depolarization (ΔF/F0, change in fluorescence (F) level) by contact with xanthophores. Changes in membrane potential in WT are much larger than in *jaguar* mutant. See also movie S2 with regard to *jaguar* cells. Error bars represent SEM. (**C**) Snapshots showing repulsive behavior of WT melanophores (M) when contacted by xanthophore (X). White dotted outline indicates the position of melanophore at 0 hours. Scale bar, 25 μm.

References and Notes

1. D. M. Parichy, J. M. Turner, *Development* **130**, 817 (2003).
2. F. Maderspacher, C. Nüsslein-Volhard, *Development* **130**, 3447 (2003).
3. M. Watanabe *et al.*, *EMBO Rep.* **7**, 893 (2006).
4. G. Takahashi, S. Kondo, *Pigment Cell Melanoma Res.* **21**, 677 (2008).
5. M. Iwashita *et al.*, *PLoS Genet.* **2**, e197 (2006).
6. H. Hibino *et al.*, *Physiol. Rev.* **90**, 291 (2010).
7. A. M. Turing, *Philos. Trans. R. Soc. London Ser. B* **237**, 37 (1952).
8. A. Nakamasu, G. Takahashi, A. Kanbe, S. Kondo, *Proc. Natl. Acad. Sci. U.S.A.* **106**, 8429 (2009).
9. H. Meinhardt, *Models of Biological Pattern Formation* (Academic Press, London, 1982).

Acknowledgments: We thank K. Kawakami for providing the Tol2 vector and Y. Kurachi, K. Furutani, M. Okada, A. Ogura, and K. Ida for helpful discussions. This study was supported by grants-in-aid for Scientific Research from the Ministry of Education, Culture, Sports, Science, and Technology of Japan [Grant-in-Aid for Scientific Research on Innovative Areas, Scientific Research on (B)] and grants from the Uehara Memorial Foundation and Mitsubishi Foundation.

Supporting Online Material

www.sciencemag.org/cgi/content/full/335/6069/677/DC1
Materials and Methods
Figs. S1 and S2
References (*10*–*13*)
Movies S1 to S4

17 August 2011; accepted 9 January 2012
10.1126/science.1212821

Graduate School of Frontier Biosciences, Osaka University, 1-3 Yamadaoka, Suita, Osaka, 565-0871, Japan.

*To whom correspondence should be addressed. E-mail: skondo@fbs.osaka-u.ac.jp

Visualizing Long-Term Memory Formation in Two Neurons of the *Drosophila* Brain

Chun-Chao Chen,[1] Jie-Kai Wu,[1] Hsuan-Wen Lin,[1] Tsung-Pin Pai,[1] Tsai-Feng Fu,[3] Chia-Lin Wu,[2] Tim Tully,[4] Ann-Shyn Chiang[1,2,5,6]*

Long-term memory (LTM) depends on the synthesis of new proteins. Using a temperature-sensitive ribosome-inactivating toxin to acutely inhibit protein synthesis, we screened individual neurons making new proteins after olfactory associative conditioning in *Drosophila*. Surprisingly, LTM was impaired after inhibiting protein synthesis in two dorsal-anterior-lateral (DAL) neurons but not in the mushroom body (MB), which is considered the adult learning and memory center. Using a photoconvertible fluorescent protein KAEDE to report de novo protein synthesis, we have directly visualized cyclic adenosine monophosphate (cAMP) response element–binding protein (CREB)–dependent transcriptional activation of *calcium/calmodulin-dependent protein kinase II* and *period* genes in the DAL neurons after spaced but not massed training. Memory retention was impaired by blocking neural output in DAL during retrieval but not during acquisition or consolidation. These findings suggest an extra-MB memory circuit in *Drosophila*: LTM consolidation (MB to DAL), storage (DAL), and retrieval (DAL to MB).

In *Drosophila*, LTM is produced by spaced repetitive training, which induces cyclic adenosine monophosphate (cAMP) response element–binding protein (CREB)–dependent gene transcription followed by de novo protein synthesis (*1*, *2*). A prominent neuroanatomical site involved with memory formation is the mushroom body (MB), which consists of γ, α′β′, and αβ neurons. Calcium-imaging studies have shown that each cell type displays a distinct and altered activity at different time durations after training (*3*). Moreover, 30 different genetic or pharmacological disruptions have suggested that the MBs are involved in both short-term memory (STM) and long-term memory (LTM) (*3*–*8*). Nevertheless, de novo protein synthesis required for LTM consolidation has never been directly visualized and/or manipulated in any targeted brain structures, including the MBs.

Visualizing de novo protein synthesis in targeted neurons. KAEDE is a green fluorescent protein (GFP), which changes its structure irreversibly to a red fluorescent protein (RFP) upon ultraviolet (UV) irradiation (*9*, *10*). We generated a transgenic *upstream activation sequence* (*UAS*)–*kaede* to monitor de novo transcriptional activities in targeted neurons. We showed that KAEDE faithfully reports the cyclic transcriptional activity of *period* (*per*) in circadian pacemaker cells (lateral neurons). Preexisting green KAEDE in the lateral neurons was photoconverted into red KAEDE in living *per-Gal4>UAS-kaede* flies exposed to UV irradiation (fig. S1, A and B). By photoconverting green KAEDE to red every 4 hours, we showed that KAEDE exhibits a diurnal cycle of de novo synthesis in the lateral neurons (Fig. 1A), parallel to the oscillation of *per* RNA (*11*). Newly synthesized green KAEDE was about 10 times as high during the night as during the day, indicated by accumulative measurement (Fig. 1A) and time lapse recording (movie S1). This de novo KAEDE synthesis in lateral neurons was reduced significantly in flies fed the protein synthesis inhibitor, cycloheximide (Fig. 1B). In contrast, red KAEDE remained at a constant level with or without cycloheximide feeding, confirming that photoconverted red KAEDE is irreversible and that spontaneous conversion of green KAEDE to red does not occur.

RICIN is a potent cytotoxic protein that inactivates eukaryotic ribosomes by hydrolytically cleaving the N-glycosidic bond (A^{4324}) of the 28*S* ribosomal RNA subunit (*12*, *13*). We obtained an effective transgenic fly carrying a cold-sensitive *UAS-ricin*^{CS} transgene, by remobilization of a P-element insertion generated previously (*14*). In *OK107-Gal4>UAS-ricin*^{CS} flies, high-temperature (30°C) RICIN^{CS} inactivated ribosomes, causing a severe MB deformation; at low temperature (18°C), however, RICIN^{CS} itself was inactive, thereby allowing normal MB development (fig. S1C).

We also visualized the effect of RICIN^{CS} on protein synthesis using KAEDE as a reporter. Using *per-Gal4* as a driver, we found that KAEDE synthesis in lateral neurons was not inhibited by RICIN^{CS} at 18°C but decreased ~80% by RICIN^{CS} at 30°C for at least 5 hours (Fig. 1C). KAEDE synthesis inhibited by activated RICIN^{CS} at permissive temperature is quickly restored to normal level after a shift to the toxin's restrictive temperature, suggesting that working ribosomes are resynthesized (Fig. 1C). Similar effects of RICIN^{CS} inhibition of protein synthesis were found in MB neurons (Fig. 1, D and E), using *OK107-Gal4*, which likely labels all MB neurons, and choline acetyltransferase (*Cha*) promoter–driving *Gal4*, which likely labels most acetylcholine-producing neurons.

Behavioral screen for neurons involved in protein synthesis–dependent memory formation. The spatiotemporal precision of *UAS-ricin*^{CS} for acutely blocking protein synthesis in small subsets of targeted neurons allowed us to identify neurons undergoing protein synthesis during LTM formation. RICIN^{CS} activated (30°C) immediately after spaced training in *Cha-Gal4* that contains ~60% of total brain neurons (*15*) impaired 1-day memory (Fig. 2A). The impairment was specific to LTM rather than anesthesia-resistant memory (ARM), because cycloheximide fed to these flies did not further reduce 1-day memory after spaced training and because activated RICIN^{CS} did not impair 1-day memory after massed training.

In this form of associative learning, olfactory information (the conditioned stimulus) is detected by sensory neurons and then is relayed by projection neurons from the antennal lobe to the MB, where it is modulated by anterior paired lateral (APL) and dorsal paired medial (DPM) neurons. Through uncharacterized interneurons, information processed in the MBs eventually reaches the central complex, including the ellipsoid body. Foot-shock punishment (the unconditioned stimulus) is thought to reach MB through dopaminergic *TH-Gal4* neurons (*16*–*18*). Unexpectedly, 1-day memory retention remained intact when RICIN^{CS} was expressed in olfactory sensory neurons (*Or83b-Gal4*), olfactory projection neurons (*GH146-Gal4*), MB modulatory neurons (*GH146-Gal4, c316-Gal4*), all MB neurons (*c247-Gal4*, *c772-Gal4*, and *OK107-Gal4*), αβ neurons (*c739-Gal4*), α′β′ neurons (*c305a-Gal4*, *E0973-Gal4*, and *G0050-Gal4*), ellipsoid body neurons (*c42-Gal4*, *c217-Gal4*, *c507-Gal4*, *Feb170-Gal4*, and *P0010-Gal4*) and dopaminergic neurons (*TH-Gal4*) and again activated immediately after spaced training (Fig. 2B). Furthermore, by limiting RICIN^{CS} expression to neurons outside of MB using a combination of *Cha-Gal4* and *MB-Gal80* (Gal80 inhibits Gal4), 1-day memory again was impaired when RICIN^{CS} was activated immediately after spaced training but not after massed training (Fig. 2C and fig. S2A). Therefore, regardless of numerous studies suggesting LTM storage in the antennal lobes (*19*), the MBs (*3*, *20*) and the ellipsoid body (*21*), our results suggest that de novo protein synthesis during LTM formation occurs in *Cha-Gal4*–expressing neurons outside of the MBs.

Next, we performed a more extensive behavioral screen for patterns of RICIN^{CS} expression that yielded 1-day memory impairments when RICIN^{CS} was activated immediately after spaced training (fig. S2B). LTM was impaired with *Gal4*

[1]Institute of Biotechnology and Department of Life Science, National Tsing Hua University, Hsinchu 30013, Taiwan. [2]Brain Research Center, National Tsing Hua University, Hsinchu 30013, Taiwan. [3]Department of Applied Chemistry, National Chi Nan University, Nantou 54561, Taiwan. [4]Dart Neuroscience, LLC, 7374 Lusk Boulevard, San Diego, CA 92121, USA. [5]Genomics Research Center, Academia Sinica, Nankang, Taipei 11529, Taiwan. [6]Kavli Institute for Brain and Mind, University of California at San Diego, La Jolla, CA 92093–0526, USA.

*To whom correspondence should be addressed. E-mail: aschiang@life.nthu.edu.tw

drivers, *cer* (*crammer*)-, *Ddc* (*Dopa decarboxylase*)-, *Trh493* (*Tryptophan hydroxylase*)-, *Trh996*-, *cry* (*cryptochrome*)-, *per*-, *CaMKII*-(X), and *CaMKII-Gal4*(III), whereas LTM was normal with *Gal4* drivers, *DVGLUT* (*Vesicular glutamate transporter*)-, *Gad* (*Glutamic acid decarboxylase 1*)-, *tim* (*timeless*)*14-27*-, *tim14-82*-, and *repo* (*reversed polarity*)–*Gal4*, the latter of which labels glial cells (Fig. 2B). LTM impairments by activated RICIN^{CS} in targeted *Gal4* neurons were confirmed again by repeating the experiment using "Cantonized" *Gal4* lines outcrossed to control flies to equilibrate genetic backgrounds (fig. S3).

Identification of individual neurons with protein synthesis during LTM formation. PER protein is necessary for LTM after courtship conditioning (*22*, *23*). We found that PER protein was also necessary for LTM after olfactory conditioning. In *per*^{0} flies, 1-day memory retention was impaired after spaced, but not after massed, training (fig. S4A). In contrast, 1-day memory after spaced training was normal in other circadian mutants, including *tim*^{03}, *tim*^{04}, *dClk*^{Jrk}, and *cyc*^{0} (fig. S4B). By blocking neurotransmission with *UAS-shi*^{ts}, a temperature-sensitive dynamin protein (*24*, *25*), we found that neural activity from *per* neurons was required for retrieval of 1-day memory after spaced training but not 3 hours or immediately after a single training session (fig. S4C). Activation of RICIN^{CS} in *per* neurons impaired 1-day memory after spaced training but not after massed training (fig. S4D). Moreover, by activating RICIN^{CS} in *per* neurons at different time windows after spaced training, we found that protein synthesis was required only during the first 12 hours of LTM formation (fig. S4D). We also evaluated activated RICIN^{CS} in MB neurons (*OK107-Gal4* and *c247-Gal4*) using a sliding 12-hour window before and after spaced training (fig. S5). One-day memory retention remained normal in every case.

We identified individual neurons by looking for overlap in expression patterns of the 9 *Gal4* driver lines in which activated RICIN^{CS} impaired LTM formation. *Ddc-Gal4* and *per-Gal4* were chosen for the initial analysis because of their distinctly different expression patterns (fig. S2B). Two *per-Gal4* neurons located at the dorsal-anterior-lateral (DAL) protocerebrum and most *Ddc-Gal4* neurons were immunopositive for DDC antibodies (fig. S6A). The two DAL neurons are good candidates for their participation in protein synthesis–dependent LTM formation because they also express *N*-methyl-D-aspartate (NMDA) receptors (dNR), which are required for LTM formation (*26*). DDC-antibody immunostaining, in fact, revealed that the DAL neurons are included in the expression patterns of all nine *Gal4* driver lines (Fig. 3A). We also used *cry-Gal80* to "subtract" expression of RICIN^{CS} in the two DAL neurons from *Cha-Gal4* and *per-Gal4* expression patterns (Fig. 3, B and C, and fig. S6B). In both cases, activated RICIN^{CS} in the remaining neurons did not affect 1-day memory after spaced training (Fig. 3, D and E), suggesting that protein synthesis for LTM formation occurred in neurons within the intersection of the *Cha-Gal4*, *per-Gal4* and *cry-Gal80* expression patterns, including the two DAL neurons. Next, we identified three new *Gal4* drivers (*E0946, G0338,* and *G0431*) with relatively limited patterns of expression, but each of which contained the DAL neurons (validated again by DDC-antibody immunostaining) (Fig. 3F). In all three cases, we found that RICIN^{CS}, when activated during the first 12 hours after training, disrupted 1-day memory after spaced training but not after massed training (Fig. 3G).

Using the same three *Gal4* drivers (*E0946, G0338,* and *G0431*), we then used *UAS-shi*^{ts} acutely to block neurotransmission from DAL neurons. One-day memory after spaced training was normal when neurotransmission was blocked (i) from 30 min before training to the first 8 hours after training, (ii) 8 to 16 hours after training, or (iii) 16 to 24 hours after training (Fig. 3H). Instead, retrieval of LTM was disrupted when neurotransmission was blocked during the test trial 1 day after spaced training (Fig. 3H). Blocking neurotransmission from DAL with these three *Gal4* drivers did not affect memory retrieval immediately or 3 hours after one training session (fig. S7).

Are there other neurons that undergo protein synthesis during LTM formation? We used *cry-Gal80* to subtract expression of RICIN^{CS} in DAL neurons from the broader expression patterns of a panel of *Gal4* driver lines. When *cry-Gal80* was combined with *cer-Gal4* and RICIN^{CS} was activated for 24 hours immediately after training, 1-day memory after spaced training was defective and 1-day memory after massed training was

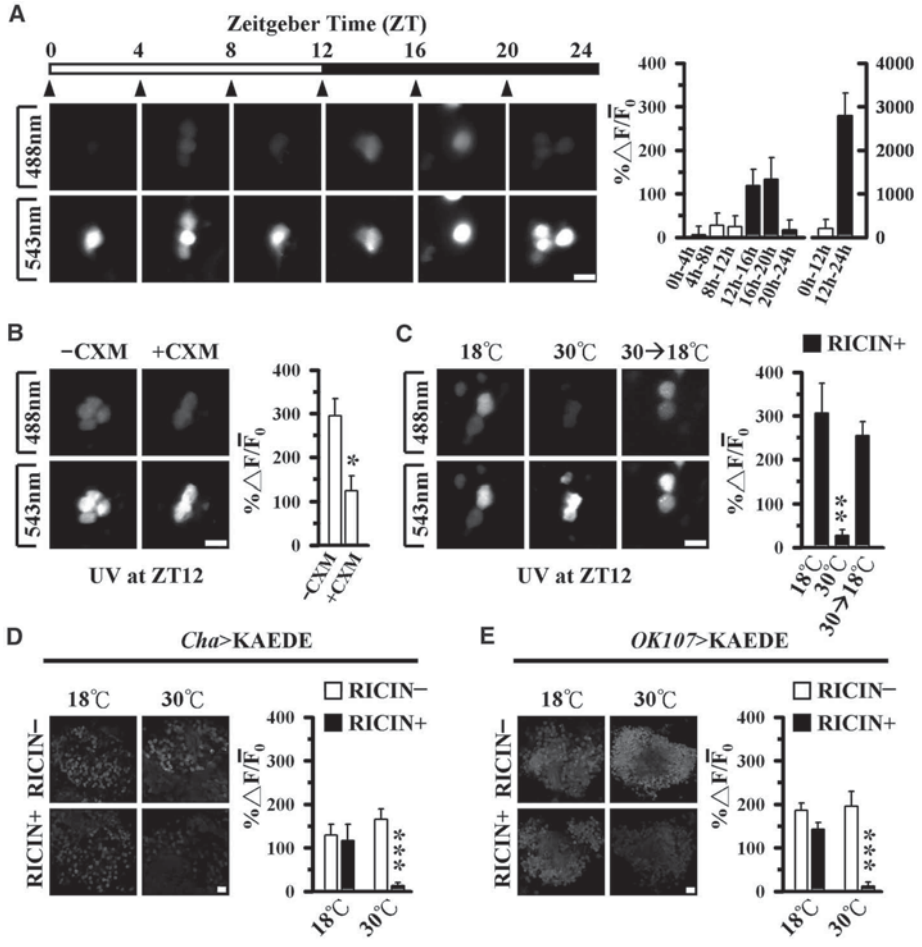

Fig. 1. Visualizing and blocking de novo protein synthesis in identified neurons. (**A**) Diurnal cycle of *per* transcriptional activity in the lateral neurons. To reset preexisting green KAEDE, living flies were UV irradiated every 4 hours (arrowheads) or every 12 hours, i.e., Zeitgeber Time (ZT) 0 or 12. Measurement of relative amount of de novo KAEDE synthesis was estimated within flies by normalizing to preexisting red KAEDE (%$\Delta F/\bar{F}_0$). Values are means ± SEM (N = 3 to 7 samples). (**B**) The effect of cycloheximide (+CXM) feeding. Images of lateral neurons were taken 5 hours after photoconversion at ZT12. Values are means ± SEM (N = 8 to 24 samples; *, $P < 0.05$). (**C**) The effect of activated RICIN^{CS}. Flies were photoconverted at ZT12 and kept (i) at 18°C (inactive RICIN^{CS}), (ii) at 30°C (activated RICIN^{CS}) during ZT12 to ZT17, or (iii) at 30°C during ZT7 to ZT12 and at 18°C during ZT12 to ZT17. Images of lateral neurons were taken at ZT17. Values are means ± SEM (N = 6 to 16 samples; *, $P < 0.05$; **, $P < 0.01$). (**D** and **E**) Effects of activated RICIN^{CS} in the MB neurons. After photoconversion, flies were kept at 18°C or 30°C for 24 hours before imaging. Values are means ± SEM (N = 10 to 15 samples; ***, $P < 0.001$). For all images, scale bar represents 10 μm. See supporting online material for more detailed legends of this and the other figures.

normal (fig. S8A), indicating that other neurons within the *cer* expression pattern also undergo de novo protein synthesis along with DAL neurons during LTM formation. In contrast, when *cry-Gal80* was combined with *Cha-Gal4*, *Ddc-Gal4*, *Trh493-Gal4*, *Trh996-Gal4*, *cry-Gal4*, *per-Gal4*, *CaMKII-Gal4*(X) or *CaMKII-Gal4*(III) and RICIN^{CS} was activated for 24 hours immediately after training, 1-day memory after spaced training remained normal (Fig. 3, D and E, and fig. S8B).

DAL axons are structurally connected with MB calyx. Using Dscam-GFP as a dendritic marker, we showed that putative DAL dendrites distributed mainly in the superior dorsofrontal protocerebrum (SDFP) region (Fig. 3I, left). Using synaptotagmin-GFP as an axon marker, we showed that DAL axons distributed widely in three brain regions: SDFP, dorsolateral protocerebrum (DLP), and inferior dorsofrontal protocerebrum (IDFP) (Fig. 3I, right) (*15*). By a close examination of *G0431-Gal4* expression pattern in the brain counterstained with DLG-antibody immunostaining, we noticed that the DAL axons and the MB calyx intersected at K5 region where dendrites belonging to pioneer αβ neurons are aggregated (*27*). Using GFP reconstitution across synaptic partners (GRASP) labeling (*28*), we verified that DAL neurons in *G0431-Gal4* and the MB pioneer αβ neurons in *L5275-LexA* (Fig. 3J, left) were structurally interconnected at the K5 region (Fig. 3J, right).

Identification of newly synthesized proteins in DAL neurons during LTM formation. Immunostaining revealed preferential expression of DDC, PER, dNR1, dNR2, CaMKII, TEQ (TEQUILA), and CRY proteins and octopamine in DAL neurons (fig. S9A). Using RNA interference (RNAi) with *UAS-perPAS-IR G2* (*29*) driven by four different *Gal4* drivers (*per-Gal4*, *Ddc-Gal4*, *G0338-Gal4*, and *G0431-Gal4*), we found that constitutive disruption of PER protein expression impaired LTM formation after spaced training but not after massed training (Fig. 4A and fig. S9, B to D). Constitutive *UAS-perPAS-IR G2* expression in ellipsoid body neurons (*Feb170-Gal4*) did not affect 1-day memory after spaced training (fig. S9E). Similarly, expressing with *G0431-Gal4*, RNAi constructs for dNR1/dNR2, CaMKII, TEQUILA, or DDC/TRH also impaired LTM formation after spaced training but not after massed training (Fig. 4, B to E). To eliminate any developmental contribution to the impairments observed above, we repeated the same set of experiments using a temperature-sensitive tub-Gal80^{ts} protein that suppresses *Gal4*-induced expression at 18°C but not at 30°C (*30*). When *G0431-Gal4*–induced RNAi expression for *per, dNR1/dNR2, CaMKII, tequila, and Ddc/Trh* genes were suppressed throughout development (18°C) and then allowed only in adults (30°C), we again observed defects in 1-day memory after spaced but not after massed training. Moreover, in each case, further inhibition of protein synthesis from feeding flies cycloheximide did not produce stronger LTM impairments (Fig. 4, F to J).

We also found that down-regulation of CRY or overexpression of CER in DAL neurons impaired 1-day memory after spaced training after constitutive, but not after adult-specific, transgenic manipulations (fig. S9, F and G). Moreover, adult-specific *Tβh^{RNAi}* expression in DAL neurons did not affect 1-day memory after spaced training (fig. S9H).

CREB2 activity in DAL neurons, but not MB neurons, is required for LTM formation. We confirmed an earlier report that 1-day memory after spaced training was impaired, but learning was normal, after constitutive expression in MB neurons by the *c739-Gal4* driver of *UAS-dcreb2-b*, which encodes a CREB repressor protein (*4*, *7*). However, learning was impaired after constitutive expression of *UAS-dcreb2-b* by two additional

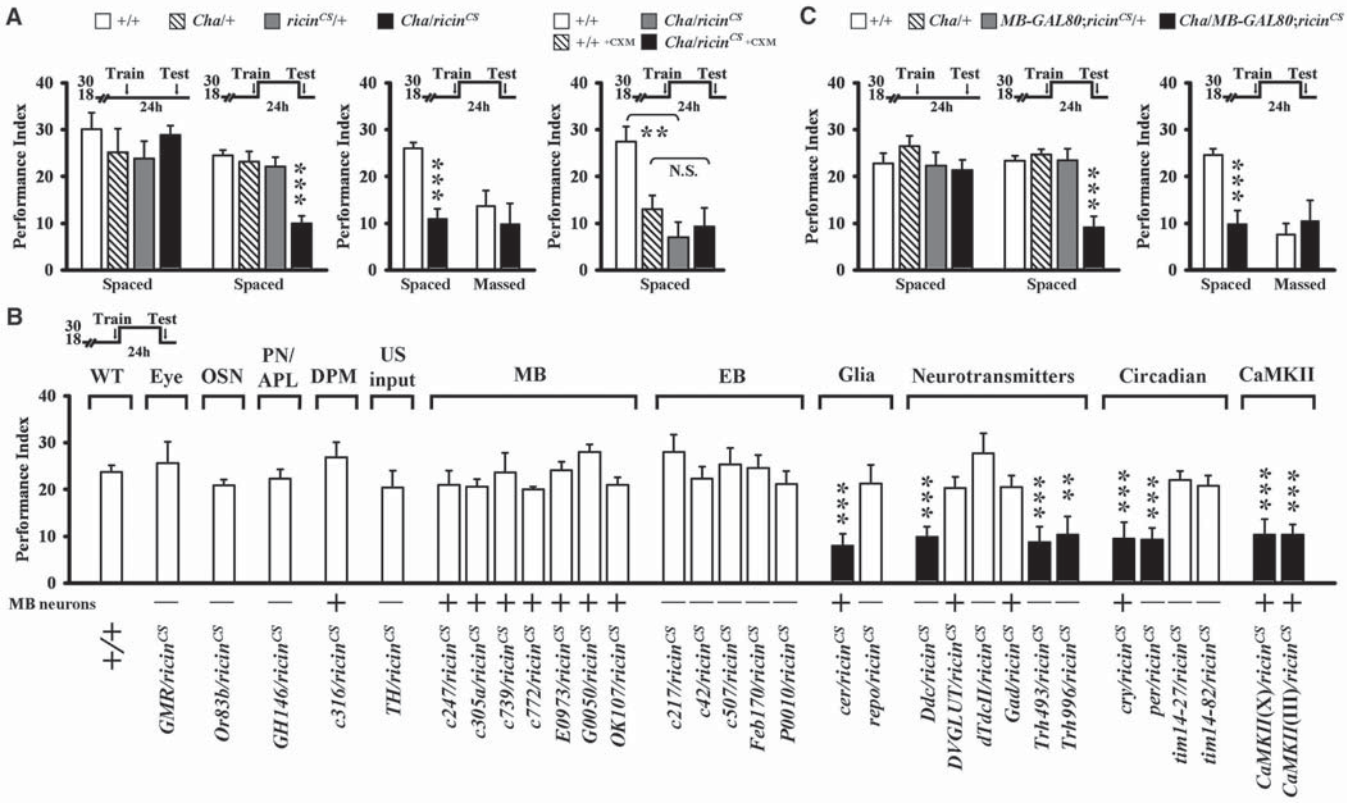

Fig. 2. Behavioral screen for neurons in which protein synthesis is required for LTM formation. (**A**) Protein synthesis is required in *Cha-Gal4* neurons for normal LTM formation. After spaced or massed training, *Cha-Gal4>UAS-ricin^{CS}* flies fed with (+) or without (–) cycloheximide (CXM) were shifted to 30°C or remained at 18°C. Values are means ± SEM (N = 12 experiments; **, $P < 0.01$; ***, $P < 0.001$; N.S., $P > 0.05$). (**B**) Behavioral screen for *Gal4* expression patterns containing neurons in which protein synthesis is required for LTM formation. All flies were subjected to spaced training, and then RICIN^{CS} was activated by keeping flies at 30°C during the 24-hour retention interval. Black bars denote significant impairments of 1-day memory. *Gal4* expression patterns containing MB neurons (+) or not (–) are indicated. Values are means ± SEM (N = 8 to 12 experiments; **, $P < 0.01$; ***, $P < 0.001$). (**C**) Protein synthesis is required for LTM formation in *Cha-Gal4*–expressing neurons outside of MB. *MB-Gal80* inhibits *Gal4* expression in the MB neurons. Values are means ± SEM (N = 12 experiments; ***, $P < 0.001$). See table S1 for a summary of *Gal4* expression patterns.

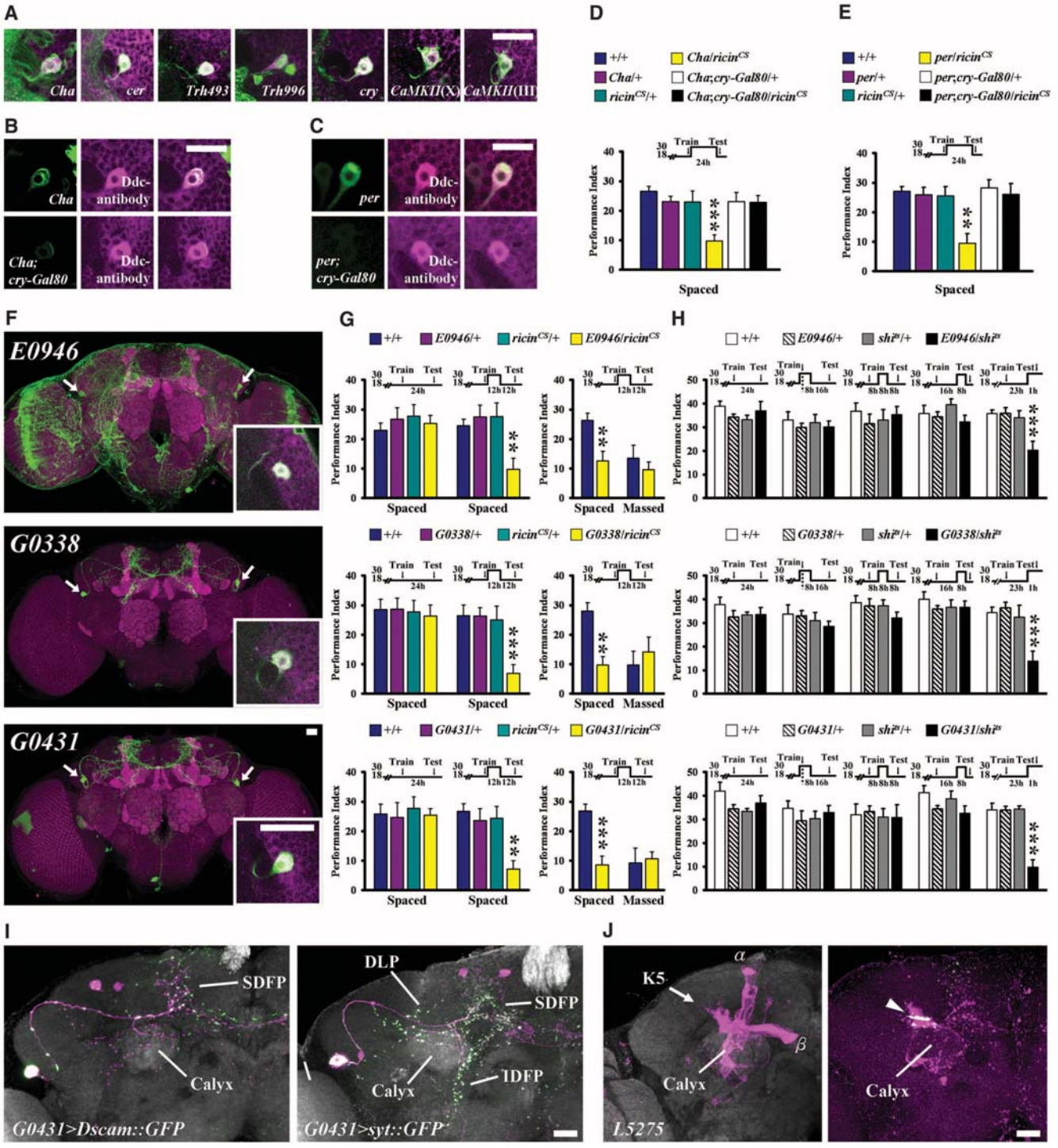

Fig. 3. DAL neurons are required for consolidation and retrieval of LTM. (**A**) The same DAL neurons contained in seven different *Gal4*, as indicated by DDC-antibody immunostaining (magenta). (**B** and **C**) DAL neurons are "subtracted" from the *Gal4* expression pattern (green) by *cry-Gal80*. (**D** and **E**) LTM formation required protein synthesis in neurons within the intersected expression between *Cha-Gal4* and *cry-Gal80* or between *per-Gal4* and *cry-Gal80*. Values are means ± SEM ($N = 12$ experiments; **, $P < 0.01$ ***, $P < 0.001$). (**F**) Three independent *Gal4* lines with more restricted expression patterns containing DAL neurons (arrow). (Inset) The identity of DAL neurons was verified using DDC-antibody immunostaining (magenta). (**G**) Protein synthesis in DAL neurons is required for LTM formation. Values are means ± SEM ($N = 8$ to 12 experiments; **, $P < 0.01$; ***, $P < 0.001$). (**H**) Neurotransmission from DAL neurons is required during LTM retrieval. One-day memory after spaced training was impaired when neurotransmission from DAL neurons was blocked (by transferring flies to 30°C for 1 hour) during the test trial (retrieval) but not during acquisition or (i) 0 to 8 hours, (ii) 8 to 16 hours, or (iii) 16 to 24 hours of the 24-hour retention interval (consolidation). Control flies kept continuously at 18°C exhibited normal 1-day memory retention. Values are means ± SEM ($N = 8$ to 12 experiments; ***, $P < 0.001$). (**I**) Polarity analysis of the DAL neuron (magenta). (Left) Putative dendrites labeled by Dscam-GFP (green). (Right) Putative axons labeled by syt-GFP (green). DLP, dorsolateral protocerebrum; IDFP, inferior dorsofrontal protocerebrum; SDFP, superior dorsofrontal protocerebrum. (**J**) Structural connections between DAL and MB neurons visualized by GRASP labeling. (Left) *L5275*-LexA expressed specifically in the MB pioneer αβ neurons. (Right) GRASP signal (arrowhead) was visualized in the K5 region. DAL and pioneer αβ neurons were labeled by CD4-antibody immunostaining (magenta). General brain structures were counterstained using DLG-antibody immunostaining [magenta in (F); grayscale in (I) and (J)]. Scale bar, 20 μm.

MB driver lines, *OK107-Gal4* and *c247-Gal4* (fig. S10, A to C). These learning defects prompted us to examine whether constitutive expression of *UAS-dcreb2-b* in MB neurons might produce any developmental defects. For all three *Gal4* driver lines, we discovered significant neuroanatomical damage in MB. In *OK107-Gal4>UAS-dcreb2-b* flies, the α′ lobe was completely missing (fig. S10D); in *c247-Gal4>UAS-dcreb2-b* or *c739-Gal4>UAS-dcreb2-b* flies, MBs had significantly fewer GFP axons compared with control flies (fig. S10, E and F), and β lobe axons occasionally crossed the midline (fig. S10F).

To eliminate these developmental defects, we used *tub-Gal80^{ts}* to limit *UAS-dcreb2-b* expression

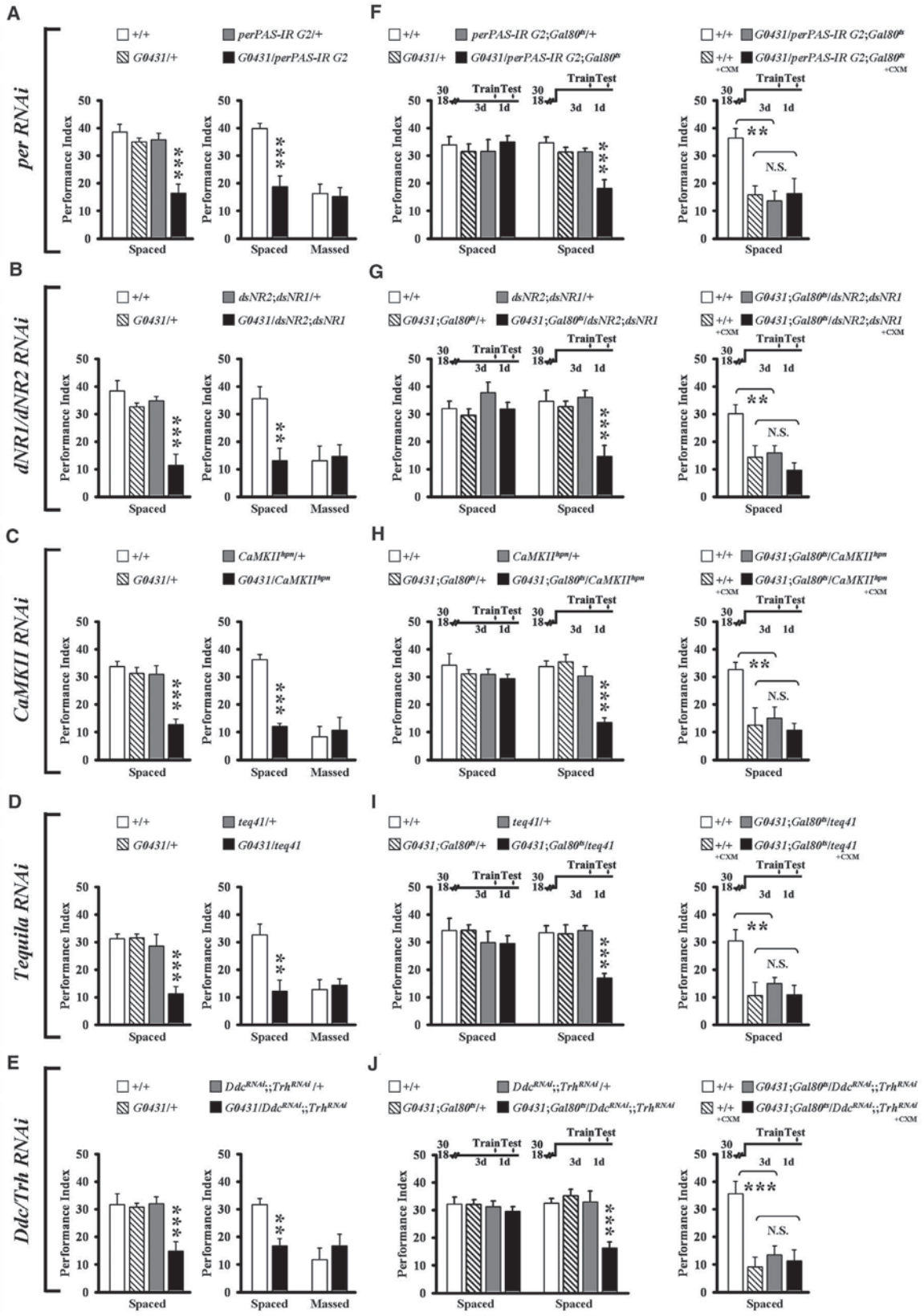

Fig. 4. RNAi-mediated disruption of specific genes in DAL neurons impairs LTM formation. (**A** to **E**) Constitutive RNAi-mediated down-regulation of PER, dNR1/dNR2, CaMKII, TEQUILA, and DDC/TRH in DAL neurons impaired 1-day memory after spaced training but not after massed training. Values are means ± SEM (N = 8 to 12 experiments; **, P < 0.01; ***, P < 0.001; N.S., P > 0.05). (**F** to **J**) Induced down-regulation of PER, dNR1/dNR2, CaMKII, TEQUILA, and DDC/TRH in the DAL neurons in adult flies impaired 1-day memory after spaced training but not after massed training. Adult flies raised at 18°C were kept at 30°C for 3 days before training to remove *tub-Gal80^{ts}*–mediated inhibition of *Gal4* activity, thereby allowing *RNAi*-mediated disruption of the target gene(s). Some groups also were fed with 35 mM cycloheximide (+CXM) 1 day before training and again until test trial. Control flies carrying the same transgenes were kept continuously at 18°C before behavioral evaluations. Values are means ± SEM (N = 8 to 12 experiments; **, P < 0.01; ***, P < 0.001; N.S., P > 0.05).

by *OK107-Gal4*, *c247-Gal4*, or *c739-Gal4* to adults (fig. S10, G to I). Under these conditions, memory retention immediately after one training session and 1-day memory after spaced training both were normal (fig. S10, J to L). MB morphology was severely damaged if these flies were kept at 30°C throughout development (fig. S10M). Note that *c739-Gal4*, but not *OK107-Gal4 or c247-Gal4*, expressed weakly also in DAL neurons (fig. S10N). In contrast, when *UAS-dcreb2-b* expression was limited to the adult stage in *Cha-Gal4>UAS-dcreb2-b;tub-Gal80^{ts}* flies, 1-day memory after spaced training, but not immediate memory after one training session, was impaired (fig. S10, O and P).

Next, we asked whether CREB2 activity is required in DAL neurons during LTM formation. Adult-specific (or constitutive) overexpression of *UAS-dcreb2-b* or RNAi-mediated down-regulation of CREB2 expression in DAL neurons impaired 1-day memory after spaced training but not after massed training (Fig. 5, A to D), and feeding with cycloheximide did not exaggerate these impairments (Fig. 5, C and D).

Visualizing transcriptional activity in identified neurons during LTM formation. Thus far, we have shown that LTM formation is impaired by acute (adult-specific) disruptions of eight different genes (i.e., *per*, *dNR1*, *dNR2*, *CaMKII*, *Teq*, *Ddc*, *Trh*, and *dcreb2*) in DAL neurons (Figs. 4 and 5). Because these disruptions existed before and after training, we wanted to determine whether spaced training itself induced expression of these genes.

CaMKII-Gal4 expresses in both MB and DAL neurons (fig. S2B). LTM formation requires normal expression of CaMKII at the time of training in *CaMKII-Gal4* neurons (*19*) and in MB neurons (*7*). When activated immediately after spaced training, RICIN^{CS} in *CaMKII-Gal4* neurons impairs 1-day memory (Fig. 2B) but, in contrast, RICIN^{CS} in MB neurons does not (fig. S4). Is the synthesis of CaMKII induced by spaced training? We used KAEDE to report the transcriptional activity of *CaMKII* for a 24-hour interval after spaced (or massed) training. After photoconversion of preexisting KAEDE (red), spaced training, but not massed training, specifically induced new KAEDE (green) in DAL neurons when *UAS-kaede* was driven by *CaMKII-Gal4* (Fig. 6A). Quantification of newly synthesized green KAEDE indicated that *CaMKII* promoter activity in the DAL neurons is induced only by spaced training, because the low baseline level of green KAEDE after massed training remained constant throughout the 24-hour interval. In MB neurons, KAEDE synthesis driven by *CaMKII-Gal4* remained at a constant low level at the tip of the α lobe or the soma of the MB after either spaced or massed training (Fig. 6A). In the DAL neurons, KAEDE synthesis driven by *per-Gal4* likewise was elevated after spaced training but not after massed training (Fig. 6B). We did not see the spaced training–induced elevation of KAEDE synthesis in any other neurons contained in *CaMKII*-Gal4 and *per*-Gal4, whether imaging at the same detection sensitivity maximized for the DAL neurons or at a lower detection sensitivity maximized for the MB or the lateral circadian neurons (fig. S11). This elevation of *CaMKII* and *per* transcriptional activities occurred mainly during the first 8 hours and then gradually declined, as indicated by monitoring KAEDE synthesis in the DAL neurons in three time regimens after spaced training (fig. S12). By using *tub-Gal80^{ts}* to limit *Gal4*-driven *UAS-dcreb2-b* expression at the adult stage, we found that spaced training–induced levels of KAEDE synthesis driven by *CaMKII-Gal4* or *per-Gal4* in DAL neurons were diminished (Fig. 6C).

Three other genes, *cry*, *Ddc* and *Trh*, were not transcriptionally up-regulated after spaced or massed training, as reported by de novo KAEDE synthesis, even though their normal functions are required in DAL neurons for normal LTM formation (Fig. 6, D to F). We also evaluated an unknown gene, in which the *G0431-Gal4* enhancer trap P element is inserted. Homozygous *G0431-Gal4/G0431-Gal4* flies exhibited normal

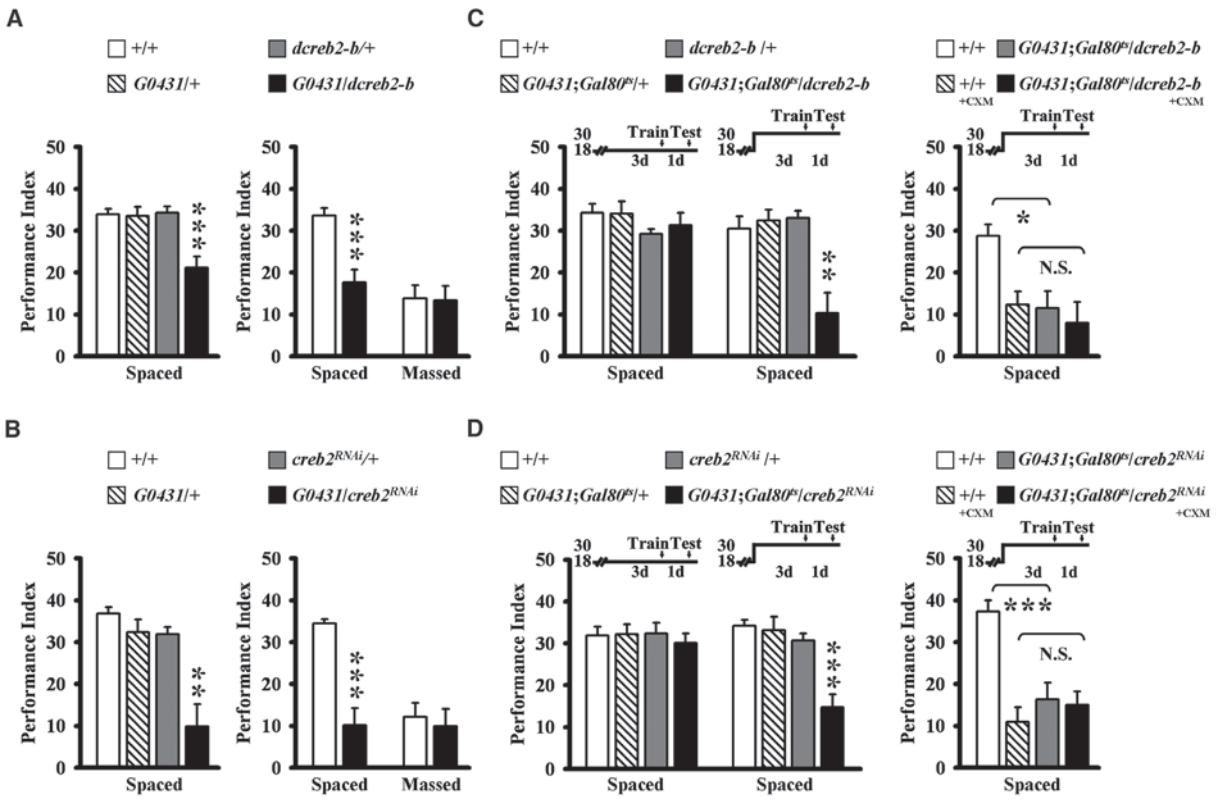

Fig. 5. CREB2 activity in DAL neurons is required for LTM formation. (**A** and **B**) Constitutive expression of *UAS-dcreb2-b* or *UAS-creb2^{RNAi}* in the *G0431-Gal4* neurons impaired 1-day memory after spaced training but not after massed training. Values are means ± SEM (N = 8 to 12 experiments; **, $P < 0.01$; ***, $P < 0.001$; N.S., $P > 0.05$). (**C** and **D**) Induced expression of *UAS-dcreb2-b* or *UAS-creb2^{RNAi}* in *G0431-Gal4* neurons impaired 1-day memory after spaced training but not after massed training. Adult flies raised at 18°C were transferred to 30°C for 3 days before training to remove *tub-Gal80^{ts}* inhibition of *Gal4* activity. Some groups also were fed with cycloheximide (+CXM) before training. One-day memory after spaced training also was evaluated for control flies carrying the same transgenes but kept continuously at 18°C. Values are means ± SEM (N = 8 to 12 experiments; *, $P < 0.05$; **, $P < 0.01$; ***, $P < 0.001$; N.S., $P > 0.05$).

1-day memory after spaced training (fig. S13). In DAL neurons of *G0431-Gal4>UAS-kaede* flies, constant low levels of KAEDE synthesis were seen throughout the 24-hour interval after spaced or massed training (fig. S13).

Discussion. We used genetically based methods to identify neurons in the *Drosophila* brain in which protein synthesis is required for LTM formation. The bilaterally paired DAL neurons satisfy several criteria to suggest that they are a site of LTM storage (*6*). First, de novo protein synthesis in DAL neurons during the first 12 hours after spaced training was required for normal LTM formation (Fig. 3G). Second, several proteins (i.e., dNR1, dNR2, PER, CaMKII, and TEQUILA) that have previously been shown to be necessary for LTM formation (*19*, *21*, *23*, *26*, *31*) were colocalized in DAL neurons (figs. S6A and S9A). Third, disruptions of PER, dNR1, dNR2, CaMKII, TEQUILA, DDC, TRH, and CREB2 in DAL neurons impaired 1-day memory after spaced (but not massed) training (Fig. 4 and Fig. 5, B and D). Fourth, expression of a repressor form of CREB2 protein in DAL neurons was sufficient

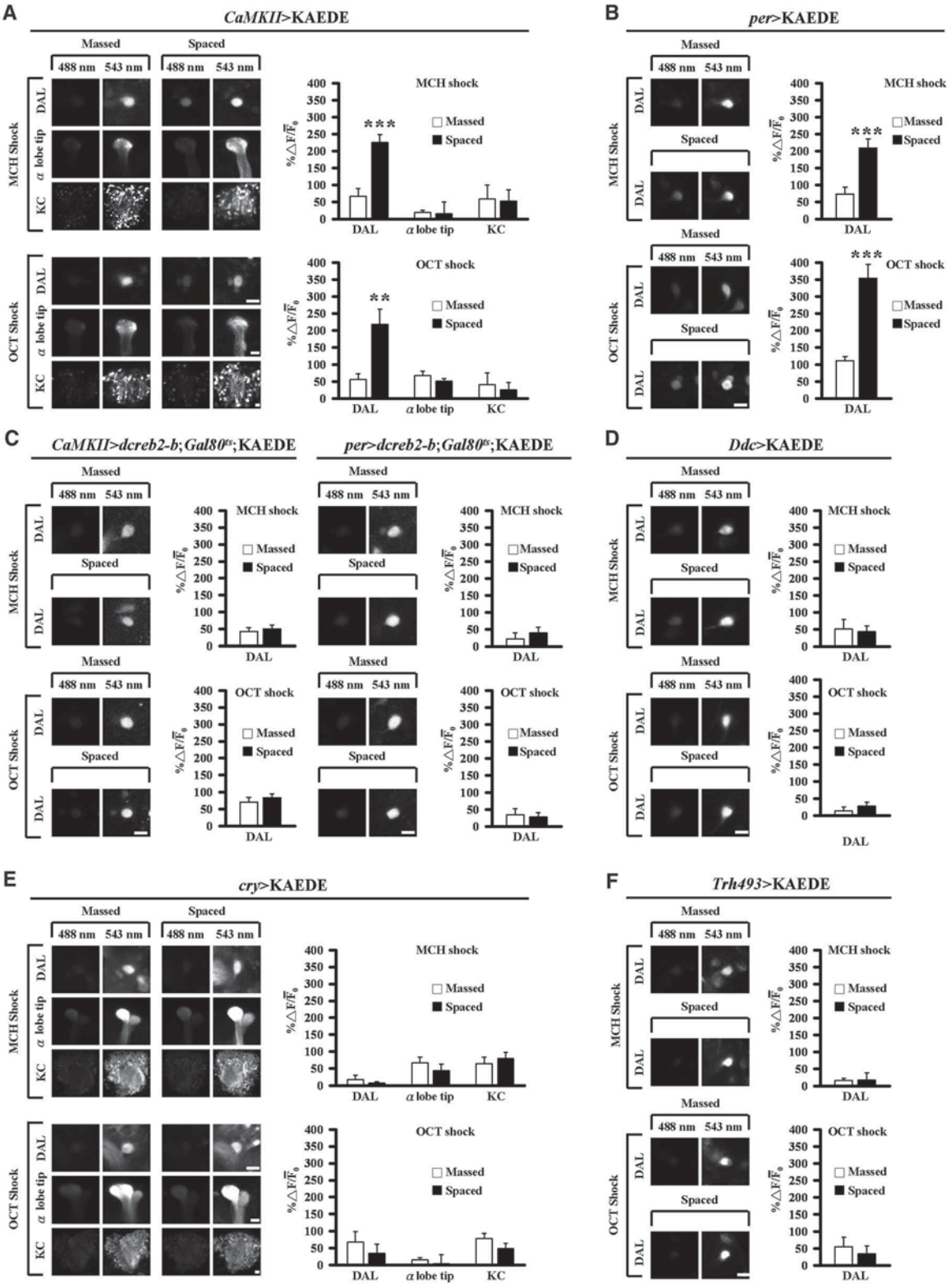

Fig. 6. (**A** to **F**) Spaced training–induced transcriptional activities. Living flies were subjected to UV irradiation to convert green KAEDE into red KAEDE just before training. KAEDE levels were quantified 24 hours after spaced or massed training to either 3-octanol (OCT) or 4-methylcyclohexanol (MCH). For each brain, a single optical slice through the cell body of a DAL neuron, MB α lobe tip, or MB cell bodies was taken under the same imaging conditions. KAEDE synthesis was determined as a ratio of new (green, 488 nm) to preexisting (red, 543 nm) KAEDE ($\%\Delta F/\bar{F}_0$). Adult specific expression of *UAS-dcreb2-b* was performed by removing *tub-Gal80^{ts}* inhibition at 30°C for 3 days before the experiment. Values are means ± SEM (N = 8 to 24 samples; **, $P < 0.01$; ***, $P < 0.001$). Scale bar, 10 μm.

to disrupt 1-day memory after spaced (but not massed) training (Fig. 5, A and C). Fifth, the transcriptional activities of *CaMKII* and *per* were elevated in DAL neurons after spaced (but not massed) training (Fig. 6, A and B). Sixth, the up-regulations of *CaMKII* and *per* in DAL neurons were CREB2-dependent (Fig. 6C). Seventh, neurotransmission from DAL neurons was required only for LTM retrieval but not for acquisition (LRN) or consolidation of LTM (Fig. 3H and fig. S7). Together, these data suggest that CaMKII and PER are bona fide "LTM proteins" synthesized in DAL neurons after spaced training.

$RICIN^{CS}$ not only allowed us to target inhibition of protein synthesis to individual neurons but also allowed us to investigate the critical window for protein synthesis during LTM formation, because of its rapid temporal control (Fig. 1C). Unexpectedly, activated $RICIN^{CS}$ did not affect LTM formation when expressed in MB neurons (Fig. 2B and fig. S5). Previous studies have shown that LTM formation involves the vertical axonal branches of αβ neurons in MBs (*20*), and LTM formation is blocked by overexpression of CREB repressor in MB [using *c739-Gal4* (*4*)]. Moreover, increases in neural activity in these structures at the time of LTM retrieval appear CREB-dependent (*4*, *7*). We clarified this apparent discrepancy by showing that (i) constitutive expression of CREB2b or $RICIN^{CS}$ in the MB neurons (using *c739-Gal4*, *OK107-Gal4*, and *c247-Gal4*) resulted in developmental defects of MB structure, along with defects in LTM (figs. S1 and S10); (ii) adult stage–restricted expression of CREB2b or activated $RICIN^{CS}$ in MB neurons yielded no detectable structural defects of MB and no LTM defects (figs. S5 and S10); (iii) adult stage–restricted expression of CREB2b or activated $RICIN^{CS}$ in DAL neurons was sufficient to impair LTM formation (Figs. 3 and 5); and (iv) spaced training–induced elevation of CaMKII occurred in DAL neurons but not in MB neurons and was diminished by expression of CREB2b (Fig. 6).

Possibly, a more stringent requirement for inhibition of protein synthesis exists in MB neurons rather than in DAL neurons. A 50% reduction of total protein synthesis in fly brains from cycloheximide feeding is sufficient to block LTM formation (*1*). Here, we show that activated $RICIN^{CS}$ in MB (or *per*-expressing) neurons results in an 80% reduction of KAEDE synthesis (Fig. 1, C to E). Also worth noting is that LTM defects in *dFmr1* mutants can be ameliorated somewhat by feeding flies inhibitors of protein synthesis (*32*). Thus, the inhibition of negative regulators of genes involved in LTM formation (in MB neurons) theoretically could enhance, rather than impair, 1-day memory after spaced training—an outcome we did not monitor in this study.

A functional memory circuit must (i) register (acquire) an experience through a persistent neural activity, (ii) consolidate (store) a lasting memory through (protein synthesis–dependent) structural or functional changes somewhere in that circuit; and (iii) retrieve a long-term memory through reactivation of (some or all) of the circuit. Neural activity in MB neurons contributes to acquisition, consolidation, and retrieval of LTM (*3*, *8*, *20*, *21*, *33*, *34*). Indeed, more than 30 different disruptions of LTM formation also diminish the calcium-based neural activity observed in αβ neurons in MB (*3*, *8*). Importantly, expression patterns of many genes involved in LTM formation suggest that other neuroanatomical regions also participate in neural activity essential for LTM formation, including glial cells (*35*), antenna lobes (*19*), asymmetrical body (*36*), ellipsoid body (*21*), many other unidentified neurons in 17 different LTM mutants (*37*), and, of course, DAL neurons. The latter are an interesting case, because neurotransmission from DAL neurons appears to be required only for retrieval, but not for acquisition or consolidation, of LTM (Fig. 3 and fig. S7). None of these data are sufficient, however, to identify the neurons in which protein synthesis–dependent memory consolidation (storage) occurs.

We provide evidence of memory consolidation in identified neurons via the combination of direct observation of protein synthesis with disruption of LTM formation through targeted inhibition of protein synthesis by activated $RICIN^{CS}$. We also found a CREB2-dependent up-regulation of CaMKII and PER after spaced but not massed training (Fig. 6, A to C), only the former of which induces LTM formation. These observations support the hypothesis that LTM consolidation occurs, at least in part, through CREB-mediated modulation of gene expression in DAL neurons (*2*, *38*). Further, our results indicate that CaMKII, PER, CREB2, DDC, TRH, dNR1, dNR2 and TEQUILA in DAL neurons are required at the time of training for normal LTM formation. In the case of DDC and TRH, however, spaced training did not up-regulate their transcription (Fig. 6, C to E), so they either are regulated posttranscriptionally or function as "basal" cellular machinery for the consolidation process.

Our data suggest a MB-DAL loop as part of the olfactory memory circuit. An olfactory experience first is communicated through olfactory sensory neurons and antennal lobe and registered in MB-APL-DPM as a neural activity (*19*, *39*–*42*). Neurotransmission from MB to DAL for consolidation (MB to DAL) occurs, and protein synthesis within DAL then yields structural and/or functional changes in DAL neural activity that communicate back to MB during retrieval (DAL to MB). Our observation that activated $RICIN^{CS}$ in neurons of the *cer-Gal4* expression pattern other than DAL still impairs LTM formation suggests that other extra-MB neurons also participate in the consolidation of LTM.

References and Notes

1. T. Tully, T. Préat, S. C. Boynton, M. Del Vecchio, *Cell* **79**, 35 (1994).
2. J. C. Yin *et al.*, *Cell* **79**, 49 (1994).
3. R. L. Davis, *Neuron* **70**, 8 (2011).
4. D. Yu, D. B. Akalal, R. L. Davis, *Neuron* **52**, 845 (2006).
5. M. Heisenberg, *Nat. Rev. Neurosci.* **4**, 266 (2003).
6. B. Gerber, H. Tanimoto, M. Heisenberg, *Curr. Opin. Neurobiol.* **14**, 737 (2004).
7. D. B. Akalal, D. Yu, R. L. Davis, *J. Neurosci.* **30**, 16699 (2010).
8. D. B. Akalal, D. Yu, R. L. Davis, *J. Neurosci.* **31**, 5643 (2011).
9. R. Ando, H. Hama, M. Yamamoto-Hino, H. Mizuno, A. Miyawaki, *Proc. Natl. Acad. Sci. U.S.A.* **99**, 12651 (2002).
10. H. Mizuno *et al.*, *Mol. Cell* **12**, 1051 (2003).
11. P. E. Hardin, J. C. Hall, M. Rosbash, *Nature* **343**, 536 (1990).
12. Y. Endo, K. Mitsui, M. Motizuki, K. Tsurugi, *J. Biol. Chem.* **262**, 5908 (1987).
13. Y. Endo, K. Tsurugi, *J. Biol. Chem.* **262**, 8128 (1987).
14. K. G. Moffat, J. H. Gould, H. K. Smith, C. J. O'Kane, *Development* **114**, 681 (1992).
15. A. S. Chiang *et al.*, *Curr. Biol.* **21**, 1 (2011).
16. T. Riemensperger, T. Völler, P. Stock, E. Buchner, A. Fiala, *Curr. Biol.* **15**, 1953 (2005).
17. A. Claridge-Chang *et al.*, *Cell* **139**, 405 (2009).
18. Y. Aso *et al.*, *Curr. Biol.* **20**, 1445 (2010).
19. S. I. Ashraf, A. L. McLoon, S. M. Sclarsic, S. Kunes, *Cell* **124**, 191 (2006).
20. A. Pascual, T. Préat, *Science* **294**, 1115 (2001).
21. C. L. Wu *et al.*, *Nat. Neurosci.* **10**, 1578 (2007).
22. M. P. Belvin, H. Zhou, J. C. Yin, *Neuron* **22**, 777 (1999).
23. T. Sakai, T. Tamura, T. Kitamoto, Y. Kidokoro, *Proc. Natl. Acad. Sci. U.S.A.* **101**, 16058 (2004).
24. J. Dubnau, L. Grady, T. Kitamoto, T. Tully, *Nature* **411**, 476 (2001).
25. S. E. McGuire, P. T. Le, R. L. Davis, *Science* **293**, 1330 (2001).
26. S. Xia *et al.*, *Curr. Biol.* **15**, 603 (2005).
27. H. H. Lin, J. S. Lai, A. L. Chin, Y. C. Chen, A. S. Chiang, *Cell* **128**, 1205 (2007).
28. M. D. Gordon, K. Scott, *Neuron* **61**, 373 (2009).
29. S. Martinek, M. W. Young, *Genetics* **156**, 1717 (2000).
30. S. E. McGuire, P. T. Le, A. J. Osborn, K. Matsumoto, R. L. Davis, *Science* **302**, 1765 (2003).
31. G. Didelot *et al.*, *Science* **313**, 851 (2006).
32. F. V. Bolduc, K. Bell, H. Cox, K. S. Broadie, T. Tully, *Nat. Neurosci.* **11**, 1143 (2008).
33. G. Isabel, A. Pascual, T. Préat, *Science* **304**, 1024 (2004).
34. J. Séjourné *et al.*, *Nat. Neurosci.* **14**, 903 (2011).
35. D. Comas, F. Petit, T. Préat, *Nature* **430**, 460 (2004).
36. A. Pascual, K. L. Huang, J. Neveu, T. Préat, *Nature* **427**, 605 (2004).
37. J. Dubnau *et al.*, *Curr. Biol.* **13**, 286 (2003).
38. R. Bourtchuladze *et al.*, *Cell* **79**, 59 (1994).
39. A. C. Keene, S. Waddell, *Nat. Rev. Neurosci.* **8**, 341 (2007).
40. X. Liu, R. L. Davis, *Nat. Neurosci.* **12**, 53 (2009).
41. C. L. Wu *et al.*, *Curr. Biol.* **21**, 848 (2011).
42. J. L. Pitman *et al.*, *Curr. Biol.* **21**, 855 (2011).

Acknowledgments: We thank S. Benzer, J. Blau, R. L. Davis, J. Hall, J. Hirsh, C. J. O'Kane, S. Kunes, L. Luo, T. Préat, M. Rosbash, S. Waddell, Y. Takamatsu, M. W. Young, and the Bloomington and Drosophila Genomics Resource Centers for fly stocks. We thank J. Hirsh, L. C. Griffith, and T. Préat for the antibodies. We also thank S. F. Teng for the preliminary test of *UAS-kaede*. This work was funded by grants from Dart Neurosciences LLC, National Science Council, and Ministry of Education to A.-S.C. C.-C.C., T.T., and A.-S.C. conceptualized the project and wrote the manuscript; C.-C.C. and A.-S.C. developed the methods and analyzed the data; C.-C.C., J.-K.W., T.-P.P., and C.-L.W carried out behavioral experiments; H.-W.L. and J.-K.W. performed imaging experiments; T.-F.F. generated the *UAS-kaede* transgenic flies; A.-S.C. supervised the project. The authors declare no competing financial interests. Correspondence and requests for materials should be addressed to A.-S.C.

Supporting Online Material

www.sciencemag.org/cgi/content/full/335/6069/678/DC1
Materials and Methods
Figs. S1 to S13
References (*43*–*45*)
Movie S1

16 August 2011; accepted 2 December 2011
10.1126/science.1212735

Structural Insight into the Ion-Exchange Mechanism of the Sodium/Calcium Exchanger

Jun Liao,[1]* Hua Li,[1,2]* Weizhong Zeng,[1,2] David B. Sauer,[1] Ricardo Belmares,[1]† Youxing Jiang[1,2]‡

Sodium/calcium (Na^+/Ca^{2+}) exchangers (NCX) are membrane transporters that play an essential role in maintaining the homeostasis of cytosolic Ca^{2+} for cell signaling. We demonstrated the Na^+/Ca^{2+}-exchange function of an NCX from *Methanococcus jannaschii* (NCX_Mj) and report its 1.9 angstrom crystal structure in an outward-facing conformation. Containing 10 transmembrane helices, the two halves of NCX_Mj share a similar structure with opposite orientation. Four ion-binding sites cluster at the center of the protein: one specific for Ca^{2+} and three that likely bind Na^+. Two passageways allow for Na^+ and Ca^{2+} access to the central ion-binding sites from the extracellular side. Based on the symmetry of NCX_Mj and its ability to catalyze bidirectional ion-exchange reactions, we propose a structure model for the inward-facing NCX_Mj.

Calcium signaling is essential for many physiological processes, including muscle contraction, cell mobility, fertilization, exocytosis, and apoptosis (*1*, *2*). One of the major players in regulating intracellular Ca^{2+} in eukaryotes is the Na^+/Ca^{2+} exchanger (NCX) (*3*–*5*), a Ca^{2+} transporter that can extrude intracellular Ca^{2+} across the cell membrane against its chemical gradient by using the downhill gradient of Na^+. For example, in cardiac myocytes, elevated cytosolic free Ca^{2+} required for muscle contraction must be removed rapidly to ensure relaxation. This clearance is carried out by the cardiac exchanger NCX1 (*6*), which extrudes Ca^{2+} into the extracellular space, and Ca^{2+} pumps, which restore Ca^{2+} into the sarcoplasmic reticulum. Several functional features of NCX define its physiological roles: It can exchange Ca^{2+} and Na^+ with a high turnover rate (*7*, *8*); the ion-exchange process is electrogenic, with a stoichiometry of three Na^+ for one Ca^{2+} (*8*–*13*); and the exchange reaction is bidirectional, depending on the membrane potential and the chemical gradient of Na^+ and Ca^{2+} (*3*). Because of its abundance in various tissues and its essential roles in Ca^{2+} homeostasis, dysfunctions of the Na^+/Ca^{2+} exchanger are associated with many human pathologies, including cardiac hypertrophy, arrhythmia, and postischemic brain damage (*3*, *14*, *15*).

Predicted to possess nine membrane-spanning helices, the transmembrane domain of the eukaryotic NCX is separated into two parts in primary sequence by a large intracellular regulatory domain (*4*, *5*, *16*, *17*). Interestingly, the removal of this intracellular domain still yields a highly active Na^+/Ca^{2+} exchanger, indicating that the transmembrane portion of the NCX constitutes the basic functional unit for ion transport (*18*, *19*). All NCX proteins contain two highly conserved homologous sequence motifs called α repeats, one on each part of the transmembrane domain, that are believed to arise from a gene-duplication event (*4*, *20*, *21*). Mutagenesis studies have demonstrated that both motifs are important for ion binding and translocation (*4*, *22*). The presence of the two homologous repeats is also the hallmark of other members of the cation-Ca^{2+} exchanger superfamily, most notably the NCKX family (*23*), a K^+-dependent Na^+/Ca^{2+} exchanger that was first found in the vertebrate eye (*24*), and microbial NCX homologs, which lack the large intracellular regulatory domain (*4*, *21*). To reveal the structural basis of the ion-exchange mechanism in NCX, we characterized the Na^+/Ca^{2+}-exchange function of an NCX homolog from *Methanococcus jannaschii*, named NCX_Mj, and determined its crystal structure to 1.9 Å resolution.

NCX_Mj functions as a Na^+/Ca^{2+} exchanger. We employed a $^{45}Ca^{2+}$ flux assay to determine the exchange function of NCX_Mj (*25*). Purified NCX_Mj was reconstituted into liposomes loaded with a buffer solution containing 120 mM NaCl, 30 mM KCl, and 1 μM $CaCl_2$ (buffered with EGTA) at pH 6.5. Ca^{2+} influx was initiated by exchanging the extraliposomal solution with a reaction buffer containing various concentrations of NaCl, KCl, and radioactive $^{45}CaCl_2$ and monitored by measuring the time-dependent accumulation of liposomal radioactivity (Fig. 1A). In the absence of any ionic gradient (the reaction buffer is the same as intraliposomal solution), we observed a slow influx of $^{45}Ca^{2+}$, probably due to the NCX_Mj-mediated Ca^{2+}/Ca^{2+} exchange (curve 1). Whereas an inward Ca^{2+} gradient promoted the influx of Ca^{2+} (curve 2, with 33 μM extraliposomal $^{45}CaCl_2$), the rate of Ca^{2+} influx was substantially enhanced by an outwardly directed Na^+ gradient (curve 3, with 60 mM extraliposomal NaCl), consistent with the behavior of

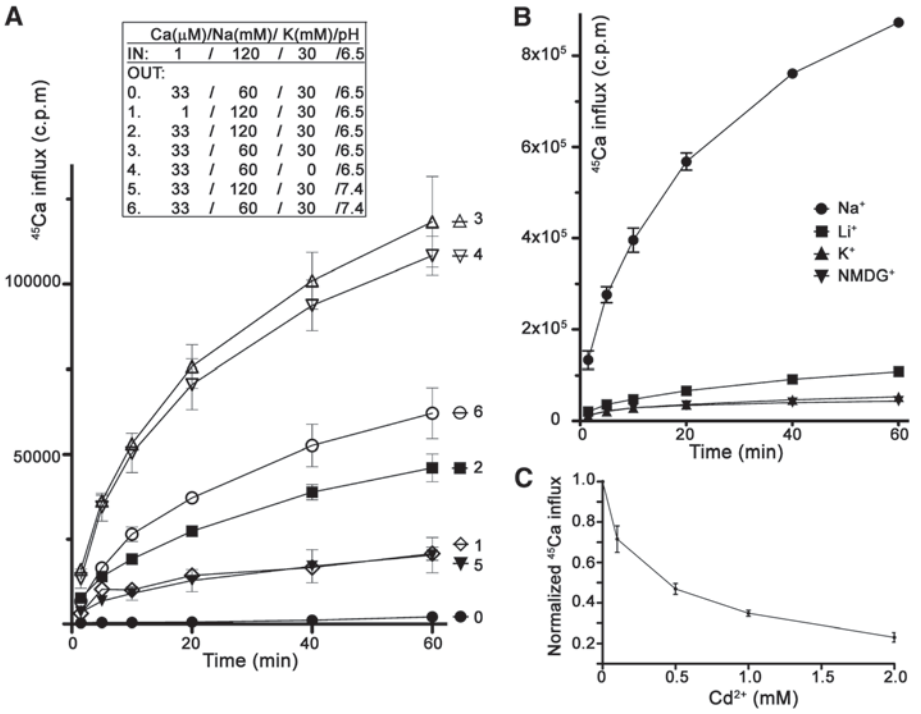

Fig. 1. $^{45}Ca^{2+}$ flux assays of NCX_Mj reconstituted liposomes. (**A**) Curves 1 to 6 show the time-dependent $^{45}Ca^{2+}$ influx with various extraliposomal reaction solutions, as listed in the inset. Curve 0 is the control assay using liposomes deficient of protein. The intraliposomal solution remains the same in all measurements. c.p.m., counts per minute. (**B**) Selectivity of NCX_Mj. The intraliposomal solution contained 120 mM of either Na^+, K^+, Li^+, or $NMDG^+$ as the only monovalent cation. The extraliposomal reaction solution contained 120 mM $NMDG^+$ and remained the same in all measurements. (**C**) Cd^{2+} blockage of NCX_Mj. The reaction solution is the same as that used for curve 3 in (A), except containing various concentrations of $CdCl_2$. The Ca^{2+} influx was terminated 20 min after adding $^{45}CaCl_2$. All data points are mean ± SEM of two independent experiments. Some data points shown in (B) contain error bars smaller than the representative symbols.

[1]Department of Physiology, University of Texas Southwestern Medical Center, Dallas, TX 75390–9040, USA. [2]Howard Hughes Medical Institute, University of Texas Southwestern Medical Center, Dallas, TX 75390–9040, USA.

*These authors contributed equally to this work.
†Present address: North Crowley High School, Fort Worth, TX 76123, USA.
‡To whom correspondence should be addressed. E-mail: youxing.jiang@utsouthwestern.edu

a Na^+/Ca^{2+} exchanger. This Na^+-facilitated Ca^{2+} influx is independent of K^+, as the removal of the extraliposomal KCl did not affect the rate of Ca^{2+} influx (curve 4). To test if NCX_Mj could be a H^+/Ca^{2+} exchanger, we performed a similar assay in an extraliposomal reaction solution of pH 7.4 (versus pH 6.5 inside). In the absence of a Na^+ gradient, the outward proton gradient actually reduces the influx of Ca^{2+} (curve 5), which can be partially alleviated by establishing an outwardly directed Na^+ gradient (curve 6), suggesting that NCX_Mj functions as a Na^+/Ca^{2+} exchanger rather than a H^+/Ca^{2+} exchanger. To confirm the Na^+ selectivity for the exchange function of NCX_Mj, we performed another set of $^{45}Ca^{2+}$ flux assays using liposomes loaded with a buffer solution containing either Na^+, K^+, Li^+, or $NMDG^+$ as the only monovalent salt. The results clearly demonstrate that intraliposomal Na^+ facilitates the Ca^{2+} influx at a much higher rate than other monovalents (Fig. 1B). The commonly observed divalent cation blockage of NCX (i.e., by Cd^{2+}) (*26*) was also tested on NCX_Mj by performing the flux assay with $CdCl_2$ in the reaction buffer. Cd^{2+} exhibits a concentration-dependent blockage of Ca^{2+} influx with a half-inhibition concentration of ~0.4 mM under our experimental conditions (Fig. 1C). Consistent with the flux assay, the exchanger-mediated Ca^{2+} uptake or extrusion was also observed in NCX_Mj expressing *Escherichia coli* cells (see supporting online material text and fig. S1).

Structural determination of NCX_Mj. We used two crystallization approaches to obtain the structure of NCX_Mj (*25*). First, the crystals were grown in the lipidic cubic phase (LCP), following a similar protocol as previously described (*27*). The LCP crystallization yielded well-diffracting crystals large enough for complete data collection with a single crystal. The crystals are of the $P2_12_12_1$ space group, with one subunit per asymmetric unit. The structure was determined by single isomorphous replacement with anomalous scattering using samarium derivatized crystals and refined to 1.9 Å (table S1). Second, a conventional crystallization approach using sitting drop vapor diffusion yielded NCX_Mj crystals in detergent, and the structure was determined at 3.6 Å using molecular replacement. The crystal structures obtained from both methods are virtually identical, demonstrating that NCX_Mj maintains the same structure in both detergent and lipid environments. Though the discussion focuses primarily on the LCP crystal structure, the lower-resolution structures in detergent provide important insight into the divalent blockage site of NCX_Mj.

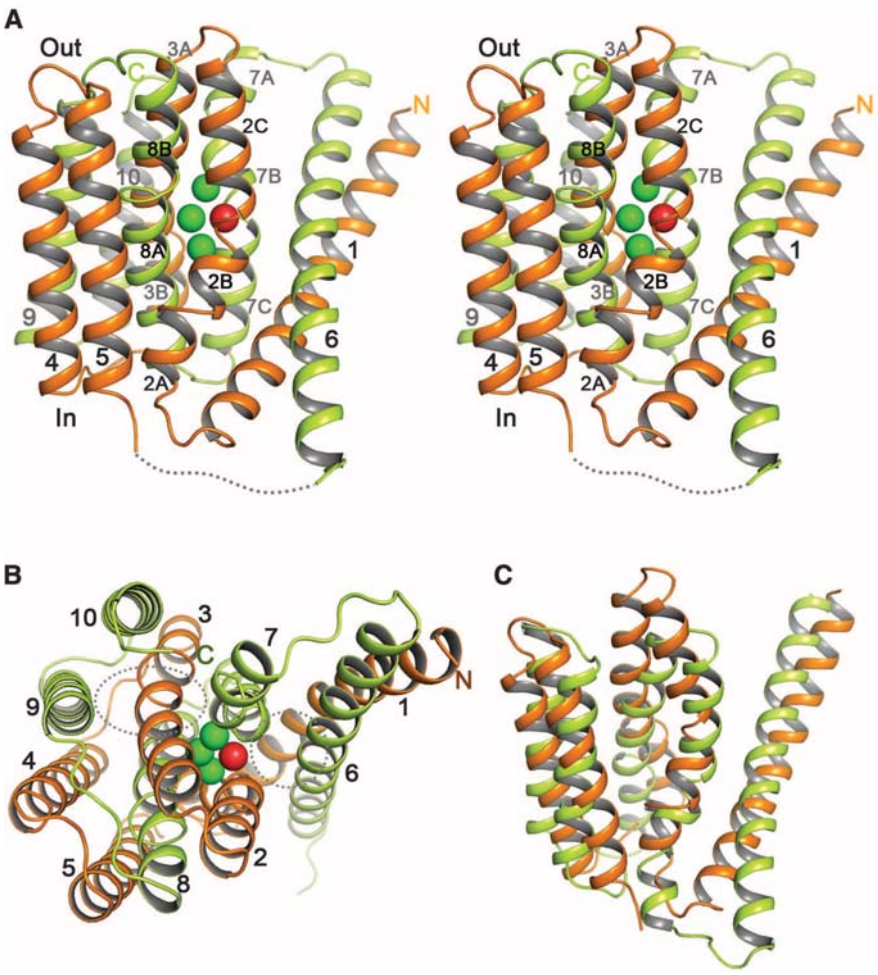

Fig. 2. Overall structure of NCX_Mj. (**A**) Stereo view of NCK_Mj viewed from the membrane. The N- and C-terminal halves are shown as orange and green ribbons, respectively. The four ion-binding sites are shown as green spheres for Na^+ and red spheres for Ca^{2+}. The dotted line represents the disordered loop between TMs 5 and 6. (**B**) View of NCX_Mj from the extracellular side. The dotted circle and oval indicate the entryways of external passages for Ca^{2+} and Na^+, respectively. (**C**) Superimposition between the N-terminal half (orange) of NCX_Mj and its inverted C-terminal half (green). All structure figures were generated in PyMOL (*40*).

Overall structure of NCX_Mj. NCX_Mj exists as a monomer in both crystal forms and contains 10 transmembrane (TM) helices, with both termini on the extracellular side (Fig. 2A and figs. S2 and S3), consistent with the predicted topology for YrbG, an NCX homolog from *E. coli* (*28*). Based on the similarity in sequence and hydrophobicity pattern between NCK_Mj and its eukaryotic counterparts, the eukaryotic NCX is likely to share the same 10-TM topology rather than the previously predicted 9-TM topology (fig. S2). Eight of the 10 helices (TMs 2 to 5 and 7 to 10) form a tightly packed core perpendicularly embedded in the membrane. TMs 1 and 6, on the other hand, are exceptionally long, with ~35 residues in each helix. They are oriented at an angle of ~45° to the membrane surface and appear to be loosely packed against the core. The two highly conserved α repeats, consisting of TMs 2 and 3 for α1 and TMs 7 and 8 for α2, are bundled in the center of the protein and surrounded by the other helices (Fig. 2B and fig. S3B). All α-repeat helices are bent into two (for TMs 3 and 8) or three (for TMs 2 and 7) segments (labeled alphabetically in Fig. 2A and fig. S2), creating a pocket in the middle of the bundle where Na^+ and Ca^{2+} bind. Beyond sequence homology, the N-terminal half of the protein shares a similar structure to the C-terminal half but with opposite topology, as though the two halves are related by a molecular dyad (Fig. 2C and fig. S3). Although structural repeats of 5-TM helices have been observed in other membrane transporters (*29*, *30*), the NCX_Mj structure represents a new fold, as a search of the structure database using DALI (*31*) yields no similar structures. The linker between the two halves in NCX_Mj is a short and disordered loop from residues 149 to 155. The equivalent linker in eukaryotic NCX is expected to be the large intracellular regulatory domain.

Na^+ and Ca^{2+} binding sites. The high-resolution structure reveals four potential cation binding sites in the protein core, at the center of the membrane (Fig. 2A). The four sites are arranged in a diamond shape, with the sites nearest to the extracellular and intracellular face labeled S_{ext} and S_{int}, respectively, and the two middle sites designated as S_{mid} and S_{Ca}, as the latter is the Ca^{2+}-specific site (Fig. 3, A and B). All residues participating in ion binding are from the two α repeats and are highly conserved in both the NCX and NCKX families of proteins (fig. S2), and mutating these residues in eukaryotic NCX leads to the loss of ion-exchange functions (*22*).

Both S_{ext} and S_{int} are surrounded by five oxygen ligands and share identical ligand chemistry

as well as geometry, with ion-ligand distances all within the range of 2.3 to 2.5 Å (Fig. 3A and fig. S4). The coordination number, ligand chemistry, and ion-ligand distances of both sites are consistent with Na^+ binding (*32*). Although Ca^{2+} has the same size and ion-ligand distances as Na^+, it tends to have more than five ligands for optimal coordination (*33*, *34*). The S_{Ca} site is surrounded by six oxygen ligands within the distances of 2.3 to 2.6 Å: two from the backbone carbonyls of Thr^{50} and Thr^{209} and four from the carboxylates of Glu^{54} and Glu^{213}; all are contributed by the signature sequence of GTSLPE (*35*) within the two α repeats. The coordination number, ion-ligand distances, and bidentate ion chelation of the two acidic side-chain carboxylates at the S_{Ca} site are characteristic of Ca^{2+} binding (*33*, *34*). To confirm that the density at S_{Ca} is from Ca^{2+}, we also collected diffraction data at a wavelength of 2.0 Å to optimize Ca^{2+} anomalous scattering. Anomalous signal is observed at the S_{Ca} site in the anomalous-difference map (Fig. 3C), confirming the specificity of Ca^{2+} binding at this site. Surrounded by the side chains of Glu^{54}, Asn^{81}, Glu^{213}, and Asp^{240}, the S_{mid} site has only four oxygen ligands within a 3 Å distance and does not appear to be optimal for either Na^+ or Ca^{2+} binding. As tetradentate ion binding is common for Na^+ but rare for Ca^{2+}, we suggest that this suboptimal site allows Na^+ binding at high concentration, which, along with S_{ext} and S_{int}, accommodates three Na^+ ions during the ion-exchange reaction. As further evidence of non-specificity at S_{mid}, we identified it as the divalent blockage site from the structure of NCX_Mj obtained by the conventional crystallization approach. In these crystals, $CdCl_2$ or $MnCl_2$ were essential additives for crystallization, and their binding at S_{mid} was determined from the anomalous-difference Fourier map (Fig. 3D). Without directly competing for the S_{Ca} site, the divalent blockers occupy the neighboring, less selective S_{mid} site, which in turn weakens or abolishes Ca^{2+} binding at S_{Ca} and may also block Na^+ translocation.

Several features of this cluster of four ion-binding sites are noteworthy and clearly related to the Na^+/Ca^{2+}-exchange function of the NCX family. First, the four sites are related by a two-fold rotational axis connecting S_{mid} and S_{Ca}, which coincides with the pseudomolecular dyad of the protein. Second, several ligands are shared by multiple sites, most notably the side-chain carboxylates from Glu^{54} and Glu^{213}, which are shared by S_{mid}, S_{Ca}, and S_{ext} (for E54) or S_{int} (for E213) (Fig. 3A and fig. S4). Third, all four sites are in close proximity, with the shortest distance of ~3.6 Å between the two middle sites (S_{mid} and S_{Ca}) (Fig. 3B). Furthermore, the proximity and presence of only three negatively charged ligands indicate that all four sites are unlikely to be occupied simultaneously. Indeed, the Fo-Fc ion-omit map clearly shows different intensity of the electron density at each site, indicating different ion occupancy (Fig. 3A).

Ion-permeation pathways and inward-outward conformational change. The NCX_Mj structure likely represents an outward-facing conformation, as two deep cavities are observed on the extracellular surface of the protein, penetrating into the protein core where Na^+ and Ca^{2+} bind and providing two independent solvent-accessible passageways for external ion access (Figs. 2B and 4A and fig. S5). One passage, surrounded by the external halves of TMs 3 (3A segment), 7 (7A and 7B segments), 9, and 10, connects the extracellular solvent to the Na^+-specific S_{ext} site. The other passage is partially surrounded by the external halves of TMs 2 (2C segment), 6, and 7 (7A and 7B segments), with an open gap between TMs 2 and 6, which is probably sealed off by the extracellular leaflet of membrane lipids, as acyl chains from monoolein were observed in the structure. This passageway allows Ca^{2+} access from the extracellular solvent to the Ca^{2+}-specific S_{Ca} site.

Whereas the NCX_Mj structure adopts an outward-facing conformation, several structural and functional features allow us to generate a feasible structure model for the inward-facing conformation. The symmetry of NCX_Mj and its ion-binding sites, as well as the bidirectional ion exchange, would suggest that the inward-facing model should maintain similar symmetry and ion accessibility but with ion-permeation pathways directed toward the intracellular side, analogous to an inverted structure of NCX_Mj. In addition, rapid bidirectional ion exchange requires a rapid conformational change between the inward- and outward-facing states, implying equivalent stability with a low-energy barrier to the transition, thus precluding a dramatic structural change between the two conformations. A superimposition of NCX_Mj and its inverted structure shows a near-perfect structural alignment over the α-repeat helix bundle but different positions for the peripheral helices of TMs 1 and 2A, as well as TMs 6 and 7A (fig. S6). The inward-facing model was generated by simply swapping these two helical regions as depicted (fig. S6). Similar approaches have been used to generate putative models in other secondary solute transporters with inverted structural repeats (*36*, *37*).

Compared to the outward-facing NCX_Mj, the inward-facing model maintains the same tightly

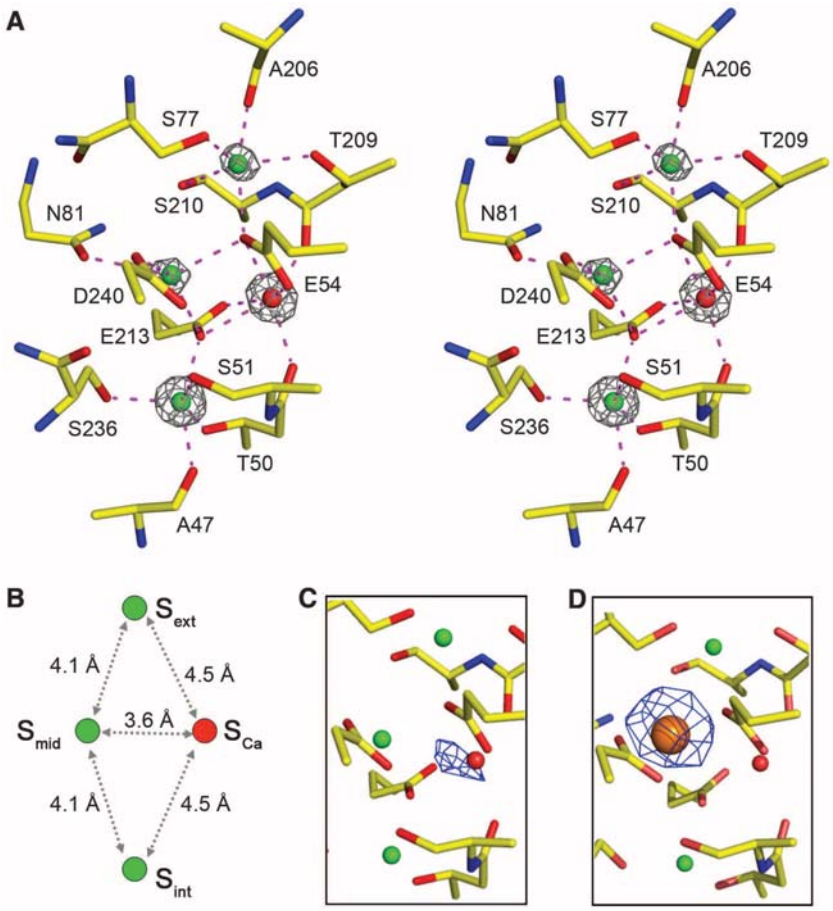

Fig. 3. Ion-binding sites of NCX_Mj. (**A**) Stereo view of the ion-binding sites. Green and red spheres represent Na^+ and Ca^{2+}, respectively. Gray mesh depicts electron density calculated from the F_o-F_c ion-omit map and contoured at 9σ. (**B**) Distances between adjacent ion-binding sites. (**C**) Density (blue mesh, contoured at 3.5σ) from the anomalous-difference Fourier map calculated using diffraction data of a LCP crystal at 2 Å wavelength indicates Ca^{2+} binding at the S_{Ca} site. (**D**) Density (blue mesh, contoured at 8σ) of bound Cd^{2+} (orange sphere) at the S_{mid} site from the anomalous-difference Fourier map. Diffraction data were collected at 2.0 Å from crystals grown in the presence of 10 mM $CdCl_2$ using the conventional crystallization method. Data from Mn^{2+}-containing crystals gave the same result.

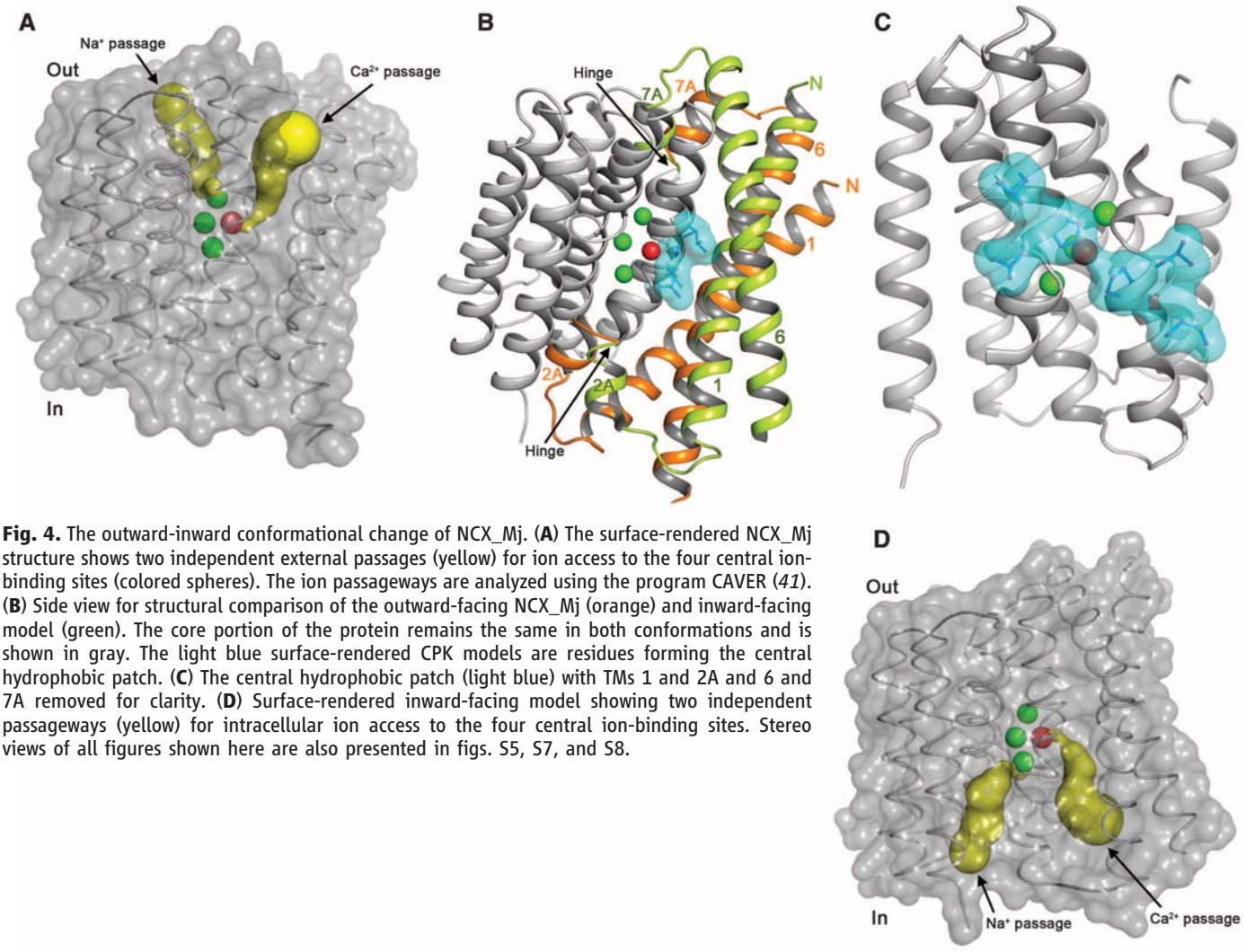

Fig. 4. The outward-inward conformational change of NCX_Mj. (**A**) The surface-rendered NCX_Mj structure shows two independent external passages (yellow) for ion access to the four central ion-binding sites (colored spheres). The ion passageways are analyzed using the program CAVER (*41*). (**B**) Side view for structural comparison of the outward-facing NCX_Mj (orange) and inward-facing model (green). The core portion of the protein remains the same in both conformations and is shown in gray. The light blue surface-rendered CPK models are residues forming the central hydrophobic patch. (**C**) The central hydrophobic patch (light blue) with TMs 1 and 2A and 6 and 7A removed for clarity. (**D**) Surface-rendered inward-facing model showing two independent passageways (yellow) for intracellular ion access to the four central ion-binding sites. Stereo views of all figures shown here are also presented in figs. S5, S7, and S8.

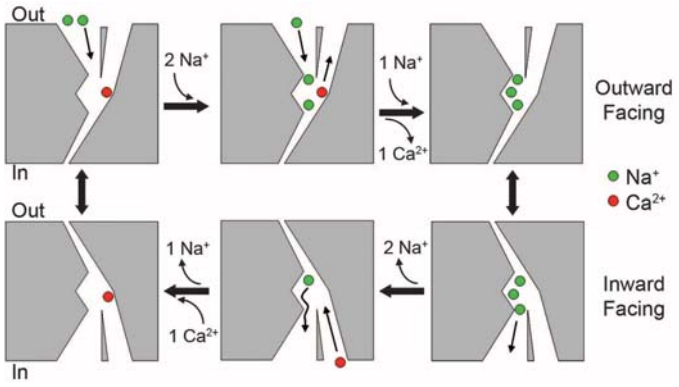

Fig. 5. Cartoon representation of Na^+/Ca^{2+} exchange of NCX in the classical $3Na^+:1Ca^{2+}$ extrusion mode.

packed core and ion-binding sites but has different packing between the peripheral helices (TMs 1, 2A, 6, and 7A) and the core (Fig. 4B and fig. S7). Without obvious steric clash, the inward-facing model retains similar hydrophobic-packing interactions between these helices and the core. The movement of TMs 1, 2A, 6, and 7A is hinged at the bends between TMs 2A and 2B and TMs 7A and 7B, and it may involve sliding across a central flat hydrophobic patch that is centered about the conserved Pro residues from the signature sequence motifs of the α repeats (Fig. 4C and fig. S8). Consequently, this proposed conformational change leads to the closure of the two outward-facing ion passageways and the formation of two inward-facing ones connecting the S_{int} and S_{Ca} sites, respectively, to the intracellular side (Fig. 4D and fig. S5B). With a simple sliding motion primarily involving two loosely packed helices, the outward and inward conformations can rapidly interchange, coupling to the alternative access of the four ion-binding sites from each side, consistent with the mechanism of rapid consecutive ion-exchange reaction in NCX (*3*, *8*, *38*, *39*).

Na^+/Ca^{2+}-exchange mechanisms. The arrangement of four central ion-binding sites with differing specificity and their alternating accessibility from each side upon conformational change reveal the structural mechanism of Na^+/Ca^{2+} exchange in NCX. Among the four sites, only S_{Ca} is specific for Ca^{2+} binding, whereas the other three are designed for Na^+ binding under physiological conditions, and their occupancy depends on the Na^+ concentration. Whereas S_{Ca} is alternatively accessible from each side, the three Na^+ sites are aligned in a winding single file with only one end being accessible in a given conformation: S_{ext} when facing outward and S_{int} when facing inward. Positioning these two identical, Na^+-specific sites on both ends ensures the selective and bidirectional Na^+/Ca^{2+}-exchange function in NCX.

The cluster of four sites in close proximity and ligand-sharing features in NCX_Mj lead us to propose a progressive antagonist effect of multiple Na^+ binding on Ca^{2+} affinity as depicted in the

cartoon representation of a simplified Na^+/Ca^{2+}-exchange reaction in the classic Ca^{2+} extrusion mode (Fig. 5). Starting with the Ca^{2+} bound, outward-facing conformation, the exchange reaction is initiated by the entry of Na^+ from the extracellular side, probably occupying the Na^+-optimized S_{int} and S_{ext} sites first. As each site competes for a negatively charged ligand with S_{Ca}, the binding of these two Na^+ ions decreases the Ca^{2+} affinity at S_{Ca} but may be insufficient for Ca^{2+} release due to the presence of high extracellular Ca^{2+} under physiological conditions. With a high external Na^+ concentration ($[Na^+]_o$), the entry of a third Na^+ ion increases Na^+ occupancy at S_{mid}, which further reduces the Ca^{2+} affinity and results in Ca^{2+} release to the extracellular side. Upon conformational change to an inward-facing state, the three bound Na^+ ions are exposed to the low intracellular $[Na^+]_i$ environment. As a weak binding site, the S_{mid} Na^+ is likely released first, possibly along with the S_{int} Na^+. The release of the bound Na^+ restores the high-affinity Ca^{2+} binding at S_{Ca}, which in turn leads to the release of the third Na^+ from S_{ext}. The conformational change reverting NCX_Mj to the Ca^{2+}-bound outward-facing state completes the cycle. This sequential binding of three Na^+ ions for the release of one Ca^{2+} explains the 3:1 stoichiometry of the Na^+/Ca^{2+}-exchange reaction and the cooperativity of Na^+ binding in activating Ca^{2+} release. This simplified exchange mechanism does not preclude other exchange ratios (*13*). For example, at high extracellular $[Na^+]_o$, the vacant S_{Ca} site upon Ca^{2+} release could also be occupied by a Na^+, resulting in a translocation of four Na^+ ions to the intracellular side. Likewise, depending on the Na^+ and Ca^{2+} concentrations, the bound Na^+ may not be completely unloaded upon Ca^{2+} binding from the intracellular side. The coexistence of these possibilities in the same transporter leads to a more complex process of Na^+/Ca^{2+} exchange and may explain the variability of the exchange ratios observed under different experimental conditions.

References and Notes

1. D. E. Clapham, *Cell* **131**, 1047 (2007).
2. M. J. Berridge, M. D. Bootman, H. L. Roderick, *Nat. Rev. Mol. Cell Biol.* **4**, 517 (2003).
3. M. P. Blaustein, W. J. Lederer, *Physiol. Rev.* **79**, 763 (1999).
4. K. D. Philipson, D. A. Nicoll, *Annu. Rev. Physiol.* **62**, 111 (2000).
5. R. DiPolo, L. Beaugé, *Physiol. Rev.* **86**, 155 (2006).
6. D. A. Nicoll, S. Longoni, K. D. Philipson, *Science* **250**, 562 (1990).
7. D. W. Hilgemann, *Biophys. J.* **71**, 759 (1996).
8. D. W. Hilgemann, D. A. Nicoll, K. D. Philipson, *Nature* **352**, 715 (1991).
9. J. P. Reeves, C. C. Hale, *J. Biol. Chem.* **259**, 7733 (1984).
10. M. P. Blaustein, J. M. Russell, *J. Membr. Biol.* **22**, 285 (1975).
11. H. Rasgado-Flores, M. P. Blaustein, *Am. J. Physiol.* **252**, C499 (1987).
12. J. Kimura, A. Noma, H. Irisawa, *Nature* **319**, 596 (1986).
13. T. M. Kang, D. W. Hilgemann, *Nature* **427**, 544 (2004).
14. D. Noble, *Science* **295**, 1678 (2002).
15. Y. Watanabe, Y. Koide, J. Kimura, *J. Pharmacol. Sci.* **102**, 7 (2006).
16. D. A. Nicoll, M. Ottolia, K. D. Philipson, *Ann. N. Y. Acad. Sci.* **976**, 11 (2002).
17. X. Ren, D. A. Nicoll, L. Xu, Z. Qu, K. D. Philipson, *Biochemistry* **49**, 8585 (2010).
18. D. W. Hilgemann, *Nature* **344**, 242 (1990).
19. S. Matsuoka, D. A. Nicoll, R. F. Reilly, D. W. Hilgemann, K. D. Philipson, *Proc. Natl. Acad. Sci. U.S.A.* **90**, 3870 (1993).
20. E. M. Schwarz, S. Benzer, *Proc. Natl. Acad. Sci. U.S.A.* **94**, 10249 (1997).
21. X. Cai, J. Lytton, *Mol. Biol. Evol.* **21**, 1692 (2004).
22. D. A. Nicoll, L. V. Hryshko, S. Matsuoka, J. S. Frank, K. D. Philipson, *J. Biol. Chem.* **271**, 13385 (1996).
23. H. F. Altimimi, P. P. Schnetkamp, *Channels (Austin)* **1**, 62 (2007).
24. H. Reiländer *et al.*, *EMBO J.* **11**, 1689 (1992).
25. Materials and methods are available as supporting material on *Science* Online.
26. T. L. Trosper, K. D. Philipson, *Biochim. Biophys. Acta* **731**, 63 (1983).
27. M. Caffrey, V. Cherezov, *Nat. Protoc.* **4**, 706 (2009).
28. A. Sääf, L. Baars, G. von Heijne, *J. Biol. Chem.* **276**, 18905 (2001).
29. S. Faham *et al.*, *Science* **321**, 810 (2008).
30. A. Yamashita, S. K. Singh, T. Kawate, Y. Jin, E. Gouaux, *Nature* **437**, 215 (2005).
31. L. Holm, P. Rosenström, *Nucleic Acids Res.* **38**, W545 (2010).
32. M. M. Harding, *Acta Crystallogr. D Biol. Crystallogr.* **58**, 872 (2002).
33. A. K. Katz, J. P. Glusker, S. A. Beebe, C. W. Bock, *J. Am. Chem. Soc.* **118**, 5752 (1996).
34. E. Pidcock, G. R. Moore, *J. Biol. Inorg. Chem.* **6**, 479 (2001).
35. Single-letter abbreviations for the amino acid residues are as follows: A, Ala; C, Cys; D, Asp; E, Glu; F, Phe; G, Gly; H, His; I, Ile; K, Lys; L, Leu; M, Met; N, Asn; P, Pro; Q, Gln; R, Arg; S, Ser; T, Thr; V, Val; W, Trp; and Y, Tyr.
36. L. R. Forrest *et al.*, *Proc. Natl. Acad. Sci. U.S.A.* **105**, 10338 (2008).
37. N. J. Hu, S. Iwata, A. D. Cameron, D. Drew, *Nature* **478**, 408 (2011).
38. D. Khananshvili, *Biochemistry* **29**, 2437 (1990).
39. M. A. Milanick, M. D. S. Frame, *Ann. N. Y. Acad. Sci.* **639**, 604 (1991).
40. W. L. DeLano, PyMOL (DeLano Scientific, San Carlos, CA, 2002); www.pymol.org.
41. M. Petřek *et al.*, *BMC Bioinformatics* **7**, 316 (2006).

Acknowledgments: We thank D. Rosenbaum for technical support with LCP crystallization, D. Hilgemann for discussion, and N. Nguyen for critical review of the manuscript. Structures shown in this report are derived from work performed at the Advanced Photon Source (19-ID and 23-ID beamlines), Argonne National Laboratory. Use of the Advanced Photon Source, an Office of Science User Facility operated for the U.S. Department of Energy (DOE) Office of Science by Argonne National Laboratory, was supported by the U.S. DOE under contract no. DE-AC02-06CH11357. We thank the beamline staff for assistance in data collection. This work was supported in part by the Howard Hughes Medical Institute and by grants from the David and Lucile Packard Foundation and the Welch Foundation (grant I-1578 to Y.J.). The atomic coordinates and structural factors have been deposited in the Protein Data Bank with the accession numbers 3V5U for the LCP crystal and 3V5S for the low-resolution crystal in detergent. The authors declare no competing financial interests.

Supporting Online Material

www.sciencemag.org/cgi/content/full/335/6069/686/DC1
Materials and Methods
SOM Text
Figs. S1 to S9
Table S1
References (*42*–*56*)

25 October 2011; accepted 21 December 2011
10.1126/science.1215759

REPORTS

One-Step Fabrication of Supramolecular Microcapsules from Microfluidic Droplets

Jing Zhang,[1] Roger J. Coulston,[1,2] Samuel T. Jones,[1,2] Jin Geng,[1,2] Oren A. Scherman,[1,2]* Chris Abell[1]*

Although many techniques exist for preparing microcapsules, it is still challenging to fabricate them in an efficient and scalable process without compromising functionality and encapsulation efficiency. We demonstrated a simple one-step approach that exploits a versatile host-guest system and uses microfluidic droplets to generate porous microcapsules with easily customizable functionality. The capsules comprise a polymer-gold nanoparticle composite held together by cucurbit[8]uril ternary complexes. The dynamic yet highly stable micrometer-sized structures can be loaded in one step during capsule formation and are amenable to on-demand encapsulant release. The internal chemical environment can be probed with surface enhanced Raman spectroscopy.

The encapsulation of materials for protection and phase separation has evolved into a major interdisciplinary research focus (*1*, *2*). Synthetic microcapsules (*3*, *4*), in which the composition of the shell structure and the core content can be controlled, have found importance in applications as diverse as cell encapsulation (*5*, *6*), drug delivery (*7*), diagnostics (*8*), catalysis (*9*), food additives (*10*), and electronic displays (*11*). Preparation of conventional polymeric microcapsules via the layer-by-layer (L-b-L) technique (*12*, *13*), although powerful, suffers from reduced encapsulation efficiencies as a result of postfabrication loading. Alternative self-assembly processes, either by forming polymersomes (*14*) or by colloidal emulsion-templating (*15*, *16*), still lack monodispersity, stability, high loading efficiency, and material diversity in the resulting microcapsules, restricting their function

[1]Department of Chemistry, University of Cambridge, Lensfield Road, Cambridge CB2 1EW, UK. [2]Melville Laboratory for Polymer Synthesis, Department of Chemistry, University of Cambridge, Lensfield Road, Cambridge CB2 1EW, UK.

*To whom correspondence should be addressed. E-mail: oas23@cam.ac.uk (O.A.S.); ca26@cam.ac.uk (C.A.)

and subsequent applications. As a subset of colloidal emulsions, microfluidic droplets (*17*) show great promise as a platform for many microcapsule fabrication techniques (*18*–*20*) on account of their monodispersity, high fabrication throughput with economic use of reagents, and ease of scaleup.

We report a class of microcapsule prepared in a single step using a microdroplet platform, combining the advantages of microfluidic droplets and supramolecular host-guest chemistry with quantitative loading efficiency. Cucurbit[8]uril (CB[8]) (*21*) is used as the host molecule because it is capable of forming stable yet dynamic complexes with guest compounds in water with extremely high affinity. Moreover, this larger CB homolog is capable of simultaneously accommodating two guests to form a 1:1:1 ternary complex in water (*21*) [with an association constant (K_a) up to 10^{15} M^{-2}] through multiple noncovalent interactions with an electron-deficient first guest such as methyl viologen (MV^{2+}) and an electron-rich second guest, such as naphthol (Np) derivatives (Fig. 1A) (*22*). The ability of CB[8] to act as a supramolecular "handcuff" was further exploited by modifying gold nanoparticles (AuNPs) and water-soluble copolymers with complementary functionalities, thereby achieving a controlled dispersion of AuNPs in a polymer network held together by CB[8] (*23*).

During microcapsule preparation, microdroplets were first generated in a microfluidic device, using a simple T-junction geometry (*24*) (Fig. 1B). The oil carrier phase was directed perpendicular to the aqueous dispersed phase, which consisted of three inlets for the aqueous solutions of CB[8], MV^{2+}-AuNPs (**1a**), and Np-containing copolymer (**2a**). Droplets were generated as the oil phase sheared off the aqueous phase, before passing through a winding channel designed for thorough mixing of the three reagents (Fig. 1C). With an oil:water flow rate ratio of 2:1, droplets were generated at a frequency of 300 Hz and exhibited a high level of monodispersity when collected on a microscope slide, as indicated by the narrow size distribution with a mean diameter of 59.6 μm (Fig. 1D) and a low coefficient of variation of 1.3%.

Individual stable microcapsules were observed immediately after dehydration of the microdroplet precursor. After 150 s, the spherical shape of the droplet was slightly distorted (Fig. 2A), until the capsules eventually collapsed on a glass surface. The individual microcapsules (Fig. 2B) can be easily isolated after the evaporation of the oil phase. The diameters of the initial droplets ($d_{droplet}$) and the corresponding microcapsules ($d_{capsule}$) decreased with the increasing ratio of the flow rate of the oil phase (Q_{OIL}) to the flow rate of the aqueous phase (Q_{AQ}) (Fig. 2C). By merely varying Q_{OIL}/Q_{AQ}, stable droplet precursors and microcapsules could be generated with a $d_{droplet}$ of 42 to 67 μm and a $d_{capsule}$ of 10 to 24 μm, with polydispersities of 0.9 ± 0.4%. Upon rehydration, rupture of some isolated microcapsules was observed, revealing their hollow nature (Fig. 2D). A scanning electron microscopy (SEM) image of a

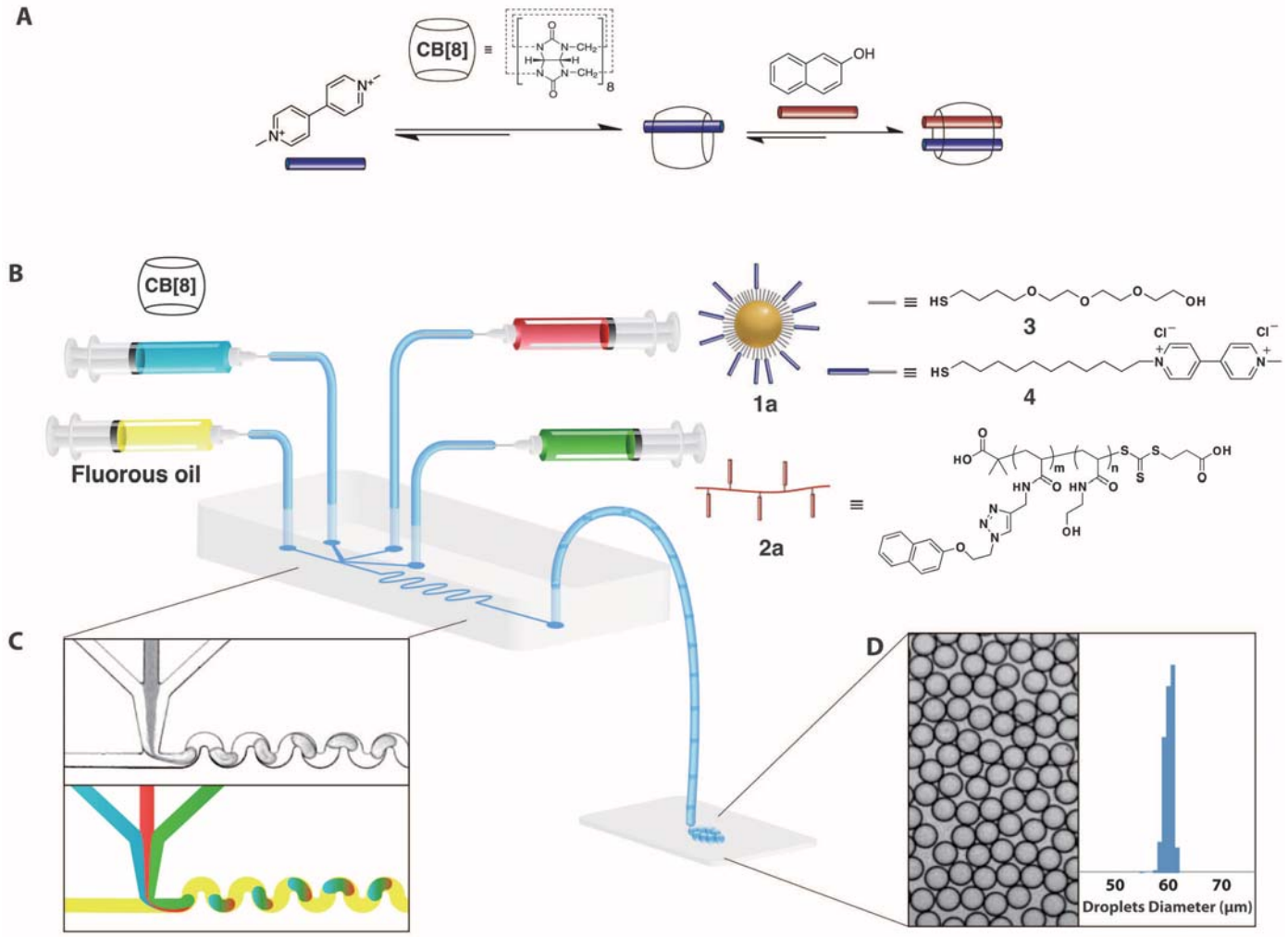

Fig. 1. (**A**) The two-step, three-component formation of the CB[8] ternary complex in water with MV^{2+} (blue) and Np (red). (**B**) Schematic representation of the microdroplet generation process using a microfluidic T-junction device, consisting of an continuous oil phase perpendicular to a combination of three aqueous solutions of CB[8], **1a** (AuNP functionalized with a mixture of neutral and viologen-containing ligands **3** and **4**), and **2a** (copolymer functionalized with Np) as the dispersed phase. (**C**) Microscopic image and the schematic of the T-junction and a wiggled channel for rapid mixing of reagents online. (**D**) The high monodispersity of microfluidic droplets is demonstrated by the narrow size distribution (diameter 59.6 ± 0.8 μm).

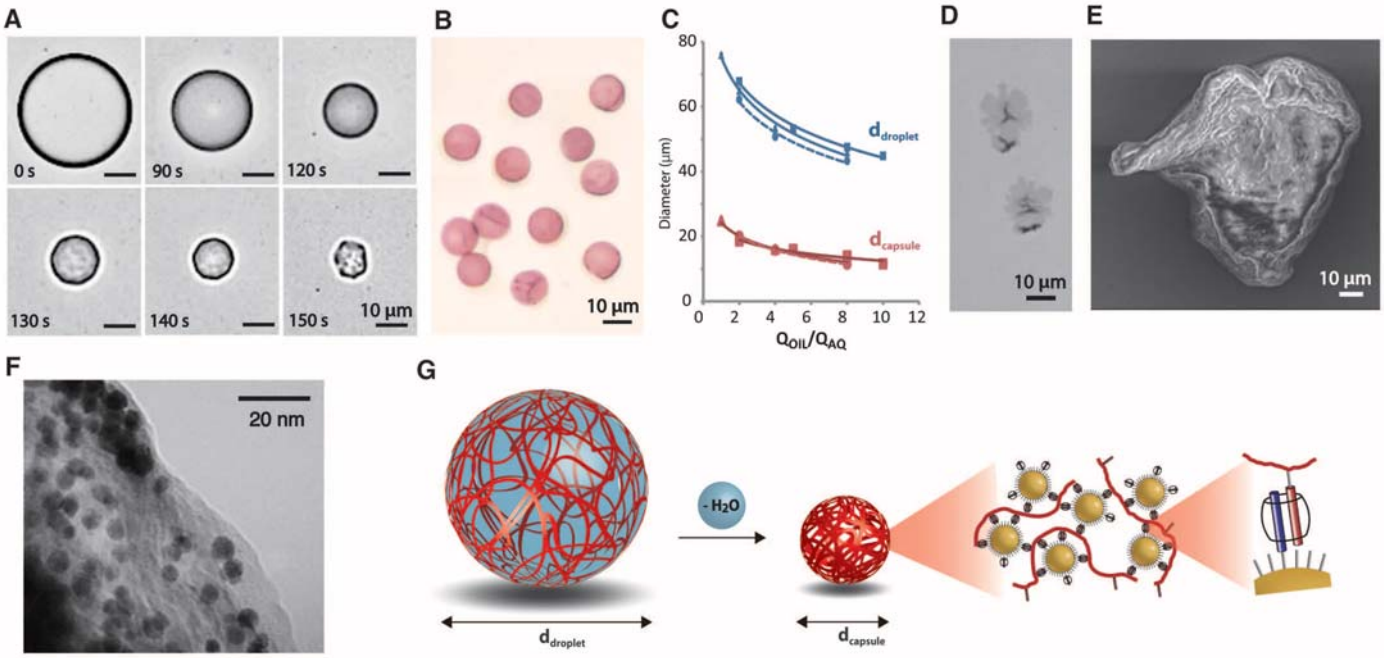

Fig. 2. (**A**) Brightfield images of the capsule formation process as the aqueous phase evaporates, resulting in a collapsed microcapsule-like structure. (**B**) Brightfield image of isolated microcapsules. (**C**) Variation in the mean diameters of initial droplets ($d_{droplet}$, blue) and corresponding stable microcapsules ($d_{capsule}$, red) as a function of the Q_{OIL}/Q_{AQ} ratio of aqueous solution for Q_{AQ} = 60 μl/hour (squares), 100 μl/hour (triangles), and 140 μl/hour (circles). (**D**) Brightfield image of burst capsules, showing the relics of the capsule shell. (**E**) SEM image of a dried microcapsule. (**F**) TEM image of the microcapsule shell, showing AuNPs approximately 5 nm in diameter dispersed in a mesh of polymer. (**G**) Schematic representation of the proposed microcapsule formation process from the initial droplet stage with a diameter $d_{droplet}$ to the dehydrated stable capsules of a diameter of $d_{capsule}$.

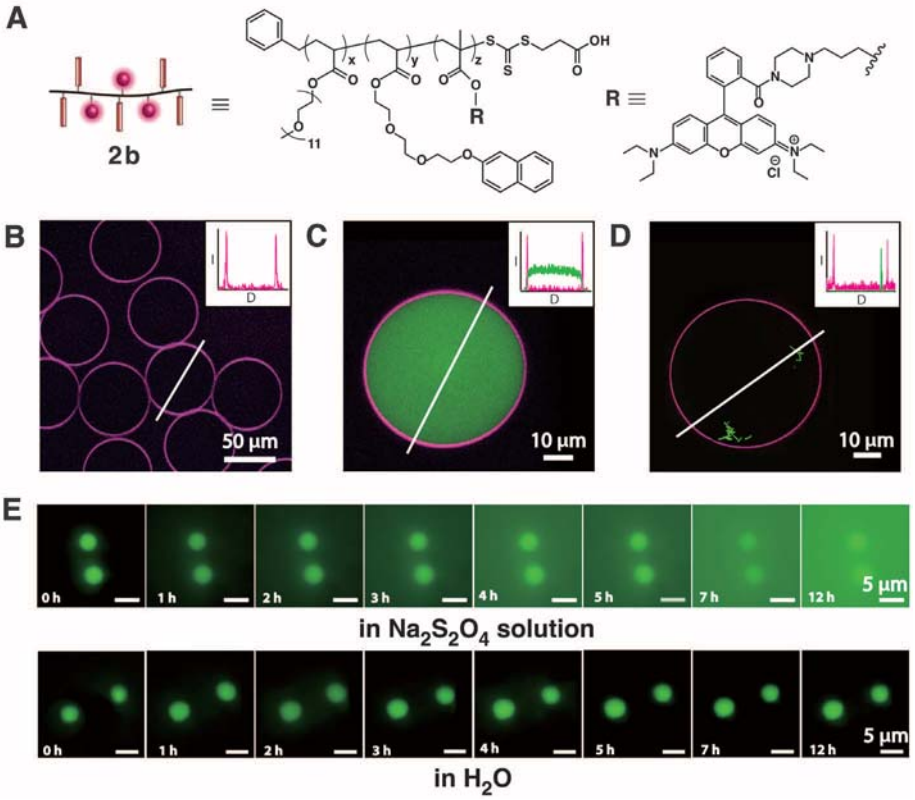

Fig. 3. (**A**) Chemical structure of rhodamine-B–containing copolymer **2b**. (**B**) LSCM image of empty capsules containing **2b** in the shell. (**C**) LSCM image of capsules containing aqueous solutions of CB[8], **1a**, **2b**, and FITC-dextran. (**D**) LSCM image of a capsule containing aqueous solutions of CB[8], **1a**, **2b**, and green fluorescent protein–expressing *Escherichia coli* cells. The inserts in (B) to (D) display the corresponding fluorescence intensity profiles (I, intensity; D, distance). (**E**) Fluorescence images of the process of disintegration of the microcapsule wall material in an aqueous solution of $Na_2S_2O_4$ or in H_2O over 12 hours (h) in a N_2 environment at 25°C.

hollow capsule that has collapsed because of a lack of internal support is shown in Fig. 2E.

A transmission electron microscopy (TEM) image (Fig. 2F) shows that the capsule shell consists of a supramolecular self-assembled network of AuNPs **1a** and copolymer **2a**, where individual AuNPs are interlinked via a mesh of the polymer. The formation of a supramolecular microcapsule is schematically represented in Fig. 2G, where the deposition of the supramolecular composite of CB[8], **1a**, and **2a** at the oil/water interface is assisted by interfacial tension stabilization through

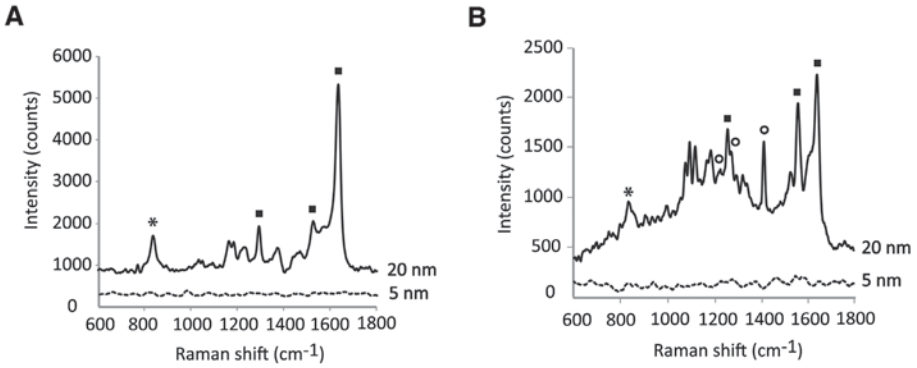

Fig. 4. (**A**) SERS spectra of empty microcapsules consisting of 5-nm-diameter and 20-nm-diameter AuNPs **1a** and **1b** using a 633-nm laser, showing characteristic peaks for CB[8] (asterisks) and MV^{2+} (squares): 830 cm^{-1}, 1630 cm^{-1}, 1560 cm^{-1}, and 1308 cm^{-1}. (**B**) SERS spectra of FITC-dextran encapsulated microcapsules consisting of AuNPs **1a** and **1b** using a 633-nm laser, showing characteristic peaks for FITC (circles) in addition to those for capsule shell materials: 1186 cm^{-1}, 1232 cm^{-1}, and 1400 cm^{-1}.

polymers and nanoparticles (*25*). The fabrication process showed that the microcapsules were resistant to heat (100°C) and reduced pressure (20 Pa), on account of the highly stable CB[8] 1:1:1 ternary complexes. Microcapsule formation was not observed when CB[8] was replaced with the smaller homolog CB[7], which is unable to form ternary complexes (*23*). Furthermore, when the AuNPs were not functionalized with the MV^{2+} ligand, no stable microcapsules were formed (fig. S1).

The microdroplet-assisted loading of water-soluble cargo was investigated by simultaneously incorporating a rhodamine-B functionality onto the polymer backbone (**2b**) (Fig. 3, A and B) and a fluorescein isothiocyanate–labeled dextran (FITC-dextran) into the capsule cavity. Aqueous solutions of **2b** and FITC-dextran were injected into the microfluidic device with solutions of CB[8] and **1a**. Droplets were collected in a reservoir, and fluorescence images were recorded with a laser scanning confocal microscope (LSCM) (*26*). The integrity of the capsule shell was not compromised by such loading, as shown by a clearly defined layer of rhodamine fluorescence confined to the water/oil interface of the droplets, whereas the interior of the capsule was filled evenly with FITC-dextran, as is apparent from the FITC fluorescence (Fig. 3C). The fluorescence intensity plot clearly shows that the rhodamine exterior is distributed in the "shell" forming outside the "cargo," whereas the FITC fluorescence is only observed inside the microcapsules. Other types of cargo were also similarly encapsulated, including bacterial cells (Fig. 3D).

The capsules benefit from properties arising from the supramolecular CB[8] host-guest network. For example, the incorporation of the rhodamine-B–containing polymer demonstrates the ease of adding customizable functionality using the supramolecular approach (*27*). Stimuli-triggered degradation of the capsules (*28*) is also possible by a one-electron reduction of the MV^{2+} moiety, leading to on-demand release of encapsulated cargo (*29*). One-electron reduction of MV^{2+} generates the radical cation $MV^{+\bullet}$, which rapidly forms a stable 2:1 $(MV^{+\bullet})_2$:⊂CB[8] inclusion complex (*30*). When microcapsules containing the 500-kD FITC-dextran were isolated into an aqueous solution of sodium dithionite ($Na_2S_2O_4$) free of oxygen, controlled dissipation of the fluorescence over time was observed (Fig. 3E). Conversely, the microcapsules failed to release the encapsulated 500-kD FITC-dextran when an N_2 atmosphere was not maintained or in the absence of $Na_2S_2O_4$. Without external stimuli, these microcapsules also allowed passive diffusion of the encapsulated cargo with appropriate molecular mass. The 500-kD FITC-dextran was retained by the microcapsules after rehydration, whereas the 10-kD counterpart was capable of diffusing freely into the external environment (fig. S2).

The incorporation of AuNPs further allows these microcapsules to be used as substrates for surface-enhanced Raman spectroscopy (SERS) (*31*–*33*). Using the modular supramolecular approach (*26*), two microcapsules were prepared, one containing 5-nm-diameter (**1a**) and a second with 20-nm-diameter (**1b**) AuNPs. When the samples were excited with a 633-nm laser, characteristic SERS signals for CB[8] and MV^{2+} were observed (Fig. 4A) (*34*). The signal strength derived from the capsules containing **1b** was much greater than those containing **1a**, because SERS field enhancement is dependent on the distance between AuNPs and the size of the AuNPs (*35*). SERS mapping of microcapsules showed that the SERS signals were uniformly localized within the capsules (fig. S3). To investigate the feasibility of detecting encapsulated materials by SERS, FITC-dextran was loaded into the microcapsules. Significant Raman enhancement of the FITC signals was observed in addition to those from CB[8] and MV (Fig. 4B). A similar dependence on the size of the AuNPs for the degree of enhancement was observed, demonstrating the potential of the porous microcapsule shell as a SERS substrate for the detection of encapsulated materials.

We have described the preparation, characterization, and application of a microcapsule held together by supramolecular host-guest 1:1:1 ternary complexes of CB[8], MV^{2+}-AuNPs, and a Np-containing copolymer at the liquid/liquid interface of microfluidic droplets. These microcapsules are produced from microdroplets in one step with high frequency and monodispersity. Upon dehydration, stable microcapsules with a hollow interior can be isolated within minutes. When an additional aqueous stream is incorporated, a wide variety of materials can be quantitatively encapsulated during capsule formation. Stimulus-triggered on-demand release of the encapsulated cargo is achieved as a result of the supramolecular host-guest chemistry incorporated in the capsule shell. Additionally, these microcapsules exhibit strong plasmonic properties on account of the AuNPs present and can be used as a SERS substrate for the encapsulated materials.

References and Notes

1. T. Wang *et al.*, *Nat. Biotechnol.* **15**, 358 (1997).
2. T. Douglas, M. Young, *Nature* **393**, 152 (1998).
3. H. N. Yow, A. F. Routh, *Soft Matter* **2**, 940 (2006).
4. S. F. M. van Dongen *et al.*, *Chem. Rev.* **109**, 6212 (2009).
5. G. Orive *et al.*, *Nat. Med.* **9**, 104 (2003).
6. A. Léonard *et al.*, *Chem. Soc. Rev.* **40**, 860 (2011).
7. L. J. De Cock *et al.*, *Angew. Chem. Int. Ed.* **49**, 6954 (2010).
8. H. Ke *et al.*, *Angew. Chem.* **123**, 3073 (2011).
9. C. S. Peyratout, L. Dähne, *Angew. Chem. Int. Ed.* **43**, 3762 (2004).
10. M. A. Augustin, Y. Hemar, *Chem. Soc. Rev.* **38**, 902 (2009).
11. B. Comiskey, J. D. Albert, H. Yoshizawa, J. Jacobson, *Nature* **394**, 253 (1998).
12. F. Caruso, R. A. Caruso, H. Möhwald, *Science* **282**, 1111 (1998).
13. E. Donath, G. B. Sukhorukov, F. Caruso, S. A. Davis, H. Möhwald, *Angew. Chem. Int. Ed.* **37**, 2201 (1998).
14. D. E. Discher, F. Ahmed, *Annu. Rev. Biomed. Eng.* **8**, 323 (2006).
15. J. Cui *et al.*, *Adv. Funct. Mater.* **20**, 1625 (2010).
16. D. Patra *et al.*, *Langmuir* **25**, 13852 (2009).
17. A. B. Theberge *et al.*, *Angew. Chem. Int. Ed.* **49**, 5846 (2010).
18. A. S. Utada *et al.*, *Science* **308**, 537 (2005).
19. S. Abraham, Y. H. Park, J. K. Lee, C.-S. Ha, I. Kim, *Adv. Mater.* **20**, 2177 (2008).
20. H. Zhang *et al.*, *J. Am. Chem. Soc.* **128**, 12205 (2006).
21. J. Kim *et al.*, *J. Am. Chem. Soc.* **122**, 540 (2000).
22. U. Rauwald, O. A. Scherman, *Angew. Chem. Int. Ed.* **47**, 3950 (2008).
23. R. J. Coulston, S. T. Jones, T.-C. Lee, E. A. Appel, O. A. Scherman, *Chem. Commun. (Camb.)* **47**, 164 (2011).
24. T. Thorsen, R. W. Roberts, F. H. Arnold, S. R. Quake, *Phys. Rev. Lett.* **86**, 4163 (2001).
25. D. Patra, A. Sanyal, V. M. Rotello, *Chem. Asian J.* **5**, 2442 (2010).
26. Materials and methods are available as supporting material on *Science* Online.
27. P. Arumugam, H. Xu, S. Srivastava, V. M. Rotello, *Polym. Int.* **56**, 461 (2007).
28. A. P. Esser-Kahn, S. A. Odom, N. R. Sottos, S. R. White, J. S. Moore, *Macromolecules* **44**, 5539 (2011).

29. A. P. R. Johnston, G. K. Such, F. Caruso, *Angew. Chem. Int. Ed.* **49**, 2664 (2010).
30. W. S. Jeon, H.-J. Kim, C. Lee, K. Kim, *Chem. Commun. (Camb.)* **38**, 1828 (2002).
31. S. Abalde-Cela *et al.*, *Soft Matter* **7**, 1321 (2011).
32. H. Hwang, S.-H. Kim, S.-M. Yang, *Lab Chip* **11**, 87 (2011).
33. W.-F. Dong, G. B. Sukhorukov, H. Möhwald, *Phys. Chem. Chem. Phys.* **5**, 3003 (2003).
34. S. Mahajan *et al.*, *Phys. Chem. Chem. Phys.* **12**, 10429 (2010).
35. J. R. Anema, J.-F. Li, Z.-L. Yang, B. Ren, Z.-Q. Tian, *Annu. Rev. Anal. Chem.* **4**, 129 (2011).

Acknowledgments: This work was supported by Engineering and Physical Sciences Research Council Basic Technology Translational grant EP/H046593/1, a European Research Council Starting Investigator Grant (ASPiRe) ERC-2009-StG-240629, and a European Union NanoSci-E+ (CUBiHOLE) grant EP/H007024/1. SERS experiments were performed with the assistance of S. Mahajan. The DH5α *Escherichia coli* strain was a kind gift from M. Welch and S. Bowden from the Department of Biochemistry, University of Cambridge. The naphthol-containing polymer was a kind gift from E. Appel from the Department of Chemistry, University of Cambridge. The authors thank X. Liu, C. A. Smith, S. Mahajan, J. J. Baumberg, and W. T. S. Huck for the helpful discussions. J.Z., R.J.C., O.A.S., and C.A. have filed a provisional application for a GB patent on the fabrication process.

Supporting Online Material
www.sciencemag.org/cgi/content/full/335/6069/690/DC1
Materials and Methods
Figs. S1 to S3
References (*36*–*40*)

18 October 2011; accepted 18 January 2012
10.1126/science.1215416

Determination of Noncovalent Docking by Infrared Spectroscopy of Cold Gas-Phase Complexes

Etienne Garand,[1] Michael Z. Kamrath,[1] Peter A. Jordan,[1] Arron B. Wolk,[1] Christopher M. Leavitt,[1] Anne B. McCoy,[2] Scott J. Miller,[1] Mark A. Johnson[1]*

Multidentate, noncovalent interactions between small molecules and biopolymer fragments are central to processes ranging from drug action to selective catalysis. We present a versatile and sensitive spectroscopic probe of functional groups engaged in hydrogen bonding in such contexts. This involves measurement of the frequency changes in specific covalent bonds upon complex formation, information drawn from otherwise transient complexes that have been extracted from solution and conformationally frozen near 10 kelvin in gas-phase clusters. Resonances closely associated with individual oscillators are easily identified through site-specific isotopic labeling, as demonstrated by application of the method to an archetypal system involving a synthetic tripeptide known to bind biaryl substrates through tailored hydrogen bonding to catalyze their asymmetric bromination. With such data, calculations readily converge on the plausible operative structures in otherwise computationally prohibitive, high-dimensionality landscapes.

A central strategy in both contemporary drug discovery and chemical synthesis exploits multiple weak or reversible hydrogen (H)–bonding interactions among embedded functional groups to achieve selective docking arrangements between complex yet flexible molecular architectures. Diverse examples include the peptidic interaction motifs underlying antibiotic activity (*1*) and asymmetric catalysis (*2*–*5*), as well as, in a larger sense, the field of supramolecular chemistry (*6*). Although simulation plays an increasingly important role in guiding these efforts (*7*–*10*), there is a clear demand for experimental methods that can probe the docking geometries of the noncovalently bonded partners. Many of the key attachment points involve complementary H-bonding between C=O, N-H, and O-H groups, with increasing evidence emerging for the special role that charged motifs (e.g., involving $-NH_3^+$ and $-CO_2^-$ interactions with neutral partners) play in enhancing noncovalent binding (*3*, *4*, *11*). In favorable cases, x-ray crystal structures, nuclear magnetic resonance, or two-dimensional vibrational spectroscopies (*12*–*14*) can yield this information, but more often the key species occur as short-lived transients that are not amenable to these approaches. Here, we demonstrate how a cryogenic vibrational spectroscopic method, carried out after the complexes are preformed in solution and then isolated in the gas phase, can be used to identify the specific C=O and N-H groups that link a small molecule to a polypeptide in a mass-selective variation of site-specific, isotope edited spectroscopy (*12*, *15*–*17*).

We focused on a protonated tripeptide catalyst, and a biaryl substrate molecule (Fig. 1), where the noncovalent docking complex is a positively charged variation of the intermediate invoked to rationalize stereoselective bromination of the substrate (*2*, *18*). The complex thus provides an archetypal example wherein multidentate interactions were designed to provide highly selective docking of a small molecule in the context of a flexible catalytic scaffold. The operative attachment motifs involve H-bonding; O-H groups on the substrate (**S**) and N-H groups on the catalyst (**C**) constitute the donors, and the O-H, =O, and –N: sites on both species can act as potential acceptors. Four important functional groups are denoted by Greek letters (α,β,γ,δ) in Fig. 1 for reference. Our goal was to elucidate experimentally which specific acceptor-donor pairs might be active in the complex formation. Structural characterization of the complex involved first establishing the spectral signatures of the intramolecular H-bonds that fold the isolated tripeptide catalyst. The sensitivity of these modes to H-bonding interactions was revealed by following how the H-bonding pattern changed when the excess proton, which dominates the H-bonded interactions in **C**, was replaced by the more mobile Na^+ ion that binds primarily through electrostatic interactions. We then determined which bonds are directly involved in a binding site that supports the docking arrangement with the biaryl substrate.

The key advance enabling vibrational spectroscopic characterization of these complexes is the recently developed ability to extract them from solution by electrospray ionization and quench them into stable local configurations by cryogenic ion processing (*19*–*21*). In this approach, the ions are first tagged with weakly bound hydrogen molecules (fig. S1) such that single-photon (linear) vibrational action spectra can be obtained by following the photoinduced mass loss accompanying excitation of vibrational resonances. In the present case, D_2 tags were used rather than H_2 because their larger molecular masses helped separate the parent and fragment signals. Such infrared (IR) spectra are obtained for mass-selected species with an instrument that integrates mass spectrometry with photofragmentation (*19*, *22*, *23*). This method is generally applicable, and yields spectra of complex ions and ion-solvent clusters cooled to around 10 K (*22*–*24*), which display intrinsic linewidths as low as 6 cm^{-1} in both the fingerprint region as well as the higher-frequency X-H stretches. Because the power requirements of the excitation source are very modest (compared to the more commonly used infrared multiple photon dissociation), the technique can be implemented with table-top laser sources (*19*, *20*), and the resulting linear absorption spectra are readily compared with calculated patterns of vibrational fundamentals.

The challenges confronting structural analysis of noncovalent interactions with IR spectroscopy are immediately evident in Fig. 1, which compares the D_2 predissociation spectrum of **C** with that of the **C-S** complex. Although both species exhibit many sharp transitions scattered throughout the mid-IR spectral region, the overall patterns are quite similar in the signature amide I region (mostly C=O stretches from 1600 to 1800 cm^{-1}) and the amide A region (largely N-H stretches from 3300 to 3500 cm^{-1}). Nonetheless, a few coarse features of the intermolecular binding ar-

[1]Sterling Chemistry Laboratory, Yale University, Post Office Box 208107, New Haven, CT 06520, USA. [2]Department of Chemistry, The Ohio State University, Columbus, OH 43210, USA.

*To whom correspondence should be addressed. E-mail: mark.johnson@yale.edu

rangement in **C-S** are evident by cursory inspection of the overall band pattern. For example, the two free O-H stretches associated with **S** (indicated by arrows at the right of Fig. 1B) are not present in the spectrum of the **C-S** complex, indicating that both O-H groups donate H-bonds to the catalyst. The other qualitative difference is that the complex does not display the strong band near 2700 cm^{-1} clearly evident in the spectrum of **C**. That feature was tentatively assigned in an earlier survey (*20*), to an N-H^+ stretch from the ionic center engaging in an intramolecular H-bond. Its absence in **C-S** thus suggests that the internal H-bond in isolated **C** is disrupted when **S** is captured in one or more of the possible binding sites.

Beyond these cursory observations, however, it is pointless to extract detailed structures by comparing these spectra with the patterns predicted for the many calculated local minima. This is especially true as multiple isomers could be formed by the quenching procedure from room temperature to ~10 K in the ion trap. The key to our approach is to unravel which amide groups contribute to the various features in the critical amide I and amide A regions that reveal H-bond activity. This, in turn, requires that transitions can be traced to local oscillators embedded in the bimolecular assembly. At the outset, it was not obvious this would be the case as peptide spectra in solution are often considered in the context of delocalized excitons comprising contributions from multiple nearly equivalent C=O oscillators (*12*, *25*). In that case, activity in the amide I region would reflect collective motions not readily traced to a particular C=O group.

To access the degree of coupling between oscillators, we first carried out a study to monitor how site-specific placement of ^{13}C in the carbonyl of the α amide (Fig. 1) affects the suite of amide I bands. The resulting spectrum (Fig. 2) reveals that only one strong band in the amide I region (at 1640 cm^{-1}) is significantly shifted (with a weak shoulder and three minor additional perturbations much lower in vibrational frequency). This effectively isolates the location of the α-C=O stretch from overlapping bands in this region and verifies that the intrinsic width of the embedded feature is small. If the C=O stretches were intimately coupled to form a delocalized band-type structure, we would expect that removal of one of them by lowering its frequency out of the band would affect the rest. The fact that nearby bands are not affected by isotopic substitution, however, establishes that the local displacement of the α-C=O is primarily responsible for its particular transition even when the normal isotope is in place at that site. This result is not typical for the behavior of biological peptides and likely reflects the unique chemical environment created by the catalytic scaffold.

The simple response of the complex series of bands to site-specific isotopic substitution raises the prospect that many such features may be embedded in the spectra that could act as local reporters of their H-bonding environments in the spirit of the pioneering work by Rizzo and coworkers (*26*). Testing this hypothesis required synthesis of many individual, isotopically labeled analogs of the two compounds central to this study (see supporting online text for details). Figure 3 summarizes the results of site-selective isotope incorporation at four key locations within the four amide groups in **C** (see fig. S2 for raw spectra). Cursory inspection of the subtracted spectra immediately establishes that mass changes at each site contribute to only one of the amide I bands, and unambiguously identifies the specific N-H groups responsible for the two bands in the amide A region. One key feature of the particular bands that dominate the response in Fig. 3 is that they typically display shifts that approach those expected for the reduced mass change arising from substitution with ^{13}C or ^{15}N in a diatomic C=O or N-H bond (36 and 8 cm^{-1}, respectively). This highlights again that these vibrational modes are all very local oscillators, in contrast to the exciton-like, delocalized picture commonly accepted in peptide spectroscopy (*12*, *25*). The local nature of these oscillators is also confirmed by normal mode analysis in the context of harmonic spectrum calculations (see fig. S3).

The band assignments obtained from isotopic substitution are summarized with the color scheme in Fig. 3A, which includes a few contributions in the amide II region. The observed locations of the N-H donor and C=O acceptor transitions in **C** provide a particularly clear picture of the intramolecular interactions that fold the protonated peptide under the conditions of this experiment. The two horizontal arrows in trace 3A depict the range of transition frequencies corresponding to nonbonded and fully H-bonded situations for the amide I and amide A regions. The experimental spectrum is consistent with the **C** structure inferred from a computational search in a previous report (*20*) and shown schematically at the top of Fig. 3. This structure features two intramolecular H-bonds indicated by the dotted lines, in one of which the β-N-H (orange) acts as an H-bond donor and is thus red-shifted by ~130 cm^{-1} from the free δ-N-H group (green) (*27*, *28*). The third N-H is associated with the charge center involved in the intramolecular H-bond and appears near 2700 cm^{-1} (N-H^+ in Fig. 1A). We can also follow the response of the two H-acceptors, where the carbonyl groups [α (red) and γ (blue)] are found ~85 cm^{-1} lower than the two free carbonyls [δ (green) and β (orange)]. In this case, the groups engaged in H-bonding are conveniently red-shifted from those that are nonbonded and appear in otherwise clear regions of the spectrum. Consequently, the lower-energy amide I doublet is traced to the two C=O groups accepting H-bonds whereas two complementary N-H stretches (amide A) are red-shifted relative to the single nonbonded N-H group near 3500 cm^{-1}.

Having considered the band shifts associated with the intramolecular H-bonds that clamp the isolated peptide, it is a useful exercise to exploit the set of site-labeled variants of the catalyst to follow the structural changes when the excess proton is replaced by a positively charged target species with a different interaction profile. We can then follow how the various bands evolve as the catalyst binds a simpler species than the multidentate biaryl guest central to this work. The

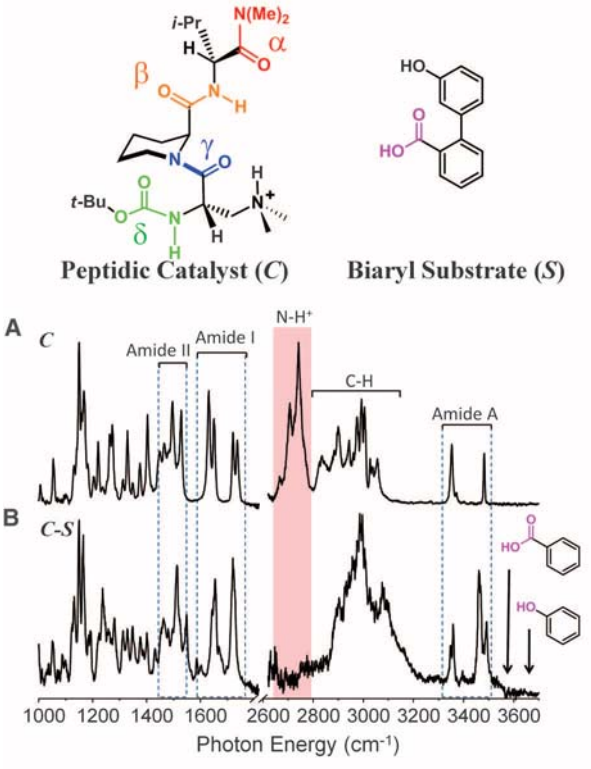

Fig. 1. The schematic structure of the peptide catalyst (**C**) and the biaryl substrate (**S**). Comparison of the infrared D_2-predissociation spectra of (**A**) **C** and (**B**) **C-S** complex. The characteristic amide regions discussed in the text are highlighted, along with the location of the intramolecular N-H^+ bond in **C**. The frequencies of free OH stretches are indicated by arrows in trace (B).

sodium ion, Na^+, provides an excellent candidate for this purpose as we expect it to strongly favor coordination to one or more of the carbonyls (*29*, *30*), and the deprotonated catalyst cannot engage in an ionic, intramolecular H-bond (largely responsible for its cyclic motif).

The D_2 predissociation spectrum of the tripeptide complexed with Na^+, $\mathbf{C}_{Na}$, is compared with that of **C** in fig. S4. The most pronounced qualitative difference is the disappearance of the intense 2720 cm^{-1} feature in the $\mathbf{C}_{Na}$ spectrum, confirming its assignment to the N-H^+ intramolecular H-bond as suggested above. The higher-frequency amide A bands are similar in the two systems, however, indicating that one of the two remaining N-H groups again participates in an intramolecular H-bond. The amide I region of $\mathbf{C}_{Na}$ still displays four distinct peaks, but their positions and intensities differ from those in **C** and the entire suite appears more compact and generally centered between the open doublets found in the **C** spectrum.

To unravel which constituents within the **C** groups are involved in the internal H-bond, as well as to establish those coordinated most closely to the ion, we followed the evolution of the various bands by using the isotopic shifts of the four sites that were studied in the protonated **C** spectra (Fig. 3). The raw data from this study are shown in fig. S5. Figure 4, A and B, compares the resulting positions of the various groups in the **C** and $\mathbf{C}_{Na}$ systems, using the same color scheme as before. Surprisingly, the most notable change going from **C** to $\mathbf{C}_{Na}$ occurs in the amide A region where the carriers of the two N-H stretch peaks are exchanged. This change implies a profound rearrangement in which the carbonyl binding of Na^+ leads the N-H of the δ amide (green) to engage in an internal H-bond while the β-N-H (orange), which acts as a donor in **C**, becomes free. Both members of the lower-energy doublet in the amide A H-bonding region are unambiguously traced to the δ amide group.

The evolution of the amide I bands from **C** to $\mathbf{C}_{Na}$ reveals the response of the C=O stretches, which are again color-coded in Fig. 4B according to amide group as indicated on the left. The α band (red), which accepted the strong ionic H-bond from the N-H^+ group in **C**, blue-shifts by 33 cm^{-1} in $\mathbf{C}_{Na}$ and changes places in energy ordering with the γ band (blue). The doublet structure of the δ amide I contribution (green) is also interesting in light of the doubling of its amide A transition, again suggesting that two closely related conformers are in play. We have confirmed that the two members of the doublet (labeled δ and δ*) are indeed due to different species by using a two-laser, isomer-selective measurement relying on photochemical hole burning (*31*), with the results shown in fig. S6. Cis and trans orientations of the *tert*-butyl (*t*-Bu) group are plausible assignments for these conformers on the basis of the calculated energies and harmonic spectra. The δ-C=O band is red-shifted relative to its position in **C** such that it overlaps the β amide I feature (orange). This points to a scenario in which three of the C=O groups interact with the ion to an appreciable extent. These qualitative features of the binding motif provide crucial constraints that narrow the computational search space and make it possible to quickly identify the local minimum that is responsible for the observed spectral features. The lowest-energy form thus obtained is displayed schematically at the left of Fig. 4B (see fig. S7 for the calculated harmonic spectra). Overall, we see that with the loss of the charged intramolecular H-bond in **C**, the peptide rearranges its conformation to accommodate the Na^+ atom by optimizing the more

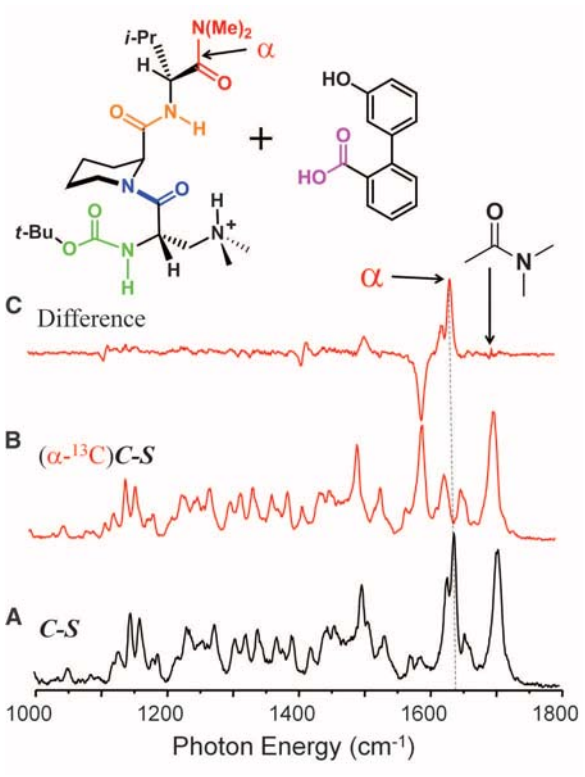

Fig. 2. IR D_2-predissociation spectrum of **C-S** with (**A**) all ^{12}C and ^{14}N, and (**B**) with α-^{13}C. The spectral changes upon isotopic labeling are highlighted in trace (**C**) which was generated by subtracting trace (B) from trace (A). Positive-going peaks in the difference spectrum indicate bands that disappear upon ^{13}C incorporation, whereas negative-going peaks reveal the location of the displaced transition, so that the mass effect manifests as a derivative-type line shape when the shift is small. The amide I frequency of isolated dimethylacetamide is indicated with an arrow.

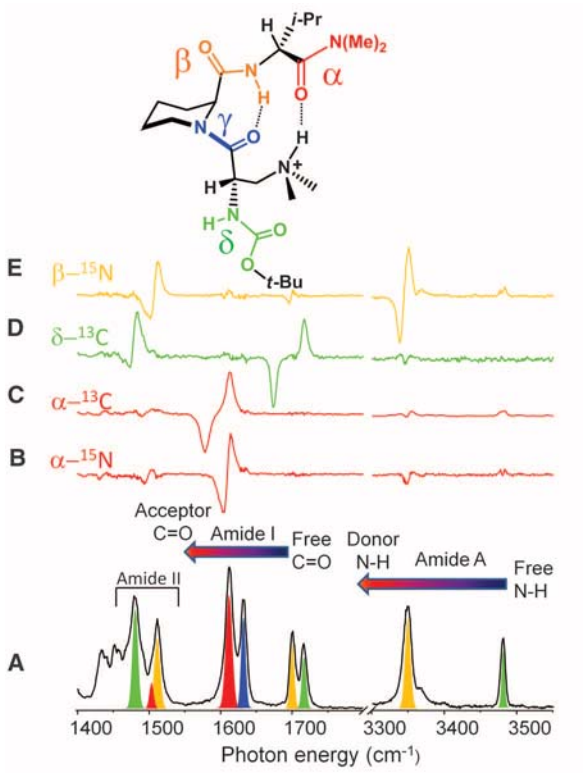

Fig. 3. (**A**) IR D_2-predissociation spectrum of **C** with all ^{12}C and ^{14}N. The spectra with heavy isotopes at the indicated positions were subtracted from trace (A) to obtain the color-coded difference spectra (**B**) to (**E**) in the four upper traces (see raw spectra in fig. S2). The color coding of the traces and peaks corresponds to the functional groups as indicated in the top schematic structure.

physical (electrostatic) interactions with three of the carbonyls (*29*, *30*). The neutral H-bond evident in the δ amide A region is then traced to the nearby tertiary amine group, while the β-N-H is rotated free as its C=O group pivots away from the ion.

We now turn to the docking motif that tethers the biaryl substrate to the peptide scaffold in the noncovalently bound complex, **C-S**. The absence of free O-H transitions (Fig. 1B) already established that both O-H groups on **S** are engaged in donor H-bonds. The positions of the **S**–CO_2H–based transitions are established by following the effect of ^{13}C placement in the acid group, with the difference spectrum displayed in fig. S8. This spectrum reveals that the acid C=O stretch is a dominant component of the higher-energy amide I feature at 1704 cm^{-1} (highlighted in purple in the color-coded spectrum in Fig. 4C). This carboxylic acid–derived transition falls about 50 cm^{-1} below the 1752 cm^{-1} value reported (*32*, *33*) for isolated benzoic acid (labeled in Fig. 4C), indicating that its C=O component is engaged as an acceptor of either a charged single H-bond or multiple neutral H-bonds. There are, indeed, two closely spaced bands in the neutral H-bonded N-H region near 3350 cm^{-1} in Fig. 4C that could in principle be engaged in such a scenario. However, the site-specific difference spectra unambiguously trace both members of this doublet to the same β-N-H group, and thus, like the $\mathbf{C}_{Na}$ system, this doubling likely results again from two isomeric forms of the adduct (labeled β and β*) in Fig. 4C. The other NH group must therefore reside in a nonbonding site; we can rule out the double donor possibility and conclude that the acid carbonyl binds to the protonated amine.

Because the basicity of the substrate is much smaller than that of the deprotonated catalyst, the complexation cannot dislodge the excess proton from its point of attachment at the tertiary amine in **C**. Although ionic H-bonding to the acid group may appear counterintuitive at first glance, it is in fact typical for organic acids, RCO_2H, to share an excess proton between their carbonyl groups in the proton-bound binary complexes ($RCOH{=}O\cdot\cdot H^+\cdot\cdot O{=}COHR'$) (*34*, *35*). This propensity is consistent with the preferential protonation of the bare carboxylic acids at the C=O to form diol-type arrangements [$R\text{-}(OH)_2^+$]. When the α-C=O is displaced by –CO_2H on **S**, the N-H^+ band is expected to blue-shift due to the lower basicity of the acid group relative to that of the (α) amide (790.1 versus 877.0 kJ/mol for gas-phase basicity, respectively) (*36*). The nature of the acid functionality is further defined by the behavior of the weaker bands at lower energy, which probe the motion of the C-OH moiety. The difference spectrum in fig. S8 reveals a transition affected by ^{13}C substitution in the acid group near 1250 cm^{-1}. This wide splitting of the two bands associated with –CO_2H (1700 and 1250 cm^{-1}) confirms that the general structure of the acid is intact (i.e., HO-C=O as opposed to a salt-bridge motif involving –CO_2^-) and is therefore acting as a strongly H-bonded domain that both accepts and donates (recall the missing free O-H discussed above) an H-bond to **C**.

To address the roles of the H-bonding sites on **C**, we again followed the evolution of the specific groups using the four isotope labels as before (raw data are in fig. S9). Like the case of the α amide depicted in Fig. 1, all sites yield definitive assignments of bands associated with the N-H donors and C=O acceptors, with the results included in the color-coded segments of the amide I and A regions in Fig. 4C. The α-C=O in **C-S** is blue-shifted relative to its position in **C**, consistent with the loss of the ionic H-bond to N-H^+, but still lies well below the range for a free C=O stretch. As a result, we conclude that it accepts a neutral H-bond. The remaining labeled transitions on the catalyst establish that the β-N-H acts as a donor whereas the δ-N-H is free. The δ-C=O (green) is red-shifted (by 20 cm^{-1}) from its uncomplexed position, establishing that it is an H-bond acceptor. Application of these constraints markedly reduces the number of possible **C-S** structures, which serves to efficiently guide the ab initio search for minimum-energy structures consistent with the empirically deduced H-bonding pattern. The most important clue derives from the assignment of the attachment occurring between the protonated amine on **C** and the acid carbonyl on **S**. Subsequent locking of the two relatively floppy moieties linked by the shared proton then involves only a relatively small number of plausible arrangements anticipated by force-field models.

These candidate structures are then sorted by the pattern of H-bonding, which reveals the only **C-S** structure consistent with the active groups presented in Fig. 4D. About 20 low-lying isomers were recovered by using electronic structure theory to identify the locally stable conformations available to the system. The structure in Fig. 4D is the global minimum identified in this computational search, being lower in energy by 0.2 eV (19.3 kJ/mol) relative to the next lower structure. The harmonic spectrum associated with this structure is indicated in Fig. 4D, which is in excellent agreement with the bands assigned by isotopic labeling. Hence, we propose the plausible assignments of other features not directly pinned down by empirical behavior of the isotopomers by the color coding in Fig. 4C. These predictions provide a solid foundation with which to confirm the structure by further labeling if desired.

The most important feature of the **C-S** structure shown in Fig. 4, C and D, is that, although different from the salt-bridge arrangement suggested to explain stereoselective bromination (*2*), the gas-phase ion complex indeed places the phenol constituent in close proximity to the catalytic dimethyl formamide functionality. Also, this docking motif is quite robust, as all site-selective

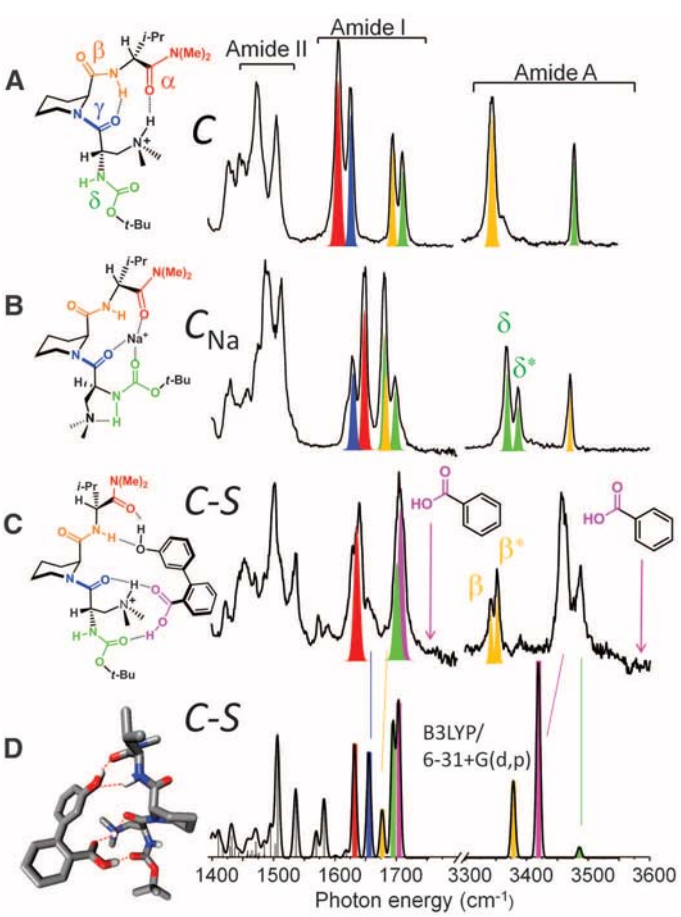

Fig. 4. Summary of amide I and A peak assignments in the (**A**) **C**, (**B**) $\mathbf{C}_{Na}$, and (**C**) **C-S** IR spectra. The color coding of the peaks corresponds to the functional groups highlighted in the corresponding schematic structures on the left. Trace (**D**) presents the **C-S** harmonic spectrum calculated at the B3LYP/6-31+G(d,p) level. The **C-S** lowest-energy structure is displayed at the left of trace (D) and displayed schematically at the left of trace (C) to highlight the interactions.

difference spectra are quite simple, with only one main band (or very close doublet) affected by substitution. Consequently, only one dominant configuration (with minor conformers arising from remote group orientation) is adopted upon extraction from solution. It is possible that removal of solvent changes the structure, and that the active species in solution could be electrically neutral, and both of these issues can be addressed with the cryogenic approach by retaining many solvent molecules and working with bulky noncoordinating counterions such as tetramethyl ammonium to explore the neutral adduct. It is nonetheless an important first step to establish that in the protonated adduct characterized here, the substrate (**S**) adopts a configuration consistent with the observed enantioselectivity of the catalyst (*2*, *5*).

The pivotal assignment of the strong contact occurring between N-H^+ and CO_2H in **C-S** relies solely on the behavior of the ^{13}C label in the acid position. This raises the importance of not only identifying whether particular groups are involved in H-bonding, but also establishing specifically which donors and acceptors are paired, at least in one contact point. One avenue to explore, therefore, is whether the intensities of both the donor and acceptor bonds can be modulated by the isotopic labeling scheme. An attractive possibility in this regard would be to monitor the combination band involving one quantum in both the donor and acceptor groups (e.g., N-H and C=O), which one would expect to be activated by the anharmonic coupling inherent in the H-bond. The presence of an isotope shift from both ^{15}N and ^{13}C labels would then confirm a specific point contact.

This procedure yields a microscopic picture of a docking arrangement, sufficiently constraining the possible structures such that electronic structure theory can be efficiently used to converge on a unique minimum-energy structure within an otherwise computationally prohibitive, high-dimensionality landscape. The method appears general and likely to become a central tool for the characterization of processes that depend on supramolecular associations.

References and Notes

1. D. H. Williams, B. Bardsley, *Angew. Chem. Int. Ed.* **38**, 1173 (1999).
2. J. L. Gustafson, D. Lim, S. J. Miller, *Science* **328**, 1251 (2010).
3. M. S. Taylor, E. N. Jacobsen, *Angew. Chem. Int. Ed.* **45**, 1520 (2006).
4. A. G. Doyle, E. N. Jacobsen, *Chem. Rev.* **107**, 5713 (2007).
5. J. L. Gustafson, D. Lim, K. T. Barrett, S. J. Miller, *Angew. Chem. Int. Ed.* **50**, 5125 (2011).
6. J. M. Lehn, *Proc. Natl. Acad. Sci. U.S.A.* **99**, 4763 (2002).
7. K. H. Bleicher, H. J. Böhm, K. Müller, A. I. Alanine, *Nat. Rev. Drug Discov.* **2**, 369 (2003).
8. J. Bajorath, *Nat. Rev. Drug Discov.* **1**, 882 (2002).
9. W. L. Jorgensen, *Science* **303**, 1813 (2004).
10. B. K. Shoichet, *Nature* **432**, 862 (2004).
11. L. J. Prins, D. N. Reinhoudt, P. Timmerman, *Angew. Chem. Int. Ed.* **40**, 2382 (2001).
12. S. Ham, S. Cha, J. H. Choi, M. Cho, *J. Chem. Phys.* **119**, 1451 (2003).
13. C. L. Perrin, J. B. Nielson, *Annu. Rev. Phys. Chem.* **48**, 511 (1997).
14. G. A. Jeffrey, W. Saenger, *Hydrogen Bonding in Biological Structures* (Springer-Verlag, Berlin, New York, 1991).
15. P. I. Haris, G. T. Robillard, A. A. van Dijk, D. Chapman, *Biochemistry* **31**, 6279 (1992).
16. S. Sonar *et al.*, *Nat. Struct. Biol.* **1**, 512 (1994).
17. L. Tadesse, R. Nazarbaghi, L. Walters, *J. Am. Chem. Soc.* **113**, 7036 (1991).
18. R. R. Knowles, E. N. Jacobsen, *Proc. Natl. Acad. Sci. U.S.A.* **107**, 20678 (2010).
19. M. Z. Kamrath, R. A. Relph, T. L. Guasco, C. M. Leavitt, M. A. Johnson, *Int. J. Mass Spectrom.* **300**, 91 (2011).
20. M. Z. Kamrath *et al.*, *J. Am. Chem. Soc.* **133**, 6440 (2011).
21. M. Okumura, L. I. Yeh, J. D. Myers, Y. T. Lee, *J. Chem. Phys.* **85**, 2328 (1986).
22. D. J. Goebbert, T. Wende, R. Bergmann, G. Meijer, K. R. Asmis, *J. Phys. Chem. A* **113**, 5874 (2009).
23. T. R. Rizzo, J. A. Stearns, O. V. Boyarkin, *Int. Rev. Phys. Chem.* **28**, 481 (2009).
24. J. A. Stearns *et al.*, *J. Am. Chem. Soc.* **129**, 11814 (2007).
25. L. Wang *et al.*, *J. Am. Chem. Soc.* **133**, 16062 (2011).
26. J. A. Stearns, C. Seaiby, O. V. Boyarkin, T. R. Rizzo, *Phys. Chem. Chem. Phys.* **11**, 125 (2009).
27. R. R. Gardner, G. B. Liang, S. H. Gellman, *J. Am. Chem. Soc.* **117**, 3280 (1995).
28. C. P. Rao, R. Nagaraj, C. N. R. Rao, P. Balaram, *Biochemistry* **19**, 425 (1980).
29. D. Semrouni *et al.*, *J. Am. Soc. Mass Spectrom.* **21**, 728 (2010).
30. R. C. Dunbar, J. D. Steill, J. Oomens, *Int. J. Mass Spectrom.* **297**, 107 (2010).
31. B. M. Elliott *et al.*, *J. Chem. Phys.* **129**, 094303 (2008).
32. J. M. Bakker, L. Mac Aleese, G. von Helden, G. Meijer, *J. Chem. Phys.* **119**, 11180 (2003).
33. S. G. Stepanian, I. D. Reva, E. D. Radchenko, G. G. Sheina, *Vib. Spectrosc.* **11**, 123 (1996).
34. Y. Inokuchi, N. Nishi, *J. Phys. Chem. A* **107**, 11319 (2003).
35. H. M. Lee *et al.*, *Phys. Chem. Chem. Phys.* **12**, 6278 (2010).
36. E. P. L. Hunter, S. G. Lias, *J. Phys. Chem. Ref. Data* **27**, 413 (1998).

Acknowledgments: M.A.J. thanks the Air Force Office of Scientific Research under grant FA-9550-09-1-0139. We also thank the U.S. NSF under grants CHE-091199 (M.A.J.) and CHE-0848242 (A.B.M.). S.J.M thanks the NIH under grant R01-GM068649. This work was supported in part by the Yale University Faculty of Arts and Sciences High Performance Computing facility (and staff).

Supporting Online Material

www.sciencemag.org/cgi/content/full/science.1214948/DC1
Materials and Methods
Figs. S1 to S9
References (*37*–*40*)

7 October 2011; accepted 20 December 2011
Published online 19 January 2012;
10.1126/science.1214948

A Molecular MoS_2 Edge Site Mimic for Catalytic Hydrogen Generation

Hemamala I. Karunadasa,[1,2] Elizabeth Montalvo,[1] Yujie Sun,[1,2] Marcin Majda,[1] Jeffrey R. Long,[1,3]* Christopher J. Chang[1,2,4]*

Inorganic solids are an important class of catalysts that often derive their activity from sparse active sites that are structurally distinct from the inactive bulk. Rationally optimizing activity is therefore beholden to the challenges in studying these active sites in molecular detail. Here, we report a molecule that mimics the structure of the proposed triangular active edge site fragments of molybdenum disulfide (MoS_2), a widely used industrial catalyst that has shown promise as a low-cost alternative to platinum for electrocatalytic hydrogen production. By leveraging the robust coordination environment of a pentapyridyl ligand, we synthesized and structurally characterized a well-defined Mo^{IV}-disulfide complex that, upon electrochemical reduction, can catalytically generate hydrogen from acidic organic media as well as from acidic water.

Molybdenite, or molybdenum disulfide (MoS_2), the earliest form of molybdenum to be identified from ores, is one of the most widely used catalysts in industry today as the standard for hydrodesulfurization (HDS) of petroleum (*1*). In its nanoparticulate form, MoS_2 has further demonstrated promise as an inexpensive alternative to platinum for the electrochemical and photochemical generation of hydrogen from water (*2*–*6*). As is the case with many inorganic solids, the catalytic activity of MoS_2 is localized to rare surface sites, whereas the bulk material is relatively inert (*7*–*9*). High-resolution scanning tunneling microscopy studies and theoretical calculations performed on nanoparticulate MoS_2 structures that form under sulfiding conditions implicate the formation of disulfide linkages or triangular MoS_2 units along the fully sulfided catalytically active edges of the layered structure (*10*–*14*). However, the precise molecular structures and modes of action of these sites remain elusive. Because of the bulk material's layered structure, which favors the growth of plate-like crystals, a single crystal with a large edge dimension is extremely challenging to prepare (*1*). Here, we report the synthesis of a well-defined molecular analog of the proposed MoS_2 edge structure, a side-on bound Mo^{IV}-disulfide complex. Electrochemical reduction of this mol-

[1]Department of Chemistry, University of California, Berkeley, CA 94720, USA. [2]Chemical Sciences Division, Lawrence Berkeley National Laboratory, Berkeley, CA 94720, USA. [3]Materials Sciences Division, Lawrence Berkeley National Laboratory, Berkeley, CA 94720, USA. [4]Howard Hughes Medical Institute, University of California, Berkeley, CA 94720, USA.

*To whom correspondence should be addressed. E-mail: chrischang@berkeley.edu (C.J.C.); jrlong@berkeley.edu (J.R.L.)

ecule leads to the catalytic generation of hydrogen from acidic organic media as well as from acidic water, lending support to the proposed active site morphology in the more active heterogeneous catalyst.

Recent efforts from our laboratories have explored the chemistry of the $PY5Me_2$ ligand [$PY5Me_2$ = 2,6-bis(1,1-bis(2-pyridyl)ethyl)pyridine] and the ability of its Mo^{IV}-oxo complex $[(PY5Me_2)MoO]^{2+}$ to catalyze the production of hydrogen from neutral water (*15*). Along these lines, treatment of the Mo^{II} precursor $[(PY5Me_2)Mo(CF_3SO_3)]^{1+}$ with S_8 at room temperature affords the Mo^{IV}-disulfide complex $[(PY5Me_2)MoS_2]^{2+}$ (**1**) in 74% yield (Fig. 1) (*16*). This molecule represents a rare species in molybdenum coordination chemistry (*17*–*20*) and a discrete molecular analog of the proposed triangular MoS_2 edge sites of molybdenite. A single-crystal x-ray analysis of **1** revealed a distorted pseudo-octahedral geometry around the metal center, with the MoS_2 plane twisting away from the plane of the axial pyridyl ligand by approximately 46°. The $PY5Me_2$ ligand is slightly distorted around the central metal with a mean Mo-N distance of 2.19(2) Å and a mean N-Mo-N angle of 82(6)°. The mean Mo-S distance of 2.402(2) Å, S-S distance of 2.019(1) Å and S-Mo-S angle of 49.68(3)° are similar to those reported for $Cp^*_2MoS_2$ (*21*) and $Cp^{tBu}_2MoS_2$ (*22*), and together frame a molecular MoS_2 isosceles triangle supported by the $PY5Me_2$ ligand. The longer Mo-S distance compared with the 2.254(2) Å bond length for a terminal sulfido ligand bonded to Mo^{IV} (*18*) indicates single Mo-S bonds. Similarly, the S-S bond length is close to the distance of 2.060 Å observed between S atoms in S_8 (*23*) as well as the distance between S atoms in a dinuclear Mo^V complex bearing a μ-S_2^{2-} bridging ligand (*24*), consistent with a single bond between the two S atoms.

The cyclic voltammogram on a glassy carbon disc electrode (GCDE) of a 1-mM solution of **1** in acetonitrile with 0.1 M of $(Bu_4N)PF_6$ electrolyte shows a reversible set of redox peaks at $E_{1/2}$ = 1.27 V versus the standard hydrogen electrode (SHE) (Fig. 2A), which we assigned to the $[(PY5Me_2)MoS_2]^{2+/3+}$ couple. Scanning cathodically reveals two more reversible redox couples at $E_{1/2}$ = –0.20 and –0.82 V versus SHE assigned to the $[(PY5Me_2)MoS_2]^{2+/1+}$ and $[(PY5Me_2)MoS_2]^{1+/0}$ couples. At still more negative potentials, a larger irreversible wave rising to a maximum at E_p = –1.49 V versus SHE is presumably due to an electrochemical-chemical (EC) process, perhaps involving the S_2^{2-} ligand (fig. S2).

The accessibility of multiply reduced states for the $Mo^{IV}S_2$ complex **1** prompted us to investigate its ability to reduce protons in organic solvents. The cyclic voltammogram (on a GCDE) of a 0.5-mM solution of **1** in acetonitrile containing 79 mM (160 equivalents) of acetic acid shows a sharp catalytic current after the $Mo^{III/II}$ couple with an onset potential of about –1.00 V versus SHE. The current reaches half its maximum value at –1.27 V and peaks at –1.50 V versus SHE. (Fig. 2B). The peak currents of the precatalytic waves as well as the catalytic wave vary linearly with the square root of the scan rate (fig. S4), indicating diffusion-limited redox processes, with the electrochemically active species freely diffusing in solution. The catalytic nature of the reductive wave at about –1.27 V versus SHE was verified by passing 3.00 C of charge during a bulk electrolysis. The experiment was conducted on a 55-μM solution of **1** in acetonitrile with 9 mM of acetic acid, using a glassy carbon plate electrode in a double compartment cell with the potential held at –1.09 V versus SHE for 2.75 hours. A control experiment performed under identical conditions, but without **1**, showed the accumulation of just 0.679 C of charge (fig. S5). Subtracting the background contribution of direct acid reduction leads to 10.9 equiv. of charge generated per molybdenum center, which precludes a stoichiometric reaction with respect to molybdenum. Gas chromatography of the headspace gas during the bulk electrolysis confirmed the generation of H_2.

Encouraged by this clear indication that **1** can operate as a molecular electrocatalyst in acetonitrile, we chose to explore its potential utility for the electrocatalytic reduction of protons in water, a much more attractive medium for the sustainable generation of hydrogen. Indeed, a sharp increase in current, indicative of catalytic water reduction, is evident in cyclic voltammograms (on a GCDE) of aqueous solutions of **1** at pH values of 3, 4, 5, and 6, with optimal activity observed at pH 3. We therefore conducted subsequent studies in aqueous media at pH 3 using potassium hydrogen phthalate (KHP) or sodium acetate aqueous buffers. The voltammogram (on a GCDE) of a 1.2-mM solution of **1** in aqueous acetate buffer at pH 3, acquired at a scan rate of 0.1 V/s, shows two irreversible reductions at peak potentials of −0.34 and −0.53 V versus SHE, respectively, before the onset of the catalytic current at a potential of about −0.65 V versus SHE (Fig. 2C). The voltammogram of the molybdenum-oxo compound $[(PY5Me_2)MoO]^{2+}$, taken under identical conditions, shows no catalytic activity within the solvent electrochemical window, confirming that the sulfide ligands are not hydrolyzed under acidic aqueous conditions. As observed in acetonitrile solution, the current response of the redox events of **1** on the glassy carbon electrode in acidic water shows a linear dependence on the square root of the scan rate, which is indicative of a diffusion-controlled process (figs. S6 and S7). A controlled potential electrolysis of a 92-μM solution of **1** in 3 M aqueous acetate buffer at pH 3 conducted using a glassy carbon rod electrode in a double-compartment cell at −0.75 V versus SHE for 1 hour led to the accumulation of 2.42 C of charge. In the absence of **1**, an identical experiment led to the passage of only 0.015 C of charge (fig. S8). Subtraction of this background activity affords 14.3 equiv. of charge per molybdenum center, establishing the catalytic nature of the reduction. To determine whether deposition on the electrode occurs during an extended electrolysis, the electrode was carefully rinsed with distilled water and examined using molybdenum K-edge x-ray absorption spectroscopy, which indicated no molybdenum species present to the limit of x-ray fluorescence measurement (monolayer). Furthermore, the electronic adsorption spectra of the solution before and after the 1-hour electrolysis show that the $(PY5Me_2)Mo$ unit remains intact during that period (fig. S9).

Because of the background activity of direct water reduction at the glassy carbon electrode at high overpotentials, subsequent experiments were conducted on a mercury electrode, where no direct water reduction occurs below overpotentials of about −1 V (overpotential being the difference between the applied potential and the thermodynamic potential for water reduction at the same pH) (*25*). Similar to the data obtained on a glassy carbon electrode, a cyclic voltammogram on a mercury drop electrode recorded at a

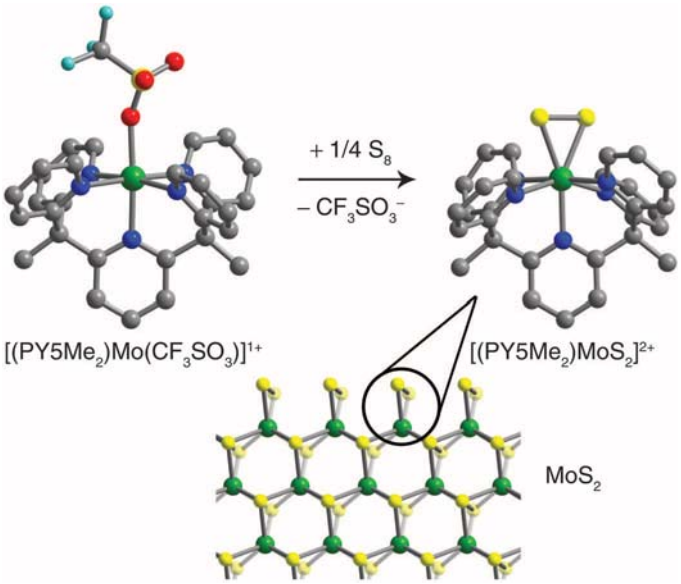

Fig. 1. Reaction of $[(PY5Me_2)Mo(CF_3SO_3)]^{1+}$ with sulfur to form $[(PY5Me_2)MoS_2]^{2+}$ (**1**, top), and a model of the layered structure of MoS_2 (bottom), highlighting the proposed surface reconstruction to give disulfide-terminated edge sites. The molecular structures depicted at the top are the results of single-crystal x-ray analyses. Green, yellow, light blue, red, blue, and gray spheres represent Mo, S, F, O, N, and C atoms, respectively; H atoms are omitted for clarity.

scan rate of 0.5 V/s shows two reductions, with a sharp wave corresponding to the first reduction at –0.16 V versus SHE, followed by a quasireversible couple at $E_{1/2}$ = –0.38 V preceding the catalytic current (Fig. 2D). To probe the nature of the first reduction process, we investigated the pH dependence of the cathodic peak potential (V_c), summarized in the Pourbaix diagram depicted in Fig. 4 (assuming electrochemical reversibility for this redox couple). Here, V_c declines linearly with rising solution pH at a slope of –59.8 (±0.8), which is within experimental error of the ideal value of –59 mV, corresponding to the association of one proton with the electron transfer (*25*). The observed pH dependence, taken together with the irreversibility of this peak, suggests a geometric distortion about the metal center consistent with the formation of a protonated reduced Mo-disulfide unit or cleavage of a Mo-S bond. Formation of a S-H bond is the first step in the proposed pathway for electrocatalytic proton reduction at MoS_2 nanoparticle edge sites (*10*), as well as in dinuclear $(CpMo\mu\text{-}S)_2S_2CH_2$ complexes (*26*). Protonation of the bridging sulfido ligand is also proposed for H_2 evolution by the nitrogenase enzyme (*27*). Furthermore, terminal S-H bonds at the edges of MoS_2 HDS catalysts have been assigned, which has led to speculation that such species are the source of H_2 for the hydrogenation of the desulfurized molecules (*28*). In contrast, the second reductive wave does not show a similar pH dependence, leading us to hypothesize that this process involves one electron reduction of the complex, which upon subsequent reduction and protonation forms the catalytically active species. Close contact between metal centers adsorbed on the electrode may also facilitate a multinuclear pathway, perhaps through the formation of S-H bonds that could homolytically or heterolytically cleave to yield H_2.

Analysis of the peak current of the cathodic and anodic scans of the second quasireversible redox couple as a function of scan rate (fig. S10) shows a linear relation, consistent with adsorption of the molecules on the electrode surface. Stabilization of the reduced molybdenum complexes through adsorption on the Hg electrode would be consistent with the positive shift of the redox events compared with the diffusion-limited redox processes observed with glassy carbon electrodes (*25*). For an idealized adsorption, which assumes reversible electron transfer with no interaction between adsorbed species, the number of electrons that give rise to the wave corresponds to $90.6/\Delta E_{p,1/2}$, where $\Delta E_{p,1/2}$ is the width of the wave at half the maximum current (*25*). At scan rates of 200 to 1000 mV/s, a mean width of 74(2) mV is observed for the anodic scan, which indicates a one-electron process. By observing the current response to variations in scan rate, we can quantify the coverage of metal sites on the electrode surface to be 3.4 to 3.6×10^{-10} mols/cm^2. A rough calculation of the footprint of **1**, obtained using the dimensions from the crystal structure, suggests monolayer coverage on the electrode [see supporting online material (SOM)]. Due to possible increases in surface area of the mercury when the pool is stirred during electrolysis, we use an estimated surface coverage of 10^{-10} mols/cm^2 for subsequent hydrogen evolution rate calculations.

The cyclic voltammogram of a 130-μM solution of **1** at pH 3 shows a catalytic current with an overpotential of about −400 mV (−0.58 V versus SHE) (Fig. 3B). The catalytic performance of $[(PY5Me_2)MoO]^{2+}$ was once again evaluated at the same pH to establish that **1** did not form the molybdenum-oxo complex under aqueous, reducing conditions. As depicted in Fig. 3B, $[(PY5Me_2)MoO]^{2+}$ shows the onset of a catalytic current at an overpotential of −700 mV (−0.88 V versus SHE) under the same conditions. Thus, using the disulfide complex **1** gives an improvement of 300 mV in overpotential with respect to the analogous oxo complex for water reduction at pH 3. Controlled potential electrolysis experiments were conducted to assess the rate of hydrogen production at various overpotentials. Identical measurements were performed with and without the catalyst to subtract the background activity at each applied potential. Figure S11 shows the charge accumulated over 1-min intervals, with applied overpotential increasing from −428 mV until a saturation value of 6.36 C is reached at −828 mV (due to the voltage between the working and auxiliary electrodes exceeding the maximum voltage obtainable by the potentiostat at high current densities). Under these conditions, the pH change of the solution, as well as quantitative gas chromatographic analysis of the electrolysis-cell headspace, indicated that the catalyst performs at close to 100% Faradaic efficiency, where every electron is used for the generation of hydrogen (see figs. S12 and S13 and SOM). At an overpotential of −828 mV, the observed turnover frequency (TOF) reached a maximum of 280 moles of H_2 per mole of catalyst per second.

We also evaluated the catalytic properties of **1** using a sample of California seawater, which was buffered at pH 3 by the addition of acetic acid and sodium acetate. As shown in Fig. 3C, the rates of hydrogen evolution for a given overpotential were similar to those observed in the studies conducted in distilled water, but with an even higher optimal TOF of 480 moles of H_2 per mole of catalyst per second at an overpotential of −780 mV. This result highlights the robustness of the catalyst to the impurities found in seawater.

To assess the long-term stability of the catalyst, an extended electrolysis was conducted in a 3 M pH 3 acetate buffer at an overpotential of

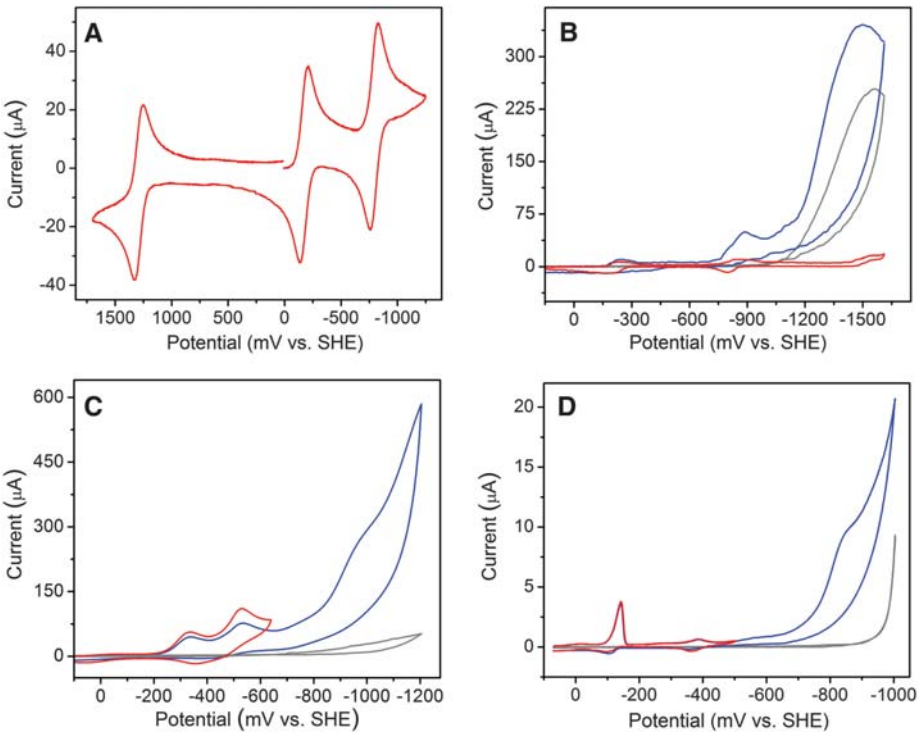

Fig. 2. Cyclic voltammograms on a glassy carbon disc electrode (A = 7.07 × 10^{-2} cm^2) of (**A**) an acetonitrile solution containing 1 mM of $[(PY5Me_2)MoS_2](CF_3SO_3)_2$ (**1**) and 0.1 M of $(Bu_4N)PF_6$ at a scan rate of 0.1 V/s; (**B**) acetonitrile solutions containing 0.5 mM of **1** and 0.1 M of $(Bu_4N)PF_6$ in the presence (blue line) and absence (red line) of 160 equiv. of acetic acid (79 mM), or 79 mM of the acid alone (gray line), at a scan rate of 0.1 V/s; (**C**) 1 M aqueous acetate buffer at pH 3 in the presence (red and blue lines) and absence (gray line) of 1.1 mM of **1** at a scan rate of 0.1 V/s. (**D**) Cyclic voltammograms on a mercury drop electrode (A ~ 1.16 × 10^{-2} cm^2) of 0.05 M aqueous KHP buffer at pH 3 in the presence (red and blue lines) and absence (gray line) of 160 μM of **1** at a scan rate of 0.5 V/s. In (C) and (D), the red line indicates the initial scan and the blue line indicates the subsequent scan.

−780 mV (Fig. 3D). The total turnover number (TON) reached ~3.5×10^3 moles of H_2 per mole of catalyst, showing that the catalyst is stable for long durations in aqueous media. This value is the lower bound for the catalyst lifetime using the total number of molecules in solution. Calculating the TON using the surface coverage of catalyst molecules on the electrode affords 1.9×10^7 moles of H_2 per mole of catalyst. We report both numbers because we do not yet know the rate of exchange of the surface layer with the molecules in solution during the 23-hour period.

Comparing the electronic adsorption spectrum of a solution of the catalyst electrolyzed for 1 hour against a control shows that the $(PY5Me_2)Mo$ unit remains intact during this period (fig. S14).

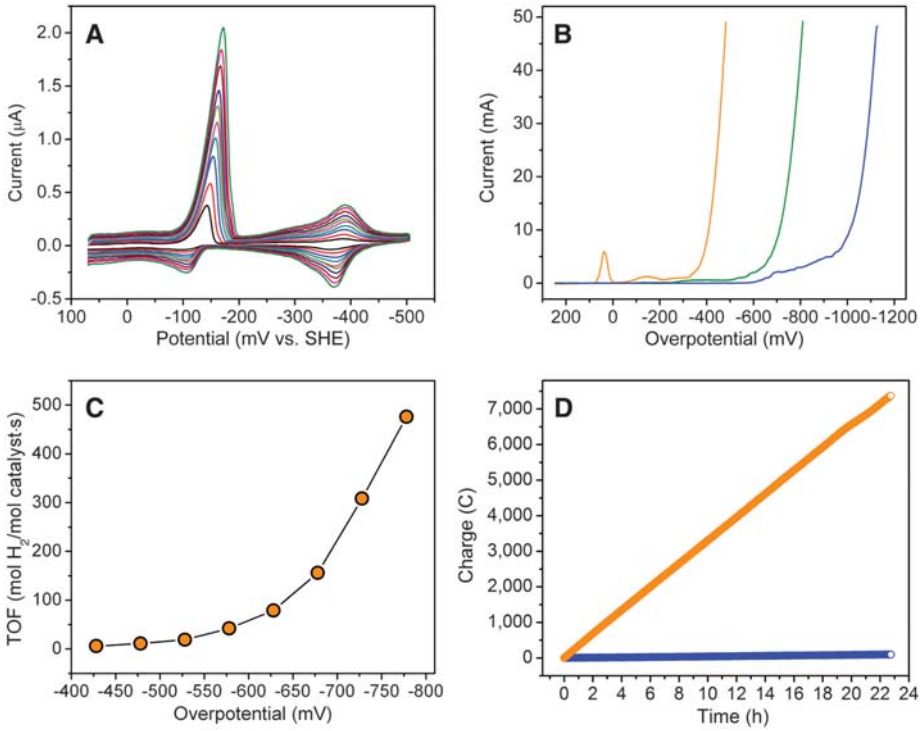

Fig. 3. (**A**) Scan rate dependence of precatalytic waves for a 160-μM solution of $[(PY5Me_2)MoS_2](CF_3SO_3)_2$ (**1**) in 0.05 M aqueous KHP buffer at pH 3, at scan rates ranging from 100 to 1000 mV/s in 100 mV/s increments on a mercury drop electrode ($A \sim 11.6 \times 10^{-3}$ cm^2). (**B**) Cathodic scans of 130-μM solutions of **1** (orange line) or $[(PY5Me_2)MoO](CF_3SO_3)_2$ (green line) in 1 M aqueous acetate buffer at pH 3 and of the buffer solution alone (blue line), on a mercury pool electrode ($A = 19.6$ cm^2) at a scan rate of 100 mV/s. (**C**) TOF versus overpotential for a 170-μM solution of **1** in seawater maintained at pH 3 with 1 M acetate buffer. The background solvent activity has been subtracted from the data. (**D**) Charge buildup over time from electrolysis of a 66-μM solution of **1** (orange circles) in 3 M aqueous acetate buffer at pH 3, compared with the electrolyte solution alone (blue circles), with the cell operating at an overpotential of −780 mV. Overpotential = applied potential − E(pH 3).

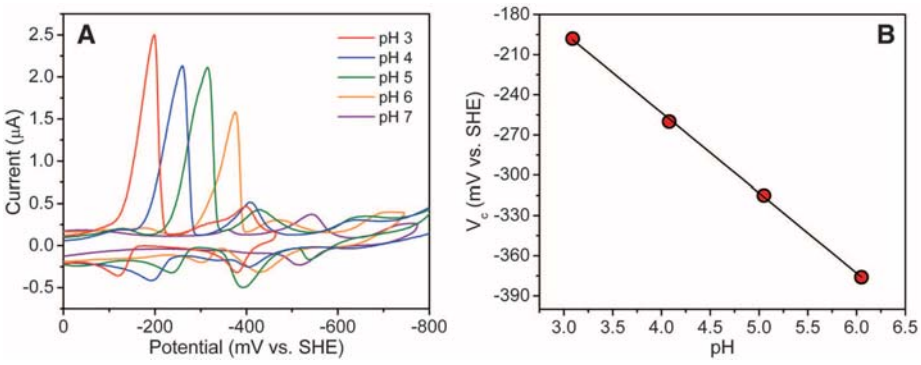

Fig. 4. (**A**) Cyclic voltammograms of 0.3-mM solutions of $[(PY5Me_2)MoS_2](CF_3SO_3)_2$ (**1**) in 0.05 M aqueous KHP buffers at pH values ranging from 3 to 7 on a Hg drop electrode at a scan rate of 1 V/s. (**B**) Pourbaix diagram showing the dependence of the peak potential of the first reductive wave on the solution pH: A linear fit gives a slope of −59.8 (± 0.8).

In addition, a ^{1}H nuclear magnetic resonance study to quantify the amount of free ligand in solution after a 12-hour electrolysis indicated that less than 3% is lost from the initial catalyst loading, further supporting the stability of this molecular species under reductive, aqueous conditions (see SOM for details). However, adsorption on the mercury surface complicates the characterization of the catalytically active species, which we cannot as yet unambiguously identify. The analogous studies performed using glassy carbon electrodes in organic and aqueous media, where the catalyst is not adsorbed on the electrode surface, support a molecular species as a competent catalyst.

This first-generation molybdenum-disulfide complex exhibits considerably higher stability and comparable TOFs to hydrogenase enzymes (which show rates from 10^2 to 10^4 s^{-1}) (*29*, *30*), albeit with greater overpotentials. For comparison, water-tolerant cobalt-based molecular catalysts attached to glassy carbon electrodes can achieve TOFs of ~90 s^{-1} at an overpotential of −400 mV (*31*), and experimentally determined TOFs ranging from 2.3×10^{-4} to 2.2×10^{-3} s^{-1} at overpotentials ranging from −690 to −1040 mV have been reported for a cobalt complex on a mercury electrode (*32*); an analogous Co complex bearing the $PY5Me_2$ ligand shows a TOF of ~0.3 s^{-1} at an overpotential of −900 mV on a mercury electrode (*33*). Furthermore, TOFs of ~0.07 s^{-1} at the equilibrium potential have been reported for carbon-supported $[Mo_3S_4]^{4+}$ clusters (*34*), which are susceptible to desorption from the electrode. Other examples of molecular catalysts attached to electrodes display lower activity and lifetimes in aqueous solution (*35*–*37*). A key advantage of **1** is the ability to form a layer of MoS_2 units, analogous to constructing a sulfided edge of MoS_2, where the dimensions of the layer can be defined by the size and shape of the electrode. Here, the electronic structure of the MoS_2 units, and thereby perhaps the activity, stability, and required overpotential for proton reduction, may be adjusted through ligand modifications accessible through synthetic chemistry.

The ability to prepare, characterize, and evaluate molecular analogs of the active components of inorganic solids has broad implications for the design and optimization of functional metal sites, not the least of which is control over the density of these units. For example, recent electronic structure calculations conducted on nanoparticulate MoS_2 indicate that only a quarter of the edge sites are used for hydrogen production (*10*). Increasing the number of active edge sites per unit volume by tailoring progressively smaller nanostructures or changing the electronics of the system to increase the enthalpy of hydrogen adsorption is a major challenge in inorganic materials and nanoscience. We present an alternative strategy using discrete molecular units, which in principle can be tailored to give a high density of catalytically active metal sites without the rest of the inactive bulk material.

References and Notes

1. R. Prins, V. H. J. De Beer, G. A. Somorjai, *Catal. Rev. Sci. Eng.* **31**, 1 (1989).
2. B. Hinnemann *et al.*, *J. Am. Chem. Soc.* **127**, 5308 (2005).
3. T. F. Jaramillo *et al.*, *Science* **317**, 100 (2007).
4. Y. Li *et al.*, *J. Am. Chem. Soc.* **133**, 7296 (2011).
5. X. Zong *et al.*, *J. Am. Chem. Soc.* **130**, 7176 (2008).
6. D. Merki, S. Fierro, H. Vrubel, X. Hu, *Chem. Sci.* **2**, 1262 (2011).
7. G. A. Somorjai, M. A. Van Hove, *Prog. Surf. Sci.* **30**, 201 (1989).
8. S. T. Ceyer, *Annu. Rev. Phys. Chem.* **39**, 479 (1988).
9. G. Ertl, *Angew. Chem. Int. Ed. Engl.* **29**, 1219 (1990).
10. B. Hinnemann *et al.*, *J. Am. Chem. Soc.* **127**, 5308 (2005).
11. J. V. Lauritsen *et al.*, *J. Catal.* **221**, 510 (2004).
12. J. C. Duchet, E. M. van Oers, V. H. J. de Beer, R. Prins, *J. Catal.* **80**, 386 (1983).
13. J. V. Lauritsen *et al.*, *Nat. Nano.* **2**, 53 (2007).
14. L. P. Hansen *et al.*, *Angew. Chem. Int. Ed. Engl.* **50**, 10153 (2011).
15. H. I. Karunadasa, C. J. Chang, J. R. Long, *Nature* **464**, 1329 (2010).
16. F. Gloaguen, T. B. Rauchfuss, *Chem. Soc. Rev.* **38**, 100 (2009).
17. S. J. Smith, C. M. Whaley, T. B. Rauchfuss, S. R. Wilson, *Inorg. Chem.* **45**, 679 (2006).
18. V. J. Murphy, G. Parkin, *J. Am. Chem. Soc.* **117**, 3522 (1995).
19. F. A. Cotton, G. Schmid, *Inorg. Chem.* **36**, 2267 (1997).
20. H. Kopf, S. K. S. Hazari, M. Leitner, *Z. Naturforsch. B: Chem. Sci.* **33b**, 1398 (1978).
21. J. H. Shin, D. G. Churchill, B. M. Bridgewater, K. Pang, G. Parkin, *Inorg. Chim. Acta* **359**, 2942 (2006).
22. J. H. Shin *et al.*, *J. Chem. Soc. Dalton Trans.* **11**, 1732 (2001).
23. A. F. Wells, *Structural Inorganic Chemistry* (Clarendon Press, Oxford, ed. 4, 1975).
24. P. D. Smith, D. A. Slizys, G. N. George, C. G. Young, *J. Am. Chem. Soc.* **122**, 2946 (2000).
25. A. J. Bard, L. R. Faulkner, *Electrochemical Methods* (Wiley, New York, 1980).
26. A. M. Appel, D. L. DuBois, M. R. DuBois, *J. Am. Chem. Soc.* **127**, 12717 (2005).
27. I. Dance, *J. Am. Chem. Soc.* **127**, 10925 (2005).
28. N. Y. Topsoe, H. Topsoe, *J. Catal.* **139**, 641 (1993).
29. M. Frey, *ChemBioChem* **3**, 153 (2002).
30. J. A. Cracknell, K. A. Vincent, F. A. Armstrong, *Chem. Rev.* **108**, 2439 (2008).
31. L. A. Berben, J. C. Peters, *Chem. Commun.* **46**, 398 (2010).
32. B. D. Stubbert, J. C. Peters, H. B. Gray, *J. Am. Chem. Soc.* **133**, 18070 (2011).
33. Y. Sun *et al.*, *J. Am. Chem. Soc.* **133**, 9212 (2011).
34. T. F. Jaramillo *et al.*, *J. Phys. Chem. C* **112**, 17492 (2008).
35. R. M. Kellett, T. G. Spiro, *Inorg. Chem.* **24**, 2378 (1985).
36. B. J. Fisher, R. Eisenberg, *J. Am. Chem. Soc.* **102**, 7361 (1980).
37. P. V. Bernhardt, L. A. Jones, *Inorg. Chem.* **38**, 5086 (1999).

Acknowledgments: Initial synthetic and electrochemical studies were supported by the Department of Energy (DOE) Lawrence Berkeley National Laboratory Helios Solar Energy Research Center (51HE112B to C.J.C.). Further electrochemical studies are based on work performed by the Joint Center for Artificial Photosynthesis, a DOE Energy Innovation Hub, supported through the Office of Science of the U.S. Department of Energy under award DE-SC0004993 (J.R.L.). C.J.C. is an investigator with the Howard Hughes Medical Institute. We thank B. Lassalle, J. Yano, and V. Yachandra for obtaining the x-ray absorption spectroscopy spectra; J. Breen for fabrication of electrochemical cells; Y. Hwang for assistance with gas chromatography; A. T. Iavarone for obtaining the mass spectra; and the University of California President's Postdoctoral Fellowship program for support of E.M. Structural parameters for **1** are available free of charge from the Cambridge Crystallographic Data Centre under identification number CCDC-798834. A patent has been filed by Lawrence Berkeley National Laboratory based on the results presented herein.

Supporting Online Material

www.sciencemag.org/cgi/content/full/335/6069/698/DC1
Materials and Methods
Figs. S1 to S14
Tables S1 and S2
References

27 October 2011; accepted 22 December 2011
10.1126/science.1215868

Near-Field Deformation from the El Mayor–Cucapah Earthquake Revealed by Differential LIDAR

Michael E. Oskin,[1]* J Ramon Arrowsmith,[2] Alejandro Hinojosa Corona,[3] Austin J. Elliott,[1] John M. Fletcher,[3] Eric J. Fielding,[4] Peter O. Gold,[1] J. Javier Gonzalez Garcia,[3] Ken W. Hudnut,[5] Jing Liu-Zeng,[6] Orlando J. Teran[3]

Large [moment magnitude (M_w) ≥ 7] continental earthquakes often generate complex, multifault ruptures linked by enigmatic zones of distributed deformation. Here, we report the collection and results of a high-resolution (≥nine returns per square meter) airborne light detection and ranging (LIDAR) topographic survey of the 2010 M_w 7.2 El Mayor–Cucapah earthquake that produced a 120-kilometer-long multifault rupture through northernmost Baja California, Mexico. This differential LIDAR survey completely captures an earthquake surface rupture in a sparsely vegetated region with pre-earthquake lower-resolution (5-meter–pixel) LIDAR data. The postevent survey reveals numerous surface ruptures, including previously undocumented blind faults within thick sediments of the Colorado River delta. Differential elevation changes show distributed, kilometer-scale bending strains as large as ~10^3 microstrains in response to slip along discontinuous faults cutting crystalline bedrock of the Sierra Cucapah.

Over the past century, most damaging continental earthquakes have arisen from multifault ruptures along incompletely mapped fault arrays (*1*). Quantifying this hazard is limited by inadequate understanding of the mechanisms by which faults link together to generate large earthquakes (*2*) and the difficulty of deducing large, multisegment events from paleoseismic records of ancient fault slip (*3*). Observations of fresh earthquake surface ruptures are critical to unraveling these problems because these most clearly illuminate relations between the paleoseismic record of faulting (at the surface) and seismic energy release that occurs predominantly at depth. In addition to the role of geometric fault segmentation in controlling the potential sizes of earthquakes (*3*), other important relations include the distribution of slip with depth (*4*, *5*) and the related problem of distributed deformation adjacent to faults (*5*–*8*). Well-studied earthquake surface ruptures in California (*9*–*11*) and elsewhere (*12*–*15*) have shown that earlier geologic observations may miss essential components of fault-zone deformation and underestimate the potential for ruptures to jump between faults.

The 4 April 2010 El Mayor–Cucapah sequence is a recent example of a large earthquake generated by a complex, multisegment fault rupture (*16*, *17*). Several faults—many but not all of which were mapped previously (*18*, *19*)—linked together to produce this moment magnitude (M_w) 7.2 earthquake. Because most evidence for ancient fault activity comes from the disruption of landforms by meter-scale fault slip, high-resolution light detection and ranging (LIDAR) topographic surveys (>1 sample/m^2) are valuable for delineating the extent of ancient ruptures, the detailed geometry and offsets in recent earthquakes (*20*), and, thus, the types of earthquakes that are likely to occur in the future. By immediately surveying the El Mayor–Cucapah surface rupture and comparing these measurements to pre-event LIDAR topography collected in 2006 by the Instituto Nacional de Estadística y Geografía (INEGI), we quantify both slip and spatially distributed warping associated with the faults that ruptured together in this earthquake.

To examine differential motion of the ground surface due to the earthquake, we removed the geoid correction from the pre-event LIDAR and subtracted the resulting ellipsoid heights from postevent LIDAR smoothed over a 2.5-m–radius window (*21*). The resulting elevation-difference map shows apparent vertical motion of the ground surface (Fig. 1 and fig. S1). In areas of steep slopes,

[1]Department of Geology, University of California, Davis, 1 Shields Avenue, Davis, CA 95618, USA. [2]School of Earth and Space Exploration, Arizona State University, Tempe, AZ 85287–1404, USA. [3]Centro de Investigación Científica y de Educación Superior de Ensenada, Carretera Ensenada-Tijuana no. 3918, Zona Playitas, C.P. 22860, Ensenada, Baja California, México. [4]Jet Propulsion Laboratory, California Institute of Technology, 4800 Oak Grove Drive, Pasadena, CA 91109, USA. [5]United States Geological Survey, 525 South Wilson Avenue, Pasadena, CA 91106, USA. [6]National Key Laboratory of Earthquake Dynamics, Institute of Geology, China Earthquake Administration, 1# Huayanli, Dewai Avenue, Beijing 100029.

*To whom correspondence should be addressed. E-mail: meoskin@ucdavis.edu

apparent vertical motions are correlated with slope facing direction. This arises from horizontal displacement of topographic ridgelines due to fault slip, as well as from residual systematic distortion present in the pre-event LIDAR survey swaths. We focus here on the elevation alone, for which airborne LIDAR data are most sensitive, in two example areas with extensive pre-event topographic slopes of less than 3°, where the observed elevation-differences are primarily due to tectonic vertical motion of the land surface.

The Paso Inferior accommodation zone (PIAZ) (Fig. 2) illustrates the trade-off in fault slip and distributed deformation among a set of fault strands within the northern Sierra Cucapah. The dominant sense of fault motion here is east-side-down dextral-normal slip, stepping northwestward to structurally lower faults. This pattern mimics the overall rupture throughout the Sierra Cucapah (Fig. 1B), which is more complex in the near-field than inferred from other remote-sensing data (*17*). Nearby outcrops and mapped geologic relations (*19*) indicate that the PIAZ largely involves crystalline bedrock buried by a thin (<<1 km) cover of alluvium. LIDAR-derived elevation differences show how this thinly mantled bedrock deformed in a distributed manner in response to slip along the PIAZ fault array (*21*). Gradients in fault throw (vertical component of slip) determined from fault-scarp mapping and LIDAR-derived elevation differences produce along-fault shear strains, $\gamma \leq 500$ microstrains (μstr). Elevation-differences also reveal that similar magnitudes of strain have accrued via warping between fault strands. For example, profile X-X′ (Fig. 2B and fig. S2) shows 1.1-m net down-to-the-northeast (NE) vertical motion via a combination of 1.6-m throw over two faults, and an overall southwest (SW)–directed tilt that reaches a maximum of 7×10^{-4} radians (rads). The block between the two faults displays an additional component of warping, with tilt ranging from 6×10^{-4} rads SW to 2×10^{-4} rads NE, yielding a bending strain $\gamma = 400$ μstr. Shear strains exceed 1000 μstr as slip trades off between west- and east-dipping faults (fig. S3). These bending strains persist well away (>100 m) from faults observed in the field and mapped from post-event LIDAR. However, small faults with <3 cm of vertical displacement cannot be detected from the LIDAR, and faults with <1 cm of slip were generally not mapped in the field.

Faulting within the PIAZ includes minor SW-down dextral-normal slip along the Laguna Salada fault, which last ruptured in 1892 with up to 5 m of dextral-normal slip, producing an earthquake exceeding M_w 7 (*9*). Surface slip in 2010 along the reactivated portion of the Laguna Salada fault tapers southeastward away from the PIAZ, diminishing to zero within a few hundred meters. Elevation differences adjacent to the Laguna Salada fault show recovery of the 2010 slip via near-field folding (within 200 m of the fault) of the down-thrown block (Fig. 2B). This short-wavelength deformation implies that this fault slip was shallow.

The Indiviso fault zone is a previously unknown array of faults, first detected from radar pixel tracking (*17*), that cut recent sediments of the Colorado River delta. The postevent LIDAR data reveal an unusual style of surface rupture expressed as linear shear zones, 10 to 50 m across, that form kilometer-length curvilinear steps in the elevation of the low-relief delta-plain (Fig. 3). We detect up to 0.5 m of distributed, down to the SW displacement, with maximum tilt approaching 2×10^{-2} rads at the center of the shear zones. This tilt is greater than that observed in the bedrock-dominated Sierra Cucapah, but still too subtle to be detected by traditional field techniques. Detection of lateral slip is generally not possible in the nearly flat landscape. However, where linear cultural features, such as canal levees, cross the Indiviso fault, the LIDAR data are useful for reconstructing their pre-event geometry and determining offsets (fig. S4). We find dextral displacement of similar magnitude (0.5 m) collocated with the zone of vertical deformation. This oblique slip has consistent sense, but lower magnitude than that indicated by far-field observations (*17*).

The shear strains associated with slip along the Indiviso fault are an order of magnitude higher than those observed in between faults in the PIAZ. The paucity of discrete faulting here suggests that unconsolidated, fluid-saturated delta sediments do not localize shear deformation as readily as crystalline rocks and alluvial fan deposits of the Sierra Cucapah. Extensive liquefaction in the delta region, expressed by numerous sandblow and lateral-spreading features, indicates loss of shear strength of the uppermost sediments

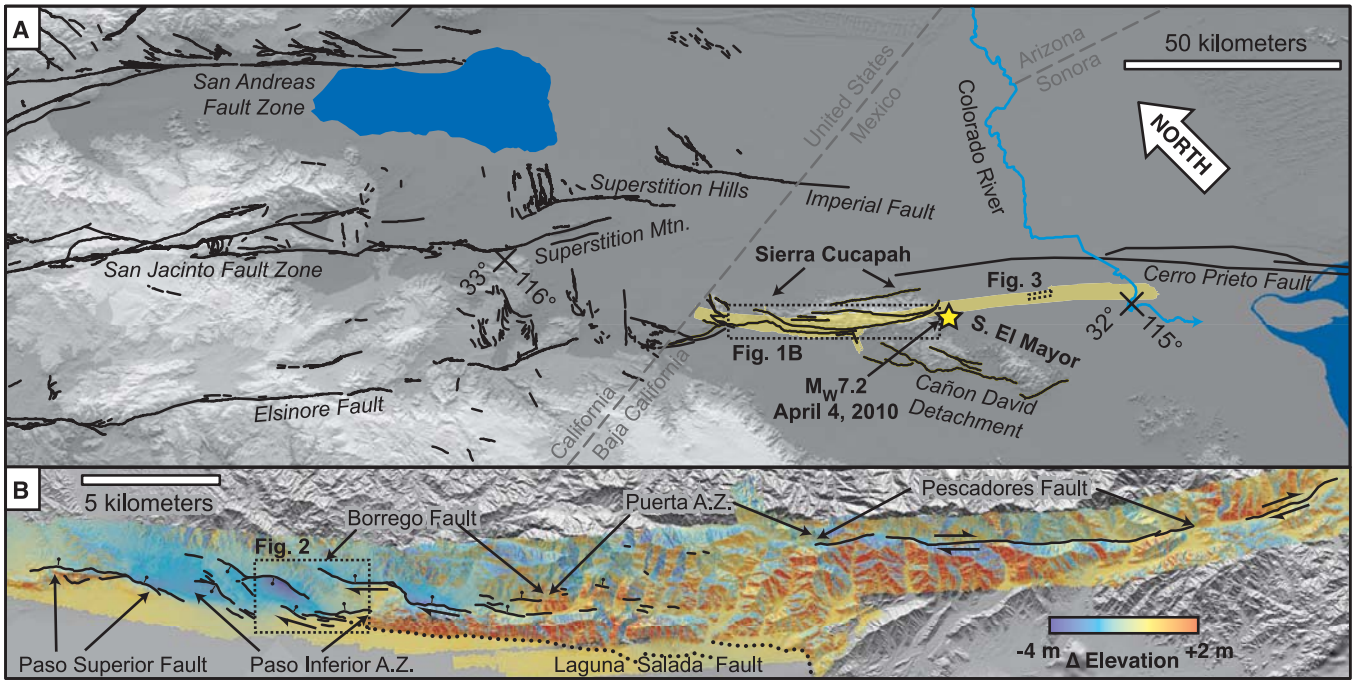

Fig. 1. Setting of El Mayor–Cucapah earthquake surface rupture and LIDAR scan. (**A**) Regional active fault map compiled from pre-earthquake sources (*18*, *19*). The elongate yellow region denotes the extent of the postearthquake LIDAR survey. (**B**) LIDAR-derived height-difference map (post- minus pre-earthquake) for the Sierra Cucapah (see fig. S1 for a more detailed version). Fault ruptures mapped from scarps in postevent LIDAR data are shown as black lines. The black dotted line is the trace of the 1892 Laguna Salada fault rupture (*9*). Distributed deformation across the Paso Inferior and Puerta accommodation zones separate localized slip along principal faults.

during earthquake shaking, which probably contributed to the distributed expression of fault slip here. The uniformity of the width of the zone of folding over several kilometers along strike (Fig. 3) indicates that the fault tip lies at a uniform depth below the surface, consistent with reactivation of an existing, but buried oblique-slip fault.

The comprehensive, near-field deformation illuminated with high-resolution topography and its comparison with pre-event data reveal substantial, shallow, distributed deformation surrounding faults that slipped during the earthquake. An elastic rheology with embedded displacement discontinuities provides a simple model to explain much of the smooth, kilometer-scale warping adjacent to faults (Fig. 2 and figs. S2 and S3). Using a three-dimensional elastic dislocation model (Fig. 2C), with oblique-normal fault slip determined from field observations, we reproduce the overall pattern of subsidence and uplift, as well as key details such as warping of the footwall of the Borrego fault and reactivation of the shallow portion of the Laguna Salada fault due to stress transfer between faults of the PIAZ. Large near-field strains emerge from the interaction of faults that slipped in the shallow crust and greatly exceed the level of strain recovered from interseismic elastic deformation across a single locked fault zone. The differential LIDAR does not directly indicate the processes by which the high strains were accommodated. Coseismic slip along numerous small faults may have led to the observed deformation; however, its close correspondence with modeled surface displacements (Fig. 2B) supports the inference that it arose largely as a direct, elastic response to slip along the mapped, discontinuous major faults of the PIAZ.

Though the distribution of strain we observe is compatible with the elastic dislocation model, its magnitude (>10^3 μstr) may exceed shallow crustal rock strength. Intact granite will indefinitely support elastic shear strains above 3×10^3 μstr in the uppermost crust (*22*), but fractured rock masses are substantially weaker, especially within fault zones (*23*). Near-field distributed deformation from the Landers earthquake apparently changed from elastic to anelastic deformation at ~1 to 2×10^3 μstr (*24*). Coseismic, shallow strains in areas of structural complexity may commonly approach this elastic limit, as implied by steep coseismic slip gradients documented at stepovers (*25*) and where ruptures terminate at asperities (*26*). Because brittle rock strength is time-scale dependent (*22*), large, nearly instantaneous elastic strains induced by coseismic fault slip may be transformed into permanent deformation by dis-

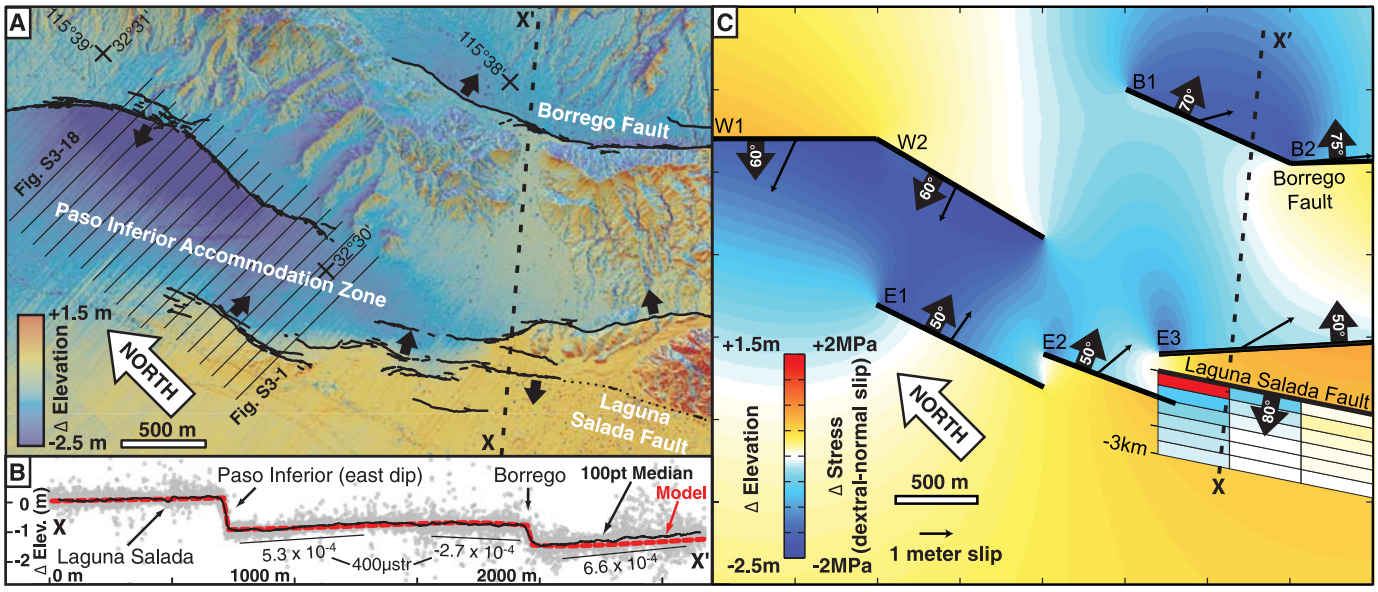

Fig. 2. Differential LIDAR and elastic model of the southern half of the PIAZ. (**A**) Elevation difference map showing distributed deformation as slip steps from the NW Borrego fault into the PIAZ. East-west striping in height difference reflects noise in the pre-event LIDAR. Black arrows show fault dip direction. (**B**) Swath profile of elevation difference along line X-X′ in (A). Points are within 50 m of the line as plotted. Outlier points result from noise and lateral displacement of locally steeper topography and vegetation (fig. S2). (**C**) Elastic model, using rectangular dislocations (table S1) and Poisson's ratio of 0.3, constructed in Coulomb (*31*), showing vertical surface deformation due to imposed slip along the PIAZ fault array. The model does not reproduce fault-slip gradients, and some faults extend beyond the domain shown. Slip vectors point in the direction of motion of the fault hanging wall. Modeled slip vectors match field observations of fault slip in the area shown, with the exception of faults E1 to E3, where normal slip is 30% above the observed values to match the elevation-difference map. Coulomb stress change for oblique dextral-normal slip (rake 135°) along the Laguna Salada fault is shown for 500-by-500–m patches, from the surface to 3-km depth, projected to the surface. Stress was calculated with a shear modulus of 3 GPa, which is appropriate for damaged fault-zone rock (*23*).

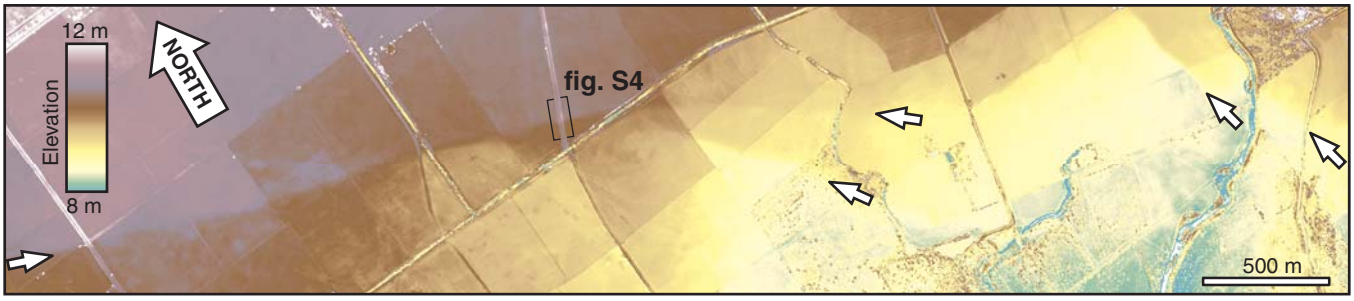

Fig. 3. Postearthquake LIDAR-derived topography (4 m of total relief) along a portion of the Indiviso fault (see Fig. 1 for location). Arrows highlight end points of shear zones recognized from topographic steps. Other elevation steps and lineaments are canals or boundaries of leveled agricultural fields.

tributed yielding mechanisms, such as granular flow (*5*, *6*) or velocity-strengthening slip along pervasively distributed fractures (*27*). Distributed yielding is commonly expressed along faults as fault-related folds, rock fabrics, topographic uplift, and gradients in cumulative slip and slip-rate (*8*, *28*–*30*). The time scale of this distributed yielding could be essentially coseismic or take months, and it may be difficult to distinguish from other coseismic deformation. Postseismic dilatancy recovery (*6*) could provide indirect evidence of its occurrence.

If a substantial fraction of plate-boundary motion is absorbed as distributed deformation in zones of structural complexity, surface rupture and strong ground motion hazard may be underpredicted. Paleoseismic measurements will underestimate fault slip rates at depth due to this unaccounted deformation. In addition to slip rate, maximum earthquake size may also be misjudged due to incomplete knowledge of the linkages between faults. These problems modestly affect hazard from fast-slipping, well-localized primary plate-boundary faults but can lead to severe underestimation of hazard away from primary faults where large ($>M_w$ 7) earthquakes along secondary fault arrays dominate strong ground motions (*1*). As exemplified by the highly segmented El Mayor–Cucapah surface rupture and similarly sized historic events in southern California (*9*–*11*), anticipating the sizes of the largest earthquakes along secondary fault arrays and the shaking and rupture hazards that these pose to critical facilities and lifelines requires careful attention to the extent and connectivity of mapped active faults. Scarp-forming paleoearthquakes along short fault segments, accompanied by large along and off-fault strains, provide key hazard information, as such events probably involved adjacent fault segments as parts of a larger surface rupture.

References and Notes

1. P. England, J. Jackson, *Nat. Geosci.* **4**, 348 (2011).
2. R. Harris, S. Day, *Geophys. Res. Lett.* **26**, 2089 (1999).
3. S. G. Wesnousky, *Nature* **444**, 358 (2006).
4. G. King, S. Wesnousky, *Bull. Seismol. Soc. Am.* **97**, 1833 (2007).
5. Y. Fialko, D. Sandwell, M. Simons, P. Rosen, *Nature* **435**, 295 (2005).
6. E. J. Fielding, P. R. Lundgren, R. Bürgmann, G. J. Funning, *Nature* **458**, 64 (2009).
7. W. Huang, A. Johnson, *J. Geophys. Res.* **115**, B03408 (2010).
8. E. Shelef, M. Oskin, *J. Geophys. Res.* **115**, B05308 (2010).
9. K. Mueller, T. Rockwell, *Bull. Geol. Soc. Am.* **107**, 8 (1995).
10. K. Sieh *et al.*, *Science* **260**, 171 (1993).
11. J. Treiman, K. Kendrick, W. Bryant, T. Rockwell, S. McGill, *Bull. Seismol. Soc. Am.* **92**, 1171 (2002).
12. J. Liu-Zeng *et al.*, *Bull. Seismol. Soc. Am.* **100**, 2615 (2010).
13. P. Haeussler *et al.*, *Bull. Seismol. Soc. Am.* **94**, S23 (2004).
14. Y. Klinger *et al.*, *Bull. Seismol. Soc. Am.* **95**, 1970 (2005).
15. M. Berberian *et al.*, *Geophys. J. Int.* **136**, 671 (1999).
16. E. Hauksson *et al.*, *Pure Appl. Geophys.* **168**, 1255 (2011)
17. S. Wei *et al.*, *Nat. Geosci.* **4**, 615 (2011).
18. C. Jennings, *Fault Activity Map of California and Adjacent Areas, with Locations and Ages of Recent Volcanic Eruptions*, scale 1:750,000, *Geologic Data Map no. 6* (California Division of Mines and Geology, Sacramento, CA, 1994).
19. J. Fletcher, R. Spelz, *Geosphere* **5**, 385 (2009).
20. K. Hudnut, A. Borsa, C. Glennie, J. Minster, *Bull. Seismol. Soc. Am.* **92**, 1570 (2002).
21. Materials and methods are available on *Science* Online.
22. D. A. Lockner, *J. Geophys. Res.* **103**, 5107 (1998).
23. E. Cochran *et al.*, *Geology* **37**, 315 (2009).
24. R. Michel, J. Avouac, *J. Geophys. Res.* **111**, B03408 (2006).
25. A. J. Elliott, J. F. Dolan, D. D. Oglesby, *J. Geophys. Res.* **114**, B02313 (2009).
26. I. Manighetti, M. Campillo, C. Sammis, P. Mai, G. King, *J. Geophys. Res.* **110**, B05302 (2005).
27. C. Marone, C. Scholz, *Geophys. Res. Lett.* **15**, 621 (1988).
28. J. Kaven, S. Martel, *J. Struct. Geol.* **29**, 1463 (2007).
29. E. Kirby *et al.*, *Tectonics* **26**, TC2010 (2007).
30. K. Blisniuk *et al.*, *J. Geophys. Res.* **115**, B08401 (2010).
31. S. Toda, R. Stein, J. Lin, V. Sevilgen, Coulomb 3 stress change modeling software, http://earthquake.usgs.gov/research/modeling/coulomb.

Acknowledgments: LIDAR data acquisition supported by an NSF RAPID grant (EAR-1039168 and 1039147), with additional support from the Southern California Earthquake Center (supported by NSF-EAR-0106924 and U.S. Geological Survey grant 02HQAG0008) and Consejo Nacional de Ciencia y Tecnología (grant CB-2007-81463). Part of this research was supported by NASA's Earth Surface and Interior Focus Area and performed at the Jet Propulsion Laboratory, California Institute of Technology. Y. Fialko, D. Sandwell, J. Galetzka, and A. Gonzalez assisted with Global Positioning System data acquisition and processing. C. Crosby, D. Haddad, O. Kreylos, A. Morelan, and T. Sato provided editorial and computational assistance. The National Center for Airborne Laser Mapping gathered and processed the postevent LIDAR data, distributed at OpenTopography (http://opentopography.org/id/OTLAS.122010.32611.1). We thank INEGI for granting access to the pre-event LIDAR data used for this study. Pre-event LIDAR digital elevation model and derived elevation difference data for the Sierra Cucapah rupture zone are available in the supporting online material.

Supporting Online Material

www.sciencemag.org/cgi/content/full/335/6069/702/DC1
Materials and Methods
Figs. S1 to S4
Table S1
Databases S1 and S2

9 September 2011; accepted 13 January 2012
10.1126/science.1213778

Propagation of Slow Slip Leading Up to the 2011 M_w 9.0 Tohoku-Oki Earthquake

Aitaro Kato,* Kazushige Obara, Toshihiro Igarashi, Hiroshi Tsuruoka, Shigeki Nakagawa, Naoshi Hirata

Many large earthquakes are preceded by one or more foreshocks, but it is unclear how these foreshocks relate to the nucleation process of the mainshock. On the basis of an earthquake catalog created using a waveform correlation technique, we identified two distinct sequences of foreshocks migrating at rates of 2 to 10 kilometers per day along the trench axis toward the epicenter of the 2011 moment magnitude (M_w) 9.0 Tohoku-Oki earthquake in Japan. The time history of quasi-static slip along the plate interface, based on small repeating earthquakes that were part of the migrating seismicity, suggests that two sequences involved slow-slip transients propagating toward the initial rupture point. The second sequence, which involved large slip rates, may have caused substantial stress loading, prompting the unstable dynamic rupture of the mainshock.

Laboratory and theoretical studies have proposed that earthquakes are preceded by a nucleation process where stable, slow rupture growth develops into unstable, high-speed rupture within a confined zone on a fault (*1*–*5*). The nucleation process has been discussed actively in association with the occurrence of foreshocks near the mainshock hypocenters and the presence of short-duration initial phases in the records of some earthquake events (*6*–*10*). A recent study on the 1999 moment magnitude (M_w) 7.6 Izmit, Turkey, earthquake suggested the possibility that the mainshock was preceded, for 44 min, by a phase of slow slip at the base of the brittle crust (*11*). If this kind of premonitory slow-slip behavior also precedes other large earthquakes, its knowledge should have crucial implications for earthquake prediction and risk assessment. It is, therefore, essential to scrutinize seismic records of other large, well-recorded earthquakes in search of similar nucleation processes.

The 11 March 2011 Tohoku-Oki earthquake was the first M_w 9 event to be recorded by a dense network of continuous and broad–frequency-range seismic stations. The extremely large spatial extent of the event (up to ~500 km) is expected to help study how it nucleated, providing an invaluable opportunity to elucidate preparatory processes for earthquake generation. The Tohoku-Oki earthquake ruptured a megathrust fault off the eastern shore of northern Honshu, Japan, where the Pacific plate is subducting beneath a continental plate at a convergence rate of 10 cm/year. According to the Japan Meteorological Agency (JMA) catalog, the mainshock was preceded by foreshock sequences lasting 23 days (*12*), starting with a burstlike seismicity in mid-February. The largest foreshock was a M_w 7.3 event that took

Earthquake Research Institute, The University of Tokyo, Tokyo, Japan.

*To whom correspondence should be addressed. E-mail: akato@eri.u-tokyo.ac.jp

place along the plate interface on 9 March (Fig. 1). The foreshock sequences occurred in proximity to the initiation point of the mainshock rupture and were located near the deepest end of the area of the largest cumulative coseismic slip (*13*). After the M_w 7.3 foreshock, the seismicity from the JMA catalog appeared to migrate toward the mainshock epicenter, which was interpreted as a propagation of afterslip (*14*).

Although the JMA routinely determines hypocenters across the Japanese islands, a large portion of the foreshock sequences is missing from its catalog, mainly because the burstlike seismicity and the aftershocks associated with the M_w 7.3 event tended to be masked by overlapping arrivals of waves from different earthquakes (low signal-to-noise ratios). We therefore applied a matched-filter technique (*15*–*17*) to detect missing events with the use of continuous three-component velocity seismograms recorded at 14 stations along the Pacific coast (Fig. 1) between 13 February and 11 March (*18*). We used all 333 earthquakes in the JMA catalog for the same period as the template events and looked for events that strongly resembled them. The correlation coefficient between a template event waveform and a target waveform was calculated on every component at every station and was averaged throughout. When the mean correlation peak exceeded a threshold level [eight times the standard deviation (*17*)], it was labeled as a positive detection (fig. S1). After removing multiple counts, our matched filter technique identified 1416 events, more than four times the number in the JMA catalog.

In a space-time diagram of all detected events (Fig. 2), we recognize two distinct sequences of earthquake migration in the trench-parallel direction toward the epicenter of the M_w 9.0 mainshock. Both sequences took place between the epicenters of the M_w 7.3 foreshock and the mainshock, and they overlap considerably in space (Fig. 1).We refer to this overlap area as the "earthquake migration zone" (EMZ). The JMA catalog shows a similar pattern, but the migrations are less conspicuous because of the sparser data coverage.

The first migration sequence started in mid-February at a speed of ~2 km/day near the epicenter of the M_w 7.3 foreshock and later sped up to 5 km/day (red dashed lines in Fig. 2). The width of the seismically active zone also expanded slightly with time in the trench-parallel direction. This pattern could be explained by a succession of several independent afterslip sequences, each associated with a moderate earthquake (*19*). The whole migration sequence, which stopped in late February near the mainshock epicenter, was followed by a lull in foreshock activities that lasted for ~8 days.

A second migration sequence broke out just after the M_w 7.3 foreshock at an average speed of ~10 km/day. Its migration front, slowing down with time, is well approximated by a parabolic curve describing a diffusive process (*14*). Seismic activities in the EMZ, corresponding to the second migration sequence, peaked at a delay of about half a day after the M_w 7.3 foreshock. The northern part (outside the EMZ) saw an immediate, abrupt increase in the number of earthquakes, which decreased with time monotonically, according to the modified Omori law (Fig. 2).

About 90% of all migrating Tohoku-Oki foreshocks with moderate-to-large magnitudes located within the EMZ had low-angle thrust faulting mechanisms similar to the mainshock. They also included small repeating earthquakes that had identical mechanisms and identical locations (denoted by red stars in Figs. 1 and 2) (*18*), which are considered to be recurrent ruptures on potentially seismic patches of a fault to overtake quasi-static slip in the aseismically creeping areas outside (*20*–*23*). Therefore, the most plausible explanation for these migration sequences is the propagation of slow-slip events within the EMZ along the plate interface toward the initiation point of the M_w 9.0 mainshock rupture. The slow-slip migration speeds of 2 to 10 km/day are comparable to those of episodic-tremor and slow-slip events found along deeper extensions of warm subduction zones (*24*, *25*). This also supports our interpretation of the foreshock migration as propagation of slow slip.

We next estimated the time history of interplate slipping induced by slow-slip transients along the plate interface based on the analysis of the small repeating earthquakes. We identified the repeating earthquakes, applying the same technique as used in a previous study (*23*), to the JMA catalog (red stars in Fig. 2) (*18*). The slip in each event was calculated based on a unique scaling relation between the seismic moment and the fault slip for repeating earthquakes (*20*). The slip estimates were totaled within each of the four regional divisions shown in Fig. 3A, and the sum was divided by the number of repeating earthquake sequences within the corresponding division. In addition, our matched-filter technique enabled us to detect many events that were found to resemble the repeating earthquakes (green stars in Fig. 2). They are located in the close vicinity of, but not exactly on, fault patches where the corresponding repeating earthquakes occur. Their activities may provide a clue to the time evolution of aseismic creep outside the seismic patches (Fig. 3B).

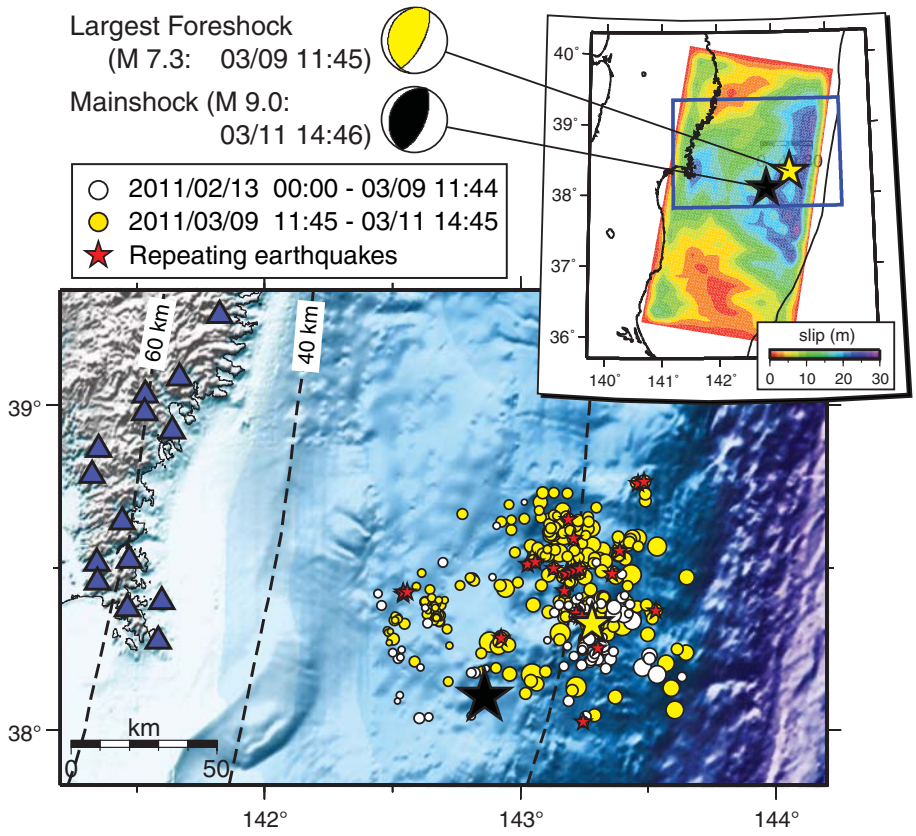

Fig. 1. Foreshocks and the mainshock rupture. Map of the foreshock region of the 2011 Tohoku-Oki earthquake, including the epicenters of the 11 March M_w 9.0 mainshock (black star), the 9 March M_w 7.3 largest foreshock (yellow star), and all 333 events in the JMA catalog between 13 February and 11 March 2011 (white and yellow circles scaled to magnitude). Blue triangles, seismic stations; dashed lines, iso-depth contours of the plate boundary at 20-km intervals (*34*); red stars, epicenters of small repeating earthquakes in the JMA catalog, identified as such based on a previous study (*23*). **(Inset)** Distribution of the total mainshock slip, imaged by a finite-source modeling using global broadband seismograms (*13*). Yellow/white and black/white spheres denote focal mechanisms of the largest foreshock and the mainshock, respectively.

Transient slip first started to build up to the south of the M_w 7.3 epicenter (divisions c and d in Fig. 3B) and continued to do so from mid- to late February at speeds far larger than the plate convergence rate. This increase in the slip rates coincided with the first sequence of earthquake migration toward the epicenter of the M_w 9.0 mainshock. After the M_w 7.3 foreshock, the amount of transient slip increased abruptly to the north of the M_w 7.3 epicenter, though it slightly slowed down logarithmically with time (a to c in Fig. 3B), a phenomenon commonly observed in afterslip following M_w 7 to 8 plate-interface earthquakes along the Japan and Kuril trenches (*26*–*28*). Within the EMZ, in contrast, slip increased at a rate of ~6 mm/hour, or up to 600 times the plate convergence rate (V_{pl}), during that final phase (c and d in Fig. 3B). Thus, the current study provides strong evidence for the propagation of slow-slip events toward the M_w 9.0 epicenter, based on the two sequences of earthquake migration accompanied by the repeating earthquakes.

The cumulative slip before the M_w 9.0 mainshock averaged ~20 cm across all four regional divisions. This converts to an estimated total moment release by the slow-slip transients worth up to M_w ~7.1, assuming that a fault with a 90–by–90-km^2 dimension (comparable to the foreshock region) slipped homogeneously (rigidity: 30 GPa). This assumption means that both seismic and aseismic slip coexisted on this fault. Geodetic measurements on land (Global Positioning System) detected transient deformation after the M_w 7.3 foreshock (*29*), whose moment release roughly coincided with that estimated in this study. This is consistent with the presence of the second slow-slip sequence documented in this study, although the geodetic measurements were not able to recognize their propagation toward the mainshock hypocenter because the land-based geodetic instruments are not sensitive to small amounts of off-shore fault slip.

The M_w 7.3 foreshock occurred near the northern end of the EMZ after the first migration of slow slip toward the M_w 9.0 mainshock hypocenter. In contrast, the mainshock nucleated near the southern end of the EMZ after the second migration, which was faster than the first one. Interestingly, the propagation of slow slip stopped in both cases near the mainshock hypocenter (Fig. 2). This suggests that the initiation point of the mainshock rupture was resistive enough to withstand the stress concentration caused by the oncoming slow-slip transients. A recent numerical modeling of the Tohoku-Oki earthquake also indicated that a shallow, highly resistive patch should be present close to the foreshock area to generate a M_w 9 earthquake (*30*).

The propagation of slow slip could be interpreted as part of the nucleation process, but there was no power-law acceleration in the slip and rupture growth to the mainshock origin of the type predicted by preslip models (*1*–*5*). In addition, the mainshock was not preceded by accelerating occurrences of foreshocks close to the mainshock hypocenter as reported for the 1999 Izmit earthquake (*11*). It should nevertheless be noted that the second sequence of slow slip had much larger slip rates and a larger migration speed than the first sequence (Figs. 2 and 3).

The slip rates involved in the second sequence of slow slip were also larger than those previously reported for transient slip after other earthquakes. In fact, the second sequence released approximately one-half of the moment of the M_w 7.3 Tohoku-Oki foreshock in only 2 days (*29*). In contrast, slow-slip transients (afterslip) after previous M_w 7 to 8 earthquakes along the Japan and Kuril trenches had slip rates of less than 4 cm/day (150 times the V_{pl}) during the first few days (*27*, *31*) and needed more than a few months to release half the moment of the mainshock (six events in table S1) (*26*, *32*).

It is conceivable that the first sequence of slow slip in the Tohoku-Oki focal region had weakened the plate interface within the EMZ,

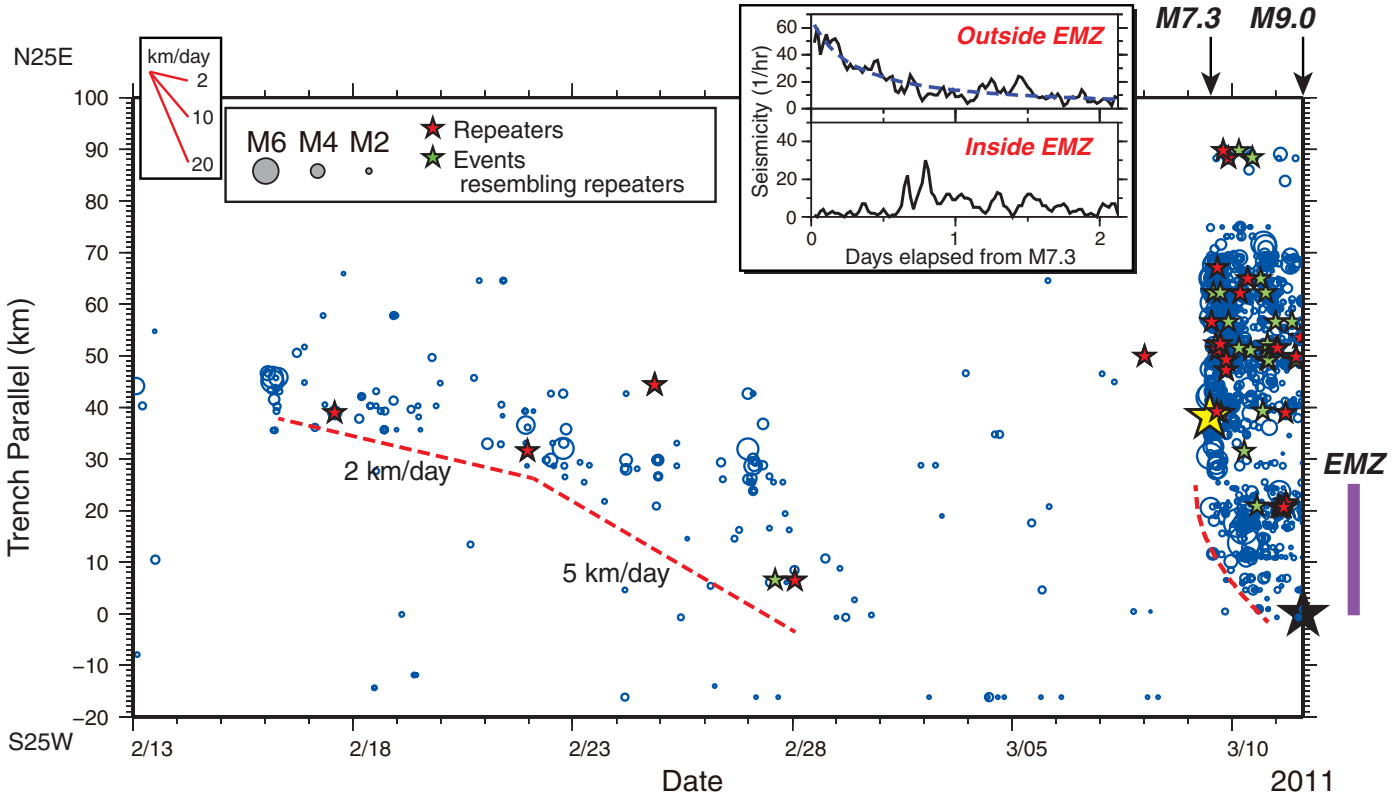

Fig. 2. Earthquake migration toward the rupture initiation point of the mainshock. Space-time diagram of all detected events between 13 February and the mainshock origin time, with earthquake origin locations indicated in terms of the distance along the trench axis (blue circles scaled to magnitude). Red dashed lines, approximate locations of the fronts of earthquake migration; red stars, repeating earthquakes in the JMA catalog (*23*); green stars, newly detected events that were found to resemble those repeating events; black star, M_w 9.0 mainshock; yellow star, M_w 7.3 largest foreshock. (**Inset**) Time variations in seismicity rates inside and outside the EMZ after the M_w 7.3 largest foreshock. The blue dashed curve denotes the least-squares fitting of the modified Ohmori law.

which facilitated slip (*33*). A subsequent, second sequence of slow slip, which had large slip rates, may have caused substantial stress loading onto the prospective hypocenter of the M_w 9.0 mainshock and prompted the initiation of unstable dynamic rupture there.

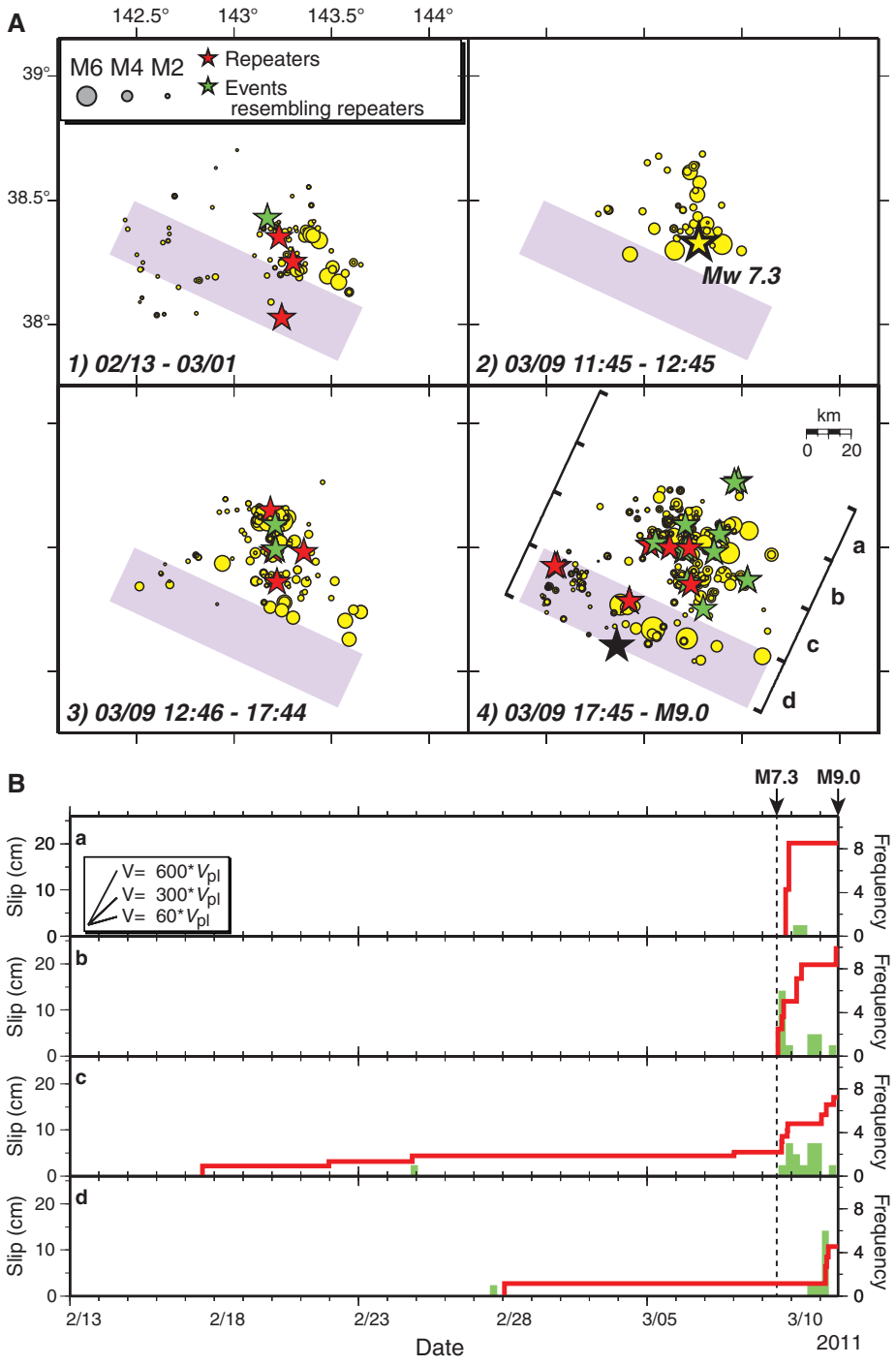

Fig. 3. Space-time characteristics of the two sequences of migrating slow-slip transients. (**A**) Map of all detected earthquakes (yellow circles scaled to magnitude) in different time windows. Red stars, repeating earthquakes in the JMA catalog; green stars, newly detected events that were found to resemble the repeating events; black star, M_w 9.0 mainshock; yellow star, M_w 7.3 largest foreshock; light purple rectangles, EMZ as defined in this study. (**B**) Average cumulative quasi-static slip in each of the four regional divisions shown in (A), plotted against time from 13 February to the mainshock origin (red lines). Green bars, combined frequencies, in successive 6-hour intervals, of newly detected events that were found to resemble repeating earthquakes; Black vertical dashed line, occurrence time of the largest foreshock. Line segments in the inset denote slopes corresponding to 60, 300, and 600 times the plate convergence rate.

References and Notes

1. J. H. Dieterich, *J. Geophys. Res.* **84**, 2161 (1979).
2. M. Ohnaka, *Tectonophysics* **211**, 149 (1992).
3. B. Shibazaki, M. Matsu'ura, *Geophys. Res. Lett.* **19**, 1189 (1992).
4. M. Ohnaka, L. Shen, *J. Geophys. Res.* **104**, 817 (1999).
5. N. Lapusta, J. R. Rice, Y. Ben-Zion, G. Zheng, *J. Geophys. Res.* **105**, 23765 (2000).
6. D. A. Dodge, G. C. Beroza, W. L. Ellsworth, *J. Geophys. Res.* **101**, 22371 (1996).
7. W. L. Ellsworth, G. C. Beroza, *Science* **268**, 851 (1995).
8. J. Mori, H. Kanamori, *Geophys. Res. Lett.* **23**, 2437 (1996).
9. R. E. Abercrombie, J. Mori, *Nature* **381**, 303 (1996).
10. J. J. McGuire, M. S. Boettcher, T. H. Jordan, *Nature* **434**, 457 (2005).
11. M. Bouchon *et al.*, *Science* **331**, 877 (2011).
12. F. Hirose, K. Miyaoka, N. Hayashimoto, T. Yamazaki, M. Nakamura, *Earth Planets Space* **63**, 513 (2011).
13. S. Ide, A. Baltay, G. C. Beroza, *Science* **332**, 1426 (2011).
14. R. Ando, K. Imanishi, *Earth Planets Space* **63**, 767 (2011).
15. D. R. Shelly, G. C. Beroza, S. Ide, *Nature* **446**, 305 (2007).
16. Z. Peng, P. Zhao, *Nat. Geosci.* **2**, 877 (2009).
17. N. Aso, K. Ohta, S. Ide, *Geophys. Res. Lett.* **38**, L08303 (2011).
18. Materials and methods are available as supporting material on *Science* Online.
19. T. Matsuzawa, N. Uchida, T. Igarashi, T. Okada, A. Hasegawa, *Earth Planets Space* **56**, 803 (2004).
20. R. M. Nadeau, L. R. Johnson, *Bull. Seismol. Soc. Am.* **88**, 790 (1998).
21. Z. Peng, Y. Ben-Zion, *Geophys. J. Int.* **160**, 1027 (2005).
22. T. Chen, N. Lapusta, *J. Geophys. Res.* **114**, B01311 (2009).
23. T. Igarashi, *Geophys. Res. Lett.* **37**, L20304 (2010).
24. H. Dragert, K. Wang, T. S. James, *Science* **292**, 1525 (2001).
25. K. Obara, *J. Geophys. Res.* **115**, B00A25 (2010).
26. K. Heki, S. Miyazaki, H. Tsuji, *Nature* **386**, 595 (1997).
27. S. Miyazaki, P. Segall, J. Fukuda, T. Kato, *Geophys. Res. Lett.* **31**, L06623 (2004).
28. N. Uchida *et al.*, *Gondwana Res.* **16**, 527 (2009).
29. S. Miyazaki, J. J. McGuire, P. Segall, *Earth Planets Space* **63**, 637 (2011).
30. N. Kato, S. Yoshida, *Geophys. Res. Lett.* **38**, L00G04 (2011).
31. Y. Yagi, M. Kikuchi, T. Nishimura, *Geophys. Res. Lett.* **30**, 2177 (2003).
32. H. Suito, T. Nishimura, M. Tobita, T. Imakiire, S. Ozawa, *Earth Planets Space* **63**, 615 (2011).
33. H. Houston, B. G. Delbridge, A. G. Wech, K. C. Creager, *Nat. Geosci.* **4**, 404 (2011).
34. J. Nakajima, A. Hasegawa, *Geophys. Res. Lett.* **33**, L16309 (2006).

Acknowledgments: We thank M. Nakatani for helpful comments and suggestions and the National Research Institute for Earth Science and Disaster Prevention, Tohoku Univ., and JMA for allowing us to use waveform data from their permanent stations. JMA provided us with an earthquake catalog. This study was supported by the Ministry of Education, Culture, Sports, Science and Technology of Japan, under its Observation and Research Program for Prediction of Earthquakes and Volcanic Eruptions.

Supporting Online Material

www.sciencemag.org/cgi/content/full/science.1215141/DC1
Materials and Methods
Fig. S1
Table S1
References (*35*–*37*)

11 October 2011; accepted 6 January 2012
Published online 19 January 2012;
10.1126/science.1215141

Structure-Based Mechanistic Insights into DNMT1-Mediated Maintenance DNA Methylation

Jikui Song,* Marianna Teplova, Satoko Ishibe-Murakami, Dinshaw J. Patel†

DNMT1, the major maintenance DNA methyltransferase in animals, helps to regulate gene expression, genome imprinting, and X-chromosome inactivation. We report on the crystal structure of a productive covalent mouse DNMT1(731-1602)–DNA complex containing a central hemimethylated CpG site. The methyl group of methylcytosine is positioned within a shallow hydrophobic concave surface, whereas the cytosine on the target strand is looped out and covalently anchored within the catalytic pocket. The DNA is distorted at the hemimethylated CpG step, with side chains from catalytic and recognition loops inserting through both grooves to fill an intercalation-type cavity associated with a dual base flip-out on partner strands. Structural and biochemical data establish how a combination of active and autoinhibitory mechanisms ensures the high fidelity of DNMT1-mediated maintenance DNA methylation.

In mammals, DNA methylation predominantly occurs on the carbon-5 position of cytosines within CpG dinucleotides (*1*–*4*) and is critically maintained by DNMT1 during DNA replication (*5*). DNMT1 is composed of a C-terminal methyltransferase domain and an N-terminal regulatory domain, linked by a conserved $(Gly\text{-}Lys)_n$ repeat (fig. S1A). The N-terminal domain contains sequences that mediate interactions of DNMT1 with other proteins (*6*, *7*), a nuclear localization sequence, a target recognition sequence that localizes DNMT1 to the DNA replication fork (*8*), a zinc finger CXXC (Cys-X-X-Cys) domain that specifically recognizes unmethylated CpG DNA (*9*, *10*), and a pair of bromo-adjacent homology (BAH) domains (*11*). The methyltransferase domain of DNMT1 is further folded into two subdomains, designated as the catalytic core and the target recognition domain (TRD).

We have determined the crystal structure of a productive complex of truncated mouse DNMT1 (mDNMT1) with DNA (Fig. 1A), which contrasts with our previously determined autoinhibitory structure of the mDNMT1-DNA complex (*12*). The complex contains mDNMT1(731-1602), which encompasses both BAH domains and the methyltransferase domain, bound to DNA within a (mCpG)-(fCpG) dinucleotide context. The complementary 12-mer DNA duplex is composed of a central 5-methylcytosine (mC)–containing hemi-mCpG step on the parental strand, positioned opposite to a 5-fluorocytosine (5fC)–containing fCpG step (*13*) on the target strand. The complex was produced by enzymatically cross-linking the 5fC on the DNA target strand to the reactive cysteine positioned in the catalytic pocket of mDNMT1 (fig. S1B).

Superposition of the structures of the productive (this study) and autoinhibited (*12*) mDNMT1-DNA complexes demonstrates that the largest conformational change is centered within the catalytic loop of mDNMT1 (Fig. 1B and fig. S2). In the productive covalent complex, the catalytic loop (in green) is followed by a straight α helix (green helical segment in inset of Fig. 1B) and penetrates into the DNA minor groove (Fig. 1C), forming extensive protein-DNA contacts (see below), whereas in the autoinhibitory structure of the complex, the α helix following the catalytic loop has a kink at the N-terminal end (purple helical segment in inset of Fig. 1B), and the catalytic loop (in purple) is excluded from the DNA minor groove by the autoinhibitory linker (in blue) (Fig. 1D).

Structural Biology Program, Memorial Sloan-Kettering Cancer Center, New York, NY 10065, USA.

*Present address: Department of Biochemistry, University of California, Riverside, CA 92521, USA.
†To whom correspondence should be addressed. E-mail: pateld@mskcc.org

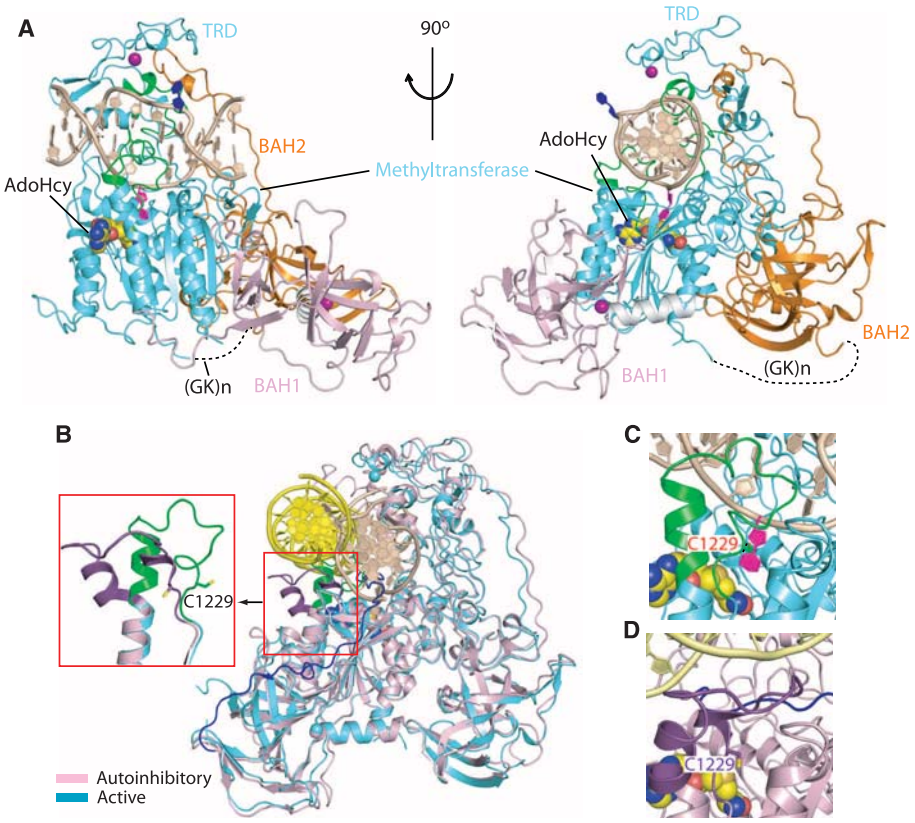

Fig. 1. Structural overview of mDNMT1(731-1602) bound covalently to a hemi-mCpG site. (**A**) Ribbon representation of the covalent complex in two orthogonal views. The BAH1, BAH2, and methyltransferase domains are colored light pink, orange, and cyan, respectively; DNA and zinc ions are barley and purple, respectively. The disordered $(Gly\text{-}Lys)_n$ linker [(GK)n] is shown as black dashed lines, the 5-methyl group from mC6 is green, the flipped-out target fC7′ is purple, the flipped-out C from parental strand is blue, the catalytic loop and TRD loops 1 and 2 are green, and the bound AdoHcy is in a space-filling representation. (**B**) Structural superposition of the covalent mDNMT1(731-1602)–DNA complex with the autoinhibited mDNMT1(650-1602)–DNA complex. The bound DNA in the covalent complex is in beige with the protein in cyan; they are yellow and cyan in the autoinhibited complex. The catalytic loop (expanded view in inset) is colored purple in the autoinhibited complex and green in the covalent complex. The CXXC-BAH1 domain linker is in dark blue in the autoinhibited complex. The inset highlights the transition from a straight helix (green) in the productive covalent complex to a kinked helix (purple) in the autoinhibited complex. (**C**) Close-up view of the catalytic loop (in green) in the covalent mDNMT1 (731-1602)–DNA complex (this study). (**D**) Close-up view of the catalytic loop (in dark brown) in the autoinhibited mDNMT1(650-1602)–DNA complex (PDB: 3PT6). The side chain of residue Cys^{1229} is shown in stick representation.

mDNMT1(731-1602)–mediated cytosine methylation kinetics on DNA 14-mer substrates containing single central hemi-mCpG versus unmodified CpG sites (fig. S3A) yielded kinetic (k_{cat} and k_{cat}/K_M) parameters similar to those previously measured for mDNMT1(717-1602) (fig. S3B and table S1) (*12*); the relative velocity of methylation of hemi-mCpG DNA substrate was greater than that of its CpG DNA counterpart by a factor of ~10 (fig. S3C).

The DNA duplex (Fig. 2A) is embedded in the catalytic cleft of mDNMT1, with the fC7′ of the target strand looped out of the helix and inserted into the catalytic pocket of the methyltransferase domain, where it is methylated and anchored through covalent bond formation with the reactive cysteine (Cys^{1229}) (Fig. 2B and fig. S4A). The fC7′ is surrounded by strictly conserved residues from the catalytic core (fig. S4), as initially observed for bacterial M.*Hha*I-DNA (*14*) and M.*Hae*III-DNA (*15*) complexes, and is in proximity to the *S*-adenosyl homocysteine (AdoHcy) (fig. S5).

Although the CXXC domain and the CXXC-BAH1 linker together play an autoinhibitory role in preventing methylation of unmethylated CpG sites by DNMT1 (*12*), DNMT1 retains considerable substrate preference toward hemi-mCpG steps in the absence of these two elements (fig. S3), which suggests that the methyltransferase domain by itself encodes capabilities for evaluating the methylation status of the substrate.

In the current structure of the productive mDNMT1-DNA complex, the methyl group attached to the C-5 position of mC6 on the parental strand is directed toward a hydrophobic segment within the TRD domain (Fig. 2C). In particular, the indole ring of a tryptophan (Trp^{1512}) slides into the DNA major groove upon complex formation and is partially stacked with the base of mC6, and, together with other hydrophobic residues (Cys^{1501}, Leu^{1502}, Leu^{1515}, and Met^{1535}), forms a shallow concave surface harboring the 5-methyl group of mC6 (Fig. 2C). This observation establishes the molecular basis for intrinsic preference of DNMT1 toward hemi-mCpG DNA substrates.

The formation of the productive mDNMT1-DNA complex involves infiltration of the DNA from both major (two TRD loops) and minor (catalytic loop) grooves (Fig. 1A and fig. S6), with the TRD domain undergoing concerted movement toward the DNA major groove by about 2 to 3 Å upon complex formation (Fig. 1B). We observe a large helical distortion around the central hemi-mCpG site resulting in the opening of an intercalation-type cavity 7.5 Å in length along the DNA helical axis (fig. S7, A and B). The side chain of Met^{1235} from the catalytic loop inserts into the DNA from the minor groove and occupies the space vacated by the extruded fC7′ on the target strand (Fig. 2, D and E). The side chain of Lys^{1537} from TRD loop 2 inserts into the DNA from the major groove and occupies the adjoining empty space on the parental strand (Fig. 2, D and E), which results from translation of the stacked orphan guanine (G7) by one step along the DNA helix toward the 3′ end, thereby flipping out the immediate downstream residue C8 (Fig. 2D). The antiparallel alignment of the side chains of Met^{1235} and Lys^{1537} is stabilized by a single hydrogen bond and further buttressed by the indole ring of Trp^{1512} (Fig. 2, D and E), with these distortions (fig. S8A) distinct from helical distortions reported for bacterial DNA methyltransferases (fig. S8, B and C). The mC6-G6′ Watson-Crick pair (Fig. 2F) and G7 of the noncanonical G7•G8′ pair (Fig. 2G) that bracket the intercalation site are recognized

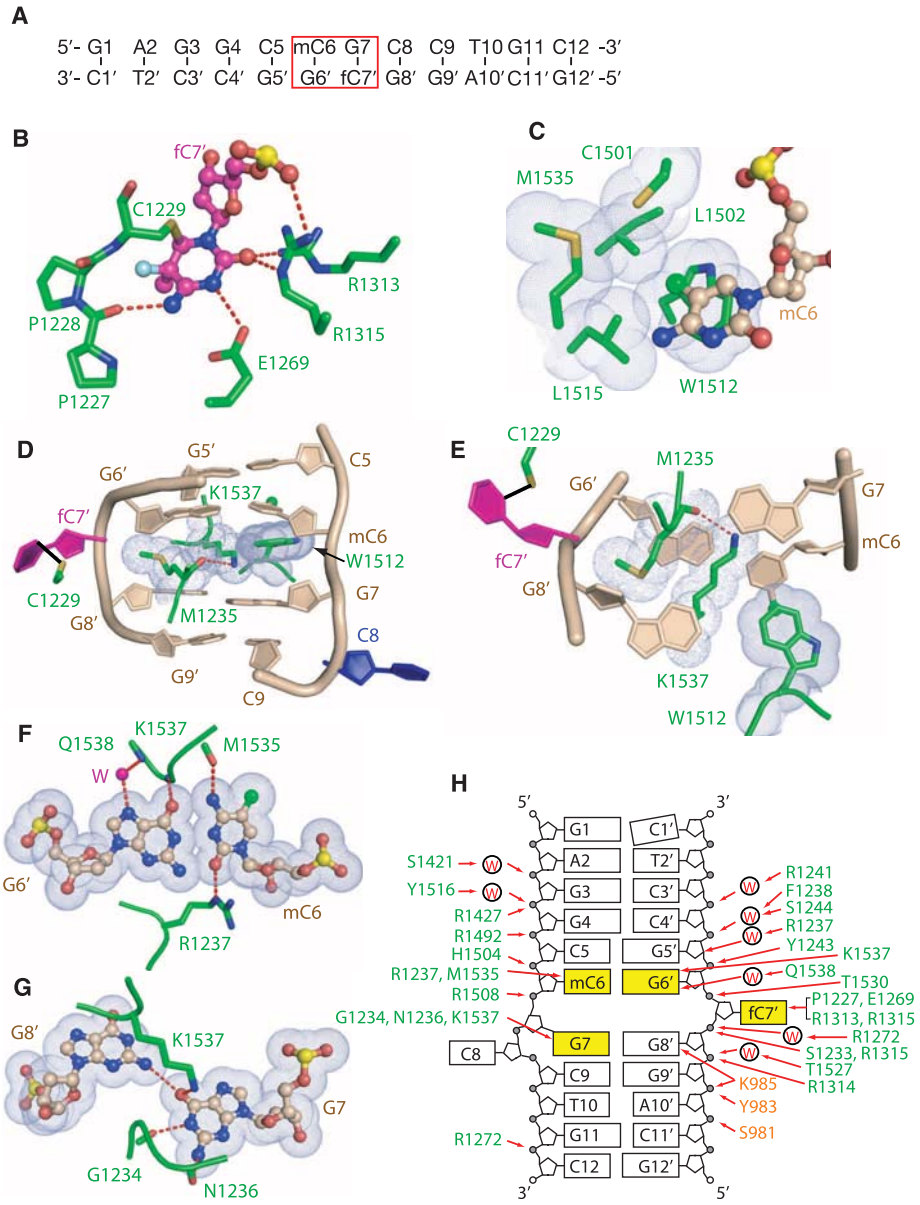

Fig. 2. Insertion of amino acid side chains into the intercalation-like distortion of the bound DNA and base-specific recognition at the hemi-mCpG site in the covalent mDNMT1-DNA complex. (**A**) Sequencing and numbering system of the hemi-mCpG–containing 12-mer duplex. (**B**) Stabilization of the flipped-out target cytosine fC7′ (light blue ball) in the active site of the enzyme. (**C**) The 5-methyl group (green ball) of mC6 is anchored within a hydrophobic concave surface of mDNMT1. (**D**) Insertion of side chains of Met^{1235} and Lys^{1537} into the intercalation-type space, and buttressing by indole ring of Trp^{1512}. The covalent bond between the sulfur atom of Cys^{1229} and the C6 atom of the target cytosine fC7′ is shown as a dark line. (**E**) End-on view of Met^{1235} and Lys^{1537} side chain insertion in the covalent complex. (**F**) Direct and water-mediated (labeled with purple W) hydrogen bond interactions target the Watson-Crick mC6-G6′ base pair from both grooves. (**G**) Stabilization of the repositioned guanine G7 through hydrogen-bonding interactions. (**H**) Schematic tabulation of direct and water-mediated hydrogen bond and electrostatic interactions between mDNMT1 and DNA in the covalent complex. Abbreviations for amino acids: C, Cys; E, Glu; F, Phe; G, Gly; H, His; K, Lys; L, Leu; M, Met; N, Asn; P, Pro; Q, Gln; R, Arg; S, Ser; T, Thr; W, Trp; Y, Tyr.

by elements from both the TRD and the catalytic core (Fig. 2H; stereo views in fig. S9, A and B).

The catalytic loop (residues 1227 to 1243) inserts into and spans both strands of the minor groove (Fig. 3A), making a network of direct and water-mediated contacts with mC6 and G7 on the parental strand, fC7′ on the target strand, and the phosphate backbone on either side of fC7′ (stereo view in fig. S10). In addition, both TRD loop 1 (residues 1501 to 1516) and loop 2 (residues 1530 to 1537) insert into and span both strands of the major groove centered about the hemi-mCpG step (fig. S6). TRD loop 1 contacts the phosphate backbone of the parental strand (Fig. 3B; stereo view in fig. S11), whereas TRD loop 2 is involved in base-specific recognition of the hemi-mCpG step and the DNA cavity (Fig. 3C; stereo view in fig. S12). Both TRD loops participate in formation of the hydrophobic concave surface that recognizes the 5-methyl group of mC6. Other DNA-interacting residues in the methyltransferase domain include Arg^{1272}, Arg^{1314}, Ser^{1421}, Arg^{1427}, Arg^{1492}, and Thr^{1527} (Fig. 2H and fig. S13).

Formation of the covalent mDNMT1-DNA complex is further accompanied by the conformational change within the BAH2 domain, whose helical tip moves toward the DNA along with the TRD (fig. S14). As a result, the side chains of three residues (Ser^{981}, Tyr^{983}, and Lys^{985}) immediately C-terminal to the tip, which are disordered in both free mDNMT1 and the autoinhibited mDNMT1-DNA complex, become ordered and engage in interactions with the phosphate backbone of the DNA target strand (Fig. 3D).

Guided by the structural analysis, we mutated a number of key and evolutionarily conserved residues (fig. S15) to monitor their impact on DNA methylation. First, we mutated residues lining the shallow concave surface that harbors the 5-methyl group of mC6. We observe that the Trp^{1512} → Ala mutant is essentially catalytically dead (Fig. 3E and fig. S16, A and B), consistent with the observation by a previous study (*16*) and the role of Trp^{1512} in base-stacking with the 5-methylcytosine. All other single mutants had their methylation rates reduced by factors of 2 to 4 for hemi-mCpG DNA substrate (Fig. 3E and fig. S16A) and by factors of 3 to 4 on unmethylated CpG substrate (Fig. 3E and fig. S16B); these findings suggest that the overall hydrophobic environment generated by a cluster of residues, rather than individual residues, is likely to play a dominant role in dictating the substrate specificity of mDNMT1.

Among residues that insert into the DNA intercalation site, the Met^{1235} → Ala mutant lost major catalytic activity on both hemi-mCpG and CpG DNA substrates (Fig. 3E and fig. S16, C and D). By contrast, the Lys^{1537} → Ala mutant exhibited a factor of 2 reduction in methylation rate for hemi-mCpG DNA substrate but an unanticipated factor of 2 increase in methylation rate on unmethylated CpG substrate (Fig. 3E and fig. S16, C and D). We have no definitive explanation for the latter result, but it is conceivable that such altered enzymatic behavior could arise from the impact of the Lys^{1537} → Ala mutation on the side chain orientations of Trp^{1512} and mC6 (Fig. 2C), which in turn could influence the substrate recognition.

Additional methylation kinetics were also performed for the Arg^{1237} → Ala mutant and for the Ser^{981} → Ala, Tyr^{983} → Ala, Lys^{985} → Ala triple mutant. In accordance with the structural analysis, both mutations show reduced catalytic activities upon DNA methylation (Fig. 3E and fig. S16, E and F). Taken together, our enzymatic

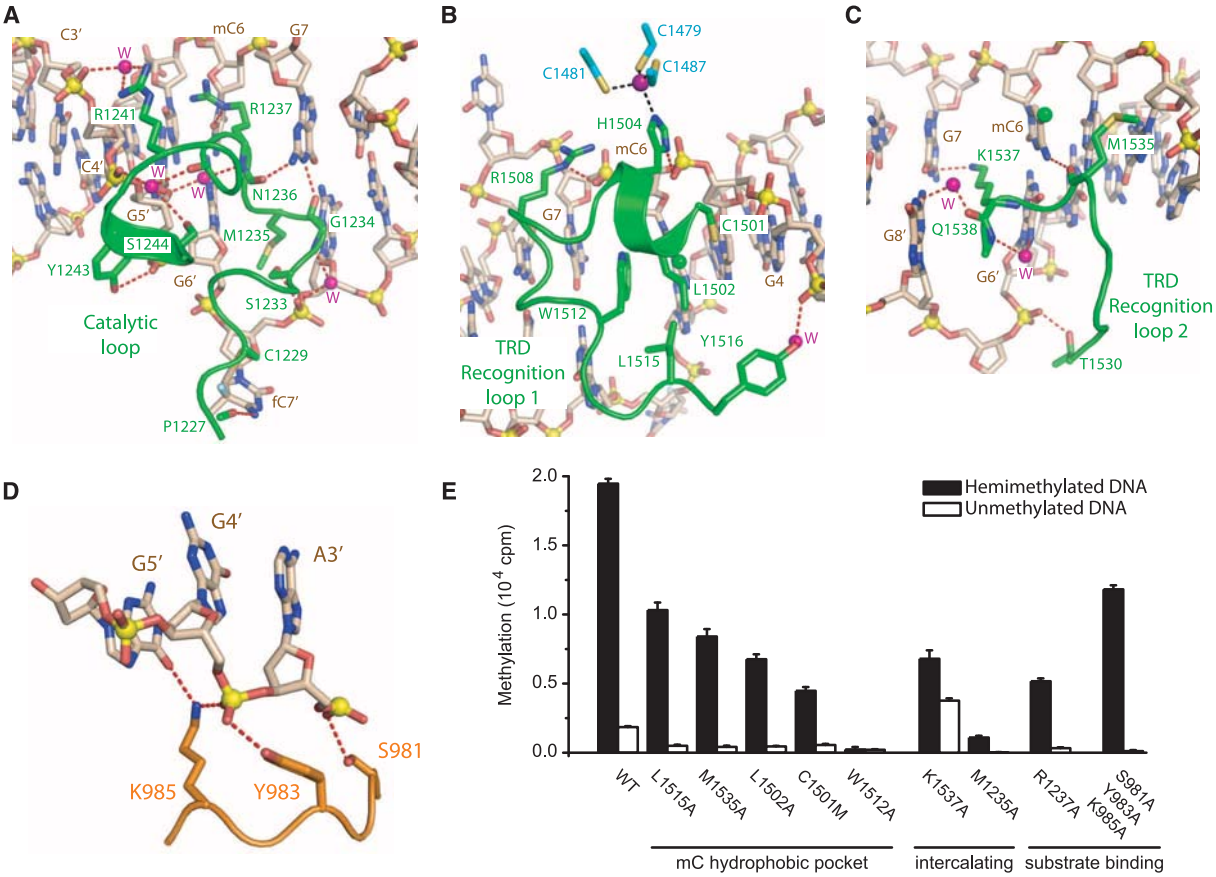

Fig. 3. Insertion of the catalytic loop and a pair of TRD loops into the grooves centered about the hemi-mCpG site in the covalent mDNMT1-DNA complex. (**A**) Catalytic loop–DNA interactions. (**B**) TRD loop 1–DNA interactions. The imidazole ring of His^{1504} bridges the zinc finger with the backbone phosphate of mC6. (**C**) TRD loop 2–DNA interactions. (**D**) Intermolecular hydrogen-bond interactions between side chains of a segment of the BAH2 loop and DNA in the complex. (**E**) Methylation activities of mDNMT1(731-1602) and its mutants involving amino acids that line the mC-recognizing hydrophobic surface, or insert into the intercalation-type cavity, and catalytic and BAH2 loop residues involved in substrate recognition. Methylation activities were monitored after reaction on hemi-mCpG DNA substrate (black bars) or unmodified CpG DNA substrate (white bars) for 10 min. Error bars represent SD calculated from two measurements.

methylation assays on selective mDNMT1 mutants appear to support structure-based molecular insights into substrate recognition by DNMT1.

Maintenance of DNA methylation patterns during cell division is crucial to animal development. DNMT1 is tethered to the DNA replication fork and is the major player in maintaining DNA methylation patterns during replication. The current structure of the productive mDNMT1-DNA complex, when combined with our earlier structure of the corresponding autoinhibited complex (*12*), establishes that two distinct but mutually supportive mechanisms are used by DNMT1 to ensure faithful maintenance of DNA methylation patterns after replication. As unmethylated CpG dinucleotides emerge from the replication complex, such sites are protected from de novo methylation by the autoinhibitory mechanism. On the other hand, as hemimethylated CpG sites emerge from the replication complex, specific recognition by the TRD domain of DNMT1 makes such sites optimal targets for maintenance DNA methylation. These two mechanisms, working in tandem and mutually supportive of each other, together with anticipated regulation by other proteins in the replication complex (such as UHRF1), ensure the fidelity of DNMT1-mediated maintenance DNA methylation.

References and Notes

1. X. Cheng, R. M. Blumenthal, *Structure* **16**, 341 (2008).
2. M. G. Goll, T. H. Bestor, *Annu. Rev. Biochem.* **74**, 481 (2005).
3. J. A. Law, S. E. Jacobsen, *Nat. Rev. Genet.* **11**, 204 (2010).
4. M. M. Suzuki, A. Bird, *Nat. Rev. Genet.* **9**, 465 (2008).
5. E. Li, T. H. Bestor, R. Jaenisch, *Cell* **69**, 915 (1992).
6. L. S. Chuang *et al.*, *Science* **277**, 1996 (1997).
7. M. R. Rountree, K. E. Bachman, S. B. Baylin, *Nat. Genet.* **25**, 269 (2000).
8. H. Leonhardt, A. W. Page, H. U. Weier, T. H. Bestor, *Cell* **71**, 865 (1992).
9. J. H. Lee, K. S. Voo, D. G. Skalnik, *J. Biol. Chem.* **276**, 44669 (2001).
10. M. Pradhan *et al.*, *Biochemistry* **47**, 10000 (2008).
11. I. Callebaut, J. C. Courvalin, J. P. Mornon, *FEBS Lett.* **446**, 189 (1999).
12. J. Song, O. Rechkoblit, T. H. Bestor, D. J. Patel, *Science* **331**, 1036 (2011).
13. D. G. Osterman, G. D. DePillis, J. C. Wu, A. Matsuda, D. V. Santi, *Biochemistry* **27**, 5204 (1988).
14. S. Klimasauskas, S. Kumar, R. J. Roberts, X. Cheng, *Cell* **76**, 357 (1994).
15. K. M. Reinisch, L. Chen, G. L. Verdine, W. N. Lipscomb, *Cell* **82**, 143 (1995).
16. K. Takeshita *et al.*, *Proc. Natl. Acad. Sci. U.S.A.* **108**, 9055 (2011).

Acknowledgments: Supported by funds from the Abby Rockefeller Mauze Trust and STARR and Maloris Foundations (D.J.P.). We thank T. Bestor and M. Goll for helpful discussions, and the staff of the NE-CAT beamlines at the Advanced Photon Source, Argonne National laboratory, for access and assistance with data collection. The structure of the complex has been deposited under accession no. 4DA4 in the Protein Data Bank.

Supporting Online Material

www.sciencemag.org/cgi/content/full/335/6069/709/DC1
Materials and Methods
Figs. S1 to S17
Tables S1 and S2
References (*17*–*21*)

26 September 2011; accepted 12 January 2012
10.1126/science.1214453

Structure and Allostery of the PKA RIIβ Tetrameric Holoenzyme

Ping Zhang,[1] Eric V. Smith-Nguyen,[2] Malik M. Keshwani,[1,3] Michael S. Deal,[2] Alexandr P. Kornev,[2,3] Susan S. Taylor[1,2,3]*

In its physiological state, cyclic adenosine monophosphate (cAMP)–dependent protein kinase (PKA) is a tetramer that contains a regulatory (R) subunit dimer and two catalytic (C) subunits. We describe here the 2.3 angstrom structure of full-length tetrameric RIIβ$_2$:C$_2$ holoenzyme. This structure showing a dimer of dimers provides a mechanistic understanding of allosteric activation by cAMP. The heterodimers are anchored together by an interface created by the β4-β5 loop in the RIIβ subunit, which docks onto the carboxyl-terminal tail of the adjacent C subunit, thereby forcing the C subunit into a fully closed conformation in the absence of nucleotide. Diffusion of magnesium adenosine triphosphate (ATP) into these crystals trapped not ATP, but the reaction products, adenosine diphosphate and the phosphorylated RIIβ subunit. This complex has implications for the dissociation-reassociation cycling of PKA. The quaternary structure of the RIIβ tetramer differs appreciably from our model of the RIα tetramer, confirming the small-angle x-ray scattering prediction that the structures of each PKA tetramer are different.

Cyclic adenosine monophosphate (cAMP)–dependent protein kinase (PKA), a ubiquitous serine/threonine protein kinase, exists in mammalian cells as an inactive tetrameric holoenzyme composed of a regulatory (R) subunit dimer and two catalytic (C) subunits. cAMP binding to the R subunits releases the active C subunits, allowing them to phosphorylate specific substrate proteins. The two classes of R subunit, RI and RII, each have α and β isoforms, and these functionally nonredundant isoforms are a primary mechanism for achieving specificity in PKA signaling (*1*). Deletion of RIα, for example, is embryonically lethal (*2*), whereas RIIβ knockout mice have a lean phenotype and are not susceptible to diet-induced insulin resistance (*3*, *4*). Depletion of RIIβ reverses the obesity syndrome of agouti mice (*5*). RIIβ is the predominant isoform in brain and adipose tissue (*2*, *6*). RII subunits are typically anchored to membrane proteins through high-affinity binding to adenosine kinase–anchoring proteins (AKAPs).

The crystal structure of the C subunit revealed the conserved kinase core shared by all members of the protein kinase superfamily (*7*, *8*). It is bilobal with a large, helical C lobe (Fig. 1A) that facilitates substrate recognition and provides the catalytic machinery for phosphoryl transfer and a smaller, more dynamic beta-rich N lobe that is associated mostly with adenosine triphosphate (ATP) binding (*7*, *9*, *10*). The C-terminal tail (C tail), a conserved feature of kinases belonging to the AGC subfamily, serves as a cis-regulatory element that wraps around both lobes and primes the C subunit for catalysis (*11*).

Each R subunit (Fig. 1A) contains an N-terminal dimerization/docking (D/D) domain, followed by a flexible linker containing an inhibitor site (IS) that docks to the active-site cleft of the C subunit in the holoenzyme. At the C terminus are two tandem highly conserved cyclic nucleotide-binding domains (CNB-A and CNB-B) (*12*). PKA is anchored to specific sites in the cell by binding of an AKAP amphipathic helix to the D/D domain (*13*, *14*). RII ISs have a Ser at their phosphorylation site (P site) and are both substrates and inhibitors, whereas RI subunits with Gly or Ala at their P site are inhibitors and pseudosubstrates. Phosphorylation of the P-site Ser in RII slows the rate of association with C subunit (*15*, *16*), and formation of holoenzyme in cells is influenced substantially depending on whether the P-site residue is a substrate or a pseudosubstrate (*12*, *17*). In contrast to RII subunits, forming a high-affinity type I holoenzyme with RI subunits requires Mg_2ATP (*18*).

Complexes of R and C subunits, first described with truncated monomeric R subunits, showed for the first time how the C subunit was inhibited by R and how the complex was activated by cAMP (*19*–*22*). These RIα, RIIα, and RIIβ heterodimeric complexes also showed that the R subunits undergo a dramatic conformational change as they release cAMP and bind to C subunit. However, in the absence of cAMP, PKA in cells exists as a tetramer, and only a full-length tetrameric holoenzyme structure will explain how PKA is assembled in its physiological state and how it acquires its allosteric properties. A model of the (RIα)$_2$:C$_2$ holoenzyme was proposed recently (*23*),

[1]Howard Hughes Medical Institute, University of California, San Diego, La Jolla, CA 92093–0654, USA. [2]Department of Chemistry and Biochemistry, University of California, San Diego, La Jolla, CA 92093–0654, USA. [3]Department of Pharmacology, University of California, San Diego, La Jolla, CA 92093–0654, USA.

*To whom correspondence should be addressed. E-mail: staylor@ucsd.edu

but so far there is no full-length tetrameric structure of PKA. Furthermore, although different PKA holoenzyme isoforms have similar domain organizations, each holoenzyme, based on small-angle x-ray scattering (SAXS), has a different quaternary structure (*24*, *25*); perhaps most notable is the difference between RIIα and RIIβ holoenzymes (*24*). SAXS showed that both RII homodimers are elongated; however, RIIβ holoenzyme becomes compact, whereas RIIα holoenzyme remains extended. To understand the structural and functional nonredundancy of the PKA isoforms requires structures of tetrameric holoenzymes.

To crystallize a tetrameric $RII\beta_2:C_2$ holoenzyme, we generated wild-type RIIβ(1-416), and, in an effort to stabilize the holoenzyme, we also expressed and purified two mutants that abolished high-affinity binding of cAMP in CNB-A [RIIβ(R230K)] and CNB-B [RIIβ(R359K)], respectively. Only the RIIβ(R230K) holoenyme produced well-diffracting crystals. The crystal structure of the tetrameric $RII\beta(R230K)_2:C_2$ holoenzyme (labeled as $RII\beta^*_2:C_2$) was solved at 2.3 Å (Fig. 1, fig. S1, and table S1). Although residues 1 to 103, 122 to 129, and 394 to 416 of RIIβ and residues 1 to 13 of C are missing in the electron density, we validated by using gel electrophoresis that the full-length $RII\beta_2:C_2$ complex is in the protein crystal. The absence of density for the N-terminal D/D domain and the following linker is likely related to the flexible nature of this region.

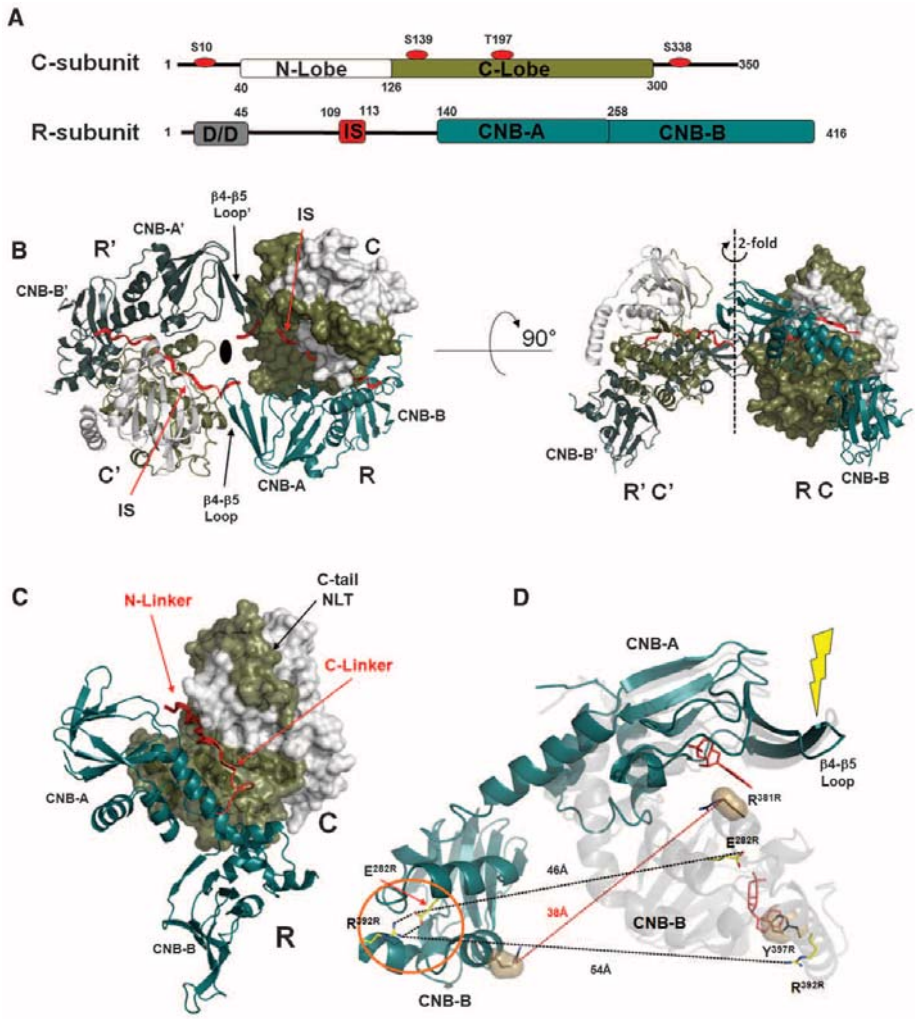

Fig. 1. Overall view of the $RII\beta^*_2:C_2$ tetrameric holoenzyme. (**A**) Domain organization and color coding of the R and C subunits. The four red spheres indicate the phosphorylation sites in C subunit. (**B**) Structure of the $RII\beta^*_2:C_2$ tetrameric holoenzyme. The N lobe of the C subunit is white; the C lobe and C tail are tan. The N-linker segment of the R subunit that contains the IS and docks to the active-site cleft of the C subunit is shown as a red ribbon. One heterodimer is labeled as RC, and its twofold symmetry mate is labeled as R′C′. The twofold axis position is shown as a black oval (left) and dotted line (right). (**C**) One RIIβ:C heterodimeric holoenzyme structure in the $RII\beta^*_2:C_2$ tetrameric holoenzyme. (**D**) RIIβ undergoes dramatic conformational changes upon binding to the C subunit. RIIβ bound to the C subunit is shown on the left and bound to cAMP shown on the right (PDB ID code 1CX4, in black). The salt bridge Glu^{282R}-Arg^{392R} formed upon binding to the C subunit is shown in an orange circle.

The structure confirms the SAXS predictions (*24*) that the highly extended RIIβ dimer folded up into a compact holoenzyme (fig. S2). The compact, doughnut-shaped tetramer contains two R:C heterodimers (labeled RC and R'C') with a rotational twofold symmetry through the central cavity (Fig. 1, B and C). This structure also reveals the dramatic changes that take place in the RIIβ subunit as it releases cAMP and binds to C subunit (Fig. 1D). In the cAMP-bound state, two hydrophobic capping residues (Arg^{381R} for CNB-A and Tyr^{397R} for CNB-B) are bound to the adenine rings of cAMP (*26*, *27*). These two residues move away from the cAMP binding sites in the holoenzyme (38 Å for Arg^{381R}) and are kept in this distal location by a holoenzyme-specific salt bridge between Arg^{392R} and Glu^{282R} (Fig. 1D). This salt bridge is important for allosteric activation (*20*, *22*) and is conserved in all R-subunit isoforms (*12*).

The C subunits are well separated, whereas each R subunit contacts the neighboring R:C heterodimers by using the highly conserved but isoform-specific β4-β5 loop in the CNB-A domain (fig. S3). This loop is exposed to solvent in the free cAMP-bound R subunit (Fig. 1D) and also in the heterodimer (*20*, *22*); however, in the tetramer it reaches over to the opposite dimer and creates an extensive interface. The area of each interface between the two heterodimers, which are strictly twofold rotational symmetry related, is ~500 $Å^2$. The major site of contact is to the C-terminal tail of the opposite C subunit, specifically the active-site tether (AST, residues 320 to 339) segment. The C tail (residues 301 to 350 in PKA) is a highly conserved feature of all AGC kinases (*11*). Residues 301 to 318, referred to as the C-lobe tether, are anchored firmly to the C lobe, whereas residues 336 to 350, referred to as the N-lobe tether, are anchored through a hydrophobic motif to the N lobe. The intervening AST segment, typically disordered in the absence of nucleotide, becomes an integral part of the ATP binding site when nucleotide is bound. A conserved Phe-Asp-Asp-Tyr (FDDY) motif (residues 327 to 330) in this region, in particular Phe^{327C} and Tyr^{330C}, are part of the hydrophobic pocket that anchors the adenine and ribose rings of ATP. When either residue is replaced with Ala, enzymatic activity is lost and affinity for ATP is reduced (*28*, *29*). In the holoenzyme, the β4-β5 loop docks to the back of the FDDY motif, pushing it and the entire N lobe into a fully closed conformation even though the nucleotide is absent. The β4-β5 loop also interacts with a portion of the R-subunit N linker from the opposite heterodimer. The details of these interactions are described in fig. S3.

Ordering of the C tail and the N lobe by the β4-β5 loop into a closed conformation independent of ATP is one of the most striking features of the RIIβ tetrameric holoenzyme and distinguishes it from the heterodimer and from all previous structures of the C subunit, which are only in a closed conformation when ATP and two magnesium ions are bound (Fig. 2A). In this structure,

Ser^{53C} at the tip of the Gly-rich loop interacts with the backbone carbonyl of the P-site Ser^{112R}, and this is a hallmark of the closed conformation. Ser^{112R} also forms hydrogen bonds with catalytic loop residues Asp^{166C} and Lys^{168C} (Fig. 2A). In the RIα heterodimer, the C subunit is also in a closed conformation that requires Mg_2ATP, whereas in the RIIα heterodimer, where high-affinity binding does not require Mg_2ATP (*18*), the C subunit is in an open conformation with an empty ATP binding pocket and a disordered C tail (Fig. 2B) (*20*, *22*). Comparing temperature factors (B factor) of C subunits in different R:C complexes reveals regions of relative order and disorder (Fig. 2B and table S2). The nucleotide-bound RIα(91-379):C heterodimer is in a fully closed conformation and has low B-factors both in the N and C lobe (Fig. 2B and table S2). In contrast, the nucleotide-free RIIα(90-400):C dimer has high B factors in the N lobe, and the C tail is partially disordered, consistent with its open conformation (Fig. 2B). The apo nucleotide-free tetrameric holoenzyme, similar to the nucleotide-bound RIα complex, has low B factors in both lobes, which reflects its closed conformation and ordered C tail (Fig. 2B).

The allosteric properties of the RIIβ holoenzyme are also different from the RIIβ heterodimer and from the other three PKA isoforms. The activation constant (K_a) for activation of the RIIβ tetramer by cAMP is 584 nM, and this is significantly higher than the K_a for other holoenzymes [101 nM for RIα (*30*), 29 nM for RIβ (*31*), and 137 nM for RIIα (Fig. 4A)]. It is also higher than the K_a of 65nM for RIIβ heterodimer (Fig. 3). The increased K_a for the RIIβ tetrameric holoenzyme can be explained by the extensive interfaces between the two heterodimers, where the phosphate-binding cassette (PBC) docking site for cAMP in CNB-A is juxtapositioned directly against the ATP binding site in N lobe of the C subunit in the opposite heterodimer (Fig. 3B). The Hill coefficient for the RIIβ tetramer is 1.7, in contrast to 0.65 for the heterodimers, which indicates that allostery is unique to the tetramer. The considerable cross-talk between the two CNB domains and the between the two heterodimers is also reflected by several mutations. When the CNB-B domain is deleted entirely, for example, the K_a for activation is 60 nM and the Hill coefficient is reduced to 1.2, indicating that there is still substantial allosteric cross-talk between the two CNB-A domains (*31*, *32*) (Fig. 3C). When the cAMP binding site in the CNB-A domain is deleted, the K_a for activation is very high, 13 μM, confirming that cAMP binding to CNB-A is essential for activation. However, when the B domain is mutated, the enzyme still has a similar K_a for activation (490 nM), but all cooperativity is lost. The molecular basis for this complex allostery could simply not be appreciated in the absence of the holoenzyme structure.

Given that the ATP binding chamber in the C subunit is perfectly formed and locked into a closed conformation, we hypothesized that ATP could diffuse into this pocket without breaking

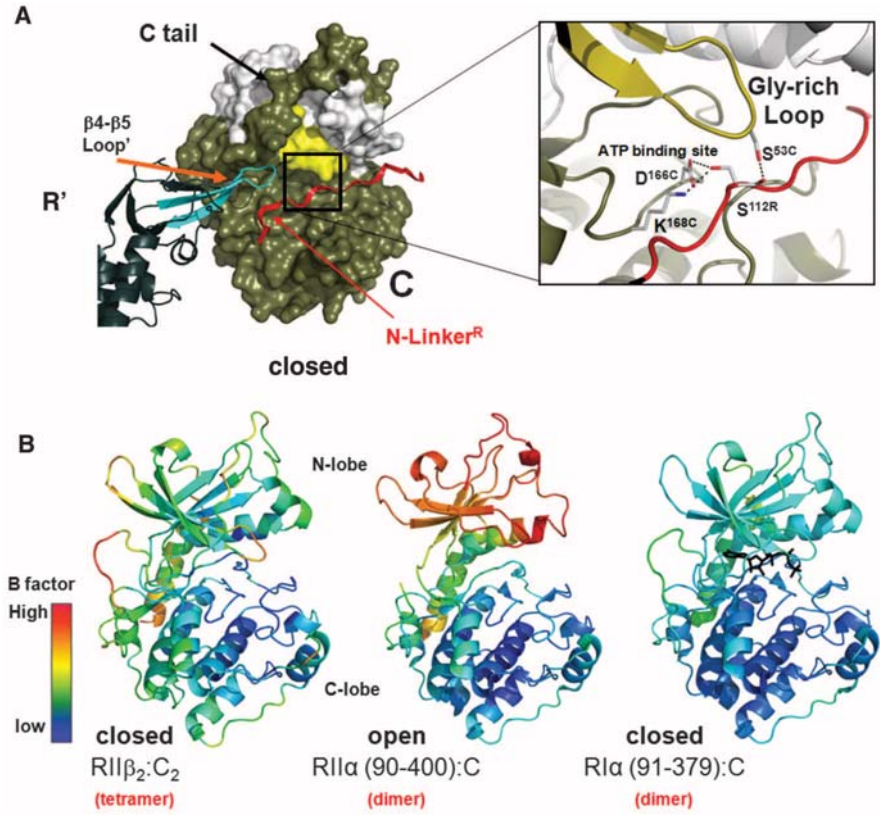

Fig. 2. C subunit is in a closed conformation. (**A**) The active site of the C subunit in the RIIβ*$_2$:C$_2$ tetrameric holoenzyme is fully closed in the absence of ATP. S, Ser; K, Lys. (**B**) The conformation and B factors analysis of the C subunit in three holoenzyme structures. The left bottom is the scale bar for B factors.

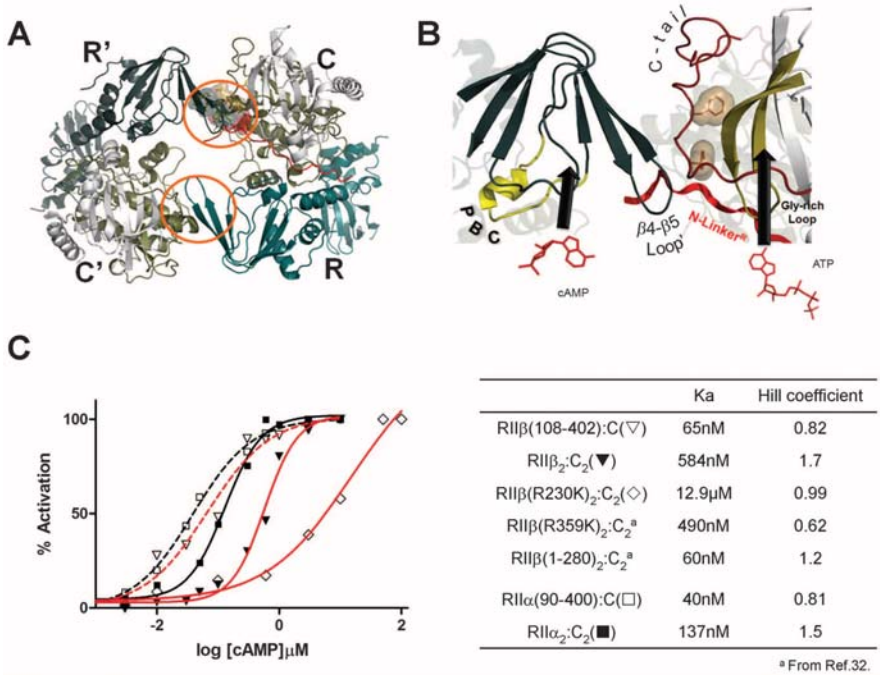

	Ka	Hill coefficient
RIIβ(108-402):C(▽)	65nM	0.82
RIIβ$_2$:C$_2$(▼)	584nM	1.7
RIIβ(R230K)$_2$:C$_2$(◇)	12.9μM	0.99
RIIβ(R359K)$_2$:C$_2$[a]	490nM	0.62
RIIβ(1-280)$_2$:C$_2$[a]	60nM	1.2
RIIα(90-400):C(□)	40nM	0.81
RIIα$_2$:C$_2$(■)	137nM	1.5

[a] From Ref.32.

Fig. 3. Allosteric cAMP activation mechanism for the RIIβ holoenzyme. (**A**) Overall interactions of the RC and R′C′. The two symmetry-related interfaces are shown in orange circles. (**B**) The binding site for cAMP to CNB-A′ in R′C′ heterodimer (left arrow) is juxtapositioned directly against the ATP binding site (right arrow) in the N lobe of the C subunit in the symmetry-related RC dimer. (**C**) Activation of holoenzymes by cAMP. The K_a values for activation were measured as a function of cAMP. Each holoenzyme is designated as follows: RIIα(90-400):C(□), RIIβ(108-402):C(▽), RIIα$_2$:C$_2$(□), WT RIIβ$_2$:C2(▼), and RIIβ*$_2$:C$_2$(◇).

the crystal lattice. We thus soaked the apo crystals with MgATP (materials and methods). The resulting crystals, solved to a resolution of 3.1 Å (table S1), showed that nucleotide had diffused into the active site. However, instead of finding ATP, we found the reaction products, Mg_2ADP and the phosphorylated RIIβ subunit (Fig. 4 and fig. S5). This is the first time that we have trapped both reaction products in the active-site cleft, and such a complex has also not been observed for other protein kinases. Even trapping a transition state complex has been challenging, and PKA is one of the few examples where this has been possible (*33*). The overall $RII\beta^P{}_2{:}C_2{:}(Mg_2ADP)_2$ structure closely resembles the apo $RII\beta^*{}_2{:}C_2$ structure (fig. S5) with a Cα root mean square deviation (RMSD) of 0.67 Å. The C subunit still remains in a closed conformation and still has low B factors in both the C and N lobe (table S2). The B factors in the phosphorylated inhibitor site of RIIβ are also low. There is an ~5 Å shift of the tip residue Ser^{53C} in the Gly-rich loop from its position in the apo structure, which is sufficient to break the hydrogen bond between the Ser^{53C} and Ser^{112R} (Fig. 2A and fig. S5). Thus, the $RII\beta^P{}_2{:}C_2{:}(Mg_2ADP)_2$ tetramer contains a perfectly formed stable reaction chamber that allows for catalysis, but the reaction products were trapped. We hypothesize that this complex may be a physiologically relevant state for the RIIβ holoenzyme.

Typically the $RII\beta_2{:}C_2$ holoenzyme is colocalized through AKAPs with protein phosphatases (PPs) (*34*). For example, calcineurin, a calcium-activated phosphatase, and PKA RII holoenzymes are colocalized at the C terminus of AKAP79/150 (*34*). Because the RII inhibitor sites are excellent substrates for calcineurin, it has been assumed that the RIIβ subunit is dephosphorylated by calcineurin to facilitate its reassociation with C subunits (*15*, *16*). However, a recent report suggests that the RII subunits in cardiac myocytes are mostly phosphorylated in the absence of forskolin (*35*). Although this observation needs to be further validated, our structure suggests that in cells the inactive $RII\beta_2{:}C_2$ holoenzyme, once formed, may be primed to have its R subunits autophosphorylated (Fig. 4C) given the high availability of cytoplasmic MgATP. This presents the following scenario. Cooperative cAMP activation leads to dissociation of the C subunits from the $RII\beta^P$ homodimer. Nearby phosphatases like calcineurin, localized in close proximity to the RII holoenzyme (*34*, *36*), can then modulate PKA activity by dephosphorylating the $RII\beta^P$ subunit when calcium levels are elevated, thereby facilitating the regeneration of inactive $RII\beta_2{:}C_2$ holoenzyme (*15*, *16*). This apo $RII\beta_2{:}C_2$ holoenzyme can then get autophosphorylated with cytoplasmic MgATP yet stay in an inactive form (Fig. 4C) until cAMP levels are elevated again.

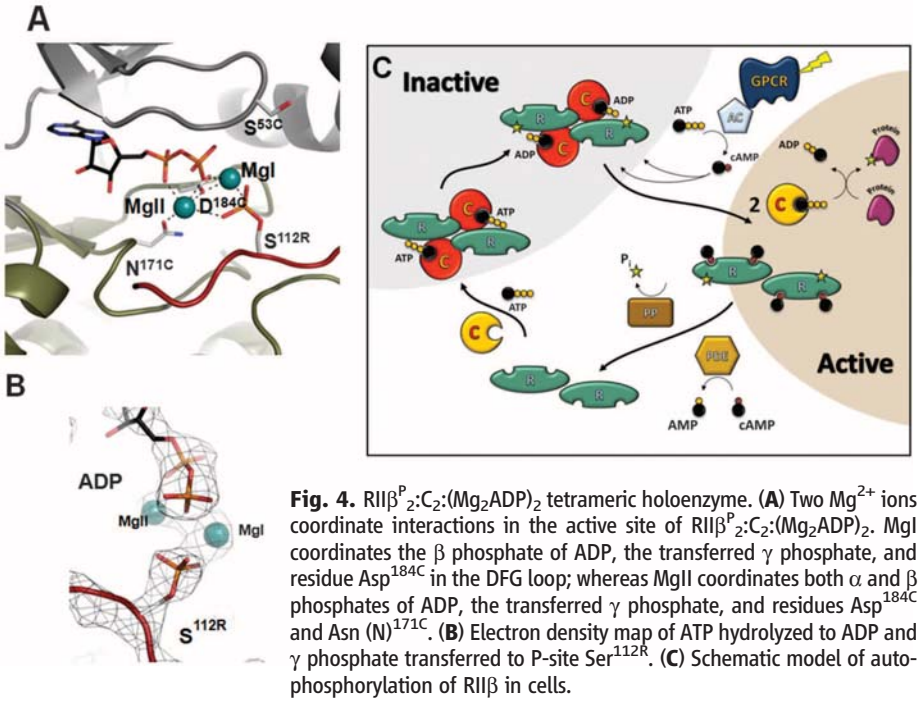

Fig. 4. $RII\beta^P{}_2{:}C_2{:}(Mg_2ADP)_2$ tetrameric holoenzyme. (**A**) Two Mg^{2+} ions coordinate interactions in the active site of $RII\beta^P{}_2{:}C_2{:}(Mg_2ADP)_2$. MgI coordinates the β phosphate of ADP, the transferred γ phosphate, and residue Asp^{184C} in the DFG loop; whereas MgII coordinates both α and β phosphates of ADP, the transferred γ phosphate, and residues Asp^{184C} and Asn (N)^{171C}. (**B**) Electron density map of ATP hydrolyzed to ADP and γ phosphate transferred to P-site Ser^{112R}. (**C**) Schematic model of autophosphorylation of RIIβ in cells.

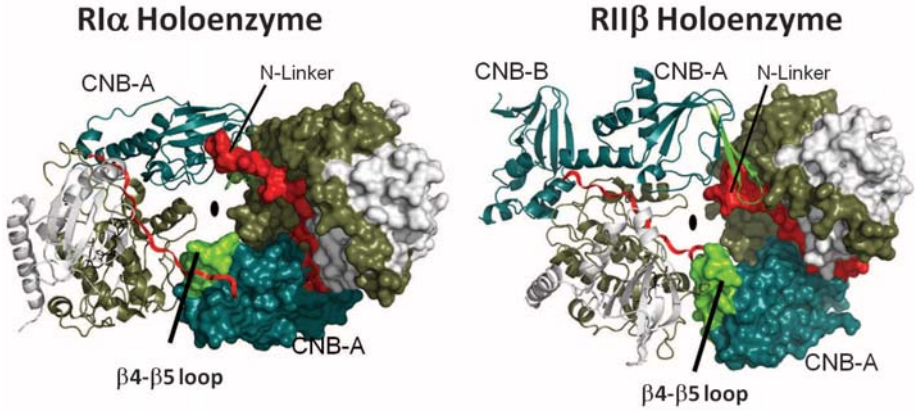

Fig. 5. Comparison of $RI\alpha_2{:}C_2$ model (3PVB) and $RII\beta^*{}_2{:}C_2$ structure. Although each holoenzyme creates a twofold symmetry, the interface is completely different in the two tetramers. The N-linker is red and β4-β5 loop is green. The axes of symmetry are also indicated by the black ovals.

Anchoring of RII holoenzymes near membranes is mediated by the D/D domain binding to AKAPs, and, from the position of the traced N linker of the two RIIβ chains (fig. S6) and the available space in crystal packing, the position of the missing D/D domain can be predicted. In our RIIβ structure, the first 13 residues of the C subunit are disordered, whereas in the free C subunit the myristyl group is folded into a hydrophobic pocket in the C lobe of the C subunit (*37*). Fluorescence anisotropy studies showed that binding of the RIIβ subunit causes the myristylated N tail to become more flexible and dynamic, and, in contrast to free C and the RIα tetramer, the RII holoenzyme interacts with membrane vesicles (*38*). When the RIIβ holoenzyme is targeted by AKAPs to membrane proteins, the exposed myristyl groups will likely be on the same surface as the AKAP, which provides an opportunity for multivalent membrane anchoring. The holoenzyme targeted to membranes also has the potential to interact with other signaling proteins, such as adenylylate cyclases (ACs), heterotrimeric guanine nucleotide–binding (G) proteins, G protein–coupled receptors (GPCRs), and phosphodiesterases (PDEs) in addition to AKAPs, and thus could contribute to the assembly of larger macromolecular complexes. These interactions would create enormous opportunities for synergy that now need to be considered more rigorously.

A comparison of our model of the RIα tetrameric holoenzyme (*23*) with the RIIβ holoenzyme (Fig. 5 and fig. S7) shows how isoform-specific quaternary structures can be created even though the tertiary structures of the heterodimers are remarkably similar for RIα, RIIα (*20*, *22*), and RIIβ. By forming a dimer of dimers, a twofold axis of symmetry is created in the tetrameric holoenzyme; however, the specific interface between

the dimers is different for each R-subunit isoform. In each case, however, the β4-β5 loop in the R subunit appears to serves a specificity determinant for docking between the two heterodimers. By comparing the RIIβ tetramer with a model of the RIα holoenzyme, we see how distinct quaternary architectures can be created. It is only by comparing the full-length holoenzymes that we can appreciate that the functional nonredundancy of the PKA isoforms is also reflected in the structural nonredundancy of these isoforms. Correlating these structural differences with functional consequences will be our next challenge.

References and Notes

1. P. S. Amieux *et al.*, *J. Biol. Chem.* **277**, 27294 (2002).
2. P. S. Amieux *et al.*, *J. Biol. Chem.* **272**, 3993 (1997).
3. D. E. Cummings *et al.*, *Nature* **382**, 622 (1996).
4. S. A. Schreyer, D. E. Cummings, G. S. McKnight, R. C. LeBoeuf, *Diabetes* **50**, 2555 (2001).
5. T. A. Czyzyk, M. A. Sikorski, L. Yang, G. S. McKnight, *Proc. Natl. Acad. Sci. U.S.A.* **105**, 276 (2008).
6. G. McConnachie, L. K. Langeberg, J. D. Scott, *Trends Mol. Med.* **12**, 317 (2006).
7. D. R. Knighton *et al.*, *Science* **253**, 407 (1991).
8. G. Manning, D. B. Whyte, R. Martinez, T. Hunter, S. Sudarsanam, *Science* **298**, 1912 (2002).
9. X. Cheng, C. Phelps, S. S. Taylor, *J. Biol. Chem.* **276**, 4102 (2001).
10. D. A. Johnson, P. Akamine, E. Radzio-Andzelm, M. Madhusudan, S. S. Taylor, *Chem. Rev.* **101**, 2243 (2001).
11. N. Kannan, N. Haste, S. S. Taylor, A. F. Neuwald, *Proc. Natl. Acad. Sci. U.S.A.* **104**, 1272 (2007).
12. J. M. Canaves, S. S. Taylor, *J. Mol. Evol.* **54**, 17 (2002).
13. F. S. Kinderman *et al.*, *Mol. Cell* **24**, 397 (2006).
14. M. G. Newlon *et al.*, *EMBO J.* **20**, 1651 (2001).
15. M. Diskar, H. M. Zenn, A. Kaupisch, A. Prinz, F. W. Herberg, *Cell. Signal.* **19**, 2024 (2007).
16. R. Rangel-Aldao, O. M. Rosen, *J. Biol. Chem.* **251**, 3375 (1976).
17. B. R. Martin, T. J. Deerinck, M. H. Ellisman, S. S. Taylor, R. Y. Tsien, *Chem. Biol.* **14**, 1031 (2007).
18. F. W. Herberg, S. S. Taylor, *Biochemistry* **32**, 14015 (1993).
19. S. H. Brown, J. Wu, C. Kim, K. Alberto, S. S. Taylor, *J. Mol. Biol.* **393**, 1070 (2009).
20. C. Kim, C. Y. Cheng, S. A. Saldanha, S. S. Taylor, *Cell* **130**, 1032 (2007).
21. C. Kim, N.-H. Xuong, S. S. Taylor, *Science* **307**, 690 (2005).
22. J. Wu, S. H. J. Brown, S. von Daake, S. S. Taylor, *Science* **318**, 274 (2007).
23. A. J. Boettcher *et al.*, *Structure* **19**, 265 (2011).
24. D. Vigil, D. K. Blumenthal, S. S. Taylor, J. Trewhella, *J. Mol. Biol.* **357**, 880 (2006).
25. W. T. Heller *et al.*, *J. Biol. Chem.* **279**, 19084 (2004).
26. H. M. Berman *et al.*, *Proc. Natl. Acad. Sci. U.S.A.* **102**, 45 (2005).
27. T. C. Diller, N. H. Xuong, S. S. Taylor, *Protein Expr. Purif.* **20**, 357 (2000).
28. M. Batkin, I. Schvartz, S. Shaltiel, *Biochemistry* **39**, 5366 (2000).
29. J. Yang *et al.*, *J. Biol. Chem.* **284**, 6241 (2009).
30. F. W. Herberg, S. S. Taylor, W. R. Dostmann, *Biochemistry* **35**, 2934 (1996).
31. G. G. Cadd, M. D. Uhler, G. S. McKnight, *J. Biol. Chem.* **265**, 19502 (1990).
32. K. M. Zawadzki, S. S. Taylor, *J. Biol. Chem.* **279**, 7029 (2004).
33. P. Madhusudan, N. H. Akamine, S. S. Xuong, Taylor, *Nat. Struct. Biol.* **9**, 273 (2002).
34. S. F. Oliveria, M. L. Dell'Acqua, W. A. Sather, *Neuron* **55**, 261 (2007).
35. S. Manni, J. H. Mauban, C. W. Ward, M. Bond, *J. Biol. Chem.* **283**, 24145 (2008).
36. D. D. Hall *et al.*, *Biochemistry* **46**, 1635 (2007).
37. J. Zheng *et al.*, *Protein Sci.* **2**, 1559 (1993).
38. M. Gangal *et al.*, *Proc. Natl. Acad. Sci. U.S.A.* **96**, 12394 (1999).

Acknowledgments: We thank members of the Taylor laboratory for helpful discussions and the Advanced Light Source (beam line 8.2.2) staff of Lawrence Berkeley National Laboratory for beam access and help with data collection. This work was supported by NIH grant GM34921 (S.S.T.). Coordinates and structure factors have been deposited in the Protein Data Bank (PDB) with accession numbers 3TNP and 3TNQ.

Supporting Online Material

www.sciencemag.org/cgi/content/full/335/6069/712/DC1
Materials and Methods
Figs. S1 to S7
Tables S1 and S2
References (*39*–*42*)

14 September 2011; accepted 3 January 2012
10.1126/science.1213979

The Crystal Structure of TAL Effector PthXo1 Bound to Its DNA Target

Amanda Nga-Sze Mak,[1]* Philip Bradley,[2]* Raul A. Cernadas,[3] Adam J. Bogdanove,[3] Barry L. Stoddard[1]†

DNA recognition by TAL effectors is mediated by tandem repeats, each 33 to 35 residues in length, that specify nucleotides via unique repeat-variable diresidues (RVDs). The crystal structure of PthXo1 bound to its DNA target was determined by high-throughput computational structure prediction and validated by heavy-atom derivatization. Each repeat forms a left-handed, two-helix bundle that presents an RVD-containing loop to the DNA. The repeats self-associate to form a right-handed superhelix wrapped around the DNA major groove. The first RVD residue forms a stabilizing contact with the protein backbone, while the second makes a base-specific contact to the DNA sense strand. Two degenerate amino-terminal repeats also interact with the DNA. Containing several RVDs and noncanonical associations, the structure illustrates the basis of TAL effector–DNA recognition.

TAL effectors are proteins that are injected into plant cells by pathogens in the bacterial genus *Xanthomonas*. There they enter the nucleus, bind to effector-specific promoter sequences, and activate the expression of individual plant genes, which can either benefit the bacterium or trigger host defenses (*1*, *2*). In each TAL effector, a variable number of tandem amino acid repeats (which are usually 34 residues in length), terminated by a truncated "half repeat," mediates DNA recognition. Each of the repeats preferentially associates with one of the four nucleotides in the target site (*3*, *4*). The repeats are located centrally in the protein between N-terminal sequences required for bacterial type III secretion and C-terminal sequences required for nuclear localization and activation of transcription (Fig. 1A).

The nucleotide specificity of individual TAL effector repeats is encoded by two adjacent residues (located at positions 12 and 13) called the repeat-variable diresidue (RVD) (Fig. 1, B and C) (*4*). More than 20 unique RVD sequences have been observed in TAL effectors, but just seven—HD, NG, NI, NN, NS, "N*" (which corresponds to a 33-residue repeat in which the RVD appears to be missing its second residue), and HG—account for nearly 90% of all repeats (*5*) and, respectively, specify C, T, A, G/A, A/C/T/G, C/T, and T (*3*, *4*). These relationships enable prediction of targets for existing TAL effectors and engineering of artificial TAL effectors that bind DNA sequences of choice. Consequently, TAL effectors have received much attention as DNA-targeting tools (*6*).

Nearly all TAL effector binding sites observed in nature are preceded by a T (*3*, *4*). Notably, the protein sequence immediately preceding the canonical TAL effector repeats bears some similarity to the repeat consensus. It has therefore been suggested that this region of the protein may participate in DNA binding by forming a cryptic repeat structure that specifies the T (*7*).

[1]Division of Basic Sciences, Fred Hutchinson Cancer Research Center, 1100 Fairview Avenue North, A3-025 Seattle, WA 98019, USA. [2]Division of Public Health Sciences, Fred Hutchinson Cancer Research Center, 1100 Fairview Avenue North, M1-B514 Seattle, WA 98109, USA. [3]Department of Plant Pathology and Microbiology, Iowa State University, 351 Bessey Hall, Ames, IA 50011, USA.

*These authors contributed equally to this work.
†To whom correspondence should be addressed. E-mail: bstoddar@fhcrc.org

A recent nuclear magnetic resonance structural study of 1.5 repeats of TAL effector PthA, and an accompanying small-angle x-ray scattering study of the entire protein, indicated that an isolated TAL effector repeat is largely α-helical, similar to a tetratricopeptide (TPR) fold, and that the full-length protein compacts upon DNA binding (*8*). However, in that study, it was unclear to what extent the structure of repeats in the context of the entire protein might differ from that of an isolated repeat, and the manner in which individual repeats associate with contiguous DNA base pairs was not resolved.

A protein construct corresponding to residues 127 to 1149 of the 23.5 repeat TAL effector PthXo1 from the rice pathogen *Xanthomonas oryzae* (Fig. 1 and fig. S1) was crystallized bound to a 36–base pair DNA duplex (table S1) containing the target sequence found in the rice genome along with flanking sequences ending in short 3′ overhangs. The structure was determined with a high-throughput computational approach in which structural models built with the Rosetta software package (*9*) were iteratively refined and selected, guided by molecular replacement searches (fig. S2). The best model was subsequently validated with a variety of model-free features of electron density, including anomalous difference peaks calculated from a selenomethionyl derivative (fig. S3). The final structure was refined to 3.0 Å resolution to values for R_{work}/R_{free} of 0.264/0.294 and excellent geometry (Table 1).

The structure consists of a relatively unperturbed B-form DNA duplex, with 23 consecutive bases of the target site intimately engaged in the major groove by a superhelical arrangement of TAL effector repeats (Fig. 2). The overall dimensions of the protein-DNA complex are approximately 60 Å by 60 Å by 90 Å. The quality of the electron density is excellent from repeat 1 through the middle of repeat 22, and then becomes less well defined.

All of the repeats in the DNA-bound PthXo1 structure form highly similar two-helix bundles (Fig. 1C). The helices span positions 3 to 11 and 14 to 33, locating the RVD in a loop between them. A proline located at position 27 creates a kink in the second helix that appears to be critical for the sequential packing and association of tandem repeats with the DNA double helix. The packing of consecutive helices within and between individual repeats is left-handed, in contrast to the right-handed packing of helices found in TPR proteins (*10*). The modular architecture of the TAL effector repeats is reminiscent of the mitochondrial transcription terminator mTERF (*11*) and the RNA-binding attenuation protein TRAP (*12*); however, interactions of those proteins with their nucleic acid targets are structurally distinct from those of TAL effectors with DNA and lack modular correspondence to single nucleotides.

Sequence-specific contacts of PthXo1 to the DNA are made exclusively by the second residue in each RVD to the corresponding base on the sense strand. In contrast, the side chain at the first position of each RVD contacts the backbone carbonyl oxygen of position 8 in each repeat, constraining the RVD-containing loop (Fig. 3). Additional, nonspecific contacts to the DNA are made by a lysine and glutamine found at positions 16 and 17. The average root mean square deviation between backbone atoms in any two repeats in the PthXo1 structure is ~0.8 Å for all atoms; it is slightly greater for the 33-residue N* repeats, which are missing one residue in the RVD loops (fig. S4). The positions within the core of individual repeats are occupied entirely by small aliphatic residues, whereas several positions in the interface between repeats correspond to polar residue pairs.

The PthXo1-DNA structure displays five HD-containing repeats (all aligned to cytosines), four NG repeats and one HG repeat (aligned to thymines), one additional NG repeat aligned to cytosine, seven NI repeats (aligned with four adenosines and three cytosines), two NN repeats (both opposite a guanosine), and two N* repeats paired to cytosines (Fig. 1A). The observed contacts by individual repeats (Fig. 3) correlate well with their specificity and fidelity (or lack thereof) that have been described via bioinformatic and genetic analyses. The sole NS in PthXo1 and one additional N* are located in the last full repeat and the half repeat, respectively, which are disordered in the structure.

In the HD RVDs, the aspartate residue makes van der Waals contacts with the edge of the corresponding cytosine base and a hydrogen bond to the cytosine N4 atom. Contacts between cytosine bases in protein-DNA complexes and charged acidic side chains, which exclude alternative base identities via physical and electrostatic clash, have been observed in a wide variety of solved sequence-specific protein-DNA complexes (*13*).

Both the NG and HG repeats make a contact in which the backbone α carbon of the glycine residue forms a nonpolar van der Waals interaction with the methyl group of the opposing thymine base (average distance ~3.3 Å). At the one position where an NG is aligned opposite a cytosine base, the backbone carbonyl and α carbon of the same glycine residue displays a less favorable, far more distant contact (~6 Å).

The second asparagine residue in the NN RVDs is positioned to make a hydrogen bond with the N7 nitrogen of an opposing guanine base. This RVD associates with either guanosine or adenine with roughly equal frequency (*3*, *4*, *14*); the availability of an N7 nitrogen in either purine ring appears to explain that observation (*13*).

PthXo1 contains two 33-residue N* repeats (7 and 22). Because RVDs are followed immediately by two conserved glycine residues, this repeat is equivalent to an NG repeat in which one of those glycine residues is missing. The crystal structure indicates that the deletion results

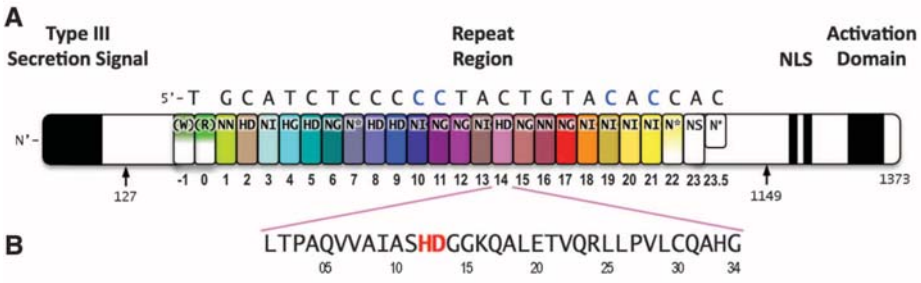

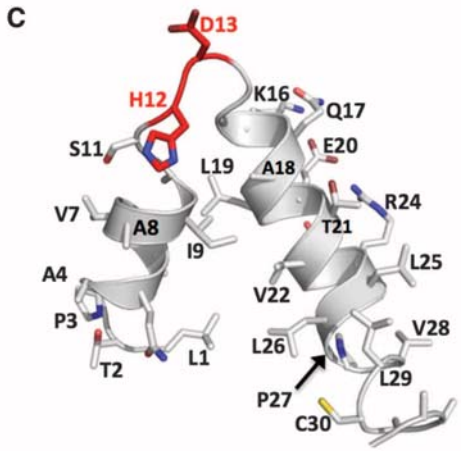

Fig. 1. (**A** and **B**) Domain organization of PthXo1 and (**C**) structure of a single TAL effector repeat. TAL effectors contain N-terminal signals for bacterial type III secretion, tandem repeats that specify the target nucleotide sequence, nuclear localization signals (NLS), and a C-terminal region that is required for transcriptional activation. PthXo1 contains 23.5 canonical repeats (color coded to match Fig. 2) that contact the DNA target found in the promoter of the rice *Os8N3* gene (*15*). Blue bases correspond to positions in the target where the match between protein and DNA differs from the optimal match specified by the recognition code (*3*, *4*). Arrows indicate the start and end of the crystallized protein construct. In the structure, repeats 22 to 23.5 are poorly ordered, as are the C termini of the two N-terminal cryptic repeats. The sequence and structure of a representative repeat (number 14) is shown; RVD residues (HD) that recognize cytosine are shown in red. Single-letter abbreviations for the amino acid residues are as follows: A, Ala; C, Cys; D, Asp; E, Glu; G, Gly; H, His; I, Ile; K, Lys; L, Leu; N, Asn; P, Pro; Q, Gln; R, Arg; S, Ser; T, Thr; and V, Val.

in a truncated RVD loop that extends less deeply into the DNA major groove, with the glycine at position 13 located a considerable distance (>6 Å) from the corresponding sense strand base. Consistent with this observation, the observed specificity of the N* repeat is relatively lax (*4*).

Finally, NI, which is the second most common RVD overall, accounting for roughly 20% of all TAL effector repeats, occurs seven times in PthXo1 and displays an unusual contact pattern to adenosine or cytosine bases. The aliphatic side chain of the isoleucine residue is observed to make nonpolar van der Waals contacts to C8 (and N7) of the adenine purine ring, or to C5 of the cytosine pyrimidine ring. These contacts would appear to necessitate desolvation of at least one polar atom in the adenosine ring, without the formation of a compensating hydrogen bond, and might therefore reasonably be expected to represent a reduced-affinity interaction.

N-terminal to the canonical repeats, the PthXo1 structure reveals two degenerate repeat folds that appear to cooperate to specify the conserved thymine that precedes the RVD-specified sequence (Fig. 4). We have designated these as the 0th and –1st repeats. Residues 221 to 239 and residues 256 to 273 each form a helix and an adjoining loop that resembles helix 1 and the RVD loop in the canonical repeats; the remaining residues in each region are poorly ordered. Those two N-terminal regions converge near the 5′ thymine base, with the indole ring of tryptophan 232 (in the –1st repeat) making a van der Waals contact with the methyl group of that base. Mutation of the thymine reduces TAL effector activity at the target (*3*, *15*). Tryptophan-232, as well as the surrounding residues, is highly conserved across available, intact TAL effector sequences. Some TAL effectors efficiently target sequences preceded by a cytosine rather than a thymine (*14*, *16*). Though less favorable, the packing of tryptophan 232 would be expected to accommodate this substitution.

In addition to revealing folding and interactions of the N-terminal cryptic repeats with the 5′ end of the DNA target site and illustrating the functions of the six most common repeat types in TAL effector–DNA recognition, the structure provides a basis for prediction of structures that are not represented. For example, an alignment of the 35-residue repeat type found in some TAL effectors with the more common 34-residue repeat type found in PthXo1 (fig. S5) indicates that the additional residue (a proline) at position 33 would be located within the relatively disordered turn region that connects the helices of one repeat to the next. The 35-residue repeat therefore can be predicted to be functionally indistinguishable from the 34. Likewise, although the sole NS repeat in PthXo1 is in an apparently disordered part of the protein-DNA complex, the overall homogeneity of the repeat structures and the consistent role of the first RVD residue in stabilizing the RVD loop to facilitate specific contacts of the second residue with the DNA should make it possible to computationally model the potential nucleotide interactions of NS, as well as those of rare or artificial RVDs.

Table 1. Crystallographic data and refinement statistics. WT, wild type; SeMet, selenomethionine; RMSD, root mean square deviation; ALS, Advanced Light Source; APS, Advanced Photon Source.

Data statistics		
Dataset	WT	SeMet
X-ray source	ALS 5.0.2	APS 21-ID-F
Wavelength (Å)	1.177	1.378
Space group	$P2_12_12_1$	$P2_12_12_1$
Unit cell (Å)	a = 95.6	a = 100.7
	b = 248.5	b = 247.8
	c = 54.6	c = 54.2
Resolution (Å)	50–3.0 (3.11–3.0)	50–4.0 (4.14–4.0)
R_{merge} (%)	0.121 (0.431)	0.087 (0.139)
I/σ (I)	9.3 (3.5)	10.3 (3.7)
Redundancy	5.6 (4.9)	4.9 (5.0)
Completeness (%)	96.6 (90.4)	95.8 (97.7)
Mosaicity (°)	0.8	0.8
Unique reflections	25841	11591
Refinement		
R_{work}	0.264	
R_{free}	0.294	
Protein atoms	6086	
DNA atoms	1552	
Heteroatoms (waters)	216	
RMSD bond lengths (Å)	0.021	
RMSD bond angles (°)	2.4	
Average B factor (Å^2)	85.1	
Ramachandran (% core, allowed, generous, disallowed)	73.6%, 26.4%, 0%, 0%	

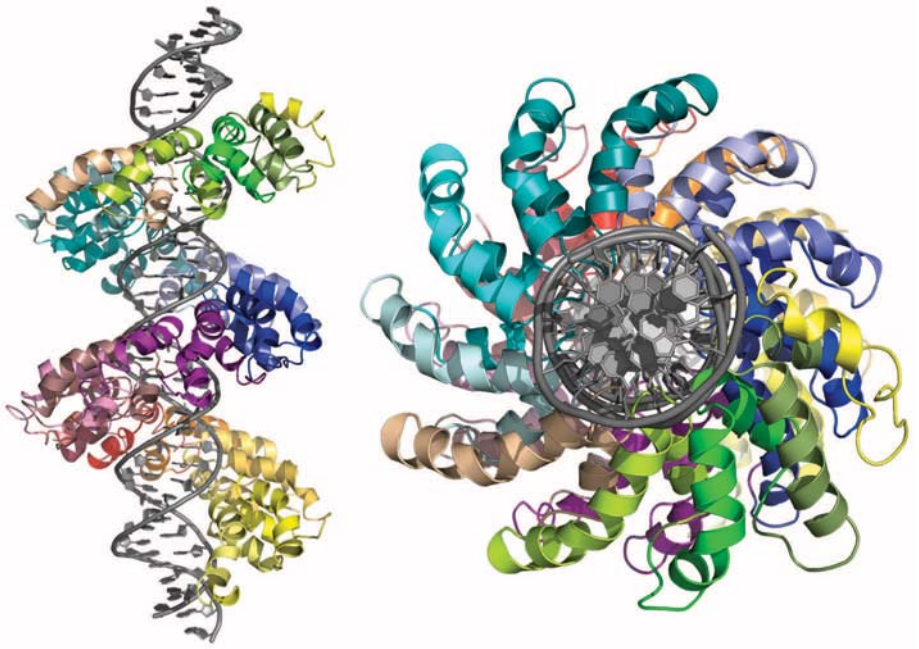

Fig. 2. Structure of the PthXo1 DNA binding region in complex with its target site. The coloring of individual repeats matches the schematic in Fig. 1.

The protein-DNA complex studied leaves some questions unanswered, such as the structure of the N- and C-terminal portions of TAL effectors that are, respectively, required for translocation and interaction with host transcriptional

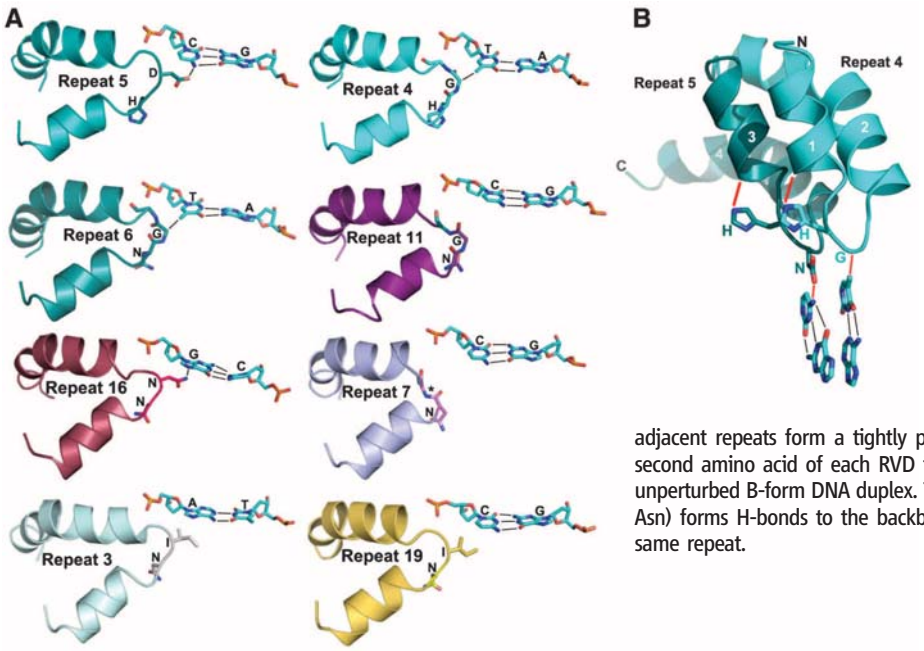

Fig. 3. Topology and contacts between TAL effector repeats and DNA bases. (**A**) Eight distinct combinations of RVDs and DNA bases are observed in the structure. HD (repeat 5) forms a steric and electrostatic contact with cytosine; HG (repeat 4) and NG (repeat 6) both form nonpolar interactions between the glycine α-carbon and the thymine methyl group. A "mismatch" between NG and a cytosine (repeat 11) results in a longer distance from the RVD to the base. NN associates with either guanine (repeat 16) or with adenine (which would interact with the same N7 nitrogen of the purine base). NI forms a desolvating interface with either adenine (repeat 3) or cytosine (repeat 19). The reduction in loop length by one residue in the N* RVD (repeat 7) results in an increased distance to the base. (**B**) Two adjacent repeats form a tightly packed left-handed bundle of helices that position the second amino acid of each RVD in proximity to corresponding consecutive bases in an unperturbed B-form DNA duplex. The first residue of each RVD (position 12, either His or Asn) forms H-bonds to the backbone carbonyl oxygen of amino acid position 8 of the same repeat.

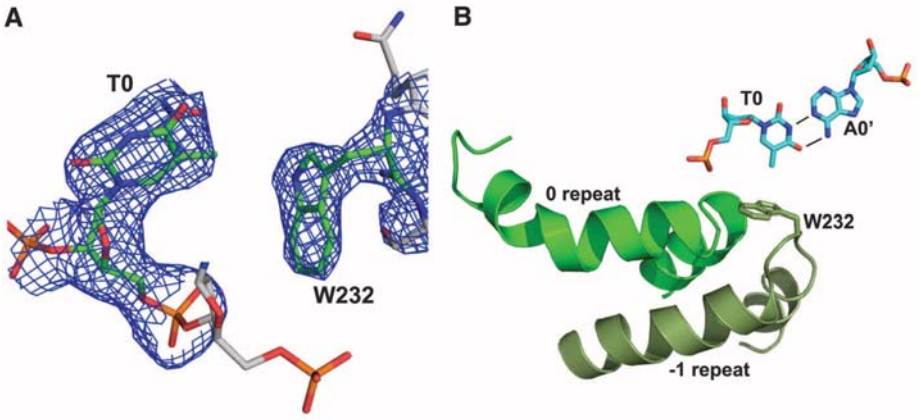

Fig. 4. N-terminal cryptic repeats and contacts with 5′ thymine. (**A**) 2*Fo-Fc* electron density maps contoured around thymine at position "0" and tryptophan 232 in the "–1" repeat. (**B**) Residues 221 to 239 and residues 256 to 273 each form a helix and an adjoining loop that resembles helix 1 and the RVD loop in the canonical repeats; the remaining residues in each region are poorly ordered. W232 forms a nonpolar van der Waals contact with the methyl carbon of the thymine base at position 0.

machinery. As well, because of the observed disorder at either end, it does not yet precisely define the minimal TAL effector–DNA binding domain. However, by demonstrating the essential features that accomplish interaction specificity, the structure provides a foundation for more accurately predicting and efficiently exploiting TAL effector–DNA targeting. More fundamentally, it reveals the hitherto enigmatic structural nature of a simple solution that an important group of pathogens has evolved to manipulate host gene expression in a specific yet highly adaptable manner.

References and Notes

1. S. Kay, S. Hahn, E. Marois, G. Hause, U. Bonas, *Science* **318**, 648 (2007).
2. P. Römer *et al.*, *Science* **318**, 645 (2007).
3. J. Boch *et al.*, *Science* **326**, 1509 (2009).
4. M. J. Moscou, A. J. Bogdanove, *Science* **326**, 1501 (2009).
5. J. Boch, U. Bonas, *Annu. Rev. Phytopathol.* **48**, 419 (2010).
6. A. J. Bogdanove, D. F. Voytas, *Science* **333**, 1843 (2011).
7. A. J. Bogdanove, S. Schornack, T. Lahaye, *Curr. Opin. Plant Biol.* **13**, 394 (2010).
8. M. T. Murakami *et al.*, *Proteins Struct. Funct. Bioinf.* **78**, 3386 (2010).
9. A. Leaver-Fay *et al.*, *Methods Enzymol.* **487**, 545 (2011).
10. L. D. D'Andrea, L. Regan, *Trends Biochem. Sci.* **28**, 655 (2003).
11. N. Jiménez-Menéndez *et al.*, *Nat. Struct. Mol. Biol.* **17**, 891 (2010).
12. N. H. Hopcroft *et al.*, *J. Mol. Biol.* **338**, 43 (2004).
13. R. Rohs *et al.*, *Annu. Rev. Biochem.* **79**, 233 (2010).
14. J. C. Miller *et al.*, *Nat. Biotechnol.* **29**, 143 (2011).
15. P. Römer *et al.*, *New Phytol.* **187**, 1048 (2010).
16. Y. Yu *et al.*, *Mol. Plant Microbe Interact.* **24**, 1102 (2011).

Acknowledgments: This project was funded by NIH (grants RL1 OCA833133 to B.L.S., R01GM098861 to B.L.S. and A.J.B., and R01 GM088277 to P.H.B.), NSF grant 0820831 to A.J.B., and a Searles Scholars Fellowship to P.H.B. A.N-S.M. was supported by a training grant from the Northwest Genome Engineering Consortium. We thank the staff of the Advanced Light Source beamline 5.0.2 and L. Doyle, B. Shen, R. Takeuchi, J. Bolduc, and C. Schmidt for technical assistance and advice; T. Edwards and M. Clifton for collecting SeMet data; and C. Pabo for helpful discussion. A.J.B. is an inventor on a patent application titled "TAL effector-mediated DNA modification" (US-2011/0145940-A1 and PCT/US2010/059932). This intellectual property, co-owned by Iowa State University and the University of Minnesota, has been licensed to Cellectis. The refined coordinates and corresponding x-ray intensities for the PthXo1-DNA structure have been deposited in the RCSB Protein Database (accession code 3UGM).

Supporting Online Material

www.sciencemag.org/cgi/content/full/science.1216211/DC1
Materials and Methods
Figs. S1 to S5
Table S1
References (*17*–*29*)

4 November 2011; accepted 21 December 2011
Published online 5 January 2012;
10.1126/science.1216211

Structural Basis for Sequence-Specific Recognition of DNA by TAL Effectors

Dong Deng,[1,2]* Chuangye Yan,[2]* Xiaojing Pan,[1,2]* Magdy Mahfouz,[3] Jiawei Wang,[1] Jian-Kang Zhu,[4] Yigong Shi,[2]† Nieng Yan[1,2]†

TAL (transcription activator–like) effectors, secreted by phytopathogenic bacteria, recognize host DNA sequences through a central domain of tandem repeats. Each repeat comprises 33 to 35 conserved amino acids and targets a specific base pair by using two hypervariable residues [known as repeat variable diresidues (RVDs)] at positions 12 and 13. Here, we report the crystal structures of an 11.5-repeat TAL effector in both DNA-free and DNA-bound states. Each TAL repeat comprises two helices connected by a short RVD-containing loop. The 11.5 repeats form a right-handed, superhelical structure that tracks along the sense strand of DNA duplex, with RVDs contacting the major groove. The 12th residue stabilizes the RVD loop, whereas the 13th residue makes a base-specific contact. Understanding DNA recognition by TAL effectors may facilitate rational design of DNA-binding proteins with biotechnological applications.

TAL (transcription activator–like) effectors (TALEs) are major virulence factors secreted by bacteria of the genus *Xanthomonas* that cause diseases in plants such as rice and cotton (*1*–*4*). TALEs, also known as AvrBs3/PthA family effectors (*5*, *6*), are injected into plant cells through a type III secretion system and interfere with cellular activities through transcriptional activation of specific target genes (*1*, *7*–*9*). TALEs share a common domain organization that enables them to be imported into nuclei and act as transcriptional activators (*10*–*13*).

The central DNA binding domain of TALEs consists of 1.5 to 33.5 tandem repeats (TAL repeats), with each repeat recognizing one specific DNA base pair (*14*, *15*). Each TAL repeat contains 33 to 35, mostly 34, highly conserved amino acids (*16*, *17*). Within each repeat, two hypervariable residues at positions 12 and 13 (also known as RVDs for repeat variable diresidues) confer DNA specificity (*14*, *15*). The code of DNA recognition by RVDs has been deciphered by both experimental (*14*) and computational (*15*) approaches. The frequently occurring RVDs His/Asp (HD), Asn/Gly (NG), and Asn/Ile (NI) recognize cytosine (C), thymine (T), and adenine (A), respectively (*1*, *18*). DNA binding by TAL repeats is modular, allowing engineering of DNA-binding proteins by assembly of TAL repeats with designed RVDs, for example, for use in targeted gene activation (*14*, *18*, *19*). Despite these advances, how TAL repeats specifically recognize DNA remains unknown.

We investigated an artificially engineered TAL effector, dHax3 (*20*) (fig. S1). The central domain of dHax3 (residues 270 to 703), containing 11.5 TAL repeats, was crystallized in the space group $C222_1$ (*21*). The structure was determined by Ta_6Br_{12}-based multiwavelength anomalous diffraction and refined to 2.4 Å resolution (tables S1 and S2 and fig. S2A). There is one molecule in each asymmetric unit. In the crystals, crystallographically independent molecules are arranged to form a continuous right-handed, superhelical assembly (fig. S2B). The structurally well-defined region of DNA-free dHax3 (residues 303 to 675) forms exactly 11 repeats, starting from the second half of repeat 1 and ending at repeat 11.5 (Fig. 1A). The superhelical assembly has an external diameter of about 60 Å.

Each TAL repeat in dHax3 contains 34 amino acids, with residues 3 to 11 forming a short α helix (designated as "a") and residues 15 to 33 constituting an extended, bent α helix (designated as "b"). The two helices are connected by a short loop consisting of RVD and an invariant amino acid Gly at position 14 (Fig. 1B and fig. S1). This loop is hereafter referred to as the RVD loop. Reflecting the high degree of sequence conservation (fig. S1), all 11 repeats exhibit a nearly identical conformation (Fig. 1B and fig. S2C). Helices a and b within each repeat closely stack against each other through extensive van der Waals contacts (Fig. 1B). The angle between the helices distinguishes the TAL repeat from other known

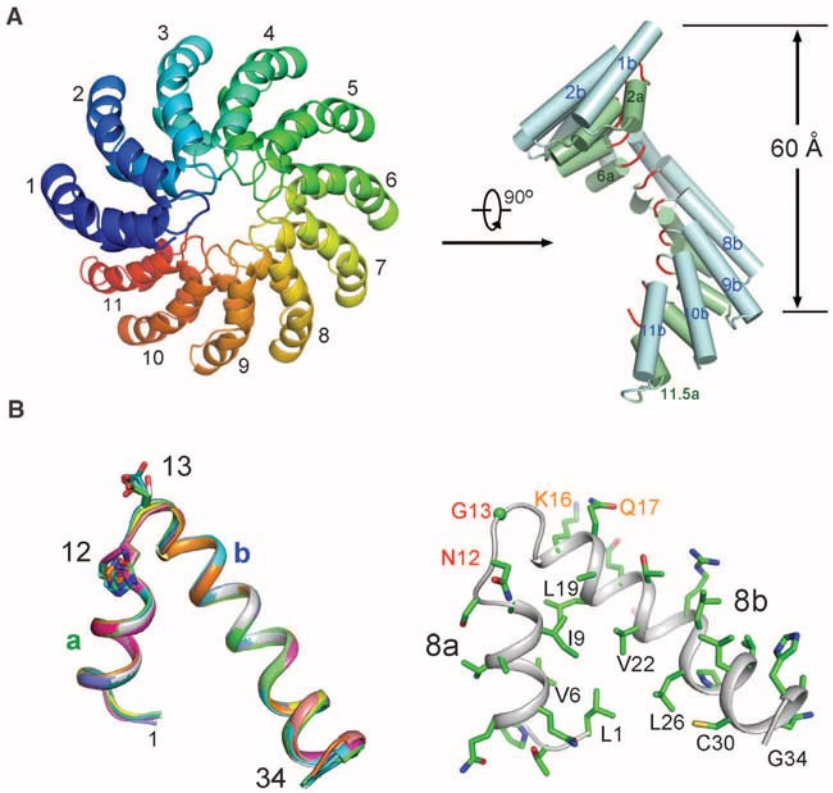

Fig. 1. Structure of the TAL repeats in DNA-free dHax3. (**A**) The 11 TAL repeats of dHax3 form a right-handed superhelical assembly. Two perpendicular views are presented with the RVDs highlighted in red in the right image. (**B**) All TAL repeats exhibit a nearly identical conformation. Each repeat is organized into short (a) and long (b) α helices connected by a short loop where the two (RVDs at positions 12 and 13 are located. All structure figures were prepared with PyMOL (*30*). Single-letter abbreviations for the amino acid residues are as follows: A, Ala; C, Cys; D, Asp; E, Glu; F, Phe; G, Gly; H, His; I, Ile; K, Lys; L, Leu; M, Met; N, Asn; P, Pro; Q, Gln; R, Arg; S, Ser; T, Thr; V, Val; W, Trp; and Y, Tyr.

[1]State Key Laboratory of Bio-Membrane and Membrane Biotechnology, Tsinghua University, Beijing 100084, China. [2]Tsinghua-Peking Center for Life Sciences, Center for Structural Biology, School of Life Sciences and School of Medicine, Tsinghua University, Beijing 100084, China. [3]Center for Plant Stress Genomics and Technology, King Abdullah University of Science and Technology, Thuwal 23955-6900, Kingdom of Saudi Arabia. [4]Department of Horticulture and Landscape Architecture, Purdue University, West Lafayette, IN 47907, USA.

*These authors contributed equally to this work.
†To whom correspondence should be addressed. E-mail: shi-lab@tsinghua.edu.cn (Y.S.); nyan@tsinghua.edu.cn (N.Y.)

α-helical repeat modules such as HEAT (*22*) and TPR (*23*), in which the two helices are nearly parallel to each other. A nuclear magnetic resonance (NMR) structure of 1.5 TAL repeats in the protein PthA was previously reported (*24*); however, our TAL repeat structure exhibits major differences from that in PthA (fig. S2, D and E).

The 11 TAL repeats of dHax3 complete a full helical turn; the RVD loops form the innermost spiral with a pitch of 60 Å per turn (Fig. 1A). The 11 a helices form an internal layer along the superhelical axis, whereas the 11 b helices constitute an external layer (Fig. 1A). These structural features suggest a DNA-binding model in which the DNA molecule is placed within the TAL superhelical assembly along the axis.

We crystallized a binary complex between dHax3 (residues 231 to 720), which encompasses the entire 11.5 TAL repeats, and a 17–base pair (bp) DNA binding element (*20*), with 5′-TGTCCCTTTATCTCTCT-3′ as the sense strand. The structure was determined by molecular replacement at 1.85 Å resolution (table S2 and fig. S3A). There are two complexes in each asymmetric unit (fig. S3B). The two protein molecules (designated A and B) can be superimposed with a root mean square deviation (RMSD) of 1.2 Å over 447 Cα atoms (fig. S3C). Because these two complexes exhibit identical features for most repeats, we mainly describe structural analysis on molecule A.

In the complex structure, dHax3 comprises 12 repeats (residues 289 to 691), with the C-terminal 0.5 repeat contributed by nonconserved amino acids (Fig. 2). These repeats are capped by three and two short α helices at the N and C termini, respectively (Fig. 2). Similar to DNA-free dHax3, all repeats exhibit a nearly identical conformation except RVD loops in repeat 6 of molecule A and repeat 5 of molecule B (figs. S3D and S4). The superhelical dHax3 structure tracks along the major groove of the DNA duplex. The conformation of the 17-bp DNA is largely B-form (table S3), with 11 base pairs per turn and a pitch of about 35 Å.

In the structures of both DNA-free and DNA-bound dHax3, there are 11 TAL repeats per helical turn (Fig. 3A). Comparison of any corresponding repeat between these two structures reveals little difference, with an RMSD of 0.25 to 0.34 Å over about 30 Cα atoms (Fig. 3B). However, the superhelical pitch is reduced from 60 Å in DNA-free form to about 35 Å in the DNA-bound form (Fig. 3A). Whereas the main chains of the first 22 amino acids are precisely superimposed, subtle conformational variations accumulate for residues 23 to 34, resulting in notable differences between the positions of the Cα atoms in Gly[34] (Fig. 3B). Such differences are gradually amplified over an increasing number of repeats (fig. S5), ultimately resulting in the compression of the superhelical assembly in the DNA-bound form. Such conformational plasticity is consistent with the predominantly van der Waals interactions between adjacent TAL repeats, which can tolerate minor distance shifts (Fig. 3, C and D, and fig. S6). The ability to undergo substantial conformational changes appears to be a conserved feature for superhelical assemblies exemplified by Armadillo repeats in β-catenin (*25*) and HEAT repeats in keryopherin α (*26*) and the scaffold subunit of protein phosphatase 2A (PP2A) (*27*). The conformational plasticity of the TAL repeats, which was previously noted (*24*), is likely essential for the function of TALEs.

Analysis of the electrostatic surface potential reveals a stripe of positively charged amino acids along the inner ridge of the dHax3 superhelical assembly (Fig. 4A and fig. S7A). Each phosphate group in the sense strand of the DNA duplex is accommodated in a shallow surface pocket along the basic stripe (Fig. 4A, left). Lys[16] and Gln[17], which are located at the beginning of helix b in each repeat, contribute to the positive electrostatic potential for interaction with the negatively charged phosphate (Fig. 4A, right). Interaction with the phosphate group of DNA duplex, invariant among repeats 1 through 11, is mediated by hydrogen bonds (fig. S7, B and C).

The two hypervariable residues in the RVD loops, positioned in close proximity to the sense strand in the DNA major groove (Fig. 4B), play different biochemical roles. Residue 12, either His or Asn in the 11.5 TAL repeats of dHax3 (fig. S1), does not directly contact DNA. Instead, the side chains of His[12] and Asn[12] point away from DNA bases, each making a direct H bond to the carbonyl oxygen atom of Ala[8], which is invariant and located at the C-terminal end of helix a in each TAL repeat (Fig. 4C). Thus, the primary role of residue 12 in TAL repeats is not to directly recognize DNA but to stabilize the local conformation

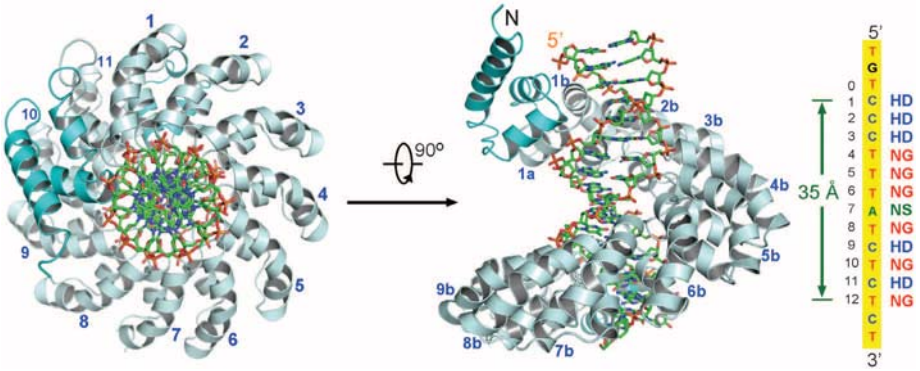

Fig. 2. Overall structure of dHax3 bound to DNA. The superhelical structure of dHax3 (residues 231 to 720) binds to the major groove of DNA. Shown on the right are the DNA sequence of the sense strand and the corresponding RVDs in TAL repeats of dHax3. dHax3 contains 11.5 repeats with flanking N- and C-terminal helices shown in cyan. Two perpendicular views are presented, with the DNA duplex shown in sticks.

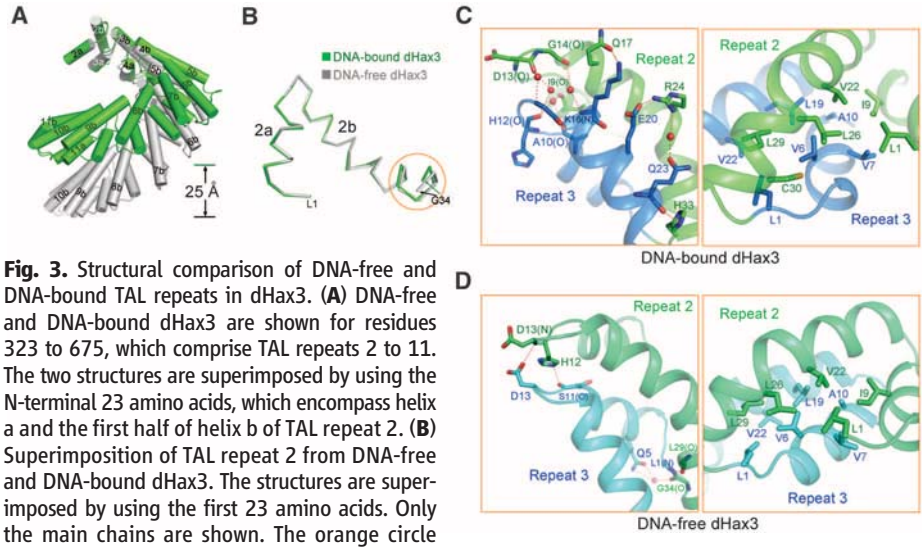

Fig. 3. Structural comparison of DNA-free and DNA-bound TAL repeats in dHax3. (**A**) DNA-free and DNA-bound dHax3 are shown for residues 323 to 675, which comprise TAL repeats 2 to 11. The two structures are superimposed by using the N-terminal 23 amino acids, which encompass helix a and the first half of helix b of TAL repeat 2. (**B**) Superimposition of TAL repeat 2 from DNA-free and DNA-bound dHax3. The structures are superimposed by using the first 23 amino acids. Only the main chains are shown. The orange circle highlights where the structures exhibit variations. (**C**) Interrepeat interactions in the DNA-bound dHax3. TAL repeats 2 and 3 are shown here. The H bonds and van der Waals interactions are shown in the left and right images, respectively. Water molecules are shown as red spheres, and H bonds are represented by red dashed lines. (**D**) Interrepeat interactions in the DNA-free dHax3.

of the RVD loops. Supporting this analysis, there is a water-mediated H bond between the imidazole group of His^{12} in TAL repeat 1 and the carboxylate oxygen atom of Asp^{13} in repeat 2 (Fig. 4C). Identical interaction is observed between His^{12} of repeat 2 and Asp^{13} of repeat 3. These structural findings demonstrate that His^{12} or Asn^{12} contributes indirectly to DNA binding by stabilizing the proper conformation of the RVD loops, which allows residue 13 to specifically recognize DNA bases.

Among the more than 20 codes identified for DNA recognition by TALE RVDs, some are more frequently observed than others (*1*, *18*). The TAL repeats in dHax3 use three codes, in which the two hypervariable residues HD, NG, and NS specifically recognize the DNA bases C, T, and A, respectively (*20*). These three codes account for about half of all cases reported (*1*). The structure of DNA-bound dHax3 provides a satisfying explanation to these codes. In the case of HD→C, the carboxylate oxygen atom of Asp^{13} accepts a H bond from the amine group of cytosine in TAL repeats 1 to 3, 9, and 11 (Fig. 4D). In the case of NS→A, the hydroxyl group of Ser^{13} in TAL repeat 7 donates a H bond to the N7 atom of adenine (Fig. 4D). Compared with HD, NS is nonselective in that it can recognize all four bases (*14*). Similar to adenine, guanine also contains a N7 atom, which is likely recognized by Ser^{13} in the same manner. Recognition of cytosine or thymine may require a slightly different conformation of the RVD loop, a scenario awaiting further structural evidence.

The correlation between NG and the base T is intriguing. Instead of providing any specific interaction, the placement of Gly at position 13 allows sufficient space to accommodate the 5-methyl group of thymine (Fig. 4E). In TAL repeats 4, 8, 10, and 12, the distance between the Cα of Gly^{13} and the 5-methyl group of thymine is between 3.4 and 3.7 Å, allowing van der Waals interaction. Substitution of Gly with any other residue would likely introduce steric clash with the 5-methyl group of thymine, providing a structural explanation for the observation that recognition of the base T usually requires Gly at position 13 (*1*). However, in repeats 5 of molecule A and 6 of molecule B, the distance between Gly-Cα and the 5-methyl group of thymine is more than 5 Å. We speculate that mutation of Gly^{13} to an amino acid with a short side chain may be tolerated here.

Both the structure and the mode of DNA binding by the TAL repeats differ from those of other known DNA-binding domains such as zinc-finger domain, basic leucine zipper motif, and helix-turn-helix motif (fig. S8). The modular nature of the DNA-TAL repeats is also different from that of known RNA-binding proteins such as trp RNA-binding attenuation protein (TRAP) (*28*). The closest entry from an exhaustive search of the Protein Data Bank (PDB) using DALI (*29*) is the structure of DNA-bound MTERF1 (mitochondria transcription terminator 1) (fig. S8), which also exhibits a superhelical conformation

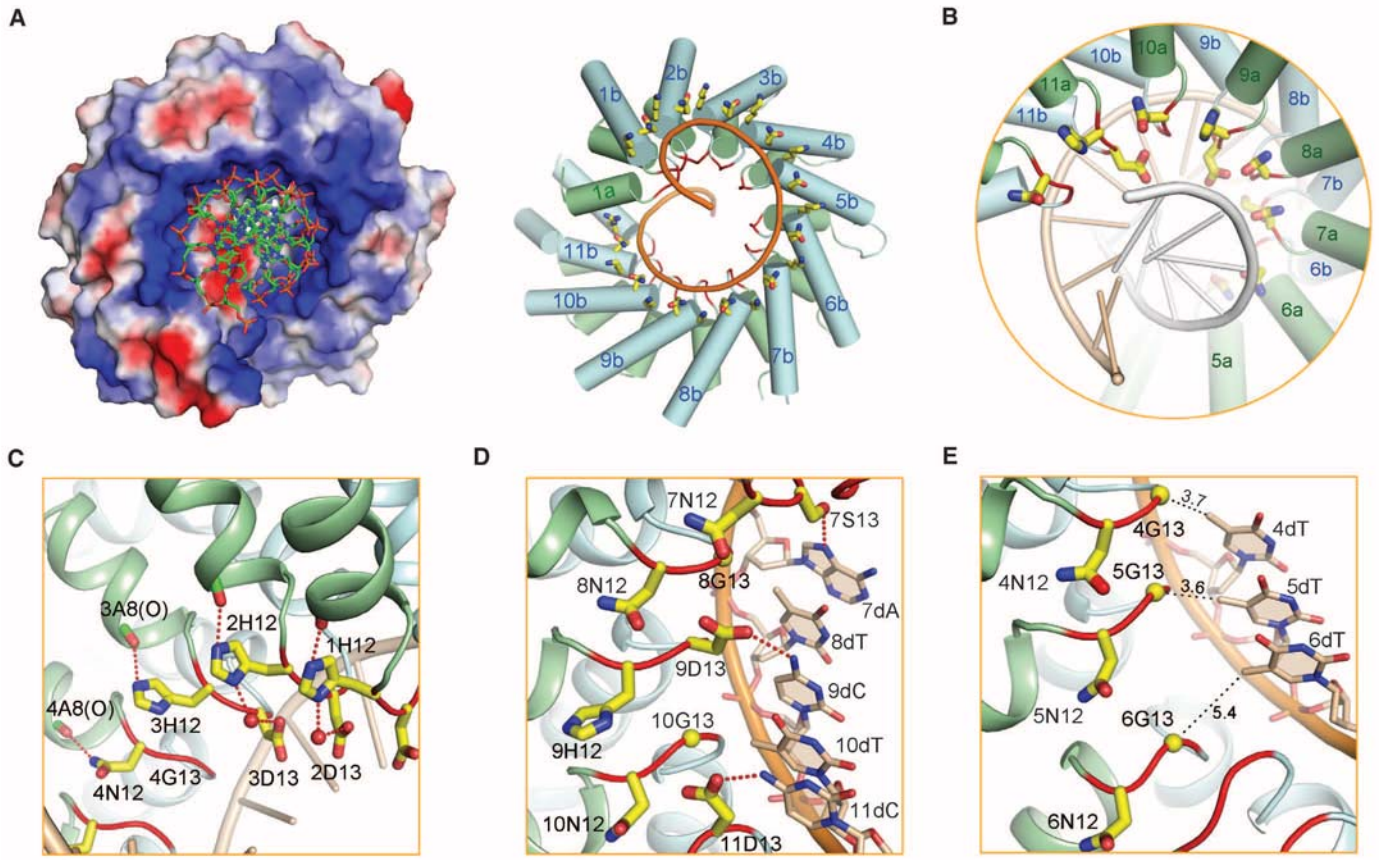

Fig. 4. DNA recognition by TAL repeats. (**A**) The phosphate groups of the DNA sense strand is embraced by the positively charged ridge of the dHax3 TAL repeats. The surface electrostatic potential was calculated with PyMOL (*30*) (left). The invariant residues Lys^{16} and Gln^{17} (yellow sticks), located at the beginning of helix b in each TAL repeat, contribute to the positive electrostatic potential (right). The RVD loops are highlighted in red. (**B**) The two hypervariable residues in each TAL repeat are placed in the major groove of DNA. The sense and antisense strands of DNA are colored gold and gray, respectively. (**C**) The hypervariable residues at position 12 do not contact DNA bases. These residues, either His or Asn in dHax3 repeats, form hydrogen bonds with the carbonyl oxygen of Ala^{8} in the same repeat, which may help stabilize the conformation of the RVD loop. When consecutive repeats containing HD are present, His^{12} forms a water-mediated H bond with Asp^{13} from the previous repeat. (**D**) The hypervariable residues at position 13 are direct determinants of DNA base specificity. Shown here are repeats 7 to 11 and the corresponding nucleotides from the DNA sense strand. (**E**) Recognition of base T by NG. A close-up view on the RVD loops in TAL repeats 4 to 6 in molecule A is shown. Note that the RVD loop of repeat 6 adopts a conformation different from all other RVD loops. All distances are shown in the unit of Å.

and has a Z score of 7.0 and RMSD of 3.2 Å over 184 aligned Cα atoms with dHax3. However, the MTERF motif comprises two α helices and one 3_{10}-helix, with considerable conformational variation among repeats. In addition, MTERF1 binding results in substantial unwinding of DNA duplex (fig. S8).

Our structural investigation provides explanation for about half of the frequently used codes for DNA recognition by TAL repeats. Among the remaining codes, how NI and NN recognize the bases A and G/A, respectively, remains to be elucidated. We suspect that the second Asn residue of NN may favor G/A through a specific H bond. Some of the less frequently used codes can also be explained by our available structural information. For example, explanation for the code ND→C should be similar to that for HD→C, which was observed here (Fig. 4D). On the other hand, rationalization for the code XG→T is likely the same as that for NG→T (Fig. 4E). Because 5′-methylcytosine is similar to T, we suspect that XG might also be able to recognize 5′-methylcytosine.

Our study represents a step toward comprehensive rationalization of sequence-specific DNA recognition by TAL repeats. Many questions remain. It is yet to be seen whether the arrangement of 11 repeats per turn is unique to dHax3 or a common feature of all TAL repeats. Although the base T is required for repeat "0" (*14*, *20*), our structure of DNA-bound dHax3 does not provide an intuitive clue, because T at position zero is not particularly coordinated by either the N-terminal domain or the adjacent repeats (fig. S9). Nonetheless, visualization of the modular, base-specific recognition by the TAL repeats may greatly facilitate rational design of novel DNA-binding proteins with a range of pragmatic applications.

References and Notes

1. J. Boch, U. Bonas, *Annu. Rev. Phytopathol.* **48**, 419 (2010).
2. J. Bai, S. H. Choi, G. Ponciano, H. Leung, J. E. Leach, *Mol. Plant Microbe Interact.* **13**, 1322 (2000).
3. K. Gu *et al.*, *Nature* **435**, 1122 (2005).
4. F. F. White, B. Yang, *Plant Physiol.* **150**, 1677 (2009).
5. U. Bonas, J. Conrads-Strauch, I. Balbo, *Mol. Gen. Genet.* **238**, 261 (1993).
6. S. Swarup, Y. Yang, M. T. Kingsley, D. W. Gabriel, *Mol. Plant Microbe Interact.* **5**, 204 (1992).
7. S. Schornack, A. Meyer, P. Römer, T. Jordan, T. Lahaye, *J. Plant Physiol.* **163**, 256 (2006).
8. S. Kay, U. Bonas, *Curr. Opin. Microbiol.* **12**, 37 (2009).
9. D. Büttner, U. Bonas, *FEMS Microbiol. Rev.* **34**, 107 (2010).
10. U. Bonas, R. E. Stall, B. Staskawicz, *Mol. Gen. Genet.* **218**, 127 (1989).
11. C. M. Hopkins, F. F. White, S. H. Choi, A. Guo, J. E. Leach, *Mol. Plant Microbe Interact.* **5**, 451 (1992).
12. S. Kay, S. Hahn, E. Marois, G. Hause, U. Bonas, *Science* **318**, 648 (2007).
13. P. Römer *et al.*, *Science* **318**, 645 (2007).
14. J. Boch *et al.*, *Science* **326**, 1509 (2009); 10.1126/science.1178811.
15. M. J. Moscou, A. J. Bogdanove, *Science* **326**, 1501 (2009); 10.1126/science.1178817.
16. S. Kay, J. Boch, U. Bonas, *Mol. Plant Microbe Interact.* **18**, 838 (2005).
17. S. Schornack, G. V. Minsavage, R. E. Stall, J. B. Jones, T. Lahaye, *New Phytol.* **179**, 546 (2008).
18. T. Cermak *et al.*, *Nucleic Acids Res.* **39**, e82 (2011).
19. A. J. Bogdanove, D. F. Voytas, *Science* **333**, 1843 (2011).
20. M. M. Mahfouz *et al.*, *Proc. Natl. Acad. Sci. U.S.A.* **108**, 2623 (2011).
21. See supporting material on Science *Online*.
22. M. R. Groves, N. Hanlon, P. Turowski, B. A. Hemmings, D. Barford, *Cell* **96**, 99 (1999).
23. T. Kajander, A. L. Cortajarena, S. Mochrie, L. Regan, *Acta Crystallogr.* **D63**, 800 (2007).
24. M. T. Murakami *et al.*, *Proteins* **78**, 3386 (2010).
25. A. H. Huber, W. J. Nelson, W. I. Weis, *Cell* **90**, 871 (1997).
26. E. Conti, M. Uy, L. Leighton, G. Blobel, J. Kuriyan, *Cell* **94**, 193 (1998).
27. Y. Xu *et al.*, *Cell* **127**, 1239 (2006).
28. A. A. Antson *et al.*, *Nature* **401**, 235 (1999).
29. L. Holm, P. Rosenström, *Nucleic Acids Res.* **38**, W545 (2010).
30. W. L. DeLano, on www.pymol.org (2002).

Acknowledgments: We thank J. He and Q. Wang at Shanghai Synchrotron Radiation Facility (SSRF) beamline BL17U and K. Hasegawa and T. Kumasaka at the Spring-8 beamline BL41XU for on-site assistance. This work was supported by funds from the Ministry of Science and Technology (grant numbers 2009CB918801, 2009CB918802, and 2011CB910501); projects 30888001, 91017011, and 31070644 of the National Natural Science Foundation of China; and Tsinghua University 985 Phase II funds. Coordinates and structure factors for the DNA-free and DNA-bound structures have been deposited with the Protein Data Bank under accession codes 3V6P and 3V6T.

Supporting Online Material

www.sciencemag.org/cgi/content/full/science.1215670/DC1
Materials and Methods
Figs. S1 to S9
Tables S1 to S3
References (*31*–*44*)

24 October 2011; accepted 21 December 2011
Published online 5 January 2012;
10.1126/science.1215670

Rescued Tolerant CD8 T Cells Are Preprogrammed to Reestablish the Tolerant State

Andrea Schietinger,[1,2] Jeffrey J. Delrow,[3] Ryan S. Basom,[3] Joseph N. Blattman,[1,2]* Philip D. Greenberg[1,2]†

Tolerant self-antigen–specific CD8 T cells fail to proliferate in response to antigen, thereby preventing autoimmune disease. By using an in vivo mouse model, we show that tolerant T cells proliferate and become functional under lymphopenic conditions, even in a tolerogenic environment. However, T cell rescue is only transient, with tolerance reimposed upon lymphorepletion even in the absence of tolerogen (self-antigen), challenging the prevailing paradigm that continuous antigen exposure is critical to maintain tolerance. Genome-wide messenger RNA and microRNA profiling revealed that tolerant T cells have a tolerance-specific gene profile that can be temporarily overridden under lymphopenic conditions but is inevitably reimposed, which suggests epigenetic regulation. These insights into the regulatory mechanisms that maintain or break self-tolerance may lead to new strategies for the treatment of cancer and autoimmunity.

T cell tolerance to self-antigens is required to prevent autoimmunity and arises through both central and peripheral mechanisms. Central tolerance occurs in the thymus through the process of negative selection, where developing thymocytes are deleted if they react too strongly to self-antigens presented by major histocompatability complex (MHC). Central tolerance is incomplete, however, because not all peripheral self-antigens are adequately presented in the thymus. Thus, self-reactive T cells that escape negative selection must be inactivated in the periphery by deletion, suppression by regulatory T cells, and/or cell-intrinsic programs to create a state of functional unresponsiveness (*1*). Peripheral tolerant CD8 T cells are phenotypically similar to antigen-experienced CD8 T cells but cannot proliferate in response to antigen stimulation (*2*). The rules governing this proliferative defect are not fully understood, but continuous exposure to self-antigen (tolerogen) is thought to be required (*3*–*5*). Many cancer antigens are self-antigens, and tolerance to these proteins can impede antitumor T cell responses. A critical challenge in tumor immunology is to develop strategies that break T cell tolerance to tumor/self-antigens without causing unacceptable autoimmune injury. Thus, it is necessary to define the molecular program

[1]Department of Immunology, University of Washington (UW), Seattle, WA 98195, USA. [2]Program of Immunology, Fred Hutchinson Cancer Research Center (FHCRC), Seattle, WA 98109, USA. [3]Genomics Shared Resource, FHCRC, Seattle, WA 98109, USA.

*Present address: School of Life Sciences, Arizona State University, Tempe, AZ 85287, USA.
†To whom correspondence should be addressed. E-mail: pgreen@u.washington.edu

underlying functional impairment of tolerant T cells and to understand the regulatory mechanism(s) that maintain or break self-tolerance.

We developed a double transgenic mouse model of CD8 T cell tolerance to a self-antigen that is also a potential target tumor antigen (*6*, *7*). T cell receptor transgenic mice (TCR_{GAG}) were engineered with CD8 T cells specific for the Friend murine leukemia virus (FMuLV) GAG epitope, an immunodominant antigen from the FMuLV-transformed mouse leukemia cell line, FBL (fig. S1A). These mice were crossed to a second transgenic mouse strain, Alb:GAG, which selectively expresses the *gag* transgene in hepatocytes under control of the albumin promoter (fig. S1B). In double transgenic TCR_{GAG}×Alb:GAG mice, TCR_{GAG} CD8 T cells are only partially deleted in the thymus (Fig. 1A), yielding peripheral CD8 T cells expressing high levels of the GAG-specific TCR that appear antigen-experienced as evidenced by their $Ly6C^{hi}$ and $CD44^{hi}$ immunophenotype (Fig. 1B). Despite the presence of high avidity, self-antigen–specific TCR_{GAG} CD8 T cells in the periphery, TCR_{GAG}×Alb:GAG mice show no signs of autoimmune liver injury. The peripheral T cells from TCR_{GAG}×Alb:GAG mice, in contrast to functional naïve or $CD44^{hi}/CD62L^{hi}$ memory TCR_{GAG} CD8 T cells, are tolerant and unable to proliferate in response to immunization with a highly immunogenic recombinant *Listeria monocytogenes* strain expressing GAG (LM-GAG) (Fig. 1C).

Maintenance of T cell tolerance has been reported to require continual exposure of T cells to self-antigen (*3*–*5*). Therefore, we transferred tolerant T cells into wild-type B6 hosts. Three weeks after transfer, recipient mice were infected with LM-GAG. Transferred tolerant T cells did not expand, demonstrating that the function of self-reactive CD8 T cells is not necessarily restored by removal from the tolerizing environment (Fig. 1D).

We previously showed that rescue could be achieved by inducing proliferation through alternative signaling pathways, for example, exogenous interleukin-15 (IL-15) in vitro (*8*, *9*). Because "forcing" tolerant T cells to proliferate appeared to abrogate tolerance, we investigated whether tolerant T cells could be rescued in vivo by lymphopenia-mediated homeostasis-driven proliferation (HP). During lymphopenia-driven HP, T cells proliferate independently of cognate antigen encounter, driven by interactions with MHCs expressing nondeleting self-peptides and/or by homeostatic cytokines (*10*). Tolerant T cells were transferred into sublethally irradiated congenic B6 or Alb:GAG recipients (fig. S2). Tolerant T cells underwent HP in both nontolerogenic and tolerogenic hosts (Fig. 2A). Proliferation was more extensive in GAG self-antigen–expressing hosts, suggesting that TCR signaling, even by a tolerogen, augmented lymphopenia-driven HP. To determine whether the proliferating tolerant T cells were rescued, lymphopenic Alb:GAG or B6 recipients were immunized in vivo 21 days posttransfer with LM-GAG (fig. S2B). Tolerant T cells expanded dramatically to LM-GAG not only in B6 but also in tolerogenic Alb:GAG recipients (Figs. 2, B and C, and 3B, left). To evaluate whether HP and rescue were dependent on the homeostatic cytokines IL-15 and/or IL-7, tolerant T cells were transferred into lymphopenic (i) Alb:GAG mice, (ii) Alb:GAG $Il15^{-/-}$ mice, or (iii) Alb:GAG $Il15^{-/-}$ mice treated with neutralizing IL-7 monoclonal antibody (mAb). Although HP was less efficient in $Il15^{-/-}$ and anti–IL-7–treated $Il15^{-/-}$ hosts (Fig. 2D, top), tolerant T cells still expanded in response to LM-GAG (Fig. 2D, bottom), suggesting that neither IL-15 nor IL-7 was absolutely required for HP-mediated rescue of tolerant T cells.

Sublethally irradiated lymphopenic mice slowly recover lymphocyte numbers and are lymphoreplete by 3 to 4 months (fig. S2A). At this time, very few transferred tolerant T cells incorporated bromodeoxyuridine (BrdU) or expressed Ki67, suggesting that the cells were no longer actively cycling (Fig. 3A). To determine whether rescued tolerant T cells post-HP remained functional, we immunized lymphoreplete hosts with LM-GAG 3 to 4 months posttransfer. T cells rescued in tolerizing Alb:GAG hosts and functional at day 22 (Fig. 3B, left) were once again tolerant (Fig. 3B, right, and fig. S3). Unexpectedly, tolerant T cells rescued by HP in nontolerogenic B6 mice also reacquired tolerance. "Retolerized" T cells

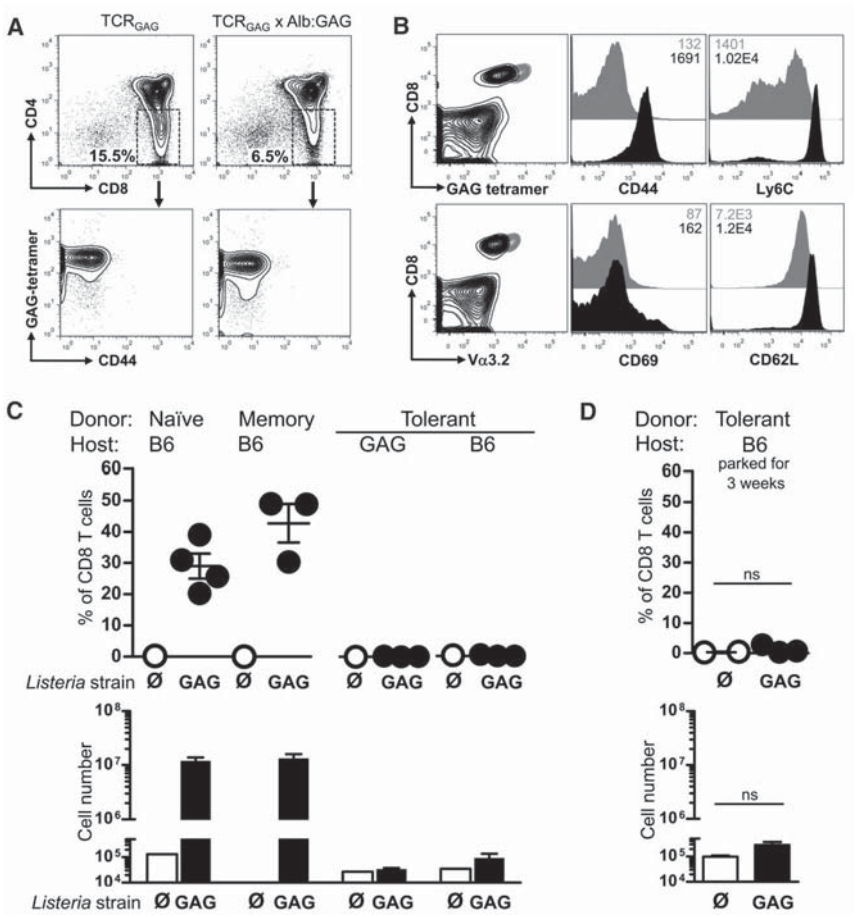

Fig. 1. Peripheral tolerant TCR_{GAG} CD8 T cells are phenotypically different and functionally impaired compared with naïve and memory TCR_{GAG} CD8 T cells. (**A**) Flow cytometric analysis of thymocytes from TCR_{GAG} (naïve) and TCR_{GAG}xAlb:GAG (tolerant) mice. Thymocytes were stained for CD4 and CD8, and single-positive CD8 thymocytes were analyzed for expression of CD44 and TCR by H2-D^b/GAG-tetramer binding. (**B**) Flow cytometric analysis of splenocytes from naïve (gray) and tolerant (black) mice. All $CD8^+$ cells are GAG-tetramer$^+$ and Vα3.2$^+$, and histograms are gated on $CD8^+$ cells. Inset numbers indicate mean fluorescence intensity (MFI). (**C**) Totals of 10^6 naïve, 10^5 memory, or 10^6 tolerant T cells were transferred intravenously into B6 and/or Alb:GAG hosts and infected 1 day later with 3×10^7 colony-forming units (cfu) of LM-GAG (solid circle) or LM-Ø (open circle) as control. Percent (top) and cell numbers (bottom) of donor T cells in spleens were determined 7 days postinfection. (**D**) A total of 5×10^5 tolerant T cells (Thy1.2) were transferred intravenously into B6 hosts (Thy1.1), and 3 weeks later mice were infected with 3×10^7 cfu of LM-GAG (solid circle) or control LM-Ø (open circle). At 7 days postinfection, splenocytes were analyzed for cell expansion. All results are representative of at least two or three independent experiments with two to four mice per group. Error bars show SEM. ns, not significant.

isolated from lymphoreplete B6 or Alb:GAG mice produced only limited amounts of the pro-inflammatory cytokines interferon (IFN)-γ and tumor necrosis factor (TNF)–α upon peptide stimulation, in contrast to rescued T cells (Fig. 3C). Thus, lymphopenia-mediated tolerance rescue was transient, with tolerance reestablished in lymphoreplete hosts even in the absence of the tolerogen.

Eukaryotic cells, including T cells, do not divide indefinitely and ultimately enter a phase of replicative senescence, known as the Hayflick limit (*11*). To determine whether tolerance reacquisition post-HP resulted from replicative senescence, we transferred retolerized T cells from lymphoreplete mice into a second set of lymphopenic recipients. After a second round of HP, retolerized T cells again responded to LM-GAG

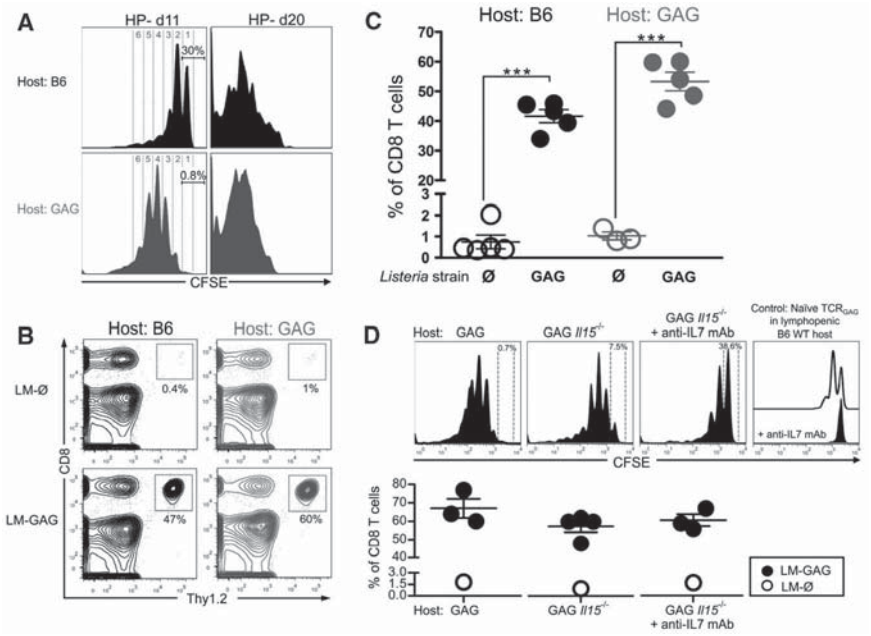

Fig. 2. Tolerant T cells undergo HP and become functional under lymphopenic conditions, even in a tolerogenic environment. (**A**) About 2×10^5 to 3×10^5 carboxy-fluorescein-succinimidyl ester (CFSE)–labeled tolerant T cells were transferred (intravenously) into lymphopenic Alb:GAG or B6 WT mice (Thy1.1) 1 day after total body irradiation (TBI; 5Gy). At 11 and 20 days later, CFSE dilution of transferred tolerant T cells was analyzed by flow cytometry. Histograms are gated on $CD8^+$ $Thy1.2^+$ cells. Inset numbers show % of cells that did not proliferate, and numbers of cell divisions are indicated. (**B** and **C**) At 22 days after adoptive transfer of 0.5×10^5 to 1×10^5 tolerant T cells into lymphopenic Alb:GAG or B6 hosts, mice were immunized with 3×10^7 cfu of LM-GAG or LM-Ø. At 7 days postinfection, peripheral blood was analyzed for expansion of transferred tolerant T cells. Results are representative of at least five independent experiments. ***$P < 0.0001$. (**D**) (Top) CFSE-labeled tolerant T cells were transferred into lymphopenic (Thy1.1) Alb:GAG mice, Alb:GAG *Il15*$^{-/-}$ mice, or Alb:GAG *Il15*$^{-/-}$ mice treated with neutralizing mAb against IL-7 (anti-IL7) 1 day after TBI, and spleen cells were analyzed 12 days later (top). To confirm the efficacy of anti-IL7 treatment, we transferred CFSE-labeled, naïve T cells into lymphopenic B6 wild-type (WT) mice (open histogram) or B6 mice treated with neutralizing anti-IL7 (solid histogram); 12 days later spleen cells were analyzed. Histograms are gated on $CD8^+$ $Thy1.2^+$ cells. (Bottom) At day 22 after transfer, mice were immunized with LM-GAG or LM-Ø, and 7 days later spleens were assessed for expansion of donor T cells. Results are pooled from two independent experiments with a total of five to seven mice per group.

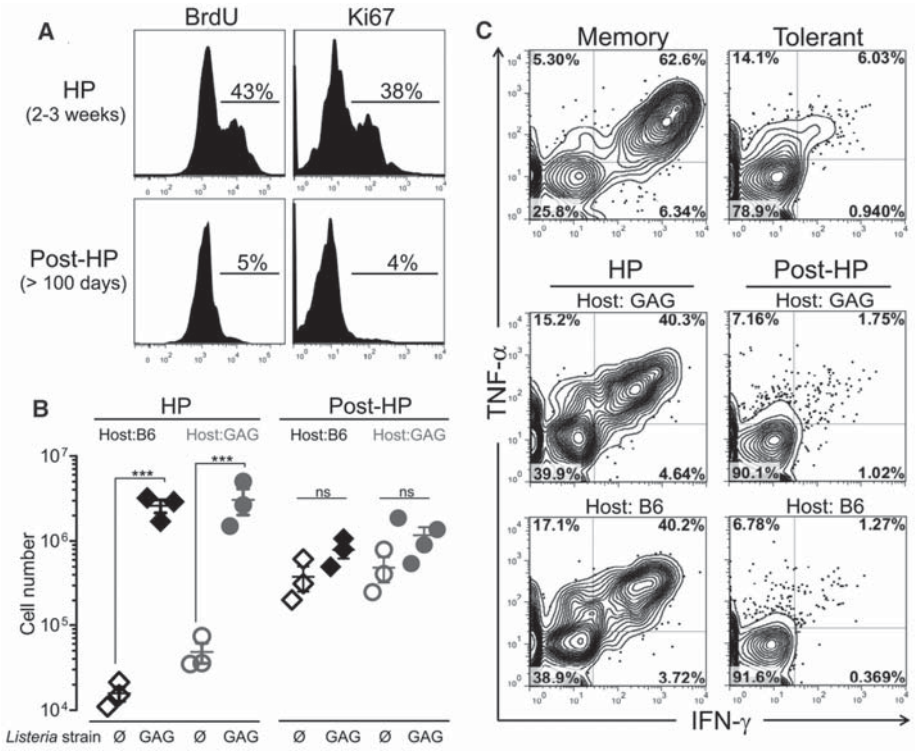

Fig. 3. Rescued T cells reacquire tolerance in lymphoreplete hosts even in the absence of the tolerogen. (**A**) Flow cytometric analysis of proliferation of tolerant T cells determined by BrdU incorporation (left) and Ki67 staining (right) 2 to 3 weeks after transfer into lymphopenic mice (top) and at >3 to 4 months after transfer, when recipients had become lymphoreplete (bottom). Histograms are gated on $CD8^+$ $Thy1.2^+$ splenocytes. Percents of BrdU-positive and Ki67-positive transferred T cells are shown. (**B**) At 3 weeks (HP) or >3 to 4 months (post-HP) after transfer into lymphopenic Alb:GAG or B6 (Thy1.1) mice, mice were immunized with 3×10^7 cfu of LM-GAG or LM-Ø. At 7 days postinfection, splenocytes were analyzed for expansion of transferred T cells. Data show mean ± SEM. For B6 hosts, ***$P < 0.0001$; for GAG hosts, ***$P = 0.0007$. (**C**) Intracellular TNF-α and IFN-γ production by tolerant T cells isolated 10 to 14 days (HP) or >3 to 4 months after transfer (post-HP) into irradiated Alb:GAG or B6 hosts. Memory and tolerant T cells are shown as control (top). Results are representative of at least three independent experiments.

immunization, indicating that retolerized T cells were not senescent and could be "re-rescued" (fig. S4).

The unexpected finding that tolerant T cells undergoing HP become functional in tolerogenic hosts and reacquire tolerance in nontolerogenic hosts suggested that peripheral tolerance is maintained by TCR-independent signaling pathways. Molecular signatures have been identified for T cells in functionally unresponsive states, including exhausted CD8 T cells during chronic viral infection (*12*, *13*), tumor-specific CD8 T cells in metastases (*14*), and anergic CD4 T cells (*15*), but the gene expression profile of tolerant self-antigen–specific T cells has not been determined. We performed microarray analysis of naïve, memory, tolerant, rescued (lymphopenic tolerogenic hosts), and retolerized (lymphoreplete nontolerogenic hosts) TCR_{GAG} CD8 T cells (fig. S5). Principal component analysis (PCA) (Fig. 4A) and K-means clustering (Fig. 4B and table S1) revealed that tolerant T cells harbor a tolerance-specific gene signature markedly distinct from those of naïve and memory T cells. To identify genes and pathways critical for maintenance of unresponsiveness, we determined which genes were preferentially expressed in tolerant T cells compared with their naïve and memory counterparts: Clusters 9 and 13 (164 genes) were identified as "tolerance-specific" gene sets representing uniquely overexpressed genes, including negative regulators of cell signaling and proliferation, transcription factors, and phosphatases (Fig. 4, B and C, and fig. S6A) (*16*). *Lag3*, an inhibitory coreceptor detected on exhausted CD8 T cells during chronic viral infection and tumor-infiltrating T cells, was one of the most highly expressed genes in tolerant T cells (*17*, *18*) (Fig. 4, C and E). Gene ontology classification of tolerance-specific genes revealed that genes modulating cell cycle, cell division, nucleosome assembly, mitosis, and DNA replication were also highly overrepresented

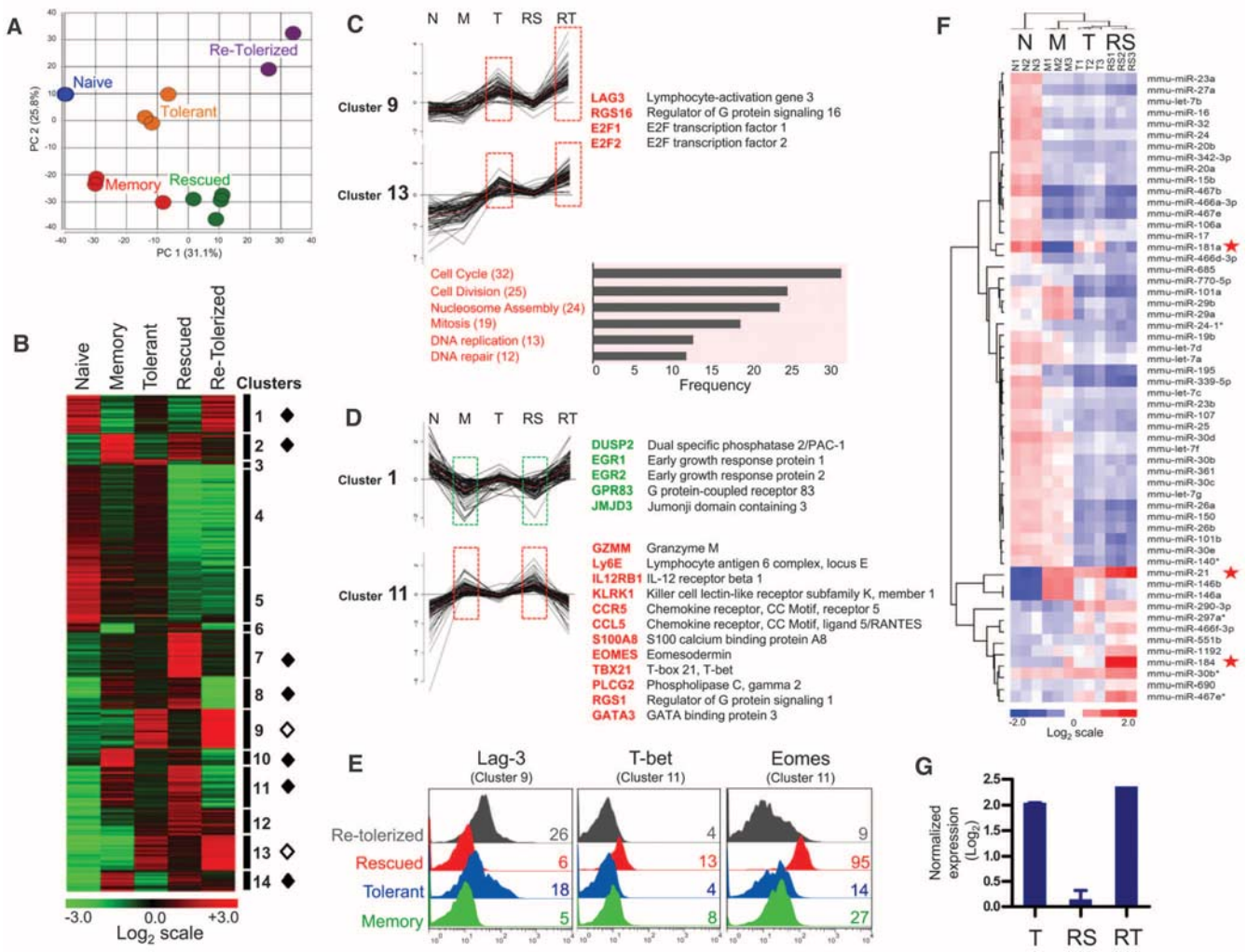

Fig. 4. Genome-wide mRNA and miRNA expression profiling of naïve, memory, tolerant, rescued, and retolerized TCR_{GAG} CD8 T cells. (A to D) mRNA expression profiling. (**A**) PCA of the indicated cell populations. A total of 56.9% of the variation in samples was revealed in the first two principal components. For naïve, memory, and tolerant T cells, $n = 3$; for rescued, $n = 4$; and for retolerized, $n = 2$. (**B**) K-means clustering was used to partition differentially expressed genes into 14 distinct clusters. Transcript levels for all clusters are shown for naïve, memory, tolerant, rescued, and retolerized T cell subsets. The heat map shows log_2-transformed expression intensities that were median-centered at the probe level. Higher expression is displayed in red, and lower expression in green. Rescue-associated gene sets indicated by solid diamonds; tolerance-specific gene clusters, open diamonds. (**C**) (Top) Selected genes from tolerance-specific clusters 9 and 13. (Bottom) Biological processes [Gene Ontology (GO) terms] enriched in tolerant and retolerized T cells. Genes associated within each cluster and GO are listed in fig. S6, A and B. (**D**) Selected genes from rescue-associated clusters 1 and 11. Additional clustering data are provided in fig. S6C. (**E**) Flow cytometric validation of Lag-3, T-bet, and Eomes expression in memory, tolerant, rescued, and retolerized T cells. Numbers indicate MFI. Data are representative for three independent experiments. (**F**) MiRNA microarray. Heat map of two-way hierarchical clustering of miRNAs and T cell samples. Each row represents a miRNA, and each column represents a sample [naïve (N); memory (M); tolerant (T); rescued (RS) T cells]. Higher expression is displayed in red and lower expression in blue; $P < 0.001$. Red stars indicate the miRNAs that are differently expressed in T compared with RS. (**G**) Expression of miR-181a in T, RS, and retolerized (RT) T cells determined by quantitative real-time PCR and normalized to miR-34a and miR-let7a. Error bars show SEM.

and up-regulated. These genes included histone proteins, minichromosome maintenance proteins, kinesins, cell division cycle proteins, and proteins of the spindle assembly and mitotic checkpoint complex (Fig. 4C and fig. S6, A and B). When tolerant T cells underwent HP in lymphopenic tolerogenic hosts, the tolerance gene signature was largely replaced by a signature remarkably similar to that of memory T cells (Fig. 4, A to E). Rescued T cells not only down-regulated tolerance-specific genes but expressed 475 additional genes at levels similar to those in memory T cells. We classified these genes into seven "rescue-associated" gene sets (clusters 1, 2, 7, 8, 10, 11, and 14), suggesting that functional impairment of tolerant T cells is due to the expression of tolerance-specific genes and lack of rescue-associated genes. Genes down-regulated in rescued and memory T cells (cluster 1, 84 genes) included the negative regulators and transcription factors *Dusp2* and *Egr1*/*Egr2* and the histone demethylase *Jmjd3* (*19*, *20*) (Fig. 4D and fig. S6C). Genes significantly up-regulated in rescued and memory T cells (clusters 2, 7, 8, 10, 11, 14; 391 genes) included (i) effector molecules *Infg*, *Prf1*, *Gzmm*, and *Grn*; (ii) master transcription factors controlling effector T cell function *Tbx21* (*21*), *Eomes* (*22*), *Gata3*, and *Stat4* (*23*); and (iii) chemokine and cytokine molecules *Cxcr3*, *Ccr5*, *Ccl5*, and *Il12r*β (Fig. 4, D and E, and fig. S6C). Rescued T cells re-tolerized in nontolerogenic hosts lost the rescue-associated gene signature and reestablished a program similar to that of tolerant T cells (Fig. 4, B to E, and fig. S6, A to C). Thus, T cells "remember" the tolerance program established during the initial encounter(s) with self-antigen in the periphery, raising the question of how such memory is encoded. This likely reflects epigenetics, the regulation of gene expression by mechanisms other than changes in the DNA sequence that is organized at multiple levels involving DNA methylation, histone modifications, nucleosome organization, and noncoding RNAs [e.g., microRNA (miRNA)]. Indeed, we found that transcripts of numerous genes regulating chromatin modification were enriched in tolerant and retolerized T cells (e.g., *Jmjd3*, *Dnmt1*, *Hat1*, *Hdac2*, *Hdac3*, etc.; fig. S7).

We focused on one critical aspect of epigenetic regulation of gene expression by asking whether specific miRNA expression changes might contribute to distinct mRNA expression profiles (*24*). Genome-wide miRNA profiling of naïve (N), memory (M), tolerant (T), and rescued (RS) T cells revealed that N, M, and T had distinct miRNA expression patterns. RS only differed from T in expression of three miRNAs: miR-21, miR-184, and miR-181a (Fig. 4F). miR-21 and miR-184 were overexpressed in RS compared with T, whereas miR-181a was decreased. miR-21 and miR-184 regulate cell proliferation and are overexpressed in many human cancers (*25*), suggesting that increased levels of miR-21 and miR-184 in RS may be due to ongoing proliferation rather than specifically associated with rescue. We therefore focused on miR-181a and confirmed by quantitative real-time polymerase chain reaction (PCR) that miR-181a was highly expressed in T and RT but low in M and RS (Fig. 4G and fig. S8A). Furthermore, miR-181a expression in M, RS, T, and RT inversely correlated with mRNA levels of known and predicted target genes compiled from published reports pointing to miR-181a as a possible key epigenetic regulator of tolerance (fig. S8, B to D). Previous studies showed that increasing miR-181a expression in CD4 T cells decreases TCR signaling threshold and increases antigen sensitivity (*26*, *27*). Our finding suggests that miR-181a plays a different role in CD8 T cells, negatively regulating cell function.

Many eukaryotic somatic cells, including T cells, exist in a state of cellular quiescence—a reversible nonproliferative state. Cognate antigen stimulation triggers T cells (e.g., naïve and memory) to exit the quiescent state, enter the cell cycle, and undergo clonal expansion. This ability to maintain quiescence while retaining the capacity to rapidly proliferate is tightly orchestrated by transcription factors, cell cycle regulators, and checkpoints, including DNA replication, chromatin organization, and chromosome segregation proteins (*28*, *29*). In contrast to naïve or memory T cells, whose transcriptional machinery is poised to enter the cell cycle upon antigen stimulation, we propose that TCR signaling in tolerant T cells is disengaged from cell cycle reentry control mechanisms. Lymphopenia provides a window of opportunity during which alternative signaling pathways enable tolerant T cells to proliferate independently of cognate antigen encounter, creating a permissive state where epigenetic control is temporarily superseded, allowing tolerant T cells to respond to antigen. However, after the mediator(s) of lymphopenia-mediated rescue disappear, T cells exit the cell cycle and become quiescent, and epigenetic control is once again reimposed, leading to restoration of the tolerant phenotype (fig. S9).

We have delineated the molecular program of tolerant, self-antigen–specific CD8 T cells and identified lymphopenia as a therapeutic opportunity to rescue, expand, and use tolerant T cells for cancer immunotherapy. Because lymphopenia-mediated rescue is only transient, with reestablishment of tolerance dictated by epigenetic memory, permanent rescue of tolerant T cells will require strategies to erase tolerance-specific epigenetic memory. However, an alternative strategy, repeated induction of lymphopenia leading to re-rescue of tolerant T cells, could be the basis for a new approach to cancer immunotherapy. Conversely, lymphopenia has been associated with exacerbation of autoimmunity (*30*), including graft-versus-host disease after autologous stem cell transplant (auto-GVHD), which is usually self-limited (*31*). Our findings not only point to a cell-intrinsic molecular mechanism for lymphopenia-associated autoimmune diseases but also explain their transient nature.

References and Notes

1. D. L. Mueller, *Nat. Immunol.* **11**, 21 (2010).
2. R. H. Schwartz, *Annu. Rev. Immunol.* **21**, 305 (2003).
3. S. Choi, R. H. Schwartz, *Semin. Immunol.* **19**, 140 (2007).
4. F. Ramsdell, B. J. Fowlkes, *Science* **257**, 1130 (1992).
5. B. Rocha, C. Tanchot, H. Von Boehmer, *J. Exp. Med.* **177**, 1517 (1993).
6. C. Ohlén *et al.*, *J. Exp. Med.* **195**, 1407 (2002).
7. J. Morimoto, X. Tan, R. M. Teague, C. Ohlén, P. D. Greenberg, *J. Immunol.* **178**, 6849 (2007).
8. R. M. Teague *et al.*, *Nat. Med.* **12**, 335 (2006).
9. R. M. Teague *et al.*, *Immunity* **28**, 662 (2008).
10. K. M. Williams, F. T. Hakim, R. E. Gress, *Semin. Immunol.* **19**, 318 (2007).
11. L. Hayflick, P. S. Moorhead, *Exp. Cell Res.* **25**, 585 (1961).
12. E. J. Wherry *et al.*, *Immunity* **27**, 670 (2007).
13. M. Quigley *et al.*, *Nat. Med.* **16**, 1147 (2010).
14. L. Baitsch *et al.*, *J. Clin. Investig.* **121**, 2350 (2011).
15. F. Macián *et al.*, *Cell* **109**, 719 (2002).
16. M. Murga *et al.*, *Immunity* **15**, 959 (2001).
17. S. D. Blackburn *et al.*, *Nat. Immunol.* **10**, 29 (2009).
18. J. F. Grosso *et al.*, *J. Clin. Investig.* **117**, 3383 (2007).
19. M. Safford *et al.*, *Nat. Immunol.* **6**, 472 (2005).
20. Y. Yin, Y. X. Liu, Y. J. Jin, E. J. Hall, J. C. Barrett, *Nature* **422**, 527 (2003).
21. A. M. Intlekofer *et al.*, *Nat. Immunol.* **6**, 1236 (2005).
22. E. L. Pearce *et al.*, *Science* **302**, 1041 (2003).
23. W. E. Thierfelder *et al.*, *Nature* **382**, 171 (1996).
24. H. Guo, N. T. Ingolia, J. S. Weissman, D. P. Bartel, *Nature* **466**, 835 (2010).
25. P. P. Medina, M. Nolde, F. J. Slack, *Nature* **467**, 86 (2010).
26. P. J. Ebert, S. Jiang, J. Xie, Q. J. Li, M. M. Davis, *Nat. Immunol.* **10**, 1162 (2009).
27. Q. J. Li *et al.*, *Cell* **129**, 147 (2007).
28. I. Yusuf, D. A. Fruman, *Trends Immunol.* **24**, 380 (2003).
29. B. R. Cairns, *Nature* **461**, 193 (2009).
30. S. Datta, N. Sarvetnick, *Trends Immunol.* **30**, 430 (2009).
31. R. J. Jones *et al.*, *Lancet* **333**, 754 (1989).

Acknowledgments: We thank S. Funk, C. Fowler, X. Tan, C. Chou, the other members of the Greenberg lab, and M. Philip for technical support and helpful discussion; the Abkowitz lab for providing the hemavet; M. Black from the UW Flow Cytometry Core Lab; J. Cao from the Immune Monitoring Shared Resource; and A. Dawson from the Genomics Shared Resource at the FHCRC. This work was supported by NIH grants R01 CA033084 (to P.D.G.), K01 CA117985 (to J.N.B.), and P30 CA015704-35 (to J.J.D. and R.S.B.); a grant FND 7008-08 from the Korea Research Institute of Bioscience and Biotechnology (to P.D.G.); and a Pilot and Feasibility Project Award (from P30 DK 56465 to B. Torok-Storb) (to A.S.). A.S. was supported by the Irvington Institute Fellowship Program of the Cancer Research Institute. All of the data reported in this paper are tabulated in the main text and in the supporting online material. The microarray data have been deposited in the Gene Expression Omnibus (GEO accession number GSE32025).

Supporting Online Material

www.sciencemag.org/cgi/content/full/science.1214277/DC1
Materials and Methods
Figs. S1 to S9
Table S1
References (*32*–*42*)

21 September 2011; accepted 12 December 2011
Published online 19 January 2012;
10.1126/science.1214277

Gordon Research Conferences

frontiers of science

2012 "Session II" Meeting Schedule and Preliminary Programs

2012 "Session II" Meetings will be held between June and August in New England and North Carolina in the United States, and internationally in Italy, Switzerland and Hong Kong. A list of preliminary programs appears on the following 22 pages. For detailed programs, fees, site/travel information and online application, visit our web site at **www.grc.org**.

During the summer of 2010, elevated seawater temperatures caused an extensive bleaching event affecting both corals and gorgonians in Bocas del Toro, Panama. As seawater temperatures continue to increase, coral bleaching events are becoming more frequent throughout the tropics. The GRC on the Metabolic Basis of Ecology in 2012 will have a special focus on understanding how multiple dimensions of global change will impact ecosystems, communities, and organisms by altering temperature and key resources such as carbon dioxide, nitrogen, and phosphorus. Photo by Raphael Ritson-Williams, Smithsonian Marine Station at Fort Pierce. Submitted by James J. Elser & Melanie E. Moses, Co-Chairs, 2012 Metabolic Basis of Ecology GRC. The Metabolic Basis of Ecology GRC will take place July 22-27, 2012 at the University of New England in Biddeford, Maine.

NEW!
Introducing: **Gordon Research Seminars**

Gordon Research Seminars (GRS) *are 2-day meetings that precede a corresponding GRC. They provide a unique opportunity for* ***graduate students, post-docs and other young investigators*** *to share in the GRC experience.* ***58*** *Gordon Research Seminars will be held during Session II 2012.*

In the preliminary program listing on the following pages, look for highlight boxes like the one shown below. These labels appear below the listing for any GRC that has an associated Gordon Research Seminar and contain the title, date, and chair information for the GRS.

LOOK FOR:

Atomic & Molecular Interactions
Jul 14-15, 2012
Chair: Amanda S. Case
Associate Chair: Julia H. Lehman

For more information about any Gordon Research Seminar, including preliminary program outlines, deadline dates, online application and more, please visit the GRC web site at www.grc.org.

The list of meetings, topics and speakers begins below (discussion leaders, where known, are noted in italics).

*Note: **Gordon Research Seminars (GRS)** are listed in boxes below their associated Gordon Research Conference, where applicable. Gordon Research Seminars are 2-day meetings that precede an associated GRC, designed for graduate students, post-docs, and other young scientists to present and exchange new data and cutting edge ideas.*

ATOMIC & MOLECULAR INTERACTIONS

Jul 15-20, 2012
Stonehill College, Easton, MA
Chair: Timothy S. Zwier
Vice Chair: Sharon Hammes-Schiffer

- **Single-Collision and Intramolecular Interactions I** (*Timothy Zwier* / Kopin Liu / Arthur Suits / Laurie Butler)
- **Clusters and Solvation** (*David W. Pratt* / Marsha Lester / Joel Bowman / Gary Douberly / Dor Ben-Amotz)
- **Single-Collision and Intramolecular Interactions II** (*Takayuki Ebata* / Hanna Reisler / Martin Head-Gordon / Andrew Orr-Ewing)
- **Excited State Interactions** (*Wolfgang Domcke* / Anne Zehnacker-Rentien / Samuel Leutwyler / Spiridoula Matsika / Todd Martinez)
- **Charges and Excited States in Solution and on Ice** (*Sharon Hammes-Schiffer* / David Vanden Bout / David McCamant / Bruce Kay)
- **Interactions at Interfaces, Surfaces, and Aerosols** (*David Nesbitt* / Alec Wodtke / Ruth Signorell / John Tully / Gil Nathanson)
- **Conformations and Folding** (*Philippe Dugourd* / Tom Rizzo / John Straub / Ashok Deniz)
- **Interactions under Extreme Conditions** (*Stephen Klippenstein* / Gerard Meijer / Ian R. Sims / Craig Taatjes / Russell Hemley)
- **Longer (Range), Shorter (Timescales), Stronger (Fields), Weaker (Interactions)** (*Martin Quack* / Ken Jordan / Steve Leone / Tim Softley)

Atomic & Molecular Interactions
Jul 14-15, 2012
Chair: Amanda S. Case
Associate Chair: Julia H. Lehman

NEW! AUDITORY SYSTEM

Jul 8-13, 2012
Bates College, Lewiston, ME
Chair: Dan H. Sanes
Vice Chair: Ruth Anne Eatock

- **From Ears to Aural Communication** (*Lisa Goodrich* / Anthony Ricci / Peter Narins / Andrew Oxenham)
- **Bottom-up and Top-down Development** (*Olivia Bermingham-McDonogh* / John Brigande / Gwenaelle Géléoc / Adrián Rodríguez-Contreras / Lisa Goodrich / Mark Wallace)
- **The Vulnerabilities of Ear and Brain** (*Adrián Rodríguez-Contreras* / Sharon Kujawa / Steven Green / Bradley May)
- **Filtering and Modulation of Sensory Signals** (*Kathy Cullen* / Elizabeth Olson / Harunori Ohmori / Leonard Kaczmarek / Laura Hurley / Alexander Reyes)
- **Processing and Plasticity** (*Robert Shepherd* / Andrej Kral / Daniel Polley / Lina Reiss)
- **Encoding and Decoding Sensory Signals** (*Ranulfo Romo* / Steven Colburn / Manuel Malmierca / Kathleen Cullen / Yale Cohen / Steven Lomber)
- **Multisensory Integration** (*Steve Lomber* / Ranulfo Romo / Dora Angelaki / Charles Schroeder)
- **Repairing the Transducer and Processor** (*Tony Ricci* / Jennifer Stone / Charley Della Santina / Mark Warchol / Robert Shepherd / Andrew Groves)
- **Substrates of Aural Communication** (*Yale Cohen* / Kamal Sen / Jeffrey Wenstrup / Robert Liu)

Auditory System
Jul 7-8, 2012
Chair: Allison Coffin
Associate Chair: Sean J. Slee

BACTERIAL CELL SURFACES

Jun 24-29, 2012
Mount Snow Resort, West Dover, VT
Chairs: Kevin D. Young & Tracy Palmer
Vice Chairs: Yves V. Brun & Lotte Sogaard-Andersen

- **Cell Division** (*Joe Lutkenhaus* / Mariana Pinho / Harold Erickson / Silvia Bulgheresi)
- **Protein Secretion** (*Ian Henderson* / Joseph Mougous / Harris Bernstein / Anne Delcour / Jorge Galan)
- **Outer and Inner Membranes** (*Jan Tommassen* / Daniel Kahne / Matt Hutchings / Meta Kuehn)
- **Cell Morphogenesis** (*Yves Brun* / K.C. Huang / Nina Salama / Rut Carballido Lopez / Zemer Gitai)
- **Surface Interactions** (*Lotte Sogaard-Andersen* / Liz Sockett / Arash Komeili / Ry Young)
- **Motility, Chemotaxis and Surface Structures** (Judy Armitage / Tam Mignot / Gabriel Waksman / Dennis Claessen)
- **Cell Wall** (*Tom Bernhardt* / Yves Dufrene / Ivo Boneca / Matt Waldor)
- **Protein Localization** (*Jeff Errington* / Marcia Goldberg / Hung Ton-That / Kumaran Ramamurthi / Christine Jacobs-Wagner)
- **Transduction, Transport and Stress** (*Tom Silhavy* / Kathleen Postle / Alan Grossman / Tracy Raivio)

BARRIERS OF THE CNS
Bridging Barriers to Treat CNS Disease

Jun 17-22, 2012
Colby-Sawyer College, New London, NH
Chair: Quentin Smith
Vice Chair: Margareta Hammarlund-Udenaes

- **Keynote Presentation: Barrier Modeling** (*Quentin Smith* / Tetsuya Terasaki / Damir Janigro)
- **Barrier Structure and Function** (*Richard Keep, Karen Mark* / Lester Drewes / Danica Stanimirovic / Ulrich Bickel / Farida Sohrabji)
- **Barrier Permeability and Signaling** (*Pierre-Olivier Couraud, Joan Abbott* / Richard Daneman / Stefan Liebner / Weihong Pan)
- **Barrier Imaging** (*M. Waleed Gaber* / Tavarekere Nagaraja / Bill Rooney / Kullervo Hynynen / Stina Syvänen)
- **Other Barrier Systems** (*Hazel Jones* / Robert Thorne / Ken-ichi Hosoya / Sarah Thomas / Jean-Francois Ghersi-Egea)
- **Barrier Transporters** (*David Miller, Reina Bendayan* / Jean-Michel Scherrmann / Elizabeth Hopper-Borge / Ian Simpson / Anika Hartz / Anne Mehringer)
- **Drug Delivery** (*Margaretta Hammarlund-Udenaes, David Smith* / Alexander Kabanov / Li Di / Romeo Cecchelli / Michel Demuele)
- **Barrier Alterations in Disease** (*Damir Janigro* / Jim Connor / Maria Deli / Greg Bix)
- **Angiogenesis and Brain Tumors** (*Gert Fricker* / Ed Neuwelt / Olaf Van Tellingen / Clinton Stewart)

Barriers of the CNS
Jun 16-17, 2012
Chair: Rajendar K. Mittapalli

BIOANALYTICAL SENSORS

Jun 17-22, 2012
Salve Regina University, Newport, RI
Chair: Steven A. Soper
Vice Chairs: Susan Lunte & Paul S. Cremer

- **Keynote Presentations** (*Steven Soper* / Harold Craighead / Charles Lieber)
- **Novel Recognition Elements/Reporters, Industrial Applications and Funding Opportunities** (*Weihong Tan* / Elizabeth Hall / Isiah Warner / Terry Fetterhoff / Avraham Rasooley / Aleksandr Simonian)
- **In Vivo Sensing** (*Susan Lunte* / Jonathan Sweedler / Robert Kennedy / Martyn Boutelle)
- **Engineered Surfaces** (*Paul Cremer* / Suichi Takayama / Frederick Höök / Jeanne Pemberton / Robin McCarley)
- **Bio-Electrochemical Sensing** (*Richard Durst* / Richard Crooks / Kevin Plaxco / Ingrid Fritsch)
- **Nanopores and Nanochannels** (*Jeffrey Schloss* / Daniel Branton / Paul Bohn / J. Michael Ramsey / Suzanna Siwy)
- **Young Investigator Presentations** (*Zeev Rosenzweig* / Jayne Garno / Amy Palmer / Katherine Willet / Lane Barker)
- **Microfluidics for Bioanalytical Sensing** (*Frances Ligler* / Luke Lee / Andrew de Mello / Antje Baeumner / Yoshinubo Baba)
- **Single Molecule Sensing** (*Shuming Nie* / Nancy Xu / Daniel Chiu / Marcus Sauer)

Bioanalytical Sensors
Jun 16-17, 2012
Chair: Sarah E. Brunker
Associate Chair: Aytug Gencoglu

BIOCATALYSIS

Jul 8-13, 2012
Bryant University, Smithfield, RI
Chairs: Stefan Lutz & Hans-Peter Meyer
Vice Chairs: Joelle N. Pelletier & Oliver May

- **Past, Present and Future of Biocatalysis** (*Stefan Lutz* / Jay Keasling)
- **Design and Engineering of Biocatalysts** (*Yashuhisa Asano* / Uwe Bornscheuer / Pimchai Chaiyen / Andrew Griffiths)
- **Design and Engineering of Processes** (*Oliver May* / John Woodley / Toni Glieder)
- **Cascade Reactions and Synthetic Biology** (*Joelle Pelletier* / Kristala Jones / Sven Panke / Claudia Schmidt-Dannert)
- **Round-Table Discussion: Trends in Applied Biocatalysis** (*Hans-Peter Meyer*)
- **Biocatalysts in Synthesis** (*John Woodley* / Yashuhisa Asano / David Berkowitz / Sarah O'Connor)
- **Future Challenges and Opportunities for Biocatalysis** (*Uwe Bornscheuer* / Jon Dordick / Vincent Rotello)

Gordon Research Conferences: "Session II" 2012 Preliminary Programs *(continued)*

- **Industrial Biocatalysis**
  (*Gjalt Huisman* / Jeffrey Moore / Ling Hua / Kai Baldenius)
- **Future Challenges in Green Chemistry**
  (*Hans-Peter Meyer* / Joe Pont / Paul Anastas)

Biocatalysis
Jul 7-8, 2012
Chair: Helge Jochens
Associate Chair: Aram Panay

BIOELECTROCHEMISTRY

The Body Electric: Understanding the Role of Endogenous Electric Fields in Development, Regeneration and Cancer and Utilizing Electric Fields to Treat Diseases
Jul 1-6, 2012
Il Ciocco Tuscany Resort, Lucca (Barga), Italy
Chair: Christine E. Pullar
Vice Chair: David A. Dean

- **Electroporation and the Brain - Responses and Imaging**
  (*Julie Gehl* / Raphael Davalos / Faisal Mahmood)
- **Voltage Gradients / Endogenous Electric Fields (EF) in Development / Regeneration**
  (*Ann Rajnicek* / Mike Levin / Nestor Oviedo / Ana Caterina Certal)
- **Biological Responses to Nanosecond and Picosecond Pulses**
  (*Damijan Miklavcic* / Shu Xiao / Ken-ichi Yano / Tom Vernier)
- **Mechanisms for Sensing EFs/Voltage**
  (*Colin McCaig* / Matias Simons / Hans-Hermann Gerdes / Yasushi Okamura)
- **Cell Biology of Gene Transfer - During and After the Pulse**
  (*Justin Tiessie* / Marie-Pierre Rols / Ziv Reich / Mark Kay)
- **EFs/Ion Flow and EF Pulses in the Detection/ Treatment of Cancer/Diseases**
  (*Lluis Mir* / Rich Nuccitelli / Mustafa Djamgoz / Mattia Ronchetti / Yoram Palti)
- **DNA Electroporation and Immunity - Modulation of the Immune Response**
  (*Richard Heller* / Emanuela Signori / Uta Griesenbach)
- **Modeling/Techniques and Biosensors for the In Vivo Study of Bioelectricity**
  (*Frank Hart* / Hidekazu Tsutsui / Dany Adams / Magda El-Shenawee)
- **Hot Topic Presentations**
  (*David Dean*)

Bioelectrochemistry
Jun 30 - Jul 1, 2012
Chair: Chloe Mauroy
Associate Chair: Gaurav Basu

BIOGENIC HYDROCARBONS & THE ATMOSPHERE

Reaching across Scales: From the Molecule to the Globe
Jun 24-29, 2012
Bates College, Lewiston, ME
Chairs: Christine Wiedinmyer & Paul Palmer
Vice Chairs: Allison L. Steiner & Janne Rinne

- **Biogenic Hydrocarbons and the Atmosphere: Past and Present**
  (*Almut Arneth* / Peter Harley / Daniel Jacob)
- **Hydrocarbon Production within the Biosphere**
  (*Todd Rosentiel* / Jonathan Gershenzon / Claudia Schmidt-Dannert / Claudia Vickers)
- **Ecological Roles of Biogenic Hydrocarbons**
  (*Russell K. Monson* / Monika Hilker / Kolby Jardine)
- **Ecosystem-Atmosphere Interactions**
  (Dennis Baldocchi / Marcy Litvak / Richard Phillips)
- **Early Career Scientist Presentations**
  (*Allison Steiner, Janne Rinne*)
- **Biogenic Hydrocarbons and Atmospheric Chemistry**
  (*Jonathan Williams* / Annmarie Carlton / Alastair Lewis / Xuemei Wang)
- **Biogenic Hydrocarbons, Aerosols, and Climate**
  (*Delphine Farmer* / Astrid Kiendler-Scharr / Thanos Nenes)
- **Using Observations to Better Quantify Biogenic Hydrocarbons**
  (*Colette Heald* / Allen Goldstein / Michael Barclay / Doug Worsnop)
- **Biogenic Hydrocarbons into the Future**
  (*Nick Hewitt* / Alex Guenther)

A complete eye induced on a tadpole's gut by molecular manipulation of bioelectric patterning cues. While anterior neural field cells were thought to be the only cell type competent to form eye tissues, tweaking of transmembrane potential into a specific voltage range induces even tissue far outside of the head to form whole eyes. Courtesy of Sherry Aw, Vaibhav Pai and Michael Levin. Submitted by Christine E. Pullar, Chair, Bioelectrochemistry GRC.

NEW! BIOINSPIRED MATERIALS

Jun 24-29, 2012
Davidson College, Davidson, NC
Chairs: Ashutosh Chilkoti & Jeffrey A. Hubbell
Vice Chair: Phillip B. Messersmith

- **Reprogramming the Genetic Code**
  (*Vince Conticello* / David Tirrell / Bernhard Geierstanger)
- **Biomimetic Systems**
  (Joanna Aizenberg / Anneliese Barron / Gabriel Lopez)
- **New Developments in Polypeptides and Peptoids**
  (*Manfred Schmidt* / Tim Deming / Ron Zuckerman)
- **Protein Based Materials**
  (*Jin Kim Montclare* / Lynne Regan / Hongbin Li / Chris Elvin)
- **Materials and Devices with DNA**
  (*Thom LaBean* / Ned Seeman / Paul Rothemund)
- **Self-Assembled Peptides**
  (*Tanja Weil* / Carol Hall / Rein Ulijn / Ehud Gazit)
- **Carbohydrate-Based Materials**
  (*Alyssa Panitch* / Kristi Kiick / Peter Seeberger)
- **Biomedical Applications of Bioinspired Materials**
  (*Molly Stevens* / David Mooney / Ravi Bellamkonda / Elliott Chaikof)
- **Complexity in Self-Assembly**
  (*Martien Cohen-Stuart* / Virgil Percec / M.G. Finn)

BIOMINERALIZATION

Aug 12-17, 2012
Colby-Sawyer College, New London, NH
Chair: Peter Fratzl
Vice Chair: Marc D. McKee

- **Mineral Nucleation and Growth Paradigms**
  (*Jim De Yoreo* / Derk Joester / Dirk Zahn / Asher Schmidt / Wim Noorduin / James Weaver)
- **Molecular and Cellular Regulation and Control of Biomineralization**
  (*Malcolm Snead* / Michael Paine / Viola Vogel / Henry Margolis / Dirk Schüler)
- **Skeletal Evolution**
  (Philip Donoghue / Adam Summers)
- **Silica Biomineralization**
  (*Rivka Elbaum* / Jian Feng Ma / Carole Perry)
- **Structure-Function Relations in Mineralized Tissues**
  (*Lia Addadi* / Markus Buehler / Wendy Shaw / Boaz Pokroy / Ali Miserez)
- **Principles of Biomineralization That Might Influence Our Thinking in Materials Science and Engineering**
  (*Joanna Aizenberg* / Kenneth Sandhage / Markus Linder / Mehmet Sarikaya / Seung-Wuk Lee)

Biomineralization
Aug 11-12, 2012
Chair: Mason N. Dean
Associate Chair: Sergio Bertazzo

BIOORGANIC CHEMISTRY

Jun 10-15, 2012
Proctor Academy, Andover, NH
Chairs: Mary Kay H. Pflum & Russell C. Petter
Vice Chairs: Jumi Shin & Grant K. Walkup

- **Frontiers in Medicinal Chemistry**
  (James Bradner / Paul Richardson)
- **Chemical Biology and Ecology**
  (Phil Cole / Peter Tonge/ Christina Grozinger)
- **Challenging Drug Targets**
  (Jared Cummings / Chris Straub / Adrian Whitty)
- **Chemical Proteomics**
  (Minkui Luo / Craig Crews / Benjamin Cravatt)
- **Community Forum: How to Make a Small Molecule Modulator to Every Biological Target**
  (Jon Overington / Michael Foley / Barry Morgan)
- **Nucleic Acid Chemistry and Biology**
  (Anne Baranger / Tamara Hendrickson / Samie Jaffrey)
- **Enabling Methods for the Bioorganic Community**
  (Sirano Dhe-Paganon / Michael MacCoss / Heather Carlson)
- **Biosynthesis of Natural Products and Sugars**
  (Kevin Walker / Jon Thorson / Xi Chen)
- **Frontiers in Bioorganic Chemistry**
  (Thomas Kodadek / Christopher Schofield / Carlos Garcia-Echeverria)

BIOPOLYMERS
Jun 3-8, 2012
Salve Regina University, Newport, RI
Chairs: Angel E. Garcia & Enrique De La Cruz
Vice Chair: Ivet Bahar

- **Keynote Presentations**
  (Lila Gierach / Klaus Schulten)
- **Molecular Crowding**
  (Margaret Cheung / Gilad Haran / Adrian Elcock)
- **Intrinsically Disordered Proteins and Amyloids**
  (Rohit Pappu / Dave Thirumalai / Peter Tessier / Ruth Nussinov)
- **Electrostatic Effects and Solutions**
  (M. Thomas Record / Roland Netz / Jose Manuel Sanchez-Ruiz / Theresa Head-Gordon)
- **Molecular Assemblies**
  (Ekaterina Grishchuk / Ahmet Yildiz / Dave Odde / Antonina Roll-Mecak / Tim Lohman)
- **Membrane Protein Folding and Dynamics**
  (Mei Hong / Karen Fleming / Nieng Yan / Helmut Grubmuller)
- **Nuclei Acid Dynamics**
  (Hashim Al Hashimi / Daniel Hershlag / Harald Schwalbe / Anjum Ansari)
- **Folding and Design**
  (Neils Andersen / Dan Raleigh / Lisa Lapidus / George Makhatadze)
- **Probing Protein Dynamics**
  (Dorothy Kern / Bertil Halle / Gerhard Hummer / Raphael Bruschweiler)

BRAIN ENERGY METABOLISM & BLOOD FLOW
Aug 12-17, 2012
Colby College, Waterville, ME
Chair: Joseph C. Lamanna
Vice Chair: Ute Lindauer

- **Metabolic Aspects of Neuroprotection and Conditioning**
  (*Costantino Iadecola* / Miguel Perez-Pinzon / Sarah Milton)
- **Tissue Stress and Oxygen Availability**
  (*Howard Prentice* / Tony Lee / Keith Webster / Goran Nilsson)
- **Neuroinflammation**
  (*Jaroslaw Aronowski* / Sunghee Cho / John Hallenbeck)
- **Ischemia-induced Organelle Damage in Mitochondria, Golgi and the ER and the Consequences of Organelle Dysfunction and Metabolism in Postischemic Brain**
  (*Gary Fiskum* / Bingren Hu / Frank Sharp / Midori Yenari)
- **Energy Substrate Metabolism**
  (*Michelle Puchowicz* / Jaime Ross / Ursula Sonnewald)
- **Near Infrared Spectroscopy and EPR Technical Advances and Clinical Applications**
  (*Martin Wolf* / Clare Elwell / Turgut Durduran / Jim Liu)
- **Control of Vascular Resistance in the Brain**
  (*Robert Bryan* / Marilyn Cipolla / Sean Marelli)
- **Energy Metabolism & Microcirculation in Cerebral Ischemia & Spinal Cord Injury**
  (*Gary Rosenberg* / R. Christian Crumrine / Juan Carlos Chavez / Richard Benton)
- **Keynote Presentation: Gas Channels**
  (Walter F. Boron)

Brain Energy Metabolism & Blood Flow
Aug 11-12, 2012
Chair: Clare Howarth

CARDIAC REGULATORY MECHANISMS
Jun 10-15, 2012
Colby-Sawyer College, New London, NH
Chairs: Elizabeth Murphy & Karin R. Sipido
Vice Chair: Mark E. Anderson

- **Novel Methods for Studying Cardiovascular Disease**
  (*Steven Houser* / Howard Rockman / Karl-Ludwig Laugwitz / Eva Van Rooij)
- **Mitochondrial Signaling and Cardiac Function**
  (*Robert Balaban* / Paul Brookes / Godfrey Smith / Peipei Ping / Luca Scorrano / Yasemin Sancak / Elena Dedkova)
- **Ion Channel Protein Defects and Arrhythmias**
  (*David Eisner, Henry Colcraft* / David Yue / Stephane Hatem / Thomas Hund)
- **The Intersection of Signaling Kinases and Hypertrophy**
  (*Walter Koch, Edward Lakatta* / Joan Heller-Brown / Mark Sussman / Elizabeth McNally / Roberta Gottlieb / Jeffrey Erickson)
- **New Mechanisms and Targets for Redox Signaling**
  (*Mark Anderson, Bjorn Knollmann* / Jun Sadoshima / Barbara Casadei / Jennifer Van Eyk)
- **Signaling Via Contractile Proteins**
  (*Litsa Kranias* / Mathias Gautel / Lucie Carrier / John Solaro / Jeff Robbins / Jolanda Van der Velden)
- **Novels Regulation of Ca^{2+} Dynamics**
  (*Donald Bers* / Jonathan Lederer / Hector Valdivia / William Louch / Katharine Dibb)
- **The Importance of Location in Signaling**
  (*Yibin Wang* / David Kass / Daria Mochly-Rosen / Christian Soeller / Niall Macquaide)
- **Keynote Presentation: The Mitochondrial Ca^{2+} Uniporter: New Insights on Ca^{2+} Regulation**
  (*Jeffery Molkentin* / Rosario Rizzuto)

Cardiac Regulatory Mechanisms
Jun 9-10, 2012
Chair: Mark J. Kohr
Associate Chair: Shirin Doroudgar

CATALYSIS
From Fundamentals to Application
Jun 24-29, 2012
Colby-Sawyer College, New London, NH
Chair: Bruce R. Cook
Vice Chair: John R. Regalbuto

- **Catalysis: New Advances and Applications**
  (*Udayshankar Singh* / Avelino Corma)
- **Advances in Surface Science and Characterization**
  (*Donna Chen* / Bert Weckhuysen / Beatriz Roldan / Adriano Zecchina)
- **Advances in Theory and its Application to Catalysis**
  (*Annastasia Alexandrova* / Jens Norskov / Karsten Reuter)
- **Organometallic Catalytic Systems: Homogeneous to Heterogeneous**
  (*Aditya Bhan* / Christophe Coperet / Justin Notestein / Edmund 'Ted' Carnahan)
- **Perspectives on Catalytic Mechanisms**
  (*Kristi A. Fjare* / Fabio Ribeiro / Manos Mavrikakis)
- **Closing the Pressure Gap, Fundamentals to Application**
  (*Michael Reynolds* / Jingguang Chen / Abhaya Datye / Stig Helveg)
- **Advances in Photocatalysis**
  (*Thomas Jaramillo* / Jae Sung-Lee / Kazunari Domen)
- **New Frontiers in Catalysis in Energy Systems**
  (*Elise Fox* / Yang Shao-Horn / Daniel Resasco / Chris Marshall)
- **Catalysis: Impact and Future Directions**
  (*Jane C. Cheng* / Alexis Bell)

CELL BIOLOGY OF THE NEURON
Jun 24-29, 2012
Waterville Valley Resort, Waterville Valley, NH
Chairs: Kelsey Martin & Peter Scheiffele
Vice Chairs: Graeme W. Davis & Nils Brose

- **Keynote Presentation**
  (Erik Jorgensen)
- **Synapse Assembly and Stability**
  (Ann-Marie Craig / Jan Pielage / Matthew Dalva / Anirvan Ghosh)
- **Imaging Neuronal Function**
  (Alice Ting / Bernardo Sabatini / Tim Ryan / Silvio Rizzoli)
- **RNA Transport and Regulation**
  (Claudia Bagni / Jennifer Darnell / Yishi Jin / Rosalind Segal)
- **Motors and Transport**
  (Erika Holzbaur / Tom Schwarz / Valeria Cavalli / Caspar Hoogenraad)
- **Polarity, Axon Growth and Regeneration**
  (Franck Polleux / Frank Bradke / Christine Holt / Frank Gertler)
- **Channels, Plasticity and Homeostasis**
  (Grae Davis / Paul Garrity / Yukiko Goda)
- **Neuronal Circuit Development**
  (Paula Arlotta / Wesley Grueber / Robert Datta / Amparo Palmer)
- **Neuronal Signaling Mechanisms**
  (Nils Brose / Gilbert Di Paolo / Aaron DiAntonio / Josh Kaplan)

CELL DEATH
Jul 15-20, 2012
Il Ciocco Tuscany Resort, Lucca (Barga), Italy
Chair: John M. Abrams
Vice Chair: Eric H. Baehrecke

- **Keynote Presentations: Reminiscence on a Diversion into Cell Death and Bcl-2 Family Proteins: Location, Relocation, Translocation**
  (Martin Raff / Richard Youle)
- **Death Pathways and Networks**
  (*Vishva M. Dixit* / Avi Ashkenazi / Seamus J. Martin / Doug Green / Sally Kornbluth)
- **Death Effectors and Effective Engineering**
  (Shigekazu Nagata / James A. Wells / Kodi Ravichandran / Guy Salvesen)
- **Bcl2 Proteins and the Mitochondriome**
  (*Doug Green* / David Andrews / Jean-Claude Martinou / Loren Walensky / Emily Cheng)
- **Cells Getting RIPed**
  (*Domagoj Vucic* / Xiadong Wang / Junying Yuan / Pascal Meier / Hao Wu)
- **Noncanonical Death Pathways**
  (Beth Levine / Michael Overholtzer / Valina Dawson / Christine J. Watson / Vishva M. Dixit)
- **Disease Mechanisms**
  (*Gerry Melino* / J. Marie Hardwick / Andreas Strasser / Andreas Villunger / Maya Saleh)
- **Oncogenic Connections**
  (Karen Vousden / Laura Attardi / Marcus Peter / Guido Kroemer)
- **Clinical Translation and Therapeutics**
  (*Huseyin Mehmet* / Vishva M. Dixit / Henning Walczak / Marc Tessier-Lavigne)

CELLULAR & MOLECULAR FUNGAL BIOLOGY
Jun 17-22, 2012
Holderness School, Holderness, NH
Chairs: Judith Berman & Alex Andrianopoulos
Vice Chairs: James B. Anderson & Jennifer Lodge

- **Evolutionary and Population Genomics**
  (*Bruce McDonald* / Maitreya Dunham / Paul Magwene / Mat Fisher / Antonis Rokas)

Gordon Research Conferences: "Session II" 2012 Preliminary Programs *(continued)*

- **Genome Organization and Expression**
  (*Michael Frietag* / Mark Caddick / James Fraser / Martijn Rep / Brendan Cormack / Anja Forche / Michael Donaldson)
- **Sex and Development**
  (*Amy Gladfelter* / Richard Bennett / Christina Hull / Kirsten Nielsen / Stefanie Pöggele)
- **Cell Biology**
  (*Steve Harris* / Michael Bolker / Ane Sesma / Michelle Momany / Philippe Silar / Eduardo Espeso / Deb Bell-Pederson)
- **Organismal Interactions**
  (*Nick Talbot* / Chris Schardl / Regine Kahmann / Fritz Muhlschlagel / Natalia Requena)
- **Host-Pathogen interactions**
  (*Anita Sill* / Melanie Wellington / Chad Rappleye / Raymond St. Leger / Aaron Mitchell / Rob Wheeler / Nicole Donofrio)
- **Energy Metabolism and Biomass Production**
  (*Louise Glass* / Jamie Cate / Kiyohiko Igarashi / Suzanne Lantz / Jens Nielsen)
- **Systems Biology**
  (*Elaine Bignell* / Kate Pollard / Martin Kupiec / Suzanne Noble / Maurizio Del Poeta / Ivana Gudelj / Tim Hughes)
- **Hot Topic Presentations**
  (*Jenny Lodge, Jim Anderson*)

CERAMICS, SOLID STATE STUDIES IN
New Insights and New Paradigms for Fracture and Deformation
Aug 12-17, 2012
Mount Holyoke College, South Hadley, MA
Chair: Martha Mecartney
Vice Chair: Monika Backhaus-Ricoult

- **Deformation and Fracture Issues in Ceramics for Electrochemical Applications**
  (*Dan Mumm* / Raj Bordia / Shen Dillon)
- **Design of Ceramics for Extreme Environments**
  (*Sylvia Johnson, Marina Pascucci* / David Marshall / Richard Todd / Biljana Mikijelj)
- **Plastic Deformation under Electric Fields**
  (*Gary Messing* / Rishi Raj / I-Wei Chen)
- **New Designs and Novel Microstructures**
  (*Susan Krumdieck, John Nuchka* / Erica Corral / Joanna McKittrick / Brian Cox)
- **Utilizing Porosity**
  (*David Green* / Reinhold Dauskardt / Kathy Faber)
- **New Developments in Thermal and Thermo-mechanical Properties**
  (*Bill Fahrenholtz / Trudy Kriven* / David Clarke / Ivar Reimanis / Greg Hilmas)
- **Nanoscale Mechanical Behavior**
  (*George Pharr* / Robert Cook / Izabela Szlufarska)
- **Grain Boundary and Interfacial Control of Fracture and Deformation**
  (*Greg Rohrer, Martin Harmer* / Michael Hoffmann / Wayne Kaplan / Yuichi Ikuhara)
- **Keynote Presentation: The New Multidisciplinary Frontier**
  (*Martha Mecartney* / Brian Lawn)

COMPUTATIONAL CHEMISTRY
Jul 22-27, 2012
Mount Snow Resort, West Dover, VT
Chair: Julia E. Rice
Vice Chair: Jay W. Ponder

- **Reactions in the Condensed Phase**
  (Ken Houk / Walter Thiel)
- **Condensed Phase Quantum Chemistry I**
  (Christian Ochsenfeld / Roland Lindh / Benadette Mennucci)
- **Condensed Phase Quantum Chemistry II**
  (Emily Carter / Thomas Miller)
- **Water Structure and Dynamics**
  (*Ken Jordan* / Sotiris Xantheas / Giulia Galli / Teresa Head-Gordon)
- **Force Field Developments I**
  (*Christopher Bayly* / Alex MacKerell / Will Noid)
- **Force Field Developments II**
  (Pengyu Ren / Adri van Duin)
- **Astrochemistry**
  (*Timothy Lee* / Lou Allamandola / Daniel Crawford / Helen Fraser)
- **Biomolecular Simulations**
  (*Adrian Mulholland* / Adrian Roitberg / Darrin York / Riccardo Baron)
- **Industrial Applications**
  (William Swope)

CORRELATED ELECTRON SYSTEMS
Correlations and Topology in Electron Systems
Jun 24-29, 2012
Mount Holyoke College, South Hadley, MA
Chairs: Eva Y. Andrei & Steven A. Kivelson
Vice Chairs: N Peter Armitage & Joerg Schmalian

- **Graphene**
  (Konstantin Novoselov / Antonio H. Castro-Neto / Philip Kim / Oscar Vafek)
- **Topological Aspects of Electronic Systems**
  (Young Beck Kim / Claudio Chamon / Bertram Halperin / Joel Moore / Aaron Kapitulnik / Andrei Bernevig / Weida Wu)
- **Interplay of Magnetism & Superconductivity**
  (Seamus Davis / Sudip Chakravarty / Bernhard Keimer / Eun-Ah Kim / Henry Alloul / Suchitra Sebastian / Jenny Hoffman)
- **Quantum Critical Points in Metals**
  (Subir Sachdev / Sean Hartinoll / Andrew Mackenzie / Andrei Chubukov / Louis Taillefer / Gillbert Lonzerich)
- **Systems Far From Equilibrium**
  (Thiery Giamarchi / Randy Hulet / Natan Andrei)
- **New Directions**
  (Yoshi Maeno / Peter Abamonte / Mark Fromhold)
- **Topological Insulators**
  (Phuan Ong / Laurens Molenkamp / Vidya Madhavan)
- **Advances in Low Dimensional Systems**
  (Ray Ashoori / Amir Yacobi / Jeanie Lau)
- **Last Minute Developments**
  (Herald Hwang / Andrea Cavalleri / Xuan Gao / Nigel Hussey)

Correlated Electron Systems
Jun 23-24, 2012
Chair: Babak H. Seradjeh

CORROSION - AQUEOUS
Jul 8-13, 2012
Colby-Sawyer College, New London, NH
Chair: David W. Shoesmith
Vice Chair: Narasi Sridhar

- **Biomaterials**
  (*Barbara Shaw* / Jeremy Gilbert / Frank Witte)
- **Stress Corrosion Cracking**
  (*Roger Newman* / Preet Singh / Lionel Fournier / Rob Kelly)
- **Localized Corrosion Processes/Corrosion Probes**
  (*Patrik Schmutz* / Chiang-Jian Lin / James Sullivan)
- **Coatings**
  (*Michael Rohwerder* / Arjan Mol / Rudy Buchheit / Dominique Thierry)
- **Minerals / Amorphous Metals**
  (*Mary Ryan* / Markus Valtiner / Annett Gebert)
- **Oxide Films**
  (*Sanna Virtanen* / James Noël / Shriram Ramanathan / Kurt Hebert)
- **Infrastructure**
  (*Ralf Posner, Yves van Ingelgem* / Carmen Andrade)
- **Atmospheric Corrosion**
  (*Jerry Frankel* / Heather Allen / Ivan Cole / Phillippe Dillman)
- **Public Issues**
  (*Narasi Sridhar* / Marc Edwards)

Corrosion - Aqueous
Jul 7-8, 2012
Chair: Ralf Posner
Associate Chair: Yves Van Ingelgem

NEW! CRYSTAL ENGINEERING
Jun 10-15, 2012
Waterville Valley Resort, Waterville Valley, NH
Chair: Robin D. Rogers
Vice Chairs: Christer Aakeröy & Mike J. Zaworotko

- **Nanocrystals**
  (*Anja Mudring* / Helmut Coelfen / Christoph Janiak)
- **Nucleation, Crystal Growth, and Solid State Reactivity**
  (*Peter Vekilov* / Jennifer Swift / Lia Addadi / Miguel Garcia Garibay)
- **Polymorphism and Crystal Structure Prediction**
  (*Maryjane Tremayne* / Joel Bernstein / Gautam Desiraju)
- **Functional Porous Materials**
  (*Joseph Hupp* / Lee Cronin / Song Gao / Shengqian Ma)
- **Magnetism and Conductivity**
  (*John Schlueter* / Marc Fourmigué / Hiroshi Yamamoto)
- **Design, Synthesis, and Properties of Co-Crystals**
  (*Alicia Beatty* / Nair Rodriguez-Hornedo / Susan Bourne / Fabrizia Grepioni)
- **Industrial Applications of Crystal Engineering**
  (*Susan Reutzel-Edens* / Luisa de Cola / Bill Jones)
- **Coordination Polymers**
  (*Adam Matzger* / Jing Li / Kumar Biradha / Stuart Batten)
- **Halogen Halogen and Other Weak Interactions**
  (*T.N. Guru Row* / Pierangelo Metrangolo / Jane Murray / Peter Politzer)

Crystal Engineering
Jun 9-10, 2012
Chair: Mohamed H. Alkordi

DEFECTS IN SEMICONDUCTORS
Aug 12-17, 2012
University of New England, Biddeford, ME
Chair: Evan R. Glaser
Vice Chair: Christian M. Wetzel

- **Spintronics/Quantum Information**
  (*Michael Thewalt* / Ben Murdin / Kazunori Sato)
- **Diamond**
  (*Paul Barclay* / Fedor Jelezko)
- **Point Defects in Nitrides**
  (*Bruno Meyer* / N.T. Son)
- **Extended Defects in Nitrides**
  (*Philomela Komninou* / Michelle Moram)
- **Metal Oxides I**
  (*Tim Veal* / Anderson Janotti / Oliver Bierwagen)
- **Metal Oxides II**
  (*Steve Durbin* / Len Brillson)
- **Complex Oxides**
  (*Mike Stavola* / Marianne Tarun / Marek Skowronski)
- **Photovoltaic/Solar Cell Materials**
  (*Wladek Walukiewicz* / Eric Mazur / John Murphy)
- **Silicon Carbide**
  (*Bill Mitchel* / Hidekazu Tsuchida)
- **Graphitic Materials**
  (*Ado Jorio* / Ulrich Starke / Steve Louie)

- **Doping of Nanostructures**
  (*Pavle Radonovic* / Steve Erwin / Uri Banin / David Norris)
- **New Frontiers in Chalcogenide Semiconductors**
  (*Kang Wang* / Qi-Kun Xue)
- **Novel Defect-Sensitive Detection/Imaging Techniques**
  (*Filip Tuomisto* / Lincoln Lauhon / Steve Pennycook)
- **Keynote Presentation: Defect Spectroscopy - Quo Vadis**
  (*Evan Glaser* / Martin Stutzmann)

DIFFRACTION METHODS IN STRUCTURAL BIOLOGY

Jul 15-20, 2012
Bates College, Lewiston, ME
Chair: Ana Gonzalez
Vice Chair: Anastassis Perrakis

- **Highlights in Structure Solution**
  (*Andrew Leslie* / Bill Weiss / Andrea Musacchio)
- **Getting the Best Out of Your Data: Crystallization and Data Collection**
  (*James Holton* / Anthony Kossiakoff / Elspeth Garman / Aina Cohen / Gerard Bricogne)
- **Runway Models**
  (*Jane Richardson* / Robbie Joosten / Gerard Kleywegt / Zbyszek Dauter)
- **Complementary Methods**
  (*Eddie Snell* / Axel Brunger / John Tainer / Arwen Pearson / Piet Gros)
- **Driving Methods Development: Challenging Cases**
  (*Tassos Perrakis* / Parto Ghosh / Poul Nissen / Jon Grimes)
- **Getting the Best Out of Your Data: Data Analysis**
  (*Airlie McCoy* / Frank di Maio / Jeffrey Headd / Dominika Borak / Kay Diederichs)
- **Ultimate Sources**
  (*Janet Smith* / Thomas Schneider / Vivian Stojanoff / Sol Gruner)
- **Poster Presentations**
  (*Paul Adams*)
- **Structural Biology at XFEL**
  (*John Spence* / Tomas Eikeberg / Thomas White / Sebastien Boutet)

NEW! DRINKING WATER DISINFECTION BY-PRODUCTS

Aug 5-10, 2012
Mount Holyoke College, South Hadley, MA
Chair: Manolis Kogevinas
Vice Chair: Michael Plewa

- **Global Clean Water**
  (*Mark Nieuwenhuijsen* / Stuart W. Krasner / Benito Marinas)
- **Methods to Identify DBPs**
  (*Tanju Karanfil* / Xiangru Zhang / Xingfang Li / Bill Mitch)
- **Swimming Pools: Chemistry and Respiratory Effects**
  (*Judy LaKind* / Ernest Blatchley / Alfred Bernard / Christian Zwiener)
- **DBP Toxicology and Mechanisms**
  (*David DeMarini* / Michael Plewa / Matias Attene-Romas / Sid Hunter)
- **Identification of Emerging DBPs**
  (*Aaron Dotson* / Ina Kristiana / Michael Templeton)
- **Exposure Assessment and Evaluation of Mixtures**
  (*Benjamin Blount* / John Nuckols / Manolis Kogevinas)
- **DBP Formation: Pharmaceuticals and Energy Extraction Activities**
  (*Stephen Duirk* / Jeanne VanBriesen / Ching-Hua Huang)
- **New Epidemiological Evidence on DBPs, Human Cancer and Reproductive Effects**
  (*Patrick Levallois* / Cristina Villanueva / Laura Bean-Freeman / Sylvaine Cordier)
- **Future in Research on DBPs**
  (*Susan Richardson* / Susan Richardson)

DRUG CARRIERS IN MEDICINE & BIOLOGY

Translational Drug Carriers: From Design and Understanding Mechanism of Action to Clinical Use

Aug 12-17, 2012
Waterville Valley Resort, Waterville Valley, NH
Chairs: Vladimir R. Muzykantov & Joseph M. Desimone
Vice Chairs: Heather D. Maynard & Paul A. Burke

- **Vascular Delivery, Targets and Barriers**
  (*Silvia Muro* / Jan Schnitzer / Ingrid Molema / Shad Thaxton)
- **Translational Studies, Clinical Trials and Combination Therapies**
  (*David Scheinberg* / Lawrence Mayer / Ruth Duncan / Renata Pasqualini)
- **Local, Pulmonary, GI and CNS Delivery: Barriers, Transporters, Devices**
  (Justin Hanes / Krystof Bankiewicz / Randy Mrsny)
- **Emerging Technologies, Materials, Carriers and Mechanisms**
  (*Sasha Kabanov* / Omid Farokazhad / Hamid Ghandehari / Efrosini Kokkoli / Tyrone Porter)
- **Natural Carriers (Cells, Proteins and Peptides)**
  (*Phil Law, William Zamboni* / Catherine Bollard / Mauro Magnani / Jennifer R. Cochran)
- **Carriers for Vaccines and Antigen Delivery**
  (*Joe De Simone* / Nathalie Garcon / Tarek Fahmy / Sam Lai / Bolyn Hubby)
- **Latest News and Young Voices**
  (*Heather D. Maynard, Paul A. Burke*)
- **Intracellular Delivery, Trafficking & Cellular Barriers**
  (*Jan Schnitzer* / Chad Mirkin [keynote] / Paula Hammond / Silvia Muro)
- **Biological Response to Delivered Drugs and Genes**
  (*Leaf Huang, Vlad Muzykantov* / William Zamboni / Carol H. Miao)

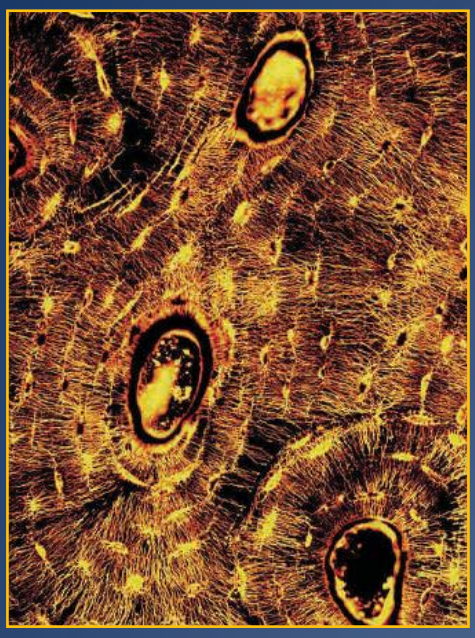

Osteocyte network in bone, revealed by confocal light microscopy. Courtesy of Michael Kerschnitzki and Wolfgang Wagermaier. Submitted by Peter Fratzl, Chair, Biomineralization GRC.

DRUG METABOLISM

Celebrating the Future of Drug Metabolism

Jul 8-13, 2012
Holderness School, Holderness, NH
Chair: Erin Schuetz
Vice Chair: James B. Mangold

- **Keynote Presentation: Drug Metabolism: The Good, The Bad and The Ugly**
  (Stephen G. Sligar)
- **Metabolomics Meets ADME**
  (*Frank Gonzalez* / Ian Wilson / Sanjay K. Nigam / Xiaochao Ma / Sabrina M. Ronen)
- **Predicting Metabolism using Cytochrome P450 Structure**
  (*Steven A. Wrighton* / Eric F. Johnson / Emily E. Scott / James R. Halpert)
- **Environmental and Dietary Factors Affecting Drug Metabolism and Response**
  (*Kenneth Thummel* / Mary Paine / Francis Levi / Erik Eliasson / Allan Rettie)
- **Time Dependent Inhibition**
  (*Andrew Parkinson* / Andrew Parkinson / Stephen D. Hall / Scott R. Obach)
- **Mice with Human Livers or Human ADME Genes for Drug Disposition Studies**
  (*Robert H. Tukey* / C. Roland Wolf / Robert van Waterschoot / Robert Tukey / John Bial)
- **Graduate Student and Post-Doc Presentations**
  (*Henry Strobel*)
- **"Back to the Future"**
  (*John D. Schuetz* / Koen van de Wetering / Gerhard Ecker / Irwin Arias)
- **New Ideas and Technologies**
  (*Tom Rushmore* / Rafel Witek / Rick King)

NEW! DRUG RESISTANCE

A Multidisciplinary Exploration of Similarities in Drug Resistance in Rapidly Evolving Diseases

Jul 29 - Aug 3, 2012
Stonehill College, Easton, MA
Chairs: Margaret A. Riley & Celia A. Schiffer
Vice Chair: Sally Blower

- **The Drug Resistance Challenge: Setting the Stage**
  (*John Coffin* / Marie-Pierre de Bethune)
- **Drug Resistance Evolution**
  (*Bruce Levin* / Leah Cowen / Tim Clackson)
- **Drug Resistance Epidemiology**
  (*Thomas O'Brien* / Robert Shafer / Cristain Tomasetti)
- **Predicting Drug Resistance**
  (*Dan Andersson* / Sally Blower / Michael Gottesman / Amy Anderson)
- **Limiting Resistance Emergence**
  (*Jean Patel* / Patrick Tranel / Roy Kishony)
- **Designing Drugs That Last**
  (*David Spiegel* / Andrew Greenstein / Arnold Edward / Robert Dorit)
- **Novel Drug Targets to Avoid Resistance**
  (*Manuel Navia* / Juswinder Singh / Carol Sibley)
- **Multidisciplinary Approaches to Tackling Drug Resistance I**
  (*Jennifer Leeds* / Judith Berman / Ronald Swanstrom / Richard Slayden)
- **Multidisciplinary Approaches to Tackling Drug Resistance II**
  (*Ray Schinazi* / Susan Bates / Michael Miller)

ELECTRODEPOSITION

Electrochemical Materials Synthesis and Applications

Jul 29 - Aug 3, 2012
University of New England, Biddeford, ME
Chair: Andrew A. Gewirth
Vice Chair: Kyoung-Shin Choi

- **Keynote Presentations**
  (Nenad Markovic)
- **Electrodeposition of Materials for Electronics**
  (Jae Jong Kim / Nosang Myung)
- **Electrodeposition for Thermoelectrics**
  (Clotilde Boulanger / Kornelius Neilsch)
- **Electrodeposition for Batteries**
  (Doron Aurbach / Amy Prieto)
- **Electrodeposition for Solar Energy**
  (Stephen Maldonaldo / Daniel Lincot)

- **Characterization of Electrodeposition**
  (Kohei Uosaki / Jeff Greeley / Suzanne Jarvis)
- **Late Breaking News Presentations**
  (*Kyoung-Shin Choi*)
- **Novel Electrodeposition Concepts (Ionic Liquids)**
  (Alexander Kuhn / Frank Endres)
- **Electrodeposition for Fuel Cells**
  (Hong Yang)

Electrodeposition
Jul 28-29, 2012
Chair: A. Wouter Maijenburg
Associate Chair: Leah B. Sheridan

ELECTRON DONOR-ACCEPTOR INTERACTIONS

Aug 5-10, 2012
Salve Regina University, Newport, RI
Chairs: James K. McCusker & Bo Albinsson
Vice Chairs: David H. Waldeck & C. Michael Elliott

- **Donor-Acceptor Interactions and Chemical Synthesis**
  (*Paula Diaconescu* / David W.C. MacMillan / Christopher Chang / Fabrice Odobel)
- **Quantum Effects in Donor-Acceptor Systems**
  (*Mark Ratner* / Gregory Scholes / Alan Aspuru-Guzik / Lin Chen / Sean Shaheen)
- **Proton-coupled Electron Transfer**
  (*Daniel Nocera* / Judith Klinman / Alexei Stuchebrukhov / James Mayer)
- **Bridging the Gap between Electron Transfer and Magnetism**
  (*Natia Frank* / Daniel Gamelin / Gemma Solomon / David Shultz / Christiane Timmel)
- **Biological and Bio-inspired Systems**
  (*Claudia Turro* / Mary Beth Williams / Karen Brewer / Licheng Sun)
- **Dye-Sensitized Solar Cells**
  (*Thomas Hamann* / Anders Hagfeldt / Elena Galoppini / Gerald Meyer / Maria Abrahamsson)
- **Dynamics and Mechanisms of Donor-Acceptor Interactions**
  (*Antonin Vlcek, Jr.* / Niels Damrauer / Oliver Wenger / Kelly Gaffney)
- **OPVs, BHJs, and Advanced Characterization of DA Devices**
  (*Garry Rumbles* / Dirk Guldi / Alison Walker / Michael Strano / John Marohn)
- **Poster Presentations / Keynote Presentation**
  (*C. Michael Elliott, David Waldeck, Michael Wasielewski* / Thomas A. Moore [keynote])

Electron Donor-Acceptor Interactions
Aug 4-5, 2012
Chair: Allison M. Brown
Associate Chair: J. Andrew Kouzelos

ELECTRONIC PROCESSES IN ORGANIC MATERIALS
Exploring the Fundamentals of Organic Electronics

Jun 3-8, 2012
Il Ciocco Tuscany Resort, Lucca (Barga), Italy
Chairs: George G. Malliaras & Richard H. Friend
Vice Chairs: Seth R. Marder & Rene Janssen

- **Novel Materials for Organic Electronics**
  (*Seth Marder* / Iain McCulloch / Peter Bäuerle)
- **Electronic Structure and Interfaces**
  (*David Cahen* / David Ginger / Norbert Koch / Hisao Ishii)
- **Polymer Morphology**
  (*Georges Hadziioannou* / Ullrich Steiner / Thomas Russell)
- **Charges and Excitons**
  (*David Vanden Bout* / Ronald Österbacka / Greg Scholes / Carlos Silva)
- **Interface with Biology**
  (*Annalisa Bonfiglio* / Magnus Berggren / Guglielmo Lanzani)
- **Organic Devices I**
  (*Dago de Leeuw* / Karl Leo / Peter Ho / Reinder Coehoorn)
- **Modeling of Organic Materials**
  (*Claudia Ambrosch-Draxl* / Mark Ratner / Leonidas Tsetseris)
- **Organic Devices II**
  (*René Janssen* / Héctor Abruña / Jun Takeya / Jenny Nelson)
- **Ionic Materials and Devices**
  (*Olle Inganäs* / Gui Bazan / Henk Bolink)

Electronic Processes in Organic Materials
Jun 2-3, 2012
Chair: Dorthe M. Eisele

ELECTRONIC SPECTROSCOPY & DYNAMICS

Jul 22-27, 2012
Bates College, Lewiston, ME
Chairs: Bern Kohler & Edward R. Grant
Vice Chairs: Samuel Leutwyler & David M. Jonas

- **Coherent Electronic Energy Transfer in Biology**
  (*Gregory Scholes* / Alan Aspuru-Guzik / Jennifer Ogilvie / Greg Engel / Birgitte Whaley)
- **Excited State Spectroscopy**
  (*Helen Fielding* / Robert Field / Albert Stolow)
- **Electronic Spectroscopy of Cold and Ultracold Molecules**
  (*Tim Softley* / Gerard Meijer / Heather Lewandowski / Takamasa Momose / Jan Michael Rost)
- **Liquid Microjet Photoelectron Spectroscopy**
  (*Stephen Bradforth* / Bernd Winter / Daniel Neumark)
- **Transformation and the Resolution Revolution**
  (*Kevin Lehmann* / Nathalie Picqué / David Chandler / Trevor Sears / Peter Loock)
- **Time-resolved X-ray Spectroscopy**
  (Lin X. Chen / Stephen Leone)
- **Excited State Dynamics**
  (*Spiridoula Matsika* / Leticia Gonzalez / Eberhard Riedle / Tahei Tahara / Villy Sundström)
- **Excitonics**
  (*Keith Nelson* / Anna Köhler / Uri Banin)

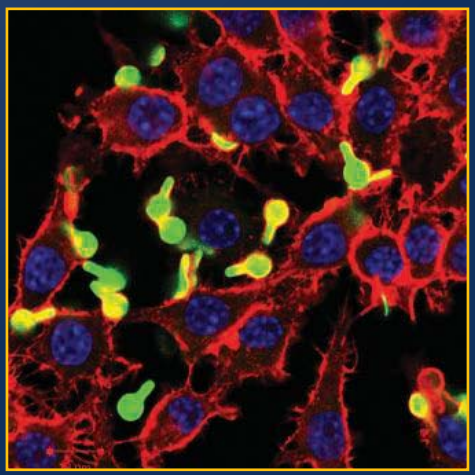

Lollipop particles: Investigating asymmetric particle effects on macrophage phagocytosis. Courtesy of Tammy Shen and Anuradha Gullapalli. Submitted by Vladimir R. Muzykantov & Joseph M. Desimone, Chairs, Drug Carriers in Medicine & Biology GRC.

ENDOTHELIAL CELL PHENOTYPES IN HEALTH & DISEASE

Jul 29 - Aug 3, 2012
Il Ciocco Tuscany Resort, Lucca (Barga), Italy
Chair: Susan Quaggin
Vice Chair: S. Ananth Karumanchi

- **Hypoxia and the Endothelium**
  (*Ananth Karumanchi* / Gregg Semenza)
- **The Endothelium in Development**
  (*Victoria L. Bautch* / Anne Eichmann / Mark L. Kahn / Victoria L. Bautch / Eli Keshet)
- **Extrinsic Cues That Modulate Endothelial Behaviour**
  (*Christer Betsholtz* / Christiana Ruhrberg / Christer Betsholtz / Ralf H. Adams)
- **Model Systems and the Endothelium**
  (*Brant M. Weinstein* / Renata Pasqulini / Wadith Arap / Brant Weinstein / Katie Bentley)
- **The Future of Endothelial Biology: Bioengineering, Progenitor Cells and Nano Technology**
  (*Janet Rossant* / Mervin Yoder / Shahin Rafii)
- **Signaling and the Endothelium**
  (*Elisabetta Dejana* / Tatiana Byzova / Helmut Augustin / Elisabetta Dejana / Michael Simons)
- **Targeted Therapeutics and the Endothelium**
  (*Dontscho Kerjaschki* / Napoleone Ferrara / Kari Alitalo)
- **Diseases of the Endothelium**
  (*William C. Aird* / Martin Friedlander / Dean Li / Jens Titz / Radu V. Stan)
- **Metabolism, Inflammation, and the Endothelium**
  (*Jordan S. Pober* / Ulf Eriksson / Peter Nawroth / George L. King)

Endothelial Cell Phenotypes in Health & Disease
Jul 28-29, 2012
Chair: Marie A. Jeansson
Associate Chair: Iacovos Michael

ENERGETIC MATERIALS

Jun 17-22, 2012
Mount Snow Resort, West Dover, VT
Chair: Michael R. Zachariah
Vice Chair: Leanna M.G. Minier

- **Opportunities and Needs**
  (*Su Peris* / Cliff Bedford / Wing Tsang / Rich Behrens)
- **Synthesis**
  (*Tom Klapotke* / Carl Kristie / Nikolj Latypov / Stefan Schnieder / Jesse Sabatini)
- **Clusters to Nanoparticles Based Materials**
  (*Puru Jenna* / Will Castleman / Kit Bowen / Bryan Eichhorn)
- **Reactive Materials**
  (*Ed Driezin* / Steve Son / Arvind Varma / Alex Rogachev / Florence Baras)
- **Advanced Diagnostics**
  (*Joel Carney* / Marcia Cooper / Tom Lagrange / Andrezj Miziolek)
- **Computational Chemistry**
  (*Prya Vishista* / Adri Van Duin / Don Thompson / Ed Byrd / Rhiadd Manna)
- **Simulation**
  (*Mel Baer* / Hugh James / S. "Bala" Balachandar / Elaine Oran)
- **Shock Physics**
  (*Dana Dlott* / Naresh Thadhani / Andrew Higgins / David Williamson / Mike Armstrong)
- **Combustion**
  (*Rich Yetter* / Fan Zhang / Luigi Deluca / Stephan Thynell)

ENVIRONMENTAL ENDOCRINE DISRUPTORS
Jun 3-8, 2012
Mount Snow Resort, West Dover, VT
Chair: Andrea C. Gore
Vice Chairs: Susan Jobling & Louis J. Guillette

- **Keynote Presentation: Endocrine Disruptors, Society, and Public Policy**
  (*Andrea C. Gore* / Paul Anastas / Pete Myers)
- **Women's Health and Environmental Endocrine Disruptors**
  (*Ana Soto* / Suzanne Fenton / Evanthia Diamanti-Kendarakis / Barbara Cohn)
- **Men's Health and Environmental Endocrine Disruptors**
  (*Zengrong Sun, Sheela Sathyanarayana* / Shanna Swan / Niels Jorgensen)
- **Gene-Environment Interactions, Epigenetics, and EEDs**
  (*Jerrold Heindel* / Cheryl Walker / Dana Dolinoy / Barbara Hales)
- **Thyroid and Immune System Disruptors**
  (*R. Thomas Zoeller* / Barbara Demeneix / Rodney Dietert)
- **Neuroendocrine Disruptors**
  (*Emilie Rissman* / GianCarlo Panzica / Heather Patisaul / Vance Trudeau)
- **Resolving Controversies in Endocrine Disruption**
  (*Fred vom Saal* / Joe Braun / Daniel Zalko)
- **Evolution in a Contaminated Environment**
  (*Brandon Moore* / Charles Tyler / David Crews / Andrew Whitehead)
- **Endocrine Disruptors and Ecosystems**
  (*Louis Guillette, Susan Jobling* / Thea Edwards / Lori Schwacke)

Environmental Endocrine Disruptors
Jun 2-3, 2012
Chair: Brandon Moore
Associate Chair: Deena M. Walker

ENVIRONMENTAL SCIENCES: WATER
Grand Challenge Frontiers in the Aquatic Environmental Sciences
Jun 24-29, 2012
Holderness School, Holderness, NH
Chair: David L. Sedlak
Vice Chair: Paul G. Tratnyek

- **Planetary Safe Operating Spaces**
  (*William Schlesinger*)
- **Biotransformation and Biocatalysis**
  (*Larry Wackett* / Vassily Hatzimanikatis)
- **Crises Driven Science**
  (*Jerry Schnoor* / Elizabeth Kujawinski / Kelvin Gregory)
- **Redox and Radical Processes**
  (*David Waite* / Jae-hong Kim / Michael Sander / Chad Vecitis)
- **Exposure, Toxicity, Risk**
  (*Nancy Denslow* / April Gu)
- **Microbial Community Structure & Function**
  (Katherine McMahon / Susann Müller / Ludmila Chistoserdova)
- **Emerging Contaminants**
  (*Susan Richardson* / Brian Mader)
- **Colloids & Nanoparticles**
  (*Menachem Elimelech* / Heileen Hsu-Kim / Young-Shin Jun / Eric Hoek)
- **Lifetime Achievement in Aquatic Sciences**
  (*Phil Gschwend* / Ron Hites)

Environmental Sciences: Water
Jun 23-24, 2012
Chair: Marcella L. Card
Associate Chair: Matthew A. Limmer

ENZYMES, COENZYMES & METABOLIC PATHWAYS
Jul 15-20, 2012
Waterville Valley Resort, Waterville Valley, NH
Chairs: Gregory D. Reinhart & Steven Rokita
Vice Chairs: Vahe Bandarian & Catherine L. Drennan

- **Pathways from Structure to Output**
  (Hazel Holden / Janet Smith / Lori Giver)
- **Mechanism of DNA Repair**
  (Zhibao Zhuang / Maria Spies / Wolf-Dietrich Heyer / Cheryl Arrowsmith)
- **Assigning Function and Targeting Inhibition**
  (Steve Almo / Tom Meek / Stewart Fisher)
- **Engineering Catalysis**
  (Reinhard Sterner / Margaret Glasner)
- **Engineering Pathways**
  (Sven Panke / Chris Voight)
- **Membranes as an Essential Component of Structure and Activity**
  (Josh Wand / Falk Harnisch)
- **Enzyme and Metabolic Regulation**
  (Bill DeGrado / Michael Marletta / Kim Orth / Gerald Carlson)
- **Assembly and Maintenance of Metallo-Cofactors in Enzymes**
  (Joan Broderick / David Barondeau / Deborah Zamble)
- **Catalysis Based on Thiols, Selenium and More**
  (Richard Armstrong / Vadim Gladyshev / Kate Carroll)

FLOW & TRANSPORT IN PERMEABLE MEDIA
Jun 24-29, 2012
Les Diablerets Conference Center, Switzerland
Chair: Tissa H. Illangasekare
Vice Chair: Hamdi A. Tchelepi

- **Flow Regimes in Porous Media Systems**
  (*Lynn Bentham* / Jean Roberts / Ken Sorbie)
- **Moving Across Scales**
  (*Dong Zhang* / Alex Tartakovsky / Xiao-Hui Wu / Sabine Attinger)
- **Re-Visiting Relative Permeability**
  (*Martin Blunt* / Kishore Mohanty / Rink van Dijke)
- **Innovation in Methods and Approaches for Process Identification in Multiscale Porous Media Systems**
  (*Helge Dahle* / Malgorzata Peszynska / Brent Linquist / Knut Andreas Lie)
- **Coupling of Porous Media to Free Fluid Flow Systems**
  (*Rainer Helmig* / Marc Parlange / Peter Lehmann)
- **Detection and Characterization of Changes - Reactive and Bio Processes**
  (*Alberto Guadagnini* / Mira Olson / Markus Hilpert / Qinjun Kang)
- **Optimizing Subsurface Storage Mass and Energy and Their Extraction**
  (*Sally Benson* / Catherine Noiriel / Curt Oldenburg)
- **Alternate Energy Systems and Sources**
  (*Brad Mallison* / Rajesh Parwar / Bob Kee)
- **Bio- Fluid Mechanics for Bio-Tissues and Life in Bio-Porous Media**
  (*Dani Or* / John Crawford / Fan Yuan)

Flow & Transport in Permeable Media
Jun 23-24, 2012
Chair: Sarah E. Gasda
Associate Chair: Vahid Joekar-Niasar

NEW! FRAGILE X AND AUTISM-RELATED DISORDERS
From Basic Neuroscience to Improved Clinical Care
Jun 10-15, 2012
Stonehill College, Easton, MA
Chair: Elizabeth M. Berry-Kravis
Vice Chair: Jennifer C. Darnell

- **Keynote Presentation**
  (Mark Bear)
- **Activity-Dependent Protein Synthesis in Neurons**
  (*Joel Richter* / Mauro Costa-Mattioli / Eric Klann / Ray Kelleher / Emily Osterweil)
- **Temporal and Cell-Specific Functions of FMRP**
  (*Jen Darnell* / Xinyu Zhao / Jay Gibson / Kendal Broadie)
- **The Presynaptic Compartment**
  (*Justin Fallon* / Michael Sutton / Deanna Benson / Craig Garner / Mike Akins / Christine Holt)
- **Circuits**
  (*Peter Kind* / Anis Contractor / Rhiannon Meredith / Karl Deisseroth)
- **The Molecular Basis of Autism, FXS and Developmental Cognitive Disorders I**
  (*Seth Grant* / Catalina Betancur / Tom Sudhof / Luis Parada)
- **The Molecular Basis of Autism, FXS and Developmental Cognitive Disorders II**
  (*Kim Huber* / Gary Bassell / Len Kaczmerak / Lu Chen)
- **Outcome Measures in Fly, Mouse and Man**
  (*Len Abbeduto* / Tom Jongens / Rich Paylor / David Hessl / Allan Reiss)
- **Clinical Trials of Targeted Treatments**
  (Randi Hagerman / Mustafa Sahin / Paul Wang / Eriene Wasef / George Apostal)

FUEL CELLS
Aug 5-10, 2012
Bryant University, Smithfield, RI
Chairs: Thomas A. Zawodzinski & Thomas Jarvi
Vice Chairs: Peter N. Pintauro & Elena R. Savinova

- **Beyond Hydrogen?**
  (*Tom Zawodzinski, Tom Jarvi* / John Deutch / Mark Johnson)
- **Can We Operate at or Above 1V?**
  (*Nenad Markovic* / Piotr Zelenay / Plamen Atannasov / Victor Batista)
- **Electrodes in Hot, Dry Systems**
  (*Thomas Steenberg* / Sanjeev Mukerjee / Alex Papandrew)
- **RFBs and Metal-Air Batteries**
  (*Gabriel Vieth* / Mike Perry / M. Stanley Whittingham)
- **Emerging Fuel Cells**
  (*Matthew Mench* / Grigorii Soloveichik)
- **Improving Conductors**
  (Mark Tuckerman / Andrew Herring / Nitash Balsara)
- **Understanding 3-D Electrodes**
  (*Bryan Pivovar* / Kunal Kanar)
- **Durability**
  (*Lesia Protsailo* / Christina Roth / Dane Morgan)
- **Poster Presentations**
  (*Peter Pintauro, Elena Savinova*)

GEOCHEMISTRY OF MINERAL DEPOSITS
Jul 15-20, 2012
Proctor Academy, Andover, NH
Chair: John Muntean
Vice Chairs: Robert P. Moritz & Jon Hronsky

- **Frontiers in Economic Geology Research**
  (Christoph Heinrich / Murray Hitzman / Antonio Arribas)
- **Metallogenic Provinces and Epochs: The Role of Upper Mantle/Lower Crust Inheritance**
  (*Richard Arculus* / Norman Pearson)
- **Sediment Hosted Copper Systems: Focus on the African Copper Belt**
  (*Murray Hitzman*)

- **Magmas, Fluids and Metals**
  (*Adam Simon* / Andreas Audétat)
- **Iron Oxide-Copper-Gold-Systems**
  (*Luis Fontboté* / Mark Barton)
- **Active Submarine and Subaerial Hydrothermal Systems**
  (*Mark Hannington, Stuart Simmons* / Julie Rowland)
- **Distal Expressions of Large Gold and Copper Systems**
  (*David Cooke* / Bruce Gemmell / Scott Halley)
- **Dynamics of Ore Systems**
  (*Richard Tosdal*)
- **Rare Earth Element Systems**
  (*Anthony Williams-Jones*)

GRANULAR & GRANULAR-FLUID FLOW
Jul 22-27, 2012
Davidson College, Davidson, NC
Chair: Karen E. Daniels
Vice Chair: Bulbul Chakraborty

- **Continuum Mechanics**
  (*Bulbul Chakraborty* / Joseph Goddard / Ken Kamrin)
- **Wet & Suspended Particles**
  (*Daniel Bonn* / Martin Brinkmann / James Gilchrist / Anke Lindner)
- **Charged Particles**
  (*Dietrich Wolf* / Daniel Lacks / Troy Shinbrot)
- **Granular Gases**
  (*Aparna Baskaran* / Jonathan Machta / Matthias Sperl)
- **Geophysical Phenomena**
  (Douglas Jerolmack / Karen Mair)
- **Acoustics & Vibration**
  (*Corey O'Hern* / David Johnson / Vincenzo Vitelli / M. Lisa Manning)
- **Friction & Shear**
  (*Deniz Ertas* / Gioacchino Viggianni / Liran Goren)
- **Penetration & Drag**
  (*Stéphane Douady* / Evelyne Kolb / Ernesto Altshuler)
- **Earthquakes & Labquakes**
  (*Karen Daniels* / Paul Johnson)

NEW! GRAPHITIC CARBON MATERIALS, CHEMISTRY AND PHYSICS OF
Jun 17-22, 2012
Davidson College, Davidson, NC
Chair: Herbert A. Fertig
Vice Chairs: Antonio Castro Neto & Liang-Shi Li

- **Opportunities and Challenges in Graphitic Carbon Materials: Fundamental Science and Applications**
  (*Antonio Castro Neto* / Kostya Novoselov / Mildred Dresselhaus)
- **Graphene Allotropes: Novel Physics and Applications I**
  (*Maria Vozmediano* / Paul McEuen / Allan MacDonald / Nancy Sandler)
- **Graphene Allotropes: Chemistry I**
  (*Xiangfeng Duan* / Rod Ruoff / Richard Kaner)
- **Graphene Allotropes: Novel Physics and Applicatons II**
  (*Alessandra Lanzara* / Sankar Das Sarma / Claire Berger / Philip Kim)
- **Graphene Allotropes: Chemistry II**
  (*Liang-shi Li* / Robert Haddon / Klaus Muellen)
- **Carbon Materials: Applications for Energy I**
  (*Allen Siedle* / Jie Liu / Prashant Kamat)
- **Young Investigator Presentations**
  (*Feng Wang* / Jeannie Lau / Kian Ping Loh / Jing Kong)
- **Graphitic Materials: Applications for Energy II**
  (*Matthias Schwab* / Liming Dai / Michael Strano)

GREEN CHEMISTRY
Jul 22-27, 2012
Il Ciocco Tuscany Resort, Lucca (Barga), Italy
Chairs: Karen I. Goldberg & Steve Howdle
Vice Chairs: Kenneth Seddon & Mark A. Harmer

- **CO_2 Utilization**
  (*Elsje Alessandra Quadrelli* / Andrew Bocarsly / Martina Peters)
- **Polymers and Materials**
  (*Ana Aguiar Ricardo* / Charlotte Williams / Ludwik Liebler / Rachel O'Reilly / Catia Bastioli)
- **Catalysis**
  (*Istvan Horvath* / Jurgen Klankermeyer / David Milstein / Alan Goldman)
- **Bio-inspired and Biorenewables**
  (*Emilio E. Bunel* / Henry Bryndza / Markus Antonietti / Jennifer Holmgren / William Kruper)
- **Designing Green Chemicals**
  (Julie Zimmermann / Paul Anastas)
- **Greener Approaches to Organic Synthesis**
  (*Andrew Wells* / Jin-Quan Yu / Johannes G. De Vries)
- **Assessing our Progress Toward a Sustainable Future**
  (*Mike Heinekey* / John Warner / panel discussion)
- **Light, Energy and Fuel**
  (Mike George / Tobin Marks)
- **Green Solvents**
  (*Charlotta Turner* / Tadafumi Adschiri / Buxing Han)

Green Chemistry
Jul 21-22, 2012
Chair: Harriet Scott
Associate Chair: Margaret Scheuermann

HEMOSTASIS
Jul 22-27, 2012
Waterville Valley Resort, Waterville Valley, NH
Chair: Sriram Krishnaswamy
Vice Chair: Andrew S. Weyrich

- **Thrombosis and Hemostasis: Historical Perspectives**
  (*Charles T. Esmon* / Joel S. Bennett / Darrel W. Stafford)
- **Inflammation/Infection and Coagulation**
  (*Susan S. Smyth* / Piet Gros / Paul Kubes)
- **Thrombus Formation and its Dissolution**
  (*Jose A. Lopez* / James Whisstock / John W. Weisel / Patricia C. Liaw)
- **Defective Hemostasis**
  (*James H. Morrissey* / Rodney M. Camire / John S. "Pete" Lollar / Walter H. Kahr / Jorge DiPaolo)
- **Blood/Vessel Wall Interface**
  (*Leslie V. Parise* / Jaime Grutzendler / Robert Flaumenhaft / Rodger P. McEver)
- **Receptors and Signaling**
  (*Lawrence "Skip" Brass* / Renhao Li / Sergio Grinstein / Mark H. Ginsberg / Charles S. Abrams)
- **Regulation of Thrombus Formation**
  (*Barbara C. Furie* / James A. Huntington / Wolfgang Bergmeier / Mark L. Kahn)
- **Hot Topic Presentations**
  (*Andrew S. Weyrich*)
- **Membranes/Microparticles/Atherothrombosis**
  (*Nigel Mackman* / Roy L. Silverstein / Wolfram Ruf / Lily Jan)

Hemostasis
Jul 21-22, 2012
Chair: Robert Campbell
Associate Chair: Paul R. Hess

HETEROCYCLIC COMPOUNDS
Jun 24-29, 2012
Salve Regina University, Newport, RI
Chair: David C. Lathbury
Vice Chair: John L. Wood

- **New Strategies for Heterocycle Synthesis I**
  (*John Wood* / Mark Lautens / Eric Carriera)
- **Catalysis in Heterocycle Synthesis**
  (*Dan Elbaum* / Tamejiro Hiyama / Sherry Chemler)
- **Heterocyclic Natural Products**
  (Bill Roush / Jim Anderson)
- **Biological Aspects of Heterocyclic Chemistry**
  (*Mark Behnke* / Dennis Dougherty)
- **New Strategies for Heterocycle Synthesis II**
  (*Jon Antilla* / Tom Rovis / Amido Studer)
- **Advances in the Synthesis of Heterocyclic Compounds**
  (*Scott Sutton* / Tim Gallagher / David Chen / Yiyin Ku)
- **Targeted Heterocycle Synthesis**
  (David Black / John H. Freudenberger)
- **Mechanistic Aspects of Heterocycle Synthesis**
  (*Christopher Grote* / Donna Blackmond / Guy Lloyd-Jones)
- **New Reactions in Heterocycle Synthesis**
  (*Diane Carrera* / David MacMillan / Paul Murray)

HIGH PRESSURE, RESEARCH AT
Jun 24-29, 2012
University of New England, Biddeford, ME
Chair: Malcolm I. McMahon
Vice Chair: Gilbert Collins

- **Structure Prediction at Extreme Conditions: Are Experiments Still Necessary?**
  (*John Tse* / Yanming Ma / Richard Needs)
- **Young Investigator Presentations**
  (Miriam Marques / Amy Lazicki / Jeffrey McMahon / Stewart McWilliams)
- **New Frontiers of High Pressure Science**
  (Ray Smith / Andy Higginbotham)
- **High Density Hydrogen**
  (*Andrew Jephcoat* / Michael Eremets / Ross Howie / Stephanie Brygoo / Rus Hemley)
- **Superconductivity and Novel Dense Structure**
  (James Hamlin / Natalia Dubrovinskaia)
- **High Density Liquids and Melting**
  (Dario Alfe / Agnes Dewaele)
- **Chemistry and Biology**
  (*Paul McMillan*)
- **Geophysics, Geoscience and Planetary Science**
- **High Pressure Advances and Future Challenges**
  (*Dennis Klug*)

High Pressure, Research at
Jun 23-24, 2012
Chair: Ashkan Salamat
Associate Chair: Rachael T. Hazael

HOST-PARASITE INTERACTIONS, BIOLOGY OF
Jun 10-15, 2012
Salve Regina University, Newport, RI
Chairs: Boris Striepen & Keith R. Matthews
Vice Chairs: Steve Hajduk & Dominique Soldati-Favre

- **Co-Evolution of Host and Parasite**
  (*Jonathan Howard* / Jonathan Howard / Sabrina Krief / Bill Petri)
- **Parasite Pathogenesis and Virulence**
  (*Stephen Hajduk* / Stephen Hajduk / David Sibley / Nicholas Fasel / Ricardo Gazzinelli)
- **Host Cell Invasion and Modification**
  (*Dominique Soldati* / Dominique Soldati / Maryse Lebrun / Norma Andrews)

- **Parasite Cell Biology**
  (*Kent Hill* / Kent Hill / Photini Sinnis / Dan Goldberg / Phil Newmark)
- **Parasite Development**
  (*Isabel Roditi* / Isabel Roditi / Michael White / David Horn)
- **Host-Parasite Metabolic Interaction**
  (*Malcolm McConville* / Malcolm McConville / Elaine Holmes / Mike Ferdig / Kiaran Kirk)
- **Parasite Gene Expression Control**
  (*Elisabetta Ullu* / Elisabetta Ullu / Patricia Johnson)
- **Host Immune Response and Parasite Evasion**
  (*Yasmine Belkaid* / Yasmine Belkaid / Carolina Barillas Mury / Judy Allen / Richard Grencis)
- **Drug Action and Resistance**
  (*Dyann Wirth* / Dyann Wirth / Matt Bogyo / Deborah Smith)

IMMUNOCHEMISTRY & IMMUNOBIOLOGY

Jun 10-15, 2012
Les Diablerets Conference Center, Switzerland
Chair: Cynthia J. Guidos
Vice Chair: Adrian Hayday

- **Innate Mechanisms of Self/Non-self Discrimination**
  (Caetano Reis e Sousa / Veit Hornung / Jayne Danska)
- **Regulation and Function of Innate Lymphoid Cells**
  (*Adrian Hayday* / Yueh-hsiu Chien / Mitch Kronenberg / Marco Colonna)
- **Molecular Mechanisms of Leukocyte Development**
  (*Barbara Kee* / Boris Reizis / Jane Skok / Thomas Boehm)
- **Leukocyte Trafficking and Cell-Cell Interactions in Lymphoid Tissues**
  (*Jason Cyster* / Sanjiv Luther / Michael Sixt / Philippe Bousso)
- **Antigen Presentation and Lymphocyte Activation**
  (*Mark Davis* / Facundo Batista / Rose Zamoyska / Takeshi Saito)
- **Lymphocyte Homeostasis & Effector Cell Differentiation**
  (*Dan Littman* / David Tarlinton / Pam Fink / E. John Wherry)
- **Immune Regulation and Autoimmunity**
  (*Ann O'Garra* / Fiona Powrie / Gitta Stockinger / Alexander Rudensky)
- **Immunity to Infection**
  (*Mike Bevan* / Antonio Lanzavecchia / Marc Jenkins / Susan Kaech)
- **Host-Microbiome Interactions in Gut Homeostasis & Pathology**
  (*Yasmine Belkaid* / Gerard Eberl / David Artis / Sarkis Mazmanian)

IN VIVO MAGNETIC RESONANCE

Jul 29 - Aug 3, 2012
Colby College, Waterville, ME
Chair: Greg J. Stanisz
Vice Chair: Penny Gowland

- **Going with the Flow**
  (*Penny Gowland* / Laura Parkes / David Buckley)
- **Is SWI Only Iron?**
  (*John Schenck* / Karin Shmueli / Jens Jensen / Claudia Hillebrand)
- **Advances in Diffusion**
  (*Michael Smith* / Mark Does / Valerij Kisielev)
- **Fats & Lipids**
  (*Tom Dixon* / Holger Eggers / Houchun Harry Hu / Roy Taylor)
- **Breast MRI**
  (*Nola Hylton* / Werner Kaiser / Brian Hargreaves)
- **Newest Probes**
  (*John Kurhanewicz* / Maja Cassidy / Daniella Goldfarb / Eduard Chekmenev)
- **SNR Skyrockets**
  (*Piotr Kozlowski* / Tom Mareci / Daniel Marek)
- **Advances in Imaging Techniques**
  (*Joel Garbow* / Michael Lustig / David Feinberg / Michael Bock)
- **Less "Flashy" but Still Important**
  (*Risto Kauppinen* / Vasily Yarnykh / Louis Bouchard)

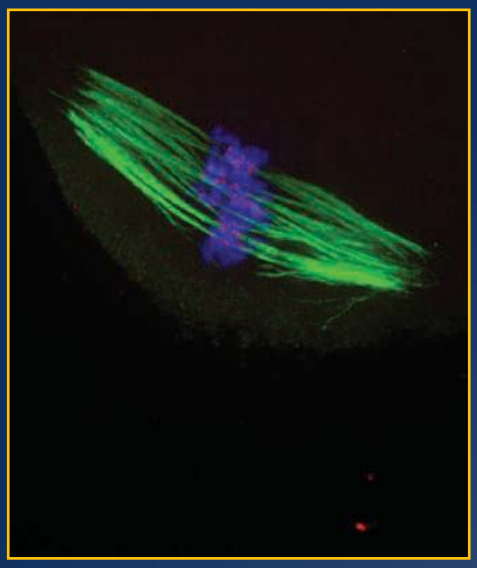

Mouse oocyte awaiting fertilization. Paired sister chromatids (in blue) are attached to the bipolar spindle (in green, after cold treatment) at kinetochores which are in the centromere region (stained with CREST serum, in red). Upon fertilization, sister chromatids are segregated and a female pronucleus is formed which will fuse with the male pronucleus to form a zygote. Courtesy of Sandra Touati and Katja Wassmann. Submitted by Nancy M. Hollingsworth, Chair, Meiosis GRC.

INDUSTRIAL ECOLOGY

The Role of Industrial Ecology in Addressing Sustainability Imperatives
Jun 17-22, 2012
Les Diablerets Conference Center, Switzerland
Chair: Sangwon Suh
Vice Chair: Helga Weisz

- **How Do We Provide Adequate Land, Water, and Nutrients to Feed the 9 Billion People That Will Inhabit the Earth by 2050?**
  (*Stefanie Hellweg* / Charles Vorosmarty / David Tilman / Faye Duchin / Kate Showers)
- **How Do We Provide Sufficient Supplies of Affordable Metals and Minerals to Support an Ever More Populous and Wealthier World?**
  (*Seiji Hashimoto* / Thomas Graedel / Jullian Alwood / John Tilton)
- **How Do We Green Rapidly Industrializing Nations and What's the Role of IE in Developing Countries?**
  (*Marian Chertow* / Heinz Schandl / Vaclav Smil / Paty Romero Lankao)
- **What Is the Role for Scenario Analysis in Formulating and Evaluating Alternative Prospects for a Sustainable Future?**
  (*Yuichi Moriguchi* / Lisa Bohunovsky / Dale Rothman)
- **What Is the Role for LCA in Informing the Policy Makers Given the Complexity of Socio-economic and Technological Interactions?**
  (*Greg Keoleian* / Thomas Ekvall / Anne-Marie Tilman)
- **Are There Sustainable Trajectories that Meet Growing Consumption Needs?**
  (Julia Steinberger / Marina Fischer Kowalski)
- **How Do We Address the Rebound Effect When Promoting Efficiency?**
  (*Roland Clift* / Walter Stahel / Steve Sorrell / Tim Gutowski)
- **What Is the Role of Industrial Ecology in Addressing Global Sustainability Imperatives?**
  (*Reid Lifset* / Edgar Hertwich / Valerie Thomas / Shinichiro Nakamura)

Industrial Ecology
Jun 16-17, 2012
Chair: James Kallaos
Associate Chair: Katherine H. Rostkowski

INORGANIC CHEMISTRY

Inorganic Chemistry: New Challenges and Opportunities
Jun 17-22, 2012
University of New England, Biddeford, ME
Chair: Michael Heinekey
Vice Chair: Keith J. Watson

- **Keynote Presentation: Recent Successes and Challenges in Olefin Metathesis**
  (*Mike Heinekey* / Richard Schrock)
- **Catalysis**
  (*Nora Radu* / Karen Goldberg / Jeff Miller / Mike Gagne / Tong Ren)
- **Energy Applications**
  (*John Lockemeyer* / Daniel Gamelin / Amy Prieto / Larry Lewis)
- **Solid State Materials**
  (*Greg Girolami* / Peidong Yang / Andreas Stein / Greta Patzke / Sarah Stoll)
- **Heavy Elements**
  (*Dave Thorn* / Polly Arnold / Karsten Meyer / Al Sattelberger)
- **Chemistry of Main Group Elements**
  (*Greg Robinson* / Ian Manners / Doug Stephan / Francois Gabbai / Parisa Mehrkodavandi)
- **Coordination Chemistry**
  (*Bahram Moasser* / Pat Holland / Ted Betley / Christina Thomas)
- **Nanotechnology / Poster Presentations**
  (*Kun Wang* / Jillian Buriak / Delia Milliron)
- **Perspectives**
  (*Keith Watson* / Rich Eisenberg)

Inorganic Chemistry
Jun 16-17, 2012
Chair: Ryan E. Cowley
Associate Chair: Reena Rahi

INTERMEDIATE FILAMENTS

Cytoskeletal and Nucleoskeletal Filaments in Normal and Diseased Cells
Jun 17-22, 2012
Bates College, Lewiston, ME
Chair: Robert D. Goldman
Vice Chair: John E. Eriksson

- **The Nuclear Lamins, Chromatin and Nuclear Architecture**
  (*Yossi Gruenbaum* / Colin Stewart / Maria Eriksson / Jan Lammerding)
- **IFs of the Nervous System: Function and Aggregation in Neurodegenerative Diseases**
  (*Elly Hol* / Mala Rao / Harish Pant / Ron Liem / Janice Robertson / Jean-Pierre Julien / Albee Messing / Milos Pekny)
- **Regulation of Cytoskeletal IF Assembly**
  (*Masaki Inagaki* / Harald Herrmann / Rudolf Leube / Cecilia Sahlgren / Nam-on Ku)
- **Cytoskeletal IF Structure and Mechanical Properties**
  (*Ueli Aebi* / Peter Burkhard / Paul Janmey / Sarah Köster / Laurent Kreplak / Sergei Strelkov / David Weitz)
- **The Dynamic Properties of Cytoskeletal IF Systems**
  (*John Eriksson* / Gaudenz Danuser / Sandrine Etienne-Manneville / Volodya Gelfand / Omar Skalli)
- **The Nuclear Lamins in Development and Disease**
  (*Gisele Bonne* / Kan Cao / Steve Adam / Chris Hutchison / Howard Worman / Yixian Zheng)
- **Cytoskeletal IF in Healthy and Diseased Cells**
  (*Yassemi Capetanaki* / Gloria Conover / Brigit Lane / Thomas Magin / Natasha Snider)

- **IF Associated Proteins and Cytoskeletal Crosstalk** (*Roy Quinlan* / Joel Eyer / Jonathan Jones / Alexander Minin / Roland Foisner / Karen Ridge / Gerhard Wiche / Georg Weitzer)
- **Functions of Epithelial Keratins** (*Diana Toivola* / Milind Vaidya / Pavel Strnad / Pierre Coulombe)

Intermediate Filaments
Jun 16-17, 2012
Chair: Takeshi Shimi

NEW! INTRINSICALLY DISORDERED PROTEINS

Jul 8-13, 2012
Mount Snow Resort, West Dover, VT
Chairs: Rohit V. Pappu & Peter Tompa
Vice Chairs: Gary W. Daugdrill & M.Madan Babu

- **Keynote Presentations I** (*Madan Babu* / Keith Dunker / Julie Forman-Kay)
- **Transcriptional Regulation and DNA Binding** (Doug Barrick / Yaakov Levy / Timothy Lohman / Remy Loris)
- **IDPs in Signal Transduction** (Jane Dyson / Richard Kriwacki / Rama Ranganathan / Michael Rosen / Susan Taylor)
- **Phase Behavior, Molecular Recognition, and Evolution of IDPs** (*Régis Pomès* / Jianhan Chen / Kyou-Hoon Han / Sonia Longhi / Ben Schuler / Eugene Shakhnovich)
- **Proteolysis of IDPs and Impact on Proteostasis Networks** (*Jim Bardwell* / Ursula Jakob / Jeff Kelly / Yosef Shaul / Alan Tunnacliffe)
- **Emerging Technologies for Studying Conformational Heterogeneity** (Martin Blackledge / Ashok Deniz / Gerhard Hummer / Claus Seidel)
- **Functionally Relevant Self-Assembly and Disease-Related Mis-Assembly of IDPs** (*Sheena Radford* / David Eliezer / Susan Lindquist / Thomas Scheibel / Joel Schneider)
- **IDP Tagging, Trafficking, and Processing** (*Patricia Clark* / Anne Bertolotti / Yuh Min Chook / Andreas Matouschek)
- **Keynote Presentations II** (*Gary Daughdrill* / Vladimir Uversky / Alan Fersht)

ION CHANNELS

Jul 8-13, 2012
Mount Holyoke College, South Hadley, MA
Chair: William R. Kobertz
Vice Chair: Colin G. Nichols

- **Data Blitz and Calcium Channels** (*Henry Colecraft* / David Clapham / David Yue)
- **Cardiac Channels** (*Andrea Brueggemann* / Gail Robertson / Nicole Schmidt)
- **Ligand-dependent Gating** (*Fran Ashcroft* / Mike Francis / Visanthi Jayarama / Mark Mayer)
- **Sodium Channels** (*Dick Horn* / Cecilia Canessa / Todd Scheuer / Bonnie Wallace)
- **Proton and Anion Channels** (*Michael Pusch* / Yuri Kirichok / Emily Liman / Merritt Maduke)
- **Permeation and Modulation** (*Clay Armstrong* / Wompil Im / Benoit Roux / Steve Brohawn)
- **Gating (Other)** (*Chris Miller* / Chris Ahern / Crina Nimigean)
- **Potassium Channels** (*Cathy Morris* / Blanche Schwappach / Stephen Tucker / Paul Slesinger)
- **Calcium Signaling** (*Alan Finkelstein* / Ilya Bezprozvanny / Anna Greka)

Ion Channels
Jul 7-8, 2012
Chair: Nazzareno D'Avanzo
Associate Chair: Maen F. Sarhan

IRON-SULFUR ENZYMES

Jun 10-15, 2012
Mount Holyoke College, South Hadley, MA
Chair: Tracey Rouault
Vice Chair: Markus Ribbe

- **Bacterial Iron Sulfur Cluster Synthesis and Origin of Life Theories** (*Richard Holm* / Dennis Dean / William Martin)
- **Mechanisms of Iron Sulfur Enzymes** (*Lance Seefeldt* / Fraser Armstrong / Brian Hoffman / Amie Boal / Joe Jarrett / Yilin Hu)
- **Biosynthesis of Complex Metal-Containing Cofactors** (*Markus Ribbe* / Yuichi Fujita / Silke Leimkuhler)
- **Basic Iron Sulfur Cluster Assembly** (*Wayne Outten* / Patricia Dos Santos / Andrew Dancis / Sandrine de Ollagnier de Choudens / Enrique Herrero / Marc Fontecave)
- **Iron Sulfur Proteins in Regulation** (*Juan Fontecilla-Camps* / Patricia Kiley / Nick Le Brun / Nicholas Rouhier)
- **Iron Sulfur Cluster Biogenesis and Human Disease** (*Paul Lindahl* / David Barondeau / Jessie Cameron / Elena Tucker / Dan Crooks)
- **Theory and Models of Complex Iron-Sulfur Clusters** (*Christopher Pickett* / Kazuyuki Tatsumi / Jonas Peters)
- **Crosstalk With Other Metals in Nature** (*Ralf Mendel* / Günther Schwarz / Russ Hille / Oliver Einsle / Wolfgang Buckel)
- **New Horizons of Iron-Sulfur Enzymes** (*Mike Johnson* / Joanne Stubbe / Barbel Friedrich)

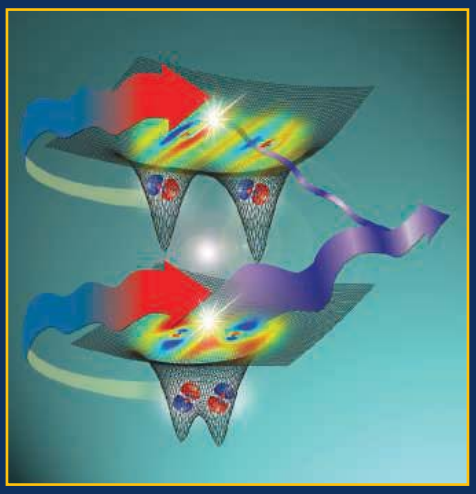

In high harmonic spectroscopy, an intense femtosecond laser removes an electron from a molecule and then drives the electron back, leading to emission of an attosecond burst of light. If a bromine molecule is dissociating, there are two possible quantum mechanical pathways. This leads to an interference in the attosecond emission that provides an image of the atoms as they come apart. Courtesy of Helene Letourneaux, National Research Council, Canada. Submitted by David Villeneuve, Chair, Multiphoton Processes GRC.

LASERS IN MEDICINE & BIOLOGY
Towards Molecular Imaging In Vivo

Jul 22-27, 2012
Holderness School, Holderness, NH
Chairs: Brian W. Pogue & Rudolf M. Verdaasdonk
Vice Chairs: Stephen A. Boppart & Arjen Amelink

- **Molecular-Guided Surgery** (*Brian C. Wilson* / John Frangioni / Vasilis Ntziachristos)
- **Molecular Imaging Agents** (*Tayyaba Hasan* / Sam Achilefu / Hisataka Kobayashi / Clemens Lowik)
- **Optical Coherence Tomography** (*Xingde Li* / Johannes DeBoer / Brett Bouma / Wolfgang Drexler)
- **Gastroenterology** (*Sharon L. Thomsen* / Thomas Suteja / Thomas D. Wang / Vadim Backman)
- **Neurons** (*Duco Jansen* / Anita Mahadevan-Jansen / Brian Bacskai / Karl Disseroth)
- **Diffuse Spectroscopy & Imaging** (*Bruce Tromberg* / Mark Brenner / Nimi Ramanumam / Maurice Aalders)
- **Photoacoustic Imaging** (*Lihong Wang* / Qing Zhu / Martin Frenz / Daniel Razansky)
- **Microscopic Molecular Imaging** (*Charles Lin* / Paul Selvin / Irene Georgakoudi / Daniel Cote)
- **Commercial Translation of Optical Technologies** (*Brad Rice* / Stefan Fry / David Benaron / Saivash Yazdanfar)

LIPOPROTEIN METABOLISM

Jun 17-22, 2012
Waterville Valley Resort, Waterville Valley, NH
Chair: Robert O. Ryan
Vice Chairs: Robert V. Farese & Joachim J. Herz

- **The Control of Lipolysis in Plasma** (*Stephen G. Young* / Ira Goldberg / Gunilla Olivecrona / Murray Huff)
- **Regulation of Cholesterol Homeostasis** (*Jay Horton* / Margrit Schwarz / Kathryn J. Moore / Peter Tontonoz / Marisa Wong Medina / Russell Debose-Boyd)
- **High-density Lipoprotein: Impact of Particle Diversity** (*Mary Sorci-Thomas* / Sean Davidson / Jay Heinecke / Daisy Sahoo)
- **Apolipoprotein B and TG Rich Lipoprotein Assembly** (*Henry Ginsberg* / Zemin Yao / Edward Fisher / Gregory Shelness)
- **Expanding Functions of LDL Receptor Family Members** (*Joachim Herz* / Bart Williams / Petra May)
- **Cholesterol Efflux, ABC Transporters and Disease** (*Yves Marcel* / Alan Tall / John Parks / Cheryl Wellington / Ira Tabas)
- **Advances in Therapy to Treat Cardiovascular Disease** (*Daniel J. Rader* / Andrew S. Plump / Roger Newton)
- **Intracellular Lipid Transport and Lipid Droplet Biology** (*Robert Farese, Jr.* / Tobias Walther / Jean Schaffer / Meng Wang)
- **State of the Art: Genomics, Proteomics and Metabolomics** (*Philippa Talmud* / Robert Hegele / Christopher R. McMaster / Chris Newgard)

Lipoprotein Metabolism
Jun 16-17, 2012
Chair: Mistuni Ghosh

LYSOSOMES & ENDOCYTOSIS
Jun 17-22, 2012
Proctor Academy, Andover, NH
Chair: Michael Marks
Vice Chair: Beverly Wendland

- **Endosomes, Lysosomes and Autophagy in Development**
  (*Lois Weisman* / Andrea Ballabio / Linton Traub / Henrik Korswagen)
- **Endosome Maturation**
  (*Mark van Zostrow, Christian Ungermann* / David Katzmann / Sylvie Urbé / Juan Bonifacino / Christopher Burd)
- **Endosomes and Lysosomes in Diabetes and Metabolism**
  (*Timothy McGraw* / Debby Thurmond / Susanna Keller / Elina Ikonen)
- **Endocytic Mechanisms**
  (*Sandy Schmid, Alexander Sorkin* / Julie Donaldson / Tom Kirchhausen / Frances Brodsky / Marino Zerial)
- **Phagocytosis and Host-Pathogen Interactions**
  (*Sergio Grinstein, Pascale Cossart* / Craig Roy / Rafael Valdivia / Olivier Neyrolles)
- **Lysosomes and Lysosome-Related Organelles**
  (*Miguel Seabra, J. Paul Luzio* / Victor Faundez / Graça Raposo / Clare Futter / Judith Klumperman)
- **New Directions**
  (*Beverly Wendland* / Roberto Weigert / Hiroshi Ohno)
- **Lysosomal Transport and Immune Function**
  (*Jacques Neefjes, Jennifer Stow* / Hidde Ploegh / Genevieve de Saint Basile / Gillian Griffiths / Willem Stoorvogel)
- **Keynote Presentation: Lipid Trafficking in the Endosomal System**
  (*Michael Marks* / Frederick Maxfield)

Lysosomes & Endocytosis
Jun 16-17, 2012
Chair: Derek C. Prosser
Associate Chair: Brenda Watt

MAMMARY GLAND BIOLOGY
Jun 10-15, 2012
Il Ciocco Tuscany Resort, Lucca (Barga), Italy
Chair: Matthew J. Smalley
Vice Chairs: Terri L. Wood & John J. Wysolmerski

- **Opening Presentation: Driving Translational Research with Basic Biology**
  (Alan Ashworth)
- **The Cellular Origins of Breast Cancer**
  (*Yi Li* / Eldad Zacksenhaus / Jose Moreira / Alexandra Pietersen)
- **Cellular Interactions in the Mammary Gland and Their Disruption in Cancer**
  (*Keith Brennan* / Patrick Derksen / Kristina Trujillo / Walid Khaled)
- **Pre-Pubertal Development**
  (*Beatrice Howard* / Marja Mikkola / Ann Ramsdell)
- **Post-Pubertal Development**
  (*Rob Clarke* / Paul Lu / Isabelle Miletich)
- **Pregnancy**
  (*Terri Wood* / Mohamed Bentires-Alj / Lothar Hennighausen / Joe Jerry)
- **Lactation**
  (*John Wysolmerski* / Evelyne Meyer / Rosa Serra)
- **Involution**
  (*Christine Watson* / Richard Clarkson)
- **Keynote Presentation**
  (*Matt Smalley* / Cathrin Brisken)

Mammary Gland Biology
Jun 9-10, 2012
Chair: Laura L. Hernandez
Associate Chair: Kristina A. Trujillo

MARINE MICROBES
Bridging the Gaps from Genomes to Biomes
Jun 24-29, 2012
Il Ciocco Tuscany Resort, Lucca (Barga), Italy
Chair: Raffaella Casotti
Vice Chair: Gabrielle Rocap

- **Perspectives in Marine Microbial Biology and Ecology**
  (*Gabrielle Rocap* / Ginger Armbrust / Carlos Pedros-Aliò)
- **Ecological Genomics**
  (*Mary Ann Moran* / Jeroen Raes / Steve Hallam / Mak Saito)
- **Debate I: The Impact of 'omics in the Field of Marine Microbes**
  (*Thomas Mock* / Jed Fuhrman / Jack Gilbert)
- **Microbes Embedded in the Environment**
  (*Jim Mitchell* / Roman Stocker / Matthias Ullrich / Rachel Foster)
- **Functional Interactions**
  (*Lisa Campbell* / Nicole Dubilier / Alison Taylor)
- **Life in Extreme Environments**
  (*Antje Boetius* / Katrina Edwards / Jan Pawloski / Alexander M. Anesio)
- **Debate II: Molecular Evolution and Endosymbiosis of Microbes**
  (*Martin T. Embley* / John Archibald / William Martin)
- **Microbial Ecology**
  (*Ramon Massana* / Mya Breitbart / Paul Berube / José Montoya)
- **Marine Microbes Powering the Future**
  (*Bruce Rittmann* / Ken Nealson / René Wijffels)

Marine Microbes
Jun 23-24, 2012
Chair: Jill A. Sohm

MECHANISMS OF EPILEPSY & NEURONAL SYNCHRONIZATION
Reorganization in the Epileptic Brain
Aug 19-24, 2012
Waterville Valley Resort, Waterville Valley, NH
Chair: Carolyn R. Houser
Vice Chairs: Jack Parent & Scott C. Baraban

- **Challenges for Epilepsy Research**
  (*David Prince* / Daniel Lowenstein / Istvan Mody)
- **Epileptogenesis: Can We Prevent It?**
  (*Douglas Coulter* / Asla Pitkänen / Tallie Baram / James McNamara / Pico Caroni)
- **Seizure Generation: Where do Seizures Begin and How Do They Spread?**
  (*Christophe Bernard* / Brian Litt / Gilles Huberfeld / Sydney Cash)
- **Circuit Analysis in Epilepsy with Optogenetics: Lighting Up a Darkened Brain**
  (*Helen Scharfman* / Karl Deisseroth / Ivan Soltesz / John Huguenard / Jin Lee)
- **Network Dynamics in Epilepsy: Novel Approaches for Dissecting the Networks**
  (*John Hablitz* / Rosa Cossart / Edward Callaway / Andrew Trevelyan)
- **Interneuron Reorganization in Epilepsy: How Many Changes Can We Find?**
  (*Monique Esclapez* / Gord Fishell / Dimitri Kullmann / Chris McBain / Paul Buckmaster)
- **Multiple Ways of Altering Excitability in Epilepsy: What Can be Targeted?**
  (*Manisha Patel* / Kevin Staley / Gary Yellen / Dane Chetkovich)
- **Developmental Epilepsies and Co-Morbidities: Are There Common Mechanisms?**
  (*John Swann* / Amy Brooks-Kayal / Peter Crino / Massimo Mantegazza / Farah Lubin)
- **Channel Reorganization in the Epileptic Brain: Do the Genetics Suggest Targets?**
  (*Jaideep Kapur* / Samuel Berkovic / Robert Macdonald / Jeffrey Noebels)

MEDICINAL CHEMISTRY
Aug 5-10, 2012
Colby-Sawyer College, New London, NH
Chair: Amy Ripka
Vice Chair: Mark A. Murcko

- **Rule-Breaker Molecules**
  (*Carl Decicco* / Nick Terrett / Julio Camarero / Percy Carter)
- **Covalent Drugs**
  (*Mark Noe* / Juswinder Singh / Wei Chen / Jack Taunton / Amy Dounay)
- **Recent Approaches to Cardiovascular Disease**
  (*Andrew Stamford* / Julien Papillon / Sven Ruf / Scott Priestly)
- **Metabolic Targets in Cancer**
  (*Janeta Popovici-Muller* / Matthew Vander Heiden / Jeff Saunders / Cindy Parrish / Richard Ward)
- **Challenges and Successes in Diabetes Discovery**
  (*Scott Edmondson* / David Moller / Philip Hipskind / William Hagmann)
- **Epigenetics**
  (*Silvana Leit* / Manfred Jung / Brian Albrecht / John Tatlock / Chun-Wa Chung)
- **Allosteric Drugs**
  (*Peter Bernstein* / Scott Kudak / Chantal Alcouffe / Jeff Conn)
- **Late-Breaking Presentations**
  (*J.C. Harmange* / Gabriel Martinez / Kim Cameron / Percy Carter / Tesfaye Biftu)
- **Keynote Presentation**
  (*Amy Ripka* / John Martin)

MEIOSIS
Jun 3-8, 2012
Colby-Sawyer College, New London, NH
Chair: Nancy M. Hollingsworth
Vice Chair: Gregory P. Copenhaver

- **The Initiation of Meiotic Recombination**
  (*Michael Lichten* / Maria Jasin / Scott Keeney / Rita Cha / Galina Petukhova)
- **Mechanisms of Meiotic Recombination I**
  (*Akira Shinohara* / Doug Bishop / Simon Boulton / Gerry Smith / Michael Lichten / Neil Hunter / Mathilde Grelon / Valerie Borde)
- **Mechanisms of Meiotic Recombination II**
  (*Scott Keeney* / Greg Copenhaver / Nancy Kleckner / Jeff Sekelsky / Peter Schlogelhofer / Franz Klein)
- **Homolog Pairing and Synapsis**
  (*Barbara Meyer* / Yasushi Hiraoka / Monique Zetka / Denise Zickler / Abby Dernberg)
- **Meiosis and Evolution**
  (*Anne Villenueve* / Peter Baumann / John Logsdon)
- **Meiotic Checkpoints and Cell Cycle Progression**
  (*Abby Dernberg* / Angelika Amon / Masayuki Yamamoto / Wolfgang Zachariae / Paula Cohen / Soni Lacefield / James Turner)
- **Chromosome Dynamics**
  (*Angelika Amon* / Anne Villenueve / Akira Shinohara / Michael Dresser / Sean Burgess)
- **Chromosome Segregation I**
  (*Julia Cooper* / Yoshinori Watanabe / Scott Hawley / Katja Wassmann / Barbara Meyer / Tatsuya Hirano / Simon Chan)
- **Chromosome Segregation II**
  (*Jeff Sekelsky* / Rolf Jessberger / Kikue Tachibana-Konwalski / Julia Cooper)

Meiosis
Jun 2-3, 2012
Chair: Michael Klutstein
Associate Chair: Ofer Rog

Gordon Research Conferences: "Session II" 2012 Preliminary Programs (continued)

MEMBRANE TRANSPORT PROTEINS
Jul 1-6, 2012
Les Diablerets Conference Center, Switzerland
Chair: Robert Edwards
Vice Chair: Poul Nissen

- **Neurotransmitter Transporters**
  (*Jonathan Javitch* / Aurelio Galli / Ulrik Gether / Baruch Kanner)
- **Structure I**
  (*Poul Nissen* / Raimund Dutzler / Daniela Stock / Da-Neng Wang / Ming Zhou)
- **Plant Transporters**
  (*Randy Blakely* / Jiri Friml / Wolf Frommer / Angus Murphy / Greg Vert)
- **Structure II**
  (*Robert Tampe* / Kaspar Locher / Doug Rees / Dirk Slotboom / Robert Stroud / Christine Ziegler)
- **Mitochondria**
  (*Baruch Kanner* / James Chou / Yuriy Kirichok / Edmund Kunji)
- **Metal Transporters**
  (*Jeff Rothstein* / Jose Arguello / Dax Fu / Svetlana Lutsenko / Edward Yu)
- **Cell Biology**
  (*Robert Edwards* / Frances Brodsky / Sergio Grinstein / John Orlowski / Rajini Rao)
- **Neuroscience**
  (*Yuriy Kirichok* / Randy Blakely / Thomas Jentsch / Deborah Nelson / Shimon Schuldiner)
- **Keynote Presentation**
  (*Robert Edwards* / William Catterall)

MEMBRANES: MATERIALS & PROCESSES
Jul 29 - Aug 3, 2012
Colby-Sawyer College, New London, NH
Chairs: Eric S. Peterson, Nieck E. Benes & Frederick Stewart
Vice Chairs: Bruce J. Hinds & Klaus-V Peinemann

- **Current Applications of Artificial Membranes**
  (*Klaus Viktor Peinemann* / Matthias Wessling)
- **Gas Separations: The Upper Bound and Beyond**
  (*Keith Murphy* / Lloyd Robeson / Ed Cussler / Ingo Pinnau)
- **Membrane Characterization Techniques**
  (*Anita Hill* / Danielle Kennedy / Majiec Haranczyk)
- **Membranes for Water Treatment**
  Ramesh Bhave / Jeffrey McCutcheon / Rong Wang / Craig Bartels)
- **Membranes in Medical Applications**
  (*Jamie Hestekin* / Andrew Zydney / Shelly Minteer / Roger Narayan)
- **New Membrane Structures and Biologically-Based Artificially Membranes**
  (*Mihai Barboiu* / Bruce Hinds / Tom Fyles / Manish Kumar)
- **Molecular Simulation and Modeling**
  (*David Brown* / Sylvie J. Neyertz / James A. Elliott)
- **Membrane Materials**
  (*Dibakar Bhattacharyya* / Andrew Livingston / Merlin Bruening / Georges Belfort)
- **Membranes, Energy, and the Future**
  (*Bill Koros* / Rob Lammertink / Paul Bryan)

Membranes: Materials & Processes
Jul 28-29, 2012
Chair: Michelle Marincel Payne

METABOLIC BASIS OF ECOLOGY
The Metabolic Basis of Ecology and Evolution in a Changing World
Jul 22-27, 2012
University of New England, Biddeford, ME
Chairs: James J. Elser & Melanie E. Moses
Vice Chairs: Andrew Clarke & Morgan Ernest

- **Current Status of Metabolic Ecology & Global Change Science**
  (*Melanie Moses* / Richard Sibly / Simon Levin)
- **Metabolic Ecology of Molecules, Cells, and Organisms**
  (*Michael Angiletta* / Graham Bell / Chen Hou / Fariba Asada Porter / Ross Carlson / David Raubenheimer)
- **Global Change and Metabolic Impacts on Molecules, Cells, and Organisms**
  (*Sue Kilham* / Warren Porter / John Sperry)
- **Metabolic Ecology in Populations and Communities**
  (*Joel Kingsolver* / Anna Joles / Rana El-Sabaawi / Jon Shik / Blake Matthews / Annette Ostling)
- **Global Change & Metabolic Impacts on Populations & Communities**
  (Amy Rosemond / Pablo Marquet / Nils Chr. Stenseth)
- **Metabolic Ecology in Communities and Ecosystems**
  (*John Schade* / Cathy Pringle / Angelica Gonzalez / Ethan White / Helmut Hillebrand)
- **Global Change & Metabolic Impacts on Communities and Ecosystems**
  (*Morgan Ernst* / Kiona Ogle / Kristina Anderson Teixeira)
- **Metabolic Ecology in Landscape, Regions, and the Biosphere**
  (*Jim Elser* / Felisa Smith / Marcus Hamilton / Mike Hartfoot / Lauren Buckley / Sharon Hall)
- **Global Change & Metabolic Impacts at Landscape, Regional, & Global Scales**
  (*Robert Sterner* / Nancy Knowlton / Josep Penuelas / Robert Sterner)

Metabolic Basis of Ecology
Jul 21-22, 2012
Chair: April J. Hayward
Associate Chair: James C. Stegen

METALS IN MEDICINE
Jun 24-29, 2012
Proctor Academy, Andover, NH
Chairs: A. Dean Sherry & Susan J. Berners-Price
Vice Chairs: Alan B. Packard & Michael J. Hannon

- **Keynote Presentations: Discovery and Translation of Metal-based Drugs**
  (*Susan Berners-Price* / Nick Farrell / Peter Sadler)
- **Imaging From Cells to Animals to Humans**
  (*Dean Sherry* / Angelique Louie / Matthew Allen / Belinda Seto / Jennifer West)
- **Pt & Non-Pt Anticancer Compounds: New Strategies for Old Problems**
  (*Nick Farrell* / Enzo Alessio / Zijian Guo / Eric Meggers)
- **Copper & Zinc in Physiology & Disease**
  (*Chris Chang* / Tom O'Halloran / Mi Hee Lim / Elizabeth Nolan / Ashley Bush)
- **Coordinating Copper: Applications in Wilson's Disease, Cancer & Alzheimer's**
  (*Kathy Franz* / Pascale Delangle / Luciano Marchio / Peter Faller)
- **Metalloproteins as Medicinal Targets**
  (*Peter Sadler* / Seth Cohen / Nour Neamati / Irit Sagi / Qizhuang Ye)
- **Iron Chemistry and Biochemistry in Disease**
  (*Jennifer Dubois* / Caroline Philpott / Barry Paw / Angela Wilks)
- **Metalloradiopharaceuticals**
  (*Alan Packard* / Zibo Li / Suzanne Lapi / John Valliant / Helmut Maake)
- **Young Investigator Presentations: Metal Complexes in Disease**
  (*Mike Hannon* / Amy Barrios / Claudio Verani / Paul Donnelly)

MICROBIAL STRESS RESPONSE
Jul 15-20, 2012
Mount Holyoke College, South Hadley, MA
Chairs: Timothy J. Donohue & Susan Gottesman
Vice Chairs: Eduardo A. Groisman & Dianne K. Newman

- **Stressful Communications Within and Between Cells**
  (*Fred Neidhardt* / Bonnie Bassler / Carol Gross / Bonnie Bassler [Alexander M. Cruickshank Lecturer])
- **Living With and Without Oxygen**
  (*John Hellman* / Patricia Kiley / James Imlay)
- **Stress of Alternate Lifestyles**
  (*Diane Newman* / Eric Masse)
- **Stress Sensing: Logic for Signal Transduction**
  (*Michael Laub* / Mark Goulian)
- **Sensing Stress: Regulatory Networks and Post-transcriptional Responses**
  (*Regine Hengge* / Gisela Storz / Tom Silhavy)
- **Living With Others: Signals Controlling Microbe-Host Interactions**
  (*Eduardo Groisman* / Margaret McFall-Ngai / Malcolm Winkler / Thad Stappenbeck)
- **Living With Others: Stress in Microbial Communities**
  (*Terry Hwa* / Richard Losick / Saeed Tavazoie)
- **Bacteria; Hibernation/Persistence**
  (*Ned Ruby* / Karen Wassarman / Kenn Gerdes)
- **DNA Damage Control**
  (*Tania Baker* / Alan Grossman / Luciano Marraffini)

MICROBIAL TOXINS & PATHOGENICITY
Jul 8-13, 2012
Waterville Valley Resort, Waterville Valley, NH
Chair: Ralph R. Isberg
Vice Chair: Michele S. Swanson

- **Keynote Presentations: The Construction and Strategies of Pathogens**
  (Stanley Falkow / Gisou van Der Goot)
- **Mechanisms of Toxin Action**
  (*Klaus Aktories* / Karla Satchell / Steven Blanke / Juliane Bubeck Wardenburg / Thijn Brummelkamp)
- **Regulatory Mechanisms of Bacterial Pathogens**
  (William Navarre / Heran Darwin / Chris Sassetti)
- **Host-pathogen Interactions**
  (*Virginia Miller* / Eric Skaar / Andreas Baumler / Victor Torres / Joan Mecsas / Matt Waldor)
- **Genetic Variation in Pathogens**
  (*Howard Ochman* / H. Steven Seifert / Roy Kishony / Sebastien Gagneux)
- **Innate Immune Protection from Pathogens**
  (*Mary O'Riordan* / Daniel Portnoy / Lynda Stuart / Jeffery Dangl / Veit Hornung / Russell Vance)
- **Microbiome in Health and Disease**
  (*Lora Hooper* / Sarkis Mazmanian / Wendy Garrett / Eric Pamer)
- **Hijacking of Cell Function**
  (*Zhao-Qing Luo* / Craig Roy / Stephane Meresse / Christoph Dehio / Raphael Valdivia / GRS Speaker)
- **Opportunities and Pitfalls in Molecular Analysis of Pathogens**
  (B. Brett Finlay / Clifton Barry)

Microbial Toxins & Pathogenicity
Jul 7-8, 2012
Chair: Zachary D. Dalebroux
Associate Chair: Aimee L. Richard

MITOCHONDRIA & CHLOROPLASTS
Jul 29 - Aug 3, 2012
Bryant University, Smithfield, RI
Chair: Alice Barkan
Vice Chair: Luca Scorrano

- **Organelle Evolution and Inheritance**
  (*Ian Small* / Trevor Lithgow / Volker Knoop)

- **Biogenesis of Mitochondria and Chloroplasts** (*Francis-Andre Wollman* / Toshiharu Shikanai / Dennis Winge / Eva Mari Aro / Agnieszka Chacinska)
- **Organellar Genomes and Gene Expression** (*Tom Fox* / Francis-Andre Wollman / Miguel Garcia-Diaz / Laurie Kaguni / Christian Schmitz-Linneweber)
- **Organellar Signalling** (Joanne Chory / Michael Frohman / Rosario Rizzuto / Markus Schwarzlander)
- **Supramolecular Organization of Energy Transducing Membranes** (*Sabeeha Merchant* / Ziv Reich / Tonio Enriquez / Werner Kuehlbrandt)
- **Systems Biology and Proteomic Approaches** (Tom Brutnell / Chris Meisinger / Sabeeha Merchant / Vamsi Mootha)
- **Organelle Morphology and Dynamics** (*Jodi Nunnari* / Thomas Langer / Kathy Osteryoung / Gia Voeltz)
- **Organelles in Stress, Autophagy, and Homeostasis** (*Luca Scorrano* / Zach Adam / Jodi Nunnari / Nika Danial)
- **Role of Organelles in Disease and Aging** (Eric Schon / S. Dinesh-Kumar / Nils-Göran Larsson)

GRS **Mitochondria & Chloroplasts**
Jul 28-29, 2012
Chair: Kamel Hammani
Associate Chair: Carsten Merkwirth

MOLECULAR & CELLULAR NEUROBIOLOGY

Jun 17-22, 2012
Hong Kong University of Science & Technology, China
Chair: Lin Mei
Vice Chair: Eric J. Huang

- **Neuronal Polarity** (*Louis Reichardt* / Mike Ehlers / Nobutaka Hirokawa / Yi-Ping Hsueh / Zhenge Luo)
- **Molecular and Cellular Basis of Behavior** (Rick Huganir [keynote] / James Bibb / Bob Horvitz / Minmin Luo / Yi Rao)
- **Axon and Dendrite Development** (*James Zheng* / Hollis Cline / David Ginty / Liqun Luo)
- **Cellular Plasticity Mechanisms** (*Yizheng Wang* / Martha Constatine-Paton / Roger Nicoll / Shuming Duan / Katherine Roche / Christian Rosenmund)
- **Synapse Development** (*Rick Rotundo* / Michael Granato / Eunjoon Kim / Nancy Ip / Kuo-Fen Lee / Patricia Salinas / Vivian Budnik)
- **Regenerative Neuroscience** (Aaron Ciechanover [keynote] / Magdalena Goetz / Guo-Li Ming / Yoshiki Sasai)
- **Circuit Development and Function I** (Gordon Fishell / Oscar Marin / Gero Miesenbock)
- **Circuit Development and Function II** (John Rubenstein / Kang Shen / Mriganka Sur / Linda Wilbrecht)
- **Molecular Basis of Brain Disorders** (*Hongjun Song* / Robert Malenka [keynote] / Eric Huang / Kozo Kaibuchi / Bai Lu / Akira Sawa / Wen-Cheng Xiong)

GRS **Molecular & Cellular Neurobiology**
Jun 16-17, 2012
Chair: Ryan Bates
Associate Chair: Amy Kit-Yu Fu

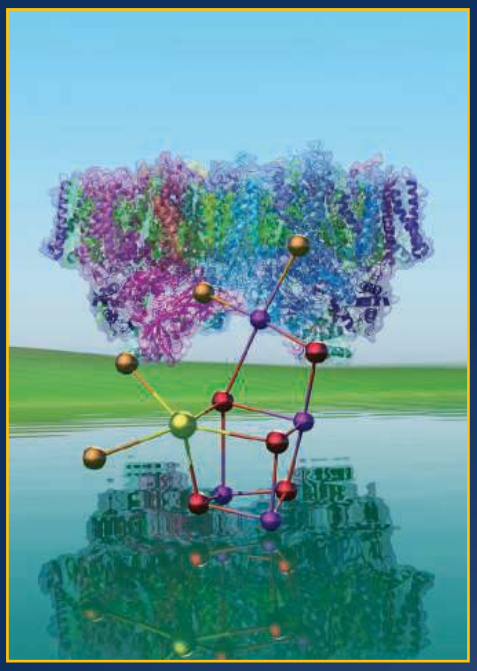

The oxygen-evolving $Mn_4CaO_5(H_2O)_4$ cluster of photosystem II (PSII) is closed up in front of the structure model of PSII dimer, newly determined at 1.9A resolution. The cluster is imaged as the heart of biological environment of the earth, sun light, blue sky, green field and natural water. Courtesy of Nobuo Kamiya, Osaka City University, Japan. Submitted by Richard J. Debus, Chair, Photosynthesis GRC.

MOLECULAR BASIS OF MICROBIAL ONE-CARBON METABOLISM

Aug 5-10, 2012
Bates College, Lewiston, ME
Chair: Julia Vorholt
Vice Chair: Thomas E. Hanson

- **Frontiers in Carbon Dioxide Fixation and Origin of Life** (*Bob Tabita* / Georg Fuchs / William Martin)
- **Novel Reactions and Pathways** (*Ivan Berg* / Mike Jetten / Sung Gyung Kang / William Whitman / Joseph Krzycki)
- **Enzyme Structure and Mechanism** (*Rolf Thauer* / Amy Rosenzweig / Squire Booker / Russ Hille)
- **Nickel Enzymes** (*Evert Duin* / Stephen Ragsdale / Seigo Shima / Catherine Drennan / Oliver Lenz)
- **Microbial Metabolism in Oxic Environments** (*Nicole Dubilier* / Colin Murrell / Marina Kalyuzhnaya / Jeremy Semrau)
- **Microbial Metabolism in Anoxic Environments** (*Harold Drake* / Ron Oremland / Vicky Orphan / Samantha Joye / Bernhard Schink)
- **Systems Perspectives** (*Chris Marx* / William Metcalf / Kathleen Scott / Daniel Segrè)
- **Chemical and Synthetic Biology** (*Sean Elliott* / Pamela Silver / Lance Seefeldt)
- **Biofuels** (*Volker Mueller* / Michael Koepke / Alfons Stams)

GRS **Molecular Basis of Microbial One-Carbon Metabolism**
Aug 4-5, 2012
Chair: Tobias J. Erb
Associate Chair: Katharina F. Ettwig

MULTIPHOTON PROCESSES
Attoseconds, Intense Fields, and Ultrafast Imaging

Jun 3-8, 2012
Mount Holyoke College, South Hadley, MA
Chair: David Villeneuve
Vice Chair: Barry C. Walker

- **Attosecond Electron Dynamics** (Mette Gaarde / Eleftherios Goulielmakis / Olga Smirnova)
- **Electron Dynamics** (Reinhard Dörner / Chris Greene / Matthias Kling)
- **ATI and Photoelectrons** (Peter Hommelhoff / Cosmin Blaga / Arnaud Rouzee)
- **Strong Fields and Sources** (François Légaré / Lars Madsen / Henry Kapteyn)
- **Free Electron Laser Experiments** (Li Fang / Nina Rohringer / Kiyoshi Ueda)
- **Imaging with X-rays** (Adam Hitchcock / John Spence)
- **High Harmonic Spectroscopy** (Markus Guehr / Caterina Vozzi / Chii-Dong Lin)
- **Photoionization Delay** (Claudio Cirelli / Marcus Dahlstrom / Martin Schultze)

MUSCLE: EXCITATION / CONTRACTION COUPLING

Jun 3-8, 2012
Les Diablerets Conference Center, Switzerland
Chairs: Francesco Zorzato & Paul D. Allen
Vice Chair: Robert T. Dirksen

- **Structure and Function of the Calcium Release Unit** (*Clara Franzini-Armostrong* / Simona Buoncompagni / Filip Van Petegem / James D. Fessenden)
- **Signal Transduction via Ryanodine Receptor, Dihydropiridine Receptor** (*Angela Dulhunty* / Kurt Beam / Werner Melzer / Vincent Jacquemond / Martin Schneider / Manfred Grabner)
- **Signaling via Accessory Proteins** (*Laszlo Csernoch* / Hiroshi Takeshima / Graham Lamb / Isabelle Marty)
- **Cardiac RyR in Health and Disease** (*Wayne Chen* / Ana Gomez / Anthony F. Lai / Sandor Gyorke / Rebecca Sitsapesan / Silvia Priori)
- **Cardiac EC Coupling** (*Hector Valdivia* / Karin Sipido / Nina Ullrich / Henry M. Colecraft)
- **Muscle Fatigue, Ageing and Repair** (*Christopher W. Ward* / Osvaldo Delbono / Jianjie Ma / Hakan Westerblad / Oliver Friedrick / David Allen)
- **Ryanodine Receptor Calcium Release Channel Regulation: the RNS/ROS Connection** (*Gerhard Meissner* / Paulina Donoso / Isaac Pessah / George G. Rodney)
- **Excitation Contraction Coupling Macromolecular Complex Related Disorders: From Molecules to Clinical Trials** (*Francesco Muntoni* / Bjorn C. Knollmann / Andrew R. Marks / Heinz Jungbluth / Steve Cannon / Susan Hamilton)
- **Round Table Discussion: New Tools to Probe Signaling in Striated Muscle** (*Eduardo Rios* / Eduardo Rios / Heping Cheng / Julio Vergara / Phillip Sasse)

MUSCULOSKELETAL BIOLOGY & BIOENGINEERING
Musculoskeletal Science: Bedside to Bench to Bedside

Aug 5-10, 2012
Proctor Academy, Andover, NH
Chair: Kurt Spindler
Vice Chair: Christopher H. Evans

- **Translational Studies on Enhancing Soft Tissue Healing** (*Martha M. Murray* / Kathleen Derwin / Joseph Iannotti / Helen Lu / William Levine / Richard Gelberman / Stavros Thomopoulos)

- **Functional Tissue Engineering**
  (*Lisa Fortier* / Wiltrud Richter / Gerjo van Osch / Jeremy Mao)
- **Knee Kinematics, Injury Prevention & Rehabilitation**
  (*Braden Fleming* / Timothy Hewett / Thomas Andriacchi / Lynn Snyder-Mackler / Scott Tashman / Louis DeFrate)
- **Mechanobiology**
  (*Robert Sah* / Gregory Jay / Jill Urban / Bob Mauck / Ed Guo)
- **Signaling and Regulation in Musculoskeletal Growth and Regeneration**
  (*Rocky Tuan* / Ben Alman / Miguel Torres / Susan Mackem)
- **Stem Cells in Health and Injury**
  (*Johnny Huard* / Jennifer Elisseeff)
- **Tendon Adhesions and End-to-End Healing**
  (*Peter Amadio* / Chunfeng Zhao / David Butler / Jin Bo Tang)
- **Biomarkers**
  (*Linda Sandell* / Francesco Dell'Accio / Yves Henrotin / Connie Chu)

MUTAGENESIS
A Delicate Balance: Cellular Mutation Pathways in Genetic Stability and Disease
Aug 19-24, 2012
Salve Regina University, Newport, RI
Chair: Bruce Demple
Vice Chair: Robert Lahue

- **Keynote Presentations**
  (Thomas A. Kunkel / Titia de Lange)
- **Branching Pathways in Mutagenesis**
  (*Robert P.P. Fuchs* / Roger Woodgate / Helle Ulrich / Josef Jiricny)
- **Oxidative Stress and Endogenous DNA Damage**
  (*Hilde Nilsen* / Paul Doetsch / David M. Wilson)
- **DNA Maintenance Pathways**
  (*Orlando Schärer* / Peter Burgers / John Tainer / Maria Falkenberg Gustafsson)
- **Recombinational Pathways, Good and Bad**
  (*Maria Jasin* / Dale Ramsden / Simon Boulton)
- **Problematic DNA Structures**
  (*Robert Lahue* / Nancy Maizels / Catherine Freudenreich / Karen Vasquez)
- **Hypermutation in the Microbial World**
  (*Jeffrey H. Miller* / Sue Lovett / Sue Jinks-Robertson)
- **Tissue-Specific and Aging-Related Mutagenesis**
  (*Christi Walter* / Myron F. Goodman / Diane Cabelof / Keith Caldecott)
- **Mutation and Disease**
  (*Lawrence A. Loeb* / Maria Blasco / Paul Modrich)

NANOSTRUCTURE FABRICATION
Jul 15-20, 2012
University of New England, Biddeford, ME
Chair: Mark A. Reed
Vice Chair: Charles T. Black

- **Perspectives on Nanofabrication and Nanodevices**
  (*Mark Reed*)
- **NanoPhotonics and Plasmonics**
  (Hong Tang)
- **Advanced Nanodevices and Concepts**
- **Nanobiology**
  (*Harold Craighead* / Oliver Schmidt / Amit Meller)
- **Novel Nanomaterials**
  (*John Randall* / Karl Berggren / Erik Bakkers)
- **To the 22nm Node and Beyond**
- **Science and the Public**
- **Nanostructures for Energy**
  (*George Maracas* / Yi Cui / Mark Brongersma / Tom Picreaux)
- **Poster Presentations**
  (*Charles Black*)

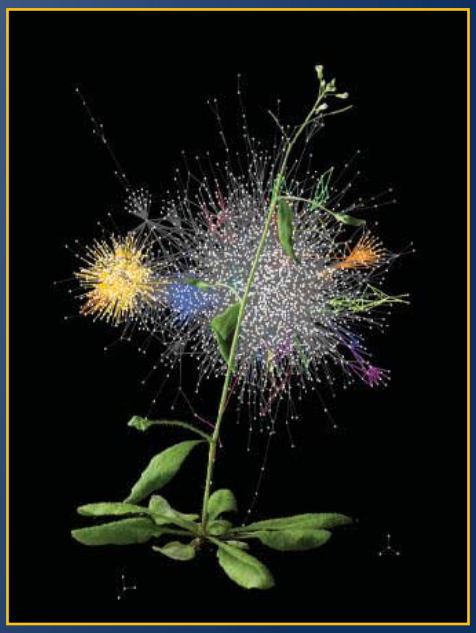

A flowering Arabidopsis thaliana plant overlaid on network map of over 6,000 protein:protein interactions (Arabidopsis Interactome Mapping Consortium. Science. 2011 333:601-607). The clusters of colors represent "communities" of interacting proteins that are enriched in specific plant processes. These data should help to enable biologists to make agricultural plants more resistant to drought and diseases and more nutritious. Photo credit: image (Joseph R. Ecker, HHMI-Salk Institute), plant (Joe Belcovson, Salk Institute), network map (Mary Galli, Salk Institute; Matija Dreze, Center for Cancer Systems Biology at the Dana-Farber Cancer Institute). Submitted by Michael R. Sussman, Chair, Plant Molecular Biology GRC.

NATURAL PRODUCTS
Jul 22-27, 2012
Proctor Academy, Andover, NH
Chair: Michael S. Van Nieuwenhze
Vice Chair: Rajinder Singh

- **Natural Product Synthesis and Applications to Chemical Biology**
  (Sergey Kozmin / Andrew Phillips)
- **Development and Application of Novel Methods for Natural Product Synthesis**
  (Tarek Sammakia / Richmond Sarpong / Glenn Micalizio)
- **Biosynthesis/Total Synthesis of Antibiotics**
  (Wilfred van der Donk / Dale Boger)
- **Biogenetic Inspired Synthesis of Natural Products**
  (Erik Sorensen / Mohammad Movassaghi / Robert Williams)
- **Discovery and Elucidation of Natural Product Biosynthetic Pathways**
  (Rebecca Goss / Ben Shen)
- **Natural Product Biosynthesis, Isolation, and Structure Determination**
  (Amy Wright / Jon Clardy / Dean Tantillo)
- **Use of Metal-mediated Methods in Natural Products Synthesis**
  (Huw Davies / Neil Garg / John Wolfe / Vy Dong)
- **Novel Synthetic Methods for Natural Product Synthesis**
  (Dan Romo / Chris Vanderwal / Matthias Christmann)
- **Chemical Synthesis of Complex Natural Products**
  (David Williams / John Wood)

NEURAL DEVELOPMENT
Aug 12-17, 2012
Salve Regina University, Newport, RI
Chair: Franck Polleux
Vice Chair: Fiona Doetsch

- **Keynote Presentations**
  (Huda Zoghbi / David Ginty)
- **Neurogenesis and Brain Patterning**
  (Wieland Huttner / Song-Hai Shi / Andrea Brand / Kenneth Campbell / Maria Lethinen)
- **Cell Type Specification**
  (Marc Freeman / Paola Arlotta / Hynek Wichterle / Yasushi Nakagawa)
- **Neural Stem Cells**
  (Yoshiki Sasai / Stewart Anderson / Marius Wernig / Guo-Li Ming)
- **Neuronal Migration and Morphogenesis**
  (Oscar Marin / Francois Guillemot / Kang Shen)
- **Wiring the Nervous System I**
  (Maya Shelly / William Harris / Dietmar Schmucker / Christine Holt / Alex Kolodkin)
- **Wiring the Nervous System II**
  (Josh Sanes / Linda Van Aelst / Wes Gruber)
- **Synaptogenesis and Circuit Formation**
  (Silvia Arber / Kim McAllister / Cagla Eroglu / Andrew Huberman)
- **Human Brain Evolution**
  (Evan Eichler / Pierre Vanderhaeghen / Arnold Kriegstein)

NEW! NEUROBIOLOGY OF BRAIN DISORDERS
Synaptic Dysfunction and Neurodegeneration
Aug 5-10, 2012
Stonehill College, Easton, MA
Chair: Jie Shen
Vice Chair: Joachim J. Herz

- **Keynote Presentations: Molecular and Synaptic Mechanisms of Autism**
  (*Donald Price* / Tom Sudhof / Michael Greenberg)
- **Mechanisms of Neurodegenerative Dementia**
  (*Jie Shen* / Bart DeStrooper / Luciano D'Adamio / Guojun Bu)
- **RNA-binding Proteins in Brain Disorders**
  (Virginia Lee / Don Cleveland / Jennifer Darnell)
- **Autophagy in Neurodegenerative Disorders**
  (*Charleen Chu* / Keiji Tanaka / Ralph Nixon / David Rubinsztein / Junying Yuan)
- **Molecular Mechanisms of Neurodegeneration**
  (*Takeshi Iwatsubo* / Joachim Herz / Hui Zheng / Christian Haass)
- **Synaptic Dysfunction in Neurodegenerative Diseases**
  (*Robert Malenka* / Harry Orr / David Sulzer / Riqiang Yan / Roberto Malinow)
- **Mitochondria and Neurodegeneration**
  (*Asa Abeliovich* / Richard Youle)
- **Pathophysiology of Autistic Disorders**
  (*Suzanne Zukin* / Mark Bear / Chris Walsh / Ray Kelleher)
- **Protein Misfolding and Aggregation in Neurodegeneration**
  (*Ted Dawson* / Greg Petsko / John Trojanowski / Susan Ackerman)

NEW! NEUROBIOLOGY OF COGNITION
Jul 8-13, 2012
Il Ciocco Tuscany Resort, Lucca (Barga), Italy
Chair: Carol A. Barnes
Vice Chair: Charles E. Schroeder

- **Oscillations: How Do They Contribute to Cognition?**
  (*Robert Desimone* / Wolf Singer [keynote] / Jessica Cardin)
- **Active Sensing**
  (*Charles Schroeder* / Robert Desimone / Marc Sommer / David Kleinfeld / Christoph Kayser)

- **Systems Connections**
  (*Earl Miller* / Pascal Fries / Stephanie Clarke / Olaf Sporns)
- **Temporal Lobe Memory**
  (*John O'Keefe* / May-Britt Moser / David Redish / Jill Leutgeb / Eleanor Maguire)
- **Aging Circuits**
  (*Lynn Nadel* / Scott Small / Mark D'Esposito / Cheryl Aine)
- **Decision Making**
  (*Tatiana Pasternak* / Daeyeol Lee / Trevor Robbins / Leslie Fellows / Xiao-Jing Wang)
- **Molecular Tools for Circuit Manipulation**
  (*Edvard Moser* / Karl Deisseroth [keynote] / Ehud Isacoff)
- **Social Cognition**
  (*Aina Puce* / Rebecca Saxe / Ralph Adolphs / Michael Platt)
- **Molecular Genetics and Disease**
  (*Robert Knight* / Dan Geschwind / Alcino Silva)

NEW! NOBLE METAL NANOPARTICLES

Jun 17-22, 2012
Mount Holyoke College, South Hadley, MA
Chair: Michael J. Natan
Vice Chair: Francesco Stellacci

- **Assemblies**
  (*Laura Fabris* / Christine Keating / Eugenia Kumacheva / So-Jung Park)
- **Plasmonics**
  (*Lilin Tay* / Naomi Halas / Harry Atwater / Teri Odom / Kallie Willetts)
- **Clusters**
  (*Royce Murray* / Thalappil Pradeep / Olga Lopez-Acevedo / Tatsuya Tsukuda)
- **Biological Applications**
  (*Michael Natan* / Itamar Willner / Molly Stevens / Shad Thaxton / Qun Huo)
- **Synthesis and Function I**
  (*Cathy Murphy* / Paul Mulvaney / Sara Skrabalak / Vince Rotello)
- **Hot Topic Presentations**
  (*Francesco Stellacci* / Sandra Van Aert / Yadong Yin / Lasse Jensen / Elena Shevchenko / Zdravka Medarova / Harold Park)
- ***In Vivo* Imaging and Model Systems**
  (*Alex Wei* / Shuming Nie / Duncan Graham / Stanislav Emelianov)
- **Catalysis**
  (*James Cookson* / Graham Hutchings / Cynthia Friend / Sheng Dai / Edman Tsang)
- **Synthesis and Function II**
  (*Jill Millstone* / Peidong Yang / Jianfang Wang / Luis Liz-Marzan)

Noble Metal Nanoparticles
Jun 16-17, 2012
Chair: Emilie Ringe
Associate Chair: Randy P. Carney

NEW! NOTCH SIGNALING IN DEVELOPMENT, REGENERATION & DISEASE

Aug 12-17, 2012
Bates College, Lewiston, ME
Chair: Raphael Kopan
Vice Chair: Alain Israel

- **Life Around Notch**
  (*Rafi Kopan* / David Holtzman / Yuh-Nung Jan / Olivier Pourquie)
- **The Cell Biology of Notch Signaling**
  (*Francois Schweisguth* / Ryoichiro Kageyama / David Sprinzak / Hugo Bellen / Martin Baron / Thomas Vaccari / Gerry Weinmaster)
- **Notch in Vascular Biology**
  (Holger Gerhardt / Ralf Adams / Yoshiko Takahashi / Michael Potente)
- **Notch in Stem and Progenitor Cells**
  (*Anna Bigas* / Taka Maeda / Irma Conboy / Andy Groves / Ben Ohlstein / Tim Schedl / Paolo Dotto)
- **Regulating Notch Activity in Disease**
  (Chris Seibel / Gavin Thurston / Christy Fryer / Yibin Kang)
- **Immunology**
  (Shahin Raffi / Freddy Radtke / Ivan Maillard / Iannis Aifantis / Jon Aster)
- **Issues Arising Presentations**
  (*Alain Israel* / Alfonso Martinez Arias)
- **Transcription, Chromatin and Notch**
  (*Irv Bernstein* / Adolfo Ferrando / Warren Pear / Brad Bernstein / Sarah Bray / Jane Johnson)
- **Structural Analysis of Components in the Notch Signaling Pathway**
  (*Doug Barrick* / Rhett Kovall / Penny Handford / Pamela Stanley / Hamad Jafar-Nejad)

NEW! NOX FAMILY NADPH OXIDASES
NOX Biology and its Translation to Human Disease and Therapy

Jun 3-8, 2012
Waterville Valley Resort, Waterville Valley, NH
Chair: Robert A. Clark
Vice Chair: Ajay M. Shah

- **Cardiovascular Diseases and NOX Enzymes**
  (*Kathy Griendling* / Ajay Shah / Robin Davisson / Jonathan Lederer)
- **Impact of NOX-Mediated ROS Signaling on ER Function and Stress Responses**
  (*Francisco Laurindo* / Agnes Görlach / Lance Terada / Karen Block)
- **Calcium-activated NOX/DUOX Enzymes - Regulation and Function**
  (*Xavier DeDeken* / David Fulton / William Nauseef / Chris Kennedy)
- **NOX Isoforms and Injury Response Patterns in Lung, Liver, and Kidney**
  (*Erzsébet Ligeti* / Constance Barazzone / Nathalie Grandvaux / Jeffrey Barnes / David Brenner)
- **Insights from Non-mammalian NOXes - Plants, Flies, Worms, Fish, Exotics**
  (*David Lambeth* / Ron Mittler / Philpp Niethammer / Franck Fieschi)
- **Structure, Function, and Regulation of NOX Enzyme Systems**
  (*Edgar Pick* / Jamel El Benna / Marie-José Stasia / Radu Dan Rudic)
- **NOX-derived ROS, Insulin Signaling, and Diabetic Pathologies**
  (*Rhian Touyz* / Amina El Jamali / Tony Tiganis / Hanna Abboud)
- **NOX Inhibitors - Status of Drug Development and Disease Targets**
  (*Ralf Brandes* / Susan Smith / Philippe Wiesel / Leonard Rybak)
- **NOX Enzymes in the Nervous System**
  (*Karl-Heinz Krause* / Michelle Block / Stefania Schiavone / Costantino Iadecola)

Nox Family NADPH Oxidases
Jun 2-3, 2012
Chair: Siobhan M. Craige
Associate Chair: Hitesh M. Peshavariya

NEW! OCEANS & HUMAN HEALTH

Jun 3-8, 2012
University of New England, Biddeford, ME
Chairs: D. Jay Grimes & Tracy K. Collier
Vice Chair: Helena Solo-Gabriele

- **Near- and Far-term Forecasting**
  (*Jay Grimes, Tom Hutchinson* / Kathryn Sullivan)
- **Emerging Contaminants**
  (*John Stegeman* / Rainier Lohmann / Evan Ward / Kara Lavender Law / Larry Brand)
- **Omics I**
  (*Lorrie Backer* / Karen Nelson / Pam Morris)
- **Climate Change and Natural Disasters**
  (*Lora Fleming* / Rita Colwell / Michael Depledge / Andreas Knecht / Tracy Collier)
- **Omics II**
  (*Karen Nelson* / Ginger Armbrust / Bob Chapman)
- **Seafood**
  (*Tom Hutchinson* / Elaine Faustman / Nicholas Ralston / Phillip Lee / Jeff Lotz)
- **Deepwater Horizon**
  (*Jay Grimes* / Terry Hazen / Dale Sandler)
- **Fecal Indicators and Marine Pathogens**
  (*Ed Laws* / Al Dufour / Ali Boehm / Jackie Woods / Jim Oliver)
- **Communicating the Importance of Oceans and Human Health**
  (*Jay Grimes, Tom Hutchinson* / Kevin Wheeler / Michael Moore / Don Rice / Juli Trtanj / Fred Tyson)

Oceans & Human Health
Jun 2-3, 2012
Chair: John J. Doyle
Associate Chairs: Carrie E. Givens & Leslie Burdett Hart

ORGANIC GEOCHEMISTRY

Jul 29 - Aug 3, 2012
Holderness School, Holderness, NH
Chair: Timothy I. Eglinton
Vice Chair: Erdem Idiz

- **Thermogenic Hydrocarbons in the Contemporary Environment**
  (*David Hollander* / Richard Camilli / Florence Schubotz / John Kessler)
- **Carbon Source-to-Sink Systems through Time**
  (*Thomas Wagner* / Niels Hovius / Guillmette Menot / Valier Galy)
- **Organic-Inorganic Associations & Interactions**
  (*Erdem Idiz* / Yves Gelinas / Martin Kennedy)
- **Isotopes of Geomolecules**
  (*Katherine Freeman* / Alex Sessions / John Eiler / Richard Robins / Anitra Ingalls)
- **Organic Hydrogeochemistry**
  (*Nicholas Drenzek* / Yongchun Tang / Everett Salas)
- **Microbial Lifestyles & Molecular Legacies**
  (*Jaap Sinninghe Damste* / Helen Talbot / Laura Villanueva / Richard Pancost / Naohiko Ohkouchi)
- **Spatially-resolved Mass Spectrometry**
  (*Thorsten Dittmar* / Jutta Niggemann / Erik Tegelaar)
- **Gas in the Bowels (of the Earth)**
  (*Barbara Sherwood-Lollar* / Chris Ballentine / Anna Martini / Alexei Milkov)
- **Frontiers in Organic Geochemistry**
  (*Francien Peterse*)

Organic Geochemistry
Jul 28-29, 2012
Chair: Francien Peterse

Gordon Research Conferences: "Session II" 2012 Preliminary Programs (continued)

ORGANIC REACTIONS & PROCESSES
Jul 15-20, 2012
Bryant University, Smithfield, RI
Chairs: Scott M. Sieburth & Jean Suffert
Vice Chairs: Matthew M. Bio & Pascal Dube

- **Methodology & Complex Molecule Synthesis I** (*Michael Willis* / Marc Snapper / Phil Baran)
- **Organometallic Reactions** (*Gregory Cook* / Chisato Mukai / Cristina Nevado)
- **Organometallic Reactions & Industrial Processes I** (*Jimmy Wu* / Elizabeth Jarvo / John Limanto)
- **Drug Discovery and Carbohydrates** (*Shawn Walker* / Laurent Hennequin / Peter Seeberger)
- **Transition Metal Catalysts and Molecular Architecture I** (*Christopher Jeffrey* / Marc Taillefer / Hideki Yorimitsu)
- **Industrial Processes II** (*Catherine Faler* / Stefan Abele / David Walsh)
- **Transition Metal Catalysts and Molecular Architecture II** (*Jared Lewis* / Mikiko Sodeoka / James Morken)
- **Methodology & Complex Molecule Synthesis II** (*Yves Troin* / Seth Herzon / Jieping Zhu)
- **Industrial Processes III** (*William Trenkle* / Albert Delmonte / Travis Ramarchuk)
- **Bioactive Molecules and Organometallic Reactions** (*Mike Harmata* / Max Malacria / Mohammad Movassaghi)
- **Industrial Processes IV** (*Joseph Fox* / Shu Yu / Albert Kruger)
- **Poster Presentations** (*Matthew Bio*)
- **Asymmetric Catalysis** (*Pascal Dube* / Eric Jacobsen)

ORGANOMETALLIC CHEMISTRY
Jul 8-13, 2012
Salve Regina University, Newport, RI
Chair: Gregory L. Hillhouse
Vice Chair: James M. Boncella

- **Carbenes in Synthesis** (*John Bercaw* / Richard Schrock / Daniel Mindiola)
- **New Frontiers** (*James Boncella* / Don Tilley / Philip Power / Trevor Hayton)
- **Synthetic Organic Applications** (*Bernadette Donovan-Merkert* / Jonathan Ellman / Dean Toste / Rubén Martín Romo / Vy Dong / Joseph Martinelli)
- **Novel Reactivity and Transformations** (*Ged Parkin* / Laura Turculet / Joshua Figueroa / Juventino Garcia / Theodore Betley)
- **Energy and Sustainability** (*John Walzer* / Marcetta Darensbourg / John Gordon / Aaron Appel)

Organometallic Chemistry
Jul 7-8, 2012
Chair: Ian Tonks
Associate Chair: Jeffery A. Byers

OSCILLATIONS & DYNAMIC INSTABILITIES IN CHEMICAL SYSTEMS
Jul 15-20, 2012
Colby College, Waterville, ME
Chair: Tomohiko Yamaguchi
Vice Chair: Dezsö J. Horváth

- **Oscillations, Patterns and Instabilities: Past 30 Years and Future** (*Irving Epstein* / Patrick De Kepper / Kenichi Yoshikawa)
- **BZ Reaction and New Chemical Oscillators** (*Richard J. Field* / Markus Hauser / Vladimir Vanag / Miklós Orbán)
- **Recent Highlights I** (*Takashi Amemiya* / Shigeru Kondo / Stefan C. Müller)
- **Nonlinear Phenomena in Materials Science** (*John A. Pojman* / Qui Tran-Cong Miyata / Anna C. Balazs / Ryo Yoshida)
- **Entropy Production in Nonequilibrium Systems** (*Dilip Kondepudi* / Gregoire Nicolis / Koji Sawada)
- **Instabilities at Dissipative Interfaces** (*Anne de Wit* / Oliver Steinbock / Velonica Pimienta / Satoshi Nakata)
- **Recent Highlights II** (*Vilmos Gáspár*)
- **Nonlinear Dynamics in Chemical Communication** (*Raymond Kapral* / Anette Taylor / Punit Parmananda / Istvan Kiss)
- **Design of 'Robots'** (*Kenneth Showalter* / František Štěpánek / Ryo Kobayashi)

PHOSPHORYLATION & G-PROTEIN MEDIATED SIGNALING NETWORKS
Jun 10-15, 2012
University of New England, Biddeford, ME
Chair: John J. Tesmer
Vice Chair: Melanie H. Cobb

- **Structural Studies of Signaling** (Roger Sunahara / Jan Steyaert / Steve Gamblin)
- **Protein Kinase Signaling Networks** (Melanie Cobb / Tony Pawson / Forest M. White / Lawrence Lum)
- **New Biophysical Approaches for the Study of Signal Transduction** (Wayne Hubbell / Virgil Woods / Jin Zhang)
- **Signal Transduction and Disease** (Silvio Gutkind / Krzysztof Palczewski / Laura Bohn / Stefan Offermanns)
- **Lipid Mediated Signaling** (Jonathon Backer / Joan Heller-Brown / Sarah Spiegel)
- **Heterotrimeric G Protein Signaling Networks** (Alan Smrcka / Carmen Dessauer / Henrik Dohlman / Diomedes Logothetis)
- **Keynote Presentations: When G Proteins and Kinases Converge** (John Kuriyan / Kun-Liang Guan)
- **Translational Approaches in Signal Transduction** (Bryan Roth / Richard Neubig / Ben Turk / Stefan Knapp)
- **Regulation of Kinase and G Protein Pathways** (Anton Bennett / Maurine Linder / Mark von Zastrow)

Phosphorylation & G-Protein Mediated Signaling Networks
Jun 9-10, 2012
Chair: Angeline M. Lyon
Associate Chair: Benita Sjogren

PHOTONUCLEAR REACTIONS
Aug 5-10, 2012
Holderness School, Holderness, NH
Chair: Misak M. Sargsian
Vice Chairs: Ronald A. Gilman & Ulrike Thoma

- **Frontier News** (*Latifa Elouadrhiri* / Gerald Miller / Maria Spiropulu / Kevin McFarland / Katherine Myers)
- **The Internal Spatial and Spin Structure of the Nucleon I** (*Wally Melnitchouk* / Stanley Brodsky / Sebastian Kuhn / Alberto Accardi / Stefano Forte / Gail Dodge / Ariel Bodek / Brian Raue)
- **The Internal Spatial and Spin Structure of the Nucleon II** (*Patrizia Rossi* / Alessandro Bachetta / Carlos Munos Camacho / Stepan Stepanyan / Ami Rostomyan / Xin Qian)
- **Hadronic Spectrum and QCD I** (*Volker Burkert* / Mike Pennington / Lothar Tiator / Andrey Sarantsev / Derek Glazer / Reinhard Beck / Irene Zonta / Teresa Pena)
- **Hadronic Spectrum and QCD II** (*Douglas Higinbotham* / Robert Edwards / Tanja Horn / Diego Bettoni / Curtis Meyer)
- **Nuclear Forces and Few Body Systems** (*Sabine Jeschonnek* / William Detmold / Evgeny Epelbaum / Haiyan Gao / Simon Sirca / Werner Boeglin / Todd Averett)
- **Probing Exotic Matter in Nuclei** (*Lawrence Cardman* / Bradley Sherrill / Abhay Deshpande / Heinz Clement / Satoshi N. Nakamura)
- **Nuclear Structure at Small Distances and QCD** (*Claudio Ciofi degli Atti* / Mark Strikman / Larry Weinstein / Nadia Fomin / Chiara Mezzetti / Eliezer Piasetzky / Yordanka Ilieva / Kawtar Hafidi)
- **Standard and New Physics with Photo and Electroweak Processes** (*Robert McKeown* / Wolfram Weise / Jocelyin Monroe / Wick Haxton)

PHOTOSYNTHESIS
Jul 8-13, 2012
Davidson College, Davidson, NC
Chair: Richard J. Debus
Vice Chair: David Kramer

- **Structural Aspects of Photosynthesis** (*Jim Barber* / Nobuo Kamiya / Petra Fromme)
- **Photosynthetic Oxygen Production - Spectroscopy and Modeling** (*Gary Brudvig* / Junko Jano / K.V. Lakshmi / Takumi Noguchi / Philipp Kurz)
- **Photosynthetic Oxygen Production - Computational Aspects** (*Victor Batista* / Per Siegbahn / Marilyn Gunner)
- **Light Harvesting and Photoprotection** (*Naomi Ginsberg* / Peter Walla / Herbert van Amerongen / Ann McDermott / Alfred Holzwarth)
- **Enzymatic Hydrogen Production** (*Maria Ghirardi* / Iftach Yacoby / Oliver Lenz)
- **Secondary Electron/Proton Transfer Reactions** (*David Kramer* / Tony Crofts / Mike Bowman / Daniel Picot / Fabrice Rappaport)
- **Rewiring Reaction Centers to Outperform Natural Photosynthesis** (*John Golbeck* / Lisa Utschig / Noam Adir)
- **Artificial Photosynthesis** (*Ana Moore* / Etsuko Fujita / Heinz Frei / Tom Moore / Steve Reece)
- **Keynote Presentation: Sunlight-Driven Hydrogen Formation by Membrane-Supported Photoelectrochemical Water Splitting** (Nathan Lewis)

Photosynthesis
Jul 7-8, 2012
Chair: Gary F. Moore

PHYSICS RESEARCH & EDUCATION
Astronomy's Discoveries and Physics Education
Jun 17-22, 2012
Colby College, Waterville, ME
Chairs: Charles H. Holbrow & Peter Shaffer
Vice Chairs: Mel Sabella & Matthew J. Lang

- **The Physics in Astronomy's Discoveries and Technologies**
- **Exoplanets: New Worlds** (*Sara Seager* / Dave Charbonneau)
- **Astronomy in Physics Courses** (*Mario Belloni* / Dan Reichart / Larry Marschall / Todd Timberlake / Wolfgang Christian)

- **Observational Cosmology: New Horizons**
- **Teaching Physics with Astronomy: Pitfalls and Opportunities**
  (*Sidney Wolff* / Ed Prather)
- **Frontiers of Astronomy's Instruments and Detectors**
  (*Randolph Peterson*)
- **Stars**
  (*Peter Parker*)
- **Gravity and High Energy Astrophysics**
  (Duncan Brown / Lucy Fortson / Greg Bothun)
- **Astronomy Based Materials for Teaching Physics: What Should They Be? Who Will Make Them?**
  (Ed Prather / Sidney Wolff / Greg Bothun)

PLANT & MICROBIAL CYTOSKELETON

Aug 12-17, 2012
Proctor Academy, Andover, NH
Chair: Laurie G. Smith
Vice Chair: Fred Chang

- **Principles of Cytoskeletal Assembly and Structure**
  (*David Drubin* / David Agard [keynote] / Phong Tran / Bruce Goode)
- **Actin Assembly, Organization and Dynamics**
  (*Tom Pollard* / David Kovar / Magdalena Bezanilla / Arash Komeili / Anja Geitmann)
- **Cytoskeleton and Cell Wall Assembly**
  (*Tony Bretscher* / David Ehrhardt [keynote] / K.C. Huang / Hiroo Fukuda / Ethan Garner)
- **Microtubule Assembly, Organization and Dynamics**
  (*Susan Dutcher* / Geoff Wasteneys / Ram Dixit / Thomas Surrey / Bela Mulder / Jeff Errington)
- **Hot Topic Presentations**
  (*Wallace Marshall*)
- **Cytoskeleton-Based Motility**
  (*Chris Staiger* / Jake Baum / Roger Hangarter / Iva Tolic-Norrelykke / Sam Reck-Petersen / Ke Hu)
- **Mitosis**
  (*Fred Chang* / Kerry Bloom [keynote] / Bo Liu)
- **Cytokinesis**
  (*Jeff Errington* / Mohan Balasubramanian / Amy Gladfelter / Piet de Boer / Erin Goley)
- **Polarized Cell Growth**
  (*David Ehrhardt* / Fulvia Verde / Danny Lew / Dan Szymanski / Ying Fu)

PLANT CELL WALLS

Cell Wall Research in a Post-Genome World
Aug 5-10, 2012
Colby College, Waterville, ME
Chair: Jocelyn K. Rose
Vice Chair: Mary L. Tierney

- **Cell Wall 'Omics': Moving Beyond Model Systems**
  (*Jocelyn Rose* / Chris Somerville / John Vogel / Staffan Persson)
- **Cell Wall Growth and Morphogenesis**
  (*Maureen McCann* / Dan Cosgrove / Herman Höfte)
- **Cell Walls, Signaling and Environmental Interactions**
  (*Nick Carpita* / Julia Davies / Jens Tilsner / Giulia de Lorenzo)
- **Cell Wall Evolution**
  (*Zoé Popper* / William Willats / Jochen Zimmer / Stephen Fry)
- **Cellulose Structure and Synthesis**
  (*Deborah Delmer* / Seth DeBolt / Mei Hong / Simon Turner)
- **Matrix Glycan Structure and Synthesis**
  (*Ken Keegstra* / Breeanna Urbanowicz / Markus Pauly)
- **Non-polysaccharide Wall Components**
  (*Mary Tierney* / Lacey Samuels / John Ralph / Jose Estevez)
- **Cell Wall Disassembly and Degradation**
  (*Debra Mohnen* / Harry Brumer / Kiyohiko Igarashi)
- **Cell Wall Imaging and Analytical Tools**
  (*Paul Knox* / Andy Round / David Ehrhardt / Federica Brandizzi)

GRS Plant Cell Walls
Aug 4-5, 2012
Chair: Gregory Buda

PLANT MOLECULAR BIOLOGY

Genomic Approaches to Plant Signaling Systems
Jul 15-20, 2012
Holderness School, Holderness, NH
Chair: Michael R. Sussman
Vice Chair: Steven P. Briggs

- **Keynote Presentation: The Arabidopsis Interactome**
  (*Michael Sussman* / Joe Ecker)
- **Epigenomics and the RNA World**
  (*Craig Pikaard* / Vicki Chandler / Vincent Colot / Robert Martienssen)
- **Systems Biology: The Plant Proteome, Metabolome and Ionome**
  (*Mary Lou Guerinot* / Katja Baerenfaller / Lloyd Sumner)
- **Hormone Receptors I (Auxin, Jasmonates, GA)**
  (*Mark Estelle* / Sheng-Yang He / Alain Goossens / Tai Ping Sun)
- **Hormone Receptors II (ABA, Cytokinins, Ethylene, Sugars)**
  (*Sean Cutler* / Alan Jones / Shoqun Zhang / Zhenbiao Yang)
- **Receptor Kinases and the Phosphorylome**
  (*Jo Chory* / Remko Offringa / Antje Heese / Jen Sheen)
- **Pathogen Signaling**
  (*Steve Briggs* / Xinnian Dong / Alisa Huffaker)
- **Symbiotic Receptor Kinases and Calcium Signaling**
  (*Joe Ecker* / Jean-Michel Ane / Giles Oldroyd)
- **What are the Limits of Plant Genetics/Plant Breeding?**
  (*Simon Chan* / Rob Dirks / Dan Voytas)

Plasmonic chirality: Circularly polarized light interacts with a chiral gold nanostructure. By measuring differences between left- and right-hand circularly polarized light, the strongly enhanced optical chirality of the gold nanostructure can be determined. Courtesy of Sven Hein and Harald Giessen, University of Stuttgart, Germany. Submitted by Nader Engheta, Chair, Plasmonics GRC.

PLANT SENESCENCE

Epigenetic, Genetic, and Signaling Processes in Senescence
Jul 8-13, 2012
Stonehill College, Easton, MA
Chairs: James J. Giovannoni & Karin Krupinska
Vice Chairs: Andreas M. Fischer & Shimon Gepstein

- **Keynote Presentation: New Paradigms in Plant Senescence - Higher Order Regulation**
  (*Karin Krupinska* / Hervé Vaucheret)
- **Transcriptional Control of Senescence Processes**
  (*Susheng Gan* / Vicky-Buchanan-Wollaston / Karin Krupinska / Susheng Gan)
- **Protein Degradation and Senescence**
  (*Andreas Fischer* / Juan Guiamet / Kohko Yoshimoto)
- **Epigenetics and Chromatin Remodeling in Plant Senescence**
  (*Hervé Vaucheret* / Hong Gil Nam / Klaus Humbeck)
- **Epigenetics of Fruit Senescence**
  (*James Giovannoni* / Phillipe Gallusci / Graham Seymour / James Giovannoni)
- **Senescence and Postharvest Biology**
  (*Peter Davies* / Ian Ferguson / Christopher Watkins)
- **Senescence and Plant Productivity**
  (*Preben Bach Holm* / Celine Masclaux-Daubresse)
- **Stress and Stress-Related Signaling Systems in Plant Senescence**
  (*Shimon Gepstein* / Christine Foyer)
- **Organelle and Hormone Cross-Talk During Plant Senescence**
  (*Karin Krupinska* / Dario Leister)

PLASMA PROCESSING SCIENCE

Plasma Processing Science & Societal Grand Challenges
Jul 22-27, 2012
Bryant University, Smithfield, RI
Chair: Richard Van De Sanden
Vice Chair: Jane P. Chang

- **Plasmas and Renewable Energy I**
  (George-Felix Leu / Antonella Milella)
- **Plasmas and Health, Plasma-Enabled Medicine**
  (*P. Favia* / A. Fridman / Deborah O'Connell / Hidenori Akiyama)
- **Plasma Modelling**
  (*Vladimir Nagorny* / Stephane Pasquiers / Mark Kushner)
- **Plasma Surface Interactions/Treatment**
  (*Jane Chang* / Nicholas Gherardi / Daphne Pappas / Achim von Keudell)
- **Controlling Plasma Complexity**
  (*Satoshi Hamaguchi* / Demetre Economou / Amy E. Wendt)
- **Plasma and Nanotechnology**
  (Kenya Ostrikov / Xiangguo Li / Chris Hodson)
- **Plasmas and Renewable Energy II**
  (Greg De Temmerman / Ursel Fantz)
- **Plasmas and Environment**
  (*T. Nozaki* / Ken Okazaki / Stefan Welzel / Marc Bacon)
- **Multi-Phase Plasmas**
  (*Khaled Hassouni* / Makoto Kambara / Vittorio Colombo)

GRS Plasma Processing Science
Jul 21-22, 2012
Chair: Sameer Kalghatgi
Associate Chair: Robert P. Geiger

Gordon Research Conferences: "Session II" 2012 Preliminary Programs *(continued)*

PLASMONICS
Light-Matter Interaction at the Nanoscale
Jun 10-15, 2012
Colby College, Waterville, ME
Chair: Nader Engheta
Vice Chair: Mark L. Brongersma

- **Active, Tunable, Flexible Plasmonics**
  (*Harry Atwater* / Thomas Ebbesen / Vladimir Shalaev / Mark Stockman)
- **Plasmonics and Electron Beams**
  (*Peter Nordlander* / Albert Polman / Christian Colliex / Nikolay Zheludev / Javier Garcia de Abajo)
- **New Materials for Plasmonics and Metamaterials**
  (*Cherie Kagan* / Alexandra Boltasseva / Chris Murray / Costas Soukoulis)
- **Plasmonic Nanoantennas and Resonators**
  (*Harald Giessen* / Rashid Zia / Hideki Miyazaki / Andrea Alu / Meir Orenstein)
- **Optical Forces and Momentum**
  (*Michelle Povinelli* / Henri Lezec / Byoungho Lee / Reuven Gordon)
- **Longer-Wavelength Plasmonics**
  (*Mikhail Noginov* / Shanhui Fan / Jean-Jacques Greffet / David Norris / Silvio Hrabar)
- **Plasmonics in Biology and Chemistry**
  (*Pol van Dorpe* / Catherine Murphy / Luke Lee / Bengt Kasemo)
- **Plasmonic and Quantum Devices**
  (*Ulrike Woggon* / Pierre Berini / Francisco Garcia-Vidal / Uriel Levy / Anatoly Zayats)
- **Perspectives and Predictions**
  (*Mark Brongersma* / Naomi Halas)

Plasmonics
Jun 9-10, 2012
Chair: Ashkan Vakil
Associate Chair: Alok Vasudev

POLYMER PHYSICS
Jul 22-27, 2012
Mount Holyoke College, South Hadley, MA
Chair: Scott T. Milner
Vice Chair: John M. Torkelson

- **Nanostructured Materials by Design**
  (Thomas Epps / Marc Hillmyer / Hiroshi Jinnai / Randall Kamien)
- **Physics of Biomolecules**
  (Carlos Bustamante / John Marko)
- **Robust Gels and Responsive Networks**
  (Jian Ping Gong / Fred Mackintosh)
- **Local Probes of Glassy Behavior**
  (Chris Stafford / John Torkelson)
- **Physics of Semicrystalline Polymers**
  (Pat Brant / Greg Rutledge / Anthony Ryan)
- **Polymeric Surfactants**
  (Maria Santore / Lynn Walker)
- **Rheology and Nonlinear Flow Behavior**
  (Suzanne Fielding / Alexei Likhtman / Shi-Qing Wang)
- **Polymers for Energy, Electronics, and Biology**
  (Michel Armand / George Malliaras / Alberto Salleo / Grant Willson)

Polymer Physics
Jul 21-22, 2012
Chair: Amanda McDermott
Associate Chair: Nicholas B. Tito

POST-TRANSCRIPTIONAL GENE REGULATION, THE BIOLOGY OF
Jul 15-20, 2012
Salve Regina University, Newport, RI
Chair: Manuel Ares
Vice Chair: Melissa Moore

- **RNA-Processing Dysfunction in Disease**
  (*Mariano Garcia-Blanco* / Adrian Krainer / Maurice S. Swanson / Tom Cooper / Jane Wu)
- **miRNA Biogenesis and Function**
  (*Shobha Vasudevan* / Joan Steitz / Javier Caceres / Peter Sarnow / Victor Ambros)
- **Translation Mechanisms**
  (*Wendy Gilbert* / Rachel Green / Jonathan S. Weissman / Chris Burge)
- **Co-Transcriptional RNA Processing Mechanisms**
  (*Tracy Johnson* / Karla Neugebauer / Xiang-Dong Fu / Gideon Dreyfuss / David Bentley / Nick Proudfoot)
- **Noncoding RNA Expression and Function**
  (Gordon Carmichael / John Rinn / Davide Corona)
- **Global Approaches to Post-Transcriptional Gene Regulation**
  (*Jeremy Sanford* / Brent Graveley / Matthias Hentze / Rachel Brem / Gene Yeo / Gary Schroth)
- **RNA Localization**
  (Kelsey Martin / Vivian Budnik / Robert H. Singer / Anne Ephrussi)
- **Splicing Mechanisms**
  (*Melissa Jurica* / Anna Pyle / Jonathan Staley / Christine Guthrie)
- **Regulation of RNA Decay**
  (*Melissa Moore* / Jens Lykke-Anderson / Lynne Maquat)

An acantharian - a single-celled eukaryotic organism (protist) from an open ocean ecosystem - showing strontium sulfate spines and a pseudopodial network strewn along the spines. Courtesy of David Caron, USC. Submitted by Raffaella Casotti, Chair, Marine Microbes GRC.

PROPROTEIN PROCESSING, TRAFFICKING & SECRETION
Jul 15-20, 2012
Colby-Sawyer College, New London, NH
Chair: Lloyd D. Fricker
Vice Chair: John W. Creemers

- **Protein Trafficking and Secretion: Classical and Unconventional Pathways**
  (*Annik Prat* / Thomas Braulke / Robert Chow / Janice Mayne)
- **The Secretory Pathway from ER to Exit - Focus on Proinsulin and Diabetes**
  (*Gary Thomas* / Don Steiner / Bill Balch / Chris Rhodes / Joshua Zimmerberg / Peter Arvan / Michele Solimena)
- **New Developments in Proprotein Processing: PCs and Beyond**
  (*Richard Mains* / Iris Lindberg / Lakshmi Devi / Betty Eipper)
- **Imaging Techniques to Study Protein Trafficking and Secretion**
  (*Ron Holz, Daniel Constam* / Jennifer Lippincott-Schwartz / Tom F. Martin / Arun Anantharam / Ed Stuenkel / Daniel Mesnard)
- **Carboxypeptidases in Peptide Processing and Disease**
  (*Y. Peng Loh* / Peter Lyons / William Wetsel / Rina Rosin-Arbesfeld / Yong Cheng)
- **Protein Trafficking and Signaling**
  (*Jan Christian, Yanzhuang Wang* / Scott Emr / Christof Niehrs / Loydie Jerome-Majewska / Mihaela Serpe)
- **Hot Topics in Proprotein Processing, Trafficking, and Secretion**
  (*John Creemers*)
- **Genetics and the Secretory Pathway**
  (*Bob Fuller, Paul Taghert* / John Creemers / Michael Blackman / Deborah Andrews / Michael Nonet / Jason Mills)
- **Proprotein Processing, Trafficking and Secretion in Disease**
  (*An Zhou* / Nabil Seidah / Robert Day / Majid Khatib)

Proprotein Processing, Trafficking & Secretion
Jul 14-15, 2012
Chair: Jonathan H. Wardman
Associate Chair: Vincent Pruniau

PROTEIN COFACTORS, RADICALS & QUINONES
Jul 29 - Aug 3, 2012
Mount Holyoke College, South Hadley, MA
Chair: Joseph T. Jarrett
Vice Chair: Carrie M. Wilmot

- **Towards a Molecular Understanding of Ribonucleotide Reductase Catalysis**
  (JoAnne Stubbe / Catherine Drennan / J. Martin Bollinger)
- **Radical Enzymes That Catalyze Post-Translational or Post-Transcriptional Modifications**
  (Osamu Nureki / Vahe Bandarian / Mohammed Atta)
- **Roles for Protein-Derived Cofactors in Enzyme Catalysis**
  (Martha Stipanuk)
- **Something Old, Something New: Radical SAM Enzymes**
  (Joan Broderick / Frank Raushel / Susan Wang)
- **Oxygen-Dependent Radical Enzymes**
  (Carsten Krebs / Justine Roth)
- **Biophysical Methods and Theory**
  (Brian Hoffman / Aimin Liu / Gary Gerfen)
- **Enzymes Important in Human Biochemistry or Health**
  (Ah-Lim Tsai / Minae Mure)
- **Amine Oxidases, Quinones, and Quinone Biogenesis**
  (Judith Klinman / Victor Davidson / Carrie Wilmot)
- **Radical Enzymes in Bioenergy and Biomaterials-Related Pathways**
  (Amy Rosenzweig / John Peters)

PROTEOGLYCANS
Jul 8-13, 2012
Proctor Academy, Andover, NH
Chair: Robert J. Linhardt
Vice Chair: Nicholas Shworak

- **Late Breaking Presentations**
  (*Jerry Turnbull, Renato Iozzo*)
- **Biosynthesis and Catabolism**
  (*Lena Kjellén, Marion Kusche-Gullberg* / Jian Liu / Hinke Multhaupt)
- **Developmental Biology**
  (*Joe Yost, Hiroshi Nakato* / Christine B. Kern)

- **Structure/Analysis/Glycomics**
  (*Barbara Mulloy, Joseph Zaia* / Jon Amster / Cindy Larive)
- **Signaling and the Interactome**
  (*Pascal Zimmerman, David Fernig* / Alan Rapraeger / A. Radu Aricescu)
- **Cancer**
  (*Ralph Sanderson, Alan Rapraeger* / Nikos Karamanos / Steve Pals)
- **Neural, Muscular and Skeletal Diseases**
  (*Yu Yamaguchi, Dick Heinegard* / James Fawcett)
- **Stem Cells and Regenerative Medicine**
  (*Lola Reid, Jennifer Elisseeff* / Cathy Merry / Xingbin Ai)
- **Cardiovascular and Inflammation**
  (*Nick Shworak, Pyong Park* / Paul Noble / Renato Iozzo)

Proteoglycans
Jul 7-8, 2012
Chair: Sarah M. Knox
Associate Chair: Thomas E. Neill

PROTEOLYTIC ENZYMES & THEIR INHIBITORS
Proteolysis: The Most Important Post Translational Modification Regulating Biology, Life and Death of Every Cell
Jun 17-22, 2012
Il Ciocco Tuscany Resort, Lucca (Barga), Italy
Chair: Klaudia Brix
Vice Chair: James C. Whisstock

- **The Active Site of Proteases**
  (*Wolfram Bode* / Antonio Baici / Guy S. Salvesen / Bonnie F. Sloane / James C. Whisstock)
- **Animal Models for Studies on Proteolysis**
  (*Christoph Peters* / Margarete S. Heck / Annik Prat / Thomas Reinheckel)
- **Networking in Proteolysis - Proteomics, Degradomics**
  (*Walter Stöcker* / Christopher M. Overall / Irit Sagi)
- **Proteolysis in Signaling Events**
  (*Nabil G. Seidah* / Judith Clements / Matthew Freeman / Sin Urban)
- **Proteases in Infectious and Tropical Diseases**
  (*Ben M. Dunn, James McKerrow* / Sheena McGowan / Jan Potempa)
- **Proteases in Wound Healing, Metastasis, Fibrotic Diseases**
  (*Agnes Noel, Bonnie F. Sloane* / Galia Blum / Dieter Brömme / Mark Gorrell / Johanna Joyce / Daniel Madsen)
- **Protease Inhibitors and Their Biological Significance**
  (*F. Xavier Aviles* / F. Xavier Gomis-Rüth / James A. Huntington / Robert N. Pike / Daniel Lawrence / Henning Stennicke)
- **Proteases and Inhibitors in Translational Approaches**
  (*Bob Lazarus* / Matthew S. Bogyo / Hans-Ulrich Demuth / Christopher Scott / Boris Turk)
- **Perspectives in Proteolysis**
  (*James C. Whisstock*)

Proteolytic Enzymes & Their Inhibitors
Jun 16-17, 2012
Chair: Sheena McGowan

NEW! QUANTUM SCIENCE
Aug 12-17, 2012
Stonehill College, Easton, MA
Chairs: Mikhail Lukin & Atac Imamoglu
Vice Chairs: Hans Briegel & David J. Wineland

- **Quantum Information Theory and Many-body Systems**
  (*Ignacio Cirac* / Frank Verstraete / Lorenza Viola)
- **Topological Quantum Systems**
  (*Bertrand Halperin* / John Preskill / Daniel Gottesman)
- **Hybrid Quantum Systems**
  (*Eugene Polzik* / Serge Haroche / Oskar Painter / Kouichi Semba)
- **Quantum Biology**
  (*Birgitta Whaley* / Hongkun Park / Greg Scholes)
- **Quantum Dynamics of Strongly Correlated Systems**
  (*Ana Maria Rey* / Eugene Demler / Hakan Tureci / Immanuel Bloch)
- **Metrology and Many-body Physics**
  (*Ronald Walsworth* / Jun Ye / David Wineland)
- **New Directions**
  (*Peter Zoller* / Vladan Vuletic / Philippe Grangier / Philipp Treutlein)
- **Outstanding Challenges**
  (*Steven Girvin* / Amir Yacoby / Andreas Wallraff / Chris Monroe)
- **Quantum Simulations**
  (*Tilman Esslinger* / Markus Greiner / Rainer Blatt)

RADIATION CHEMISTRY
Radiation Driven Processes in Physics, Chemistry, Biology and Industry
Jul 29 - Aug 3, 2012
Proctor Academy, Andover, NH
Chair: William A. Bernhard
Vice Chair: Jay A. Laverne

- **Keynote Presentations: From Energy Absorption to Disease**
  (*Marianne Sowa, Wendy Pogozelski* / Nigel Mason / William Morgan)
- **Track Structure and Low Energy Electrons**
  (*Simon Pimblott* / Michael Dingfelder / Leon Sanche / Uwe Hergenhahn)
- **Young Investigator Presentations**
  (*Slywia Ptasinska, Jim Wishart*)
- **DNA and Proteins**
  (*Amanda Bryant-Friedrich, Maria Davidkova* / Elspeth Garman / Jean-Luc Ravanat / Tetsuro Majima)
- **Irradiated Polymers for Industrial/Medical Applications**
  (*Mohamad Al-Sheikhly, Erzsébet Takács* / Walter Voit / Piotr Ulański)
- **Space Radiation Chemistry/Biology**
  (*Susanna Widicus Weaver, Thom Orlando* / Naoki Watanabe / Ralf Kaiser / Reggie Hudson)
- **Dosimetry Following a Radiological Incident**
  (*Tulsi Mukherjee, Steve Swarts* / Harold Swartz / Francois Trompier)
- **Nanoparticles and Surface Interfaces**
  (*Mats Jonsson* / Jean-Philippe Renault / Nikolay Petrik / Xavier Coqueret / Clelia Dispeneza)
- **Nuclear Power and Waste Management**
  (*Clara Wren* / Francis Livens)

Radiation Chemistry
Jul 28-29, 2012
Chair: Paul J. Black
Associate Chair: Pamela A. Yakabuskie

ROCK DEFORMATION
Feedback Processes in Rock Deformation
Aug 19-24, 2012
Proctor Academy, Andover, NH
Chair: Peter Kelemen
Vice Chair: Wenlu Zhu

- **Instabilities Leading to Failure at High Confining Pressure I**
  (*Steve Kirby* / Michel Bestmann / Erland Schulson)
- **Instabilities Leading to Failure at High Confining Pressure II**
  (*Jessica Warren* / Bruno Reynard / Yuri Podladchikov / Virginia Toy)
- **Fluid-Assisted Slow Slip, Earthquakes and Fracture I**
  (*Harry Green* / Nicholas Brantut / Olga Sergienko / Nadia Lapusta)
- **Fluid-Assisted Slow Slip, Earthquakes and Fracture II**
  (*Tom Heaton* / Georg Dresen / Nick Austin / Scott Johnson)
- **Reaction-Driven Cracking**
  (*Peter Kelemen* / Bjørn Jamtveit / François Renard / Ray Fletcher)
- **Dynamic Triggering of Earthquakes**
  (*Heather Savage* / Emily Brodsky / David Shelley / Karen Mair)
- **Localized Fluid Transport and Deformation**
  (*Ben Holtzman* / Dave Kohlstedt / Erik Rybacki / Jamie Connolly / Jan Ludvig Vinningland)
- **Localized Fluid Transport and Reaction**
  (*Marc Spiegelman* / Russell Detwiler / Laura Hebert / Rich Katz)
- **Density Instabilities, Diapirs, and Crustal Growth**
  (*Mark Behn* / Clare Warren / Kelin Wang / Gene Humphreys)

SALT & WATER STRESS IN PLANTS
Jun 24-29, 2012
Chinese University of Hong Kong, China
Chairs: Julian I. Schroeder & Teun Munnik
Vice Chairs: Michael R. Blatt & Eduardo Blumwald

- **Whole Plant Responses & Trait Discovery**
  (*Mark Tester* / Rana Munns / Julia-Bailey Serres)
- **ABA and Salinity Stress Signalling**
  (*Hans Bohnert* / Erwin Grill / Jianhua Zhang / Jiang Kang Zhu)
- **Stress Trait Breeding, QTL & NextGen Sequence Mapping**
  (*Peter Langridge* / Zhikang Li / Tom Greene)
- **Systems Biology of Stress**
  (*Dorothea Bartels* / José R. Dinneny / Kazuko Yamaguchi-Shinozaki)
- **From Molecular Biology to Field**
  (*Eduardo Blumwald* / Michael Metzlaff / Lizhong Xiong)
- **Ways in Which Basic Research Advances and New Tools Can Serve the Growing Needs of Global Agriculture**
  (*Julia Bailey-Serres, Julian Schroeder, Jianhua Zhang, Teun Munnik* / open discussion for all participants)
- **Ion Transport**
  (*Mike Blatt* / Tomoaki Horie / Rainer Hedrich)
- **Metabolism & Omics**
  (*Mel Oliver* / Antonio Tiburco / Lahiri Majumder)
- **Signal Transduction**
  (*Teun Munnik* / Shintaro Munemasa / Sneh Lata Singla-Pareek)
- **Extremophiles and Quantitative Trait Mapping**
  (*Jill Farrant* / Anna Amtmann / Roberto Tuberosa)

SCIENCE & TECHNOLOGY POLICY
Science and Technology Policy in Global Context
Aug 5-10, 2012
Waterville Valley Resort, Waterville Valley, NH
Chairs: Susan Cozzens & Jack Stilgoe
Vice Chair: Jennifer Kuzma

- **Keynote Presentations: What is Globalization?**
  (*Albert H. Teich* / Sheila Jasanoff / Raphael Kaplinsky)
- **Global Movement of Scientists and Engineers**
  (*Sallie Ann Keller* / Carolina Canibano / Josh DeWild / Bruce Weinberg / Kathryn Zippel)
- **Building Global Scientific Institutions**
  (*Kerri Ann Jones* / Sara Farley / Terttu Luukkonen / David Stonner)
- **Global Collaboration in Knowledge Production**
  (*John Boright* / Kaitlin Christensen / Stephen Perz / Caroline Wagner / Marcus Ynalvez)

Gordon Research Conferences: "Session II" 2012 Preliminary Programs *(continued)*

- **Global Issues in Intellectual Property** (*Vaughn Turekian* / Heloise Emdon / Sunil Mani / Bhaven Sampat)
- **Innovation Strategy under Globalization** (*David Guston* / Susanna Borras / Dan Breznitz / Stephanie Shipp / Francisco Veloso)
- **Inclusive Innovation for Inclusive Development** (*Jameson Wetmore* / Dinesh Abrol / Adrian Ely / Judith Sutz)
- **Global Governance of Technologies** (*Michele Garfinkel* / Kathy Hudson / Clark Miller / Peter Newell / Henk Zandvoort)
- **The Global Research Community in Science, Technology, and Innovation Policy** (*Kaye Husbands Fealing* / Gabriela Dutrenit / Ann Kingiri / Rongping Mu)

Science & Technology Policy
Aug 4-5, 2012
Chair: Logan D.A. Williams
Associate Chair: Thomas Woodson

NEW! SCIENTIFIC METHODS IN CULTURAL HERITAGE RESEARCH
Non-Destructive Imaging and Micro-Analysis in Cultural Heritage
Jul 29 - Aug 3, 2012
Mount Snow Resort, West Dover, VT
Chairs: Heinz-Eberhard Mahnke & Marco Leona
Vice Chairs: Francesca Casadio & Philippe Walter

- **Complex Materials: Case Studies from the Old and the New World** (*Ernst Pernicka* / Ira Rabin / Jose Luis Ruvalcaba Sil)
- **Structures at the Nanoscale** (*Karen Trentelman* / Marc Walton / Xiu Zhen Janice Li / Tim Wess)
- **Hard X-Rays: From Large Scale Facilities to Tabletop Sources** (*Ercan Alp* / Eric Dooryhee / Marie Jacquet)
- **Structures at the Microscale I: The Role of Spectroscopy** (*Sandra Lopez Varela* / Costanza Miliani / Marine Cotte / Carol Hirschmugl)
- **Panel 1: The Role of Large Scale Facilities in Cultural Heritage Studies** (*Uwe Bergmann, Koen Janssens*)
- **Structures at the Microscale II: From Bio-Organic Heritage to Modern Art** (*Ioanna Kakoulli* / Catherine Higgitt / Jennifer Mass)
- **Structures at the Macroscale** (*Marie-Claude Corbeil* / Robert van Langh / Eberhard Lehmann / Katja Kleinert)
- **Panel 2: New Trends in Chemistry for Cultural Heritage Studies** (*Christian Amatore*)
- **Lasers: From Molecules to Macrostructure** (*Y. Lawrence Yao* / Richard van Duyne / Piotr Targowski)
- **Imaging and Depth Profiling** (*Kaori Fukunaga* / John Delaney / Margriet van Eikema Hommes / Bernhard Bluemich)
- **Interdisciplinary Investigations in Archaeology** (*Markus Reindel* / Friederike Seyfried [keynote])

SIGNAL TRANSDUCTION BY ENGINEERED EXTRACELLULAR MATRICES
Jul 8-13, 2012
University of New England, Biddeford, ME
Chair: Karen Hirschi
Vice Chair: Jason A. Burdick

- **Keynote Presentations** (*Karen Hirschi* / Christopher Chen / David Cheresh)
- **Engineering Adhesion and Signaling** (Catherine Picart / Andreas Garcia / Margaret Gardel)
- **Cellular Mechanotransduction** (*Robert Mauck* / Martin Schwartz / Valerie Weaver / Ning Wang)
- **3D Matrices** (*Andy Putnam* / Mathias Lutolf / Sarah Heilshorn / David Mooney)
- **Matrix Remodeling** (*Johnna Temenoff* / Viola Vogel / George Davis / Sharon Gerecht)
- **Engineering Stem Cell Niches** (*Robin Lovell-Badge* / Todd McDevitt / Kam Leong / Adam Engler)
- **Engineering Tissue Function** (*Charles ffrench-Constant* / Gordana Vunjak-Novakovic / Michael Sheetz)
- **Tissue Patterning** (*Jason Burdick* / Shulamit Levenberg / Lance Davidson / Kate Bentley)
- **Imaging and Quantification of Tissue Formation** (*Charles Little* / Brenda Rongish / Michel Modo / Victoria Bautch)

Signal Transduction by Engineered Extracellular Matrices
Jul 7-8, 2012
Chair: Kyle J. Lampe
Associate Chair: Brendan Purcell

SIGNALING BY ADHESION RECEPTORS
Jun 24-29, 2012
Colby College, Waterville, ME
Chair: Martin Schwartz
Vice Chair: Martin J. Humphries

- **Keynote Presentation** (Mina Bissell)
- **Integrin Signaling to the Cytoskeleton and Cell Migration** (*Gaudenz Danuser* / David Calderwood / Mark Ginsberg)
- **Cadherin Signaling to the Cytoskeleton**(*James Nelson* / Alpha Yap / Karl Matter)
- **Cadherin Signaling in Growth and Differentiation** (*Elaine Fuchs* / Denise Montell / Dietmar Vestweber)
- **Integrin Signaling in Growth, Differentiation and Survival** (*Valerie Weaver* / Eun-Gook Kim / Lester Lau)
- **Mechanotransduction by Cell Adhesion Receptors** (*Clare Waterman* / Michael Sheetz / Johan de Rooij)
- **Signaling by Other Adhesion Receptors** (*Michael Simons* / Eleni Tzima / Erik Sahai)
- **The Hippo/YAP Pathway** (*Barry Gumbiner* / Jeff Wrana / Stephan Piccolo)
- **Systems Biology Approaches to Adhesion Receptor Biology** (*Martin Humphries* / Alexander Bershadsky / Joan Brugge)

Signaling by Adhesion Receptors
Jun 23-24, 2012
Chair: Mei R. Ng
Associate Chair: Kimberly M. Stroka

NEW! SINGLE MOLECULE APPROACHES TO BIOLOGY
Understanding Life at a Higher Resolution
Jul 15-20, 2012
Mount Snow Resort, West Dover, VT
Chairs: Julio M. Fernandez & Stefan W. Hell
Vice Chairs: Hermann Gaub & Michelle Wang

- **Keynote Presentation: Synergy between Single Molecule Simulations and Single Molecule Experiments - Applications to Biomolecular Motors** (*Stefan Hell* / Martin Karplus)
- **Origin and Fate of Proteins** (*Xiaowei Zhuang* / Joseph D. Puglisi / Robert T. Sauer / David Rueda)
- **Physical Principles of Life** (*Shimon Weiss* / Sunney Xie / Olga Dudko / Ruben Gonzalez)
- **Active Motion or Random Diffusion?** (*David Clapham* / Eric Greene / Carlos Bustamante / Yossi Klafter)
- **Building Blocks of Living Cells** (*Michelle Wang* / Jeff Gelles / Viola Vogel / Holger Stark)
- **Sensing and Acting at the Nanoscale** (*Kevin Plaxco* / Yale Goldman / Latha Venkataraman / Timothy Springer)
- **From Molecular Mechanics to Physiology** (*Hermann Gaub* / Matthias Rief / Sergi Garcia-Manyes / Helmut Grubmuller)
- **Molecules and Superresolution Microscopy** (*Taekjip Ha* / Jörg Wrachtrup / Silvio Rizzoli / Xiaowei Zhuang)
- **Nanoswitches in Action** (*Timothy Springer* / Steve Block / Johan Elf)
- **Keynote Presentation** (*Julio M. Fernandez* / Toshio Yanagida)

SOLID STATE CHEMISTRY
Design and Properties of Materials for Energy and Environment Applications
Jul 22-27, 2012
Colby-Sawyer College, New London, NH
Chair: Antoine Maignan
Vice Chair: Susan M. Kauzlarich

- **Synthesis and Discovery of Novel Materials** (*R.J. Cava* / Paul Attfield / Angela Moeller / Ling Chen)
- **Solid State Chemistry for Energy** (*Claude Delmas* / Jeff Snyder / Atsuo Yamada / Amy Prieto)
- **Functional Oxides** (*Hans Conrad Zur Loye* / Mas Subramanian / Patrick Woodward / Sabajit Banerjee)
- **New HTCs, Multiferroics and Magnetocalorics** (*Miguel Alario Franco* / Shintaro Ishiwata / Richard Brutchey)
- **Nanostructured Materials** (*Ram Seshadri* / Darrell G. Schlom / Giulia Galli / Javier Vela-Becerra)
- **Porous Solids for Applications** (Bradley F. Chmelka / Susumu Kitagawa)
- **Lighting Materials** (*Amparo Fuertes* / Stephen Forrest / Julie J. Brown / H.T. 'Bert' Hintzen)
- **Advances in Characterization** (*K.R.P. Poeppelmeier* / Staf Van Tendeloo / Paolo G. Radaelli)
- **Non-Oxide Materials** (*Gordon J. Miller* / Franck Di Salvo / Michael Shatruk / Richard B. Kaner)

STEREOCHEMISTRY
Jul 29 - Aug 3, 2012
Salve Regina University, Newport, RI
Chairs: Michael J. Martinelli & Vittorio Farina
Vice Chairs: Joel Hawkins & Helma Wennemers

- **Stereoselective Synthesis** (*Helma Wennemers* / Yoshito Kishi / Tohru Fukuyama)
- **Asymmetric Synthesis** (Jay Siegel / Richmond Sarpong / Vy Dong / Dawei Ma)
- **Stereochemistry in Process R&D** (Ian Davies / Sèbastien Lemaire / Steven Ley)
- **Stereoselective Catalysis** (Scott Miller / Pavel Kocovsky / Elizabeth Jarvo / Matthew Gaunt)
- **Materials and Stereochemistry** (Robert Grubbs / David Amabilino / Heather Maynard)

- **Biocatalysis and Enzymology**
  (Manfred Reetz / Nikki Pohl / Daniel Mink / Christina Grozinger)
- **Medicinal Stereochemistry**
  (Ada Yonath / Jacquelyn Gervay-Hague / Punit Seth)
- **Stereoselective Synthesis**
  (Craig Forsyth / Jonathan Reeves / George Moniz / Jon Rainier)
- **Stereoselective Catalysis**
  (*Joel Hawkins* / Scott Denmark / Ei-ichi Negishi)

SYNAPTIC TRANSMISSION

Jul 29 - Aug 3, 2012
Waterville Valley Resort, Waterville Valley, NH
Chair: Felix E. Schweizer
Vice Chair: Peter Jonas

- **Synaptic Transmission: from Molecules to Mechanisms and Circuits**
  (*Felix Schweizer, Peter Jonas* / Eve Marder / James E. Rothman)
- **Calcium Channels, Domains and Sensors**
  (Stephen M. Smith / Elise Stanley / Ed Chapman / Tobias Moser)
- **Vesicle Fusion, Fusion Pores, SNAREs**
  (Robert Zorec / Manfred Lindau)
- **Synaptic Diversity: Ribbon Synapses**
  (Teresa Nicolson / Marlies Knipper / Henrique von Gersdorff)
- **Postsynaptic Signaling and Receptor Trafficking**
  (Isabel Pérez-Otaño / Seth Grant)
- **Diversity of Synaptic Plasticity**
  (*Chris McBain* / Pablo Castillo / Catherine Woolley / Nick Spitzer)
- **Synaptic Structure**
  (*Kristen Harris* / Erik Jorgensen / Antoine Triller)
- **Synaptic Basis of Brain Disorders**
  (*Kamran Khodkhah* / Maria Spillantini / Jane Sullivan / Lisa Monteggia)
- **Synaptic Transmission in Microcircuits**
  (Mathew Larkum / Jill Leutgeb / Carl Petersen)

TETRAPYRROLES, CHEMISTRY & BIOLOGY OF

Jul 22-27, 2012
Salve Regina University, Newport, RI
Chair: Harry A. Dailey
Vice Chair: Martin J. Warren

- **Hot Topics: Short Talks Selected from Abstracts**
  (*John Phillips*)
- **Vitamin B12**
  (*Ruma Banerjee* / Yan Kang / Montsettat Eilas-Arnanz / David Rosenblatt / Markos Koutmos)
- **Bacterial Tetrapyrrole Metabolism**
  (*Gunhild Layer* / Susana Lobo / Nicole Frankenburg-Dinkel / Celia Goulding)
- **Chemistry of Tetrapyrroles**
  (*Emma Raven* / Dilek Dogutan / P.L. Dutton / Yi Lu / Christiane Knappke)
- **Heme in Physiological Processes**
  (*Pavel Martasek* / Anthony Kettle / Eileen Jaffe / Feng Guo)
- **Tetrapyrroles in Disease States**
  (*Peter Meissner* / David Bishop / Sarah Ducamp / Barry Paw / Miguel P. Soares)
- **Tetrapyrrole Metabolism in Parasites and Pathogens**
  (*Amy Medlock* / Neil Hammer / Iqbal Hamza / Akhil Vaidya)
- **Tetrapyrroles in Photosynthetic Organisms**
  (*Neil Hunter* / Robert Blankenship / Min Chen / Roman Sobotka / Stefan Hortensteiner)
- **Keynote Presentation: Human Porphyrias - What We Know, What We Don't Know**
  (*Michael Badminton* / Jean-Charles Deybach)

Minimalism in radiation sculptured therapeutic nanogels. Sterile nanogels can be generated by electron-beam irradiation from dilute polymer aqueous solutions and covalently decorated with different biological moieties. By combination of different complementary building blocks, virtually infinite and controlled structures can be formed with precise site recognition functions, responsive shells or programmed supramolecular assembly patterns. Courtesy of Clelia Dispenza, Speaker, Radiation Chemistry GRC. Submitted by William A. Bernhard, Chair, Radiation Chemistry GRC.

THIN FILM & SMALL SCALE MECHANICAL BEHAVIOR

Jul 22-27, 2012
Colby College, Waterville, ME
Chair: John Balk
Vice Chair: Neville R. Moody

- **Mechanisms Governing Small-Scale Mechanical Behavior**
  (*Daniel Kiener* / Peter Gumbsch)
- **Plasticity in Confined Volumes**
  (Marc Fivel / Daryl Chrzan)
- **Indentation and Small-Scale Compression Testing**
  (Easo George / Erica Lilleodden)
- **Nanomechanics of Battery Materials**
  (*Robert McMeeking* / Yang-Tse Cheng)
- **Advances in Test Techniques for Materials at Small Length Scales**
  (*David Bahr* / Corrine Packard / Maarten de Boer)
- ***In-situ* Mechanical Testing and Characterization**
  (Chris Eberl / Johann Michler)
- **Size Effects in Mechanical Behavior**
  (Andrew Bushby / Jun Lou)
- **Mechanical Behavior of Biological Materials**
  (Vicky Nguyen / Michelle Dickinson)
- **Keynote Presentation: Mechanics for Bio-Integrated Electronics**
  (John Rogers)

GFS Thin Film & Small Scale Mechanical Behavior
Jul 21-22, 2012
Chair: Nicolas J. Briot
Associate Chair: Sofie Burger

NEW! THIOL-BASED REDOX REGULATION & SIGNALING

The Molecular Underpinnings of Redox Regulation and Oxidative Stress

Jul 29 - Aug 3, 2012
Bates College, Lewiston, ME
Chair: Leslie B. Poole
Vice Chair: Michel B. Toledano

- **Foundations of Thiology**
  (*Vadim Gladyshev* / Leopold Flohé / Ben Cravatt)
- **Chemical Biology of Regulatory Thiol Modifications**
  (*Cristina Furdui* / Dan Liebler / Kate Carroll / Jason Held / Andy Snyder / Jakob WInther)
- **Molecular Details of Thiol Switches**
  (Ursula Jakob / Nick Tonks / Franscisco Cejudo)
- **NO and H2S Signaling**
  (*Colin Thorpe* / Neil Hogg / Jay Zweier / Beatriz Alvarez / Ruma Banerjee / Chris Chang)
- **Localized ROS and Redox Signaling**
  (*Vsevolod Belousov* / Dean Jones / Masuko Ushio-Fukai / John Engelhardt)
- **Thiol-Based Enzymes and Oxidant Defense**
  (*Luise Krauth-Siegel* / Sue Goo Rhee / Andy Karplus / Luis Netto / Akhilesh Reddy)
- **Molecular Mechanisms of Redox Regulation of Signaling and Disease Processes**
  (*Toren Finkel* / Yvonne Janssen-Heininger / Boudewijn Burgering / Sang Won Kang)
- **Protein Folding in the Endoplasmic Reticulum and Mitochondrial Intermembrane Space**
  (*Roberto Sitia* / Neil Bulleid / Kostas Tokatlidis / Billy Tsai)
- **Chemical Biology of Reactive Oxygen and Sulfur Species**
  (*Dennis Templeton* / Tobias Dick / Mike Murphy)

GFS Thiol-Based Redox Regulation & Signaling
Jul 28-29, 2012
Chair: Erika Bechtold
Associate Chair: Matthieu Depuydt

NEW! TRANSGLUTAMINASES IN HUMAN DISEASE PROCESSES

Jul 15-20, 2012
Davidson College, Davidson, NC
Chair: Kapil Mehta
Vice Chair: Mauro Piacentini

- **Keynote Presentation: Transglutaminases - The Past and Next Decade**
  (Davies PJA)
- **Transglutaminases and Celiac Disease**
  (*Laszlo Fesus* / Katri Lindfors / L.J. Meyers / Ludwig Sollid)
- **Transglutaminases and Neurological Disorders**
  (*Anne-Marie Van Dam* / Ray Truant / Nancy Muma / Beisha Tang)
- **Transglutaminases and Cancer**
  (*Daniel Matei* / Richard Cerione / R.J. Ablin / Dong-Sup Lee / Soichi Kojima)
- **Transglutaminases and Inflammation**
  (*T.S. Johnson* / Stephanie Watts / Soo-Youl Kim / B.S. Tang / Barry Fanburg)
- **Transglutaminases in Bone and Skin Pathology**
  (*Mari Kaartinen* / Laszlo Muszbek / Richard Eckert / Aki Ichinose / Louis Tong)
- **Transglutaminases as Transcription Regulators**
  (*Gail Johnson* / Tristan Croll / Kevin D. Brown / Santosh Kumar / Rajiv R. Ratan)
- **Clinical Applications of Transglutaminases**
  (*Mauro Piacentini* / Jeff Keillor / Martin Griffin / Keith M. Rich)
- **Recent Developments in Transglutaminases (Short Talks)**
  (*Paul Birckbichler, Kapil Mehta*)

TRIBOLOGY
Paths of Dissipation
Jul 8-13, 2012
Colby College, Waterville, ME
Chair: Alfons Fischer
Vice Chair: Roland Bennewitz

- **Extreme Environments**
  (*Somuri Prasad* / W. Gregory Sawyer / Philip Shipway)
- **Computer Simulations**
  (*Izabela Szlufarska* / Michael Moseler / Dik Schipper / Kenneth Holmberg)
- **Friction and Wear on the Microscale**
  (*Kathryn Wahl* / Thomas Scharf / Thierry A. Blanchet)
- **Friction and Adhesion on the Nanoscale**
  (*Robert Carpick* / Andre Schirmeisen / Scott Perry)
- **Tribomaterial - Microstructural & Chemical Alterations**
  (*Martin Dienwiebel* / Pascal Bellon / Wilfried T. Tysoe)
- **Tribocorrosion**
  (*Anne Neville* / Stefano Mischler / Anna Igual Munoz / Margaret Stack)
- **Lubrication - From Boundary to Ultra-Low Friction**
  (*Ashlie Martini* / Maria-Isabel de Barros Bouchet / Nicholas Spencer / Susan Perkin)
- **Biotribology or Tribiology**
  (Lawrence Marks / Markus A. Wimmer / Mark Rainforth)

VIBRATIONAL SPECTROSCOPY
Aug 5-10, 2012
University of New England, Biddeford, ME
Chairs: Franz M. Geiger & Edwin L. Sibert
Vice Chairs: Arthur L. Utz & Mischa Bonn

- **Vibrational Motions in Chemical Reactions**
  (*Tim Zwier* / Brooks Pate / Andrew Orr-Ewing)
- **Vibrational Dynamics in Materials and Energy Conversion**
  (*Nancy Levinger* / Tim Lian / Aaron Massari / Abe Nitzan / John Asbury)
- **Vibrational Dynamics in Biology**
  (Sharon Hammes-Schiffer / Shaul Mukamel)
- **Vibrations at Interfaces**
  (*Sylvie Roke* / Ron Shen / Jim Skinner / Akihiro Morita / Paul Cremer)
- **Spatially Resolved Vibrational Spectroscopy**
  (*Mischa Bonn* / Steve Baldelli / Carol Hirschmugl)
- **Vibrational Spectroscopy in the Environment**
  (Lynn Russell / Mitchio Okumura / Vicki Grassian / Anne McCoy)
- **Vibrational Spectroscopy in Catalysis**
  (*Art Utz* / Bert Weckhuysen / Victor Batista)
- **New Methods for Probing Structure and Dynamics**
  (*Ted Heilweil* / Dan Neumark / Tucker Carrington / Hans-Dieter Meyer)
- **Retrospective and Prospective**
  (*Fleming Crim* / Mark Johnson)

VISUAL SYSTEM DEVELOPMENT
Aug 19-24, 2012
Colby-Sawyer College, New London, NH
Chair: Helen McNeill
Vice Chair: Brian Link

- **Keynote Presentations**
  (*Helen McNeill, Brian Link* / Larry Zipursky / Joshua Sanes)
- **Stem Cell and Proliferation I**
  (*Tom Reh* / Derek Van der Kooy / Georg Halder)

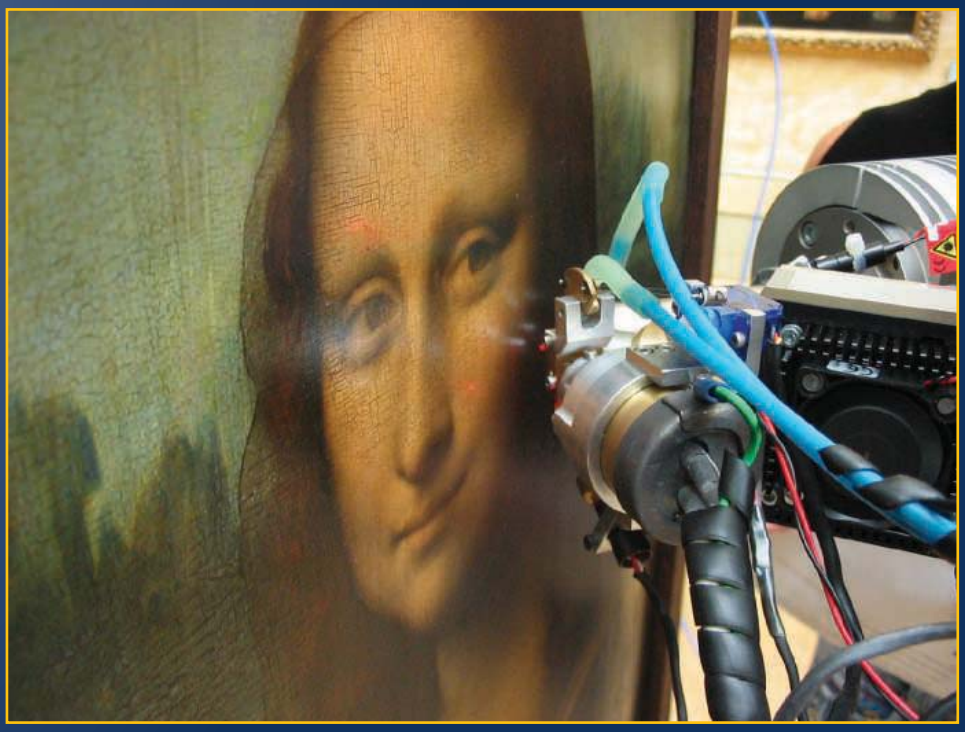

X-ray fluorescence analysis of the Mona Lisa painting in the Musée du Louvre. Courtesy of Philippe Walter, (c)ESRF, A. Solé. Submitted by Heinz-Eberhard Mahnke & Marco Leona, Chairs, Scientific Methods in Cultural Heritage Research GRC.

- **Stem Cell and Proliferation II**
  (*Tom Reh* / Edward Levine / Yoshiki Sasai)
- **Chromatin and Competence**
  (*Michael Dyer* / Itsuki Ajioka / Jessica Treisman / Monica Vetter)
- **Glia**
  (*Edward Levine* / Christian Klambt / Iris Salecker / Seth Blackshaw)
- **Non-Neural Tissue Development**
  (*Tiffany Cook* / Richard Lang / Jeffrey Gross)
- **Circuitry and Synapses**
  (Botond Roska / Takahisa Furukawa / Lisa Goodrich)
- **Morphogenesis and Trafficking**
  (*Marek Mlodzik* / Don Ready / Ching-Hwa Sung / Nic Tapon)
- **Emerging Topics in Vision Research**
- **Evolution**
  (*Claude Desplan* / William Jeffery)
- **Signaling and Transcription I**
  (*Michel Cayouette* / Tom Reh / David Lubensky / Erika Bach)
- **Signaling and Transcription II**
  (Valerie Wallace / Joe Corbo / Graeme Mardon)
- **Disease Mechanisms**
  (*Brian Link* / Brian Brooks / Richard Maas)

WATER & AQUEOUS SOLUTIONS
Aug 12-17, 2012
Holderness School, Holderness, NH
Chair: Dor Ben-Amotz
Vice Chair: Douglas Tobias

- **When Oil and Water Meet I**
  (*Noam Agmon* / Boris Akhremitchev / Gilbert Walker / Shekhar Garde)
- **Molecular Water-Ballet**
  (*Peter Rossky* / Andrei Tokmakoff / Peter Hamm / Casey Hynes / Song-I Han)
- **Exotic Flavors of Water I**
  (*Nobuyuki Matubayasi* / Alan Soper / Anders Nilsson / Rich Saykally)
- **When Oil and Water Meet II**
  (*Kersti Hermansson* / Ruth Lynden-Bell / Valeria Molinero / William Ducker / Ben Widom)
- **Exotic Flavors of Water II**
  (*Pablo Debenedetti* / Austen Angell / Tom Markland / David Chandler)
- **Charges on the Edge I**
  (*Sylvie Roke* / James Beattie / Pavel Jungwirth / Steve Rick / Lyudmila Slipchenko)
- **Charges on the Edge II**
  (*Nancy Levinger* / Maria Fernandez-Serra / Susan Rempe / Mike Fayer)
- **Coming to Life**
  (*Lorna Dougan* / Dmitry Matyushov / Gerhard Hummer / Josh Wand / Irit Sagi)
- **Keynote Presentation / Poster Presentations**
  (*Paul Cremer* / Karen Meech)

Water & Aqueous Solutions
Aug 11-12, 2012
Chair: Sapna Sarupria
Associate Chair: Robin C. Underwood

Apply online now at ***www.grc.org*** *and be a part of the experience...*

Join us at a GRC or GRS in 2012!

GRC would like to formally acknowledge and congratulate our 2012 Alexander M. Cruickshank Award Lecturers:

Bonnie Bassler (Microbial Stress Response), **Angela M. Belcher** (Renewable Energy: Solar Fuels), and **Naomi Halas** (Noble Metal Nanoparticles)

The Board of Trustees of the Gordon Research Conferences established the Alexander M. Cruickshank Lectures to honor the many years of service to the organization by the former director, Dr. A.M. Cruickshank. Three awards are given annually - one for each of the principal subdisciplines of the Conferences, namely the Biological, Chemical, and Physical Sciences.

New Products: General Lab Equipment

ZOOM MICROSCOPE

The Axio Zoom.V16 combines the typical benefits of stereomicroscopes such as zoom optics and long working distances with the higher resolutions of traditional light microscopes. In comparable image fields, the Axio Zoom.V16 offers a 2.5 times higher resolution and 10 times brighter fluorescence than stereomicroscopes. With a 16x zoom range, the Axio Zoom.V16 surpasses all comparable microscopes currently available. An extensive line of accessories enables configurations precisely tailored to many different applications. An illumination concept specially developed for zoom microscopes delivers considerably higher fluorescence illumination intensity, with even the smallest fluorescent structures remaining visible. The Axio Zoom.V16 incorporates totally new approaches not only to visual observation, but also to imaging. Higher apertures substantially reduce the depth of field ranges in the focal plane. Structured illumination with the Apotome.2 slider system makes it possible to generate optical sectional images and 3-D reconstructions of the specimens.

Carl Zeiss
For info: 800-509-3905 | www.zeiss.de

LOW VOLUME MICROPLATE

The MicroMax Low Volume Microplate offers researchers the benefit of measuring up to 64 samples per plate on the SpectraMax microplate readers. The elegant simplicity of the MicroMax design provides remarkable flexibility, ideal for multiuser environments. The customer can use either 2 or 4 µL samples, and will have a variety of cleaning options available: simply wiping the slide, autoclaving, or replacing the slides. The unique, no-hinge design offers great uniformity with no maintenance and simplifies the cleaning process. Perfect for core labs, bioprocessing quality control/manufacturing environments, biorepositories, and molecular diagnostics labs, the 8- or 16-channel pipettor compatibility of 24- or 64-sample plates, respectively, enables fast determinations of a wide range of samples including DNA, RNA, and proteins. The MicroMax Low Volume Microplates are compatible with all SpectraMax readers. The low-volume plates have ready-to-use application specific protocols in SoftMax Pro Data Analysis and Acquisition Software for seamless integration.

Molecular Devices
For info: 800-635-5577 | www.moleculardevices.com

SPECTROPHOTOMETERS

The new Ultrospec series of dual beam, ultraviolet-visible spectrophotometers provides research scientists with a choice of smart instruments with diverse capabilities to deliver reproducible results, precision, and ease of use to match a variety of user requirements. The series includes Ultrospec 7000/7000PC for day-to-day laboratory activities, Ultrospec 8000/8000PC, and the top of the range 9000/9000PC system for demanding assays. Each version is available as either a standalone or PC-controlled system. The Ultrospec range benefits from the following features: dual-beam instrument (with a variety of bandwidths); color touchscreen (for standalone product); USB data and PC connectivity; European Pharmacopoeia research compatibility (8000/9000 models); Datrys Standard (option to upgrade to Datrys Life Science or Datrys CFR); Equation Editor software; and extended range of accessories available such as thermostatting, Bluetooth, and Datrys software options.

GE Healthcare
For info: 800-526-3593 | www.gelifesciences.com

ANALYTICAL LAB BALANCE

The Kern ABT high-precision laboratory analytical balance automatically recalibrates itself under four scenarios: every four hours, after temperature fluctuations of 0.5°C (0.9°F), when switching from standby to weighing, and after being reconnected to its power source. Prior to a recalibration the balance alerts technicians, who can postpone the process until their weighing operation is complete. The laboratory balance automatically outputs GLP/ISO data to a PC or printer. Two models of this fast-responding electronic analytical balance operate in dual weighing ranges. Four other single weighing range models are available. All are tailor-made for organizations demanding high-precision electronic scales delivering stable temperature behavior, a short stabilization time, and excellent weighing precision even with samples at the edge of the pan. The versatile ABT analytical balances also accommodate piece counting, recipe weighing, percentage determination, suspended weighing capabilities, metric/non-metric operation, and feature large LCD displays.

Tovatech
For info: 973-913-9734 | www.tovatech.com

H_2O_2 INCUBATOR-DECONTAMINATION SYSTEM

The unique hydrogen peroxide vapor decontamination option provides complete decontamination while limiting incubator downtime to less than three hours. The automated H_2O_2 cycle protects user safety and can be validated, if desired, ensuring compliance with the highest cGMP, GLP, and GRP standards. Available with Sanyo's MCO-19AIC CO_2 and MCO-19M multi-gas incubators, the H_2O_2 system enables full decontamination and incubator cleaning to be completed in less than a morning. As this is a low temperature process there is no heat stress on electrical components and zero impact on adjacent equipment and the surrounding environment. All interior components and the CO_2 sampling loop are decontaminated in situ, bypassing the need for a separate autoclave cycle. Following a seven-minute H_2O_2 vaporization, the ultraviolet lamp switches on for 90 minutes, reducing the H_2O_2 to water vapor and oxygen. The incubator's interior fan circulates air throughout the chamber during the entire cycle.

Sanyo
For info: +31-765-433833 | www.eu.sanyo.com

Electronically submit your new product description or product literature information! Go to **www.sciencemag.org/products/newproducts.dtl** for more information.

Newly offered instrumentation, apparatus, and laboratory materials of interest to researchers in all disciplines in academic, industrial, and governmental organizations are featured in this space. Emphasis is given to purpose, chief characteristics, and availability of products and materials. Endorsement by *Science* or AAAS of any products or materials mentioned is not implied. Additional information may be obtained from the manufacturer or supplier.

Science

This is an abbreviated version of *Science*'s Information for Authors. Complete Information for Authors is available at www.sciencemag.org/about/authors.

Science is a weekly peer-reviewed journal that publishes significant, original scientific research, plus reviews and analyses of current research and science policy. We welcome submissions from all fields of science and from any source. Competition for space in *Science* is keen, and many papers are returned without in-depth review. Priority is given to papers that reveal novel concepts of broad interest.

PEER-REVIEWED MANUSCRIPTS

Research Articles (up to ~4500 words or ~5 pages in print) are expected to present a major advance. Research Articles include an abstract, an introduction, up to six figures or tables, sections with brief subheadings, and a maximum of about 40 references.

Reports (up to ~2500 words or ~3 pages in print) present important new research results of broad significance. Reports should include an abstract, an introductory paragraph, up to four figures or tables, and a maximum of about 30 references.

Brevia (1 page; about 800 words and one figure or table, and a maximum of about 10 references) are short peer-reviewed papers presenting novel results of broad general interest.

In the above manuscripts, materials and methods, along with other information needed to support the conclusions, should be presented as supplementary materials.

Reviews (4 print pages, on average) describe new developments of interdisciplinary significance and highlight unresolved questions and future directions. They include an abstract, an introduction that outlines the main point, sections with brief subheadings, and a maximum of about 40 references. Most Reviews are solicited by the editors, but unsolicited submissions are considered occasionally.

COMMENTARY

Science's Commentary section presents analysis by scientists and other experts on issues of interest to *Science* readers.

Policy Forums (1000 or up to 2000 words) present issues at the intersection between science and society that relate to science policy.

Education Forums (1000 or up to 2000 words) present essays on science education and its practice, from preschool through postgraduate education. (Research results related to education should be submitted to the Reports section.)

Books *et al.* (up to 1000 words) present reviews of current books, multimedia, exhibitions, and films of interest to *Science* readers.

Perspectives (up to 1000 words) analyze recent research developments but do not primarily discuss the author's own work. Book reviews, Education and Policy Forums, and Perspectives are frequently solicited by the editors, but unsolicited contributions will be considered.

Letters (up to 300 words) discuss material published in *Science* in the last 3 months or issues of general interest. Letters should be submitted online (www.submit2science.org) and are edited for clarity and space.

COMMENTS

Technical Comments (up to 1000 words, 2 figures or tables, and 15 references) are published online and discuss the core conclusions and/or methodology of research published in *Science* within the previous 3 months. A brief abstract is included in the Letters section of the print edition. Technical Comments should not present new data or other previously unpublished work nor be based on new findings/concepts that would not have been accessible to the authors when the target paper was written. Pertinent comments on noncentral aspects of a paper should be submitted as online comments.

Authors of Technical Comments should contact the authors of the target paper before submitting their manuscript, and should submit to *Science* the evidence of any correspondence. Technical Comments may be peer-reviewed. We hope to post accepted Technical Comments promptly online along with a formal reply from the authors of the original paper.

Online Comments. Brief online comments can be submitted on papers or news stories from the full-text view on *Science* Online and will be evaluated promptly. Authors are identified and must agree to our terms and conditions (http://comments.sciencemag.org/terms).

Science Contact Information

Phone: (1)-202-326-6550 (USA)
(44)-1223-326500 (UK)

E-mail: science_editors@aaas.org (USA)
science@science-int.co.uk (Europe)

MANUSCRIPT SELECTION

We are committed to the prompt evaluation and publication of submitted papers through our fully electronic submission and review process. Papers are assigned to a staff editor who has knowledge of the field(s) discussed in the manuscript. Most submitted papers are rated for suitability by members of the Board of Reviewing Editors (see the masthead). The editors at *Science* consider their advice in selecting papers for in-depth review. Authors of papers that are not highly rated are notified promptly, by e-mail only, within 2 weeks. Membership in AAAS is not a factor in selection.

Papers selected for in-depth review are reviewed by at least two anonymous referees. Reviewers are contacted before being sent a paper and are asked to return comments within 2 weeks. We are able to expedite the review process for papers that require rapid assessment. Papers selected for publication are edited to improve accuracy and clarity and to shorten, if necessary. Most papers are published 4 to 8 weeks after acceptance; selected papers are published rapidly online in *Science* Express (www.sciencexpress.org).

Papers cannot be resubmitted over a disagreement on interest or relative merit. If a paper was rejected on the basis of serious reviewer error, resubmission may be considered. Papers submitted to *Science* but not accepted for publication may be eligible for publication in *Science Signaling* or *Science Translational Medicine*.

SUBMISSION REQUIREMENTS

Authorship. All authors must agree to be so listed and must have seen and approved the manuscript and its submission to *Science*. Any changes in authorship must be approved in writing by all the original authors. Submission of a paper that has not been approved by all authors will result in immediate rejection without appeal.

Submitting a Manuscript or Letter

Science accepts submissions of manuscripts and letters only through our Web site: www.submit2science.org. We are not able to accept submissions by e-mail. Your submission should include a cover letter containing a statement of the paper's main point, any information needed to ensure a fair review process, and names of colleagues who have reviewed the paper for you.

PDF copies of related papers (see submission requirements) should be sent as a PDF by e-mail to science_editors@aaas.org along with your Web submission number.

Published by AAAS

Prior publication. *Science* will not consider any paper or component of a paper that has been published or is under consideration elsewhere. Distribution on the Internet may be considered prior publication and may compromise the originality of the paper. Reporting the main findings of a paper in the mass media may compromise the novelty of the work and thus its appropriateness for *Science*. Please contact the editors with questions regarding these policies.

Human studies. Informed consent must have been obtained for studies on humans after the nature and possible consequences of the studies were explained. All research on humans must have approval from the author's institutional review board (IRB) or equivalent body.

Animal care. Care of experimental animals must be in accordance with the author's institutional guidelines.

Related papers. Copies of papers submitted to other journals by any of the authors that relate to the paper submitted to *Science* must be included with the submission.

Unpublished data and personal communications. Citations to unpublished data, in-press papers, and personal communications cannot be used to support claims in the paper.

Dual use. Authors and reviewers are expected to notify editors if a manuscript could be considered to report dual-use research of concern. Papers identified as such will be brought to the attention of the Editor-in-Chief for further evaluation. If necessary, outside reviewers with expertise in the area will be consulted.

Manuscript Preparation

(See www.sciencemag.org/about/authors for more information.)

Titles should be no more than 96 characters for Reports, Research Articles, and Reviews, and 64 characters for Brevia.

One-sentence summaries should be submitted for all papers.

Abstracts explain to the general reader why the research was done and why the results are important. The abstract should present, in no more than 125 words, background information to convey the context of the research, describe the results, and draw general conclusions.

Text starts with a brief introduction describing the paper's significance, which should be intelligible to readers in other disciplines. Technical terms should be defined. Symbols, abbreviations, and acronyms should be defined the first time they are used. All tables and figures should be cited in numerical order.

References and notes are numbered in the order in which they are cited, first through the text, then through the text of the references, then through the figure and table legends, and finally through the supplementary materials. Each reference should have a unique number; do not combine references or embed references in notes. Do not use op. cit. or ibid. Titles can be included in references and will appear in our online version. There should be only one reference list, containing all of the citations in the paper and in the supplementary materials.

Acknowledgments, including complete funding information; a statement indicating the availability of data, including accession numbers; and any information related to authorship conflict of interest should be gathered into an unnumbered note at the end of the references.

Tables should be included at the end of the references and should supplement, not duplicate, the text. The first sentence of the table legend should be a brief descriptive title. Every vertical column should have a heading, consisting of a title with the unit of measure in parentheses. Units should not change within a column.

Figure legends should be double-spaced and in numerical order. The figure title should be given as the first line of the legend. No single legend should be longer than ~200 words. Nomenclature, abbreviations, symbols, and units used in a figure should match those used in the text. Units should be metric and follow SI conventions.

Supplementary Materials are posted permanently on *Science* Online, are linked to the manuscript, and are freely available. Files can include materials and methods, figures, tables, and video or audio clips that are important for the integrity of the paper.

Figures should be submitted as part of the online submission or, if necessary for large files only, on a CD or DVD. No part of a figure may be selectively manipulated. When figures are assembled from multiple gels or micrographs, a line or space should indicate the border between two original images. See our online Information for Authors for information on preparing art.

CONDITIONS OF ACCEPTANCE

Authorship, funding, and conflict of interest. All authors must disclose all affiliations, funding sources, and financial or management relationships related to a paper, including those that could be perceived as potential sources of bias, before acceptance. *Science* now requires all authors of accepted papers to affirm their contribution to a paper and agree to our policies on data and materials availability. The senior author from each group is required to have examined the raw data that his/her group has produced.

Data deposition. Before publication, large data sets, including but not limited to microarray data, protein or DNA sequences, and atomic coordinates and structure factors for macromolecular or chemical structures, must be deposited in an approved database, an accession number must be included in the published paper, and the deposited information must be released at the time of publication. Electron micrograph maps must also be deposited. Approved databases are listed online. Large data sets with no appropriate repository must be housed as part of the supplementary materials at *Science*, or when this is not possible, on the author's Web site, provided that a copy of the data is held in escrow at *Science* to ensure availability to readers.

Data availability and materials sharing. After publication, all data and computer codes necessary to understand, assess, and extend the conclusions of the manuscript must be available to any reader of *Science*, and all reasonable requests for materials must be fulfilled. Before acceptance, *Science* must be informed of any restrictions on sharing of materials (materials transfer agreements or patents, for example) applying to materials used in the reported research.

License and access policies. Authors retain copyright but must agree to grant to *Science* an exclusive license to publish the paper in print and online. Any author whose university or institution has policies or other restrictions limiting their ability to assign exclusive publication rights (such as Harvard, MIT, or Open University) must apply for a waiver or other exclusion from that policy or those restrictions. After publication, authors may post the accepted version of the paper on their personal Web site and are provided one referrer link that can be posted on a personal or institutional Web page, through which users can freely access the published paper on *Science*'s online site. *Science* allows deposition of accepted papers into repositories if mandated by funders with a release 6 months after publication and provided that a link to the final version published in *Science* is included. Original research papers are freely accessible with registration on *Science*'s Web site 12 months after publication.

Press coverage. The paper should remain a privileged document and should not be released to the press or the public before publication. Questions should be referred to the AAAS Office of Public Programs (202-326-6440).

POSITIONS OPEN

ASSOCIATE OR FULL PROFESSOR
Obesity Research
University of Iowa

The University of Iowa Carver College of Medicine is seeking a full-time faculty member in the Department of Surgery, Division of Gastrointestinal, Minimally Invasive, and Bariatric Surgery at the level of Associate or Full Professor in the tenure-track. The successful candidate for this position will be expected to participate actively in an ambitious new University of Iowa Obesity Initiative, which is a multidisciplinary initiative in obesity research and education. New faculty with expertise in basic biomedical research and in translational and community based obesity research will complement the University's existing expertise in these areas to form the core of this innovative multidisciplinary initiative. Participation in the Obesity Research Initiative will be an important component in performance evaluations. The new hire will be among the first new faculty appointments to the Fraternal Order of Eagles Diabetes Research Center.

Candidates must possess a M.D. and/or Ph.D. (or equivalent). Candidates must have an established record of research excellence, including a record of sustained external research funding with R01 funding being highly desirable and ongoing scholarly productivity. Candidates must have experience working effectively in a diverse environment and should have excellent interpersonal and leadership skills.

The new hire may be eligible for appointment as Vice Chair of Research for the Department of Surgery, appointment to a basic science department, as well as appointment to the Dr. Edward and Dordana Mason Professorship.

To apply for this position visit the University of Iowa **website: http://jobs.uiowa.edu, requisition #60275.**

The University of Iowa is an Equal Opportunity/Affirmative Action Employer. Women and minorities are strongly encouraged to apply. Applicant credentials are subject to verification; background checks will be conducted on final candidates for all positions in the University of Iowa Hospitals and Clinics.

POSTDOCTRAL/RESEARCH ASSOCIATE POSITIONS

Positions available to study the molecular signaling, gene expression and functional analysis of guanylyl cyclase/natriuretic peptide receptor by transcriptional analysis, protein phosphorylation, and intracellular trafficking in transfected cells in vitro and gene-targeted mouse models in vivo. The project one involves investigation of functional genomics by characterizing the genes involved in renal and cardiac hypertrophy and fibrosis in Npr1 gene-targeted mice. Experience in the in vivo studies of mice will be preferred. The project two involves studying the transcriptional regulation involving promoter analysis, EMSA, and CHIP both in vitro and in vivo systems. The project three involves analysis of receptor dynamics, protein phosphorylation, and intracellular trafficking using confocal and fluorescence microscopy in model cell systems. Strong background in biochemistry and molecular biology is highly desirable. The successful applicant(s) will be expected to have motivation and vision to develop independent research program. Excellent opportunities are available for academic career advancement. Send resume and list of three references to **K.N. Pandey** (**e-mail: kpandey@tulane.edu**), **Tulane University Health Sciences Center, 1430 Tulane Avenue, New Orleans, LA 70112.**
Equal Opportunity/Affirmative Employer.

POSITIONS OPEN

OPEN FACULTY SEARCH
University of Illinois at Chicago

The University of Illinois at Chicago (UIC) invites applications for a tenured faculty position at either the **ASSOCIATE** or **FULL PROFESSOR** level, starting Fall 2012.

We seek an outstanding candidate who is a leader in the field of bioinformatics, chemical biology, drug discovery, epigenetics, lipidomics, metabolomics, proteomics, or systems biology. The candidate must possess strong interpersonal, communication, and project management skills, and is expected to coordinate a multidisciplinary research program.

The successful candidate will join a vibrant community of faculty in the Chicago area, many of who are members of the Chicago Biomedical Consortium (CBC). The CBC will supplement the recruitment funds from the Searle Funds at The Chicago Community Trust. The mission of the CBC is to stimulate and nurture major research collaborations among biomedical scientists at Northwestern University, The University of Chicago, and UIC. Compensation is competitive and commensurate with experience.

For fullest consideration, please enter curriculum vitae and a brief summary of research plans online at **website: https://jobs.uic.edu** by March 15, 2012. The position will remain open until filled. *UIC is an Affirmative Action/Equal Opportunity Employer organization.*

CO-DIRECTOR of
Aquaculture Facility and Instructor of Biology

The Northern Aquaculture Demonstration Facility and the Department of Biology, University of Wisconsin–Stevens Point, has a co-director and teaching academic staff, 12-month position, beginning July 2012. Responsibilities include leading nationally recognized research, demonstration, education and outreach program in aquaculture and teaching assignments that include introductory biology courses. Research with undergraduates, department service, and student advising are expected. Ph.D. required with broad training in biology with emphasis in aquaculture or fish biology. Experience showing outreach, publications, research experience, grantsmanship, and commitment to undergraduate education are required.

Include curriculum vitae, statements of teaching philosophy and research interests, three letters of recommendation, and undergraduate and graduate transcripts. Send application materials to: **Dr. C. Yahnke, Chair; Biology Department, University of Wisconsin–Stevens Point; Stevens Point, WI 54481. Review begins 9 March 2012.** For info, **telephone: 715-346-2455, e-mail: cyahnke@uwsp.edu.**

Affirmative Action/Equal Opportunity Employer.

ASSISTANT PROFESSOR OF SURGERY

The Department of Surgery at the University of Pittsburgh seeks qualified applicants to fill a position in the Division of Surgical Oncology at the rank of Assistant Professor in the tenure stream. Outstanding individuals are encouraged to apply to conduct research in tumor immunology. Preferred M.D.-Ph.D. although either degree possible. At least five years of postgraduate experience in tumor immunology, damage associated molecular pattern molecule biology, and/or cancer biology. Should be able to work effectively within a dynamic environment and interact collaboratively with other scientists—publication record in high-ranking journals commensurate with experience.

Closing date is March 15, 2012. Candidates should reply with current curriculum vitae, a statement of research interest, and three letters of reference. Send replies to **e-mail: lotzemt@upmc.edu.**

The University of Pittsburgh is an Affirmative Action/Equal Opportunity Employer.

2012 Cold Spring Harbor Laboratory Meetings & Courses

Meetings

Meeting Date / Abstracts Due

PTEN Pathways & Targets
March 13 - 16 / January 13

Systems Biology: Global Regulation of Gene Expression
March 20 - 24 / January 13

Neuronal Circuits
March 28 - 31 / January 20

Evolution of *Caenorhabditis* and Other Nematodes
April 3 - 6 / January 27

Automated Imaging & High-Throughput Phenotyping
April 10 - 14 / January 27

Molecular Pathways in Organ Development & Disease
April 17 - 21 / February 3

Gene Expression and Signaling in the Immune System
April 24 - 28 / February 10

Molecular Chaperones & Stress Responses
May 1 - 5 / February 17

The Biology of Genomes
May 8 - 12 / February 24

The Cell Cycle
May 15 - 19 / March 2

Retroviruses
May 21 - 26 / March 9

77th Symposium: The Biology of Plants
May 30 - June 4 / March 16

Glia in Health & Disease
July 19 - 23 / May 4

Mechanisms & Models of Cancer
August 14 - 18 / June 1

Bacteria, Archaea and Phages
August 21 - 25 / June 8

Regulatory & Non-Coding RNAs
August 28 - September 1 / June 15

Translational Control
September 4 - 8 / June 22

Epigenetics & Chromatin
September 11 - 15 / June 29

Axon Guidance, Synapse Formation and Regeneration
September 18 - 22 / July 6

Dynamic Organization of Nuclear Function
September 27 - October 1 / July 13

Germ Cells
October 2 - 6 / July 20

Molecular Genetics of Aging
October 9 - 13 / July 27

Nuclear Receptors & Disease
October 30 - November 3 / August 17

Personal Genomes & Medical Genomics
November 14 - 17 / August 31

Neurodegenerative Diseases
November 28 - December 1 / September 14

Blood Brain Barrier
December 5 - 8 / September 21

Courses

Course Date / Applications Due

Protein Purification & Characterization
April 11 - 24 / January 30

Cell & Developmental Biology of *Xenopus*
April 13 - 24 / January 30

Workshop on Schizophrenia & Related Disorders
June 6 - 12 / March 15

Single Cell Analysis
June 6 - 19 / March 15

Advanced Bacterial Genetics
June 6 - 26 / March 15

Ion Channel Physiology
June 6 - 26 / March 15

Mouse Development, Stem Cells & Cancer
June 6 - 26 / March 15

Workshop on Cognitive Aging
June 13 – 17 / March 15

Computational Neuroscience: Vision
June 20 - July 3 / March 15

Statistical Analysis of Genome Scale Data
June 22 - July 3 / March 15

Frontiers & Techniques in Plant Science
June 29 - July 19 / March 15

***Drosophila* Neurobiology: Genes, Circuits & Behavior**
July 2 - 19 / March 15

Advanced Techniques in Molecular Neuroscience
July 3 - 19 / March 15

Proteomics
July 7 - 22 / March 15

Workshop on Biology of Social Cognition
July 11 - 17 / March 15

Brain Tumors
July 19 - 25 / April 15

Computational Cell Biology
July 24 - August 13 / April 15

Eukaryotic Gene Expression
July 24 - August 13 / April 15

Imaging Structure & Function in the Nervous System
July 24 - August 13 / April 15

Yeast Genetics & Genomics
July 24 - August 13 / April 15

Stem Cells
July 27 - August 5 / April 15

Genetics of Complex Human Diseases
August 7 - 13 / April 15

Programming for Biology
October 15 - 30 / July 15

X-Ray Methods in Structural Biology
October 15 - 30 / June 15

Antibody Engineering & Phage Display
October 17 - 30 / July 15

Advanced Sequencing Technologies & Applications
October 18 - 30 / July 15

Computational & Comparative Genomics
October 31 - November 6 / July 15

The Genome Access Course
April 29 - May 1, November 14 -16

Cold Spring Harbor Laboratory Meetings & Courses Program, 1 Bungtown Road, Cold Spring Harbor, NY 11724
Phone: 516 367 8346 email: meetings@cshl.edu www.cshl.edu/meetings

Chinese Academy of Sciences
Max-Planck-Gesellschaft

The Max-Planck-Gesellschaft (MPG)

is searching for the

Head of a Paul Gerson Unna Research Group of the Max Planck Society

in the field of

Skin and hair follicle morphogenesis, molecular biology of the ageing skin, and related areas

The group will be located at the

CAS-MPG PARTNER INSTITUTE FOR COMPUTATIONAL BIOLOGY (PICB)

in Shanghai

The CAS-MPG Partner Institute for Computational Biology, Shanghai Institutes for Biological Sciences, Chinese Academy of Sciences, is a joint non-profit research institution founded by the Chinese Academy of Sciences and the German Max Planck Society. Please visit the Institute's website for further information (http://www.picb.ac.cn/). The proximity to experimentally oriented, internationally competitive research institutes on the campus of the Shanghai Institutes for Biological Sciences allows close scientific cooperation and interaction between theoretical and experimental research.

The recruitment procedure will be carried out jointly by CAS and MPG. The position is limited to five years. It includes a five-year grant with research positions, running budget, and investments.

Applications should include a tabular CV, a list of publications with reprints of three selected papers, a description of major scientific achievements and a summary of future research plans. Successful candidates should be prepared to attend a symposium planned to be held in the middle of May 2012, in Shanghai. Travel and accommodation expenses will be covered.

The Max Planck Society is committed to equal opportunities and to employing individuals with disabilities.

The deadline for application is **March 16, 2012**.

Applications should be sent to:

Barbara SPIELMANN
E-mail: spielmann@gv.mpg.de
Max-Planck-Gesellschaft
Hofgartenstraße 8, 80539 München, Germany
Phone: +49-89-2108 1365, Fax: +49-89-2108 1041

Yi CHEN
E-mail: ychen@picb.ac.cn
CAS-MPG Partner Institute for Computational Biology (PICB), Shanghai Institutes for Biological Sciences (SIBS), Chinese Academy of Sciences (CAS)
320 Yueyang Road, Shanghai 200031, P.R. China
Phone: +86-21-5492 0456, Fax: +86-21-5492 0451

UAB THE UNIVERSITY OF ALABAMA AT BIRMINGHAM
http://www.uab.edu

Associate/Full Professor

Department of Neurobiology

The Department of Neurobiology at UAB invites applications for a tenured or tenure-track position in **Cognitive Epigenetics** at the rank of Associate or Full Professor. The Department is recruiting an outstanding scientist who applies studies of epigenetic molecular mechanisms to questions related to cognitive and behavioral neuroscience, learning and memory, and learning/memory disorders including aging-related memory dysfunction.

The Department of Neurobiology offers a collegial and creative environment and is housed in the Evelyn F. McKnight Brain Institute comprising three floors (approximately 75,000 square feet) of the recently built Annette and Richard Shelby Research Building. UAB is one of the leading academic medical centers in the country and the Department of Neurobiology is currently ranked among the top 20 in NIH funding among all U.S. Neuroscience Departments. More information can be found at **www.neurobiology.uab.edu**. The deadline for applications will be March 30, 2012. Applicants should provide a CV, brief description of research interests and names of 3-5 references to: Lissa LaRue, University of Alabama at Birmingham, Department of Neurobiology, 1825 University Blvd. SHEL 903, Birmingham, AL 35294-2182, E-mail: **llarue@uab.edu**

UAB is an Equal Opportunity/Affirmative Action Employer committed to fostering a diverse, equitable and family-friendly environment in which all faculty and staff can excel and achieve work/life balance irrespective of ethnicity, gender, faith, and sexual orientation. UAB also encourages applications from individuals with disabilities and veterans.

MAYO CLINIC

Postdoctoral Position – Division of Pulmonary and Critical Care Medicine

Heal the sick, advance the science, share the knowledge.

Postdoctoral positions are available immediately in the laboratory of Dr. Edward Leof at the Mayo Clinic in Rochester, Minnesota. General areas of study include:

1. Characterizing the cellular machinery and cis-acting elements mediating TGF-B receptor trafficking;
2. Delineating the mechanisms controlling cell type-specific TGF-B signaling; and
3. Investigating the role of TGF-B in the pathogenesis of lung and kidney fibrosis.

See Cancer Res. 69(1): 84-93, 2009; Dev. Cell 16(3): 433-44, 2009; Cancer Res. 70(19): 7421-30, 2010; Mol. Biol. Cell 21(22): 4009-19, 2010; and J. Biol. Chem. 286(20): 17841-50, 2011 for recent related studies.

Mayo Clinic College of Medicine is a not-for-profit organization that integrates research with clinical practices and education in a multi-campus environment. Mayo offers an attractive benefits package. Salary will be determined by the successful candidate's experience. For further information, please visit **http://www.mayo.edu/**

Please forward curriculum vitae, a summary of past accomplishments and names and e-mail addresses of three references to:

Ms. Trish Iverson
Division of Pulmonary and Critical Care Medicine
Mayo Clinic
200 First Street SW • Rochester, MN 55905
Email: iverson.patricia@mayo.edu

Mayo Clinic College of Medicine is an affirmative action and equal opportunity employer and educator.

77th Cold Spring Harbor Symposium on Quantitative Biology

The Biology of Plants

May 30 - June 4, 2012

Abstracts due March 16, 2012

Speakers:

Rick Amasino, *University of Wisconsin. Madison*
Julia Bailey-Serres, *University of California, Riverside*
James Barber, *Imperial College London, United Kingdom*
Kathryn Barton, *Carnegie Institution of Science*
David Baulcombe, *University of Cambridge, United Kingdom*
Philip Benfey, *Duke University*
Frederic Berger, *Temasek Life Sciences Laboratory, Singapore*
Dominique Bergmann, *Stanford University*
Thomas Brutnell, *Donald Danforth Plant Science Center*
Vicki Chandler, *Gordon & Betty Moore Foundation*
Xuemei Chen, *University of California, Riverside*
Joanne Chory, *The Salk Institute for Biological Studies*
Jeffrey Dangl, *University of North Carolina, Chapel Hill*
John Doebley, *University of Wisconsin, Madison*
Xinnian Dong, *Duke University*
Joseph Ecker, *The Salk Institute for Biological Studies*
Mark Estelle, *University of California, San Diego*
Wolf Frommer, *Carnegie Institution at Stanford University*
Mary Gehring, *Whitehead Institute*
Niko Geldner, *University of Lausanne, Switzerland*
Ueli Grossniklaus, *University of Zurich, Switzerland*
Sarah Hake, *USDA / University of California, Berkeley*
Stacey Harmer, *University of California, Davis*
Martin Howard, *John Innes Institute, United Kingdom*
David Jackson, *Cold Spring Harbor Laboratory*
Steven Jacobsen, *University of California, Los Angeles*
Georg Jander, *Boyce Thompson Institute*
Jonathan Jones, *John Innes Institute, United Kingdom*
Tetsuji Kakutani, *National Institute of Genetics, Japan*
Sophien Kamoun, *The Sainsbury Laboratory, United Kingdom*
Steven Kay, *University of California, San Diego*
Cris Kuhlemeier, *University of Bern, Switzerland*
Thomas Laux, *University of Freiburg, Germany*
Ottoline Leyser, *University of Cambridge, United Kingdom*
Xin Li, *University of British Columbia, Canada*
Zachary Lippman, *Cold Spring Harbor Laboratory*
Jan Lohmann, *Heidelberg Institute of Zoology, Germany*
Jeffrey Long, *The Salk Institute for Biological Studies*
Robert Martienssen, *Cold Spring Harbor Laboratory*
Marjori Matzke, *Austrian Academy of Sciences, Austria*
Stephen Mayfield, *University of California, San Diego*
Blake Meyers, *University of Delaware*
Joseph Noel, *The Salk Institute for Biological Sciences*
Jerzy Paszkowski, *University of Geneva, Switzerland*
Craig Pikaard, *Indiana University*
Scott Poethig, *University of Pennsylvania*
Eric Richards, *Boyce Thompson Institute for Plant Biology*
Patrick Schnable, *Iowa State University*
Julian Schroeder, *University of California, San Diego*
Jen Sheen, *Massachusetts General Hospital*
Dorothy Shippen, *Texas A&M University*
Pamela Silver, *Harvard Medical School*
Brian Staskawicz, *University of California, Berkeley*
Marja Timmermans, *Cold Spring Harbor Laboratory*
Keiko Torii, *University of Washington*
Jean-Philippe Vielle-Calzada, *National Laboratory of Genomics for Biodiversity, Mexico*
Richard Vierstra, *University of Wisconsin, Madison*
Olivier Voinnet, *Swiss Federal Institute of Technology Zurich, Switzerland*
Daniel Zamir, *The Hebrew University of Jerusalem, Israel*
Jian-Kang Zhu, *Purdue University*
Daniel Zilberman, *University of California, Berkeley*

Organizers:

Terri Grodzicker, Robert Martienssen,
David Stewart & Bruce Stillman
Cold Spring Harbor Laboratory

Topics:

- Stem Cells & Development
- Gametogenesis & Germ Cells
- Hormones & Signal Transduction
- Cell Division & Cell Cycle
- Regulatory RNAs
- Epigenetics
- Clocks & Rhythms
- Photosynthesis
- Genomics, Speciation & Evolution
- Stress Responses & Adaptation
- Molecular Ecology
- Host-Pathogen Interactions
- Symbiosis
- Metabolism & Biofuels

Registration, abstract submission and further information:
http://www.cshl.edu/meetings ♦ email: meetings@cshl.edu
phone: 516-367-8346 ♦ fax: 516-367-8845

Supported by the National Science Foundation, the Cold Spring Harbor Laboratory Corporate Sponsor Program, the Gatsby Charitable Foundation, and the Gordon & Betty Moore Foundation.

Image credit: Pea plant 3D model by James Whitaker, based on drawings by Gregor Mendel, an Austrian monk whose breeding experiments with garden peas, in 1866, led him to formulate the basic laws of heredity.

Poster credit: Catherine Dougherty

Vector Biologist

The Department of Pathology at the University of Texas Medical Branch in Galveston invites applications for a Vector Biologist faculty position at the Assistant, Associate or full Professor level.

The department is interested in enhancing its successful program in mosquito and tick-borne pathogens. Applicants must have a Ph.D., M.D., D.V.M., or equivalent degree in an appropriate field, with a research record related to arthropod-pathogen-vertebrate host interactions. Preference will be given to applicants with experience and capability in vector-borne disease research demonstrated by an established independent research program. Responsibilities will include establishing an innovative and externally funded vector biology research program, collaborating with others studying vector-borne pathogens, participating in intra- and inter-departmental conferences and meetings, and other activities in the department, pursuing scholarly activities to include research, publications, and presentations at national and international meetings, and teaching of graduate and medical students. Salary and academic rank are commensurate with experience. An excellent benefits package is included.

UTMB has a long history of tropical disease research and currently has a large, diverse and outstanding group of investigators working with bacteria, viruses and parasites, including those that require high containment. Emerging infectious diseases and biodefense are major foci in addition to more basic studies of pathogen biology, ecology and evolution.

UTMB has excellent research infrastructure to conduct research in BSL-2, BSL-3 and BSL-4 laboratories. Arthropod rearing and containment facilities are available for pathogen-free and pathogen-infected mosquitoes, ticks and other vectors at Arthropod Containment Levels (ACL) 2, 3, and 4. Other scientific cores provide access to state-of-the-art proteomics, genomics, electron microscopy, histopathology, virus imaging and structural biology resources. Opportunities are also available to become involved in on-going overseas field research projects.

Interested applicants should send curriculum vitae, a statement of personal and academic goals, and names of three references to: **David H. Walker, M.D., Chairman, Department of Pathology, University of Texas Medical Branch at Galveston, 301 University Boulevard, Galveston, Texas 77555-0609; dwalker@utmb.edu**.

UTMB is an Equal Opportunity, Affirmative Action Institution which proudly values diversity. Candidates of all backgrounds are encouraged to apply.

utmb Health

UNIVERSITY of WASHINGTON

HEAD of the NEUROSCIENCE DIVISION in the WASHINGTON NATIONAL PRIMATE RESEARCH CENTER and FACULTY MEMBER in the DEPARTMENT OF PHYSIOLOGY and BIOPHYSICS

The Washington National Primate Research Center and the Department of Physiology and Biophysics at the University of Washington announce a search for a Core Staff Scientist and full-time faculty member at the Assistant Professor, Associate Professor or Professor level (tenured or tenure track). Individuals appointed at the Associate Professor or Professor level will also serve as Head of the Neuroscience Division in the WaNPRC and will work with departments in the School of Medicine to develop the neuroscience research program in the WaNPRC. We seek an individual (PhD and/or MD) with outstanding scholarly achievements in the field of primate neuroscience. The individual will be expected to maintain a vigorous research program and participate in teaching and service in the Department of Physiology and Biophysics. For information about the Department of Physiology and Biophysics, see our website at **http://depts.washington.edu/pbiopage**. For information about the Washington National Primate Research Center see **http://www.wanprc.org**.

Applicants should submit a curriculum vitae, a description of research accomplishments and plans, and have three letters of reference submitted electronically to **pbsearch@uw.edu**. Review of applications will begin on **February 15, 2011**, and continue until the position is filled.

The University of Washington is building a culturally diverse faculty and strongly encourages applications from women and minority candidates. The University of Washington is an Affirmative Action/ Equal Opportunity Employer. University of Washington faculty engage in teaching, research and service.

Department Chair Biological Sciences

The University of Idaho is seeking an outstanding leader for the Department of Biological Sciences. The department consists of 25 faculty with dynamic extramurally funded research programs, with particular strengths in evolutionary biology, reproductive biology, cellular and molecular biology and biochemistry. This position represents an opportunity to lead new initiatives and guide the future growth of the department. This is a 12 month, tenured position at the rank of professor. Qualified applicants will possess a doctorate in biology or related field, a professional record sufficient to achieve tenure at a senior rank, an internationally recognized, externally funded research program, and experience in teaching at the undergraduate and graduate levels. Review of applications begins 3/15/2012. For a full description and application materials, visit **http://apptrkr.com/231629** announcement #12007021953. For questions relating to the application process, contact Gina Reid at biofac@uidaho.edu. AA/EEO

An Equal Opportunity/Affirmative Action Employer.

RYERSON UNIVERSITY

Founding Dean, Faculty of Science

Ryerson University invites nominations and applications for the position of Founding Dean, Faculty of Science with the appointment to be effective July 2012.

Located in downtown Toronto, Ryerson University is known for innovative programs built on the interaction of theoretical and practically oriented learning. Close to 100 undergraduate, graduate and doctoral-level programs, distinguished by a strong emphasis on excellence in teaching, research and creative activities, are offered to approximately 28,000 students. For more information, please visit www.ryerson.ca.

The newly created and approved Faculty of Science will distinguish itself by developing a distinctive leadership niche in research, teaching and innovation. Its four founding departments – Chemistry and Biology, Computer Science, Mathematics, and Physics – are recognized for their internationally renowned faculty and research, have established themselves as funded engines of research and innovation, and are well positioned to strengthen these foci in the future. Their programs at the masters and doctoral levels are well subscribed and encourage a robust culture of interdisciplinary scholarship, research, innovation and critical analysis. Three new PhDs in Molecular Science, Computer Science and Biomedical Physics have been recently launched.

Reporting to the Provost and Vice President Academic as part of Ryerson's senior administration, the Dean of Science will have an earned doctorate in a relevant field, an exemplary academic record, strong achievements in research, teaching, scholarly activities and service, demonstrated administrative and management capabilities in a collegial university setting, and experience in budget management and resource allocation.

The search committee will begin to consider potential candidates immediately and will continue until the position is filled. Applications should include a letter of introduction, curriculum vitae, and the names of three references (who will not be contacted without consent of the candidate), and may be forwarded electronically, in confidence, to:

Laverne Smith & Associates Inc.
1 Yonge Street, Suite 1801
Toronto, Ontario M5E 1W7
Ryersonsci@lavernesmith.com

Laverne Smith & Associates Inc. LAVERNE SMITH www.lavernesmith.com

---

Genome Sciences

OPEN FACULTY POSITION

The Department of Genome Sciences at the University of Washington is looking for a faculty member to join its Northwest Genomic Center. Research efforts in the department encompass both genetic and genomic analysis of humans and model organisms. The department also has a significant focus in technology development and in computational biology across all levels including sequence, expression, proteomics, network, and genetic analysis. For this position we are seeking individuals with expertise in human genetics and genomics, which can be computational, diagnostically, or technology based. The department invites applications in any of these areas for a full-time faculty position at the rank of RESEARCH ASSISTANT PROFESSOR (without tenure). Applicants should hold a Ph.D. and/or M.D. degree. Applications received by **March 23, 2012**, will receive full consideration. Thereafter, applications will be reviewed upon receipt until the position is filled. Candidates should **e-mail** their curriculum vitae and statement of research, and arrange to have three signed letters of reference sent to: **faculty-search@gs.washington.edu**.

For additional information that may be helpful in preparing an application, see the department's website at **http://www.gs.washington.edu**.

The University of Washington is an Affirmative Action, Equal Opportunity Employer. The University is building a culturally diverse faculty and staff and strongly encourages applications from women, minorities, individuals with disabilities and protected veterans. The University of Washington Faculty engage in teaching, research and service. The University of Washington, a recipient of the 2006 Alfred P. Sloan award for Faculty Career Flexibility, is committed to supporting the work-life balance of its faculty.

AScI
Aalto University Science Institute

Aalto University Science Institute (http://asci.aalto.fi) is an interdisciplinary research institute hosted by the Aalto University School of Science, with a mission to advance collaboration, research and ambitious new initiatives in science at the highest level.

The Institute now invites nominations and applications for

3–5 AALTO SCIENCE FELLOWS

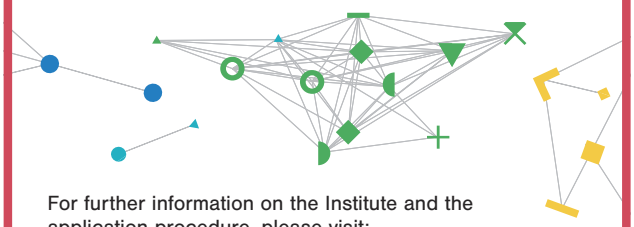

For further information on the Institute and the application procedure, please visit:
http://www.aalto.fi/en/current/jobs/teaching_and_research/

Aalto University, Finland

Aalto University

Download your free copy today.

ScienceCareers.org/booklets

Polish the critical skills you need for a successful job search.

Science Careers is offering a booklet of career advice on topics including choosing a career path, getting the most from a career fair, effective networking, marketing yourself to potential employers, and acing your job interview.

To download the booklet, just sign up for a free *Science* Careers job seeker account by visiting ScienceCareers.org/booklet. Already have an account? Just login and click the link from the "My *Science* Account" page.

Science Careers
From the journal *Science* AAAS

AMITY UNIVERSITY

INDIA'S NO.1 RANKED NON-PROFIT PVT. UNIVERSITY

Part of India's Leading Education Group .....

95,000 STUDENTS, 3,500 FACULTY, 5 UNIVERSITIES, 7 INTERNATIONAL CAMPUSES, 60,000 ALUMNI AND 2 DECADES OF EXCELLENCE IN EDUCATION.

250	250	300	300	240
patents filed by faculty in the last years	Govt. funded research projects	case-studies developed by faculty in the last one year	state-of-the-art labs	programmes across 50 disciplines

Established by the Chauhan Family more than twenty years ago, the Amity Education Group is a leading education group today, offering globally benchmarked education right from pre-schools to Ph.D. level. Starting with campuses in India, Amity today has campuses around the world and aims to add more in 25 countries over the next few years.

Amity, one of the few universities in India to offer 240 UG & PG degrees, has brought together some of the most eminent scientists, research scholars and corporate leaders from across the world, who are doing research in diverse, cutting-edge areas of science, technology and industry. Such focus on path-breaking innovations, a globally benchmarked infrastructure and outstanding faculty have resulted in Amity institutes being ranked amongst the top by India's most respected surveys.

SOME OF AMITY'S ACHIEVEMENTS

3,500 faculty & scientists – At Amity, a vibrant community of 3,500 distinguished faculty of scientists, professors, researchers and corporate professionals has been drawn from different walks of the industry who have been credited with publishing over 3,400 research papers and authoring over 500 books.

Highest number of patents filed – The Amity faculty have been credited with filing the highest number of patents by any university in India in the last one year.

India's Largest Fellowship Programme – Furthering its goal of excellence in research, Amity also offers India's Largest Ph.D. and Post-Doctoral Programme.

International Linkages – To keep abreast of the latest developments, Amity has tie-ups with over 100 global Universities, Laboratories and Research Centres spanning USA, Europe and Australia in areas of research, faculty & student exchange and curriculum development.

Future focussed Programmes – Amity has pioneered numerous degree courses in India in cutting edge areas like Solar Energy, Thin Film Technology, Nuclear Science & Technology, Postharvest Technology, Nanotechnology etc.

Recognition for research – Amity has been recognized as a Scientific & Industrial Research Organisation (SIRO) by the Govt. of India, a unique achievement by any Indian University and is a reflection of its unique initiatives in hi-end research.

State-of-the-art academic environment - Setting benchmarks only against the best universities globally, a hi-tech experience is drawn at Amity from a mix of 5 million sq.ft. of buildings, 300 state-of-the-art labs across 35 science disciplines, libraries with 4,00,000 books, periodicals & 17,000 online journals.

Top ranked institutions - Amity Institutions have been ranked among the very top in prestigious surveys by leading media including those of Law, Management, Biotechnology, Engineering, Insurance etc.

7 international campuses - Amity has emerged as India's only education group with international campuses in London, New York, Singapore, California, Mauritius, Dubai & Romania. Through centrally located campuses, the highest rating & accreditations and globally recognised degrees, these campuses carry forward Amity's rich legacy of excellence in education.

AMITY UNIVERSITY CAMPUSES IN INDIA

Amity conducts research & offers UG & PG degree programmes in over 35 disciplines of Science & Technology including: Aerospace I Agriculture I Applied Sciences I Biotechnology I Engineering - Automobile/Civil/Computer Science/Control Systems/Electronics & Comm./Electrical & Electronics/Information Technology/Instrumentation/Mechatronics/ Mechanical & Automation/Optoelectronics & Optical Comm./Power Systems /Telecom/VLSI/WIreless Comm. | Environment I Food Tech. I Forensic Sciences I Green Technology I Herbal Research & Studies I Horticulture I Marine Sc. I Medical & Allied Sc. I Microbial Sc. I Nanotechnology I Nuclear Science & Technology I Pharmacy I Physiotherapy I Post Harvest Tech. & Cold Chain Management I Space Sciences I Telecom I Virology & Immunology ***(For complete programme list, visit www.amity.edu)***

Universities or Faculty/Scientists interested in collaboration with Amity may contact at partnerships@amity.edu | Faculty interested in teaching at Amity may contact at globalfaculty@amity.edu

EPITOMICS®
BETTER ANTIBODIES • BETTER SCIENCE

SPECIAL OFFER
$129 AKT RABMABS
Find out more @
www.epitomics.com/products/promo

RabMAbs® = Better AKT Antibodies

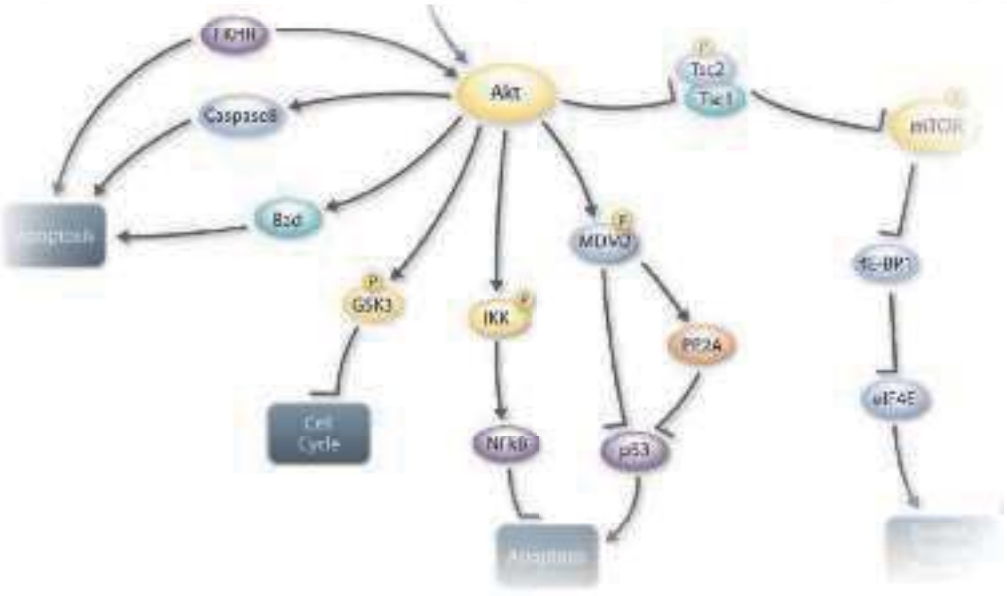

- **High quality antibodies to Akt and related proteins**
- **Validated in WB, IHC, IF, IP and FACS**
- **Over 7000 antibodies and counting**

At Epitomics, we provide a wide range of high quality antibodies to Akt and related proteins. Using our patented Rabbit Monoclonal Antibody (RabMAb®) technology, we have developed a collection of high quality Akt specific antibodies. Each Akt specific RabMAb offers superior antigen recognition of the rabbit immune system and the specificity of a monoclonal antibody.

Find out more@ www.epitomics.com/akt

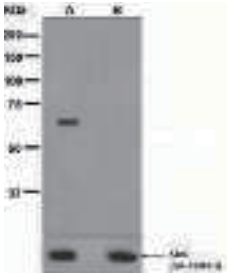

Akt1 Phospho (pT450)

Western blot analysis on NIH/3T3 cell lysate using anti-Akt1 Phospho (pT450) RabMAb (cat. #3188-1). Cells were either (A) untreated or (B) treated with Lambda Phosphatase.

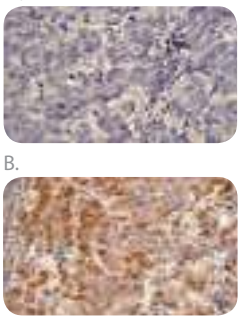

Akt1 Phospho (pS473)

Immunohistochemical staining of human cervical carcinoma tissue using anti-Phospho-Akt1 (pS473) RabMAb (cat. # 2118-1). Tissue was (A) phosphatase treated and (B) untreated.

100% SATISFACTION GUARANTEE *Antibody Satisfaction Guarantee*

www.epitomics.com

US & Canada | 1-877-772-2622
Outside NA | 650-583-6688
info@epitomics.com

Enhance your imaging results

abcam®
discover more

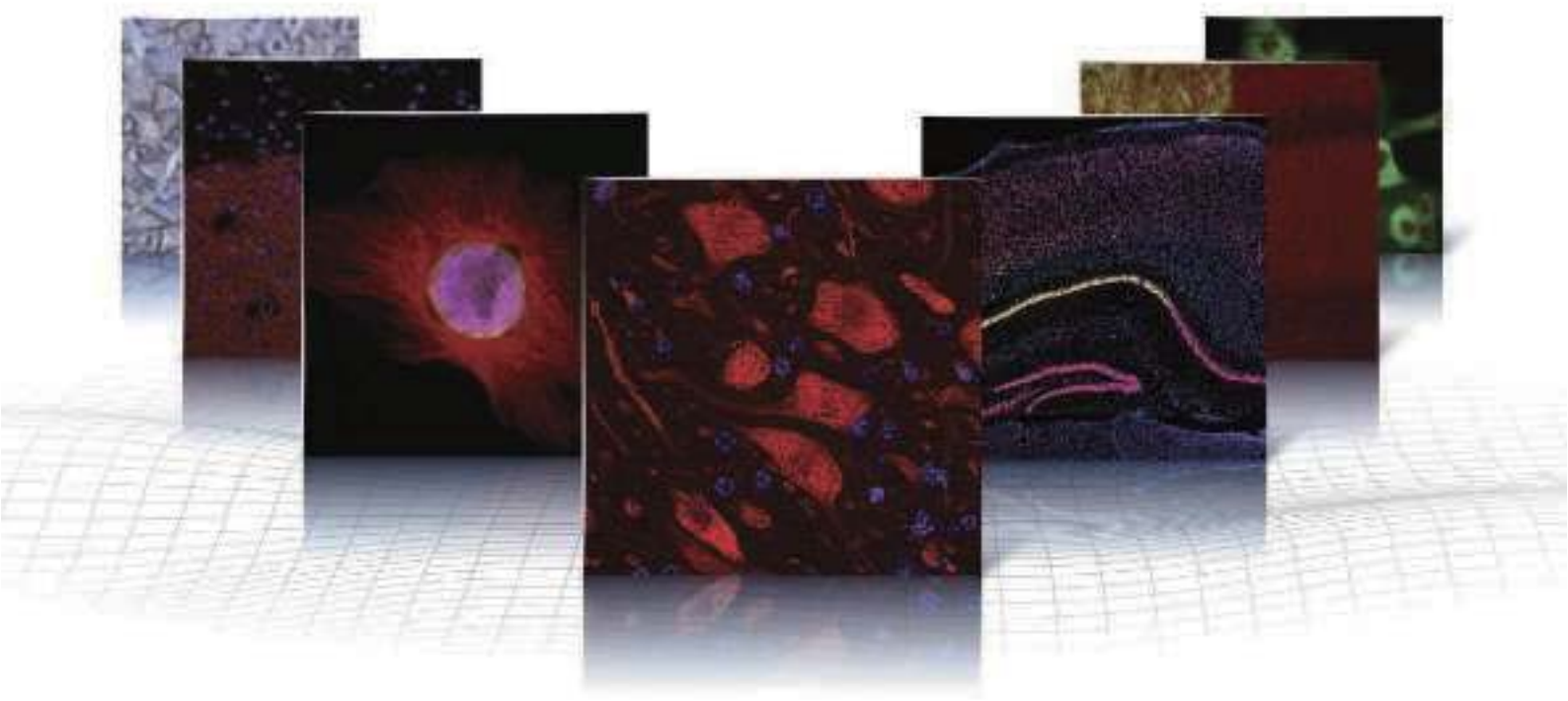

Introducing new products to help you with your research.

Recommended products

- IHC kits (include EXPOSE IHC kits)
- IHC buffers and reagents
- Pre-adsorbed secondary antibodies
- Over 2,500 secondary antibodies
- DRAQ5™ and CyTRAK Orange™

Product benefits

- Higher sensitivity and quick results
- Improved antigen retrieval and efficient blocking
- Reduced the risk of cross-reactivity
- Amplify your imaging signals
- Advanced cell or nuclear staining tools

265_11_SS

Discover more at abcam.com/imaging

Cell Cycle Analysis on the BD FACSVerse™ System

A streamlined approach to application support.

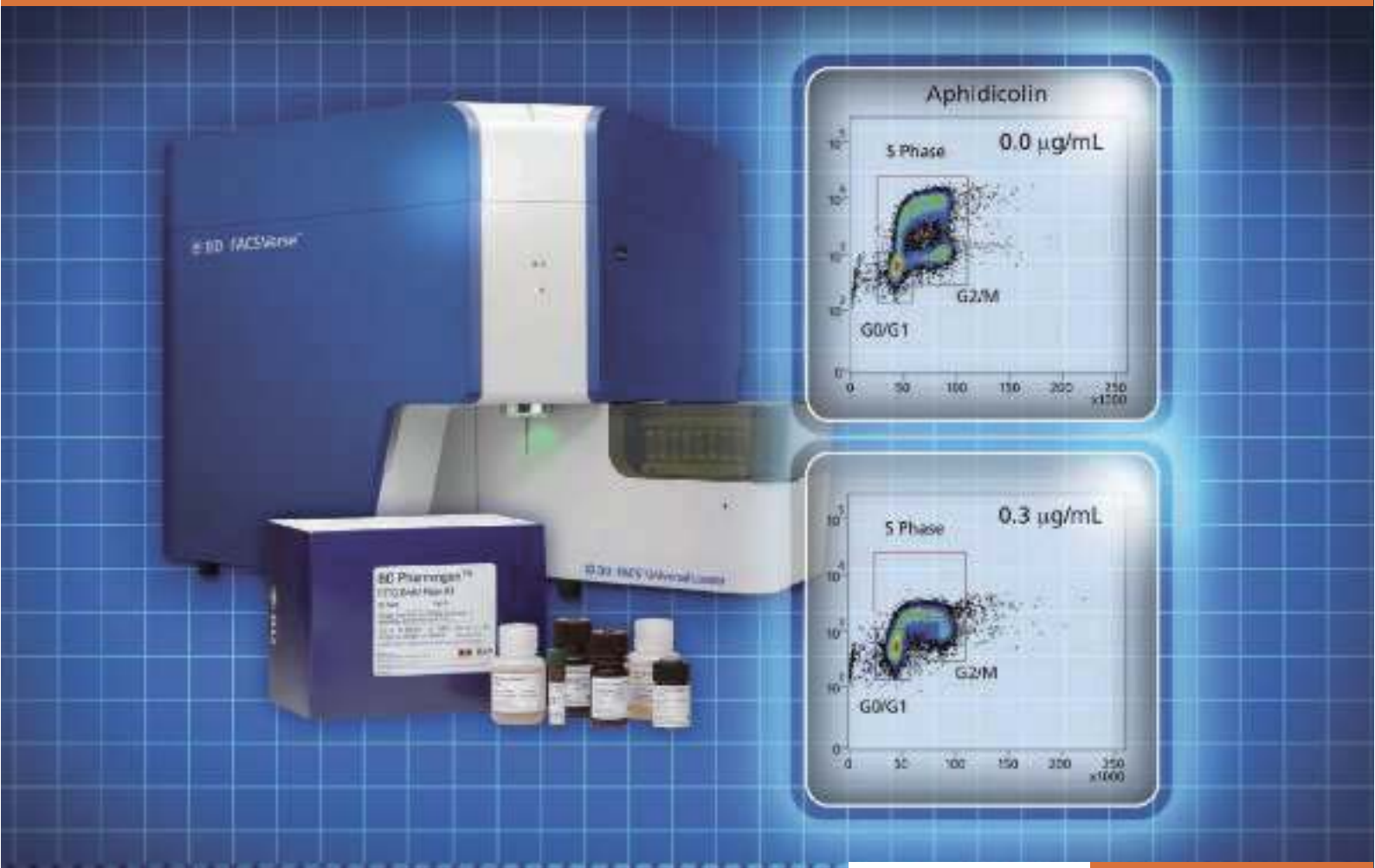

What's Really Exciting Is What's Behind it.

In the data shown, unpulsed and BrdU-pulsed Jurkat cells were analyzed to show that the BD Pharmingen™ FITC BrdU flow kit combined with the BD BrdU FITC assay can be used as a quick and easy way to assess the cell cycle.

The assay can also be customized for advanced dose response and time course experiments with multiple tubes.

New BD FACSuite™ software makes it easy to convert experiments to reusable assays with setup information, acquisition and analysis templates, gating strategies, and reports you can share with other BD FACSVerse™ systems.

The software also provides BD predefined research assays matched with BD reagent kits for reproducible results. These assays reduce the variability of data between users and among laboratories for the same application.

Download a free application note and learn more about BD FACSuite predefined assays for apoptosis, cell cycle, cell proliferation, and cytokine detection at **bdbiosciences.com/go/verse.**

Simply Brilliant.

BD

Helping all people live healthy lives

BD Biosciences
2350 Qume Drive
San Jose, CA 95131
bdbiosciences.com

SANYO

A member of the Panasonic Group

ACCELERATE YOUR growth

Experience greater cell expansion in shorter culture time

BD Falcon™ Multi-Flask
SANYO MCO-19AIC(UVH)

GREATER CAPACITY & YIELD

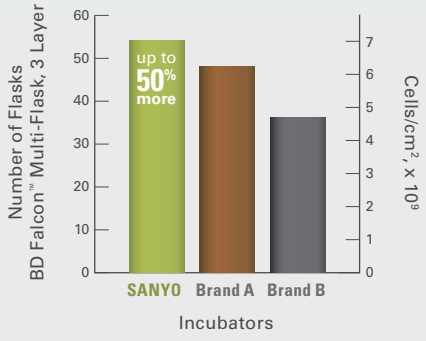

FASTER DECONTAMINATION

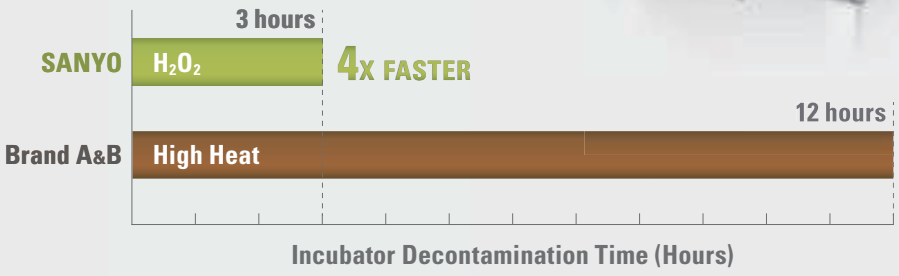

BD

Visit www.AccelerateCellGrowth.com to learn more!
Take advantage of special offers and win a FREE SANYO incubator.

**Based on 1 incubation cycle with BHK-21 cells*

Visit us at AACR!
Booth #1203

New Products: General Lab Equipment

ZOOM MICROSCOPE

The Axio Zoom.V16 combines the typical benefits of stereomicroscopes such as zoom optics and long working distances with the higher resolutions of traditional light microscopes. In comparable image fields, the Axio Zoom.V16 offers a 2.5 times higher resolution and 10 times brighter fluorescence than stereomicroscopes. With a 16x zoom range, the Axio Zoom.V16 surpasses all comparable microscopes currently available. An extensive line of accessories enables configurations precisely tailored to many different applications. An illumination concept specially developed for zoom microscopes delivers considerably higher fluorescence illumination intensity, with even the smallest fluorescent structures remaining visible. The Axio Zoom.V16 incorporates totally new approaches not only to visual observation, but also to imaging. Higher apertures substantially reduce the depth of field ranges in the focal plane. Structured illumination with the Apotome.2 slider system makes it possible to generate optical sectional images and 3-D reconstructions of the specimens.

Carl Zeiss
For info: 800-509-3905 | www.zeiss.de

LOW VOLUME MICROPLATE

The MicroMax Low Volume Microplate offers researchers the benefit of measuring up to 64 samples per plate on the SpectraMax microplate readers. The elegant simplicity of the MicroMax design provides remarkable flexibility, ideal for multiuser environments. The customer can use either 2 or 4 µL samples, and will have a variety of cleaning options available: simply wiping the slide, autoclaving, or replacing the slides. The unique, no-hinge design offers great uniformity with no maintenance and simplifies the cleaning process. Perfect for core labs, bioprocessing quality control/manufacturing environments, biorepositories, and molecular diagnostics labs, the 8- or 16-channel pipettor compatibility of 24- or 64-sample plates, respectively, enables fast determinations of a wide range of samples including DNA, RNA, and proteins. The MicroMax Low Volume Microplates are compatible with all SpectraMax readers. The low-volume plates have ready-to-use application specific protocols in SoftMax Pro Data Analysis and Acquisition Software for seamless integration.

Molecular Devices
For info: 800-635-5577 | www.moleculardevices.com

SPECTROPHOTOMETERS

The new Ultrospec series of dual beam, ultraviolet-visible spectrophotometers provides research scientists with a choice of smart instruments with diverse capabilities to deliver reproducible results, precision, and ease of use to match a variety of user requirements. The series includes Ultrospec 7000/7000PC for day-to-day laboratory activities, Ultrospec 8000/8000PC, and the top of the range 9000/9000PC system for demanding assays. Each version is available as either a standalone or PC-controlled system. The Ultrospec range benefits from the following features: dual-beam instrument (with a variety of bandwidths); color touchscreen (for standalone product); USB data and PC connectivity; European Pharmacopoeia research compatibility (8000/9000 models); Datrys Standard (option to upgrade to Datrys Life Science or Datrys CFR); Equation Editor software; and extended range of accessories available such as thermostatting, Bluetooth, and Datrys software options.

GE Healthcare
For info: 800-526-3593 | www.gelifesciences.com

ANALYTICAL LAB BALANCE

The Kern ABT high-precision laboratory analytical balance automatically recalibrates itself under four scenarios: every four hours, after temperature fluctuations of 0.5°C (0.9°F), when switching from standby to weighing, and after being reconnected to its power source. Prior to a recalibration the balance alerts technicians, who can postpone the process until their weighing operation is complete. The laboratory balance automatically outputs GLP/ISO data to a PC or printer. Two models of this fast-responding electronic analytical balance operate in dual weighing ranges. Four other single weighing range models are available. All are tailor-made for organizations demanding high-precision electronic scales delivering stable temperature behavior, a short stabilization time, and excellent weighing precision even with samples at the edge of the pan. The versatile ABT analytical balances also accommodate piece counting, recipe weighing, percentage determination, suspended weighing capabilities, metric/non-metric operation, and feature large LCD displays.

Tovatech
For info: 973-913-9734 | www.tovatech.com

H_2O_2 INCUBATOR-DECONTAMINATION SYSTEM

The unique hydrogen peroxide vapor decontamination option provides complete decontamination while limiting incubator downtime to less than three hours. The automated H_2O_2 cycle protects user safety and can be validated, if desired, ensuring compliance with the highest cGMP, GLP, and GRP standards. Available with Sanyo's MCO-19AIC CO_2 and MCO-19M multi-gas incubators, the H_2O_2 system enables full decontamination and incubator cleaning to be completed in less than a morning. As this is a low temperature process there is no heat stress on electrical components and zero impact on adjacent equipment and the surrounding environment. All interior components and the CO_2 sampling loop are decontaminated in situ, bypassing the need for a separate autoclave cycle. Following a seven-minute H_2O_2 vaporization, the ultraviolet lamp switches on for 90 minutes, reducing the H_2O_2 to water vapor and oxygen. The incubator's interior fan circulates air throughout the chamber during the entire cycle.

Sanyo
For info: +31-765-433833 | www.eu.sanyo.com

Electronically submit your new product description or product literature information! Go to **www.sciencemag.org/products/newproducts.dtl** for more information.

Newly offered instrumentation, apparatus, and laboratory materials of interest to researchers in all disciplines in academic, industrial, and governmental organizations are featured in this space. Emphasis is given to purpose, chief characteristics, and availability of products and materials. Endorsement by *Science* or AAAS of any products or materials mentioned is not implied. Additional information may be obtained from the manufacturer or supplier.

LOCATION: Jackson Park Health Club
ARTICLE: *An Electronic Second Skin*
DATE: Sep 21, 7:43am

LOCATION: University Faculty Lounge
ARTICLE: *The Visual Impact of Gossip*
DATE: Sep 21, 4:22pm

LOCATION: Gyro King
ARTICLE: *Cavemen Craved Carbs, Too*
DATE: Sep 21, 1:13pm

LOCATION: Hemlock Bar
ARTICLE: *Quantum Simulation of Frustrated Classical Magnetism in Triangular Optical Lattices*
DATE: Sep 21, 9:21pm

LOCATION: Bed
ARTICLE: *Consciousness: What, How and Why*
DATE: Sep 21, 10:56pm

A new way to look at science

The new *Science* Reader app for iPad® from AAAS puts *Science* in your hands, wherever you go. Read abstracts, career advice, and highlights from our newest journals, *Science Signaling* and *Science Translational Medicine*. Plus, AAAS members can access full text articles from *Science*. Visit iTunes App Store℠ or content.aaas.org/ipad for details.

Available on the App Store

Science
AAAS